



## City Research Online

### City, University of London Institutional Repository

---

**Citation:** El Kaddah, N.H. (1983). Water wave-structure interaction for small amplitude structural oscillations. (Unpublished Doctoral thesis, City University London)

This is the accepted version of the paper.

This version of the publication may differ from the final published version.

---

**Permanent repository link:** <https://openaccess.city.ac.uk/id/eprint/8234/>

**Link to published version:**

**Copyright:** City Research Online aims to make research outputs of City, University of London available to a wider audience. Copyright and Moral Rights remain with the author(s) and/or copyright holders. URLs from City Research Online may be freely distributed and linked to.

**Reuse:** Copies of full items can be used for personal research or study, educational, or not-for-profit purposes without prior permission or charge. Provided that the authors, title and full bibliographic details are credited, a hyperlink and/or URL is given for the original metadata page and the content is not changed in any way.

WATER WAVE-STRUCTURE INTERACTION FOR  
SMALL AMPLITUDE STRUCTURAL OSCILLATIONS

A THESIS SUBMITTED FOR THE DEGREE OF  
DOCTOR OF PHILOSOPHY IN THE DEPARTMENT OF  
CIVIL ENGINEERING AT THE CITY UNIVERSITY

BY

NASHAT HAMED EL KADDAH BSc, MSc

THE CITY UNIVERSITY

AUGUST 1983

*To My Parents*

## A B S T R A C T

The water wave/structure interaction is a complex phenomenon, which affects the prediction of the dynamic response of offshore structures. The problem arises from the interdependence of the structural response and the wave force. This interdependence is usually represented by the effect of the relative velocity and relative acceleration used in the wave force formula.

This work is carried out to investigate the effect of the water wave/structure interaction on circular cylinder for small Keulegan-Carpenter numbers and structural amplitude of oscillation. In order to achieve this an extensive experimental program, in conjunction with theoretical study was undertaken.

The study indicates that the use of modified Morison's equation taking into consideration the velocity and acceleration of the structure is not needed to predict the structural deflection. But significant difference in the force coefficients for free and fixed structure have obtained experimentally.



## ACKNOWLEDGEMENTS

During the course of the research the author received valuable advice and helpful suggestions from many persons. In particular the author wishes to express his gratitude to Dr. K. Arumugam, who supervised this work, for his constant encouragement, his valuable advice and his guidance throughout the duration of the research, without which the effective fulfilment of this work would not have been possible.

To Dr. K. S. Virdi and Mr. P. Carr for their generous help in many ways.

To the staff of The City University Civil Engineering Hydraulics Laboratory 1 whose effort is appreciated.

To my parents for providing financial and moral support. Last, but not least, to my family and friends for their love and encouragement.

# CONTENTS

	PAGE
Abstract	III
Acknowledgement	IV
Contents	V
List of Figures	X
List of Tables	XV
Notation	XVII
 Chapter 1	
Introduction	1
 Chapter 2	
Survey of Literature Related to Dynamic Response	7
2.1	
Hydrodynamic Forces	8
2.1.1	
Water Wave Theory	8
2.1.2	
Hydrodynamic Force	12
2.1.2.1	
Force on Large Bodies	14
2.1.2.1A	
Diffraction Theory	14
2.1.2.2	
Force on Small Bodies	15
2.1.2.2A	
Morison's Equation	15
2.1.2.2B	
Transverse Force	29
2.1.2.3	
Morison's Equation for Flexible Cylinder	30
2.2	
The Idealization used to Model the Structure System	31
2.2.1	
Foundation System	31
2.2.2	
Structure System	38
2.2.2.1	
The Mass Matrix	38
2.2.2.2	
The Stiffness Matrix	44

	PAGE
2.2.2.3 The Damping Matrix	44
2.3 Numerical Procedures	49
2.3.1 Time Domain and Frequency Domain Description	49
2.3.1.1 Mathematical Formulation of the Dynamic Problem in Frequency Domain Description	50
2.3.1.2 Mathematical Formulation of the Dynamic Problem in Time Domain Description	51
2.3.2 Model Superposition and Direct Intergration	52
2.3.2.1 Mathematical Formulation of the Dynamic Problem by Mode Superposition	53
2.3.2.2 Mathematical Formulation of the Dynamic Problem by Direct Integration	54
Chapter 3 Theoretical Formulation	57
3.1 Introduction	57
3.2 Wave Dynamics	57
3.2.1 Wave Description	58
3.2.2 Wave Forces	62
3.3 Structural Dynamics	67
3.3.1 The Structure Modelling	67
3.3.2 Formulation of the Equation of Structural System Response	69
3.3.3 Solution of the System	85
3.3.4 Numerical Analysis	88

	PAGE
3.4 Theoretical Formulation of the Experiment	90
3.4.1 Modelling of the Tested Structure	90
3.4.2 Digitization of Data	92
3.4.3 Determination of the Measured Wave Force	93
3.4.4 Determination of the Velocity and Acceleration of the Structure at any Level	95
3.4.5 Evaluation of the Constant $\alpha_0$ and $\alpha_1$ for the Damping Matrix	98
Chapter 4 Experimental Technique	102
4.1 Experimental Facilities	102
4.1.1 Wave Tank	102
4.1.2 Tested Structures	106
4.1.2.1 Durapipe ABS Structures	106
4.1.2.2 Aluminium Structures	113
4.2 Description of Instrumentation	118
4.2.1 Measurement Instrumentation	118
4.2.1.1 Wave Probe	118
4.2.1.2 Strain Gauges at the Base of the Structure	120
4.2.1.3 Pressure Transducers	122
4.2.1.4 Displacement Transducer	125
4.2.2 Reading Instruments	125
4.3 Calibration of the Measuring Instrumentation	129
4.3.1 Strain Gauge	
4.3.2 Displacement Transducer	130

		PAGE
	4.3.3 Pressure Transducers	132
	4.3.4 Wave Probe	134
4.4	Experiment	134
	4.4.1 Water Wave Criteria	134
	4.4.2 Structure Dynamic Properties	138
	4.4.2.1 Stiffness Test	138
	4.4.2.2 Natural Frequencies and Structural Damping	142
	4.4.3 Main Tstes	144
Chapter 5	RESULTS	
5.1	The Dynamic Properties of the Structures	164
	5.1.1 Determination of Damping Coefficients and Natural Frequencies	164
	5.1.2 Determination of Stiffness Constants	168
5.2	DATA ANALYSIS	169
	5.2.1 Wave Properties	178
	5.2.2 The Forces on Structure	180
	5.2.3 Structure Dynamic Response	182
5.3	The Results from the Experiments	183
	5.3.1 Wave and the Corresponding Forces on the Structures	183
	5.3.2 Structure's Response to the Wave Forces	217
Chapter 6	Summary and Conclusion	251

		PAGE
REFERENCES		258
APPENDICES		
	A Pressure Transducer	277
	B Preamplifier	281
	C Sinusoidal Interpolation	283
	D The Variation of the Relative Displacement $X/D$ with Time for One Cycle of the Wave	285



## LIST OF FIGURES

FIGURE NO		PAGE
(2.1.1)	The Range of Validity of Various Wave Theories 12	10
(2.1.2)	Representation of Zones of Validity of Various Wave Theories 9	11
(2.1.3)	Wave Force Theory 16	12
(2.1.4)	Direction of Velocity and Acceleration at Various Points of a Wave Cycle	18
(2.1.5)	$C_M$ Versus Keulegan-Carpenter Number 27	19
(2.1.6)	$C_D$ Versus Keulegan-Carpenter Number 27	19
(2.2.1)	Gravity Structure	32
(2.2.2)	Framed Steel Structure	32
(2.2.3)	Soil Model for Gravity Structure	33
(2.2.4)	Soil Model for Framed Steel Structure	33
(2.2.5)	Foundation Modelling	35
(2.2.6a - 2.2.6b)	Model 1 and Model 2 80	40
(3.3.1)	Modelling of the Structures	68
(3.3.2)	The Tangent Pipe Element	89
(3.4.1)	Discretization of Response and Force	91
(3.4.2)	Pressure and Shear Distribution about a Circular Cylinder	93
(4.1.1)	Wave Tank	105
(4.1.2)	The Parts of the Structures (A) and (B) before Assembly	108
(4.1.3)	Dimension of Structures (C) and (D)	110
(4.1.4)	Structure (A) and (B)	111
(4.1.5)	Structure (C) and (D)	112
(4.1.6)	Dimensions of Structures (E) and (F)	114
(4.1.7)	Structure (E) and the Four Masses	115

FIGURE NO		PAGE
(4.2.1)	Strain Gauge Installation	121
(4.2.2)	The Mounting and Connection of the Pressure Transducer to the Structure	124
(4.2.3)	Strain Gauge Amplifier, Preamplifier and Tape Recorder	128
(4.3.1)	The Test Determining the Tip Deflection due to Horizontal Load	131
(4.4.1)	Water Wave Profile	135
(4.4.2)	Typical Reflected Wave	136
(4.4.3)	Reflection Coefficient for the Wave Tank	137
(4.4.4)	Schematic Diagram of Deformation Types for Durapipe ABS	139
(4.4.5)	Typical Recording of the Strain Gauge	140
(4.4.6)	Typical Record of the Natural Frequencies and Structural Damping	143
(4.4.7)	Structure A under Test	146
(4.4.8)	Structure B under Test	147
(4.4.9)	Structure C under Test	148
(4.4.10)	Structure D under Test	149
(4.4.11)	Structure E under Test	151
(4.4.12)	Structure F under Test	152
(5.2.1)	Measured Data and the Calculated In-line and Transverse Local Force for Free Structure	172
(5.2.2)	Measured Data and the Calculated In-line and Transverse Local Force for Fixed Structure	173
(5.2.3)	Pressure Distribution across the Structure during the Wave Cycle for Free Structure	174
(5.2.4)	Pressure Distribution across the Structure during the Wave Cycle for Fixed Structure	175
(5.2.5)	F.F.T for the Wave Profile, the In-line Force and the Tip Displacement for Free Structure	176



FIGURE NO		PAGE
(5.2.6)	F.F.T for the Wave Profile, the In-line Force and the Tip Displacement for Fixed Structure	177
(5.2.7)	The Measured and Calculated Wave Profile	179
(5.2.8)	The Calculated and Measured Bending Moment	182
(5.3.1a - 5.3.1b)	Variation of $C_D$ with Reynolds Number, $1/D$ - and of $C_M$	199
(5.3.2a - 5.3.2b)	Variation of $C_D$ with Keulegan-Carpenter Number - and of $C_M$	200
(5.3.3a - 5.3.3b)	Variation of % ( $C_D$ Free (R)/ $C_D$ Fixed) with K-C Number for Structure A - and of $C_M$	201
(5.3.4a - 5.3.4b)	Variation of % ( $C_D$ Free (R)/ $C_D$ Fixed) with K-C Number for Structure B - and of $C_M$	202
(5.3.5a - 5.3.5b)	Variation of % ( $C_D$ Free (R)/ $C_D$ Fixed) with K-C Number for Structure C - and of $C_M$	203
(5.3.6a - 5.3.6b)	Variation of % ( $C_D$ Free (R)/ $C_D$ Fixed) with K-C Number for Structure D - and of $C_M$	204
(5.3.7a - 5.3.7b)	Variation of % ( $C_D$ Free (R)/ $C_D$ Fixed) with K-C Number for Structure E with no Mass at the Top - and of $C_M$	205
(5.3.8a - 5.3.8b)	Variation of % ( $C_D$ Free (R)/ $C_D$ Fixed) with K-C Number for Structure E with 1010 Grs at the Top - and of $C_M$	206
(5.3.9a - 5.3.9b)	Variation of % ( $C_D$ Free (R)/ $C_D$ Fixed) with K-C Number for Structure E with 2020 Grs at the Top - and of $C_M$	207
(5.3.10a - 5.3.10b)	Variation of % ( $C_D$ Free (R)/ $C_D$ Fixed) with K-C Number for Structure F with no Mass at the Top - and of $C_M$	208
(5.3.11a - 5.3.11b)	Variation of % ( $C_D$ Free (R)/ $C_D$ Fixed) with K-C Number for Structure F with 1010 Grs at the Top - and of $C_M$	209
(5.3.12a - 5.3.12b)	Variation of % ( $C_D$ Free (R)/ $C_D$ Fixed) with K-C Number for Structure F with 2020 Grs at the Top - and of $C_M$	210
(5.3.13)	Variation of % ( $C_D$ Free (R)/ $C_D$ Fixed) with K-C Number for all Structures	211
(5.3.14)	Variation of % ( $C_M$ Free (R)/ $C_M$ Fixed) with K-C Number for all Structures	212

FIGURE NO		PAGE
(5.3.15a - 5.3.15b)	Variation of % ( $C_D$ Free (R)/ $C_D$ Free) with K-C Number for all Structures - and of $C_M$	213
(5.3.16a - 5.3.16b)	Variation of the Structures' Response (X/D) with Reciprocal of Reduced Velocity - and with Response Parameter	232
(5.3.17a - 5.3.17b)	Variation of the (Force Frequency/Natural Frequency) with the Reciprocal of Reduced Velocity - and with Response Parameter	233
(5.3.18a - 5.3.18b)	Variation of the Phase Shift between the Structure's Response and the Force with the Reciprocal of Reduced Velocity - and with Response Parameter	234
(5.3.19)	Variation of (% $C_D$ Free (R)/ $C_D$ Fixed) with the Reciprocal of Reduced Velocity	235
(5.3.20)	Variation of (% $C_D$ Free (R)/ $C_D$ Fixed) with the Response Parameter	236
(5.3.21)	Variation of (% $C_M$ Free (R)/ $C_M$ Fixed) with the Reciprocal of Reduced Velocity	237
(5.3.22)	Variation of (% $C_M$ Free (R)/ $C_M$ Fixed) with the Response Parameter	238
(5.3.23)	Structure's Response (X/D) during the Wave Cycle for Structure A	240
(5.3.24)	Structure's Response (X/D) during the Wave Cycle for Structure B	241
(5.3.25)	Structure's Response (X/D) during the Wave Cycle for Structure C	242
(5.3.26)	Structure's Response (X/D) during the Wave Cycle For Structure D	243
(5.3.27)	Structure's Response (X/D) during the Wave Cycle for Structure E with no Mass at the Top	244
(5.3.28)	Structure's Response (X/D) during the Wave Cycle for Structure E with 1010 Grs at the Top	245
(5.3.29)	Structure's Response (X/D) during the Wave Cycle for Structure E with 2020 Grs at the Top	246
(5.3.30)	Structure's Response (X/D) during the Wave Cycle for Structure F with no Mass at the Top	247
(5.3.31)	Structure's Response (X/D) during the Wave Cycle for Structure F with 1010 Grs at the Top	248

FIGURE NO		PAGE
(5.3.32)	Structure's Response (X/D) during the Wave Cycle for Structure F with 2020 Grs at the Top	249
(1A)	The Sensing Element	278
(2A)	The Transducer Housing	280
(1B)	The Preamplifier Circuits	282
(1D - 61D)	Structure's Response (X/D) during the Wave Cycle for all the Tests on Each Structure	286-346



## LIST OF TABLES

TABLE NO		PAGE
(4.1)	Mechanical Properties of the Structures	117
(4.2)	Digitized Electric Signal for One of the Calibration Tests	153
(4.3)	Digitized Electric Signal for One of the Tests	154-163
(5.1)	Relative Damping Coefficients and Natural Frequencies	167
(5.2)	Wave Characteristics and Wave Force Coefficients for Structure A	187
(5.3)	Wave Characteristics and Wave Force Coefficients for Structure B	188
(5.4)	Wave Characteristics and Wave Force Coefficients for Structure C	189
(5.5)	Wave Characteristics and Wave Force Coefficients for Structure D	190
(5.6)	Wave Characteristics and Wave Force Coefficients for Structure E with no Mass at the Top	191
(5.7)	Wave Characteristics and Wave Force Coefficients for Structure E with 1010 Grs at the Top	192
(5.8)	Wave Characteristics and Wave Force Coefficients for Structure E with 2020 Grs at the Top	193
(5.9)	Wave Characteristics and Wave Force Coefficients for Structure F with no Mass at the Top	194
(5.10)	Wave Characteristics and Wave Force Coefficients for Structure F with 1010 Grs at the Top	195
(5.11)	Wave Characteristics and Wave Force Coefficients for Structure F with 2020 Grs at the Top	196
(5.12)	Structure's Response to the Wave Force for Structure A	220
(5.13)	Structure's Response to the Wave Force for Structure B	221
(5.14)	Structure's Response to the Wave Force for Structure C	222

TABLE NO		PAGE
(5.15)	Structure's Response to the Wave Force for Structure D	223
(5.16)	Structure's Response to the Wave Force for Structure E with no Mass at the Top	224
(5.17)	Structure's Response to the Wave Force for Structure E with 1010 Grs at the Top	225
(5.18)	Structure's Response to the Wave Force for Structure E with 2020 Grs at the Top	226
(5.19)	Structure's Response to the Wave Force for Structure F with no Mass at the Top	227
(5.20)	Structure's Response to the Wave Force for Structure F with 1010 Grs at the Top	228
(5.21)	Structure's Response to the Wave Force for Structure F with 2020 Grs at the Top	229

## NOTATION

$\phi$	Velocity potential
$\eta$	Wave surface
$P$	Pressure
$\rho$	Water density
$\dot{U}$	Water particle velocity in x direction
$v$	Water particle velocity in y direction
$w$	Water particle velocity in z direction
$g$	Gravitational acceleration
$H$	Wave height
$L$	Wave length
$h$	Water depth
$D$	Structure diameter
$F_m$	Total force
$F_D$	Drag force
$F_I$	Inertia force
$C_D$	Drag coefficient
$C_M$	Inertia coefficient
$\ddot{U}$	Water particle acceleration
$K-C$	Keulegan and Carpenter number( $U_m T/D$ )
$R_e$	Reynolds number( $U_m D/\gamma$ )
$C_L$	Transverse (lift) coefficient
$X$	Structure displacement
$\dot{X}$	Structure velocity
$\ddot{X}$	Structure acceleration
$[M]$	Mass matrix

$\{C\}$	Damping matrix
$\{K\}$	Stiffness matrix
$\{F(t)\}$	Hydrodynamic force matrix
$\{X\}$	Structure displacement matrix
$\{\dot{X}\}$	Structure velocity matrix
$\{\ddot{X}\}$	Structure acceleration matrix
$[C_s]$	Damping in the free structure matrix
$[C_f]$	Damping in the foundation matrix
$[K_s]$	Stiffness in the free structure matrix
$[K_c]$	Stiffness in the foundation matrix
$[C_s^f]$	Damping matrix for fixed based structure
$[C_s^{bb}]$	Damping matrix associated with the base degree of freedom
$[C_s^b]$	The coupling damping matrix
$[M^f]$	Diagonal mass matrix including hydrodynamic added mass
$\{\phi_J\}$	Mode shape vector
$W_J$	Frequency of the J mode
$\xi_J$	Damping ratio of the J Mode
$M_J$	Generalized mass of the J mode
$[K_s^f]$	Stiffness matrix of fixed base structure
$[K_s^b]$	Stiffness-coupling matrix
$M$	Total mass
$M_m$	Material structural and platform mass
$M_a$	Hydraulics added mass
$M_F$	Flooding and marine growth mass
$\Psi$	Volume of water displaced by structure
$\xi$	Damping coefficient

$C$	Structural damping
$C_c$	Critical damping
$\sigma_n$	Wave angular frequency ( $2\pi/T$ )
$k$	Wave number ( $2\pi/L$ )
$c_n$	Velocity of wave propagation $\frac{\sigma_n}{k}$
$a$	Wave amplitude
$L_s$	Structure length
$z$	Vertical distance from the still water level
$C'_D$	Drag coefficient for free structure
$C'_M$	Inertia coefficient for free structure
$F'$	Force exerted on free structure
$F_m$	Measured force
$S$	Element length
$\{Pt\}$	Force matrix from the modified Morison's equation
$[\tilde{C}]$	Equivalent linear damping matrix
$[C^w]$	Damping matrix using the damping coefficient in water
$[M^*]$	Generalized mass matrix
$[K^*]$	Generalized stiffness matrix
$[C^*]$	Generalized damping matrix
$\{P^*\}$	Generalized force vector
$[\phi]$	Eigen vector
$\{\omega^2\}$	Eigen value
$[\Upsilon]$	Normal co-ordinate structural displacement
$[\dot{\Upsilon}]$	Normal co-ordinate structural velocity
$[\ddot{\Upsilon}]$	Normal co-ordinate structural acceleration
$\{e(x)\}$	Error vector
$\alpha^2 e_n e_n$	Ensemble average



$\alpha_0$	Proportional factor multiplied by the mass matrix
$\alpha_1$	Proportional factor multiplied by the stiffness matrix
$f_{NY}$	Nyquist frequency ( $1/2\Delta t$ )
$\tau$	Shear distribution
$\psi$	First mode shape of the structure
FN	Natural undamped frequency of vibration
FD	Natural damped frequency of vibration
$W_n$	Natural frequency of Nth mode $W_n = 2\pi FN$
E	Modulus of elasticity
I	Second moment of area
W	Axial load
$C_{DP}$	Percentage ratio of the drag coefficient for a free structure to that for fixed structure
$C_{MP}$	Percentage ratio of the inertia coefficient for a free structure to that for fixed structure
$C_{DD}$	Percentage ratio of the drag coefficient calculated by modified Morison's equation to that calculated by Morison's equation
$C_{MD}$	Percentage ratio of the inertia coefficient calculated by modified Morison's equation to that calculated by Morison's equation
VD	Reduced velocity ( $U_m/D FN$ )
$U_m$	Maximum water particle velocity
$\bar{M}$	Effective mass
DM	Response parameter $(2\bar{M}\xi/\rho D^2 L_s) CD FN/U_m$

# CHAPTER ONE

## INTRODUCTION

At present, the exploration for energy resources has resulted in offshore structures being built in deep seas, where severe conditions of wind and waves exist; under these conditions the classical design process produces uneconomical and sometimes unsafe structures.

It has been shown in the inquiry into the collapse of Texas Tower No 4<sup>(1)</sup> that dynamic analysis will have to be used for designing of such towers.

In deep water, the interaction of a time-dependent ocean environment with a dynamically responsive structure leads to complex resonance conditions and gives rise to larger stresses than would be predicted by a quasi-static analysis. For example, Brannon et al 1974<sup>(2)</sup> have shown that the dynamic response can double the static wave load.

Laird 1962 and 1966<sup>(3, 4)</sup> has shown that the drag and inertia coefficients may vary rather widely when the structures are oscillating.

From the above it can be concluded that the investigation of the water wave/structure interaction is important for both the dynamic analysis and for the determination of the water wave force.

The existing knowledge in the fields of mechanical vibration and fluid mechanics can be used to determine the structural response. By knowing the system input of the wave profile and by applying the hydrodynamic theories, such as Airy's linear wave theory, the flow characteristics of the wave in the vicinity of the structure can be evaluated. Morison's semi-empirical force formula enables the hydrodynamic forces on the structure to be evaluated. The theory of mechanical vibration is used to compute the structural response due to these forces. The complication arises here due to the water wave/structure interaction which is the interdependence of the fluid forces and structural response.

In general the problem of the interdependence of the fluid forces and structural response is caused by the structures significant velocity and acceleration only. This may be overcome by using the relative velocity and relative acceleration in the Morison's equation which is called the modified Morison's equation.



In this thesis an investigation of this interdependence, including the effect of the structure's vibration on the force coefficients ( $C_D$  and  $C_M$ ) used in the force formula and the effect of this interdependence in the dynamic response (deflection), was carried out for the condition of low Keulegan-Carpenter numbers (1.87 - 10.69) and amplitudes of structure oscillation.

For this purpose extensive experimental work was done. Two sets of structures in different material were tested. The structures were circular cylindrical piles. The first set was PVC material and consisted of two groups. Each group had two structures with different heights. The first group was relatively stiff (the structure diameter was 0.11 metre), the second group was relatively flexible (the structure diameter was 0.0605 metre). The second set was aluminium and consisted of two structures of the same diameter (0.0574 metre), but with different height; in this set each structure was tested three times, once with no added load on top and later with different added loads on top, to give different flexibility properties of the structure. The dynamic properties of the tested structures, such as the damping coefficient, the fundamental natural frequency and the stiffness constant, were determined experimentally.

The above structures were tested for different wave conditions. At each wave condition and at each level of the structure where the pressure can be measured, the structure was tested twice, once when it was free to vibrate and once when it was prevented from vibrating. At each test, the wave profile, the pressure distribution around a certain level of the structure, the tip displacement and the bending moment at the base of the structure were measured.

The data obtained from the experiments were subjected to extensive analysis in order to predict the most appropriate wave theory for the tested wave condition and the method used for the determination of the average value of the force coefficients  $C_D$  and  $C_M$ . For the determination of the wave velocity and acceleration, the fast Fourier's analysis was utilized to obtain the free higher harmonic components in the tested wave. The least square method was used in the determination of the average value of the  $C_D$  and  $C_M$ .

For the analysis of the structural response, the structure system was idealized. The equivalent structure was assumed to be fixed at the base and the continuous member was assumed to consist of a series of pipe finite elements with discrete springs

of mass at the two end nodes. The vertical wave force was ignored and the horizontal wave force was discretized at the node point. The analysis was restricted to two dimensions.

Two methods were used in the formulation of the dynamic equation of structural response in order to find whether the water wave/structure interaction represents a significant contribution in the prediction for the case of the condition studied.

The first method included the water wave/structure interaction which will cause a nonlinear term in the partial differential equation of motion, the direct approach method was used to overcome this nonlinearity. In the second method, the water wave/structure interaction was ignored by assuming that the wave force is not modified by the motion of the structure and substituted for this assumption by using the value of the hydrodynamic damping obtained in still water for the dynamic analysis.

The numerical analyses were done by finite element method using computer program SAP IV.

The dynamic response was calculated by the mode superposition technique taking only the first three modes and using time domain description.

This work gives a clear insight into the relative influence of the structure vibration on the fluid force coefficients, (the inertia and drag coefficient). It also gives the possibility of substituting for the nonlinear hydrodynamic damping that arise from the terms of relative fluid-structure velocities by the damping coefficient in still water for obtaining the structural response.



## CHAPTER TWO

### SURVEY OF LITERATURE RELATED TO DYNAMIC RESPONSE

The flow induced vibrations are a relatively complex and diverse phenomena and heterogeneous body of research and analyses in related fields is available but is scattered through a wide variety of journals.

One of these phenomena is the water wave/structure interaction. The term, water wave/structure interaction, however, denotes only these phenomena in which an interdependence develops between the fluid dynamic forces acting on the structure and the structural response.

The inclusion of the dynamic response of an offshore structure to the water wave force complicates the determination of the structure's behaviour and water wave force.

In order to study the behaviour of these structures under dynamic loading and wave conditions, the following aspects of the problem will have to be understood and properly applied to the structure in question.

- (1) The hydrodynamic forces on the structure caused by waves
- (2) The idealization used to model the structure's system should simulate the system's response.



(3) The applicable numerical procedure must be used.

## 2.1 HYDRODYNAMIC FORCES

The determination of the hydrodynamic forces exerted by waves on structure is complex, even for slender members because of the assumptions and approximations required to predict the wave force. This requires the determination of the time histories of the loading corresponding to the design wave (i.e. velocity and acceleration time histories of wave particular with the region of each structure).

### 2.1.1 WATER WAVE THEORIES

If the flow field is assumed incompressible and irrotational, the flow field should satisfy the Laplace's equation

$$\nabla^2 \phi = 0 \quad \dots \dots \dots (2.1.1)$$

where  $\phi$  is the velocity potential.

The flow field will have to satisfy the following boundary conditions

- A - at the surface

let  $\eta(x, y, z, t)$  describe the surface S

$$\therefore \text{ the kinematic boundary } \dot{\eta}_x + V\eta_y + W\eta_z = -\eta_t \quad \dots \dots \dots (2.1.2)$$

$$\text{free surface boundary } \frac{P}{\rho} = 0 \quad \dots \dots \dots (2.1.3)$$

where  $P/\rho$  = Pressure at the free surface

then the generalized Bernoulli equation reduce to

$$\frac{\partial \phi}{\partial t} + \frac{1}{2}(\dot{u}^2 + v^2 + w^2) + gY = F(t) \quad \dots \dots (2.1.4)$$

- B - at the bottom

Let  $G(x, y, z, t)$  represent the bottom surface

$$\therefore \dot{U}G_x + VG_y + WG_z = -G_t \quad \dots \quad \dots \quad \dots \quad (2.1.5)$$

where the suffix mean differentiation with respect to the subscript.

All wave theories find close solution to the above equations by using certain assumptions to match with the physical condition of the wave (5, 6, 7).

The wave in the sea can be classified periodic, aperiodic and translatory. The regions of applicability of the various wave theories depend on the following parameters:

- (a) The wave parameters, wave height, wave length and period (H, L, T)
- (b) The position parameter water depth (h).

The limitation conditions for sinusoidal and Stokes wave were shown by Laitone 1962<sup>(8)</sup>. Wilson 1957<sup>(9)</sup>, Dean<sup>(10,11,12)</sup> and more recently Nishimuru and Isobe 1978<sup>(13)</sup> have discussed the validity of these various theories. Figure (2.1.1) shows the relation between the validities of the theories to evaluate the kinematic properties for water wave with the relation to wave and position parameter after Dean<sup>(12)</sup>, also Figure (2.1.2) after Wilson.

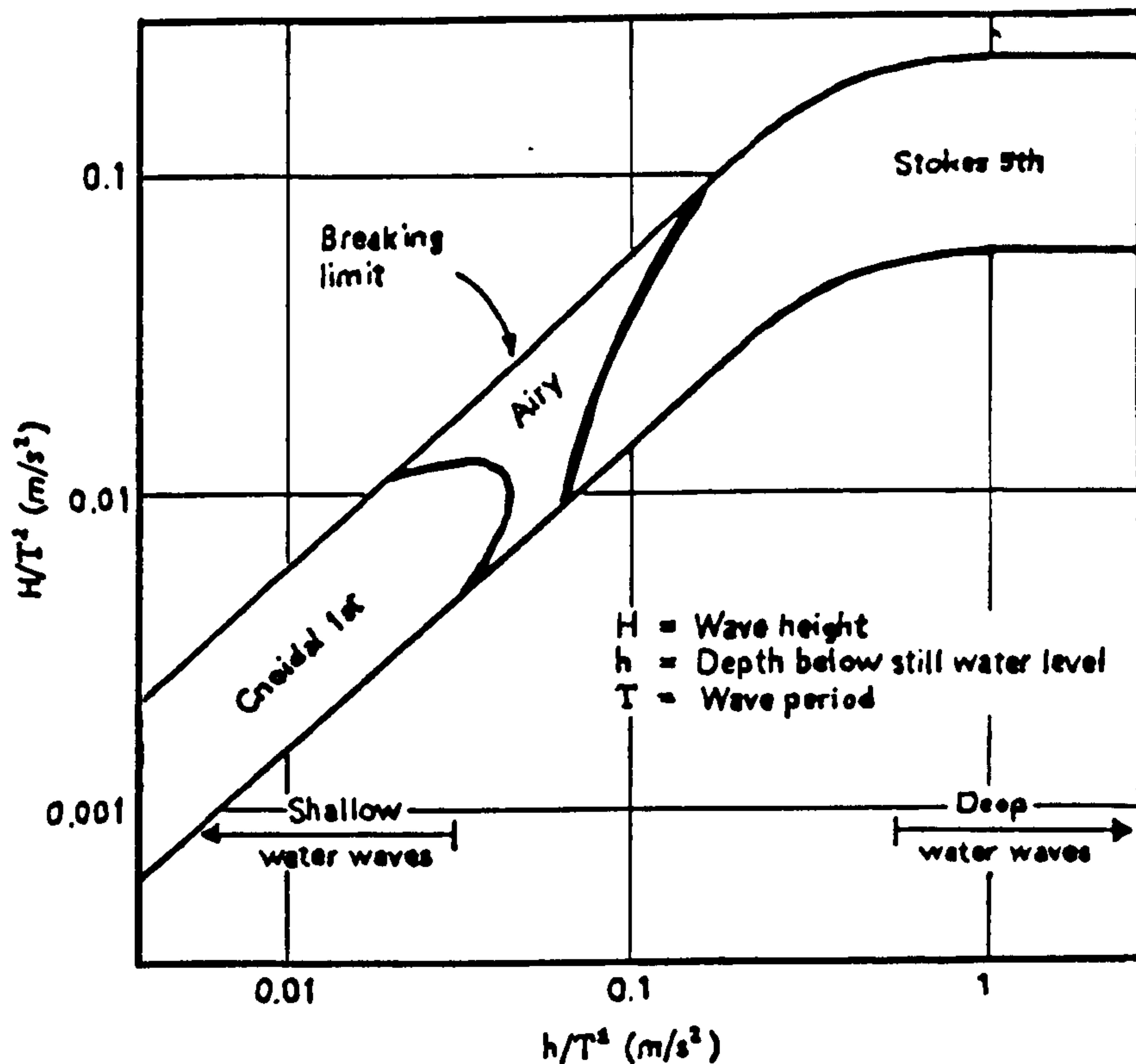


Figure (2.1.1) - The Range of Validity of Various Wave Theories.

In irregular random waves, the statistical properties will have to be determined. The random wave spectrum consist of waves having different wave-lengths and frequencies, Wiegel 1964<sup>(14)</sup> and more recently 1978<sup>(15)</sup> used several linear and non-linear representations of the ocean system.

The wave theory for the appropriate wave region is then chosen. From this, velocity and accelerations are calculated and related to the force.

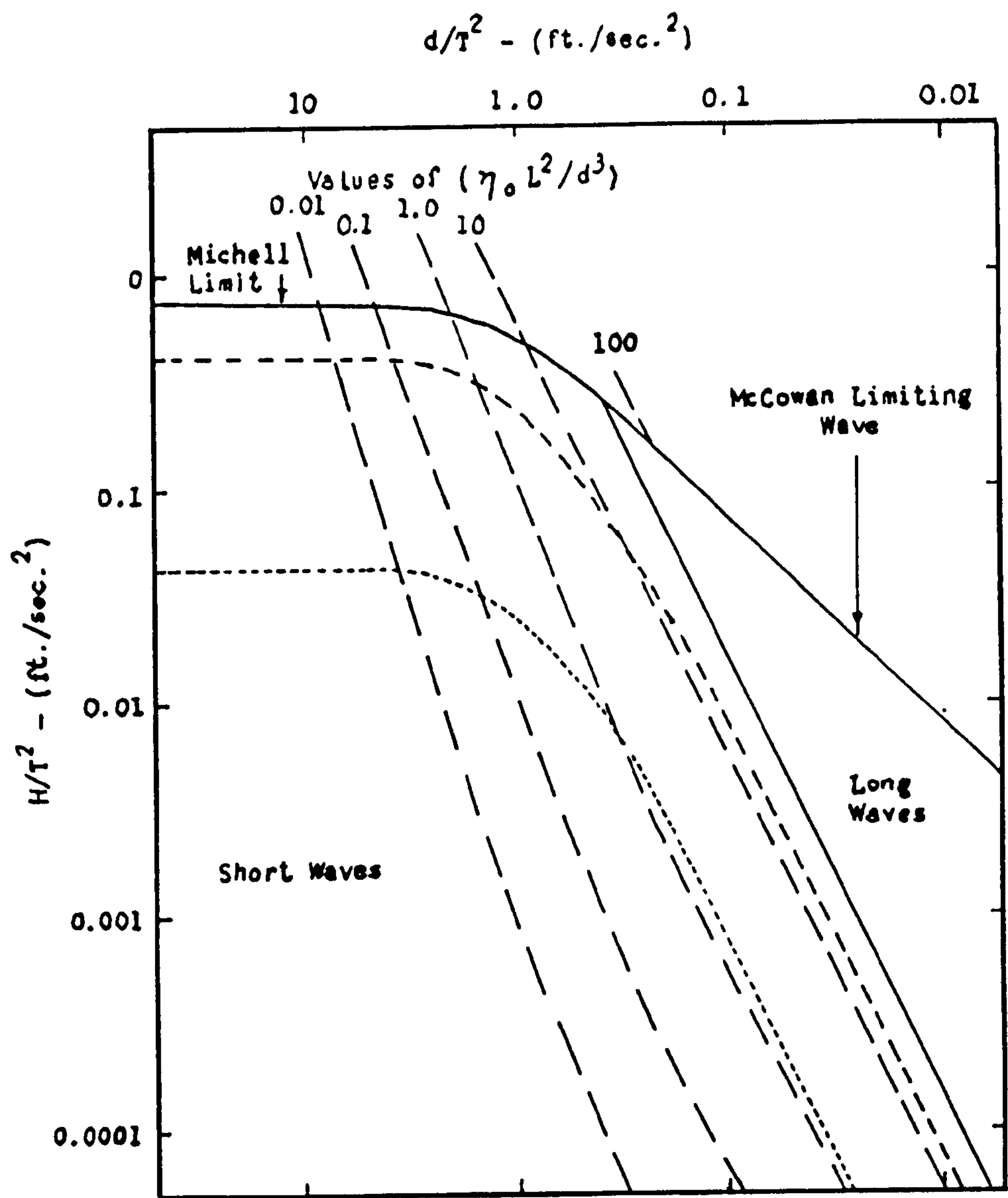


Figure (2.1.2) - Representation of Zones of Validity of Various Wave Theories.

### 2.1.2 HYDRODYNAMIC FORCE

Several approaches have been developed for evaluation of the wave forces on offshore structures. The applicability of these methods depends on the relative magnitudes of the typical dimension of the structure,  $D$ , with respect to the wave-length,  $L$ , and wave height,  $H$ . The dimensionless ratios  $H/2D$  (the wake parameter) and  $2\pi D/L$  (the scattering parameter) are key parameters which dictate the choice of the method used for wave force evaluation on offshore structure. See Figure (2.1.3) by Garrison and Rao 1977<sup>(16)</sup>.

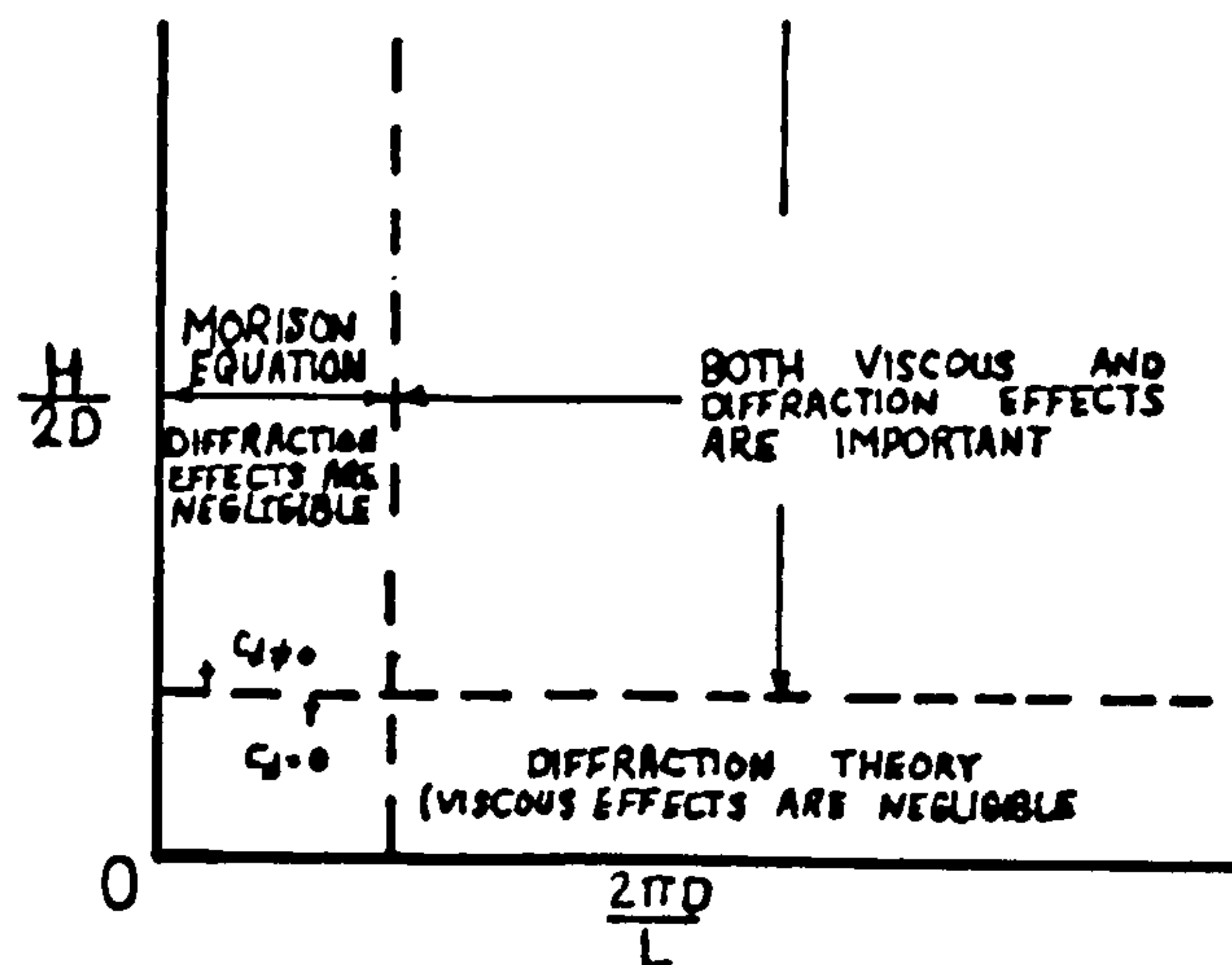


Figure (2.1.3) - Wave Force Theory.

The scattering parameter  $2\pi D/L$  controls the ratio between the incident wave and the reflected wave. For large value of  $2\pi D/L$  the structure is largely in a deflection regime. For smaller value of  $2\pi D/L$  the structure will be in the drag regimes where the incident wave plays a predominant part.

The following ratios of  $D/L$  give the approximate regime of flow

$D/L > 1$  pure reflection

$D/L \geq 0.2$  diffraction effects predominate

$D/L < 0.2$  incident wave predominate

The wake parameter  $H/2D$  controls the flow regime of the wave round the body as  $H/2D$  becomes sufficiently large, flow separation and energy dissipation in eddys are important, where the viscous effects become important and the following ratios of  $D/H$  give approximate regimes, Verley<sup>(17)</sup> 1975.

$D/H > 0.3$  inertia increasingly predominant

$D/H = 0.6$  incipience of lift (and drag)

$D/H < 0.3$  drag increasingly predominant



### 2.1.2.1 FORCE ON LARGE BODIES

#### 2.1.2.1A DIFFRACTION THEORY

For the case of diffraction where viscous effects are not important, MacCamy 1954<sup>(18)</sup> calculated the forces on cylinder subjected to regular wave using linear wave theory and Bessel function.

Spring and Monkmeyer 1974<sup>(19)</sup> outlined an analytical procedure of solution for any number of cylinders (Linear Theory) and obtained results for the case of two cylinders. Chakrabarti 1978<sup>(20)</sup> applied with slight modification, Spring and Monkmeyer (1974) method to the case of more than two cylinders.

Garrison 1974, 1978<sup>(21-22)</sup> presented the linear wave theory based on Green's function, for general structural geometries. Raman et al 1975<sup>(23)</sup> used a higher order theory to obtain analytical studies for circular cylinder. They used the perturbation method to obtain a solution for the second order theory. This resulted in a slight improvement when compared with the linear theory.

For the case of diffraction where viscous and diffraction effects were important, for the case of an isolated cylinder, Chakrabarti 1973<sup>(24)</sup>, used a fifth order waves theory. However there is an inconsistency in his solution as the fifth order wave theory was used without satisfying the free surface non-linear condition.

#### 2.1.2.2 FORCE ON SMALL BODIES

For small values of the scattering parameter " $2\pi D/L$ " and the wake parameter " $H/2D$ " where Morison's equation and diffraction theory both apply, the problem can be treated as radiated waves.

##### 2.1.2.2A MORISON'S EQUATION

As mentioned above that when scattering parameter is small Morison's equation is applied to evaluate the wave force, this equation has been formulated by Morison et al 1950<sup>(25)</sup> for the vertical cylinder. The main assumptions were,

- (a) the body has negligible effect on the waves (the wave field does not change due to the presence of the structure),
- (b) the total force on the body has two independent components.

These two component of forces are:

The drag force which results from the flow separation induced by the relative velocity of the fluid around the structure, the drag force on the body is generally made up of two terms, one a viscous and the other a pressure term, in the vast majority of cases the viscous term is negligible compared to the pressure as the viscous drag is proportional to velocity and not to the velocity squared as for the pressure drag force.



The other component is the inertia force which is due to the pressure gradient associated with the relative acceleration of the ambient fluid and is proportional to the particle acceleration.

Therefore the total force on a vertical cylindrical structure is assumed to be

$$F_T = F_D + F_I \quad \dots \quad \dots \quad \dots \quad (2.1.6)$$

Each of these time varying components has been formulated in terms of (i) Geometrical properties of the structure, (ii) fluid properties describing the flow field and (iii) some "variable coefficients"

$$\therefore d F_D(t) = C_D \frac{1}{2} \rho D \dot{U}(t) |\dot{U}(t)| ds \quad \dots \quad (2.1.7)$$

$$d F_I(t) = C_M \frac{\rho \pi D^2}{4} \ddot{U}(t) ds \quad \dots \quad \dots \quad (2.1.8)$$

where  $D$  = diameter of the cylinder

$\rho$  = water density

$\dot{U}$  = fluid particle velocity

$\ddot{U}$  = fluid particle acceleration

$C_D$  = drag coefficient

$C_M$  = inertia coefficient

In the above equations the geometrical properties of the structure appear as exposed area in the drag force term and as volume in the inertia term. But this geometry of the structure also affects the fluid flow field around the structure as shown in Blesvins 1977<sup>(26)</sup>.

The fluid properties represented in the wave velocity and acceleration in the above equations are calculated from the wave theories. Hence it is important to use the sequential wave theory in order to estimate accurately the wave force. They also affect indirectly the estimation of  $C_D$  and  $C_M$  as shown below.

The variable coefficients are the drag coefficient and the inertia coefficient. The drag force on structure is due to the pressure difference across the structure. This pressure difference is due to separation of the flow from some point on the structure creating a low pressure area behind the structure. The position at which separation occurs, the way in which it occurs and the resultant wake width all influence the pressure behind the structure. Thus the drag coefficient is used taking into account the unknown pressure difference across the structure.

The inertia force on the body is due to the fluid in the wave accelerating and as the fluid in the wave must move round the object additional accelerations are involved, related to the curvature of flow. The accelerations are dependent on the form of the wake. These accelerations induce a force field which is expressed in terms of the fluid mass it displaces.

It is clearly shown that the drag and the mass (inertia) coefficient is dependent on the geometrical properties of the structure and the fluid properties describing the flow field.

The experimental values of  $C_d$  and  $C_m$  obtained by Morison et al show some scattering and no trend as function of dimensionless parameter, Reynolds number ( $U_{\max} D/\nu$ ), where " $U_{\max}$ " is the maximum surface orbital velocity,  $D$  is the structure diameter and  $\nu$  is the kinematic viscosity of the fluid.

Because the wave flow reverses every half wave cycle as shown in Figure (2.1.4). This means that there is only a relatively short time for the wake to form before it is destroyed. Keulegan and Carpenter 1968<sup>(27)</sup> formed a dimensionless parameter which compares the time for a wake to form with the time available for it to form.

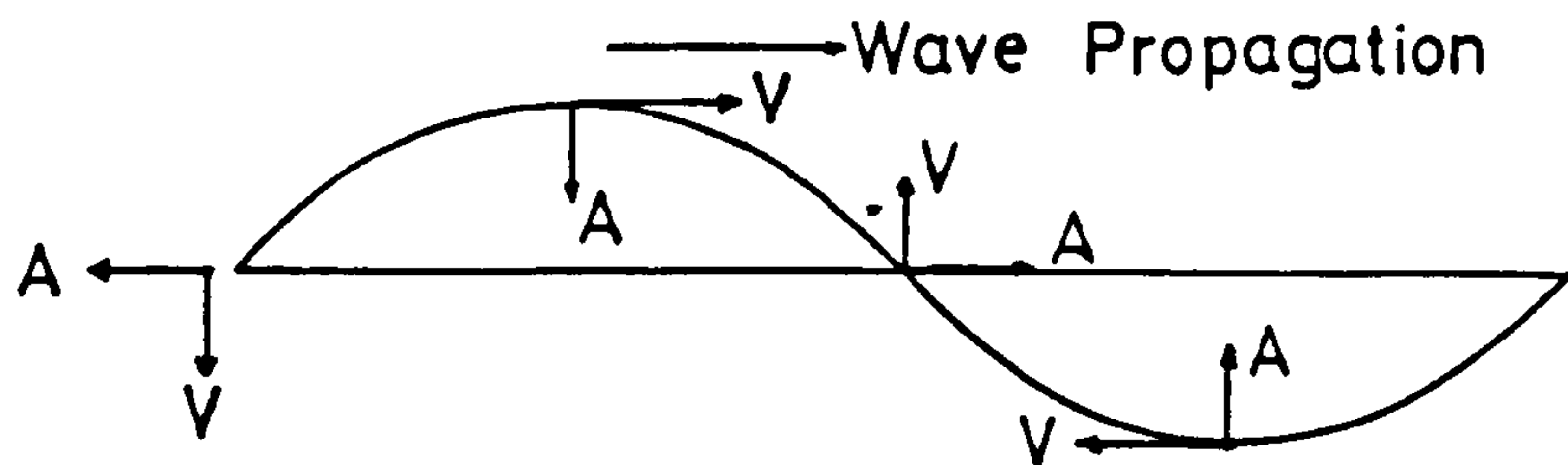


Figure (2.1.4) - Direction of Velocity and Acceleration at Various Points of a Wave Cycle.

They carried out studies both theoretically and experimentally on the force acting on cylinders in an oscillating flow field. They observed that  $C_D$  and  $C_m$  varied over a wave cycle. They correlated the cycle averaged values of  $C_D$  and  $C_m$  with the period parameter  $K-C = U_m T/D$  called the Keulegan-Carpenter number where " $U_m$ " is the maximum orbital velocity,  $T$  is the wave period and  $D$  is the diameter of the cylinder."

The variation of the average of the inertia coefficient values per cycle with the period parameter is shown in Figure (2.1.5). Similarly for the drag coefficient is shown in Figure (2.1.6).

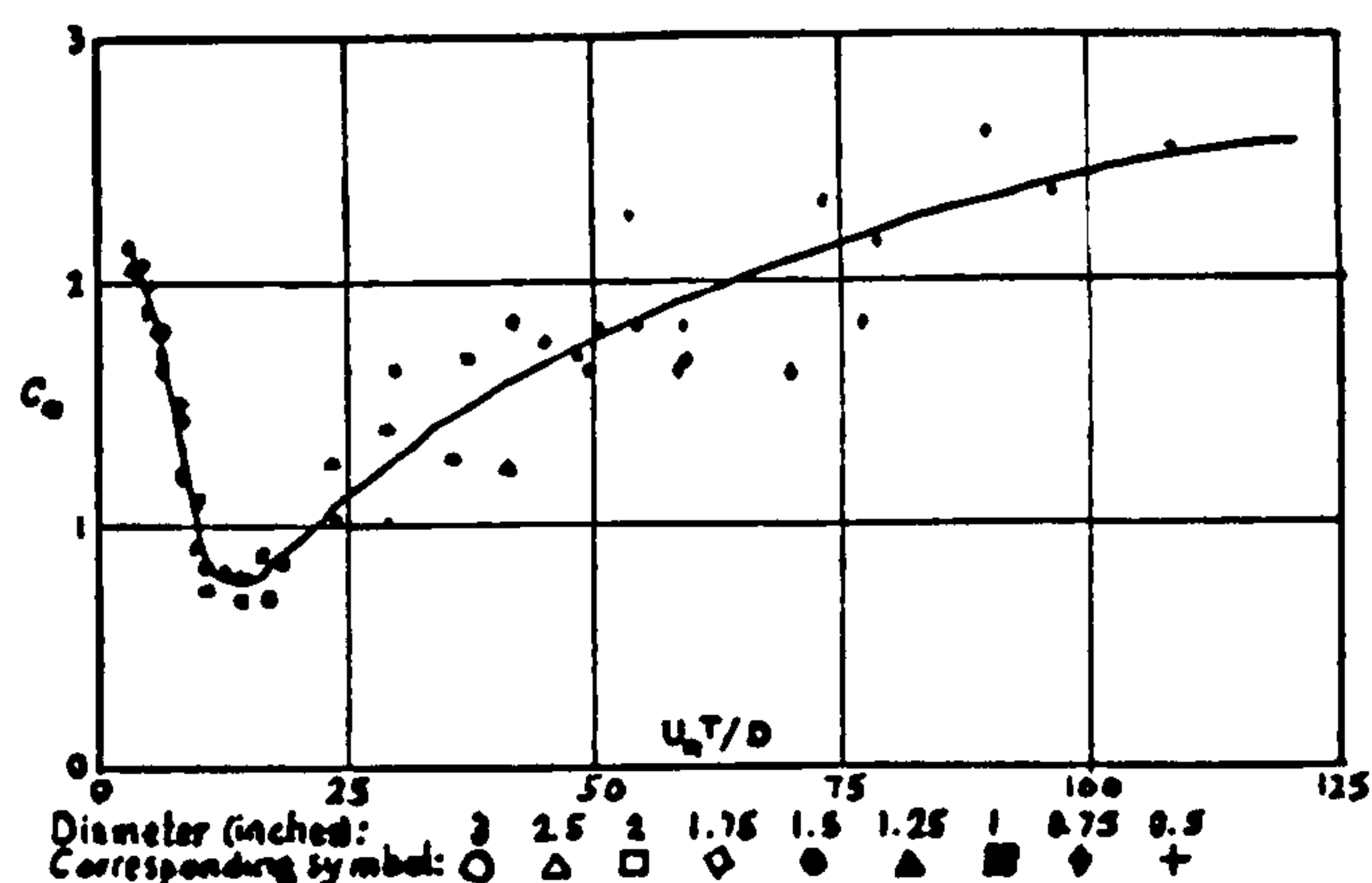


Figure (2.1.5) -  $C_M$  Versus Keulegan-Carpenter Number.

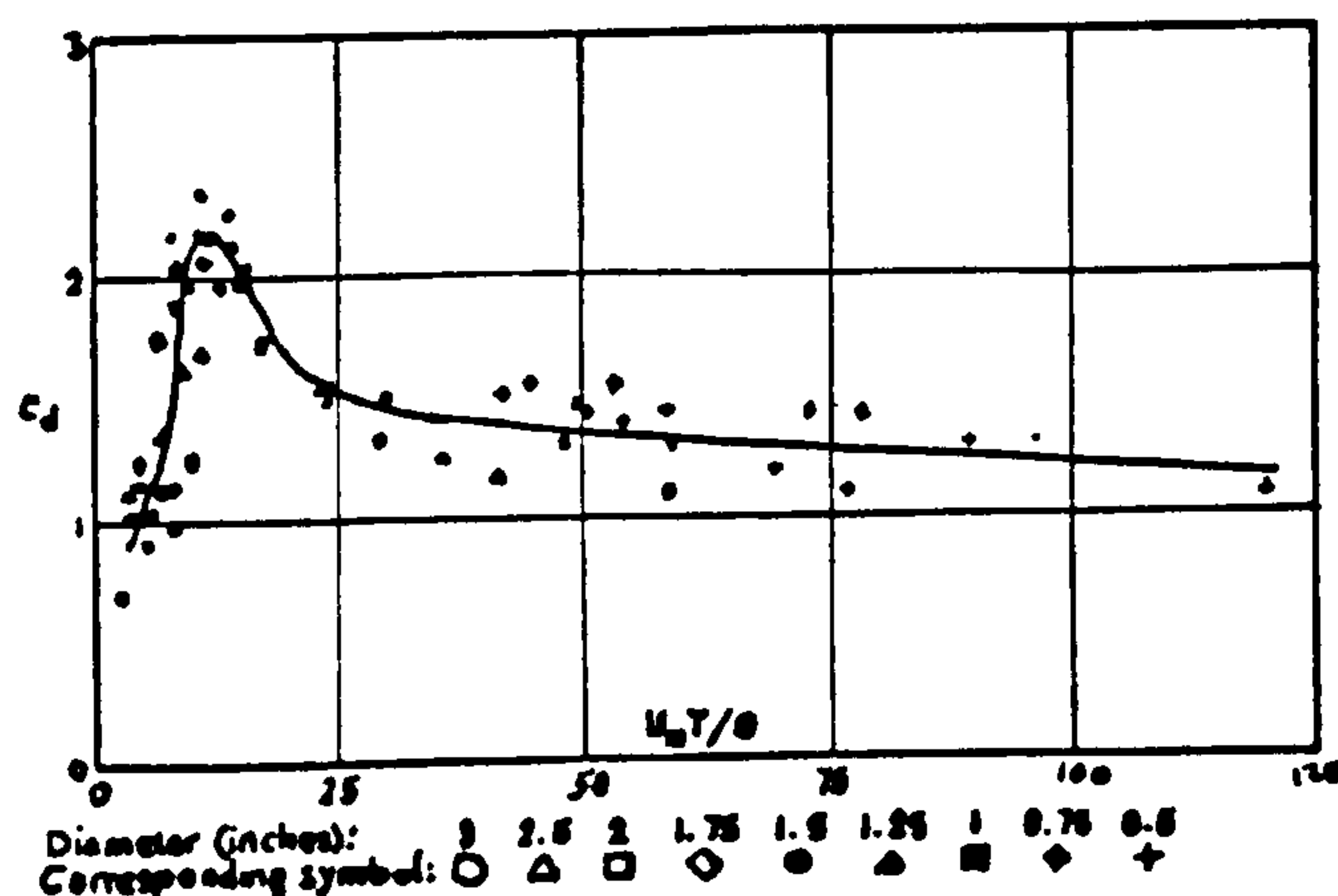


Figure (2.1.6) -  $C_M$  Versus Keulegan-Carpenter Number.

The period parameter  $K-C$  is associated with the flow separation process and eddy formation around the cylinder. When  $K-C$  is small, no separation occurs. As  $K-C$  increase, separation is initiated and eddies are formed.

In the work of Keulegan and Carpenter they did not correlate  $C_D$  and  $C_M$  with respect to Reynolds number  $R_e$ .

In order for Morison's equation to be applicable and be useful to engineers in the design of offshore structure, it was necessary to undertake a comprehensive laboratory and field tests for the purpose of determining the coefficient of drag and inertia which appear in the equation. Some of the data came from the measurements carried out in the actual sea condition (field test).

Wiegel, Beebe and Moon 1957<sup>(28)</sup> made field measurements at Pacific Coast (Davenport, California) on various sections of a 6.625 inch cylinder. They used linear wave theory, average values of  $C_D$  and  $C_M$  were obtained. They calculated  $C_M$  at zero velocity and  $C_D$  at zero acceleration, the results show considerable variations in the mean values of  $C_D$  and  $C_M$  as well as scatter.

Agerschau and Edens 1965<sup>(29)</sup> used the data obtained from Wiegel et al and used Stokes fifth-order theory. The values of  $C_D$  and  $C_M$  obtained were also scattered and show that the fifth order approach was not superior to the first order "linear theory."



Reid 1957<sup>(30)</sup> measured force on a section of an 8.625 inch cylinder in water of 30 ft depth in the Gulf of Mexico. The kinematics of the flow were calculated from the wave profile and the drag and inertia coefficient were obtained through the use of the least squares technique. Measured wave force records and those calculated using constant mean  $C_D$  and  $C_M$  values were in good agreement. Structural vibration was observed and allowed for in the analysis.

Wilson 1965<sup>(31)</sup> presented the results of wave force data from an experiment conducted with a 30 inch diameter pile in confused sea conditions in the Gulf of Mexico. He developed a numerical filter with which unwanted high frequency effects were removed from force records. Large scatter in  $C_D$  and  $C_M$  values from different wave force record analyses.

Two wave projects were undertaken at the Gulf of Mexico and the results were evaluated by several researchers; Aagaard and Dean 1970<sup>(32)</sup> by using stream function theory in the estimation of  $C_D$  and  $C_M$  with  $C_M = 1.33$  and  $C_D$  varying with Reynolds number as obtained from the data, they found agreement between calculated and measured local force maximum within 50%.

Evans 1970<sup>(33)</sup> performed his work in 100 ft depth of water with 3.7 ft diameter pile. The average pressure distribution was measured over a one foot section. The forces and their directions were calculated from it. The wave profile was recorded simultaneously with pressure. He used Stokes fifth order wave theory to calculate  $C_D$  and  $C_M$ . Calculated total forces were generally within 10% of the measured forces, and usually conservative. None of the evaluations of the data of the two projects considered the effect of currents.

Wheeler 1970<sup>(34)</sup> used another technique to represent the data of the Gulf of Mexico by predicting the velocities and accelerations by linear digital filter acting on the wave profile records. No correlation of  $C_M$  and  $C_D$  coefficient with critical parameter was reported; agreement between measured and calculated maximum local forces was within 40%.

Kim and Hibbard 1975<sup>(35)</sup> presented the results of data obtained from measurements in Australia. The test pile was 38 ft long and 12.75 inch in diameter, it was subjected to rather small amplitude waves, the agreement between the measured and calculated force was good in the drag dominated part of the wave cycle and fair in the inertia dominated region.

Heideman, Olsen and Johansson 1979<sup>(36)</sup> used two methods to evaluate the drag and inertia coefficients from the large scale experiments of space frame structure in the Gulf of Mexico. The first was the least squared error procedure for each half wave cycle. The second method consisted of evaluation of  $C_D$  over short segments of wave where drag force was dominant and of  $C_M$  over short segments in which inertia force was dominant. The force coefficients exhibited large scatter particularly for  $K-C < 20$ . The current was taken into consideration.

Bretschneider 1967<sup>(37)</sup> predicted the probability distributions of peak wave drag and inertia force from field tests carried out in California Coast at Devenport for vertical cylinder using linear wave theory, the probabilistic approach considering peak drag and inertia forces were unsatisfactory.

The reasons for discrepancies in the evaluation of  $C_D$  and  $C_M$  in field tests may be many; among the more important are:

1. Representation of the irregular wave
2. Turbulence around the structure by which the test structures are supported
3. Inaccuracy in measuring force

4. Vibration of test structure
5. Inability of wave theories to describe actual water particle motion especially if there is the possibility of a steady ocean current.

In order to eliminate most of the above discrepancies, to obtain for a wide range of data and flow conditions and to segregate each parameter which can affect the calculation of  $C_D$  and  $C_M$ , laboratory experimental tests were conducted. In the laboratory tests several experimental methods have been used in the evaluation of the drag and inertia coefficient which include:

- (a) Force measured on structure in laboratory wave
- (b) Force measured on structure in an oscillating fluid, where the motion of the particle is in straight line rather than orbital
- (c) Force measured on a cylinder constrained to move with an oscillatory motion in a stationary fluid.

The flow field characteristics of (a) are essentially different from that of (b) and (c).

Some of the experimental work which follow pattern (a) were carried out by Morison et al 1950<sup>(25)</sup> using measured moments and using linear wave theory, in calculating  $C_M$  and  $C_D$  they did not correlate well with  $d/\lambda$ ,  $D/\lambda$  or  $R_e$  for linear sinusoidal waves.

Susbielles et al 1971<sup>(38)</sup> used various methods of derivation of coefficients which included linear, stokes third and fifth order wave theory and stream function wave theory. The actual  $C_M$  and  $C_D$  range of values varied with the method of derivation. Several  $C_M$  and  $C_D$  pairs were shown to predict the same force. By using the values of the coefficients from Keulegan and Carpenter's curve the results obtained differed by 10% between the measured and the calculated.

Chakrabarti et al 1975<sup>(39)</sup> found large scatter in  $C_D$  and  $C_M$  values using Morison's equation in three-dimensional vector form with component normal to the axis of the cylinder. Measured and calculated mean forces agreed to within 10% using  $C_D$  and  $C_M$  values for individual waves. The tested structures were held at various inclinations in line with and normal to the waves.

Gaston and Ohmart 1979<sup>(40)</sup> measured the total wave force and overturning moment on a smooth and roughened 14 ft long, 1ft diameter, vertical cylinder under conditions of periodic and random waves. Drag and



inertia coefficients have been determined by the least squares method, using the measured in-line moment and predicted kinematics from the irregular stream function theory. Typical Reynolds number of the experiments were  $2 \times 10^5$  to  $3 \times 10^5$  based on the r.m.s water-particle velocity data. The results gave the average values of  $C_D$  and  $C_M$  as:

$$C_D = 0.77 \text{ and } C_M = 1.81$$

for smooth cylinder.

Experiments which seem to have shed the most light upon the fundamental behaviour of  $C_D$  and  $C_M$  are those which have been conducted in straight line oscillatory motion. The best known early experiments were those of Keulegan and Carpenter 1958<sup>(27)</sup> who utilized the linear oscillatory flow field under a node of standing wave. Their experiments showed that  $C_D$  and  $C_M$  are not constant throughout a motion cycle but, in fact, varied substantially with motion phase. More recently in a series of papers Sarpkaya et al have presented the results of an extensive series of oscillating fluid experiments using vertical U-shaped water tank. Sarpkaya (1976a, 1976b)<sup>(41 - 42)</sup> conducted a series of experiments for smooth and sand-roughened cylinders to evaluate the drag and inertia coefficients introducing "frequency parameter"  $\beta$  in which  $\beta = D^2/\nu T$  or  $\beta$  is equal to  $R_e/K-C$  parameter to represent the data of  $C_D$  and  $C_M$ . The dependence of  $C_D$  and  $C_M$  on  $\beta$  has already

been noted in connection with the discussion of the Stokes 1851<sup>(43)</sup> sphere problem. Sarpkaya 1977a<sup>(44)</sup> carried out his series of experiments for high Reynolds numbers. Sarpkaya et al 1977<sup>(45)</sup> expressed their results for  $C_D$  and  $C_M$  as function of Reynolds number, Keulegan-Carpenter number and relative roughness. For large Keulegan-Carpenter number, they obtained a different trend than Keulegan-Carpenter<sup>(27)</sup>. In general the scatter in the data is small.

Mau11 and Milliner 1978<sup>(46)</sup> examined the production and motion of vortices in a sinusoidally-oscillating flow in a small U-tube at Reynolds numbers smaller than about 4,000. They proposed that the variation of the drag coefficient during a cycle may be considered as the addition of two terms, the inertia term with  $C_M = 2.0$ , and a further term which is a function of the movement of the vortices produced.

Bearman and Graham 1979<sup>(47)</sup> measured the in-line force on several cylindrical bodies in plane oscillatory flow in a small U-tube over a range of K-C number from 3 - 70 at relatively small Reynolds number. They had noted large cycle to cycle variations in computed values of  $C_D$  and  $C_M$  even though the bulk flow in the U-tube was closely repetitive.

Force measured on a structure constrained to move with an oscillatory motion in a stationary fluid (Pattern C) help to add insight into the role played time dependence.

Most of the work of unidirectional acceleration of a body in stationary fluid conducted to establish a single force coefficient combines the effects of drag and inertia. Kiem 1956<sup>(48)</sup> showed that the single coefficient as a function of  $(d\dot{U}/dt)D/\dot{U}^2$ . This correlated the data fairly well. Also the experimental work of Laird and Johnson 1956<sup>(49)</sup> and Laird et al 1959<sup>(50)</sup> expressed the result in terms of total resistance coefficient.

Dalton et al 1976<sup>(51)</sup> and Sarpkaya and Garrison 1963<sup>(52)</sup> tried to use dimensional analysis to show that the single coefficient can be used to transform the results from the oscillating cylinder into the problem of a stationary cylinder in an oscillating fluid otherwise from Pattern C to Pattern A and B.

From the above we can see the differences in the test condition, methods of measurement and data evaluation do not permit a critical and comparative assessment of the drag and inertia coefficients obtained in each investigation. A comprehensive summary of the data on force-transfer coefficients has been presented by Hogben et al 1977<sup>(53)</sup>. The relationship between  $C_D$  and  $C_M$  has shown that there is not a unique relationship between them, independent of  $K - C$  and  $R_e$ . Hogben 1976<sup>(54)</sup> suggested

a conceptual modelling of the interaction leading to an explicit formula for the inter dependence of  $C_D$  and  $C_M$ , it is based on highly simplified and somewhat initiative reasoning.

#### 2.1.2.2B TRANSVERSE FORCE (LIFT FORCE)

Although the transverse force is not concerned in these studies it is important to mention it because this phenomenon may cause increase in in-line force and it has an important effect closely related to drag forces. The transverse force can be calculated from the equation:

$$dF_L(t) = C_L \frac{1}{2} \rho D \dot{U}_m^2 ds \quad \dots \quad \dots \quad \dots \quad (2.1.9)$$

where  $C_L$  = transverse or (Lift) coefficient. The rest of the symbols have been identified previously.

The phenomenon of the transverse force is caused by the eddy shedding and so it is likely to be influenced by the way in which the eddies are shed (this also applied to the drag force). Some of the work concern the transverse force in wave flow have been looked at by Bidde 1971<sup>(55)</sup>, Wiegel and Delmonte 1972<sup>(56)</sup>, Isaacson 1974<sup>(57)</sup> and Zedan and Rajabi 1981<sup>(58)</sup>. Some of the work concerning the transverse force in harmonically oscillating flows has been measured by Mercier 1973<sup>(59)</sup>, Sarpkaya 1975a, 1976a<sup>(60, 41)</sup> and Maul and Milliner 1978, 1979<sup>(46, 61)</sup>.

### 2.1.2.3 MORISON EQUATION FOR A FLEXIBLE CYLINDER

The original Morison equation has been modified by several investigations to cover in some sense the effect on the in-line forces of the flexibility of the structure. In particular the absolute value of the fluid velocity has been replaced by the relative one with respect to the structure's velocity, and the added mass term associated with the acceleration of the structure has been included (see Berge and Penzien 1976<sup>(62)</sup>; Moan, Haver and Vinje 1975<sup>(63)</sup>).

The modified relation is:

$$\begin{aligned} dF(t) = & ((C_M - 1) \frac{\pi D^2}{4} \rho (\ddot{U}(t) - \ddot{X}(t)) + \frac{\rho \pi D^2}{4} \ddot{U} + \\ & + \frac{1}{2} C_D \rho D |\dot{U}(t) - \dot{X}(t)| (\dot{U}(t) - \dot{X}(t)) ds \\ & \dots \dots \dots \dots \dots \dots (2.1.10) \end{aligned}$$

where  $\ddot{X}$  = The acceleration of the structure at the point under consideration

$\dot{X}$  = The velocity of the structure at the point under consideration.

The rest of the symbols have been identified previously.

Although Equation (2.1.10) is a reasonable extension of the original Morison equation, it requires experimental verification as the original form of Morison's equation has been used for the estimation of  $C_D$  and  $C_M$  in field studies.



## 2.2      THE IDEALIZATION USED TO MODEL THE STRUCTURE SYSTEM

In order to solve the static or dynamic response of any structure to the existing force it is necessary to model structure-foundation accurately to be able to establish the structure mechanism behaviour and the interaction between the superstructure and the supporting foundation.

As the offshore structure is a very complex structure and problem; Penzein and Tseng 1976<sup>(64)</sup> refer to separate the modelling of the structure foundation system into (a) a foundation system, (b) a structure system.

### 2.2.1      FOUNDATION SYSTEM

The foundation of offshore structure can be either raft foundation as those commonly used for the gravity type of structure; see Figure (2.2.1) or a piles foundation as those normally used for the framed steel type of structure, see Figure (2.2.2).

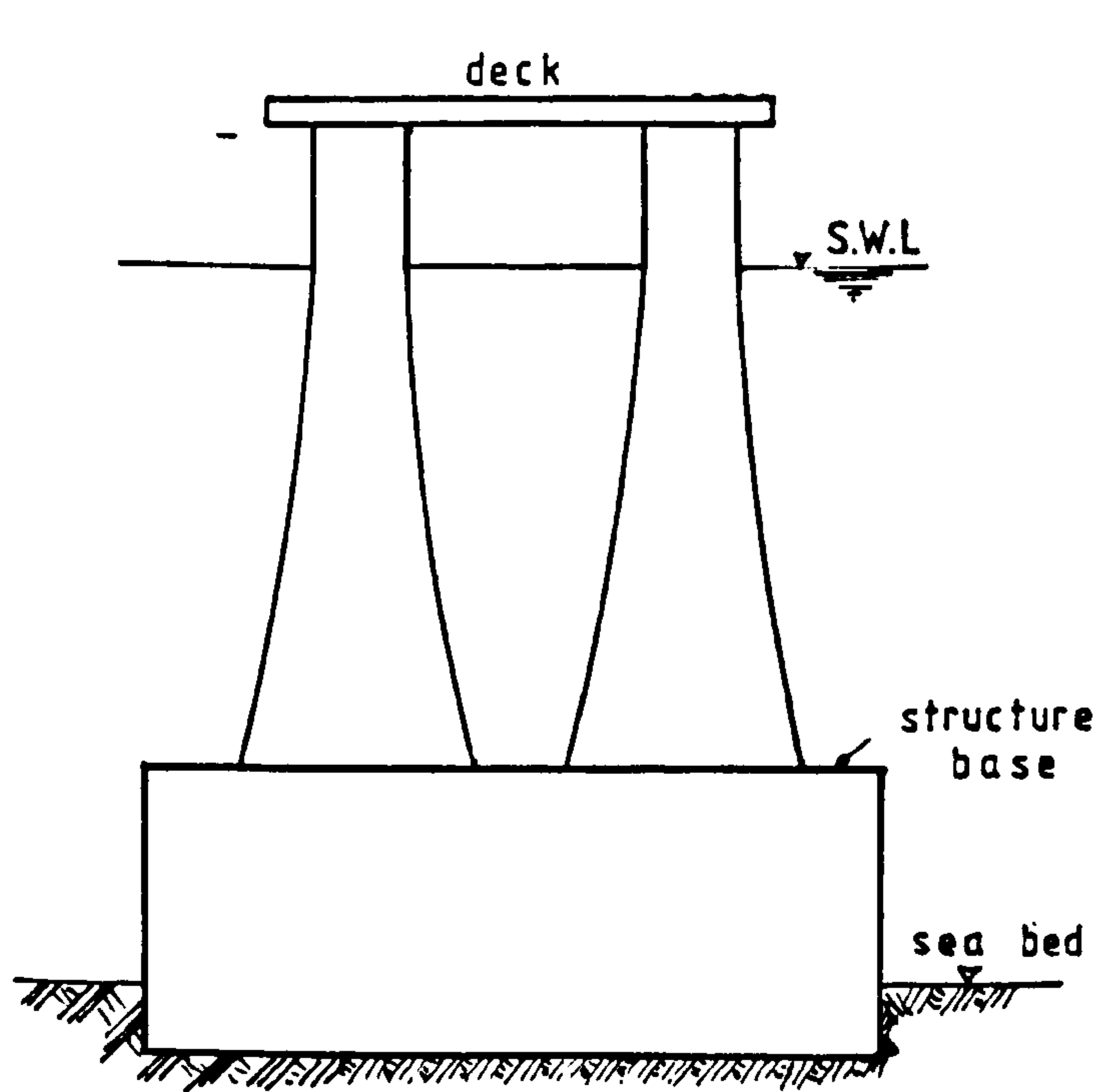


Figure (2.2.1) - Gravity Structure

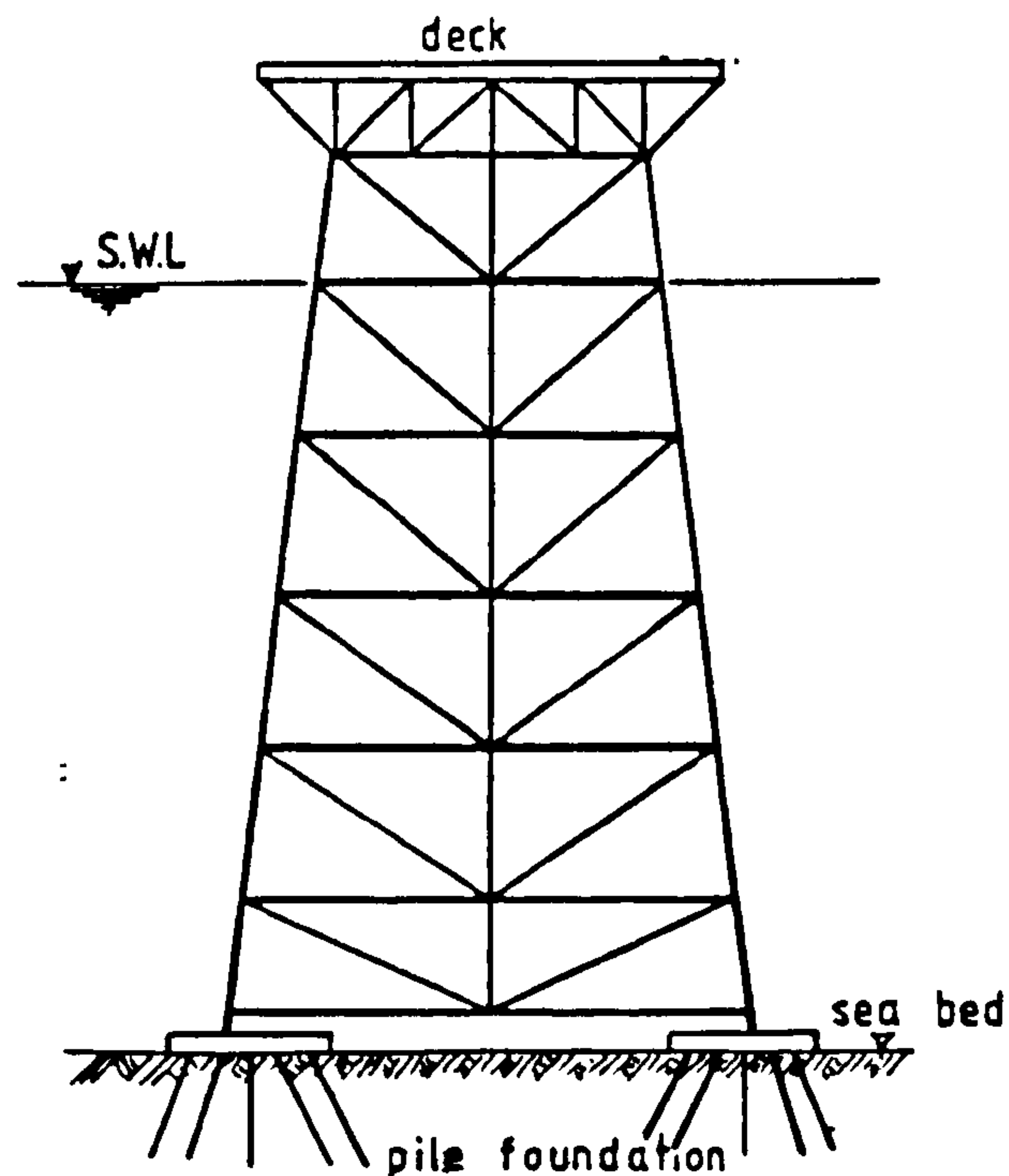


Figure (2.2.2) - Framed Steel Structure

The foundation impedance function stiffness coefficient and the damping coefficient of the foundation must be derived by performing a steady state foundation sub-structure dynamic analysis under harmonic excitation at its interface boundary. For the gravity structure Veletsos and Wei 1978<sup>(65)</sup>, Luco and Westmann 1971<sup>(66)</sup> have obtained the foundation impedance assuming a uniform elastic half space. Luco 1974<sup>(67)</sup> obtained it assuming a layered viscoelastic half-space.

Due to the presence of piles, realistic model of the foundation subsystem for framed steel structure is more complicated. Novak 1974<sup>(68)</sup> generate the foundation impedance for single pile in a uniform layer of soil founded in rigid rock. Kausel and Roessel 1975<sup>(69)</sup>

applied the finite element representation to obtain the impedance function. Tsai and Housner 1970<sup>(70)</sup>, Lysmer and Kuhlemeyer 1969<sup>(71)</sup> developed the "exact" wave transmitting boundary element.

As the foundation impedance and damping which consist of radiation damping causing loss of energy of the motion due to the soil properties hence it is frequency dependent.

A type of the soil modelling of the foundation for gravity type and framed steel type are shown in (Figure 2.2.3) and (Figure 2.2.4) respectively.

The effect of the soil parameter on the mathematical model of the foundation subsystem for the dynamic response of the structure had two principal effect according to (Taylor 1975<sup>(72)</sup> and Angelides and Conner 1979<sup>(73)</sup>).

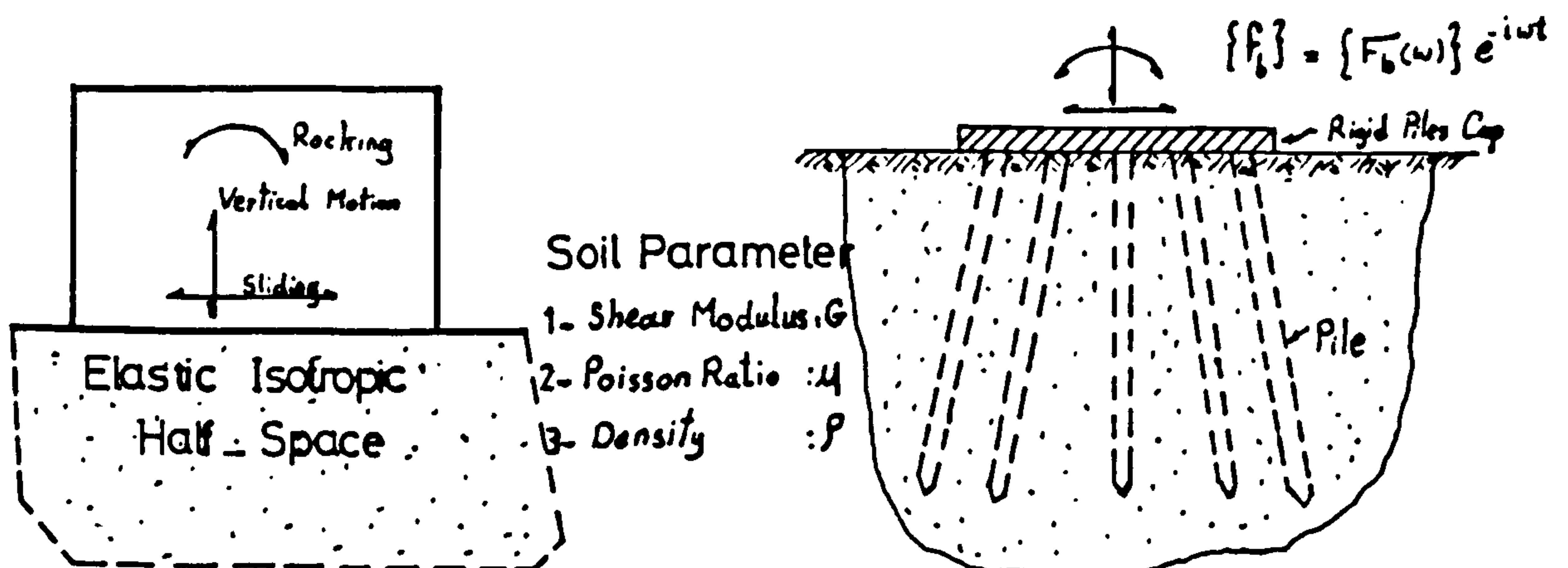


Figure (2.2.3) - Soil Model for Gravity Structure.

Figure (2.2.4) - Soil Model for Framed Steel Structure.

1. Significant shifts in the response were observed for reasonable modification in the soil properties
2. Reduction in foundation stiffness due to soil degradation increases the foundation period of the structure and the dynamic amplification of the structure response

The first point has been investigated by Moan et al 1975<sup>(63)</sup> for the shear modulus variation. The combination of the soil properties expressed in terms of damping and stiffness indicate that smaller soil damping will give higher dynamic amplification at resonance (Bell et al 1976<sup>(74)</sup>). For the soil stiffness a higher dynamic amplification is found for a higher soil stiffness (Taylor 1974<sup>(75, 72)</sup>) and that is clear due to the small amount of energy absorbed by the soil.

The second point has been investigated (e.g. Walt 1978<sup>(76)</sup>). It is important to represent the mathematical model for modelling the structure foundation interaction using the foundation impedance and damping. Figure (2.2.5) shows some of the modelling used.

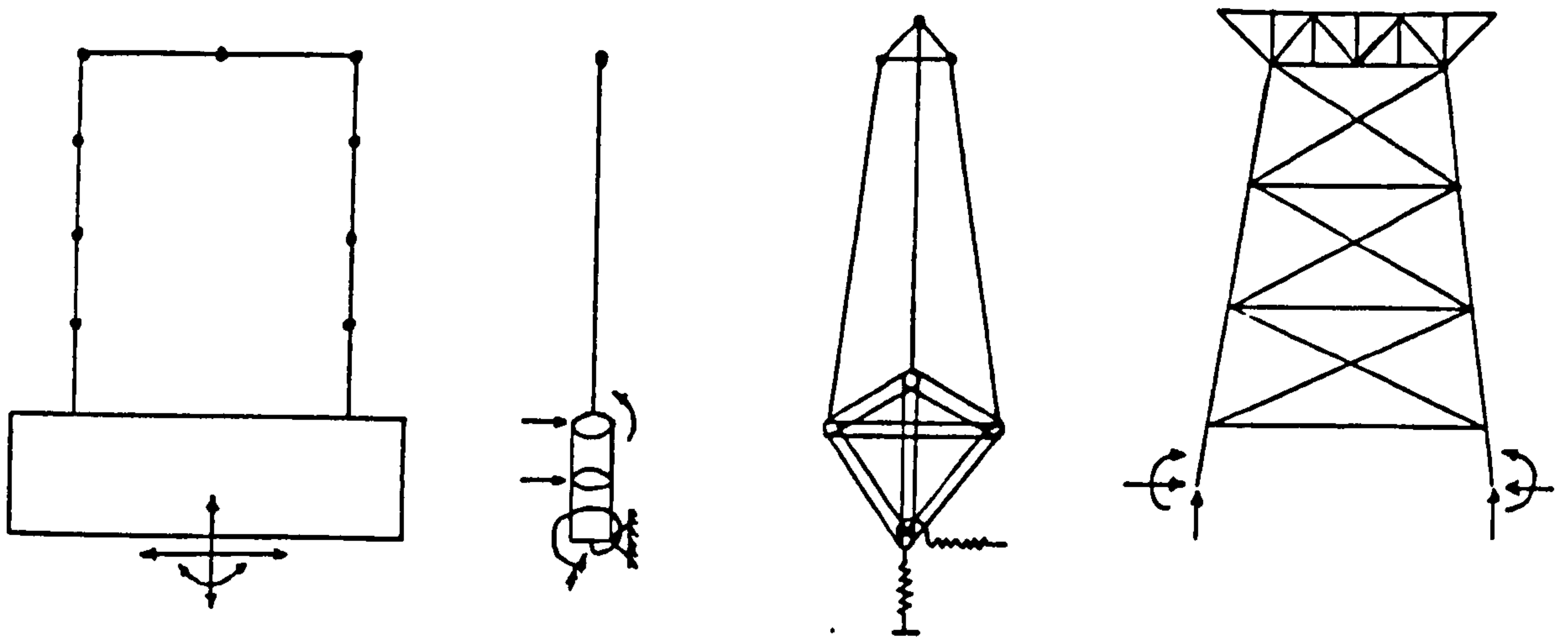


Figure (2.2.5) - Foundation Modelling.

As the foundation has been represented completely in the offshore structure the vital points now are to use the information from the foundation modelling in the analysis using the foundation structure-interaction, this point has been looked at by many professional investigators e.g. (Penzin 1976<sup>(77)</sup>, Taylor<sup>(75)</sup>). The interaction can be represented by forming the stiffness and damping matrix which are used in the equation of motion governing the dynamic analysis of the structure.

$$\begin{aligned}
 [M] \{\ddot{X}\} + [C] \{\dot{X}\} + [K] \{X\} &= \{F(t)\} \\
 \dots \quad \dots \quad \dots \quad \dots \quad \dots & \quad \quad \quad (2.2.1)
 \end{aligned}$$



where  $[M]$  = Mass matrix  
 $[C]$  = Damping matrix  
 $[K]$  = Staffness matrix  
 $\{\ddot{X}\}, \{\dot{X}\}$  and  $\{X\}$  = Acceleration, velocity and  
displacement of the structure respectively  
 $\{F(t)\}$  = Hydrodynamic force

by using the interaction between structure-foundation,  
the damping and the stiffness matrix will be

$$[C] = [C_s] + [C_f] \dots \dots \dots (2.2.2)$$

$$[K] = [K_s] + [K_f] \dots \dots \dots (2.2.3)$$

where  $[C_s]$  = Damping in the free structure  
 $[C_f]$  = Damping in the foundation  
 $[K_s]$  = Stiffness in the free structure  
 $[K_c]$  = Stiffness for the foundation

One suitable method for evaluating  $[C_s]$  is to use the  
dynamic properties of the fixed base structure along  
with the pseudo/static influence coefficient associated  
with its base degrees of freedom, i.e.

$$\text{Let } [C_s] = \begin{bmatrix} [C_s^f] & [C_s^b] \\ [C_s^b] & [C_s^{bb}] \end{bmatrix} \dots \dots \dots (2.2.4)$$

where  $[C_s^f]$  is the damping matrix for the fixed base  
structure,  
 $[C_s^{bb}]$  is the damping matrix associated with the  
base degree of freedom of the structure, and  
 $[C_s^b]$  is the coupling damping matrix,

Matrix  $[C_S^f]$  can be formulated for the fixed base structure using the relation formulated by Clough 1975<sup>(78)</sup>

$$[C_S^f] = [M^f] \begin{bmatrix} m & & & \\ \Sigma & \frac{2\zeta_J W_J}{M_J} & & \\ J=1 & \{\phi_J\}\{\phi_J\}^T & & \\ & \dots & \dots & \dots \end{bmatrix} [M^f] \quad (2.2.5)$$

where  $[M^f]$  is the diagonal mass matrix, including hydrodynamic add mass,

$m$  is the number of normal modes to be considered and

$\{\phi_J\}$ ,  $W_J$ ,  $\zeta_J$  and  $M_J$  are the mode shape vector, frequency, damping ratio and generalized mass respectively of the  $J^{\text{th}}$  normal mode.

Matrices  $[C_S^b]$  and  $[C_S^{bb}]$  can be formulated as follows:

$$[C_S^b] = - [C_S^f] [b_s] \dots \dots \dots \quad (2.2.6)$$

$$[C_S^{bb}] = [b_s]^T [C_S^f] [b_s] \dots \dots \quad (2.2.7)$$

where  $[b_s] =$  pseudo-static influence coefficient matrix which is equal to

$$[b_s] = - [K_S^f]^{-1} [K_S^b] \dots \dots \dots \quad (2.2.8)$$

In which  $[K_S^f] =$  Stiffness matrix of fixed base structure

$[K_S^b] =$  Stiffness-coupling matrix expressing the force developed in the degrees of freedom of the fixed base structure caused by the pseudo-static displacement of the base degrees of freedom.

From the above we can conclude that the understanding and evaluating the dynamic analysis of the fixed base structure should be carried out before establishing the analysis of the offshore structure with its foundation.

### 2.2.2 THE STRUCTURE SYSTEM

The structure system must be idealized so that the dynamic analysis can be made with simple systems forming the dynamic properties Mass, Stiffness and Damping of the structure.

#### 2.2.2.1 THE MASS MATRIX

The mass matrix can be formulated either by consistent mass matrix or by the lumped mass matrix, the simplest procedure for defining the mass matrix of any structure is to assume that the entire mass is concentrated at the points of which the translation displacement are defined.

The usual procedure for defining the point mass to be located at each node is to assume that the structure is divided into segments, the nodes serving as connection points.

The mass matrix of the offshore structure can be represented as

$$M = M_m + M_a + M_F \dots \dots (2.2.9)$$

where  $M_m$  = Material structural mass and the platform mass

$M_a$  = Added mass due to the displaced fluid replaced by the submerged part of the structure

$M_F$  = Flooding and marine growth mass

The part of  $M_F$  due to the flooding mass can be easily calculated and it is the mass of water occupying certain volume of structure element to make it flood. The part of  $M_F$  due to marine growth are not easy to predict due to uncertainties of the marine growth thickness over the whole structure. Heaf 1979<sup>(79)</sup> shows the effect of increased marine growth on the mass matrix. This effect appears in two ways; firstly, the increase in mass of the structure and secondly, the increase in hydrodynamic added mass due to an increase in displaced volume.

$M_m$  is the mass of the structure material plus the mass of the platform deck including all the machinery and equipment. It is easy to calculate and form the mass matrix for  $M_m$ . But the only problem associated with  $M_m$  is to choose the position and number of mass points to be taken in the analysis.

Maddox 1974<sup>(80)</sup> has conducted a study to find the best position and number of discrete mass points to be considered by using two different representation of the mass points for the same structure, as shown in figures (2.2.6A and 2.2.6B) which represent model 1 and model 2 respectively.

A comparison between the two models has shown that model 1 can be considered to be an adequate representation of the structure to be accounted for.

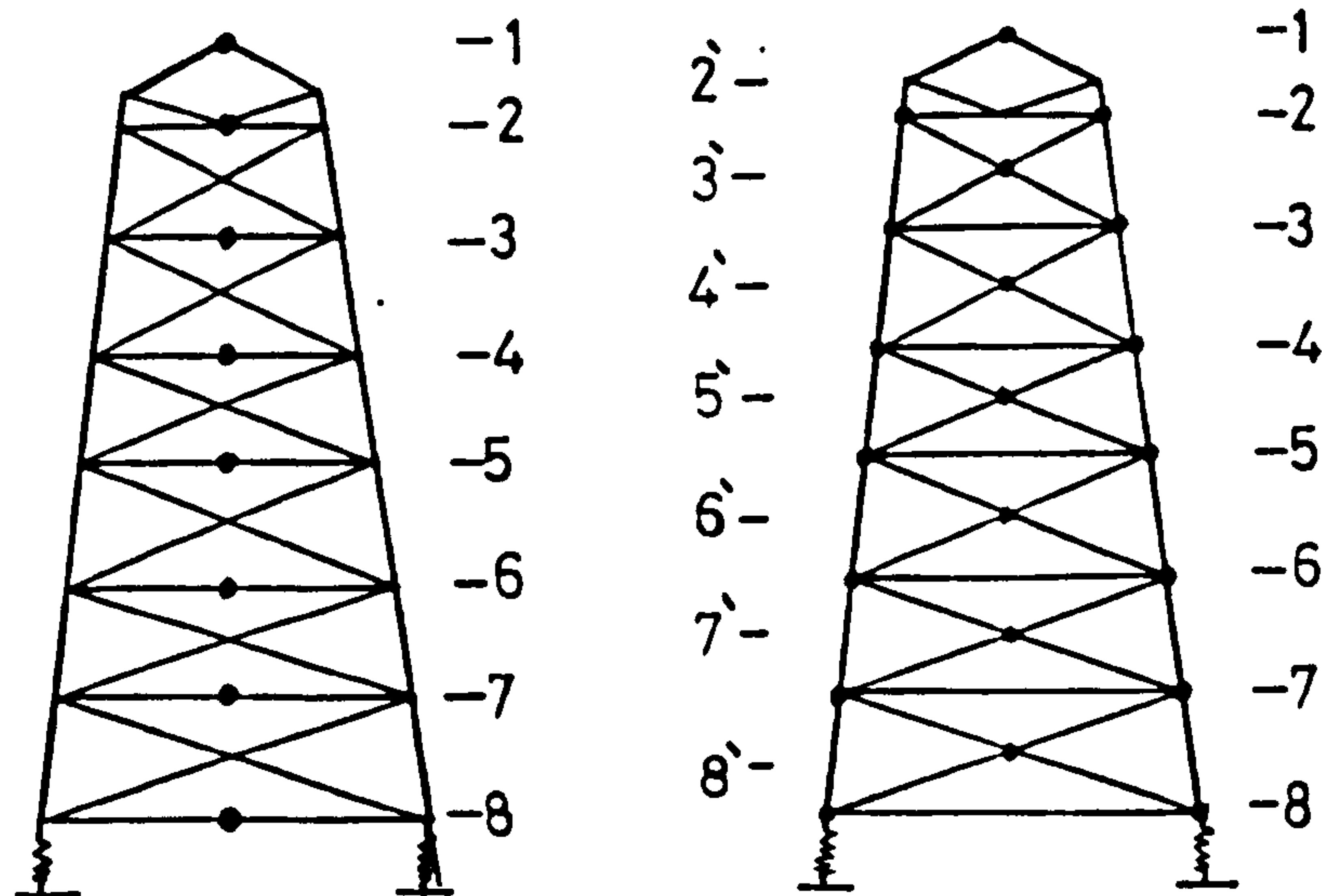


Figure (2.2.6a) - Model 1.      Figure (2.2.6b) - Model 2.

The number of discrete mass points must be considered in the analysis, because at each discrete mass point the dynamic equation of motion is set. By using a large number of discrete mass points we get a similar number of equations of motion to be solved simultaneously which requires too much computer time and a high computer capacity. This is not the only disadvantage of choosing too many lumped masses but also it gives an inaccurate solution because of the higher frequency modes which will be concluded in the solution while not being required.



From the above it is important to choose the exact number of lumped mass to be taken in the mathematical modelling of the structure. Nath and Harleman 1969<sup>(81)</sup> used one lumped mass at the platform for two massless leg structures, the experimental result shows that there is quite good agreement with the predicted analysis for deep water wave and with different space between structures. Harleman et al 1963<sup>(82)</sup> carried out experiments for four massless leg structures using one lumped mass at the platform. They show general agreement between experimental and analytical prediction. Experimental and analytical studies for one-degree of freedom of one, two and four massless towers subjected to regular and random water waves had been performed by Nath and Harleman 1967<sup>(83)</sup> taking into consideration the stress and the moment of the structures and the effects of the spacing of vertical supports on the platform deflection and also the effect of wave direction emphasis, the general agreement with the use of the one-degree of freedom. The above experiments used structure model fixed at the base and the wave structure interaction were ignored. It does not show whether the model represent any full scale real structure.

Nolan and Honsinger 1962<sup>(84)</sup> found that for the single degree of freedom approximation for the structures assuming that all masses to be concentrated at the platform level, the ratio of the maximum theoretical to experimental displacement varied from 0.5 - 1.7.

Molhotra and Penzin 1970<sup>(85)</sup> mentioned that the behaviour of a tower in water subjected to random wave forces can be represented fairly accurately by using the first and second mode or first, second and third lateral mode of vibration. Also Bege and Penzien 1974<sup>(62)</sup> concluded that at least six normal modes of vibration should be included in the three-dimensional dynamic analysis.

Wu 1976<sup>(86)</sup> concluded that the number of discrete mass points necessary to satisfy the displacement analysis is less than that required for the analysis of shear force and bending moment.

The use of a large number of lumped masses is unnecessary.

$M_a$  represent the mass of water attached to the structure and move with it as one body. The evaluation of this mass of water represented by the equation

$$M_a = (C_m - 1)\rho V \quad \dots \quad \dots \quad \dots \quad (2.2.10)$$

where  $V$  = Volume of water displaced by structure

$\rho$  = Water density

$C_m$  = Mass coefficient (inertia coefficient)

Equation (2.2.10) has a numerical coefficient which attribute uncertainties to the evaluation of the added mass. Many works assumed that  $C_M = 2.00$  which means that the added mass will be equal to the mass of water displaced by the structure.

King 1971<sup>(87)</sup> support the idea of  $C_M = 2.00$  and also mentioned that the added mass is unaffected by streaming flow and vortex shedding, as well as the added mass function was seen to be independent of frequency, amplitude and model shape. Jenssen et al 1977<sup>(88)</sup> observe that the above statement of King is not absolute as they found a variation in added mass near the surface. Sarpkaya 1981<sup>(89)</sup> dealt with the question of instantaneous value of inertia coefficient which lead to negative added mass in some parts of the wave cycle, which prove that the added mass is not a constant value during the wave cycle and also it varies due to wave and structure condition.

#### 2.2.2.2 THE STIFFNESS MATRIX

The stiffness matrix is independent of the type of the structure whether offshore or inshore. It is also independent of the solution type i.e. whether static or dynamic, although some papers state that there are changes in stiffness matrix due to the difference in the dynamic Young's modulus. (See Nath and Harleman 1969<sup>(81)</sup> and Hallam et al 1978<sup>(90)</sup>).

#### 2.2.2.3 DAMPING MATRIX

It is important to understand the general description of damping. Damping is basically a dissipation of energy due to motion. There are several possibilities for energy dissipation:

##### (i) MATERIAL DAMPING

The material damping is thought to be very small. This component may mathematically be represented as viscous damping. The damping coefficient may be assumed to be constant throughout the structure and only depend on the structure material.

##### (ii) STRUCTURAL DAMPING

The structural damping is caused by the way the structure is assembled (bracing, welding) and on the structure mechanism. The assessment of material damping is equally valid for structural damping.

### (iii) ENVIRONMENTAL DAMPING

For offshore structure the environmental damping is mainly of hydrodynamic origin. Damping forces due to movement of air above the water line are negligible compared with the hydrodynamic damping.

The above physical possibilities of damping summed together to represent and use of damping in computations. In calculations, the damping are represented by the damping coefficient which can be calculated from the equation:

$$\zeta = \frac{C}{C_c} \times 100 \quad \dots \dots \dots (2.2.11)$$

the damping coefficient is usually imagined to be constant throughout the structure which is not a good physical description (see Vugts and Hayes 1979<sup>(91)</sup>), the value of this coefficient is given in the form of a percentage of critical damping, as critical damping cannot be defined for a general N-degree of freedom, the natural period of vibration is important and to get the damping coefficient in the equation

$$C_c = 2 M W_n \quad \dots \dots \dots (2.2.12)$$

where  $M$  = mass of structure

$W_n$  = natural frequency of structure



The most vital part is to establish the appropriate damping coefficient. Several papers have been published concerning this point, some used model structures (Skepp et al 1976<sup>(92)</sup> and King 1972<sup>(93)</sup>) and others used prototype structures.

The damping coefficient of the structure can be measured by one of the three possible methods

- (a) Log-decrement measurements of decay vibration resulting from a free vibration due to tip displacement
- (b) Response measurements under known imposed excitation
- (c) Response measurements under natural excitation for offshore structure

For offshore structure methods (a) and (b) seem practical for establishing the damping coefficient, the snag in both methods has been pointed out <sup>(91)</sup>, also in the mathematical representation of the physical realities. Three main factors affect the choice of a preferable method: nonlinear effects, local damping effect and frequency dependent coefficients.

Ogilvie 1964<sup>(94)</sup> found that the choice of a damping coefficient has strong effect upon forces and displacement but it had hardly any effect on the resonant frequency.

In reviewing the work done by some offshore professional in estimating the damping coefficient, Cherry and Brady 1965<sup>(95)</sup> used the concept of autocorrelation technique for random vibration of experimental data as a method for predicting structure dynamic properties (Natural period and damping coefficient), the result concluded that reasonable estimation of structure period can be obtained from an analysis involving small amounts of data, relatively large sample sizes are required if meaningful estimates of structure damping coefficient are expected.

A method of measuring structural damping based on time delay correlation has been established by Jeary and Winney 1972<sup>(96)</sup> for random vibration experiment data has shown that the results obtained with this method is in good agreement with the results obtained from the standard decay tests. Vanmarke 1971<sup>(97)</sup> outlines a new method based on power spectral density analysis for determining period and damping values of offshore structure from field measurements of their response to wave-induced random excitation. Ruhl and Berdahl 1979<sup>(98)</sup> carried out forced vibration tests to find the damping coefficient they found that the damping coefficient is less than two percent of the fundamental group of modes and is three to five percent range for the second group of modes. They used the steady state test which show that these tests are extremely useful for determination of coefficient of damping. Also Ruhl

1976<sup>(90)</sup> conducted free vibration tests and spectral analysis of random response data to find the fundamental periods and damping coefficient using the partial spectral moment method for the random vibration.

Another way of getting the damping of offshore structures is by separating it into two parts, first the material and structure damping and second the environmental "Hydrodynamic Damping. Skop et al 1972<sup>(92)</sup> evaluated a damping empirical formula for circular cylinder, but it had not been used or proven. King 1972<sup>(93)</sup> tried the hydrodynamic damping in still water, concludes that it is pure viscous and may be described by Stokes element damping theory. His work also shows that the damping increases rapidly with water depth. Verley 1978<sup>(100)</sup> compared between the independent flow fields, i.e. by taking the damping as being the still water and the hydrodynamic added damping due to the relative velocity, his result of the analysis confirms the suggestion of using the independent flow fields for low values of the reduced velocity ( $U_r = U_m/f_n D$ ) and low expected vibration amplitude as the relative velocity assumption for calculating the hydrodynamic damping will overestimate the damping, and underestimate vibration. Verley and Moe 1979<sup>(101)</sup> carried out experimental investigation of oscillating cylinder in current and the results indicate the same conclusion of those of Verley 1978<sup>(102)</sup>, <sup>(100)</sup>. Dean et al 1979<sup>(103)</sup> in his report tried to establish values to be added, called

(implied damping) to substitute the hydrodynamic damping but in their report they could not generalize the values for the sea state.

## 2.3 NUMERICAL PROCEDURE

A realistic dynamic analysis of the fixed offshore structure is complex. Hence approximation analogous to the single-degree of freedom system is adequate. But a full and comprehensive dynamic analysis appears to be the only satisfactory way of dealing with the problem.

Two general aspects of the problem must be briefly discussed.

### 2.3.1 TIME DOMAIN AND FREQUENCY DOMAIN DESCRIPTION

A distinction in time and frequency domain analyses is governed by the manner in which the excitation is handled; (The right hand side of the equation of motion). With a description in the time domain the full time history of every quantity is involved, certain initial conditions are specified and with the loading distribution over the whole structure known as a function of time, the response of the structure may be obtained at each and every instant.



2.3.1.1      MATHEMATICAL FORMULATION OF THE DYNAMIC  
PROBLEM IN FREQUENCY DOMAIN DESCRIPTION

- Constant and frequency depended coefficient can both simply and equally be handled. These coefficients may arise from e.g. hydrodynamic and soil interaction (added mass, damping coefficient). Time dependent coefficients are strictly not admissible.
- Non-linearities in system properties (stiffness, damping) or in loading wave force can only be modelled by linearization.
- The equation of motion have the appearance of differential equation but are in fact algebraic equations (see Ogilvie 1964<sup>(94)</sup>).
- The steady state solution only is obtained, and it is obtained directly.
- For N degree of freedom and harmonic excitation, a system of 2N linear algebraic equations must be solved at each frequency. The response to a random excitation can be obtained through spectral analysis.
- An arbitrary though prescribed excitation over a short period cannot be handled in the sense that the response include transients but it can be analysed using Fourier series.



### 2.3.1.2 MATHEMATICAL FORMULATION OF THE DYNAMIC PROBLEM IN TIME DOMAIN DESCRIPTION

In the time domain with constant coefficients the equations are differential equations. Frequency dependent coefficients lead to the inclusion of retardation functions, the equations become integro-differential equations (see Ogilvie). Coefficients that are functions of time can be handled.

- The equations are differential or integro-differential equations.
- Transient and/or steady state solutions can be obtained. Initial conditions have to be specified. Number of cycles required for steady state to be reached may be large depending on initial conditions and damping.
- For N degree of freedom and harmonic excitation of a linear system under certain assumptions the set of N second order differential equations may be replaced by N simultaneous equation for every time step response, to random excitation may be obtained directly through numerical integration.
- Any non-linearity can in principle be included provided that an adequate mathematical formulation and solution procedure is available.

- The differential equations must be solved numerically with small time steps, initial conditions and a criterion to define steady state condition have to be specified.
- Numerical integration under random excitation is a time consuming process. For different excitation the whole process must be repeated. In general the random loading distributions are required.
- Any prescribed excitation can be dealt with by direct numerical integration given appropriate conditions and a reliable integration technique.

### 2.3.2 MODEL SUPERPOSITION AND DIRECT INTEGRATION

The distinction between model superposition and direct integration techniques lies in the manner by which the equation describing the behaviour of the system are dealt with.

The model superposition technique makes use of the fact that the response of a complex multi-degree of freedom system can be described as the sum of the responses of a number of one-degree of freedom system. By appropriate coordinate transformations the degrees of freedom are uncoupled, so it improves the understanding of the system properties, also the excitation has also to be

transformed to refer to the same coordinate system. The system may be continuous or discretized.

The direct integration approach, the coupled equation which in practical cases would refer to a discretized system are integrated as they stand.

#### 2.3.2.1 MATHEMATICAL FORMULATION OF THE DYNAMIC PROBLEM BY MODEL SUPERPOSITION

- The basic features of this technique is that  $N$  degree of freedom system are uncoupled into  $N$  equations each describing a single degree of freedom system. The technique is exploited when the eigenvalues of the coupled equation is real.
- The essential difficulty with model superposition is the number of modes that have to be considered.
- The system non-linearities cannot be included.
- The first requirement in an eigenvalue solution in order to find the undamped natural frequencies and mode shapes.
- The transformation to generalized coordinates is lengthy but needs to be done only once. Only the transformation of the loading function is to be represented.

- Relatively small computer can handle the problem.

#### 2.3.2.2 MATHEMATICAL FORMULATION OF THE DYNAMIC PROBLEM BY DIRECT INTEGRATION

- The coupled equation is dealt with directly.
- There are no questions of truncation of a series, the full solution is obtained.
- Non-linearities can in principle be incorporated.
- Although not a part of the solution procedure, definition of damping may be facilitated by an eigenvalue solution of the first few natural frequencies. Knowledge of the principal mode shapes also improve physical insight.
- No transformation is required.
- Large computer is required.

Two practical examples of the way in which dynamic analysis have been incorporated into particular design problems in both the time and frequency domain had been carried out by Schumm 1978<sup>(104)</sup> for steel jacket platform. It showed that the advantage of using time domain analysis are as follows:

1. The correct structure submergence for members in the region of the still water surface.
2. Drag force can be included without linearizations.
3. Relative velocity between wave and structure can be correctly accounted for.

Also in frequency domain it shows that despite the necessity to perform linearization, the frequency domain approach provides an extremely powerful tool for stochastic analysis for long term effects as it reduces the amount of data processing to a manageable size and significantly reduces computing cost over an equivalent time domain approach. It shows also that the best suited technique of the solution of mathematical model for steel platform is the model superposition technique in which case the major response of the structure can be adequately represented by the first ten or so mode shapes without a significant loss of accuracy.

Vugts 1979<sup>(105)</sup> made a comparison between the solution of mathematical model, also alternative model superposition analysis using varying numbers of modes to account for dynamic effects, supplemented by the full static solution which replaces the corresponding static component contained in the solution of the truncated model series has been used. All calculations were performed in frequency domain for two derivatives of the structure:



the first is made artificially stiff in order to make it dynamically insensitive to the wave load and the second is made artificially flexible in order to produce significant dynamic response to the prescribed wave excitation. This work indicates that pure model superposition is unacceptable if a realistic prediction of detailed member end forces and moment (and hence stresses) is the primary objective. The comparison with exact direct solutions confirm that model analysis provides reasonably reliable estimates of gross platform behaviour, expressed in terms of global horizontal displacement even when relatively few modes are used.

A considerable improvement in accuracy observed when static response of higher modes, which were truncated in the model series, has a large influence upon the number force contribution and firmly recommended that however stress recovery is the primary objective of a dynamic analysis of an offshore structure a direct solution of the equation of motion in the physical coordinates should be performed. In the stiff structure it is not necessary to perform the direct dynamic solution as it more costly than model superposition.

# CHAPTER THREE

## THEORETICAL FORMULATION

### 3.1 INTRODUCTION

The problem of determining structural interaction of cylinders in periodic waves will be examined theoretically. The model posed is a circular cylinder fixed at the base and either free or fixed at the top (i.e. free to vibrate or not) subjected to periodic waves.

The periodic wave form will be assumed to be linear. The force on the structure due to these waves will be obtained by the Modified Morison's equation as well as Morison's equation.

The dynamic structural response to waves will be calculated using mode superposition in the time domain. A finite element method is used to solve the resulting dynamical equations.

### 3.2 WAVE DYNAMICS

The accuracy of the determination of the water wave force depends on the accurate description of waves. This is needed to obtain the appropriate wave velocity and accelerations necessary for the prediction of wave forces.

### 3.2.1 WAVE DESCRIPTION

The wave flow field used in this study is assumed to be in two dimensions. Also it is assumed to be incompressible and irrotational which will satisfy Laplace's equation (2.1.1)

$$\frac{\partial^2 \phi}{\partial x^2} + \frac{\partial^2 \phi}{\partial y^2} = 0 \quad \dots \quad \dots \quad \dots \quad \dots \quad (3.2.1)$$

The bottom surface is assumed to be horizontal, rigid and impermeable and hence Equation (2.1.5) reduces to

$$\frac{\partial \phi}{\partial y} = 0 \quad \text{at } y = -h \quad \dots \quad \dots \quad \dots \quad (3.2.2)$$

The Equation (2.1.4) is linearized by neglecting the velocity components, also by assuming small amplitude wave

$$\therefore \eta = \frac{1}{g} \frac{\partial \phi}{\partial t} \quad \text{at } y = 0 \quad \dots \quad \dots \quad \dots \quad (3.2.3)$$

To satisfy the linearization of the boundary condition, the ratio between the neglected terms and terms which have been retained should be small. This is found to give:

$$ak \ll 1, \quad (\tanh Kh \text{ and } \cosh Kh \ll 1) \quad \dots \quad (3.2.4)$$

if the velocity potential is considered to be the first term  $\phi_{11}$  in a perturbation expansion

$$\phi = \phi_{11} + \phi_{12} + \phi_{13} + \dots \phi_n \quad \dots \quad (3.2.5)$$

where  $\phi_{n-1} \gg \phi_n$  for all  $n$

The ratio of  $\phi_{12}/\phi_{11}$  should be small where ( $\phi_{12}$  is the Stokes second order term)

$$\phi_{12} = \frac{3}{8} \frac{a^2 g}{C} \frac{\cosh 2k(h+z)}{\sinh^3 Kh \cosh Kh} \sin 2(kx - \sigma t) \quad \dots \quad (3.2.6)$$

To satisfy the above requirement the following condition must hold

$$a/K^2 h^3 \ll 1 \quad \dots \quad (3.2.7)$$

The wave generated contained small amplitude of higher order free harmonic waves. The wave profile was periodic

$$\therefore \eta(t + \tau) = \eta(t) \quad \dots \quad (3.2.8)$$

The experimental wave profile obtained for one wave cycle was analysed using the Fast Fourier Transform to obtain the magnitude of each of the individual free harmonic waves

$$\eta_{\text{total}} = \sum_n a_n \cos(K_n x - \sigma_n t) + b_n \sin(K_n x - \sigma_n t) \dots \dots \dots (3.2.9)$$

$$\therefore \eta_{\text{total}} = \sum_n A_n \cos(K_n x - \sigma_n t + \alpha_n) \dots (3.2.10)$$

where  $A_n$  = amplitude of the nth harmonic in the wave

$$= \sqrt{a_n^2 + b_n^2}$$

$\alpha_n$  = the phase shift relationship between the various waves (nth harmonic) and the measured from the original  $(kx - \sigma t)$  and equal to  $\tan^{-1} \frac{a_n}{b_n}$

Since Laplace's equation is linear, the velocity potential of a wave system  $\phi_{\text{total}}$  is given by the sum of the potential of the individual waves

$$\phi_{\text{total}} = \phi_1 + \phi_2 + \phi_3 + \dots \phi_n \dots \dots (3.2.11)$$

in which

$$\phi_n = \frac{A_n g}{\sigma_n} \frac{\cosh K_n (h + z)}{\cosh K_n h} \sin(K_n x - \sigma_n t + \alpha_n) \dots \dots \dots (3.2.12)$$

and the dispersion relation

$$C_n^2 = (g/K_n) \tanh K_n h \dots \dots \dots (3.2.13)$$



where

$g$  = gravitational acceleration

$\sigma_n$  = the nth wave angular frequency =  $2\pi/T_n$

$K_n$  = the nth wave number =  $2\pi/L_n$

$h$  = distance from the still water level  
to bottom

$C_n$  = velocity of the nth wave propagation  
(phase velocity) =  $L_n/T_n$

$Z$  = vertical distance measured positive upward  
from the still water level

Since the fluid particle velocity and acceleration are first derivative of  $\phi$ , they can be added because  $\phi$  is linear

$$\dot{u}_{total} = \dot{u}_1 + \dot{u}_2 + \dot{u}_3 + \dots + \dot{u}_n \dots \dots \quad (3.2.14)$$

where

$$\dot{u}_n = \frac{\partial \phi_n}{\partial x} = \frac{A_n g K_n}{\sigma_n} \frac{\cosh K_n(h+z)}{\cosh K_n h} \cos(K_n x - \sigma_n t + \alpha_n) \dots \dots \dots \quad (3.2.15)$$

and

$$\ddot{u}_n = \ddot{u}_1 + \ddot{u}_2 + \ddot{u}_3 + \dots + \ddot{u}_n \dots \dots \quad (3.2.16)$$

where

$$\ddot{U}_n = \frac{\partial \dot{U}_n}{\partial t} = A_n gK \frac{\cosh K_n(h+z)}{\cosh K_n h} \sin(K_n x - \sigma_n t + \alpha_n) \dots \dots \dots (3.2.17)$$

### 3.2.2 WAVE FORCES

The wave forces on structure will be determining using Morison's equation. This force varies with time during the wave cycle. It also varies with the position of different element along the structure. The force on the element is calculated using the average values of the drag and the inertia coefficients during the wave cycle (over the cycle  $C_D$  and  $C_M$  are assumed constant).

$$dF(t, z) = [C_{D(z)} \frac{1}{2} \rho D (\dot{U}_{total}(t, z) |\dot{U}_{total}(t, z)| + C_{M(z)} \frac{\rho \pi D^2}{4} \ddot{U}_{total}(t, z)] dz \dots (3.2.18)$$

In the case where the structure is free to vibrate the force on the element will be represented by

$$dF'(t, z) = [C'_{D(z)} \frac{1}{2} \rho D (\dot{U}_{total}(t, z) - \dot{X}_{(t,z)}) |\dot{U}_{total}(t, z) - \dot{X}_{(t,z)}| + (C'_M - 1) \frac{\rho \pi D^2}{4} (\ddot{U}_{total}(t, z) - \ddot{X}_{(t,z)}) + \frac{\rho \pi D^2}{4} \ddot{U}_{total}(t, z)] dz \dots \dots (3.2.19)$$

The corresponding bending moment at the base of the structure due to the wave force can be obtained by integrating of Equations(3.2.18) and (3.2.19) along the submerged part of the structure for the case of small structure's deflection.

For the case of free structure (cantilever)

$$M_B = \int_{z_0}^h dF_{(t,z)} z dz$$

or

$$M_B = \int_{z_0}^h dF'_{(t,z)} z dz \quad \dots \quad \dots \quad \dots \quad (3.2.20)$$

For the case of fixed structure

$$M_B = \int_{z_0}^h dF_{(t,z)} \frac{z(L_S - z)^2}{L_S} dz \quad \dots \quad \dots \quad (3.2.21)$$

where  $L_S$  = structure length.

The appropriate drag and inertia coefficients are obtained using either Equation (3.1.15) or (3.1.16) in conjunction with the measured wave force. The method of obtaining the measured wave force, the parameter  $\dot{X}_{(t, z)}$  and  $\ddot{X}_{(t, z)}$  will be shown later in this chapter.

The average values of the drag and inertia coefficients during the wave cycle can be calculated by one of the following methods:

1. Fourier analysis
2. Cross point(calculated of the drag coefficient at zero inertia force and calculating of the inertia coefficient at zero drag force)
3. Least square method

The Fourier analysis for an oscillating flow represented by

$$\dot{U} = \dot{U}_m \cos \sigma t \quad \dots \quad \dots \quad \dots \quad \dots \quad (3.2.22)$$

the average value of  $C_D$  and  $C_M$  are given by Keulegan and Carpenter (27)

$$C_D = - 0.75 \int_0^{2\pi} (F_m \cos \sigma t / \rho \dot{U}_m^2 SD) dt \quad \dots \quad (3.2.23)$$

and

$$C_M = (2\dot{U}_m T / \pi^3 D) \int_0^{2\pi} F_m \sin \sigma t / \rho \dot{U}_m^2 SD) dt \quad (3.2.24)$$

in which  $F_m$  is the measured force and  $S$  is the length of the segment over which the force was measured.

This method yields the same value of  $C_M$  as that of the least square method but with slight difference in

the value of  $C_D$ . This method is not applicable if there are free higher order harmonic waves present in the wave. The omission of the second harmonic wave will affect the value of the force coefficients (see D. I. Maull and M. G. Milliner 1979<sup>(61)</sup>).

The cross point will give discrepancies due to the difficulty in determining the region of the zero drag and zero inertia during the wave cycle.

The least square method is more applicable, as it can deal with higher harmonic component in the wave.

The least square method used is as follows

$$F_m = (f_I) C_M + (f_D) C_D \dots \dots \dots (3.2.25)$$

where

$$(f_I) = \frac{\rho \pi D^2}{4} \ddot{U}_{total}(t, z) S \dots \dots \dots (3.2.26)$$

$$(f_D) = \frac{1}{2} \rho D \dot{U}_{total}(t, z) |\dot{U}_{total}(t, z)| S \dots \dots \dots (3.2.27)$$

$$\Sigma (f_D)^2 C_M + \Sigma (f_I)(f_D) C_D = \Sigma (f_I F_m) \dots \dots \dots (3.2.28)$$

$$\Sigma (f_I)(f_D) C_M + \Sigma (f_D)^2 C_D = \Sigma (f_D F_m) \dots \dots \dots (3.2.29)$$



$$\therefore C_{D(z)} = \frac{\Sigma(f_I)^2 \Sigma(f_D F_m) - \Sigma(f_I F_m) \Sigma(f_I) (f_D)}{\Sigma(f_I)^2 \Sigma(f_D)^2 - \Sigma((f_I) (f_D))^2} \dots \dots \dots (3.2.30)$$

$$C_{M(z)} = \frac{\Sigma(F_m f_I) \Sigma(f_D)^2 - \Sigma(f_D F_m) \Sigma(f_I) (f_D)}{\Sigma(f_I)^2 \Sigma(f_D)^2 - \Sigma((f_I) (f_D))^2} \dots \dots \dots (3.2.31)$$

where  $F_m$  = measured force for the case either (fixed or free).

In the case of the modified Morison's equation is used Equation (3.2.25) becomes

$$F_m = (F_I) + (f'_I)C'_m + (f'_D)C'_D \dots \dots \dots (3.2.32)$$

where

$$F_I = - \frac{\rho \pi D^2}{4} \ddot{x}_{(t, z)} S \dots \dots \dots (3.2.33)$$

$$(f'_I) = \frac{\rho \pi D^2}{4} (\ddot{u}_{total}(t, z) - \ddot{x}_{(t, z)}) S \dots \dots \dots (3.2.34)$$

$$(f'_D) = \frac{1}{2} \rho D (\dot{u}_{total}(t, z) - \dot{x}_{(t, z)}) \dot{u}_{total}(t, z) - \dot{x}_{(t, z)} | S \dots \dots \dots (3.2.35)$$

by arranging Equation (3.2.29)

$$F'_m = (f'_I)C'_M + (f'_D)C'_D \dots \dots \dots (3.2.36)$$

the values of  $C_D(z)$  and  $C_M(z)$  can be obtained from Equations (3.2.30) and (3.2.31) using these new values of  $F'_m$ ,  $f'_I$ ,  $f'_D$ .

### 3.3 STRUCTURAL DYNAMICS

The problem of vibrating structure is solved by equilibrating the externally applied force with the inertia forces resulting from the acceleration of the structure, the elastic resistance to displacement and the energy-loss due to the structure mechanism (damping). The difficulties arises in the prediction of structural dynamic of offshore structure is due to the dependence of external applied force on the structure oscillation.

The prediction of the dynamic response of offshore structure will depend upon the idealization used to model the structure system, the formulation of the equation of structure system response and the method of solution of the structural system equations with its numerical analysis.

#### 3.3.1 THE STRUCTURE MODELLING

The structural system used in this study is modelled as follows:

- The continuous member is assumed to be series of discrete masses connected by springs (with no mass)
- The continuous wave forces are represented by point loads acting at the mass centres

Figure (3.3.1(a)) shows the actual structure and the wave force while Figure (3.3.1(b)) shows the modelled structure

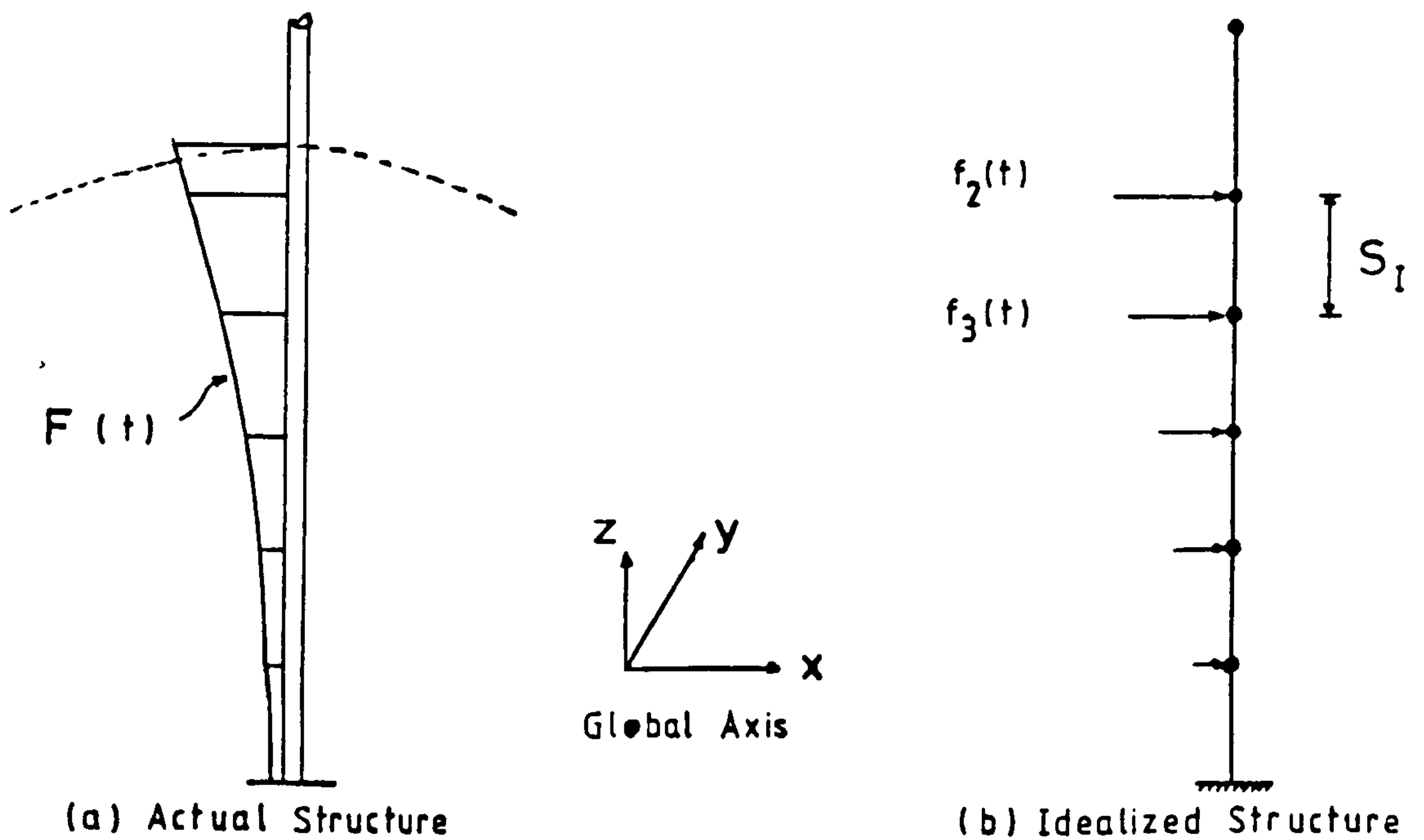


Figure (3.3.1) - Modelling of the Structures.

Further idealizations upon which the analysis is based are (a) stress is proportional to strain, (b) small deflection theory, (c) all motion is measured from the position of static equilibrium.

In this study, it is assumed that the waves travel in the positive x direction. All structural and loading variations in the y direction are therefore neglected. Thus, the number of degrees of freedom at each node is reduced to three; namely, translational displacements in the horizontal x direction and in the vertical direction, and rotational displacement about the y-axis.

### 3.3.2 FORMULATION OF THE EQUATION OF STRUCTURAL SYSTEM RESPONSE

The force on the structure including the interaction effect and noting that  $\dot{U}_o \approx \dot{U}_x$  and  $\ddot{U}_o \approx \ddot{U}_x$ , where subscript 'o' indicates that these quantities are taken at the undeflected structure location, the complete dynamic equation for the idealized structure shown in Figure (3.3.1(b)) may be written as follows

$$\begin{aligned}
& \begin{bmatrix} M_1 & 0 & 0 & 0 & 0 \\ 0 & M_2 & 0 & 0 & 0 \\ \vdots & & & & \\ 0 & 0 & 0 & 0 & M_n \end{bmatrix} \begin{Bmatrix} \ddot{X}_1 \\ \ddot{X}_2 \\ \vdots \\ \ddot{X}_n \end{Bmatrix} + \begin{bmatrix} C_{11} & C_{12} & C_{13} & \cdots & C_{1n} \\ C_{21} & C_{22} & C_{23} & \cdots & C_{2n} \\ & & & & \\ C_{n1} & C_{n2} & C_{n3} & \cdots & C_{nn} \end{bmatrix} \begin{Bmatrix} \dot{X}_1 \\ \dot{X}_2 \\ \vdots \\ \dot{X}_n \end{Bmatrix} \\
& + \begin{bmatrix} K_{11} & K_{12} & K_{13} & \cdots & K_{1n} \\ K_{21} & K_{22} & K_{23} & \cdots & K_{2n} \\ \vdots & & & & \\ K_{n1} & K_{n2} & K_{n3} & \cdots & K_{nn} \end{bmatrix} \begin{Bmatrix} X_1 \\ X_2 \\ \vdots \\ X_n \end{Bmatrix} \\
& = \begin{Bmatrix} P_1(t) \\ P_2(t) \\ \vdots \\ P_n(t) \end{Bmatrix} \dots \dots \dots \dots \dots \dots \dots \quad (3.3.1)
\end{aligned}$$

where the column matrix {P(t)} can be obtained from modified Morison's equation (3.2.19)



$$\begin{aligned}
\begin{Bmatrix} P_1(t) \\ P_2 \\ \vdots \\ P_n(t) \end{Bmatrix} &= \begin{bmatrix} 0 & 0 & 0 & 0 & 0 \\ 0 & F_{m2} & 0 & 0 & 0 \\ 0 & 0 & F_{m3} & 0 & 0 \\ \vdots & \vdots & \vdots & \vdots & \vdots \\ 0 & 0 & 0 & 0 & F_{mn} \end{bmatrix} \begin{Bmatrix} 0 & -\ddot{X}_1 \\ \ddot{U}_{o2} & -\ddot{X}_2 \\ \ddot{U}_{o3} & -\ddot{X}_3 \\ \vdots & \vdots \\ \ddot{U}_{on} & -\ddot{X}_n \end{Bmatrix} + \\
&+ \begin{bmatrix} 0 & 0 & 0 & 0 & 0 \\ 0 & F'_{m2} & 0 & 0 & 0 \\ 0 & 0 & F'_{m3} & 0 & 0 \\ \vdots & \vdots & \vdots & \vdots & \vdots \\ 0 & 0 & 0 & 0 & F'_{mn} \end{bmatrix} \begin{Bmatrix} 0 \\ \ddot{U}_{o2} \\ \ddot{U}_{o3} \\ \vdots \\ \ddot{U}_{on} \end{Bmatrix} + \\
&+ \begin{bmatrix} 0 & 0 & 0 & 0 & 0 \\ 0 & F_{D2} & 0 & 0 & 0 \\ 0 & 0 & F_{D3} & 0 & 0 \\ 0 & 0 & 0 & 0 & F_{Dn} \end{bmatrix} \begin{Bmatrix} (0 \quad -\dot{X}_1) | 0 \quad -\dot{X}_1 | \\ (\dot{U}_{o2} - \dot{X}_2) | \dot{U}_{o2} - \dot{X}_2 | \\ (\dot{U}_{o3} - \dot{X}_3) | \dot{U}_{o3} - \dot{X}_3 | \\ (\dot{U}_{on} - \dot{X}_n) | \dot{U}_{on} - \dot{X}_n | \end{Bmatrix} \\
&\dots \quad \dots \quad \dots \quad \dots \quad \dots \quad \dots \quad \dots \quad (3.3.2)
\end{aligned}$$

$$F_{mn} = \frac{\rho \pi D^2}{4} (C_{Mn} - 1) S_n$$

$$F_{Dn} = \frac{1}{2} \rho D C_{Dn} S_n$$

Equations(3.3.1) and (3.3.2) can be written as

By rearranging the above equation

72

where

$$\{F(t)\} = [\bar{F}_m] + [\bar{F}'_m] \{\ddot{U}_o\} + \\ + [\bar{F}_D] \{\dot{U}_o |\dot{U}_o|\} \dots \dots \dots (3.3.5)$$

From Equation (3.3.4) it can be seen that the water wave/structure interaction produces a hydrodynamic damping due to the drag force, which is  $[\bar{2}\dot{U}F_o]$   $\{\dot{X}\}$  and a nonlinear vector  $\{E(\dot{X})\}$  which has the form

$$\{E(\dot{x})\} = - [\bar{F}_D] \{\dot{X} |\dot{x}|\} \dots \dots \dots (3.3.6)$$

The nonlinear nature of Equation (3.3.4) necessitates an examination of solution methods for systems of nonlinear differential equation. The following methods are used for the solution of nonlinear differential equation

1. Perturbation method
2. Semilinear method

The above methods depend upon the condition that the nonlinearity in the system is small.

## PERTURBATION METHOD

In this method the nonlinear term  $\{E(\dot{X})\}$  expressed

$$\{E(\dot{X})\} = \epsilon \{E'(\dot{X})\} \quad \dots \quad \dots \quad \dots \quad \dots \quad (3.3.7)$$

where  $\{E(\dot{X})\}$  is the nonlinear damping function and

$\{E'(\dot{X})\}$  describes the shape of the nonlinearity  
and the relative magnitude is indicated  
by the parameter  $\epsilon$

when  $\epsilon = 0$  the Equation (3.3.4) reduces the equation to linear oscillations. The perturbation method is based on the assumption that, the solution of the Equation (3.3.4) permits an expansion in power of  $\epsilon$ . It is only expected to be valid for motions in which the nonlinear part of the damping force remain small in comparison with the linear part.

$$\therefore \begin{bmatrix} X_1 \\ X_2 \\ \vdots \\ \vdots \\ X_n \end{bmatrix} = \begin{bmatrix} X_{10} + \epsilon X_{11} + \epsilon^2 X_{12} + \dots \\ X_{20} + \epsilon X_{21} + \epsilon^2 X_{22} + \dots \\ \vdots \\ \vdots \\ X_{n0} + \epsilon X_{n1} + \epsilon^2 X_{n2} + \dots \end{bmatrix} \quad \dots \quad \dots \quad \dots \quad \dots \quad (3.3.8)$$

Equation (3.3.8) can be written as

$$\{X_n\} = \sum_{I=D}^{NP} \epsilon^I \{X_{nI}\} \dots \dots \dots (3.3.9)$$

where NP = an arbitrarily large integer

n = number of node point

The Ith term of the quantity represents the Ith order correction to the (I-1)th order solution for that quantity . The expansion of the shape function  $\{E'(\dot{X})\}$  by using the truncated Taylor series with respect with  $(\epsilon \Delta X)$  is

$$\begin{Bmatrix} E'(\dot{X})_1 \\ E'(\dot{X})_2 \\ \vdots \\ E'(\dot{X})_n \end{Bmatrix} = \begin{Bmatrix} E'(\dot{X})_{10} + \frac{(\epsilon \Delta \dot{X})}{1!} \frac{d'E(\dot{X})_{10}}{d\dot{x}_{10}} + \frac{(\epsilon \Delta \dot{X})^2}{2!} \frac{d'^2 E(\dot{X})_{10}}{d\dot{x}_{10}^2} + \dots \\ \vdots \\ E'(\dot{X})_{n0} + \frac{(\epsilon \Delta \dot{X})}{1!} \frac{d'E(\dot{X})_{n0}}{d\dot{x}_{n0}} + \frac{(\epsilon \Delta \dot{X})^2}{2!} \frac{d'^2 E(\dot{X})_{n0}}{d\dot{x}_{n0}^2} + \dots \end{Bmatrix} \dots \dots \dots (3.3.10)$$



∴ equation (3.3.10) can be written as

$$\{E'(\dot{X})_n\} = \sum_{I=0}^{NP} \frac{(\epsilon \Delta \dot{X}_n)^I}{I!} \left\{ \frac{d^I E'(\dot{X})_n}{d(\dot{X})_n^I} \right\} \dots \dots \quad (3.3.11)$$

where

$$\Delta \dot{X}_n = \dot{X}_{n1} + \epsilon \dot{X}_{n2} + \epsilon^2 \dot{X}_{n3} + \dots \dots \dots \quad (3.3.12)$$

Therefore insert Equation (3.3.11) into Equation (3.3.8) and substitute in Equation (3.3.4) with collecting terms having the same power of  $\epsilon$ .

The first four of these would appear as

$$\begin{aligned} & \left[ [\neg M + M_a \neg] \{\ddot{X}\}_0 + [[C] + [\neg 2\dot{U}F_D \neg]] \{\dot{X}\}_0 + \right. \\ & \quad \left. + [K] \{X\}_0 - \{F(t)\} \right] + \\ & \epsilon \left[ [\neg M + M_a \neg] \{\ddot{X}\}_1 + [[C] + [\neg 2\dot{U}F_D \neg]] \{\dot{X}\}_1 + [K] \{X\}_1 + \right. \\ & \quad \left. + \{E'(\dot{X})_0\} \right] + \\ & \epsilon^2 \left[ [\neg M + M_a \neg] \{\ddot{X}\}_2 + [[C] + [\neg 2\dot{U}F_D \neg]] \{\dot{X}\}_2 + [K] \{X\}_2 + \right. \\ & \quad \left. + \{(\dot{X})_1 \frac{dE'}{d\dot{X}} (\dot{X})_0\} \right] + \\ & \epsilon^3 \left[ [\neg M + M_a \neg] \{\ddot{X}\}_3 + [[C] + [\neg 2\dot{U}F_D \neg]] \{\dot{X}\}_3 + [K] \{X\}_3 + \right. \\ & \quad \left. + \frac{1}{2} \left( \{(\dot{X})_1^2 \frac{d^2 E'}{d\dot{X}^2} (\dot{X})_0\} + 2 \{(\dot{X})_2 \frac{dE'}{d\dot{X}} (\dot{X})_0\} \right) \right] + \dots = 0 \\ & \dots \dots \dots \quad (3.3.13) \end{aligned}$$

If Equation (3.3.12) is to be satisfied identically in  $\epsilon$ , each square bracket must separately vanish. This provides a chain of linear problems in which  $X_{I+1}(t)$  may be considered as a linear response to an excitation that is a nonlinear function of the previously determined  $X_I(t)$ .

Applying the perturbation method to the given problem leads to difficulty of deciding how many terms the solution, (3.3.9) should retain in order to fully represent the nonlinearity by a series of the type (3.3.11). Also it is necessary to establish how the computation for higher-order terms is to be executed, and what the permissible values of  $\epsilon$  should be.

#### SEMILINEAR METHOD

This method of analysis involves replacing the actual nonlinear system equation of motion (3.3.4), by a system of linear differential equation. It is possible to have the linear system to be an equivalent system by selecting the constants such that the errors arising from its use are minimal. The efficiency of this method depends, as did the perturbation method, upon the nonlinear strength of the system. If a highly nonlinear system were to be replaced by a linear one with constants selected to minimize the mean-square errors, the minimized errors might be large enough

to cast doubt upon the results. However, if the system is weakly nonlinear in the sense that its equations of motion possess linear portion which dominate the nonlinear portions (as anticipated in Equation (3.3.4)), the minimized replacement errors can be much smaller.

This method was applied to a nonlinear system with deterministic inputs by Krylov and Bogaliubov 1947<sup>(106)</sup>. The semilinear approach for the problem of offshore structure is developed as follows.

The equation of motion (3.3.4) shows that the nonlinear effects are velocity-dependent which implies that the linear replacing system of equations should be of the form

$$[\tilde{M} + M_a]\{\ddot{X}\} + [\tilde{C}]\{\dot{X}\} + [K]\{X\} + \{e(\dot{X})\} = \{F(t)\} \\ \dots \dots \dots \dots \dots \quad (3.3.14)$$

In Equation (3.3.14)  $[\tilde{C}]$  is an equivalent linear damping matrix and  $\{e(\dot{X})\}$  is the vector of velocity dependent errors introduced by having the linear system. It is the objective of the semilinear approach to minimize the elements of  $\{e(\dot{X})\}$  in some manner.

Prior to discussing the manner in which elements of  $\{e(\dot{X})\}$  will be minimized, it is necessary to study  $[\tilde{C}]$  in more detail to establish the parameters of this matrix which affect  $\{e(\dot{X})\}$ . Selection of

$\left[ [C] + [2\dot{U}_O F_D] \right]$  is aided by examining Equation (3.3.4) and substituting for  $\{E(\dot{X})\}$  from Equation (3.3.6) to obtain an alternative expression of Equation (3.3.4) as

$$\begin{aligned} & \left[ -M + M_a \right] \{\ddot{X}\} + \left[ [C] + [2\dot{U}_O F_D] + [F_D] [\dot{X}] \right] \{\dot{X}\} + \\ & + [K] \{X\} = \{F(t)\} \quad \dots \quad \dots \quad \dots \quad (3.3.15) \end{aligned}$$

where the matrix  $[F_D] [\dot{X}]$  will produce a diagonal matrix. Equation (3.3.15) shows that, the diagonal element of the damping matrix (premultiplying  $\{\dot{X}\}$ ) is a function of  $\dot{X}_n$  while the off-diagonal element is a constant, namely  $C_{mn}$ . Accordingly, it becomes sensible to take  $[\tilde{C}]$  to be given by

$$\tilde{C}_{Mn} = \begin{cases} C_{Mn} & m \neq n \\ \tilde{C}_{Mn} & m = n \end{cases} \quad \dots \quad \dots \quad \dots \quad (3.3.16)$$

where the diagonal element  $\tilde{C}_{mn}$  remain to be determined such that  $\{e(\dot{x})\}$  is minimized.

By equating Equations (3.3.4) and (3.3.14) and solve for  $\{e(\dot{x})\}$

$$\{e(\dot{x})\} = ([C] + [2\dot{U}_O F_D] - [\tilde{C}]) \{\dot{X}\} + \{E(\dot{X})\} \quad \dots \quad \dots \quad \dots \quad \dots \quad (3.3.17)$$

As a consequence of Equation (3.3.16) at the nth node point the  $\{e_n(\dot{x})_n\}$  depends only upon  $\dot{X}_n$ ,  $C_{nn}$ ,  $2\dot{U}_{on} F_{Dn}$ ,  $E_n(\dot{X})_n$  and the unknown constant of  $\tilde{C}_{nn}$

$$\therefore e_n(\dot{X})_n = (C_{nn} + 2\dot{U}_{on} F_{Dn} - \tilde{C}_{nn})\dot{X}_n + E_n(\dot{X})_n \quad \dots \quad \dots \quad \dots \quad \dots \quad (3.3.18)$$

Taking the ensemble average of  $e_n^2(\dot{x})_n$ , given as

$$\sigma_{e_n}^2 = \langle e_n^2(\dot{X}(t))_n \rangle \quad \dots \quad \dots \quad \dots \quad \dots \quad (3.3.19)$$

provides N mean-square expressions of the nth node point  $\{e_n(\dot{x})_n\}$  which can be minimized by N expressions of the form

$$\frac{\partial \sigma_{e_n}^2}{\partial \tilde{C}_{nn}} \quad \dots \quad \dots \quad \dots \quad \dots \quad (3.3.20)$$

Since Equation (3.3.18) shows that  $\tilde{C}_{nn}$  is the only unknown parameter affecting  $e_n(\dot{x})_n$ , substituting from Equations (3.3.18) and (3.3.19) into (3.3.20) leads to N equation for  $\tilde{C}_{nn}$  by performing the operations

$$\frac{\partial}{\partial \tilde{C}_{nn}} \langle ((C_{nn} + 2\dot{U}_{on} F_{Dn} - \tilde{C}_{nn})\dot{X}_n + E_n(\dot{X})_n)^2 \rangle = 0 \quad (3.3.21)$$



Differentiating inside the  $\langle \rangle$  operator is permissible, given that the ensemble average exists, and provides the  $N$  optimizing equations for  $\tilde{C}_{nn}$  as

$$\tilde{C}_{nn} = C_{nn} + 2\dot{U}_{on} F_{Dn} \frac{\sigma^2 E_n(\dot{X})_n}{\sigma^2 \dot{X}_n \dot{X}_n} \dots \dots (3.3.22)$$

with

$$\sigma^2 E_n(\dot{X})_n = \langle \dot{E}_n(\dot{X}(t))_n \cdot (\dot{X}(t))_n \rangle (a)$$

$$\sigma^2 \dot{X}_n \dot{X}_n = \langle (\dot{X}^2(t))_n \rangle (b) \quad (3.3.23)$$

That the coefficients  $\tilde{C}_{nn}$  define a true minimum is apparent in the computation leading to

$$\frac{\partial^2 \sigma^2 e_n e_n}{\partial \tilde{C}_{nn}^2} = \langle 2 \sigma^2 \dot{X}_n \dot{X}_n \rangle = 0 \dots (3.3.24)$$

The value of  $\sigma \dot{X}_n \dot{X}_n$  should be provided in order to obtain the new parameter for  $[\tilde{C}]$ . Obviously this cycle must have a beginning point, however, the selection of it is arbitrary.

The process initiates with a selection of the  $N$  diagonal terms  ${}^0\tilde{C}_{nn}$  of the equivalent damping matrix  ${}^0[\tilde{C}]$  the pre-superscript  $o$  indicates the initial approximation of a quantity, the second approximation value of  ${}^1\tilde{C}_{nn}$  will be

$${}^1\tilde{C}_{nn} = {}^0\tilde{C}_{nn} + \sqrt{\frac{8}{\pi}} F_D^0 \sigma \dot{X}_n \dot{X}_n \dots \dots \dots (3.3.25)$$

The nonlinear hydrodynamic damping force  $\{E(\dot{X})\}$  is a monotonically increasing function of  $\dot{X}$ , which means that if the initial value of  ${}^0\tilde{C}_{nn}$  underestimates the true value of  $\tilde{C}_{nn}$ ,  ${}^0\sigma \dot{X}_n \dot{X}_n$  will be in excess of its true value so that provides  ${}^1\tilde{C}_{nn}$  as a magnitude overestimate of the true value of  $\tilde{C}_{nn}$ . The reverse would be true. This process continues until convergence is defined, for all the  $N$  main-diagonal members of  $[\tilde{C}]$ . The number of cycles requires to establish convergence depends upon the initial value of  ${}^0\tilde{C}_{nn}$  and the strength of the nonlinearity.

This method requires changing of damping matrix at each step of solution until the convergence is defined.

For the present study, the investigation was done for small amplitudes of vibration so that nonlinearity in Equation (3.3.4) is very small. Therefore the problem is solved by the following two methods.

## METHOD A

In this method the governing nonlinear equation of motion is solved by the direct approach method. This method is as follows:

- 1) The governing equation of motion (3.3.4) can be rearranged as follows:

$$[\bar{M} + M_a] \{\ddot{X}\} + \left[ [C] + [\bar{2}\dot{U}_0 F_D] \right] \{\dot{X}\} +$$

$$[K] \{X\} = \{F(t)\} - \{E(\dot{X})\} \quad \dots \quad (3.3.26)$$

- 2) Neglecting the nonlinear terms  $\{E(\dot{X})\}$  for the first estimate. A set of linearized equations are solved.
- 3) Use first solution and calculate the nonlinear term  $\{E(\dot{X})\}$
- 4) Resolve Equation (3.3.26) with the calculated nonlinear term obtained from the first solution. Obtain a second solution and recalculate the nonlinear term  $\{E(\dot{X})\}$  using the second estimate of  $\dot{X}$
- 5) Repeat the process until convergence of successive iteration is obtained.

The value of  $C_D$  and  $C_M$  obtained from the test of free structure were used in forming of Equation (3.3.26).

### METHOD B

This method is based upon the assumption that for small displacement of the structure, whether the object moves in still water or the water moves about the object does not affect the value of the hydrodynamic damping.

The equation (3.3.4) will be

$$\begin{aligned} & [\sim M \sim] \{X\} + [C^w] \{\dot{X}\} + [K] \{X\} \\ & = [\sim F_m'' \sim] + [\sim F_m' \sim] \{\ddot{U}\} + [\sim F_D'' \sim] \{\dot{U} | \dot{U}\} \\ & \quad \dots \quad \dots \quad \dots \quad \dots \quad \dots \quad (3.3.27) \end{aligned}$$

where  $[C^w]$  is the damping matrix obtained by using the damping coefficient measured in water

$[\sim F_m'' \sim]$  and  $[\sim F_D'' \sim]$  are calculated by using the value of  $C_M$  and  $C_D$  obtained from the test of fixed structure.

### 3.3.3 SOLUTION OF THE SYSTEMS

The solution of the linearized system (Method (A) and Method (B)) is based upon the possibility of treating the system as having linear input-output characteristic in the sense that the principle of superposition is valid. The normal mode superposition approach is used to calculate the response of the structure. The response of the structure is given by

$$\{X\} = [\phi] \{Y\} \dots \dots \dots \quad (3.3.28)$$

where the modal matrix  $[\phi]$  is deduced for the undamped free vibration given by the eigen value problem.

$$[-M + M_a] \{-\omega^2 X\} + [K] \{X\} = \{0\}$$

$$[-\omega^2] [-M + M_a] [\phi] = [K] \{\phi\} \dots \quad (3.3.29)$$

Equation (3.3.26) or (3.3.27) is premultiplied by the transpose of the modal matrix, and the displacement  $\{X\}$  expressed in terms of the normal co-ordinate vector  $\{Y\}$ , to yield the relations

$$[-M^*] \{\ddot{Y}\} + [C] \{\dot{Y}\} + [-K^*] \{Y\} = \{P^*\} \\ \dots \dots \dots \quad (3.3.30)$$



Since the system equations comprise a self-adjoint eigen value problem and orthogonality property of the normal modes exists, where

$$\begin{aligned}
 [M^*] &= [\phi]^T [M + M_a] [\phi] \quad (\text{For Method A}) \\
 \text{or } [\phi]^T [M] [\phi] & \quad (\text{For Method B}) \quad = \text{Generalized Mass Matrix} \\
 & \dots \dots \dots (3.3.31)
 \end{aligned}$$

$$\begin{aligned}
 [K^*] &= [\phi]^T [K] [\phi] \quad (\text{For Both methods}) = \text{Generalized Stiffness Matrix} \\
 & \dots \dots \dots (3.3.32)
 \end{aligned}$$

$$\begin{aligned}
 [C] &= [\phi]^T \left[ [C] + [2\dot{U}_O F_D] \right] [\phi] \quad (\text{For Method A}) \\
 \text{or } [\phi]^T [C^*] [\phi] & \quad (\text{For Method B}) \\
 & = \text{Generalized Damping Matrix} \quad (3.3.33)
 \end{aligned}$$

$$\begin{aligned}
 \{P^*\} &= [\phi]^T \left( \left[ [F_m] + [F'_m] \right] \{\ddot{U}_O\} + [F_D] \{\dot{U}_O\} \right. \\
 & \quad \left. + [F_D] \{\dot{X}|\dot{X}|\} \right) \quad (\text{For Method A}) \\
 \text{or } &= [\phi]^T \left( \left[ [F_m] + [F'_m] \right] \{\ddot{U}_O\} + \right. \\
 & \quad \left. + [F_D] \{\dot{U}_O\} \right) \quad (\text{For Method B}) \\
 & \dots \dots \dots (3.3.34)
 \end{aligned}$$

$\{P^*\} =$  Generalized Force vector.

The coupled damping matrix  $[C]$  is symmetric but is not a diagonal matrix. The coupled damping matrix is decoupled by assuming that the damping matrix  $[C]$  satisfied the modal orthogonality condition

$$[\phi]^T [C] [\phi]_m = 0 \quad (n \neq m) \quad \dots \quad (3.3.35)$$

$\therefore$  Equation (3.2.27) become

$$[M^*] \{\ddot{Y}\} + [C^*] \{\dot{Y}\} + [K^*] \{Y\} = \{P^*\} \quad (3.3.36)$$

Equation (3.3.36) therefore represents N uncoupled linear second order differential equations. These equations can also be put in the familiar form.

$$\ddot{Y}_n + 2\omega_n \xi_n \dot{Y}_n + \omega_n^2 Y_n = \frac{P_n^*}{M_n^*} \quad n = 1, 2, \dots, N \quad (3.3.37)$$

where

$$\xi_n = \frac{C_{nn}^*}{2M_n^* \omega_n} \quad \dots \quad (3.3.38)$$

In this derivation of the normal- coordinate equations of motion it has been assumed that the normal-coordinate transformation serves to uncouple the damping forces in the same way that it uncouples the mass and stiffness.

The conditions under which this uncoupling will occur is the Rayleigh damping matrix, that is, the form of damping matrix in which Equation (3.3.35) applied.

Rayleigh showed that a damping matrix of the form

$$[C] = \alpha_0 [M] + \alpha_1 [K] \quad \dots \quad \dots \quad \dots \quad \dots \quad (3.3.39)$$

in which  $\alpha_0$  and  $\alpha_1$  are arbitrary proportionality factors, will satisfy the orthogonality condition. The method of determination of  $\alpha_0$  and  $\alpha_1$  will be shown later in this chapter.

The solution of Equation (3.3.37) can be obtained in the time domain or the frequency domain. Having determined  $Y_n(t)$ ,  $n = 1, 2, 3, \dots, N$  the displacement  $\{X\}$  can be found through Equation (3.3.28).

#### 3.3.4 NUMERICAL ANALYSIS

The analysis of the structures which used in this study, were carried out by using finite element method. The computer program SAPIV was available to analyse the dynamic response of the structures in the time domain. The structure's response was calculated by the mode superposition technique, using the first three modes only.

The structural system was analysed by using the tangent pipe element. The tangent pipe element (Figure (3.3.2)) can represent a straight segment; the elements require a uniform section and uniform material properties. The member stiffness matrix account for bending, torsional, axial and shearing deformations. The types of structure loads contributed by the pipe elements include gravity loading in the global directions, forces and moments acting at the member ends (i, j).

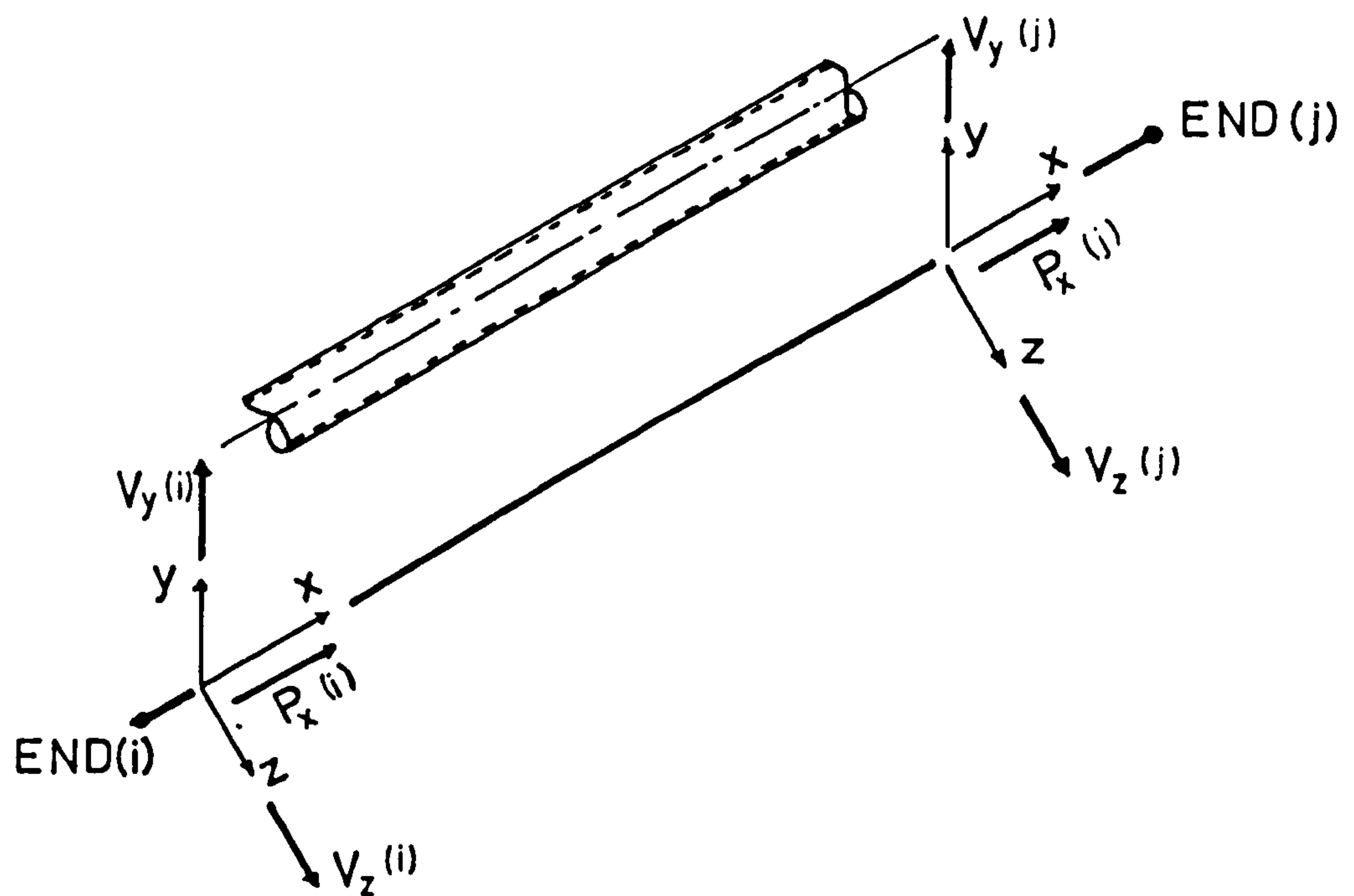


Figure (3.3.2) - The Tangent Pipe Element.

### 3.4 THEORETICAL FORMULATION OF THE EXPERIMENTS

The parameters required in the analysis of the problem were obtained experimentally. The theory and assumption behind the analysis of experimental data are shown below.

#### 3.4.1 MODELLING OF THE TESTED STRUCTURES

All the tested structures were divided into six elements. The first element had the length from the still water level to the tip of the structure and the other five elements were obtained by dividing the length from the still water level to the base of the structure. The element mass was lumped at the element ends equally. Each of these lumped mass has two degrees of freedom: (1) horizontal translation and (2) rotation. The response of the element is discretized in step-wise fashion, i.e. the response of each lumped mass represents the response of the element half way to the upper and lower lumped masses (see Figure (3.4.1)).



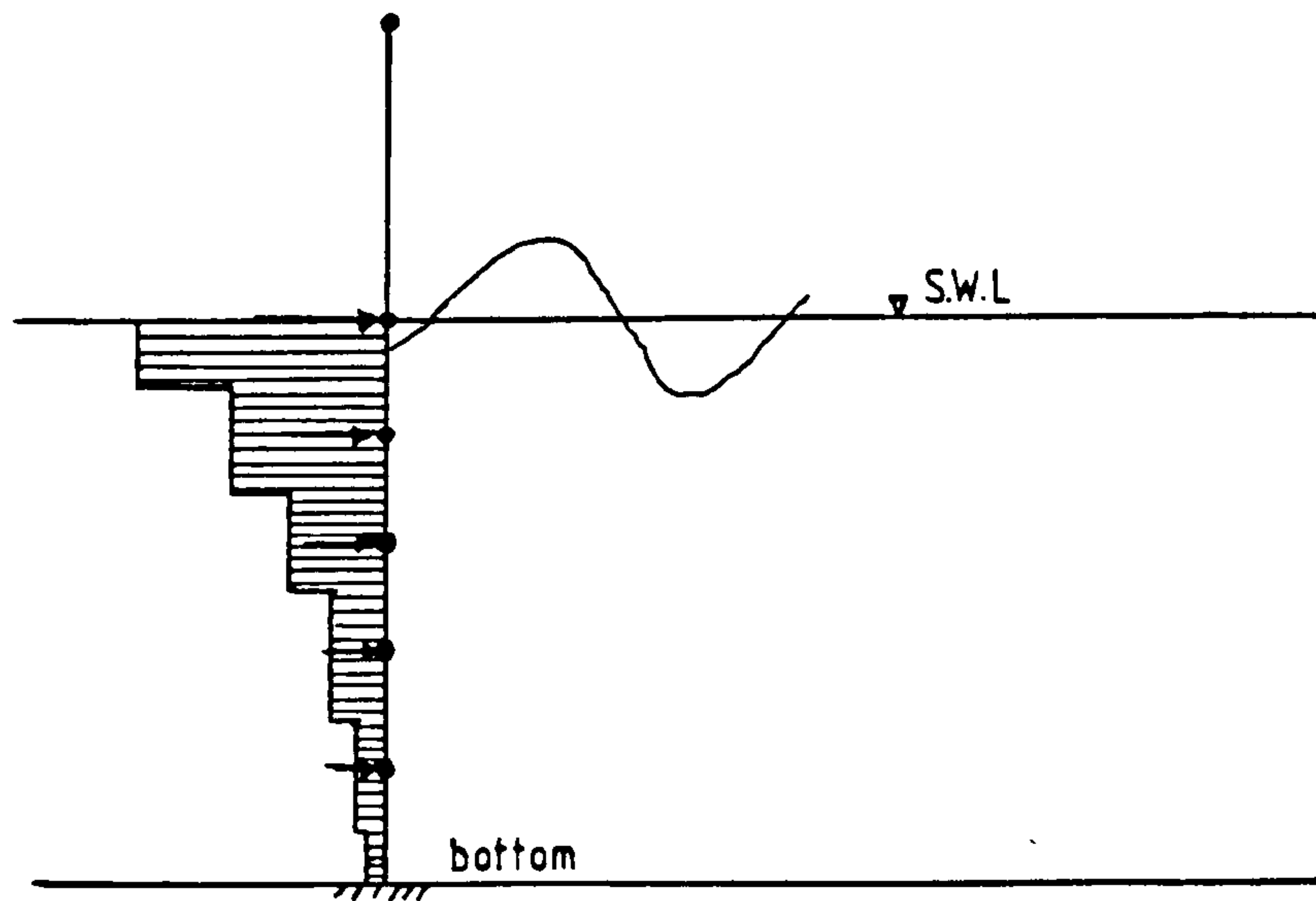


Figure (3.4.1) - Discretization of Response and Force.

The fluid orbital velocities and acceleration are discretized in the same stepwise manner as the response. Morison's equation and the modified Morison's equation are used for the evaluation of the wave force which are discretized at the lumped mass positions. Each force is evaluated for the real structure configuration and represent the contribution from half of the panels below and above that position. The net moment created by the forces about a lumped mass centre is neglected, as it will be relatively small.

### 3.4.2 DIGITIZATION OF THE DATA

The experimental data obtained were recorded in analog format. For numerical solutions this data need to be digitized in a way that it simulate the obtained analog data.

In order to maintain a proper relationship between the phase and amplitude of a given variable a suitable frequency of digitization or digitization interval had to be chosen. Otherwise aliasing could occur which is a potential source of error in an analog to digital data conversion (see Bendat and Piersol 1971<sup>(107)</sup>). The maximum frequency reasonable is called Nyquist frequency and is defined as

$$f_{NY} = \frac{1}{2\Delta t} \quad \dots \quad \dots \quad \dots \quad \dots \quad (3.4.1)$$

where  $\Delta t$  is the interval of digitization. The frequencies in the original data above this cut off frequency are folded back into the frequency range from zero to  $f_{NY}$ . Therefore, in order to choose a suitable  $\Delta t$  the maximum frequency encountered in the experiments had to be known. The observation of the analog records showed that the highest frequencies in the range of 3-4 Hz.

In general, it is a good rule to select  $f_{NY}$  to be greater than the maximum anticipated frequency. Therefore a Nyquist frequency of 25 Hz was chosen from which an interval of digitization of 0.02 seconds resulted. Any digitization below this value would have given correct results. The smaller of this interval will require more computing time.

### 3.4.3 DETERMINATION OF THE MEASURED WAVE FORCE

At any time  $t$ , the force acting on the measured level of the structure can be obtained by integration of the pressure and the shear distribution on the object surface (see Figure (3.4.2)).

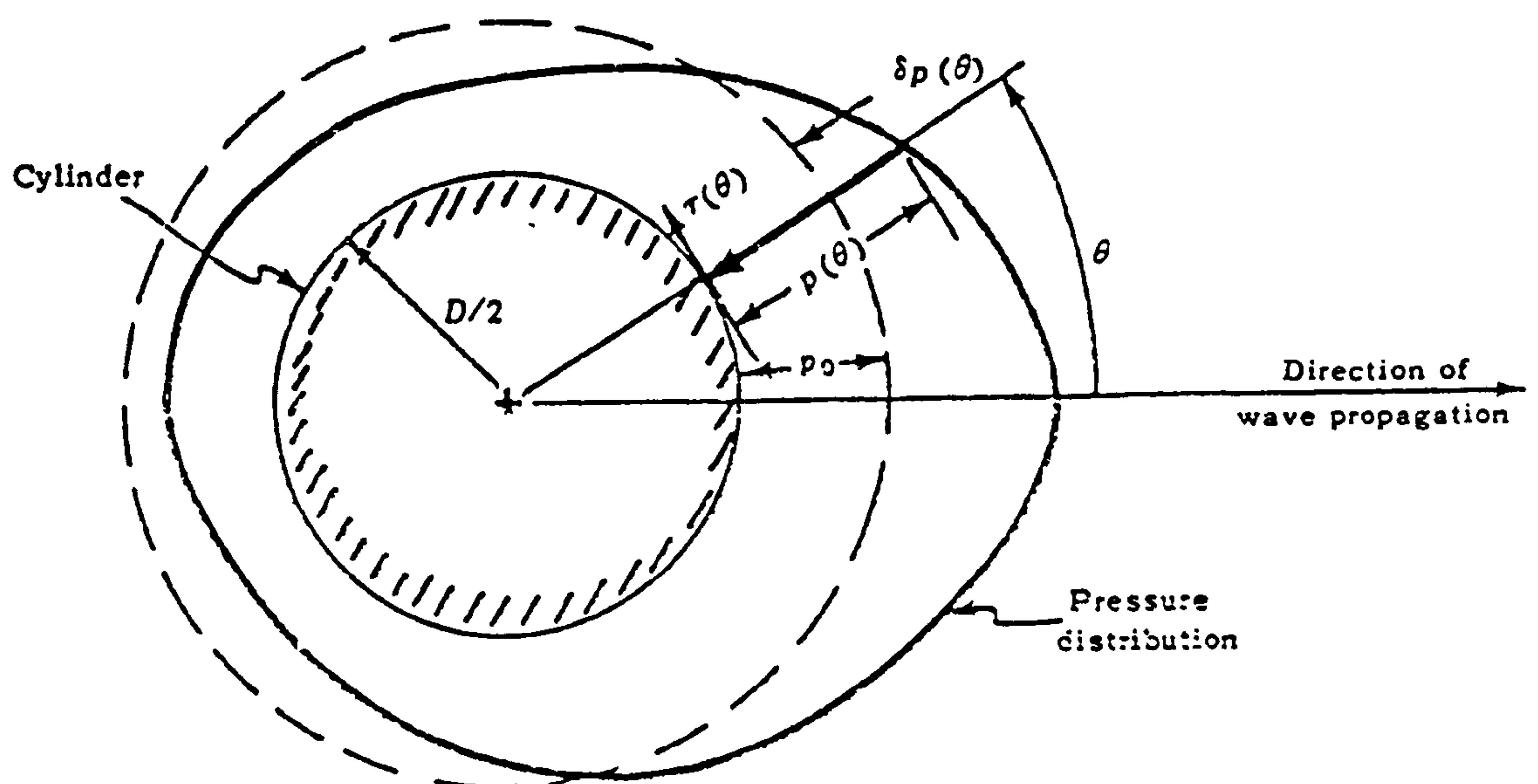


Figure (3.4.2) - Pressure and Shear Distribution about a Circular Cylinder.

$$\begin{aligned}
dF_m &= \left[ \int_0^{2\pi} \frac{D}{2} (P_o + \delta P) \cos \theta \, d\theta \right. \\
&\quad \left. + \int_0^{2\pi} \frac{D}{2} \tau(\theta) \sin \theta \, d\theta \right] ds \\
dF_m &= \left[ \frac{DP_o}{2} \int_0^{2\pi} \cos \theta \, d\theta + \int_0^{2\pi} \frac{D}{2} \delta P(\theta) \cos \theta \, d\theta \right. \\
&\quad \left. + \int_0^{2\pi} \frac{D}{2} \tau(\theta) \sin \theta \, d\theta \right] ds \\
dF_m &= \left[ \text{zero} + \int_0^{2\pi} \frac{D}{2} \delta P(\theta) \cos \theta \, d\theta \right. \\
&\quad \left. + \int_0^{2\pi} \frac{D}{2} \tau(\theta) \sin \theta \, d\theta \right] ds \quad \dots \quad \dots \quad (3.4.2)
\end{aligned}$$

As the structure has a smooth surface the force attributed to the shear distribution is negligible

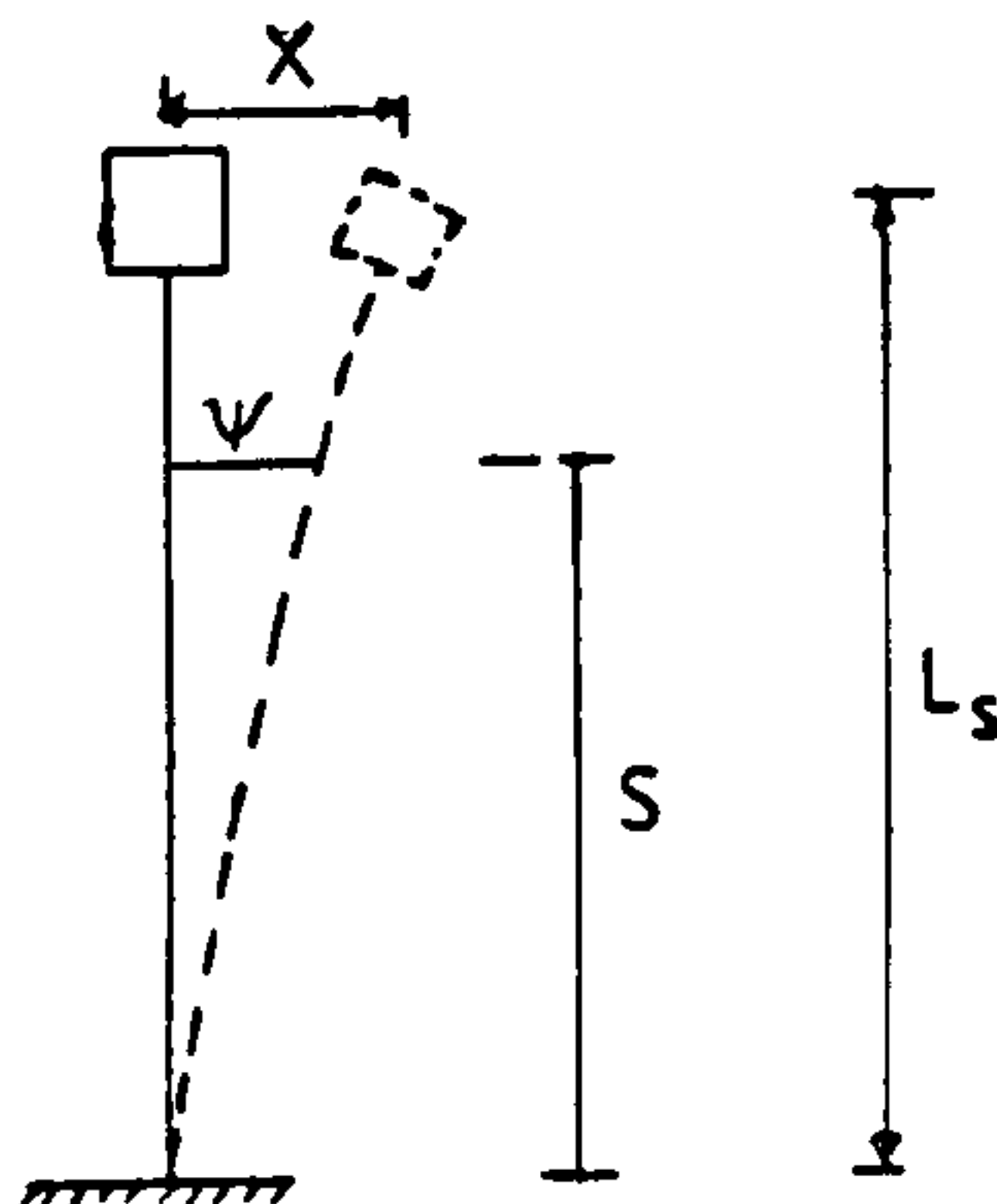
$$\therefore dF_{m(t,z)} = \int_0^{2\pi} \frac{D}{2} \delta P(\theta) \cos \theta \, d\theta \, ds \quad \dots \quad (3.4.3)$$

#### 3.4.4 DETERMINATION OF THE VELOCITY AND ACCELERATION OF THE STRUCTURE AT ANY LEVEL

The velocity and acceleration of the structure at any level (the level where the pressure were measured) were required for the determination of the force coefficients  $C_D'$  and  $C_M'$  when the modified Morison's equation was used.

The calculation of the velocity and acceleration of the structure at any level by knowing the tip displacement is based upon the assumption that, if the load distribution is similar to the deflected shape of the first mode shape and if the load frequency is smaller or equal to the first mode frequency of the structure, then only the first mode of vibration exists.

Timoshenko 1956<sup>(108)</sup> shows a solution for elastic curve,  $\psi$  as an approximation formed from a truncated series of the sum of sinusoidal shapes, each contributing to  $\psi$  for the first mode shape. The result is





$$\psi = \frac{PL_s^3}{3EI} \frac{1}{1 - \beta'} (1 - \cos \frac{\pi S}{2L_s}) \dots \dots (3.4.4)$$

where I = sectional moment of inertia

$$\beta' = \frac{4WL_s^2}{\pi^2 EI}$$

when S = L<sub>s</sub>

$$\psi = \frac{PL_s^3}{3EI} \frac{1}{1 - \beta'} \quad \text{which represent the tip displacement}$$

$$\psi = X(1 - \cos \frac{\pi S}{2L_s}) \dots \dots \dots (3.4.5)$$

Equation (3.3.5) represent the deflection at any level of the structure. As the tip displacement of the structure due to the wave forces is periodic function, it is possible to represent X by the fast Fourier transforms.

$$X = \sum_n a_n'' \sin (\frac{2\pi n}{T} \Delta t) + b_n'' \cos (\frac{2\pi n}{T} \Delta t) \dots \dots \dots (3.4.6)$$

The velocity  $\dot{X}$  at any level of the structure can be obtained by differentiation of the displacement with respect to the time

$$\dot{X} = \frac{\partial X}{\partial t}$$

$$\dot{X} = \left( \sum a_n'' \frac{2\pi n}{T} \cos\left(\frac{2\pi n}{T} \Delta t\right) - b_n'' \frac{2\pi n}{T} \sin\left(\frac{2\pi n}{T} \Delta t\right) \right) \left(1 - \cos \frac{\pi S}{2L_S}\right) \dots \dots \dots (3.4.7)$$

Also the acceleration  $\ddot{X}$  will be obtained by

$$\ddot{X} = \frac{\partial \dot{X}}{\partial t}$$

$$\begin{aligned} \ddot{X} = & \left( \sum - a_n'' \left(\frac{2\pi n}{T}\right)^2 \sin\left(\frac{2\pi n}{T} \Delta t\right) - \right. \\ & \left. - b_n'' \left(\frac{2\pi n}{T}\right)^2 \cos\left(\frac{2\pi n}{T} \Delta t\right) \right) \left(1 - \cos \frac{\pi S}{2L_S}\right) \dots \dots \dots (3.4.8) \end{aligned}$$

### 3.4.5 EVALUATION OF THE CONSTANT $\alpha_0$ AND $\alpha_1$ FOR THE DAMPING MATRIX

The Rayleigh damping matrix (Equation (3.3.39)) should satisfy the orthogonality condition. This can be demonstrated by applying the orthogonality operation which is

$$\begin{aligned} [\phi]_m^T [M] [\phi]_n &= 0 \quad m \neq n \quad (a) \\ &\dots \quad (3.4.9) \\ [\phi]_n^T [K] [\phi]_n &= 0 \quad m \neq n \quad (b) \end{aligned}$$

in both side of the equation

$$\begin{aligned} [\phi]^T [C] [\phi] &= \alpha_0 [\phi]^T [M] [\phi] + \alpha_1 [\phi]^T [K] [\phi] \\ &\dots \quad \dots \quad \dots \quad \dots \quad (3.4.10) \end{aligned}$$

as each term at the right hand side of the above equation satisfy the orthogonality condition, therefore the left hand side satisfy the orthogonality condition.

However it can be shown that an infinite number of matrices formed from the mass and stiffness matrices also satisfy the orthogonality condition:

$$[\phi]_m^T \left[ [M] \quad [M]^{-1} \quad [K] \right]^b [\phi]_n = 0 \quad -\infty < b < \infty$$

$$\dots \quad \dots \quad \dots \quad \dots \quad (3.4.11)$$

where  $[M]^{-1} = \frac{1}{[M]}$

The two basic relationships Equations (3.4.9a) and (3.4.9b) are given by exponents  $b = 0$  and  $b = 1$  in Equation (3.4.11).

Thus the damping matrix can also be made up of combination of these. In general, then, the orthogonal damping matrix may be of form

$$[C] = [M] \sum_b \alpha_b \left[ [M]^{-1} \quad [K] \right]^b = \sum_b [C_b] \dots \quad (3.4.12)$$

With this type of damping matrix it is possible to compute the damping influence coefficients necessary to provide a decoupled system having any desired damping ratios in any specified number of modes. For each mode  $n$ , the generalized damping is given by Equation (3.3.8).

$$[C_n^*] = [\phi]_n^T [C] [\phi]_n = 2 \xi_n \omega_n [M^*]_n \dots \quad (3.4.13)$$

but if  $[C]$  is given by Equation (3.4.12), the contribution of  $b$  in the series to the generalized damping is

$$[C_b]_n = [\phi]_n^T [C_b] [\phi]_n = \alpha_b [\phi]_n^T [M] [[M]^{-1} [K]]^b [\phi]_n$$

$$\dots \dots \dots \dots \quad (3.4.14)$$

$$\therefore [\phi]_n^T [M] [[M]^{-1} [K]]^b [\phi]_n = [\omega_n^2]^b [M^*]_n$$

$$\dots \dots \dots \dots \quad (3.4.15)$$

therefore

$$[C_b]_n = \alpha_b [\omega_n^2]^b [M^*]_n$$

on this basis, the damping matrix associated with any mode n is

$$[C_n^*] = \sum_b [C_b]_n = \sum_b \alpha_b [\omega_n^2]^b [M^*]_n \quad \dots \dots \quad (3.4.16)$$

Equating the right hand side of Equations (3.4.13) and (3.4.16)

$$\therefore \xi_n = \frac{1}{2\omega_n} \sum \alpha_b \omega_n^{2b} \quad \dots \dots \dots \quad (3.4.17)$$

Equation (3.4.17) in matrix form with the first two modes only is

$$\begin{Bmatrix} \xi_1 \\ \xi_2 \end{Bmatrix} = \frac{1}{2} \begin{bmatrix} 1/\omega_1 & \omega_1 \\ 1/\omega_2 & \omega_2 \end{bmatrix} \begin{Bmatrix} \alpha_0 \\ \alpha_1 \end{Bmatrix} \quad \dots \dots \dots \quad (3.4.18)$$



$$\therefore \alpha_1 = \frac{\frac{\omega_1}{\omega_2} \xi_1 - \xi_2}{\frac{1}{2}(\frac{\omega_1}{\omega_2} - \omega_2)}$$

$$\therefore \alpha_0 = \frac{\frac{\omega_2}{\omega_1} \xi_1 - \xi_2}{\frac{1}{2}(\frac{\omega_2}{\omega_1} - 1/\omega_2)}$$

The parameter required to solve the above equations for  $\alpha_1$  and  $\alpha_0$  are known except  $\xi_2$  (the damping coefficient of second mode).  $\xi_2$  was assumed to be equal to  $\xi_1$  (see Wilson and Pensica 1972<sup>(109)</sup>):

# CHAPTER FOUR

## EXPERIMENTAL TECHNIQUE

The formula used in the estimation of the hydrodynamic forces on structure with relative small diameter has empirical parameters  $C_D$  and  $C_M$  which vary with the flow field and structure characters, any investigation dealing with water wave-structure interaction involves extensive experimental work before a concrete solution can be obtained.

The aim of this experimental work is to find the relation between the force coefficients when the structure is prevented from vibration and when it is free to vibrate, under different wave and structure characteristics.

### 4.1 EXPERIMENTAL FACILITIES

#### 4.1.1 WAVE TANK

The experiments were preformed in a rectangular water tank. The dimensions of the cross section are 0.75 x 0.75 metre and 18.0 metre long. The side walls are 0.0095 metres thick glass which is suitable for visually observing the model. The water tank had a regular wave generator installed at one end with a sloping beach wave observer at the other end. At this end an extension of dimension 3.00 metre long and 1.25 x 1.25 cross section connected to the tank. This extension was built in order to help the beach to absorb the waves.

This regular wave generator is a wedge type, the wedge is connected to a 0.75 horse power motor with different speeds of rotation. The motor has a digital counter to control the speed of rotation. By changing the speed of rotation, the frequency of the displaced water by the wedge changes giving a different wave period and length. Also the wedge arm can be adjusted to give a different submerged volume of the wedge which effects the volume of displaced water, consequently effecting the wave amplitude.

From the above and also as the water depth in the tank can be changed, the wave characteristics (d, L, T, H) can be changed in order to produce waves of differing characteristics for the tests.

It is desirable to eliminate cross-waves at all times and all frequencies of the tests; so two-dimensional analysis can be carried out without discrepancies, there is a good case for mounting fins against the face of the wavemaker. The fin was a mesh, in the shape of  $\Lambda$  placed at a distance 1.00 metre from the wavemaker the width of the channel, the angle between the  $\Lambda$  shape is adjustable to give the best elimination for each wave frequency. This fin improve the efficiency in eliminating the cross-waves for the range of wave frequency 0.75 - 1.25.

Reflected waves also prove undesirable though they are often not detected or allowed for. Their energy tends to increase in time to a limiting state, allowing them to exert a corresponding influence on the experimental results. The function of the beach is simply to absorb all wave energy incident upon it as reflections will produce problems. The fact that no beach is a fully efficient absorber implies that the beach design must be related to the wave climate required for the experimental programme, and the amount of reflection that can be tolerated. The beach used in the tank was made of wood sheet having the width of the tank and maximum slope of  $9.925^{\circ}$ . The beach was efficient in absorbing the waves as defined by a "reflection coefficient", this being the ratio of the amplitudes of the primary reflected and primary incident waves.

The position of the tested structure was half way between the wave generator and beach, approximately 8.5 metre away from either of them to minimize any disturbance caused either by wave generator or the beach.

Figure (4.1.1) shows the wave tank dimension and the position of the beach and wavemaker.

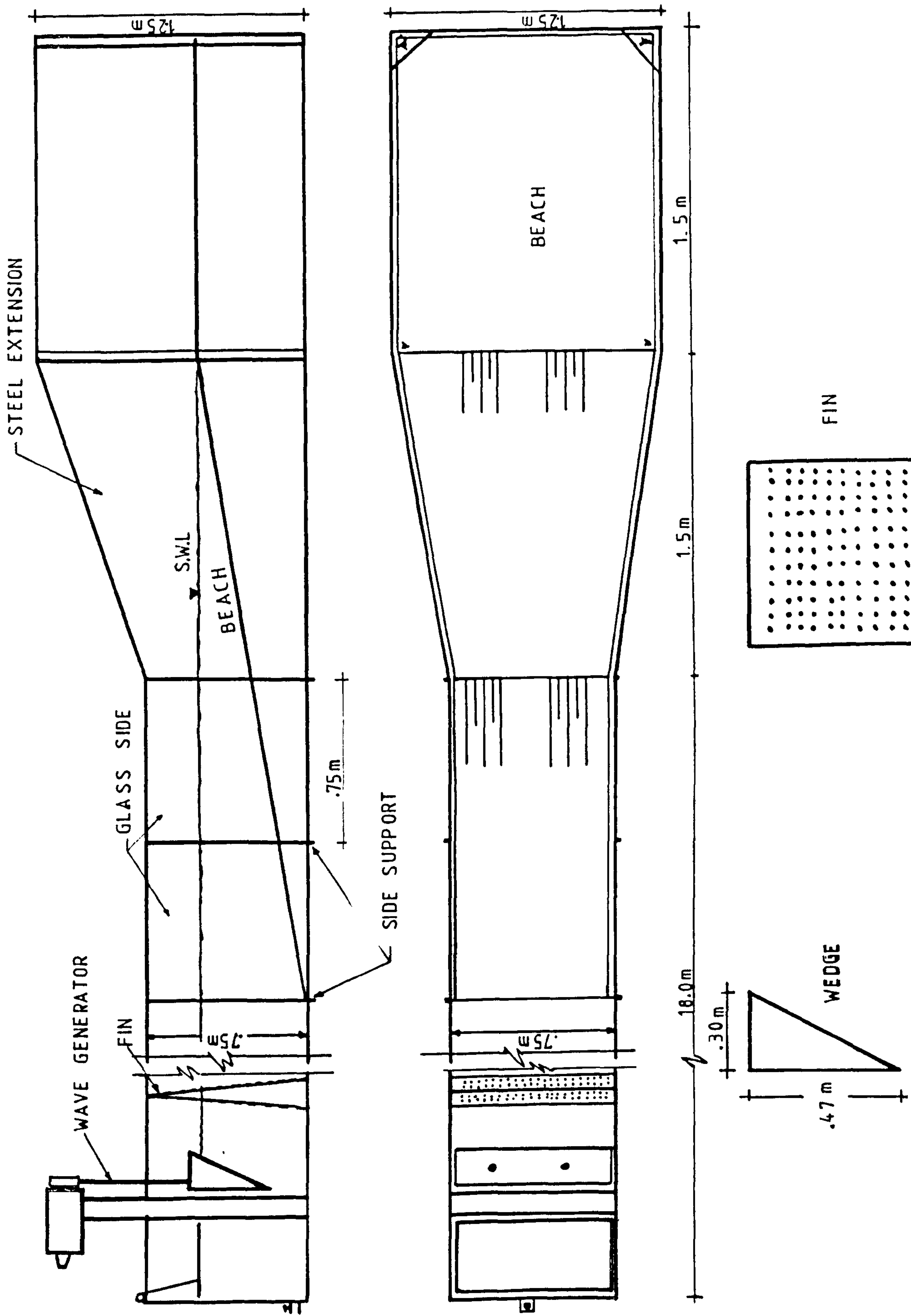


Figure (4.1.1) - Wave Tank.



#### 4.1.2      TESTED STRUCTURES

Two sets of single circular cylinder cantilever structure were tested. A cantilever was chosen because it represents the structure mechanism of the prototype structure, the cross-sectional shape of the structure was chosen to be circular in shape as it is the most common shape in the offshore structures.

The first set consists of two group of structures. The structures of this set were plastic Acrylonitril Butadiene Styrene (Durapipe ABS) tube material. This material was chosen because it afforded a cylinder that could be fixed at the bottom and also has a low modulus of elasticity which decreases the natural frequency of vibration.

The second set consists of one group of structures. The structures were made of Aluminium tube material. This material was chosen to compare between the behaviour of the first and second sets i.e. to compare the behaviour of two different dynamic properties.

##### 4.1.2.1      DURAPIPE ABS STRUCTURES

Four different structures were tested. These structures can be divided into two groups according to the structure diameter and modulus of elasticity i.e. relatively stiff and relatively flexible.

Group one consists of two structures (A) and (B), the structures consist of a 0.11 metre outside diameter tube. The tube was glued at the bottom end to a cap which was rested and glued to a heavy pipe flange with a leader. The pipe flange has six 0.0125 metre bolt holes, equally spaced to fit the imbedded six 0.0125 metre bolts in the heavy perspex sheet of a dimension of 0.75 x 1.5 metre with 0.0125 metre thickness placed on the tank floor at the mid part of the tank. Silicone vacuum grease was applied between the contact surfaces to obtain a water-tight fit.

At one level of the structure eight 0.006 metre diameter holes at equal space of the cross section ( $\theta = 45^{\circ}$ ) were made. At each of these holes a plastic PVC (hard) tube having L shape of 0.03 x 0.01 metre in dimension where the short leg were fixed to the cylinder wall and filed to give smooth surface while the long leg of the tube were connected to one end of 0.75 metre long rubber tube of 0.005 metre inside diameter, the other end of the rubber tube come out from the structure top so it can be connected to pressure transducer.

A perspex top cap with eight holes to pass the rubber tubes was placed in the top of the structure. It was used to prevent the structure from vibrating by the use of the clamp. The parts of the structure before assembly were shown in Figure (4.1.2).



Group two consists of two structures (C) and (D). The structures consist of 0.0605 metre outside diameter tube and similar parts as in group one with difference in dimension. See Figure (4.1.3).

At two levels of the group two structure were eight 0.004 metre diameter holes. A plastic PVC (soft) tube instead of the rubber tube was used as there is smaller space inside the tube structure than those of group one.

Figures(4.1.4) and (4.1.5) show the structures of groups one and two after they have been assembled.

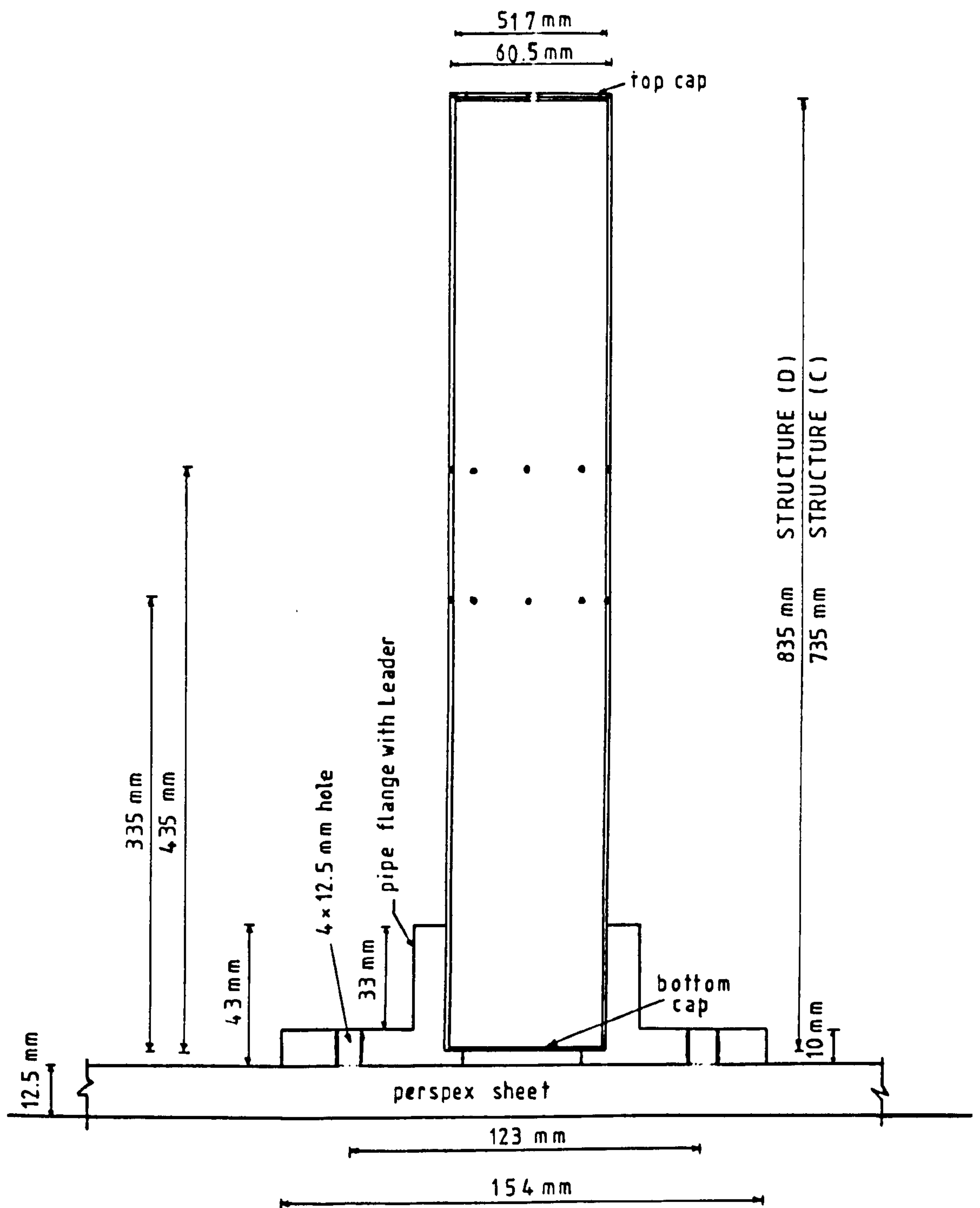


Figure (4.1.3) - Dimension of Structures (C) and (D).



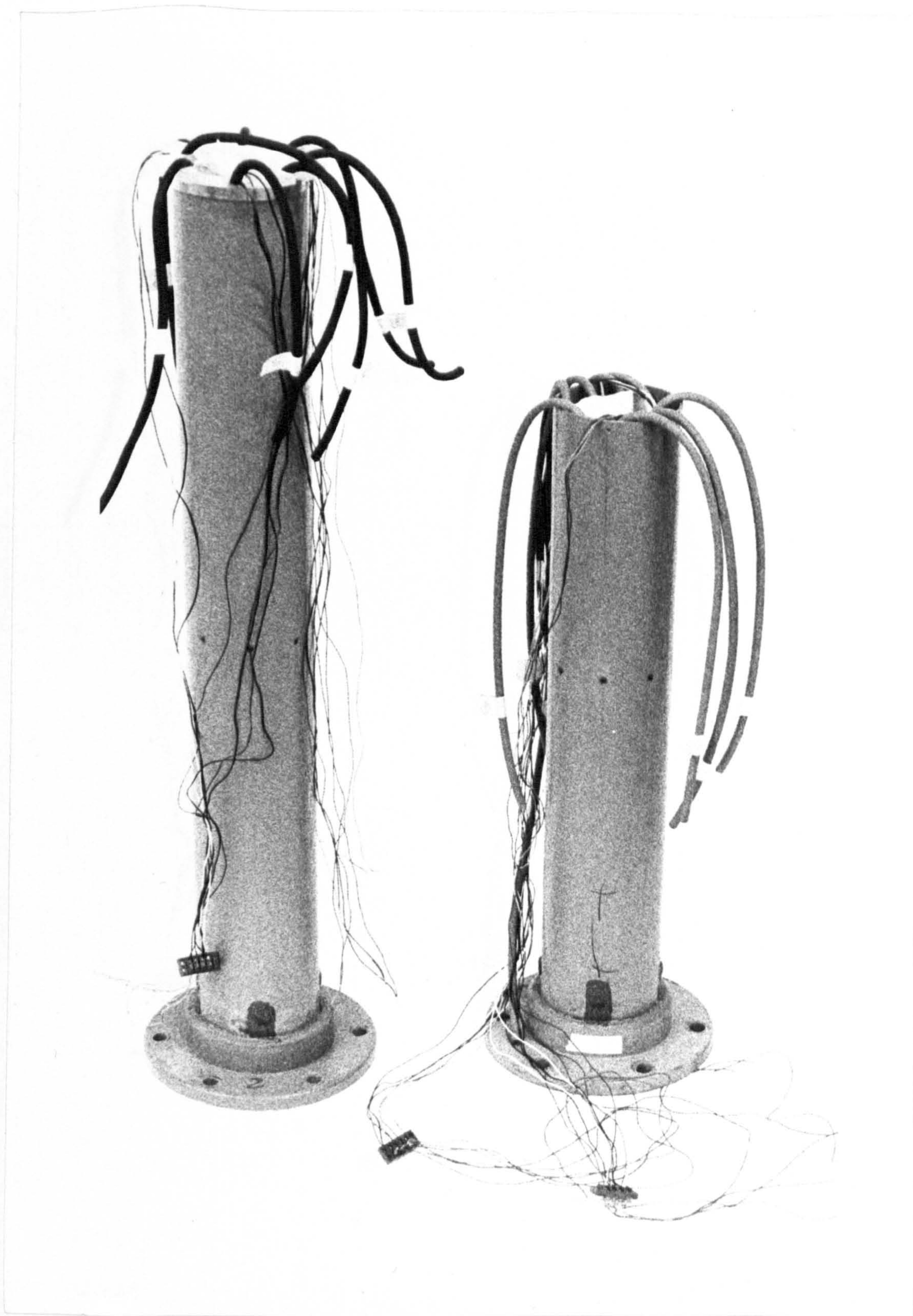


Figure (4.1.4) - Structures (A) and (B).



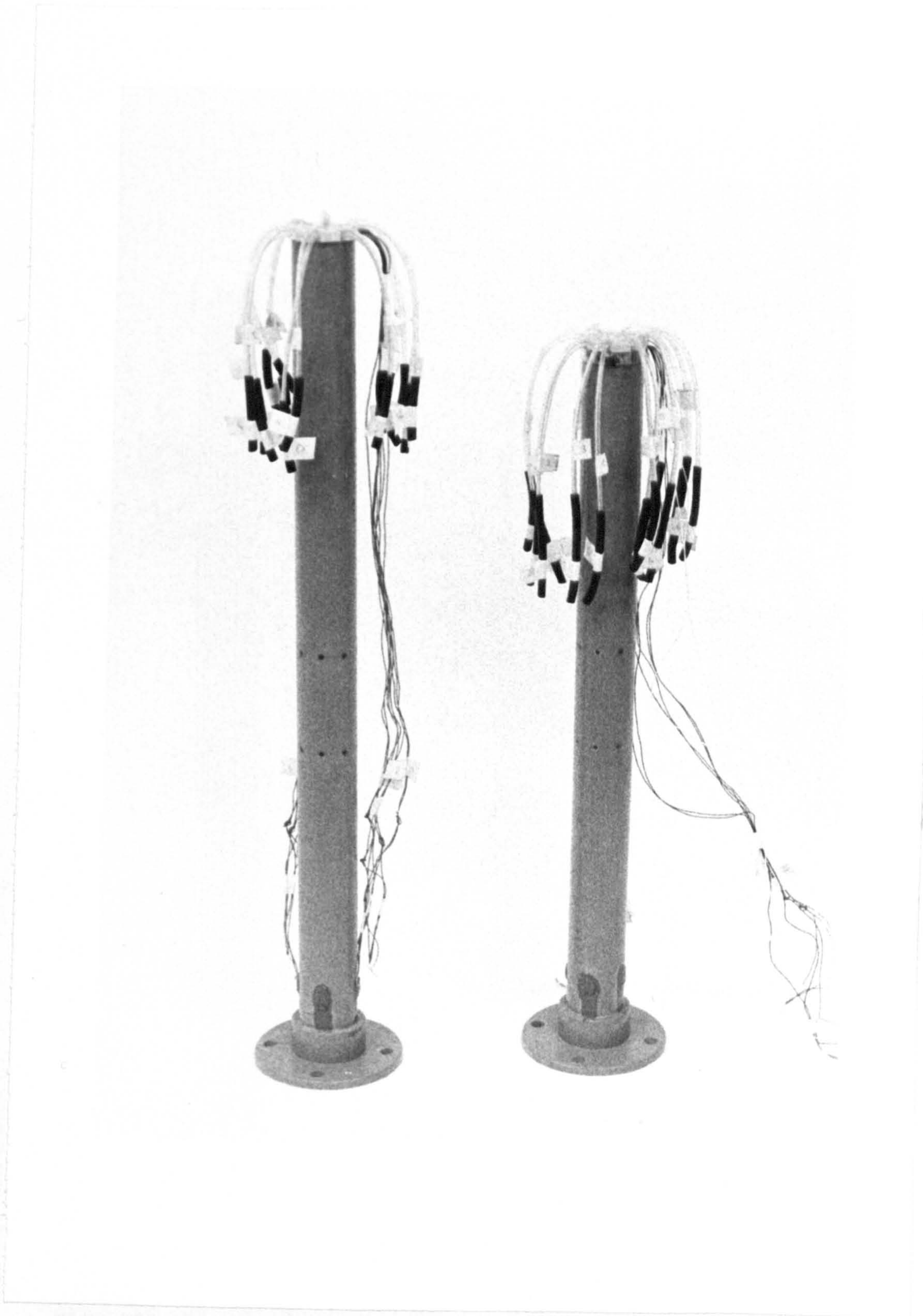


Figure (4.1.5) - Structures (C) and (D).

#### 4.1.2.2 ALUMINIUM STRUCTURES

A third group consists of two aluminium structures. Structure (E) and structure (F) each has 0.0574 metre diameter, structure (E) was 0.735 metre high and structure (F) was 0.835 metre high. A circular PVC (hard) top cap having a mass of 520 grammes was mounted at the top of the structure. It was used as a concentrated mass above the water line so that the structure would behave like a one-degree-of-freedom system when subjected to the wave, thus representing the platform of the offshore structure.

Four masses were made of steel balls contained in a plastic bag each having a mass of 505 grammes. These four masses provided two possible combinations of masses in increments of 1010 grammes. The mass was put in the top cap, the top cap was rigidly fixed by four 0.0125 metre screws to the structure so that the top cap would not wobble with respect to the tube. The top of the cap was level with the structure top.

The eight 0.004 metre diameter holes were made at three different levels of the structure. Figure (4.1.6) shows the parts and dimensions of the structures of this group. The masses and also structure (E) after assembly are shown in Figure (4.1.7).

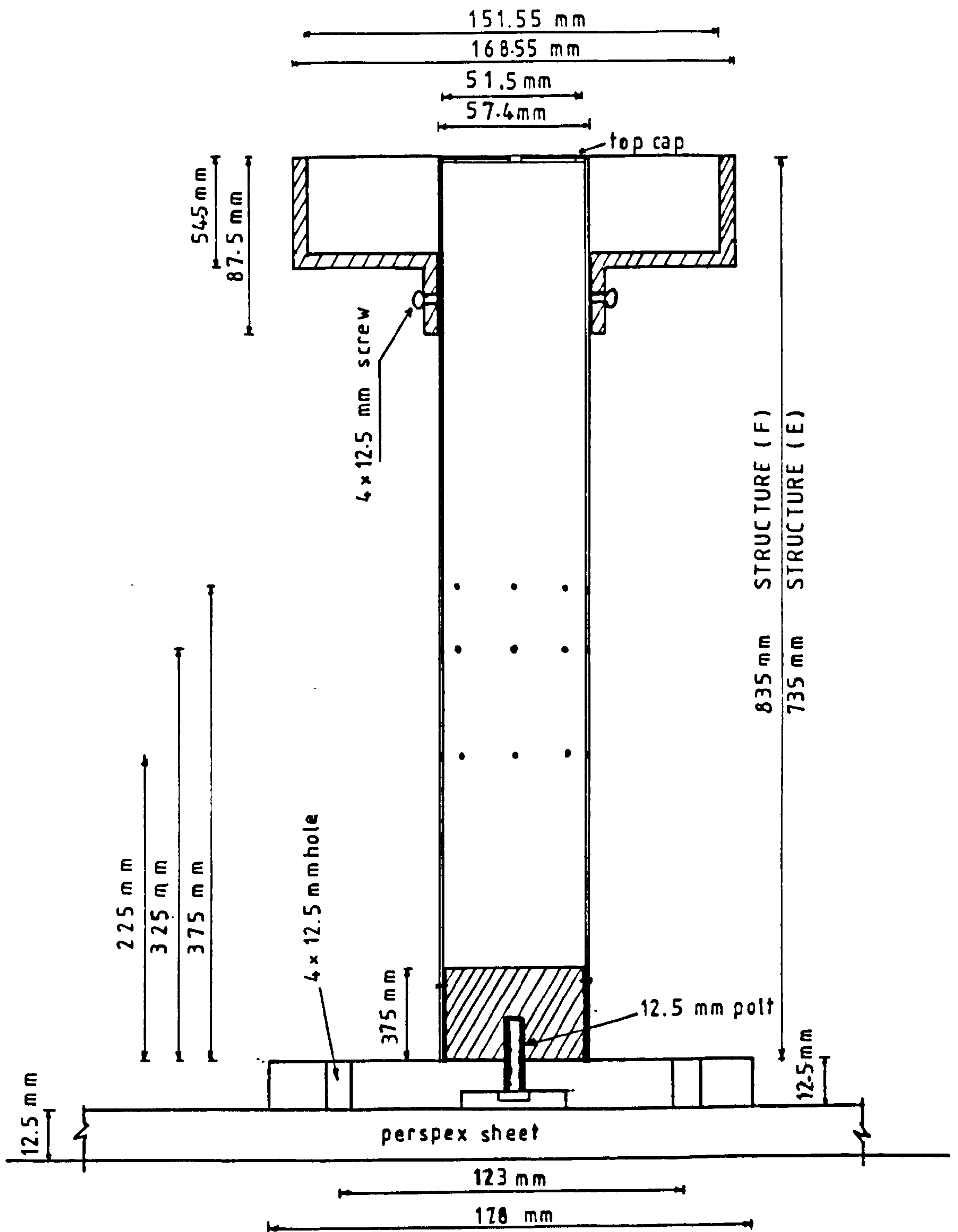


Figure (4.1.6) - Dimensions of Structures (E) and (F).



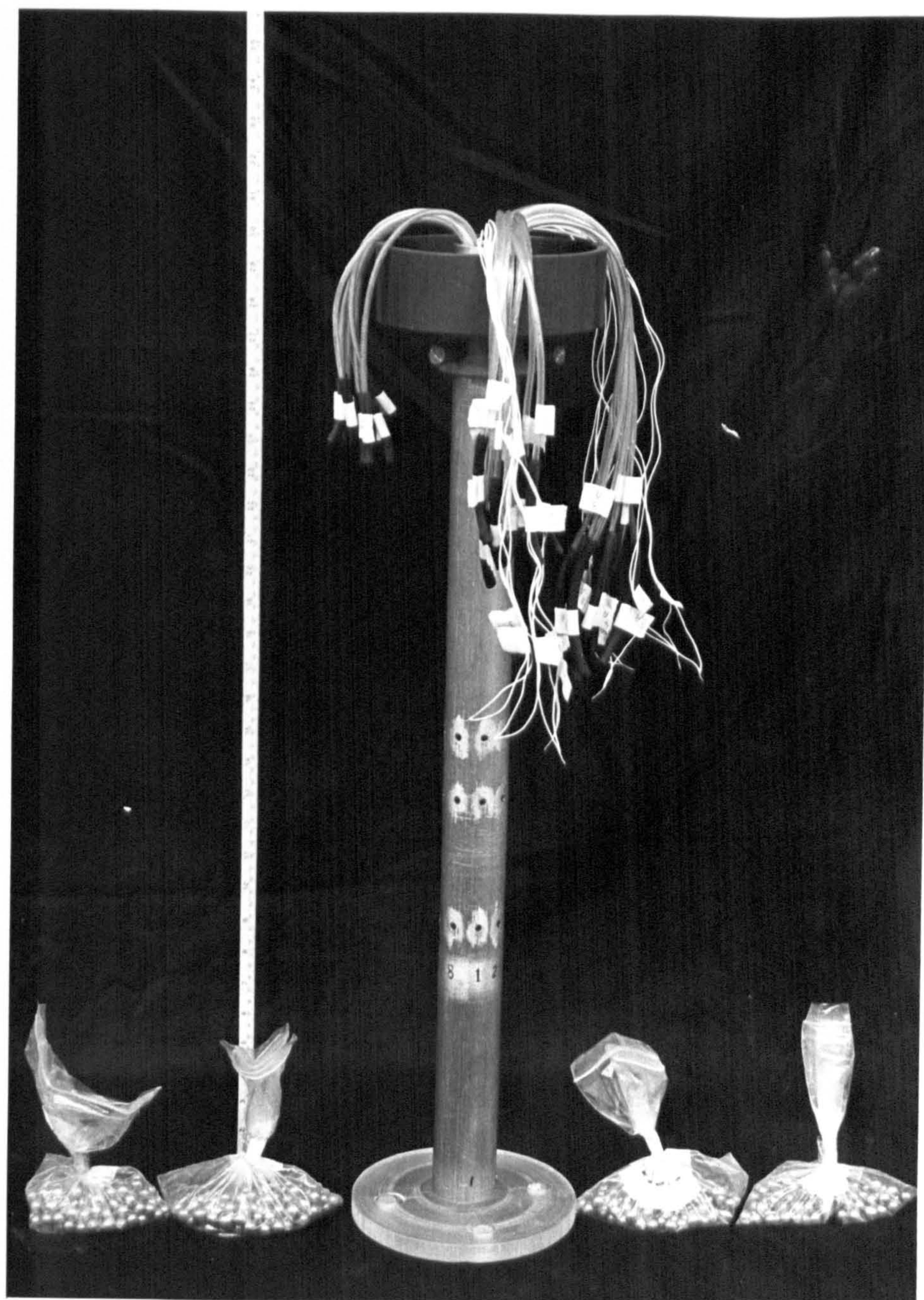


Figure (4.1.7) - Structure (E) and the Four Masses.



The mechanical properties of the structures tested are shown in Table (4.1).



Group	Structure designate	Material	Length meter	Diameter meter	Inside Diameter meter	Second Moment of area m <sup>4</sup>	Modulus of Elasticity kN/m
One	A	Durapipe ABS	0.608	0.11	0.102	1.7048 x 10 <sup>-6</sup>	1509174.8
	B		0.808	0.11	0.102	1.7048 x 16 <sup>-6</sup>	1509174.8
Two	C	Durapipe ABS	0.735	0.0605	0.0517	0.2777 x 10 <sup>-6</sup>	1509174.8
	D		0.835	0.0605	0.0517	0.2777 x 10 <sup>-6</sup>	1509174.8
Three	E	Aluminium	0.735	0.0574	0.0515	0.0822 x 10 <sup>-6</sup>	58022298.0
	F		0.835	0.0574	0.0515	0.0822 x 10 <sup>-6</sup>	58022298.0

Table (4.1) - Mechanical Properties of the Structures.

## 4.2 DESCRIPTION OF INSTRUMENTATION

All the instrumentation used in this work was electrical, some of which was commercially available and the rest was designed and built especially for this work.

The instrumentation used may be divided into the measuring instrumentation and the reading instrumentation. The instrumentation used for measuring each parameter needed in the analysis and results was designated as the measuring instrumentation, while the reading instrumentation was connected to the measuring instrumentation to give the final measured data.

### 4.2.1 MEASUREMENT INSTRUMENTATION

The measuring instrumentation was designed and placed to give the most reliable measurement without seriously affecting the characteristics and the environment of the test.

#### 4.2.1.1 WAVE PROBE

The wave probe was used to measure the wave profile. The measurement was done by detecting the change of voltage due to the change of resistance of the wire probe following the equation

$$\tilde{I} \times \tilde{R} = \tilde{V}$$

where  $\tilde{I}$  = the constant alternative current  
 $\tilde{V}$  = the variable D.C Voltage  
 $\tilde{R}$  = the variable resistance of the probe wire  
due to the change of the wave profile

Alternating current was used at the tips of the probe to avoid the polarisation of waver.

Two stainless steel wires having a diameter of 0.002 metre and a length of 0.5 metre with a resistance of 0.006 ohms per metre were used as the probe. The two wires were stretched 0.025 metre apart and fixed to a perspex plate; the perspex plate was suspended over the tank by means of an adjustable boom. This mounting facilitated the daily calibration of the probe and also aided in maintaining the probe in the proper position relative to the still water level.

There are certain disadvantages in the use of the resistance type probe. The relationship between water surface position and the electrical signal output is non-linear. Furthermore, the calibration of the system is dependent upon the conductivity of the water between the two wires. These difficulties have been overcome satisfactorily by always adjusting the position of the probe to the still water level existing in the tank and also by adding a resistance to the electrical circuits before the electrical current reaches the probe.

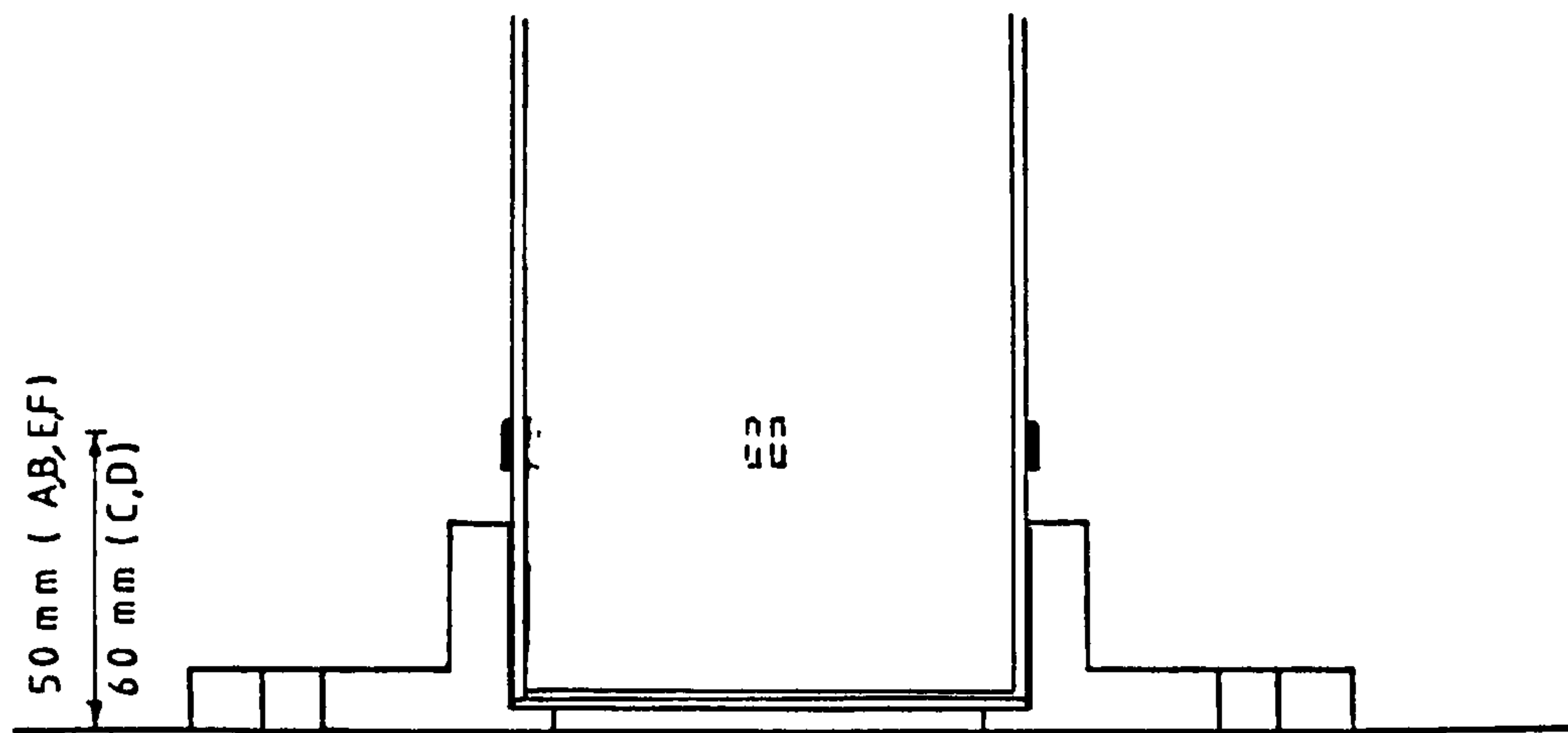
#### 4.2.1.2 STRAIN GAUGES AT THE BASE OF THE STRUCTURES

The bending moment at the base of the structure was measured with strain gauges. They were Tokyo Sokki strain gauges, type FLA-6-11, the gauges lengths were 0.006 metre and resistance of 120 ohms. For each structure two sets of gauges were used with four gauges in each set. The gauges were placed and connected as shown in Figure (4.2.1), one set was fixed to measure the bending moment in-line with the wave direction and the other perpendicular to the wave direction.

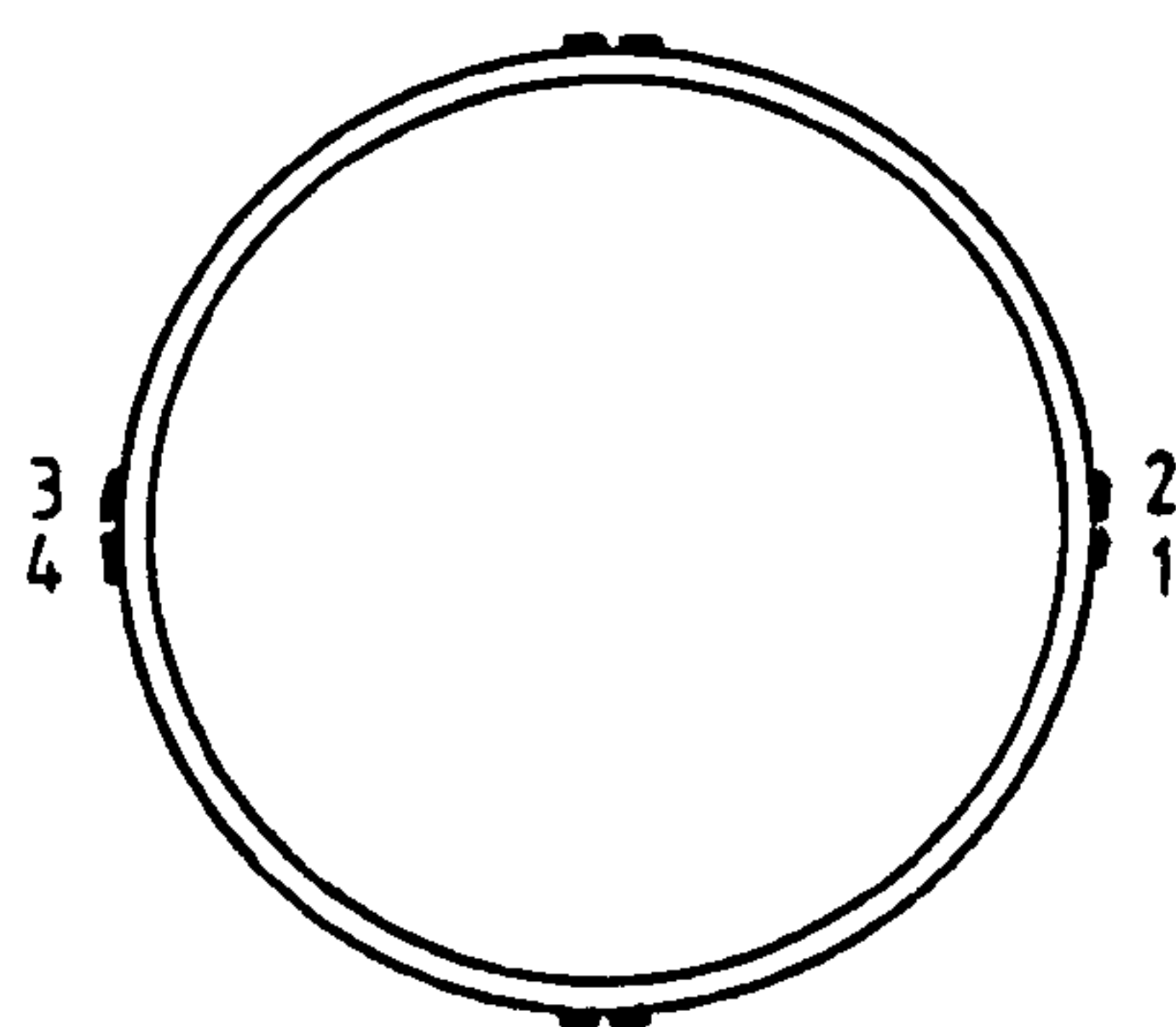
The strain gauges for the Durapipe (ABS) structures were placed outside of the cylinder and covered with watertight paint while the wires from the strain gauges were carried inside the cylinders. The reason for placing the strain gauges outside is to keep them at a constant temperature throughout the test (water temperature). For the aluminium structures the strain gauges were placed inside.

The strain gauges were connected so that only the bending moment was measured. The direct load, such as that from the concentrated mass, did not influence the strain gauge reading.

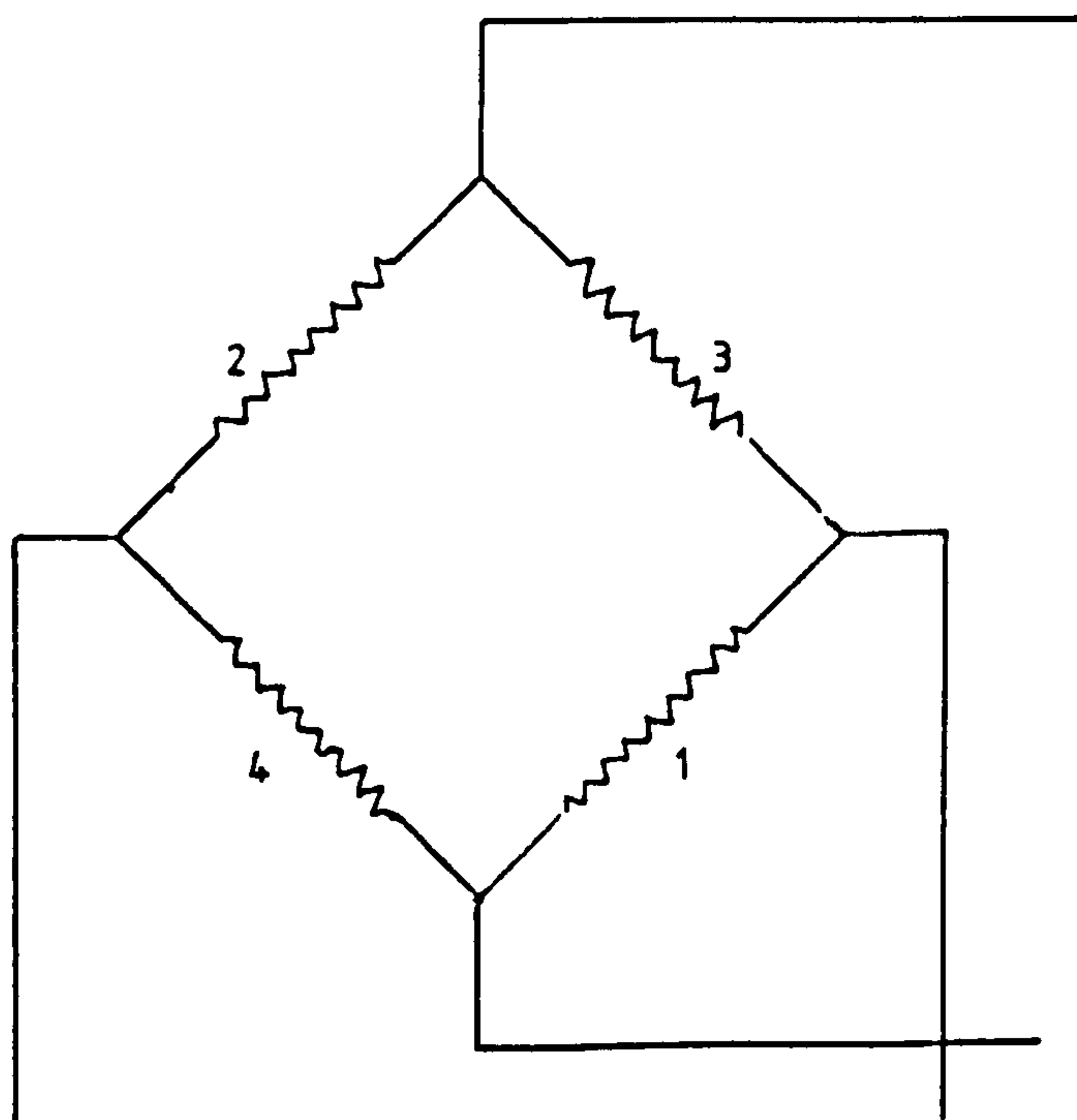
The strain gauges were aligned with respect to the tank by a vertical mark inscribed throughout the length of the cylinder and its base.



Sectional elevation of strain gauge installation



Plan view of strain gauge installation



Full Wheastone bridge of strain gauge

Figure (4.2.1) - Strain Gauge Installation.



#### 4.2.1.3 PRESSURE TRANSDUCERS

A more accurate method for measuring the force of the waves at any level of the structure is one in which the pressure is measured at equal intervals around the circumference of the structure at that level by use of pressure transducers. The total pressure force on a unit height of the cylinder may then be obtained by integrating the pressure on the individual surface elements around the circumference.

The general description of design of the pressure transducers was desirable to incorporate the following features:

1. The pressure transducers should be capable of measuring pressures from 0.01 psi to 0.5 psi
2. The output of the transducers versus the applied pressure should be linear
3. The output traces should be clean "no noise", this could be obtained by the high natural frequency of the transducer sensing element. This feature reduces the error in reading the output
4. The pressure transducers should be easily attached and removed to read the pressure at any point along the pile

Because no known commercial transducer met the requirements listed above, a special transducer shown in Appendix (A) was developed.

During the development of the transducer, a number of different types of sensing element were considered, fabricated and tested. Based on the experience obtained during these tests, the final design of the sensing element was arrived at.

Eight pressure transducers were built so that eight individual pressure readings around the circumference of the structure at the level required can be obtained at the same time.

The pressure transducers were mounted on the top of the tank. To measure the pressure at any particular points on the structure several soft tubes were connected from the various points on the structure to the transducers.

Figure (4.2.2) shows the mounting and the connection of the pressure transducers to the structure.



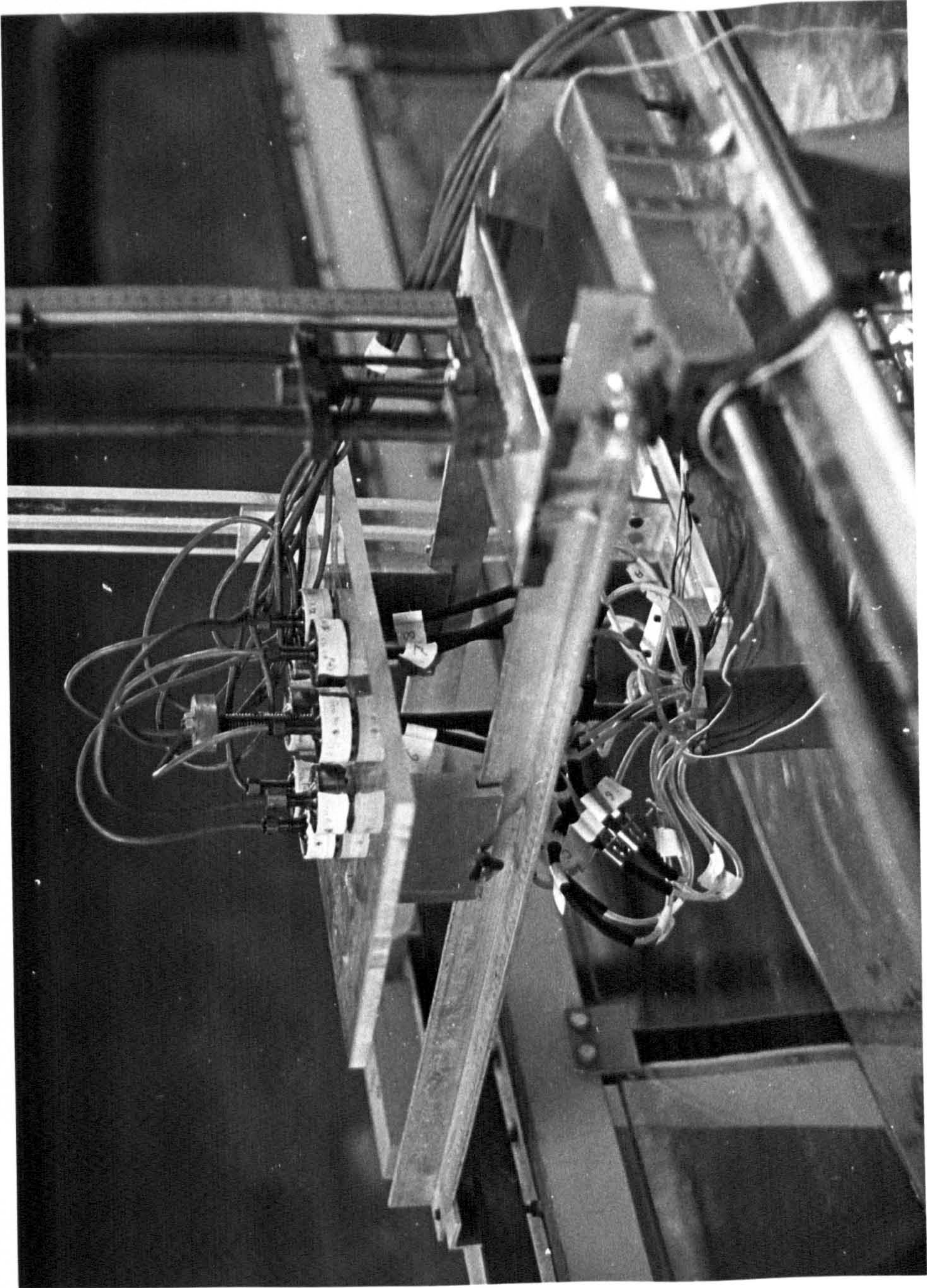


Figure (4.2.2) - The Mounting and Connection of the Pressure Transducer to the Structure.



#### 4.2.1.4 DISPLACEMENT TRANSDUCER

An inductive type of displacement transducer was attached to the tip of the structure to measure the tip displacement of the structure caused by the wave action.

This displacement transducer utilises the well proven linear variable differential transformer principle. A transducer with a free unguided armature assembly was used so that the movement of the structure will not be affected by the stiffness of the spring loaded armature. This is especially so because the wave loading on the structure is small and consequently the movement of the structure was also small.

The working range of the transducer is  $\pm 0.0125$  metre.

#### 4.2.2 READING INSTRUMENTS

The reading instruments were used in conjunction with the measuring instruments. The reading instruments were used to drive, amplify the magnitude of the electrical signal coming out from the sensing element and purify it from any noise interference in order to be able to record and digitalize it without any alteration of the actual electric signal measured.

Ten channels out of the fourteen strain gauge bridge amplifier units of the basic Sensonic amplifier were used to drive and pick up the electric signals from the two sets of the strain gauges which were fixed at the base of the structure, and also from the strain gauges of each of the pressure transducers.

Two channels of inductive amplifier units were used with the wave probe to measure the wave profile.

A RDP transducer amplifier type D7M was used to drive and amplify the electrical signal of the displacement transducer.

The low level signals "output" from the measurement instrumentation drive amplifier were converted into higher level signals and also filtered with low output impedance by using a preamplifier. The preamplifier was designed and manufactured to satisfy the necessary requirements of the signals level to be recorded. For the electric circuit of the preamplifier see Appendix (B).

The amplification and the phase shift due to filtration in the preamplifier were tested by using the output from a signal source type 471 which generates a sinusoidal waveform of 100 MV at frequency ranges between 1 Hz to 10 Hz as an input to the preamplifier. Both the output from the preamplifier and the signal source were fed into a



two channel oscilloscope type D1011 which attenuated the signal from the amplifier so that both signals of similar amplitude were displayed on the screen, the attenuation inside the oscilloscope was equal to the gain of the preamplifier. The phase shift from the two signals was negligible.

All the outputs from the preamplifier channels were recorded simultaneously by one fourteen channel RACOL tape recorder store 14D5. The electric signals were recorded at a speed of  $1\frac{7}{8}$  and at the window of recording  $\pm 2$  volt peak to peak.

Figure (4.2.3) shows the strain gauge Sensonic amplifier, preamplifier and the tape recorder.

The electric signals analogue recorded were fed to an Intercole Transmitter/Receiver model HS6202C which was connected to a PDP Compulog Intercole system in order to be digitalized at regular intervals to be saved on a floppy disc.



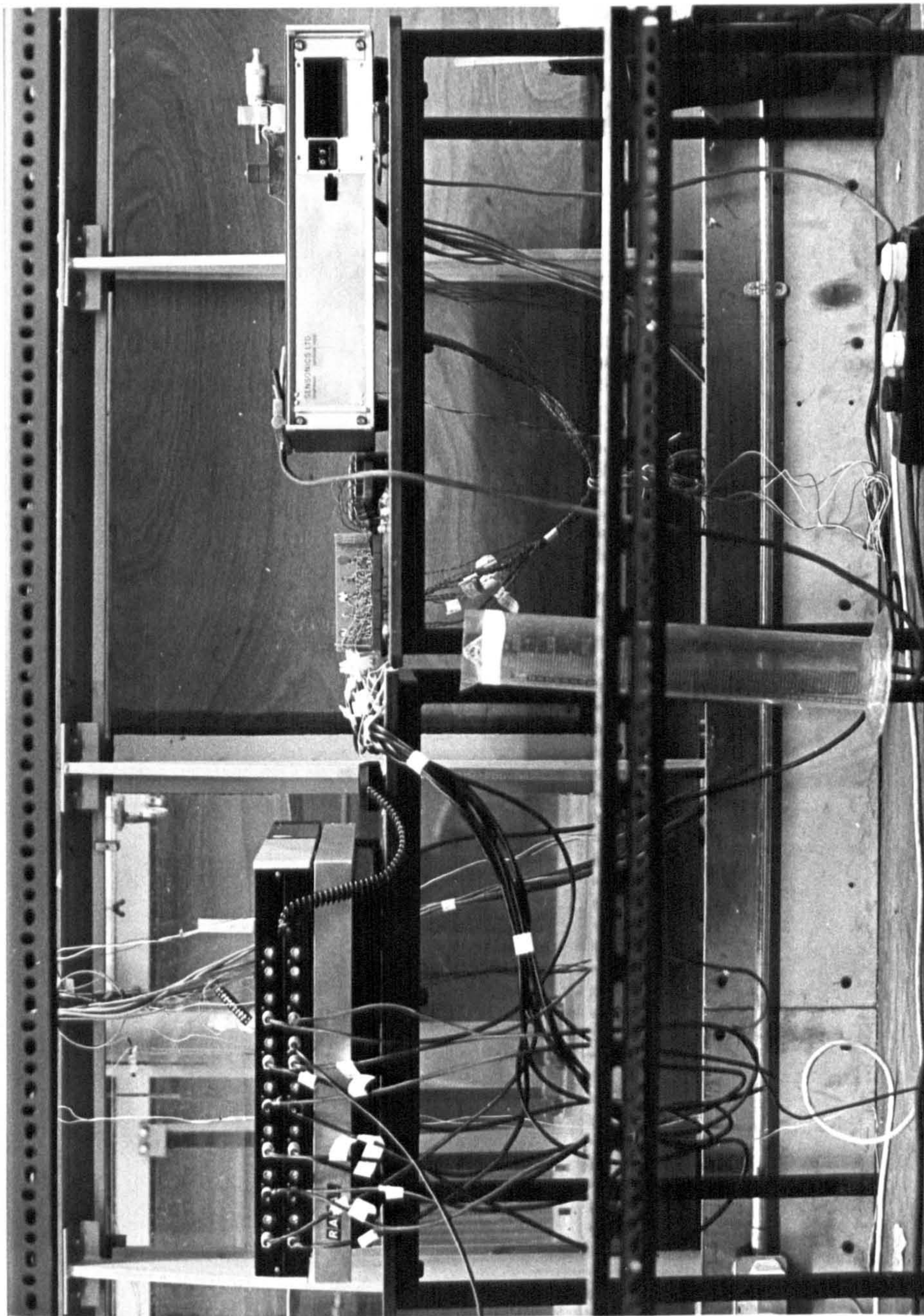


Figure (4.2.3) - Strain Gauge Amplifier, Preamplifier and the TapeRecorder.



For the calibration tests of the measuring instrumentation the structure was first located and fixed in the tank. The displacement transducer was attached to the structure and the pressure transducers were mounted, so the structure was ready for the main test. The calibration tests were done twice each day; once before and once after the main tests.

All the electric equipment was switched on and left for half an hour before the first calibration tests start in order to achieve a stable electrical signal.

#### 4.3.1 STRAIN GAUGES

The strain gauges at the base of the structure for measuring the bending moments were calibrated by applying a known horizontal load equal to 4.45 N at the top of the cylinder with a wire and pulley arrangement. This horizontal load had three increment of loading each equal to 4.45 N. For the in-line bending moment the tests were done once where the horizontal load was in the direction of the wave propagation and once in the opposite direction in order to obtain the positive and negative bending moments reading. Similar tests were carried out for the strain gauges in the transverse direction.

The bending moments at the base of the structure were calculated by multiplying the horizontal force by the distance from the top of the structure to the strain gauge. For the cases where added mass was applied at the top of the structure (third group of structures) the bending moment was calculated as the above plus the moment due to the concentrated mass at the top of the structure when the structure is in a deflection position. The deflection of the tip of the structure was determined in a previous test where a dial guage was attached to the top of the structure on the other side and on the same line with the wire so that the tip displacement due to the horizontal load were known. This test was useful also in the calibration of the displacement transducer as shown below.

Figure (4.3.1) shows the arrangement of the test determining the tip deflection.

#### 4.3.2 DISPLACEMENT TRANSDUCER

The displacement transducer was calculated at the same time as the strain gauge. The horizontal displacements were known due to the horizontal applied loads. A mark on the transducer armature was made in order to correct the relative positions between the armature and the body of the transducer.

The relationship between the horizontal displacement and the electrical signal recorded was linear.





Figure (4.3.1) - The Test Determining the Tip Deflection due to the Horizontal Load.



#### 4.3.3 PRESSURE TRANSDUCERS

The pressure transducers were calibrated for a positive gauge pressure by connecting the pressure transducers at the top of the tank with the eight holes around the circumference of the structure by the tube assembly in each structure. For that purpose the water level in the tank decreased to the level of these holes. This gave a zero gauge pressure reading. The electric signals from the pressure transducers were recorded. The water level in the tank increased by 0.025 metre which gave a gauge pressure equal to the head of water above the holes, the electric signals were recorded, the water level in the tank was again decreased to the level of these holes, again giving zero gauge pressure and the electric signals were recorded. By repeating this process with increments in the water level of 0.025 metre up to the maximum water level of 0.1 metre, the pressure transducers were calibrated for the positive pressure gauge readings.

The negative gauge pressures were obtained by disconnecting the pressure transducers from the tubes and connecting them again when the water level was 0.11 metre above the holes which give zero gauge pressure. The procedure of positive gauge pressure was reversed in order to calibrate the pressure transducers for the negative pressure gauge reading.

The calibration of the pressure transducers was done with the uppermost holes in the cases of structures with more than one holes level.

The following test was previously made in order to find the pressure losses along the length of the tube from the hole on the structure to the pressure transducer at the top of the water tank. The pressure transducer was connected to a single bore at the bottom of a graduated measuring cylinder with a single bore stopcock by 0.04 metre long rubber tube in the case of testing for 0.025 metre head of water. This was in order to keep the pressure transducer away from the water as it is not waterproof. The electric signals were recorded, water was poured down to the level 0.025 metre in the measuring cylinder then electric signal was recorded. The water was emptied from the measuring cylinder by the stopcock. A 0.75 metre long rubber tube of the same length as those used in the tests, replaced the 0.04 metre tube and the test was repeated.

The above test was repeated with different head of water pressure and different lengths of the short tube. The difference between the electric signals recorded from the short tubes and from the long tube were negligible.

#### 4.3.4 WAVE PROBE

After the position of the wires of the probe had been adjusted to the still water level the electric signal gave a zero reading. The probe was lowered by means of an adjustable boom by 0.01 metre which was equivalent to raising the water level by the same amplitude and the electric signal was recorded. This test was carried out by lowering the probe in stages of 0.01 metre until a distance of 0.1 metre was reached.

Similar tests were carried out by raising instead of lowering the wave probe to give the calibration in the case of lowering of the water level.

#### 4.4 EXPERIMENT

To achieve the main objective of the investigation, it was decided to carry out experiments in order to determine all the parameters required in the analysis, which are the water wave criteria and the structure dynamic properties.

##### 4.4.1 WATER WAVE CRITERIA

The first test was carried out to see how close small amplitude harmonic waves conformed to sinusoidal shape, and how their characteristics varied with time.

The test was done by adjusting the wedge arm and the speed of the driving motor of the wave generator. The wave profile was measured by the wave probe which was located at the position of the tested structure. The test was carried out for 45 minutes.

For conformation of sinusoidal shape a typical case is shown in Figure (4.4.1).

The variation of the wave characteristic during the test was insignificant.

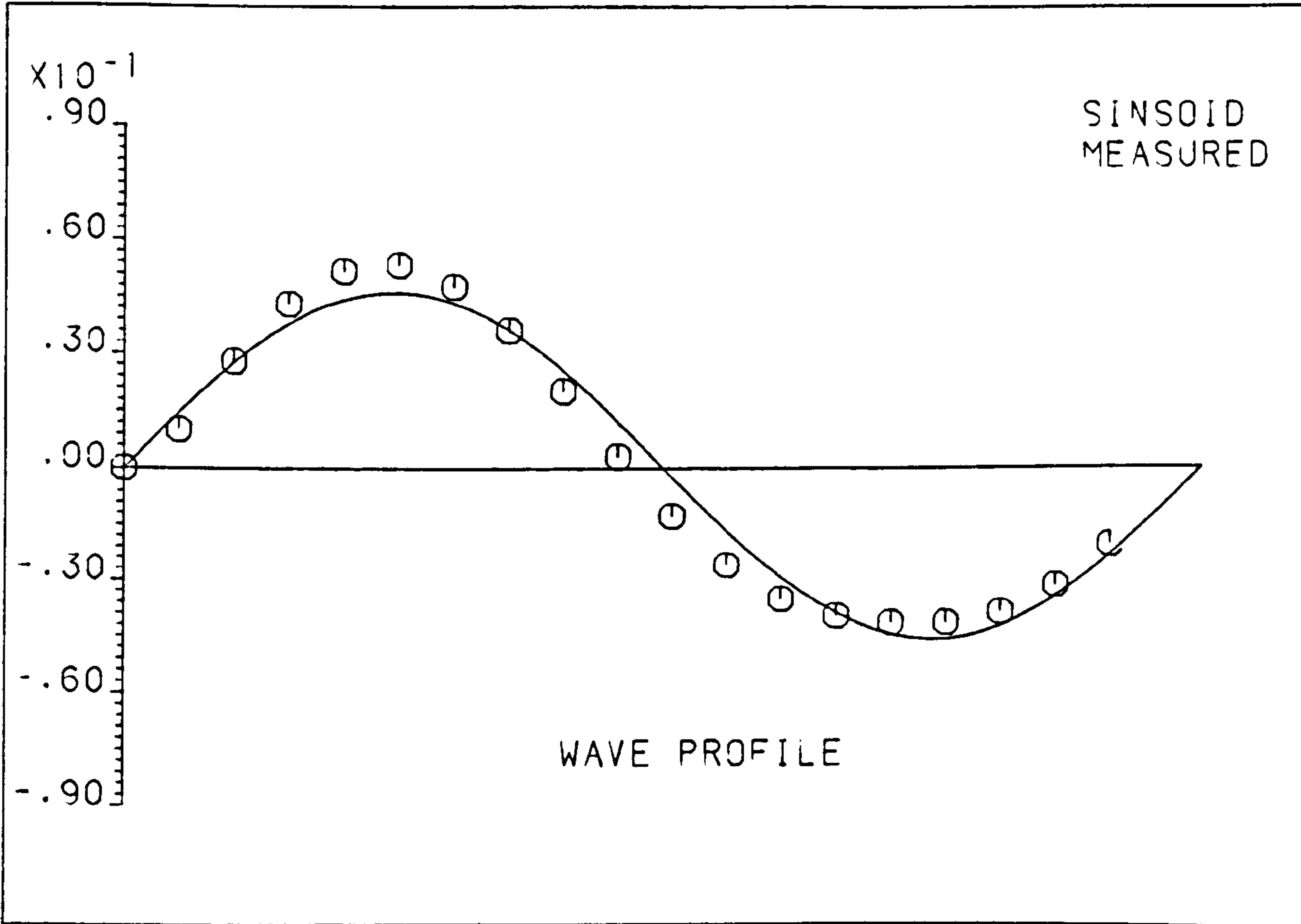


Figure (4.4.1) - Water Surface Profile.

It was necessary to check the degree of wave reflection from the beach. The amount proved to be quite small.

Eagleson and Dean 1966<sup>(110)</sup> show that a portion of a wave impinging on a sloping surface will reflect upon itself. The magnitude of the reflected wave can be expressed as a coefficient of reflection times the magnitude of the incident wave. The reflected wave will disturb the regularity of the wave surface. The crests and troughs of the resulting wave will describe an envelope as shown in Figure (4.4.2).

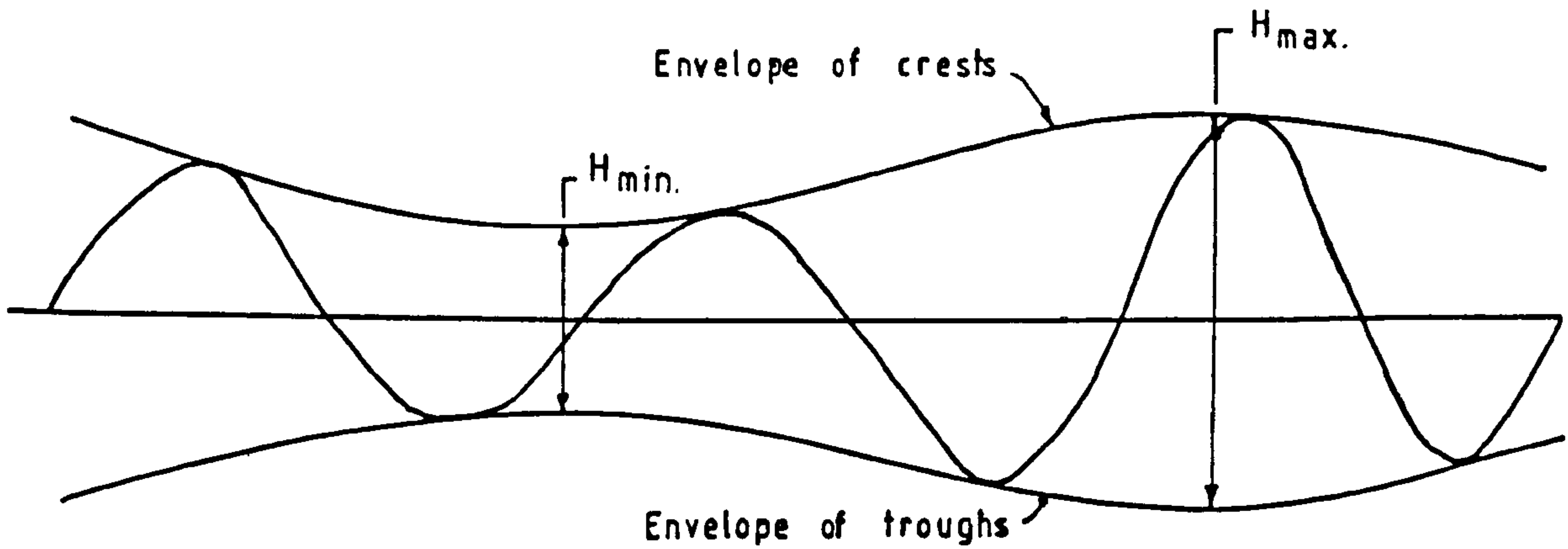


Figure (4.4.2) - Typical Reflected Wave.

It is shown in the above reference that the reflection coefficient can be obtained from:

$$K_r = \frac{H_{\max} - H_{\min}}{H_{\max} + H_{\min}} \quad \dots \quad (4.4.1)$$



where  $K_r$  = Reflection coefficient

$H_{\max}$  = Maximum wave height

$H_{\min}$  = Minimum wave height

Waves of various characteristics were tested. From the results it can be concluded that reflection was minimal, and thus it was ignored in all analysis. Figure (4.4.3) shows the result of the reflection coefficient verse wave period.

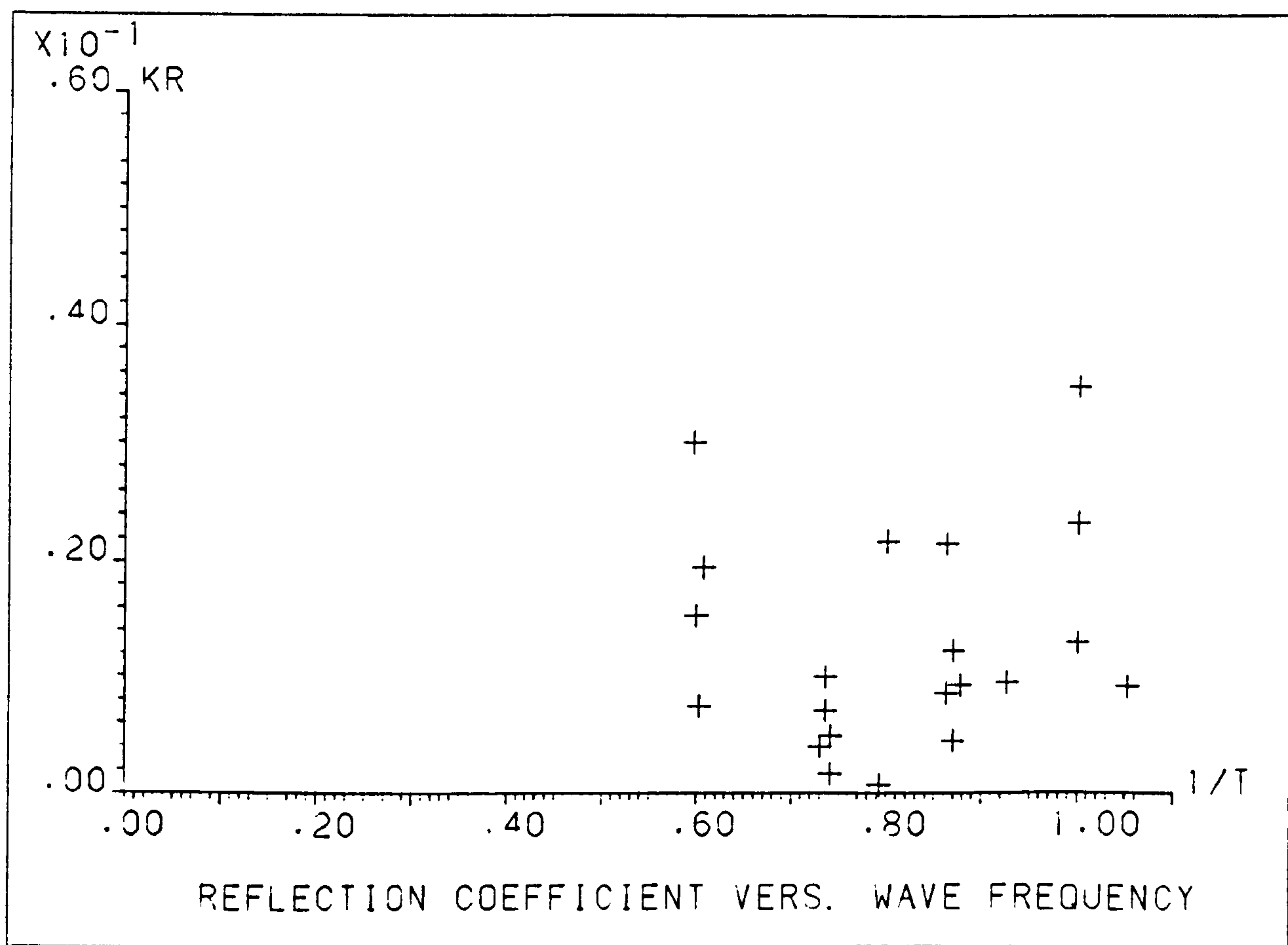


Figure (4.4.3) - Reflection Coefficient for the Wave Tank.

#### 4.4.2      STRUCTURE DYNAMIC PROPERTIES

As the determination of certain structural parameter such as stiffness, natural frequencies and damping coefficients are important to be obtained, the following experiments were carried out.

##### 4.4.2.1      STIFFNESS TEST

In the determination of the stiffness of the structure it is vital to know the rate of the deformation of the structure material, especially the Durapipe ABS structure. The Durapipe ABS is not a truly elastic material. Maxwell and Harrington 1952<sup>(111)</sup> show that the strain of this material depends on the time rate of deformation. That is, if the velocity of deformation is high enough the stress-strain curve will be linear. When the velocity of deformation becomes small or negligible, then a plastic flow takes place which is recoverable when the load is removed. There is a limit of strain however, beyond which plastic deformation is not recoverable. This can be called deformation types I, II and III and can be illustrated schematically as in Figure (4.4.4).

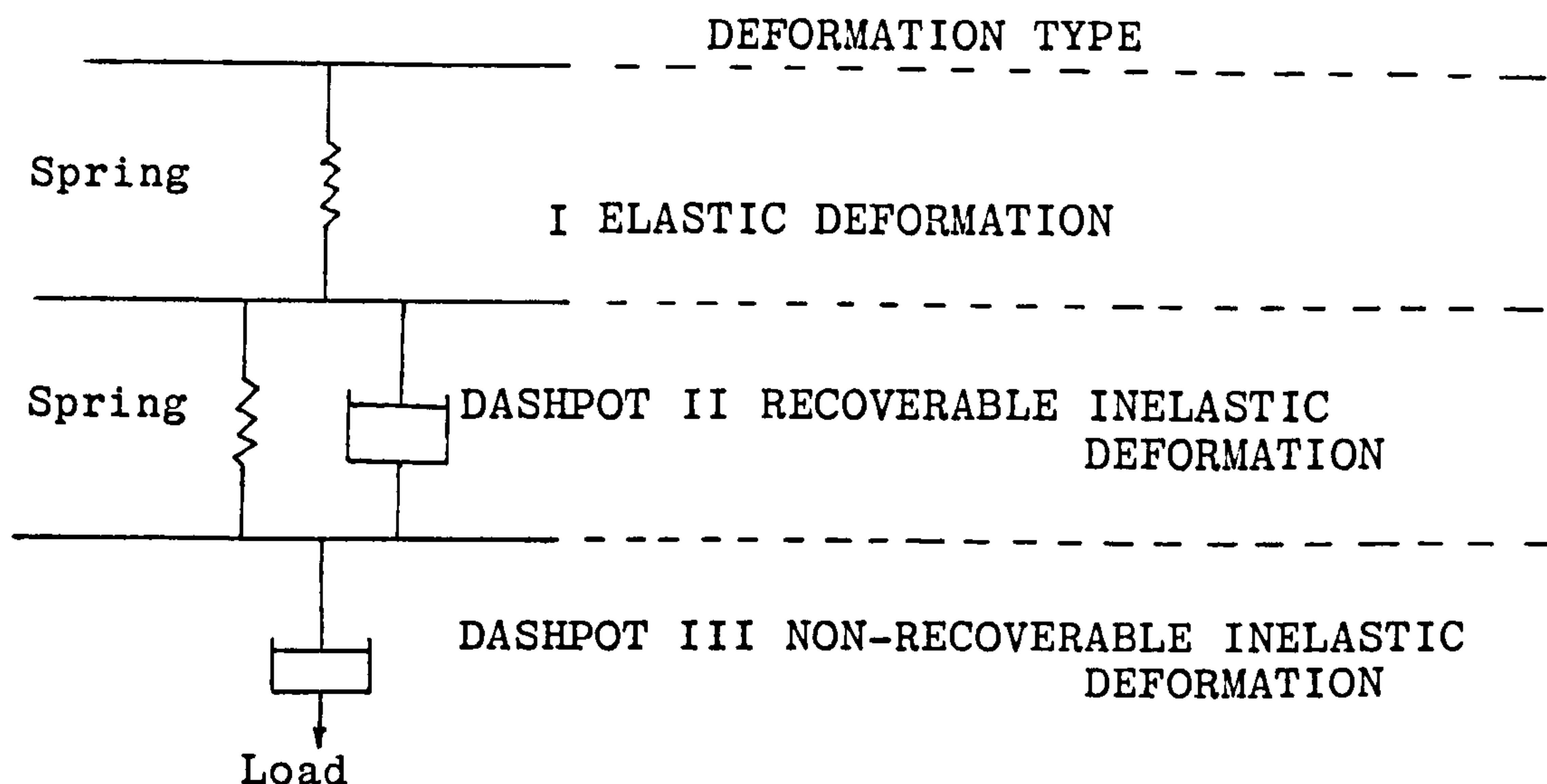


Figure (4.4.4) - Schematic Diagram of Deformation Types for Durapipe ABS.

For this work it will be shown that type I deformation occurred for the Durapipe ABS cylinders under dynamic loads.

The experimental procedure of this test was exactly as that of the calibration of the strain gauges at the base of the cylinder structure except that the output signal was taken to the Oscillograph instead of the tape recorder.

Typical records of the test procedure are shown in Figure (4.4.5), it was noted that the strain started at zero and ended at zero, indicating that type III deformation did not take place. The load was applied fairly suddenly so that a few oscillations occurred in the record. It can be seen that strain did not decrease



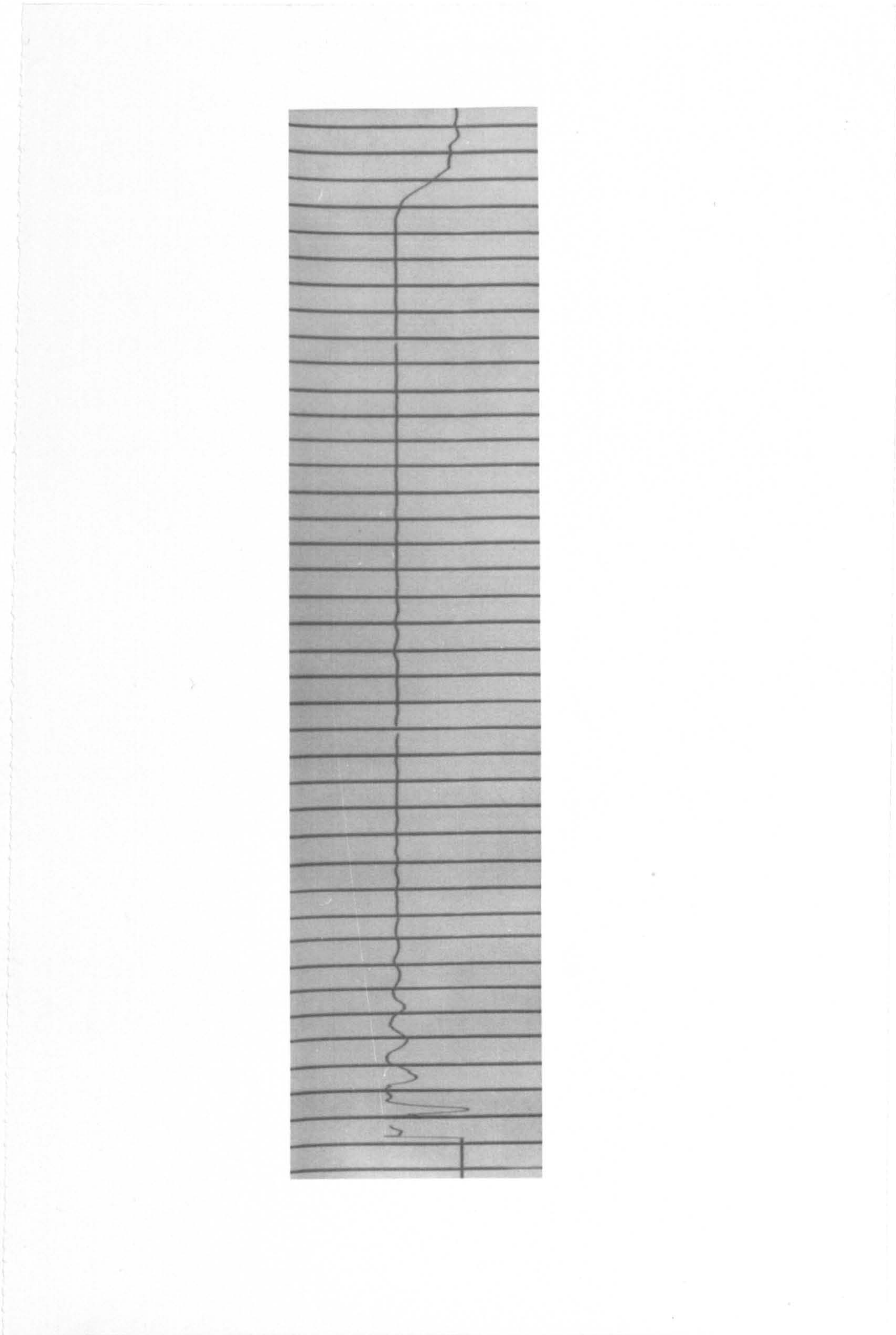


Figure (4.4.5) - Typical Recording of the Strain Gauge.



with time for constant load. If decrease showed in the strain under static load condition type II deformation would occur.

The stiffness of the cylinders was determined by the following test. The cylinder was mounted vertically as in the case of the main test and a series of weights were applied at the free end. The free end deflection corresponding to each weight was measured using a dial gauge. Graphs of load against the deflection were plotted, the slope yielding the equivalent stiffness.

#### 4.4.2.2 NATURAL FREQUENCIES AND STRUCTURAL DAMPING

For convenience, measurements of the natural frequency and damping were made simultaneously. Essentially, the scheme was to force the oscillation of the structure by means of an impulse load and then to take the reading of the strain gauge at the base of the structure. The signals were recorded on an oscillograph from which the structural damping and natural frequency in the fundamental mode could be measured.

Care was taken to make the amplitude of vibration during an impulse load test about the same as the amplitude of vibration during the experiments with waves.

In the second approach, the structures were deflected with a steady load and then released.

The natural damped frequencies of the structures were obtained from the same test records as those from which the damping coefficient were obtained.

Typical records of the test results are shown in Figure (4.4.6).

The structures were tested in air and water.



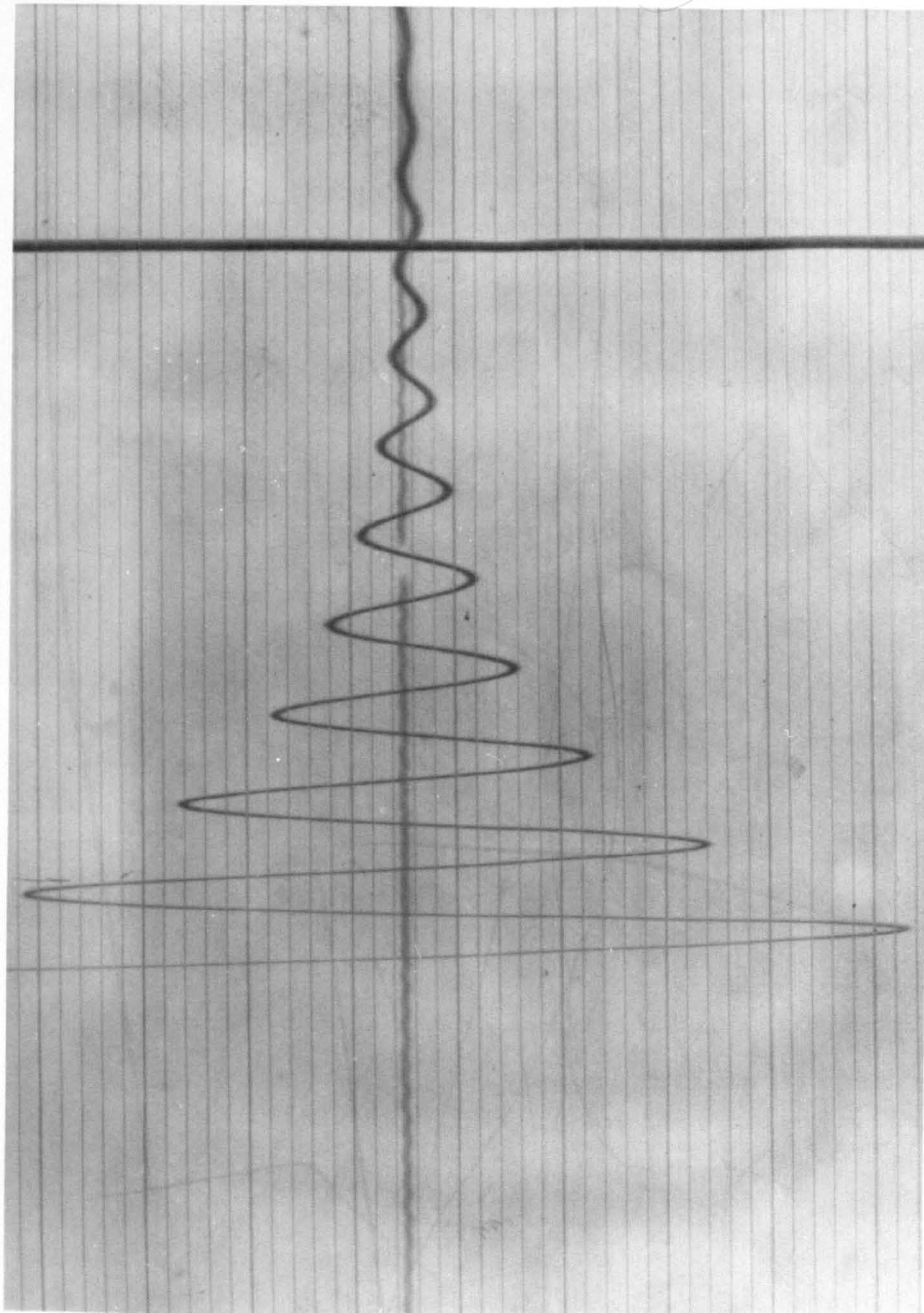


Figure (4.4.6) - Typical Record of the Natural Frequencies and Structural Damping.



#### 4.4.3 MAIN TESTS

After the structure was installed in the water tank and all the measurement instrumentation was calibrated the tests were started by adjusting the water level in the tank. The wave generator arm was fixed at the position required and then switched on; the speed of the motor which controlled the frequency of the wave was set up by the digital counter. The records were taken after a few waves passed the structure in order to establish a steady state wave and structure motion. This was approximately five minutes after the operation of the wave generator.

First the structure was acting as a cantilever "free to vibrate" the signals from the eight pressure transducers connected to one level of the structure, from the wave probe located beside the structure, from the strain gauges at the base of the structure and from the displacement transducer at the top of the structure were recorded simultaneously for 15 minutes. Then the structure was clamped from the top "Fixed Structure" by screwing a stiff shaft fixed on the top of the water tank to the top cap of the structure. The effectiveness of the clamp at the top was tested by monitoring the signal of the displacement transducer. If the signal was zero throughout the wave cycle then the structure was fully clamped. After the structure was fully fixed the signals from the measurement instrumentation were recorded for 15 minutes. The stiff



shaft was released, returning the structure to the initial condition and the signals were recorded for 15 minutes.

This process was repeated for waves of other characteristics.

For the first group of the Durapipe ABS, structures A and B which had only one level in which the pressure could be measured; for this case the above test procedure was complete for testing this group.

Figure (4.4.7) and Figure (4.4.8) show structures A and B when they were under test, respectively.

The second group of Durapipe ABS, structures C and D which had two levels at which the pressures could be measured. For that reason after the above test procedures were carried out then the second level of pressure was recorded by locking the connection between the pressure transducers and first level and by opening the connection to the second level and repeating the procedure.

Figure (4.4.9) shows structure C when it was under test and also it shows clearly the position of the wave probe. Figure (4.4.10) shows structure D under test and it also shows the way of the mounting of the displacement transducer and the stiff shaft used for clamping the top of the structure.



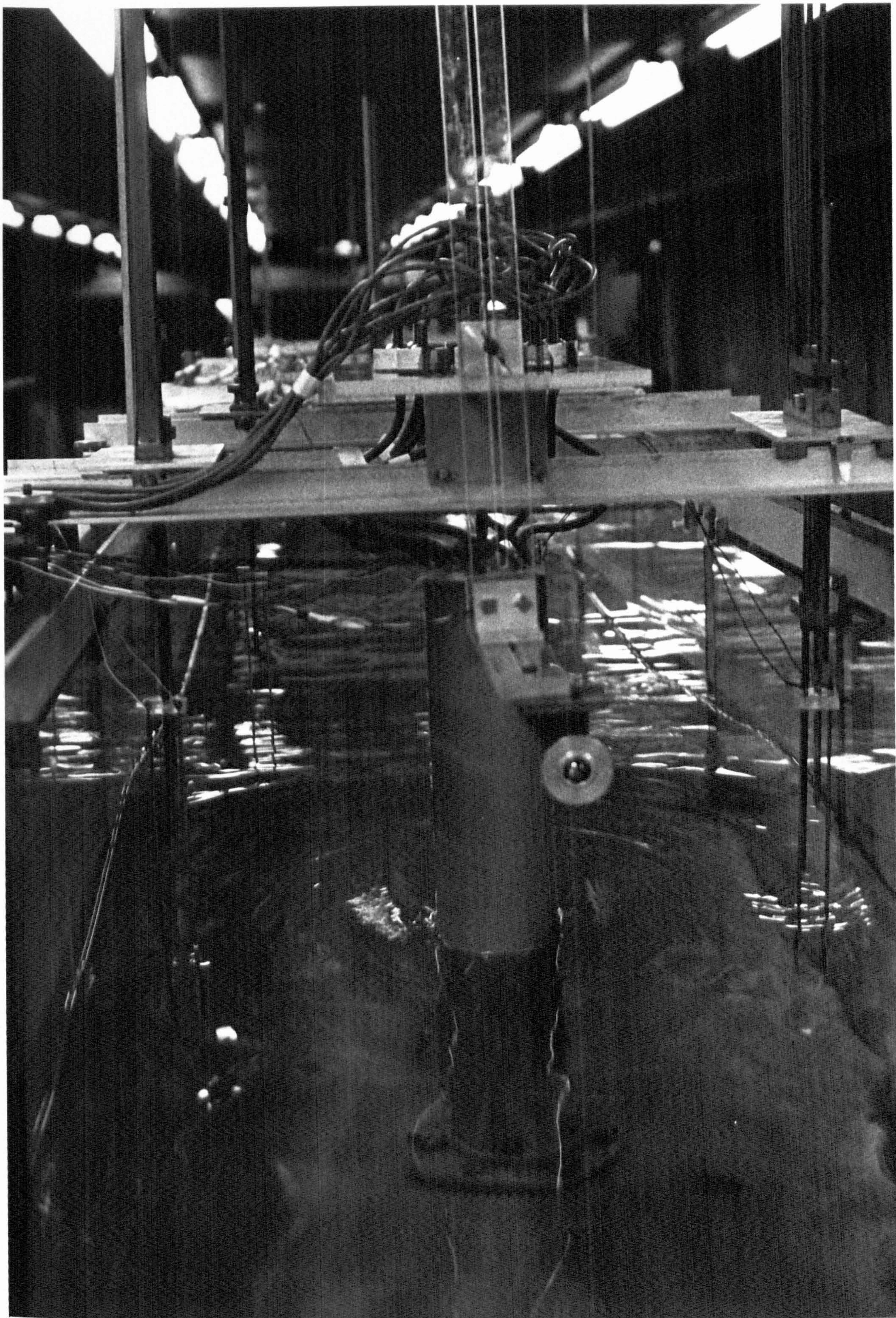


Figure (4.4.7) - Structure (A) under Test.



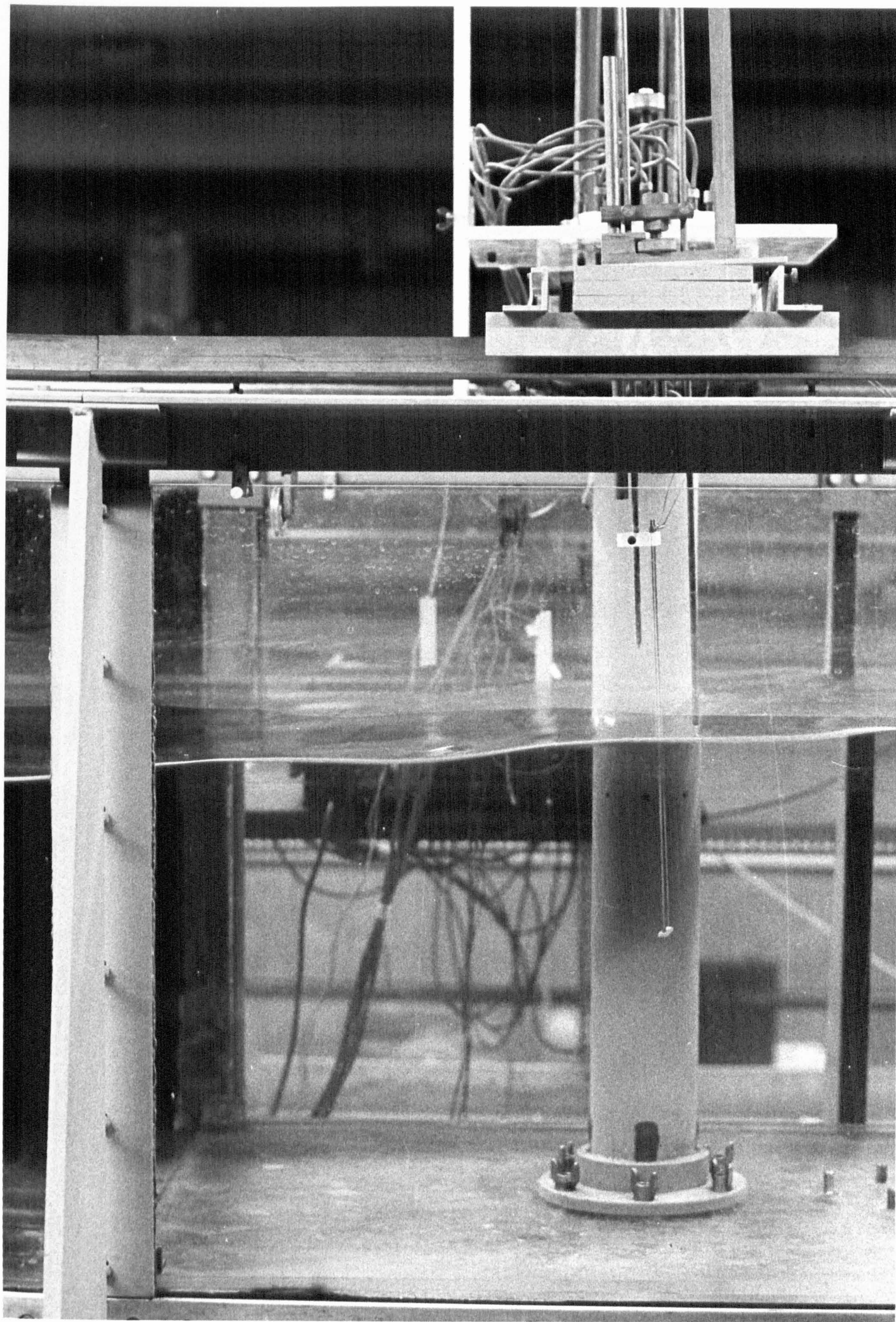


Figure (4.4.3) - Structure (B) under Test.



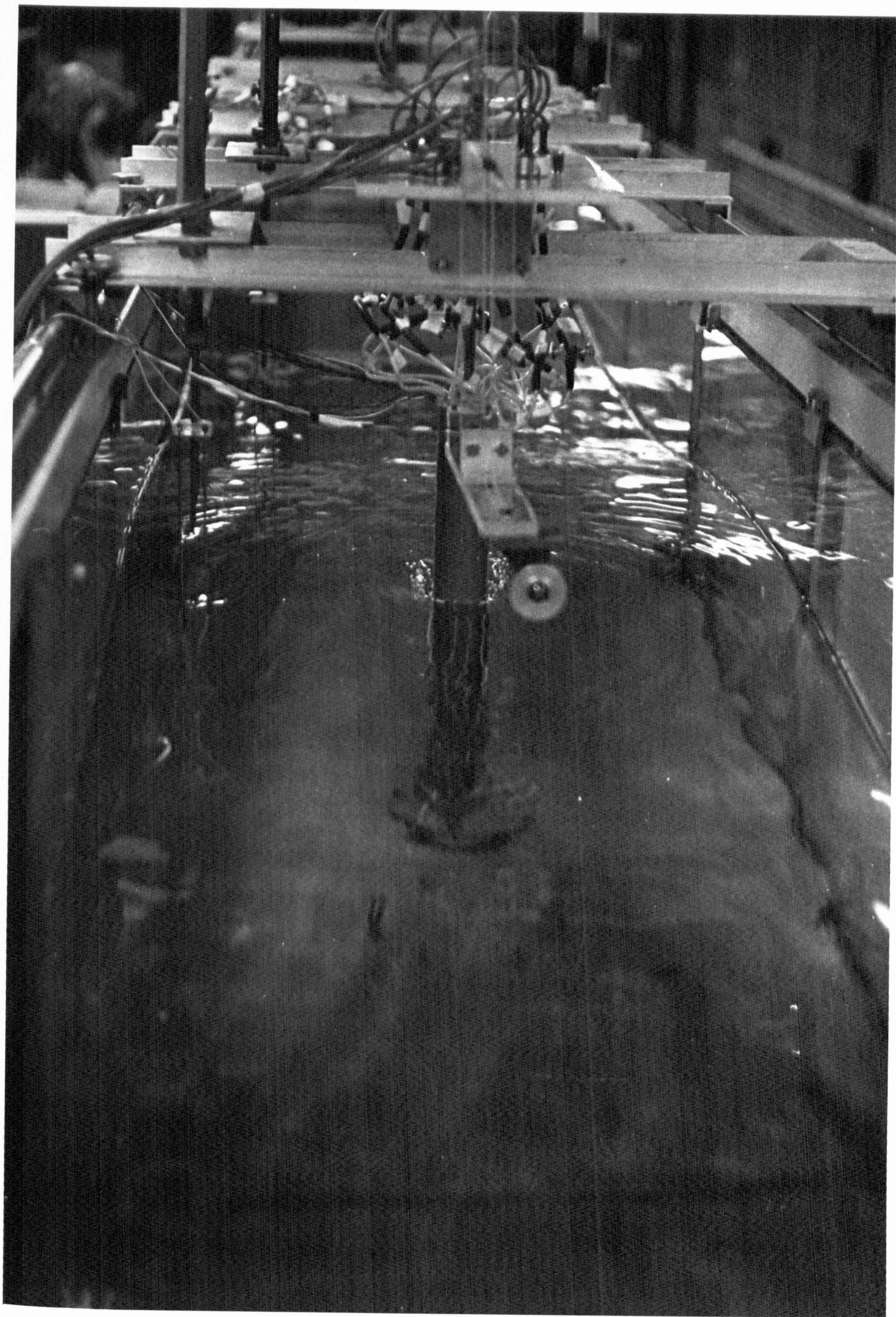


Figure (4.4.9) - Structure (C) under Test.



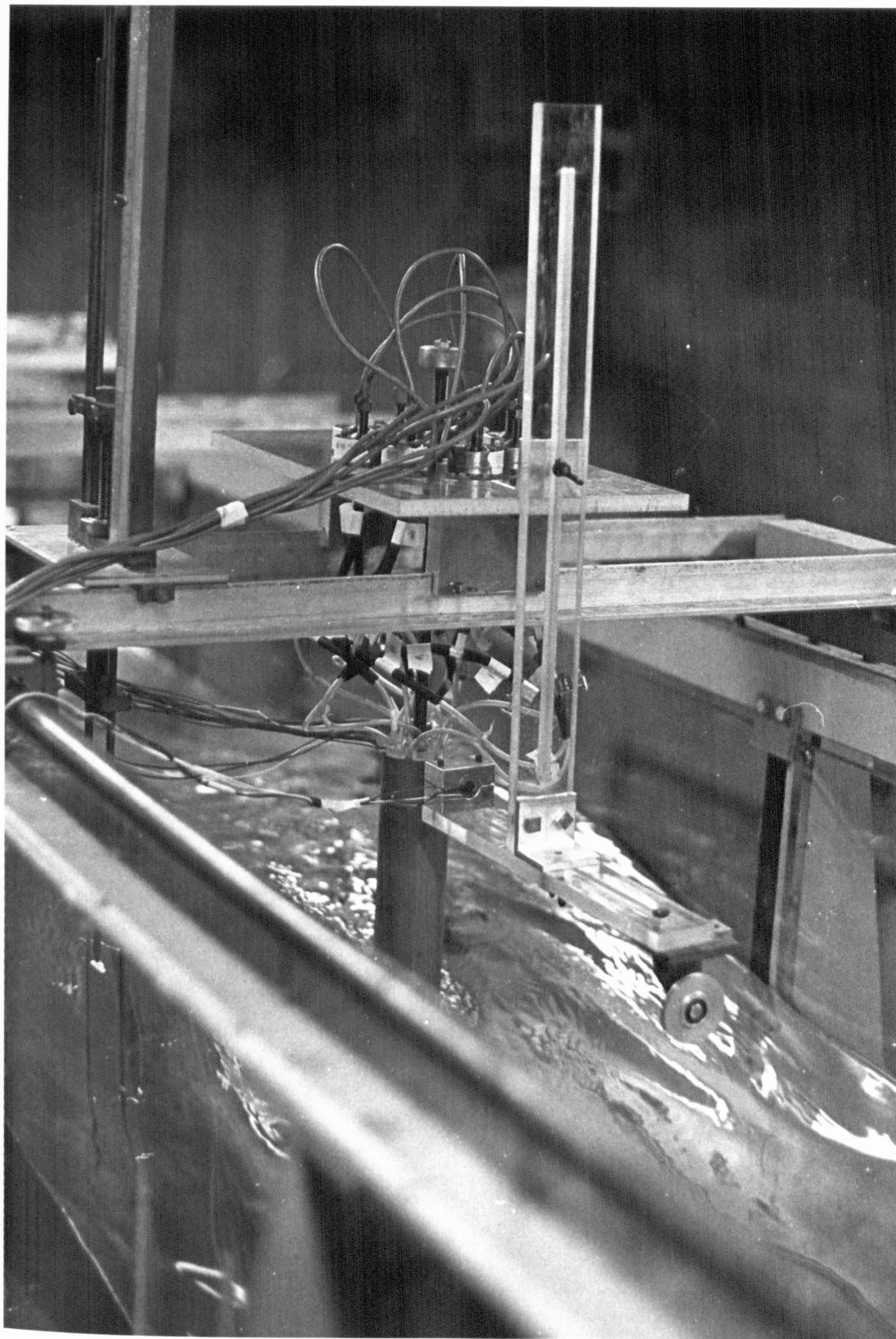


Figure (4.4.10) - Structure (D) under Test.





Figure (4.4.11) - Structure (E) under Test.



For the group of the Aluminium structures, structures E and F the test was carried out without any added mass for the highest level where the pressure can be recorded. The test was repeated for each increment of added mass for the same level of the pressure. For the other two levels which the pressure could be measured the same test procedure as used for the first level was repeated.

Figures (4.4.11) and (4.4.12) show the structure (E) and structure (F) while they were under test.

Table (4.2) shows the reading of the digitize electric signals of one of the calibration test, column one to eight are the eight pressure transducers, column nine is the strain gauge reading for the in-line bending moment while column ten is the reading of the transverse bending moment, column eleven is the reading of the displacement transducer and column twelve is the reading of the wave probe.

Table (4.3) shows the digitize electric signals reading for one of the test.



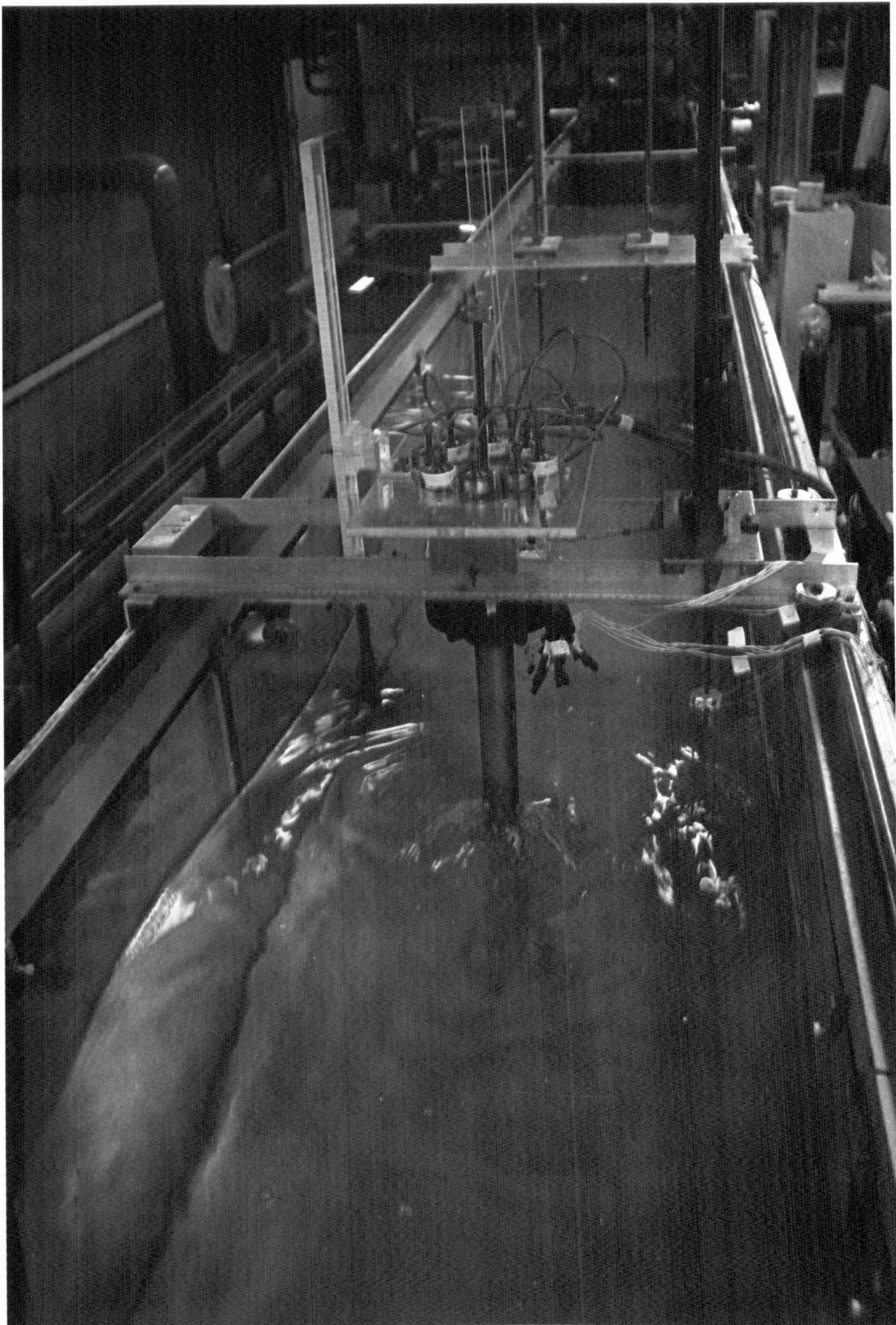


Figure (4.4.12) - Structure (F) under Test.



CALIBRATION FOR TEST UO-50 401

12	70	150										
-222	27	137	-174	-121	212	-177	3	-95	42	-45	-54	
-220	27	137	-174	-121	212	-177	3	-95	42	-45	-54	
-219	27	137	-174	-121	212	-177	3	-95	42	-45	-54	
-222	24	130	-165	-118	246	-189	3	-53	42	-35	-57	
-237	26	136	-171	-120	234	-189	-38	-33	44	-105	-50	
-240	27	138	-179	-113	223	-177	-63	-44	36	-45	-53	
-236	32	132	-170	-117	226	-186	-59	-26	41	-36	-59	
-231	31	132	-163	-121	231	-185	-50	-29	40	-35	-56	
-229	25	132	-170	-112	230	-188	-56	-32	34	-84	-64	
-237	24	134	-180	-112	219	-195	-53	-45	46	-86	-55	
-234	29	174	-169	-116	225	-196	-48	-39	46	-94	-49	
-710	-1340	555	-497	-407	663	-737	911	118	324	330	-202	
-712	-1358	551	-493	-403	661	-741	924	122	323	331	-205	
-708	-1367	554	-477	-405	664	-739	916	130	310	397	-211	
-711	-1388	561	-487	-394	650	-731	806	136	311	393	-216	
-712	-1392	557	-487	-394	651	-732	792	115	317	407	-216	
-719	-1410	547	-489	-414	651	-750	820	123	327	392	-204	
-712	-1411	562	-485	-395	652	-729	912	141	315	410	-215	
-711	-1415	556	-479	-401	662	-737	828	132	326	400	-206	
-709	-1421	557	-493	-391	654	-732	863	136	312	412	-214	
-711	-1425	557	-475	-404	661	-739	828	126	328	402	-201	
-531	-972	424	-352	-282	503	-565	501	-2	38	-76	-58	
-532	-880	428	-363	-281	496	-561	475	5	32	-71	-62	
-536	-967	418	-357	-280	493	-557	472	10	34	-76	-51	
-536	-861	416	-352	-282	494	-562	480	9	35	-68	-53	
-533	-367	421	-362	-281	491	-559	480	1	34	-68	-65	
-533	-964	424	-357	-278	495	-561	484	6	45	-78	-52	
-531	-969	425	-359	-276	490	-556	470	10	32	-61	-64	
-525	-866	420	-357	-276	502	-566	477	-2	40	-69	-59	
-530	-962	424	-349	-280	501	-565	470	-3	45	-70	-54	
-530	-964	421	-353	-279	497	-566	487	-1	39	-69	-59	
-534	-864	418	-348	-283	498	-565	453	6	763	942	-360	
-360	-1025	620	-522	-416	721	-854	870	430	758	943	-363	
-367	-1045	617	-518	-422	717	-863	972	423	765	917	-355	
-360	-1064	625	-516	-416	713	-851	971	429	758	949	-363	
-365	-1086	620	-514	-425	715	-863	974	417	760	931	-357	
-365	-1100	626	-524	-413	708	-854	862	433	756	929	-363	
-365	-1110	616	-514	-413	712	-858	863	427	760	941	-355	
-365	-1121	615	-511	-424	718	-857	871	428	755	933	-358	
-360	-1129	626	-516	-414	718	-866	877	413	755	938	-357	
-359	-1134	623	-516	-409	719	-862	871	420	757	943	-359	
-360	-1149	623	-517	-413	718	-859	874	410	756	931	-355	
-47	-85	374	-277	-190	441	-492	311	11	55	-225	-60	
-10	-65	367	-284	-190	423	-416	314	9	44	-92	-67	
-5	-38	369	-273	-187	439	-489	317	3	46	-95	-59	
-11	-37	364	-291	-194	430	-497	321	11	44	-10	-59	
-5	-19	368	-270	-139	442	-491	332	11	44	-88	-55	
-2	-13	371	-271	-181	439	-491	313	9	45	-89	-56	
-18	-14	363	-288	-183	423	-490	316	14	30	-75	-68	
-3	-5	372	-279	-173	425	-482	293	7	27	-77	-65	
-1	-1	368	-273	-180	433	-487	304	15	37	-78	-64	
1	2	371	-270	-178	435	-494	299	14	41	-87	-59	
3	4	374	-273	-170	427	-484	284	19	31	-80	-67	
-489	-1532	747	-594	-474	854	-1037	876	443	954	989	-500	
-489	-1544	746	-590	-477	854	-1039	876	445	956	993	-504	
-493	-1541	738	-596	-468	839	-1029	865	453	948	1005	-515	
-480	-1550	755	-589	-462	853	-1027	868	452	960	987	-501	
-480	-1550	749	-600	-464	841	-1029	866	480	951	1001	-513	
-485	-1549	749	-598	-466	842	-1024	868	452	949	1004	-513	
-483	-1551	742	-585	-469	855	-1037	878	440	964	988	-503	
-477	-1551	760	-599	-456	856	-1027	874	450	960	996	-504	
-484	-1548	747	-587	-470	849	-1030	882	443	961	994	-498	
-473	-1550	758	-584	-492	851	-1017	888	460	948	1001	-516	
17	-96	374	-261	-148	427	-509	308	15	-280	999	-65	
17	-86	369	-255	-150	433	-508	317	13	-266	-601	-58	
19	-88	378	-262	-143	427	-502	309	11	-266	-596	-55	
19	-76	367	-254	-151	429	-501	303	19	-277	-592	-63	
17	-79	371	-258	-146	424	-499	300	16	-276	-593	-66	
16	-79	371	-257	-158	428	-510	314	15	-270	-596	-63	
8	-88	366	-271	-155	417	-524	274	-1	-268	-608	-53	

Table (4.2) - Digitized Electric Signal for One of the Calibration Tests.

ZERO FOR TEST 40=50 S=45 (C)

12	19	150	0	0	0	0	0	0	0	0	0	0
-85	24	-102	-20	23	10	-82	38	-13	64	52	-53	
84	24	-94	-25	43	-1	65	38	-14	76	40	-45	
-87	36	-107	-11	31	11	-108	-60	-10	65	61	-55	
79	26	-102	-20	27	9	104	-45	-12	73	76	-60	
-81	26	-102	-19	25	9	-106	-32	-9	75	77	-55	
-85	26	-99	-13	23	15	102	69	-19	76	66	-57	
-83	24	-101	-27	33	6	-106	-24	-21	79	50	-49	
-83	28	-100	-17	23	9	111	46	-16	62	47	-53	
-85	25	-92	-26	33	4	-119	52	-13	76	34	-45	
-82	27	-102	-19	30	4	119	46	-6	67	51	-48	

TEST FOR STRU (C) 40=50 S=45 N=10 FREE (A)

12	128	1	0	0	0	0	0	0	0	0	0	0
-201	-241	-26	-142	-150	135	-50	374	667	-441	1442	653	
-272	-233	-28	-133	-137	134	-51	363	640	-357	1449	614	
-192	-232	-30	-139	-156	179	-52	359	676	-244	1447	557	
-175	-218	-36	-132	-157	178	-52	368	620	-121	1446	490	
-156	-208	-27	-138	-142	165	-51	316	658	4	1437	451	
-132	-194	-32	-135	-136	156	-45	308	655	119	1433	359	
-115	-129	-45	-126	-127	143	-32	275	646	222	1440	292	
-84	-154	-53	-115	-116	133	-23	238	639	331	1436	219	
-53	-123	-61	-101	-103	113	3	188	639	425	1443	136	
-12	-96	-69	-86	-99	102	-13	144	617	512	1441	50	
22	-51	-77	-78	-79	79	38	81	610	580	1439	-25	
64	-6	-104	-54	-76	77	-51	22	586	626	1448	-120	
103	38	-118	-42	-66	62	-74	-37	575	649	1450	-198	
144	78	-132	-35	-52	49	105	-90	546	657	1442	-265	
171	117	-156	-22	-30	18	146	-149	542	624	1438	-334	
185	152	-176	-8	-13	-10	128	-188	522	582	1442	-408	
192	190	-212	23	-5	-30	207	-228	505	539	1447	-484	
202	224	-229	45	9	-62	242	-275	423	482	1444	-542	
219	263	-260	60	31	-104	275	-329	479	411	1448	-599	
241	276	-267	75	48	-127	294	-352	458	362	1436	-639	
263	294	-276	83	72	-160	314	-383	445	300	1435	-673	
278	307	-287	105	89	-176	329	-398	429	235	1440	-720	
286	317	-296	109	113	-198	335	-410	423	178	1445	-739	
295	320	-296	114	125	-205	344	-424	405	123	1443	-759	
301	325	-302	124	121	-200	338	-425	386	73	1442	-771	
307	329	-311	130	125	-203	341	-437	372	14	1448	-789	
308	333	-306	130	133	-208	346	-437	351	-35	1439	-780	
308	334	-309	131	139	-219	356	-452	345	-108	1446	-785	
310	341	-312	131	139	-219	359	-453	321	-173	1445	-774	
312	344	-305	131	139	-214	353	-439	289	-230	1437	-757	
309	340	-316	141	134	-211	353	-438	278	-307	1444	-748	
311	343	-308	133	142	-212	355	-445	262	-380	1438	-714	
311	341	-309	135	143	-219	366	-453	237	-467	1445	-689	
308	345	-310	143	140	-211	360	-445	242	-542	1446	-658	
296	342	-304	133	145	-215	362	-445	230	-624	1438	-603	
275	348	-314	141	145	-216	366	-449	240	-713	1449	-564	
253	339	-311	136	151	-223	373	-424	246	-796	1450	-507	
229	326	-304	138	145	-211	361	-383	255	-863	1446	-450	
204	302	-289	123	149	-210	353	-353	272	-942	1443	-376	
181	221	-276	108	136	-196	324	-308	280	-999	1437	-305	
161	243	-264	99	120	-171	293	-262	300	-1057	1438	-235	
138	208	-245	77	102	-151	222	-227	338	-1119	1442	-158	
94	120	-225	65	75	-113	231	-163	356	-1159	1438	-84	
51	136	-214	54	50	-86	203	-112	398	-1205	1452	-10	
12	86	-130	24	41	-68	179	-56	408	-1228	1439	77	
27	47	-162	18	19	-40	147	-3	440	-1254	1439	164	
61	10	-149	-14	1	-22	126	56	472	-1264	1439	254	
93	-25	-126	-23	-29	17	94	128	492	-1262	1440	342	
123	-63	-117	-42	-50	36	77	155	528	-1260	1451	431	
143	-113	-90	-64	-63	57	53	200	541	-1217	1436	521	
164	-153	-89	-68	-94	92	36	215	571	-1177	1449	582	
182	-183	-70	-93	-102	99	28	238	627	-1105	1442	649	
199	-212	-56	-107	-122	124	-9	220	601	-1016	1439	691	
208	-214	-52	-116	-139	146	-25	293	624	-937	1454	712	
219	-229	-44	-129	-133	149	-30	300	645	-838	1449	731	
225	-232	-34	-136	-149	162	-40	317	653	-727	1444	755	
226	-243	-34	-147	-148	168	-46	329	682	-619	1445	722	
221	-244	-33	-139	-167	186	-61	344	659	-502	1444	683	
212	-244	-27	-147	-160	179	-53	332	673	-371	1440	646	
199	-236	-26	-144	-162	185	-55	338	671	-238	1439	591	
183	-225	-26	-146	-155	178	-53	316	671	-130	1440	551	
162	-219	-32	-136	-159	183	-63	307	658	-17	1443	456	
143	-204	-36	-129	-151	169	-54	287	662	97	1447	380	
120	-190	-39	-130	-137	156	-46	263	649	214	1439	316	
93	-165	-47	-121	-123	134	-28	238	644	313	1439	240	
62	-136	-64	-99	-117	122	-14	198	639	410	1450	155	
27	-102	-68	-96	-107	118	3	148	621	498	1446	68	

Continue



11	-62	-77	-31	-83	35	28	32	612	575	1440	-1
37	-20	-83	-60	-61	37	45	38	600	630	1440	-84
97	33	-112	-42	-61	76	67	-33	504	655	1449	-173
135	76	-129	-22	-55	52	64	-73	564	661	1444	-247
169	114	-143	-19	-35	30	123	-118	549	644	1442	-313
197	148	-166	-5	-14	-9	169	-190	542	591	1447	-329
192	167	-197	27	-7	-24	195	-214	520	549	1449	-468
204	214	-213	40	14	-53	233	-258	502	502	1441	-529
215	252	-235	59	33	-32	270	-305	495	443	1441	-523
236	291	-258	76	53	-112	309	-358	488	379	1450	-644
260	302	-265	86	79	-135	324	-377	470	324	1441	-676
279	307	-270	105	96	-165	342	-397	455	267	1436	-717
291	323	-275	112	113	-184	351	-403	439	214	1437	-776
298	333	-290	131	116	-184	349	-420	425	154	1450	-767
301	337	-291	124	134	-200	361	-428	417	111	1437	-768
306	340	-293	129	137	-208	368	-432	390	55	1438	-775
307	339	-290	131	139	-206	359	-428	364	-3	1438	-781
309	344	-292	130	143	-216	370	-439	350	-60	1439	-772
307	345	-296	133	144	-220	373	-446	330	-129	1438	-763
309	346	-297	131	141	-215	366	-444	306	-195	1444	-757
309	344	-301	141	139	-214	365	-449	290	-271	1447	-746
308	351	-305	136	144	-225	378	-464	280	-352	1440	-710
305	347	-309	141	133	-216	365	-457	258	-431	1447	-694
297	344	-303	127	146	-224	373	-460	253	-517	1443	-653
297	347	-305	136	138	-218	368	-452	240	-595	1439	-613
271	349	-308	136	135	-219	370	-456	243	-686	1453	-576
252	340	-308	130	145	-225	372	-441	234	-757	1438	-510
228	325	-307	132	144	-229	372	-422	256	-839	1436	-452
209	311	-299	126	143	-221	352	-377	265	-909	1442	-388
185	283	-298	117	134	-205	325	-331	294	-975	1438	-319
160	255	-268	101	121	-181	300	-281	303	-1036	1439	-244
127	227	-251	86	100	-156	273	-241	338	-1107	1451	-174
92	183	-227	66	79	-126	247	-201	359	-1148	1439	-93
54	146	-216	54	53	-98	215	-147	389	-1196	1449	-27
17	100	-194	35	33	-71	188	-89	422	-1230	1448	59
-19	47	-172	5	25	-53	169	-28	449	-1253	1442	150
-53	-10	-151	-10	-2	-28	141	45	466	-1265	1439	237
-95	-43	-137	-24	-23	-2	112	110	493	-1276	1449	327
-116	-84	-120	-40	-53	-28	85	155	519	-1262	1446	411
-141	-119	-104	-58	-74	-54	52	196	540	-1234	1448	491
-164	-150	-83	-76	-93	-71	-27	225	556	-1187	1441	568
-132	-185	-69	-96	-107	-97	7	254	574	-1120	1444	624
-197	-200	-57	-110	-120	-102	-3	284	594	-1043	1438	676
-212	-217	-52	-119	-137	-124	-23	305	612	-958	1447	694
-221	-230	-47	-125	-147	-146	-35	324	633	-967	1452	713
-228	-239	-41	-143	-151	-161	-43	345	638	-740	1441	726
-229	-253	-33	-155	-152	-166	-44	336	655	-632	1435	717
-226	-243	-39	-145	-160	-133	-53	347	667	-531	1450	689
-219	-240	-25	-158	-154	-179	-52	340	671	-408	1441	662
-210	-238	-34	-155	-157	-177	-56	330	688	-287	1438	609
-193	-226	-33	-147	-156	-175	-53	315	677	-187	1450	541
-176	-216	-42	-139	-161	-175	-65	312	662	-62	1449	469
-158	-210	-36	-148	-145	-154	-54	272	665	-49	1438	406
-137	-191	-51	-130	-144	-153	-56	264	648	-160	1440	323
-108	-170	-51	-129	-127	-138	-34	229	604	-260	1446	258
-79	-142	-63	-107	-123	-130	-20	192	646	-365	1449	170
-43	-111	-72	-92	-112	-118	-2	158	632	-460	1449	85
-7	-76	-76	-98	-93	-90	23	98	619	-535	1445	9
38	-33	-86	-74	-73	-83	39	50	599	599	1438	-68
81	13	-105	-59	-64	-63	69	-13	589	632	1438	-144
122	69	-131	-31	-62	-60	90	-58	566	643	1448	-236

FREE(A)											
12	128	1	0	0	0	180	-57	413	-1258	166	59
12	107	-196	29	32	-77	166	4	443	-1286	185	148
-27	58	-171	3	24	-58	134	79	459	-1294	200	255
-56	-1	-143	-18	1	-29	107	133	489	-1304	214	352
-98	-47	-123	-39	-19	-2	75	165	519	-1300	240	435
-125	-87	-113	-50	-48	36	46	195	535	-1263	241	526
-152	-120	-102	-67	-72	59	25	216	565	-1236	259	595
-175	-150	-84	-81	-89	79	9	248	582	-1162	265	654
-195	-183	-64	-105	-101	98	-18	292	592	-1081	271	697
-212	-204	-58	-111	-126	126	-20	311	611	-993	274	731
-225	-221	-47	-131	-133	131	-33	332	625	-896	284	744
-240	-238	-43	-143	-145	145	-47	351	639	-785	306	753
-247	-244	-39	-141	-160	168	-46	346	657	-672	316	724
-248	-251	-32	-159	-155	169	-58	354	657	-559	332	689
-244	-241	-40	-146	-167	187	-62	360	663	-427	335	657
-232	-246	-30	-154	-165	192	-56	348	671	-310	354	602
-223	-242	-25	-157	-160	192	-73	332	679	-203	356	542
-207	-240	-34	-158	-157	173	-49	321	672	-93	372	468
-188	-220	-37	-144	-153	171						

Continue



-166	-211	-31	-149	-145	159	-42	312	664	34	367	404
-141	-194	-38	-136	-135	151	-39	280	660	150	375	329
-116	-172	-55	-117	-131	145	-39	256	644	260	374	254
-95	-147	-57	-113	-115	126	-14	209	641	359	374	178
-48	-113	-69	-97	-105	112	-4	161	635	455	373	92
-8	-75	-73	-86	-91	96	20	118	618	538	366	18
-34	-28	-88	-73	-79	79	46	49	606	598	362	-64
77	22	-109	-47	-76	64	66	-13	576	630	358	-150
121	70	-123	-44	-50	40	100	-20	568	651	352	-217
158	112	-145	-26	-35	21	132	-130	556	634	352	-300
180	142	-167	-5	-30	11	151	-162	531	599	334	-374
190	175	-194	10	-9	-18	194	-287	524	543	338	-450
190	211	-223	33	5	-46	224	-252	500	497	330	-516
203	245	-235	45	29	-33	264	-307	491	440	312	-565
222	275	-256	67	52	-118	301	-348	481	375	303	-622
246	288	-266	82	69	-142	318	-371	458	326	276	-661
265	309	-278	102	82	-158	326	-362	442	260	263	-699
282	317	-293	118	99	-173	337	-402	430	201	258	-732
289	325	-292	117	119	-189	350	-422	411	141	239	-747
295	332	-294	122	129	-194	357	-427	406	94	214	-754
300	342	-301	133	123	-197	356	-429	383	29	203	-776
299	335	-302	130	130	-204	353	-446	358	-24	176	-739
301	334	-299	122	140	-215	359	-440	340	-84	147	-783
300	339	-307	133	136	-213	359	-447	327	-157	135	-787
303	340	-305	131	139	-209	358	-438	298	-213	109	-772
302	334	-302	127	145	-221	366	-452	283	-289	91	-755
302	339	-306	127	145	-222	368	-444	269	-366	80	-739
299	340	-305	127	142	-219	363	-446	248	-434	64	-707
293	342	-305	125	142	-221	368	-448	239	-517	56	-673
285	346	-311	135	135	-212	361	-443	236	-604	59	-640
268	348	-316	134	139	-218	362	-445	232	-684	59	-596
251	342	-313	134	133	-215	362	-405	237	-763	63	-550
230	328	-316	139	135	-215	360	-419	244	-936	63	-489
210	310	-303	123	141	-217	351	-385	262	-916	71	-422
185	289	-293	124	125	-197	330	-341	282	-990	84	-353
158	255	-268	103	115	-178	298	-307	290	-1043	81	-274
125	212	-254	37	95	-153	223	-250	322	-1113	101	-205
91	183	-234	64	86	-133	251	-196	337	-1156	105	-109
49	145	-218	53	54	-100	224	-147	374	-1212	139	-35
13	97	-195	28	49	-96	195	-88	398	-1242	145	59
-23	65	-180	9	29	-64	168	-39	437	-1282	172	141
-58	31	-162	-8	9	-36	136	22	462	-1299	197	233
-90	-1	-138	-27	-11	-10	110	79	469	-1303	218	324
-121	-40	-123	-43	-40	27	73	143	500	-1285	227	424
-131	-82	-103	-58	-63	56	50	191	527	-1262	241	514
-172	-134	-88	-75	-83	74	30	213	545	-1223	250	585
-192	-175	-83	-87	-102	91	12	252	573	-1178	273	632
-204	-202	-64	-97	-122	118	-10	283	583	-1103	280	679
-217	-220	-52	-119	-124	125	-12	301	614	-1024	285	716
-227	-228	-49	-127	-142	146	-37	331	625	-932	302	723
-230	-242	-39	-139	-145	155	-38	353	644	-824	301	735
-235	-246	-42	-141	-153	172	-49	362	649	-706	318	711
-232	-252	-34	-147	-161	186	-56	368	656	-596	320	688
-225	-251	-28	-150	-157	193	-52	355	670	-485	322	646
-214	-242	-28	-148	-161	187	-59	352	678	-354	326	598
-201	-239	-25	-150	-152	175	-55	337	671	-230	313	552
-184	-226	-23	-149	-150	169	-54	324	669	-114	314	487
-166	-212	-38	-139	-151	171	-54	305	649	-3	333	400
-146	-198	-38	-141	-138	151	-39	276	665	112	330	342
-117	-179	-46	-124	-136	153	-41	253	656	217	347	256
-88	-155	-57	-111	-125	138	-18	212	650	333	351	178
-56	-123	-61	-101	-111	129	-8	181	631	430	348	93
-17	-88	-70	-96	-95	103	-20	170	620	510	338	26
-27	-43	-88	-73	-89	95	-34	61	605	576	337	-56
69	2	-100	-60	-74	78	-53	-71	588	619	338	-139
112	50	-122	-43	-57	51	-89	-62	584	628	342	-218
146	91	-135	-32	-43	34	112	-116	554	633	335	-282
169	123	-161	-3	-37	18	132	-163	555	587	344	-367
184	173	-186	18	-18	-6	178	-207	526	541	345	-437
193	202	-214	40	1	-36	208	-242	508	493	339	-501
202	232	-232	54	-20	-68	249	-308	491	440	321	-549
222	268	-254	69	44	-104	279	-330	475	379	306	-598
243	290	-269	93	55	-122	304	-366	548	310	303	-650
264	296	-275	98	87	-160	326	-388	453	258	272	-672
278	317	-290	115	106	-180	338	-403	442	198	259	-708
288	323	-299	127	112	-183	339	-407	426	142	246	-737
292	322	-295	125	126	-203	353	-428	410	92	214	-744
296	332	-300	134	129	-200	344	-417	383	46	195	-769
299	334	-306	136	130	-202	347	-422	363	-6	170	-775
299	339	-306	132	134	-210	350	-433	345	-71	145	-785
298	334	-314	136	134	-210	349	-438	324	-130	119	-787
302	337	-301	131	145	-219	363	-442	311	-192	92	-768
100	338	-300	138	130	-217	344	-439	288	-240	74	-744

Continue

344	334	-307	129	143	-217	349	-438	254	-403	44	-723
299	339	-309	130	143	-217	357	-438	254	-403	44	-723
300	341	-313	131	147	-223	369	-457	254	-493	46	-700
291	342	-309	127	149	-226	365	-448	236	-564	36	-658
282	349	-311	129	147	-220	366	-444	233	-641	27	-608
261	341	-309	129	147	-220	362	-435	233	-724	35	-556
239	340	-321	135	142	-222	365	-431	245	-811	51	-510
214	316	-303	126	144	-223	355	-395	250	-880	47	-438
191	289	-294	125	130	-207	330	-361	268	-958	67	-382
164	263	-278	108	126	-189	301	-312	281	-1013	75	-298
133	239	-265	39	104	-166	274	-278	315	-1088	101	-224
104	211	-247	78	83	-130	243	-220	335	-1141	124	-146
70	171	-229	58	64	-106	221	-162	360	-1186	139	-43
33	125	-210	44	45	-79	198	-93	391	-1217	149	-22
-4	71	-189	22	28	-59	124	-22	416	-1259	175	104
-32	10	-166	-3	17	-42	156	36	449	-1278	188	215
-69	-28	-149	-21	-3	-14	122	101	464	-1279	206	314
-101	-64	-135	-32	-29	-13	92	135	499	-1289	230	405
-128	-36	-119	-43	-56	44	72	123	522	-1276	254	482
-148	-125	-95	-59	-77	72	45	212	540	-1234	261	575
-170	-151	-82	-75	-97	95	24	239	564	-1186	283	636
-190	-182	-73	-91	-113	114	27	268	577	-1113	287	685
-207	-205	-54	-115	-118	125	9	295	602	-1031	293	730
-217	-221	-58	-121	-131	146	28	324	616	-940	311	742
-226	-233	-45	-130	-143	159	36	340	635	-849	328	739
-229	-245	-32	-150	-142	162	41	352	646	-725	334	736
-229	-241	-38	-142	-159	178	52	365	650	-609	351	704

FREE(A)

-12	128	-1	0	0	0	-367	-373	253	-852	60	-489
234	340	-318	146	126	-208	361	-361	239	-887	66	-471
230	324	-308	143	145	-210	361	-361	239	-887	66	-471
206	303	-304	136	139	-198	336	-323	252	-964	79	-400
179	273	-282	121	134	-186	320	-311	275	-1027	81	-314
149	250	-264	106	119	-159	292	-276	300	-1090	106	-247
116	227	-239	80	110	-140	273	-230	305	-1131	105	-151
82	198	-223	65	85	-115	254	-174	355	-1185	133	-76
46	155	-199	38	68	-90	225	-98	371	-1205	139	16
14	109	-183	31	39	-55	191	62	402	-1235	168	99
-20	52	-164	5	27	-40	163	-81	427	-1255	186	190
-56	-2	-151	-16	2	-13	129	107	452	-1264	205	284
-82	-51	-131	-31	-20	-21	98	151	478	-1263	216	384
-118	-90	-117	-49	-42	40	83	182	510	-1251	228	478
-139	-113	-107	-54	-71	75	51	223	526	-1226	254	545
-159	-139	-78	-76	-20	91	42	252	551	-1176	259	623
-176	-167	-69	-85	-106	118	15	284	568	-1111	267	672
-193	-187	-63	-96	-120	136	-6	309	591	-1042	279	707
-204	-205	-59	-110	-131	151	-19	330	602	-947	278	735
-212	-217	-43	-122	-140	162	-30	349	617	-937	280	745
-216	-225	-37	-138	-145	178	-38	370	629	-717	286	745
-215	-227	-34	-138	-153	188	-40	373	641	-607	293	719
-210	-233	-27	-148	-151	196	-46	376	646	-478	287	688
-203	-226	-29	-151	-148	183	-38	363	663	-359	297	640
-195	-223	-27	-152	-149	188	-45	362	656	-230	295	581
-178	-215	-26	-153	-145	177	-37	342	662	-128	308	516
-159	-203	-30	-143	-143	172	-39	324	663	-11	317	442
-135	-190	-32	-130	-144	176	-37	315	646	114	320	361
-113	-168	-41	-126	-126	155	-19	278	645	209	329	286
-87	-152	-55	-106	-125	157	-19	248	635	313	340	198
-53	-126	-55	-96	-104	137	-3	202	632	406	335	124
-17	-94	-65	-84	-93	129	10	168	608	494	340	31
-24	-49	-79	-69	-79	110	-32	102	599	549	356	-59
-66	-9	-95	-51	-65	89	61	27	586	593	351	-125
106	30	-111	-35	-60	76	-80	-8	560	626	355	-207
143	80	-130	-25	-45	59	-110	-66	474	624	358	-277
168	112	-152	-8	-31	43	-132	-112	525	586	368	-350
186	152	-181	15	-14	19	-165	-158	511	551	366	-417
198	188	-199	30	7	-13	-200	-198	490	506	358	-476
202	220	-232	56	22	-44	239	-239	482	448	365	-541
221	266	-244	71	39	-83	282	-282	475	397	357	-587
246	288	-255	80	62	-108	300	-316	448	348	338	-633
269	307	-274	96	79	-142	322	-348	440	297	307	-654
286	319	-277	114	91	-150	326	-360	422	243	292	-700
295	330	-286	129	110	-171	346	-385	417	188	259	-714
302	344	-297	137	120	-178	348	-390	398	136	233	-735
307	336	-290	129	137	-187	353	-393	369	101	199	-758
312	341	-289	132	140	-194	359	-398	351	54	177	-749
310	344	-293	131	142	-196	359	-399	329	-3	146	-746
312	344	-300	135	145	-205	369	-415	324	-74	130	-747
312	348	-303	142	143	-199	364	-409	292	-132	104	-749
315	349	-298	135	145	-206	370	-415	268	-198	72	-733
315	351	-301	138	150	-209	379	-421	268	-283	62	-725
312	351	-305	146	142	-206	372	-415	240	-359	51	-716

Continue



314	348	-300	140	146	-202	323	-414	228	-433	27	-687
307	363	-308	146	142	-199	328	-419	231	-524	33	-664
293	360	-310	145	143	-203	374	-418	220	-604	21	-653
276	355	-315	145	141	-206	376	-420	226	-696	22	-587
260	349	-307	137	148	-207	384	-408	232	-771	25	-529
235	328	-300	138	147	-206	371	-370	229	-844	34	-479
212	308	-298	135	146	-207	366	-356	254	-922	42	-399
188	282	-289	128	131	-183	340	-295	276	-197	67	-358
159	253	-269	104	122	-170	314	-243	398	-1053	81	-251
129	231	-256	88	97	-136	271	-182	312	-1116	112	-177
98	197	-229	63	82	-116	242	-136	341	-1162	132	-86
61	162	-212	50	62	-96	223	-86	368	-1202	156	-5
20	126	-194	27	41	-75	192	-33	394	-1233	180	-79
-19	90	-173	10	20	-48	162	21	419	-1253	208	-169
-57	48	-152	-8	-3	-19	129	77	445	-1266	230	-266
-91	-3	-147	-29	-26	12	93	140	463	-1259	247	-351
-118	-62	-133	-41	-49	38	73	181	494	-1256	264	-446
-139	-111	-113	-68	-60	53	56	216	514	-1228	269	-527
-158	-151	-99	-84	-79	81	31	253	531	-1175	268	-599
-128	-177	-85	-95	-102	104	12	274	561	-1126	277	-654
-196	-200	-67	-109	-115	119	7	306	570	-1045	271	-697
-212	-215	-63	-116	-134	141	-19	318	597	-976	278	-711
-223	-226	-49	-130	-139	157	-30	332	612	-874	272	-733
-228	-243	-39	-150	-143	169	-41	350	619	-746	256	-734
-227	-239	-45	-149	-152	180	-45	349	640	-644	259	-713
-224	-244	-31	-157	-151	185	-51	362	635	-518	238	-696
-212	-242	-35	-152	-159	185	-54	349	641	-399	249	-645
-210	-237	-34	-158	-154	178	-58	353	643	-272	246	-601
-192	-231	-31	-157	-152	179	-58	344	641	-163	250	-535
-174	-221	-35	-150	-149	168	-44	322	650	-52	255	-473
-151	-205	-33	-154	-140	158	-41	305	640	-69	263	-396
-125	-187	-48	-133	-139	163	-39	283	639	165	290	-310
-99	-169	-55	-133	-120	142	-26	254	621	280	291	-244
-70	-150	-56	-123	-107	127	-8	212	613	379	300	-154
-34	-112	-68	-108	-91	115	8	185	604	455	314	-70
2	-75	-87	-85	-89	106	20	122	590	522	338	-30
42	-32	-99	-79	-69	91	49	58	562	574	336	-98
84	17	-119	-54	-63	62	74	-1	564	602	344	-184
122	60	-141	-28	-59	57	85	-45	538	610	356	-262
151	100	-161	-11	-44	37	119	-93	528	585	370	-333
169	137	-179	1	-26	14	150	-132	506	555	369	-404
175	174	-207	12	-7	-22	196	-192	489	522	355	-459
190	211	-230	29	14	-49	235	-243	473	483	347	-519
206	247	-253	47	21	-70	268	-270	458	426	337	-576
234	278	-264	62	49	-101	298	-348	456	366	326	-616
257	295	-280	91	55	-121	313	-367	435	315	310	-663
276	310	-286	98	88	-157	333	-388	412	262	278	-683
288	312	-285	109	109	-175	342	-399	406	211	256	-709
298	332	-289	121	120	-191	345	-405	389	157	239	-737
304	335	-296	127	130	-187	350	-412	383	107	211	-740
308	336	-299	135	129	-191	354	-423	361	46	193	-761
308	344	-307	138	132	-196	361	-433	344	-10	158	-765
315	345	-297	129	149	-208	371	-454	326	-68	122	-752
312	347	-303	140	140	-197	362	-436	300	-131	106	-756
311	349	-304	144	138	-201	367	-442	288	-210	92	-757
312	350	-304	135	148	-208	372	-440	267	-275	63	-734
313	348	-299	152	152	-214	378	-434	245	-346	51	-716
310	352	-303	136	153	-219	383	-440	238	-440	44	-698
306	353	-308	141	145	-210	382	-441	228	-520	41	-677
295	355	-305	143	143	-210	380	-438	203	-606	37	-640
276	350	-307	141	147	-210	372	-433	218	-681	29	-597
253	336	-303	133	154	-217	389	-426	225	-767	22	-536
233	314	-300	134	152	-218	385	-398	235	-845	25	-479
214	302	-293	128	144	-209	363	-336	241	-921	36	-417
193	283	-285	119	129	-189	334	-284	257	-988	53	-349
167	259	-267	109	113	-167	308	-241	280	-1050	69	-275
133	234	-249	90	101	-140	276	-205	313	-1121	98	-199
93	190	-225	66	92	-124	257	-171	336	-1162	103	-103
56	157	-208	56	67	-89	225	-127	359	-1202	127	-27
17	119	-192	41	44	-63	196	-72	388	-1239	149	-52
-15	74	-168	12	35	-43	176	-7	420	-1271	163	-147
-46	29	-154	-2	8	-18	156	67	455	-1294	192	-239
-75	-24	-135	-19	-17	14	122	138	471	-1285	206	-333
-104	-67	-114	-46	-27	29	105	187	495	-1270	212	-434
-130	-107	-100	-52	-60	66	77	222	553	-1250	235	-513

FIXED	12	128	1	0	0	0	0	0	0	0	0
272	346	-313	142	139	-193	368	-497	144	732	-772	-783
278	345	-311	137	150	-201	376	-504	157	636	-820	-773
281	348	-311	139	151	-204	377	-507	160	536	-855	-762
280	349	-311	139	150	-204	377	-510	161	431	-893	-739

Continue

279	350	-322	147	139	-197	372	-509	162	305	-908	-724
280	350	-316	138	151	-207	376	-514	166	166	-922	-692
278	351	-317	144	145	-197	320	-506	165	19	-918	-664
266	352	-318	143	144	-199	321	-512	174	-138	-909	-627
253	355	-319	145	142	-200	320	-512	176	-285	-891	-582
250	349	-317	144	147	-209	383	-516	185	-443	-863	-526
203	328	-323	135	146	-211	369	-495	129	-592	-833	-470
174	297	-312	128	147	-209	349	-451	178	-754	-790	-403
142	275	-303	124	126	-188	312	-406	129	-905	-733	-336
110	236	-285	103	117	-169	290	-360	190	-1053	-667	-261
76	204	-255	80	94	-139	254	-303	180	-1172	-614	-178
42	168	-240	65	72	-112	226	-259	183	-1298	-543	-96
5	130	-224	44	51	-84	206	-209	191	-1419	-469	-5
-33	86	-209	27	25	-54	172	-139	186	-1482	-393	75
-62	38	-189	10	5	-26	141	-69	183	-1508	-318	161
-101	-6	-160	-22	-3	-11	120	-5	182	-1517	-249	265
-135	-40	-150	-31	-35	22	92	53	110	-1524	-170	353
-165	-73	-126	-59	-50	41	74	96	176	-1524	-96	451
-182	-105	-116	-70	-77	69	46	126	175	-1526	-25	533
-204	-148	-90	-91	-90	91	24	149	168	-1522	42	614
-220	-182	-90	-92	-117	118	-16	180	158	-1518	107	663
-233	-206	-73	-104	-131	137	-19	202	150	-1517	165	712
-244	-225	-65	-115	-140	152	-35	231	156	-1519	224	729
-252	-232	-61	-131	-147	166	-39	244	162	-1522	284	737
-259	-241	-57	-136	-156	188	-49	269	152	-1496	328	723
-256	-248	-42	-152	-151	191	-54	274	152	-1431	364	713
-251	-249	-43	-156	-152	193	-55	270	152	-1356	402	684
-245	-247	-42	-153	-155	189	-58	269	162	-1250	428	642
-234	-240	-42	-143	-164	195	-67	272	152	-1130	446	586
-220	-234	-42	-142	-162	195	-70	268	154	-1010	457	529
-202	-223	-42	-146	-153	175	-68	247	154	-875	457	465
-182	-209	-44	-142	-140	162	-54	226	158	-739	458	397
-159	-191	-52	-131	-140	163	-55	209	151	-588	455	315
-134	-175	-60	-122	-127	148	-44	180	148	-438	425	251
-110	-152	-73	-105	-123	146	-39	204	147	-293	404	171
-79	-125	-78	-101	-108	121	-10	97	159	-157	381	85
-43	-89	-85	-80	-104	116	3	60	130	-8	345	5
-8	-42	-100	-78	-84	35	-28	9	152	136	292	-62
33	-3	-116	-62	-69	73	-52	-50	149	272	245	-151
68	35	-132	-50	-54	62	-81	-115	150	391	190	-228
102	80	-161	-25	-45	47	105	-161	144	498	133	-304
125	112	-177	-9	-31	26	128	-203	141	608	53	-369
146	161	-202	14	-14	-1	167	-256	132	698	-7	-440
157	209	-230	32	8	-41	219	-321	141	760	-73	-506
174	243	-244	44	27	-70	254	-413	130	803	-159	-554
192	276	-274	76	36	-89	281	-413	128	817	-232	-611
220	299	-281	87	64	-124	312	-449	128	825	-316	-647
240	307	-293	107	77	-147	328	-469	132	818	-384	-690
252	319	-296	113	104	-173	343	-481	129	822	-461	-730
262	329	-309	132	109	-175	341	-484	126	833	-535	-756
268	335	-306	128	126	-189	352	-495	137	837	-609	-764
273	340	-308	126	135	-196	361	-507	138	815	-661	-792
274	344	-317	140	131	-194	358	-509	132	794	-725	-790
274	345	-313	139	135	-194	360	-506	138	736	-774	-788
275	343	-320	142	135	-200	362	-516	143	658	-815	-791
275	345	-315	138	137	-204	371	-525	149	570	-859	-771
277	349	-314	143	136	-198	368	-518	154	467	-888	-761
273	349	-316	141	140	-202	368	-518	160	340	-910	-742
274	343	-315	133	146	-212	376	-527	165	207	-921	-716
276	351	-319	142	137	-202	370	-517	165	68	-924	-689
276	353	-328	145	137	-202	379	-521	173	-82	-912	-660
267	354	-319	135	145	-208	376	-528	175	-230	-904	-610
249	345	-315	137	151	-213	381	-529	184	-392	-866	-563
222	337	-312	138	150	-210	378	-505	185	-543	-835	-504
192	324	-301	132	149	-211	372	-471	195	-701	-792	-437
164	300	-293	131	131	-190	340	-406	191	-848	-734	-376
135	275	-273	113	113	-167	309	-340	190	-985	-684	-283
104	257	-255	92	114	-152	289	-295	198	-1124	-624	-199
71	198	-241	80	84	-116	253	-248	195	-1245	-556	-112
32	157	-218	53	73	-89	227	-206	201	-1370	-481	-36
-9	115	-199	34	52	-65	196	-153	191	-1452	-423	57
-49	77	-177	26	22	-31	161	-82	188	-1489	-347	132
-85	40	-159	7	-1	-2	128	-11	186	-1511	-265	220
-116	-16	-134	-25	-15	19	107	35	187	-1519	-189	320
-142	-64	-125	-34	-39	46	82	59	189	-1526	-116	411
-164	-112	-109	-59	-53	65	61	106	181	-1518	-55	505
-185	-149	-97	-66	-83	101	29	146	158	-1516	14	586
-205	-124	-84	-76	-103	120	10	177	170	-1519	90	652
-221	-198	-62	-98	-108	123	5	200	175	-1525	158	699
-236	-210	-55	-106	-133	142	-18	246	163	-1518	204	733
-247	-225	-54	-119	-145	157	-32	249	159	-1516	256	756
-254	-235	-47	-133	-147	166	-41	258	128	-1519	315	747
-256	-244	-45	-139	-157	182	-53	265	160	-1466	351	734

Continue



-253	-254	-39	-154	-150	-133	-55	259	155	-1588	380	710
-249	-256	-39	-147	-160	-190	-58	262	168	-1304	422	663
-243	-245	-36	-154	-157	-187	-58	253	164	-1189	439	613
-229	-232	-45	-142	-161	-194	-69	255	160	-1068	451	553
-212	-226	-40	-148	-152	-179	-56	233	166	-951	467	489
-196	-212	-41	-144	-146	-171	-52	219	162	-814	469	418
-175	-202	-47	-134	-144	-163	-49	196	157	-662	448	355
-156	-180	-62	-115	-141	-166	-48	173	155	-520	439	275
-124	-161	-60	-109	-126	-153	-36	144	151	-366	411	205
-95	-136	-73	-94	-122	-144	-25	103	148	-220	390	117
-61	-103	-78	-82	-99	-115	8	45	162	-80	352	29
-23	-70	-87	-91	-97	-104	22	-1	155	67	299	-43
15	-29	-103	-71	-74	79	47	-54	155	197	254	-131
54	18	-126	-51	-69	69	62	-102	148	327	205	-211
86	62	-144	-41	-51	44	122	-159	148	446	147	-285
113	112	-176	-17	-42	22	122	-207	138	550	86	-360
130	144	-189	-14	-15	-15	160	-318	139	641	12	-421
146	184	-216	5	-1	-41	197	-324	135	723	-58	-482
164	223	-246	30	16	-65	230	-372	125	794	-133	-540
185	256	-268	46	36	-99	275	-438	133	807	-205	-603
208	280	-284	67	56	-125	301	-473	129	816	-279	-649
231	299	-300	91	73	-146	314	-484	120	832	-363	-683
244	310	-304	101	93	-175	335	-508	132	824	-426	-722
253	320	-311	121	97	-178	332	-512	120	830	-504	-749
258	322	-313	114	119	-196	346	-523	125	835	-578	-762
262	333	-323	129	121	-197	345	-519	126	827	-636	-783
266	332	-323	131	121	-202	353	-532	133	791	-689	-800
266	335	-327	135	123	-202	353	-534	132	743	-741	-798
268	338	-322	133	132	-209	367	-546	148	678	-787	-794
268	339	-321	134	131	-203	353	-549	142	597	-841	-776
269	342	-329	138	128	-207	365	-549	155	485	-865	-776
270	341	-322	132	134	-210	361	-541	147	383	-905	-744
272	345	-316	131	143	-215	373	-552	166	246	-912	-726
271	346	-325	134	142	-217	375	-542	171	109	-910	-709
270	354	-333	144	131	-206	365	-538	170	37	-907	-677
265	358	-326	145	139	-209	378	-541	184	-190	-889	-633
245	350	-330	147	137	-207	376	-535	182	-337	-875	-584
222	336	-325	142	142	-211	380	-536	193	-496	-842	-530
195	316	-318	143	140	-204	364	-489	184	-639	-813	-463
163	280	-297	130	144	-204	355	-449	194	-797	-766	-383
139	254	-282	113	131	-197	320	-390	108	-936	-718	-308

FIXED(A)

-12	-128	1	0	0	0	-12	-128	1	0	0	0
-217	-164	-103	-90	-105	69	26	117	166	-1522	53	618
-232	-199	-77	-102	-129	-118	-25	-552	167	-1519	121	676
-246	-219	-62	-116	-142	-131	-16	174	152	-1515	171	716
-257	-227	-61	-127	-145	-143	-22	-491	165	-1531	240	732
-262	-243	-55	-130	-151	-159	-36	200	150	-1514	266	741
-265		-54	-139	-164	-173	-46	220	153	-1508	320	717
-268	-254	-47	-143	-172	-180	-50	220	159	-1445	345	707
-264	-255	-45	-149	-172	-190	-59	226	142	-1362	373	673
-258	-243	-41	-153	-164	-135	-55	219	147	-1251	397	628
-242	-240	-36	-154	-164	-130	-51	214	155	-1142	416	575
-232	-231	-41	-148	-161	-177	-49	194	156	-1018	421	511
-214	-212	-46	-135	-167	-182	-52	186	106	-930	433	439
-191	-202	-46	-133	-154	-172	-49	170	114	-729	422	375
-162	-191	-54	-124	-149	-165	-46	148	150	-587	411	310
-140	-163	-67	-111	-144	-151	-30	124	148	-433	394	227
-111	-147	-77	-101	-132	-136	-22	86	142	-297	363	152
-79	-115	-83	-99	-113	-106	4	29	136	-157	336	84
-46	-82	-96	-76	-113	-101	11	-14	142	-1	296	-13
-2	-37	-114	-70	-96	77	44	-92	150	130	245	-105
38	15	-124	-63	-90	58	68	-156	142	263	187	-127
76	51	-156	-38	-71	45	86	-206	127	390	123	-252
103	93	-172	-20	-63	27	113	-259	110	498	68	-326
123	134	-199	-13	-34	-18	154	-316	126	595	9	-398
139	181	-227	14	-21	-39	191	-367	131	688	-53	-473
154	213	-247	35	-5	-70	236	-421	122	770	-173	-522
171	247	-268	45	15	-99	273	-478	124	802	-202	-583
194	273	-286	64	33	-119	302	-512	124	817	-275	-676
215	281	-302	88	43	-136	315	-522	126	817	-337	-689
230	295	-308	99	67	-167	328	-528	121	828	-431	-718
240	310	-314	109	85	-181	332	-526	119	835	-504	-753
244	318	-325	122	90	-192	341	-536	125	830	-571	-783
244	319	-328	119	100	-206	342	-544	125	812	-642	-792
249	322	-325	116	115	-218	356	-552	128	769	-701	-810
249	327	-329	121	111	-215	351	-552	136	714	-754	-817
250	322	-325	119	123	-226	362	-559	135	649	-813	-806
253	331	-330	124	115	-217	353	-554	140	570	-859	-793
254	333	-325	123	125	-227	368	-555	150	466	-893	-788
256	336	-329	127	126	-228	372	-565	159	354	-904	-766
259	338	-329	134	124	-216	365	-548	151	241	-923	-735

Continue

256	336	-323	127	132	-228	-378	-537	166	96	-916	-712
255	343	-335	138	125	-221	-370	-547	162	-32	-921	-674
242	343	-325	125	133	-229	-378	-554	120	-181	-909	-629
234	344	-327	128	136	-229	386	-558	180	-376	-982	-595
210	334	-331	133	125	-220	-326	-543	125	-496	-854	-525
185	313	-331	134	124	-215	359	-511	175	-637	-912	-467
152	289	-320	121	126	-216	-349	-469	183	-795	-754	-403
132	230	-294	104	117	-198	319	-403	137	-934	-704	-313
103	254	-279	37	101	-176	-282	-344	139	-1069	-642	-237
72	230	-262	37	76	-138	251	-287	131	-1192	-581	-155
-36	133	-240	61	54	-111	-235	-258	188	-1323	-504	-78
-1	151	-225	45	73	-81	-201	-212	126	-1416	-444	11
-38	105	-200	17	23	-64	-183	-164	183	-1479	-372	98
-29	55	-192	-3	3	-43	-154	-97	132	-1508	-216	176
-111	-3	-169	-24	-16	-10	123	-24	181	-1520	-219	261
-144	-52	-164	-5	-45	16	84	33	165	-1513	-160	356
-123	-103	-149	-31	-72	42	-63	129	165	-1517	-38	440
-194	-144	-135	-70	-20	64	-38	107	162	-1514	-32	532
-211	-122	-107	-81	-109	86	12	136	157	-1515	27	602
-232	-194	-92	-76	-131	107	-2	156	156	-1517	38	666
-246	-220	-71	-117	-135	117	-11	126	159	-1520	142	709
-258	-232	-62	-127	-143	134	-26	208	152	-1519	197	733
-268	-246	-54	-143	-152	145	-32	218	155	-1523	245	743
-271	-258	-54	-145	-173	173	-53	237	147	-1505	290	737
-270	-265	-44	-162	-164	170	-49	226	156	-1465	329	709
-269	-268	-42	-165	-167	174	-54	225	153	-1384	358	682
-261	-258	-48	-157	-178	187	-64	229	152	-1286	391	631
-255	-253	-49	-157	-181	133	-65	226	147	-1169	416	599
-241	-242	-44	-161	-167	168	-54	219	162	-1058	428	529
-225	-232	-41	-155	-164	168	-57	202	153	-920	425	472
-205	-230	-44	-153	-154	162	-50	183	157	-786	435	401
-187	-204	-53	-145	-140	151	-42	155	153	-646	422	333
-159	-136	-67	-73	-146	149	-40	133	145	-495	339	268
-132	-163	-70	-15	-14	141	-28	101	147	-348	378	190
-99	-140	-78	-113	-123	118	-6	55	152	-201	341	111
-65	-103	-92	-17	-110	105	6	13	147	-64	306	28
-26	-60	-113	-75	-106	86	28	-45	141	80	258	-54
13	-16	-121	-64	-62	67	57	-104	147	195	221	-40
52	31	-140	-49	-84	50	74	-155	117	330	156	-209
88	73	-155	-35	-65	28	107	-219	136	438	14	-295
115	114	-190	-19	-45	-6	151	-280	142	536	35	-362
132	151	-205	2	-32	-33	184	-326	133	636	-42	-425
143	194	-227	16	-9	-64	221	-384	136	704	-95	-503
160	229	-261	44	3	-89	260	-439	132	777	-165	-563
179	255	-277	54	26	-118	293	-487	126	813	-250	-611
202	278	-291	74	46	-142	315	-518	131	815	-313	-662
223	298	-314	100	59	-160	322	-526	125	833	-393	-702
234	307	-320	108	91	-182	335	-540	137	837	-464	-730
239	316	-319	114	90	-192	338	-548	125	834	-537	-758
246	317	-318	111	109	-211	355	-560	136	813	-601	-781
248	321	-331	124	102	-207	349	-571	134	778	-661	-808
250	324	-333	128	106	-214	355	-564	135	735	-730	-798
252	330	-331	129	115	-217	357	-565	129	669	-781	-802
252	333	-331	127	116	-223	369	-569	146	586	-827	-788
255	337	-336	131	115	-217	364	-571	152	483	-855	-785
253	333	-336	128	114	-218	359	-555	155	365	-879	-775
254	334	-339	130	116	-222	365	-575	161	241	-892	-751
254	338	-335	129	121	-220	363	-570	166	122	-911	-715
254	337	-334	131	117	-218	363	-572	159	-20	-913	-683
244	332	-333	123	120	-228	365	-578	159	-172	-907	-643
237	340	-333	126	127	-231	378	-572	180	-333	-879	-604
207	337	-332	125	124	-230	377	-571	180	-484	-856	-347
182	312	-338	129	119	-222	359	-535	184	-626	-830	-469
155	298	-333	125	113	-214	348	-490	171	-780	-798	-421
128	280	-323	116	105	-201	324	-449	194	-936	-726	-361
102	247	-303	101	92	-177	293	-413	179	-1063	-677	-281
22	222	-270	74	82	-155	267	-345	184	-1195	-621	-193
40	194	-249	63	59	-128	244	-302	197	-1324	-545	-122
35	159	-232	40	47	-108	229	-258	175	-1420	-494	-26
67	120	-218	26	15	-73	186	-194	178	-1490	-405	45
96	89	-201	10	0	-45	152	-124	175	-1505	-334	131
128	17	-176	-15	-8	-27	132	-79	182	-1518	-261	222
152	-35	-168	-20	-38	-9	95	-123	129	-1522	-186	306
177	-79	-149	-40	-56	39	70	36	172	-1516	-124	413
206	-117	-132	-55	-72	64	33	67	128	-1527	-44	489
212	-147	-106	-79	-87	89	32	178	162	-1517	10	567
235	-173	-100	-81	-114	113	15	134	160	-1516	70	625
249	-195	-76	-101	-120	126	-1	157	161	-1523	133	673
258	-224	-58	-112	-134	139	-12	172	165	-1524	185	713
265	-237	-57	-123	-146	151	-27	205	160	-1522	234	725
267	-242	-48	-135	-157	168	-42	232	153	-1514	272	732
	-249	-55	-137	-171	184	-53	246	151	-1495	317	712

Continue



-262	-251	-44	-154	-163	181	-49	248	155	-1435	347	691
-261	-250	-40	-154	-165	182	-50	244	161	-1353	394	647
-253	-251	-36	-150	-169	186	-52	248	153	-1233	395	614
-241	-239	-35	-145	-166	197	-54	240	164	-1128	420	554
-227	-232	-40	-147	-164	176	-50	225	162	-1006	424	496
-207	-219	-44	-146	-155	166	-45	212	159	-971	426	450
-184	-200	-55	-129	-162	172	-52	200	148	-721	412	364

FIXED(A)

12	129	1	0	0	0	371	-584	144	576	-866	-776
258	337	-323	135	122	-209	370	-581	152	456	-398	-711
260	337	-323	139	113	-206	324	-587	162	327	-913	-755
258	336	-327	137	120	-212	378	-591	166	202	-323	-716
258	341	-327	135	123	-216	371	-578	154	76	-935	-704
257	342	-325	136	121	-211	366	-584	157	-69	-929	-676
254	341	-333	140	116	-210	371	-588	164	-217	-916	-642
249	344	-331	138	117	-211	384	-601	180	-386	-894	-599
231	341	-328	130	129	-223	329	-586	179	-541	-868	-547
204	332	-328	127	123	-228	371	-558	190	-695	-930	-490
181	321	-325	125	126	-229	346	-508	179	-845	-784	-421
154	298	-310	119	116	-211	325	-457	180	-391	-737	-340
124	256	-296	105	113	-203	284	-396	179	-1128	-683	-250
91	229	-272	92	92	-170	261	-356	185	-1264	-619	-182
60	192	-256	75	71	-145	232	-315	191	-1377	-565	-86
26	164	-242	53	52	-119	208	-273	202	-1465	-494	-11
9	123	-227	42	27	-85	186	-230	183	-1504	-417	66
46	77	-208	21	9	-66	154	-164	179	-1520	-344	156
36	27	-186	2	-14	-40	126	-88	176	-1523	-274	244
121	31	-162	-20	-33	-18	92	-18	163	-1513	-217	349
150	74	-149	-35	-57	13	27	38	168	-1512	-145	432
172	108	-128	-56	-72	36	62	68	170	-1523	-68	504
198	139	-114	-79	-87	52	34	92	164	-1528	3	573
218	168	-102	-83	-117	82	12	156	157	-1517	59	639
232	191	-91	-94	-134	106	6	140	150	-1514	107	693
248	212	-82	-108	-142	117	24	164	150	-1516	174	725
260	230	-69	-117	-161	142	32	192	153	-1523	235	736
268	236	-64	-128	-169	158	33	189	160	-1522	295	743
272	250	-50	-146	-161	155	43	200	153	-1472	312	747
270	254	-50	-152	-167	169	46	196	141	-1408	356	720
265	254	-47	-158	-170	174	56	204	150	-1305	373	694
257	252	-43	-145	-182	189	52	187	161	-1200	409	639
252	247	-44	-155	-176	172	47	192	158	-1072	422	583
240	240	-39	-156	-170	169	55	181	148	-935	416	523
224	229	-54	-141	-180	175	46	145	147	-651	409	376
204	216	-49	-144	-166	165	32	115	153	-509	402	282
184	201	-57	-132	-164	160	22	78	150	-359	374	145
153	179	-61	-124	-152	151	4	51	149	-206	330	119
129	163	-74	-110	-142	136	12	5	152	-63	293	29
99	136	-83	-99	-131	123	30	-61	146	79	258	-69
67	102	-94	-87	-120	108	58	-127	153	208	211	-157
35	72	-102	-79	-104	90	77	-164	138	343	141	-226
7	31	-116	-67	-86	66	113	-237	143	450	89	-305
48	19	-139	-49	-75	55	138	-286	136	559	22	-374
85	67	-146	-37	-59	39	172	-341	139	638	-41	-446
113	107	-170	-21	-45	24	209	-392	131	721	-112	-522
134	142	-193	0	-32	1	248	-499	135	778	-182	-580
151	198	-229	25	10	-26	280	-492	131	809	-260	-629
163	228	-254	41	3	-62	303	-517	125	828	-338	-672
182	260	-279	63	21	-96	332	-545	130	827	-407	-713
202	285	-290	87	39	-127	337	-548	126	834	-496	-743
220	299	-300	101	66	-163	356	-560	139	827	-551	-770
236	313	-312	115	87	-190	348	-558	130	827	-627	-785
246	312	-306	115	104	-192	362	-576	159	795	-682	-804
248	325	-322	134	101	-191	361	-571	144	753	-745	-808
251	329	-320	126	116	-207	373	-580	150	685	-805	-803
254	329	-322	129	115	-203	364	-567	141	615	-857	-790
256	331	-321	130	123	-214	375	-584	159	507	-884	-780
257	337	-334	141	116	-205	367	-573	154	402	-914	-759
252	337	-320	134	129	-212	380	-581	168	266	-920	-744
257	340	-328	144	115	-205	372	-576	166	138	-927	-712
255	335	-321	133	129	-219	368	-577	165	-1	-924	-688
253	341	-329	136	121	-213	382	-595	179	-160	-910	-656
253	342	-336	143	116	-207	320	-588	170	-299	-907	-604
250	344	-332	133	128	-220	371	-589	176	-463	-877	-557
244	345	-332	140	120	-209	376	-589	185	-616	-848	-496
223	346	-341	143	117	-207	352	-519	178	-764	-812	-436
199	329	-332	129	126	-222	340	-472	183	-921	-754	-378
173	303	-329	136	115	-207	309	-418	190	-1063	-699	-303
140	277	-308	115	120	-209	263	-362	185	-1196	-635	-222
105	247	-288	99	106	-187	243	-318	181	-1312	-578	-128
70	222	-269	89	80	-148	212	-269	182	-1419	-511	-43
36	183	-245	65	64	-128						
4	153	-234	50	53	-95						

Continue

-29	116	-203	27	23	-73	186	-212	195	-1480	-440	39
-61	73	-193	9	5	-48	157	-141	175	-1498	-374	126
-97	30	-178	-6	-20	-16	124	-60	172	-1508	-290	213
-131	-19	-153	-32	-31	5	100	-15	182	-1522	-210	295
-162	-63	-146	-46	-60	35	70	26	176	-1514	-150	394
-187	-99	-126	-62	-78	54	58	49	172	-1524	-72	464
-207	-136	-106	-76	-99	90	33	88	162	-1514	-14	549
-225	-167	-82	-90	-113	97	21	108	172	-1522	54	611
-241	-194	-82	-102	-141	120	-4	146	163	-1522	115	652
-251	-217	-72	-113	-145	133	-11	160	166	-1526	177	694
-262	-235	-64	-123	-161	156	-33	184	164	-1516	218	728
-268	-249	-57	-136	-169	165	-42	196	152	-1513	259	741
-270	-252	-52	-147	-173	178	-50	199	161	-1502	318	726
-268	-263	-43	-157	-179	174	-45	192	161	-1440	348	719
-264	-258	-51	-147	-183	188	-61	202	153	-1351	372	697
-253	-253	-44	-148	-180	186	-63	199	159	-1239	390	659
-243	-243	-45	-158	-169	170	-54	183	161	-1134	417	603
-232	-236	-49	-146	-175	176	-63	181	155	-997	420	549
-212	-226	-50	-141	-164	165	-54	155	153	-858	417	485
-193	-212	-48	-142	-157	159	-45	132	163	-730	426	405
-172	-194	-61	-125	-160	154	-42	107	144	-576	406	335
-143	-176	-61	-126	-140	137	-27	73	163	-433	394	244
-112	-142	-79	-106	-142	136	-19	45	151	-280	361	159
-80	-120	-83	-98	-128	122	-25	-8	149	-131	326	77
-46	-84	-94	-83	-112	102	20	-41	149	12	298	-12
-8	-43	-109	-60	-105	89	-44	-96	150	148	237	-96
31	4	-124	-52	-80	61	76	-161	157	266	135	-188
72	55	-140	-33	-62	46	101	-213	148	401	124	-257
108	97	-158	-23	-46	20	131	-254	149	500	66	-342
133	141	-189	5	-41	13	152	-317	140	597	-5	-412
150	177	-209	8	-13	-28	198	-381	107	671	-72	-469
164	218	-233	31	-2	-54	238	-434	146	749	-146	-556
181	254	-260	61	7	-68	269	-472	133	906	-234	-603
201	276	-269	66	36	-107	307	-517	139	811	-298	-658
221	294	-293	95	45	-127	320	-533	135	823	-368	-707
233	307	-297	104	66	-157	332	-544	129	933	-452	-728
243	322	-308	120	81	-180	344	-559	135	929	-520	-765
248	318	-301	117	104	-199	359	-573	143	819	-589	-784
254	322	-311	129	105	-195	356	-568	144	905	-650	-803
257	333	-306	124	118	-210	363	-576	150	766	-711	-808
259	336	-317	130	123	-214	320	-581	151	711	-769	-802
258	341	-322	137	119	-210	367	-582	148	635	-820	-799
257	337	-315	130	123	-213	371	-592	150	546	-871	-780
260	343	-313	130	128	-216	375	-597	164	434	-898	-776
259	341	-321	130	127	-222	378	-601	179	316	-915	-757
258	340	-324	125	128	-226	380	-603	170	186	-920	-740
258	336	-320	130	129	-225	380	-604	173	47	-927	-706
253	343	-325	137	121	-214	371	-570	162	-84	-930	-665
242	348	-326	138	122	-218	374	-593	171	-234	-918	-627
222	346	-325	133	131	-224	386	-606	169	-395	-890	-589
198	337	-332	143	123	-218	380	-589	137	-554	-856	-536
178	322	-327	139	126	-219	357	-553	185	-702	-823	-472
155	297	-306	122	126	-215	340	-458	192	-857	-777	-407
133	224	-288	111	113	-191	314	-445	191	-996	-720	-331
102	243	-274	93	97	-172	291	-396	204	-1133	-664	-248

Table (4.3)- Digitized Electric Signal for One of the Tests.



# CHAPTER FIVE

## RESULTS

In this chapter the results of the laboratory experiments and the theoretical work required to determine certain structural parameters(Dynamic Properties) will be covered. The experimental data analysis for the six structures will be presented, and the results obtained from these tests will be shown.

### 5.1 THE DYNAMIC PROPERTIES OF THE STRUCTURES

#### 5.1.1 DETERMINATION OF DAMPING COEFFICIENTS AND NATURAL FREQUENCIES

Damping coefficients were determined from the logarithmic decrement method as set forth by Den Hartog 1956<sup>(112)</sup>

For a single degree of freedom system, if an impulse load is applied to the mass centre, the sequential amplitudes of the oscillation are reduced by the damping in the system. For a system with linear, or viscous damping the relationship between succeeding peaks is expressed by:

$$\frac{X_{n+1}}{X_n} = e^{-2\pi\xi FN/FD} \quad \dots \quad \dots \quad \dots \quad \dots \quad (5.1.1)$$

where  $X_n$  = magnitude of the  $n^{\text{th}}$  oscillation  
 $X_{n+1}$  = magnitude of the next oscillation  
 $\xi$  = relative damping coefficient  
 $FN$  = natural undamped frequency of vibration  
 $FD$  = natural damped frequency of vibration

and

$$FD = FN \sqrt{1 - \xi^2} \quad \dots \quad \dots \quad \dots \quad \dots \quad (5.1.2)$$

For low damping as in the case of this work

$\xi^2 \ll 1$  so that

$$\ln X_{n+1} - \ln X_n = -2\pi\xi$$

or

$$\xi = \frac{1}{2\pi} \ln\left(\frac{X_n}{X_{n+1}}\right) = \frac{1}{2\pi} \times \frac{1}{n} \ln\left(\frac{X_0}{X_n}\right) \quad \dots \quad \dots \quad (5.1.3)$$

In the experiments the magnitudes of succeeding oscillations were obtained by constructing verticals at the upcrossings. The damping coefficients were determined from the smooth part of the record, after the higher modal vibration had disappeared. The decay trace was obtained by displacing the cantilever tip and releasing it. The first few cycles of motion from release were therefore occupied by the cantilever changing the imposed deflection shape to a curve compatible with a freely vibrating uniform loaded cantilever. For this



reason, the first three cycles from the start of the trace were ignored in the calculation. It was observed that over the remaining cycles, the amplitude ratio did not significantly vary with time.

Very little difference in the damping coefficient was observed from the two tests (impulse load test and tip displacement released test). The damping coefficients calculated therefrom were averaged. Each of these tests were repeated several times.

From the results, it was observed that the damping coefficients in air were less than in water and also it was noticed that the damping coefficients in water increased with the increase of water depth. This could have been due to the added hydrodynamic damping.

The natural damped frequencies of the structures were obtained although in the analysis the undamped natural frequencies were required but since the relative damping coefficients were always very small the damped frequencies were essentially equal to the undamped frequencies as can be seen from Equation (5.1.2).

Table (5.1) gives the average of the results of testing for the relative damping coefficients and the natural frequencies for the structures in both air and water.

Structure	Water Depth Meter	Relative Damping Coefficient		Natural Frequency		Remarks
		In Air	In Water	In Air	In Water	
(A)	0.45	0.043	0.045	58.9	55.4	
	0.47		0.046		55.1	
	0.50		0.048		54.8	
	0.525		0.049		54.5	
(B)	0.5	0.040	0.044	36.94	34.25	
	0.525		0.045		33.76	
	0.55		0.047		33.4	
(C)	0.5	0.030	0.034	25.8	23.35	
	0.525		0.036		22.92	
	0.55		0.037		22.49	
(D)	0.5	0.028	0.030	21.2	18.93	
	0.525		0.033		18.54	
(E)	0.5	0.064	0.067	20.6	16.07	Zero load
		0.068	0.070	15.13	12.33	1010 grams
		0.072	0.074	12.69	9.8	2020 grams
	0.525		0.069		15.64	Zero load
			0.071		12.27	1010 grams
			0.076		9.45	2020 grams
(F)	0.5	0.0625	0.065	17.65	14.65	Zero load
		0.065	0.068	13.46	10.76	1010 grams
		0.070	0.073	11.52	8.6	2020 grams
	0.525		0.067		13.8	Zero load
			0.069		10.65	1010 grams
			0.075		8.3	2020 grams

TABLE (5.1) - Relative Damping Coefficients and Natural Frequencies.



5.1.2      DETERMINATION OF STIFFNESS CONSTANTS

The values of stiffness constant obtained from the experiments were substituted into the following equation

$$\begin{aligned} W_n^2 &= K/M \quad \dots \quad \dots \quad \dots \quad \dots \quad \dots \quad \dots \quad (5.1.4) \\ FN &= W_n/2\pi \end{aligned}$$

From the above equation, the analytical values of the natural frequencies were obtained. These analytical natural frequencies were compared with those obtained by experimentation during the tests for damping coefficients in order to provide an experimental check on the analysis.

The results are shown in Table (5.1).

<u>Structure</u>	<u>FN Experimental</u>	<u>FN Analytical</u>
(A)	58.9	59.08
(B)	36.94	33.9
(C)	25.8	25.0
(D)	21.2	20.1
Mass Added at the top		
(E)      Zero	20.6	18.88
1010 grams	15.13	13.41
2020 grams	12.69	10.97
(F)      Zero	17.65	15.09
1010 grams	13.46	10.89
2020 grams	11.52	8.95

-----

TABLE (5.1)    The Experimental and Analytical Natural Frequencies

Also the values of the stiffness constant were substituted into the following equation

$$K = \frac{3EI}{L_s^3} (1-b) \dots \dots \dots (5.1.5)$$

where  $L_s$  = structure height

$$b = \frac{4WL_s^2}{\pi^2 EI}$$

From the above equation the modulus of elasticity of each structure was calculated. Small discrepancies were found between the calculated and experimental values of the modulus of elasticity and also between the calculated and experimental values of the natural frequencies. These could be due to the possibility that the wall thickness away from the end may be different from that at the end which will affect the value calculated for the sectional moment of inertia  $I$  as well as the value of mass.

## 5.2 DATA ANALYSIS

The obtained data for each setting of the wave generator, the water depth in the tank and each level on the structure where the pressure can be measured were

- (1) The wave profile
- (2) The pressure round the structure at that level



(3) The tip displacement

(4) the bending moment at the base of the structure.

The above data were taken, first when the structure was free to vibrate (Free) and second when the structure was prevented from vibrating (Fixed).

The wave profiles obtained from free structure and fixed structure for each test were compared. The difference between the wave profiles was negligible, which shows that for the waves used in the tests and for the tested structures there were no radiation waves due to the movement of the structure.

For the structures with more than one level of pressure which can be measured, the data of the wave profile, tip displacement and the bending moment, obtained from the first level, were compared with the other levels for the same condition of test. There were no differences between these data which indicates that the wave properties did not change throughout the whole time of tests and the structures' vibrations were in steady state conditions.

Figures (5.2.1) and (5.2.2) show a typical data obtained for free and fixed structure respectively. Each figure shows the wave profile, the tip displacement, the

pressures at each of the eight points due to the wave and the in-line and transverse bending moments. They also show the calculated in-line and transverse local forces at that level.

The calculated static pressure ( $\gamma\eta$ ) is plotted with the measured value of the pressure at point (1) (the static pressure is the curve without symbols). The static pressure is higher than the pressure due to the wave throughout the wave cycle as expected.

Figures (5.2.3) and (5.2.4) show the corresponding pressure distribution across the structure a time increment of the cycle equal to ( $t = T/8$ ). From the figures it can clearly be seen that the distribution of pressure around the periphery of the cylinder cross-section is not symmetrical about the axis of wave propagation. This asymmetry is attributable to the asymmetric formation and shedding of eddies which will give rise to a transverse force.

Figures (5.2.5) and (5.2.6) show the corresponding Fast Fourier's Transformation to the wave profile, in-line force and tip displacement. From the figures it can be noticed that there is a magnitude of the second harmonic in the wave profile, and they show also that the wave profile did not change for the two sets of



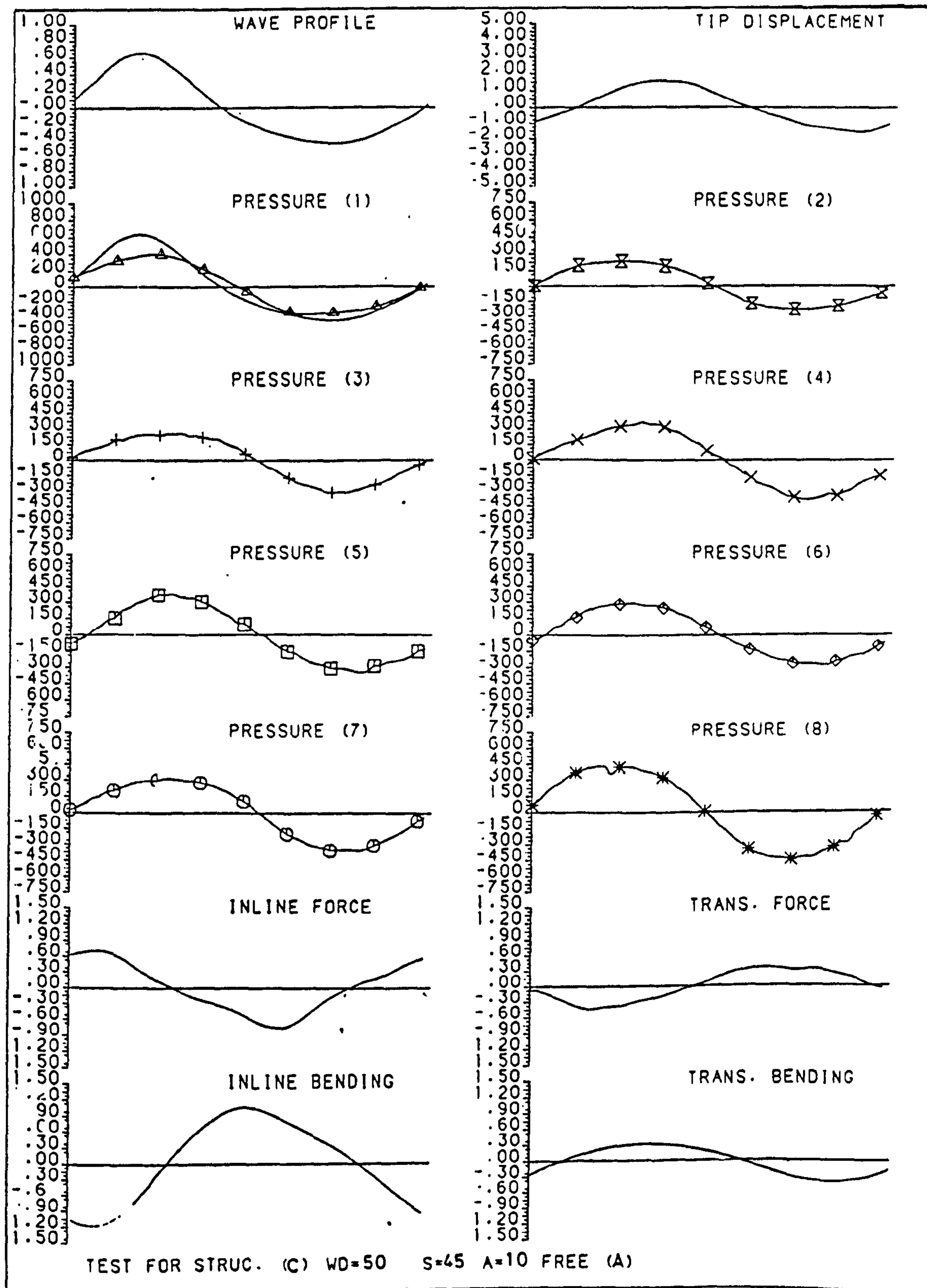


Figure (5.2.1) - Measured Data and the Calculated In-Line and Transverse Local Force for Free Structure.

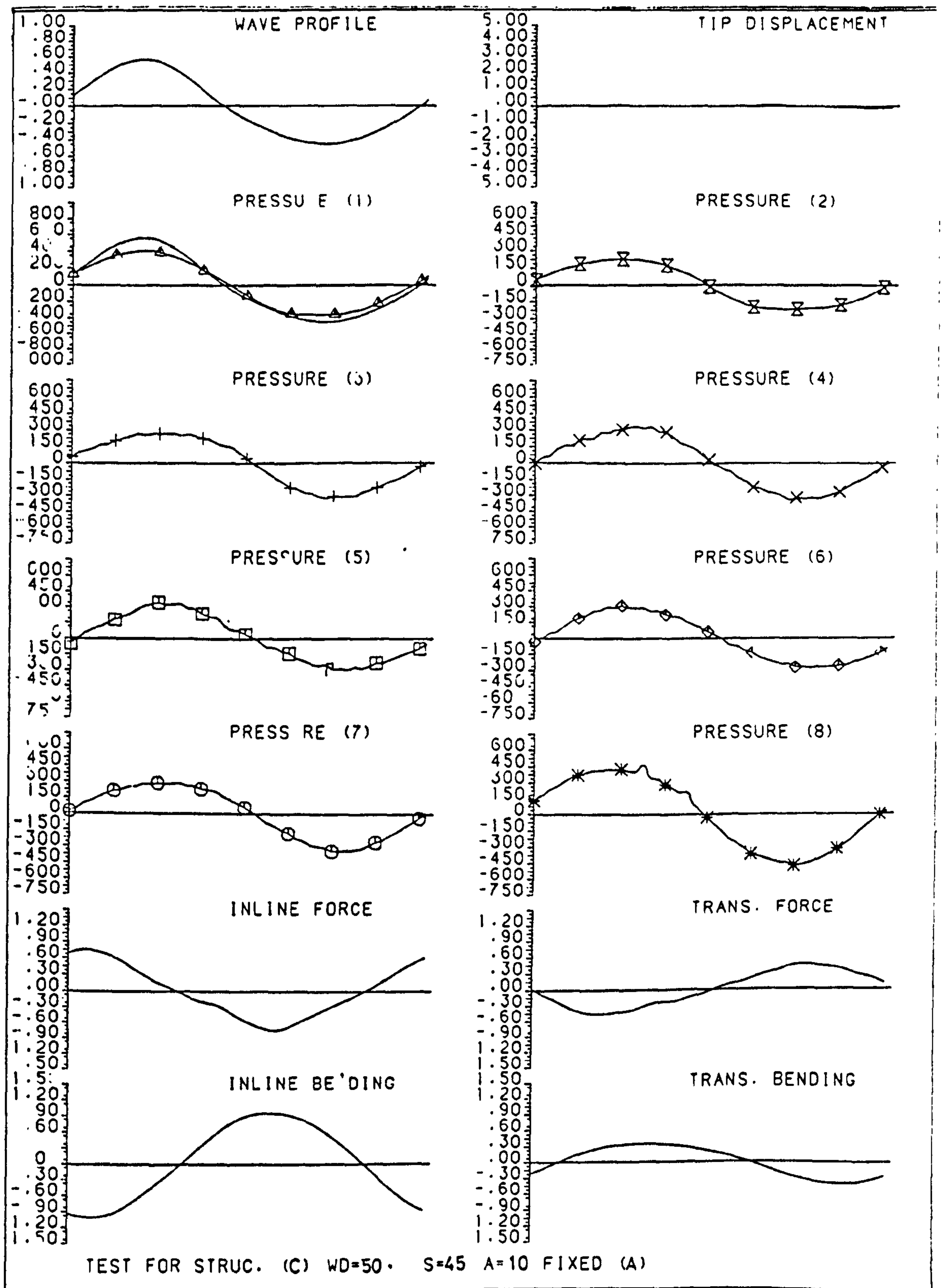


Figure (5.2.2) - Measured Data and the Calculated In-Line and Transverse Local Force for Fixed Structure.



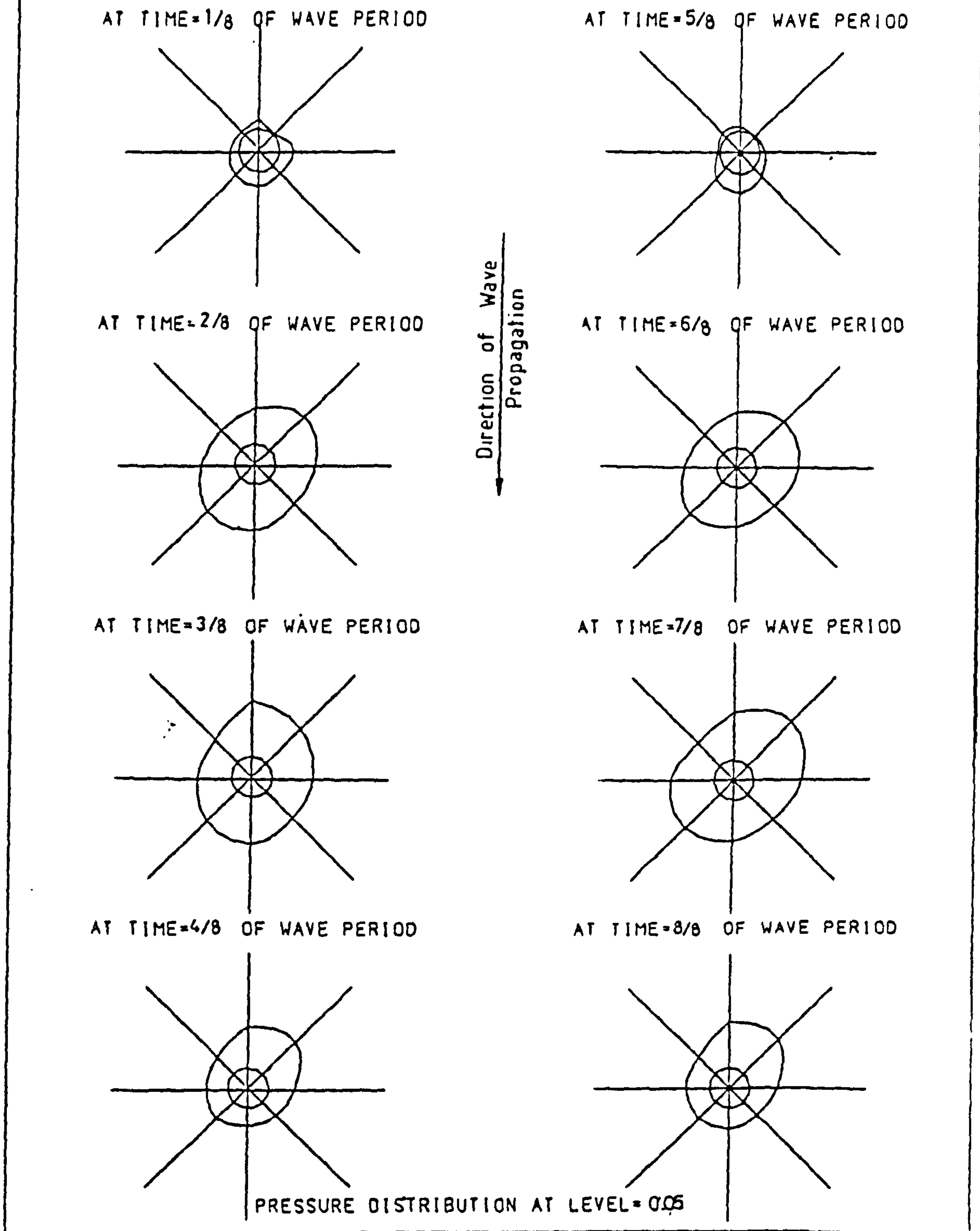
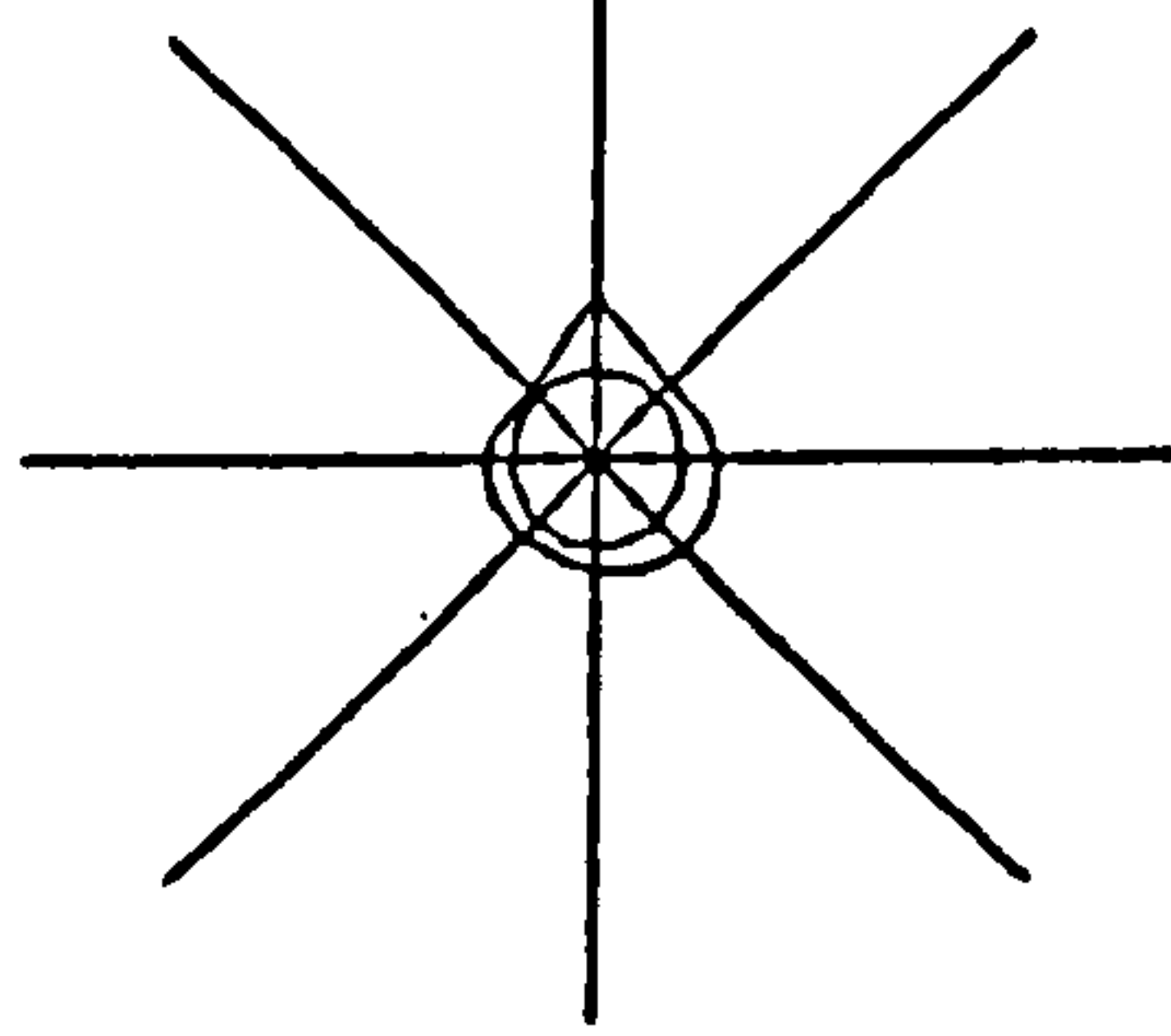
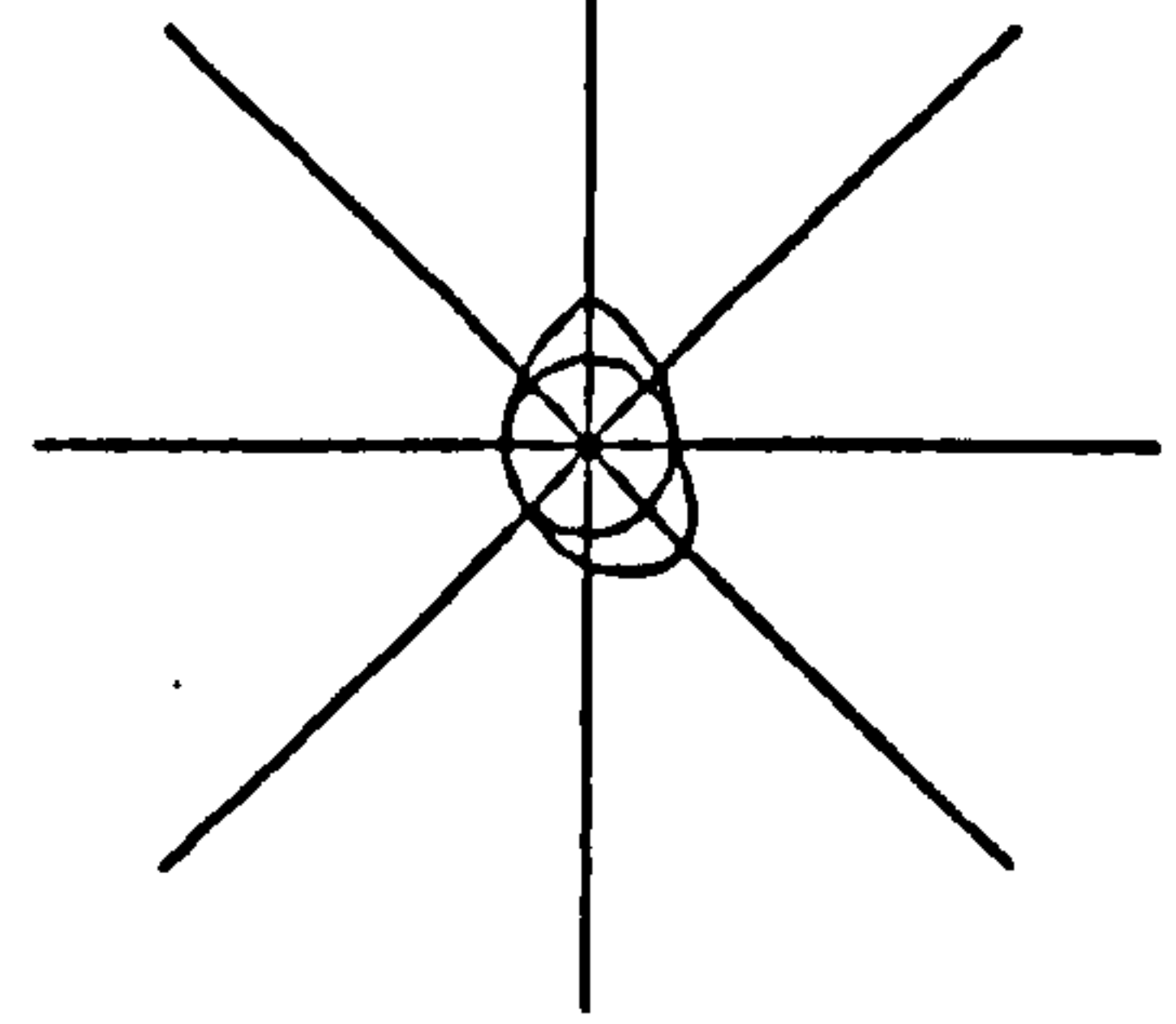


Figure (5.2.3) - Pressure Distribution across the Structure during the Wave Cycle for Free Structure.

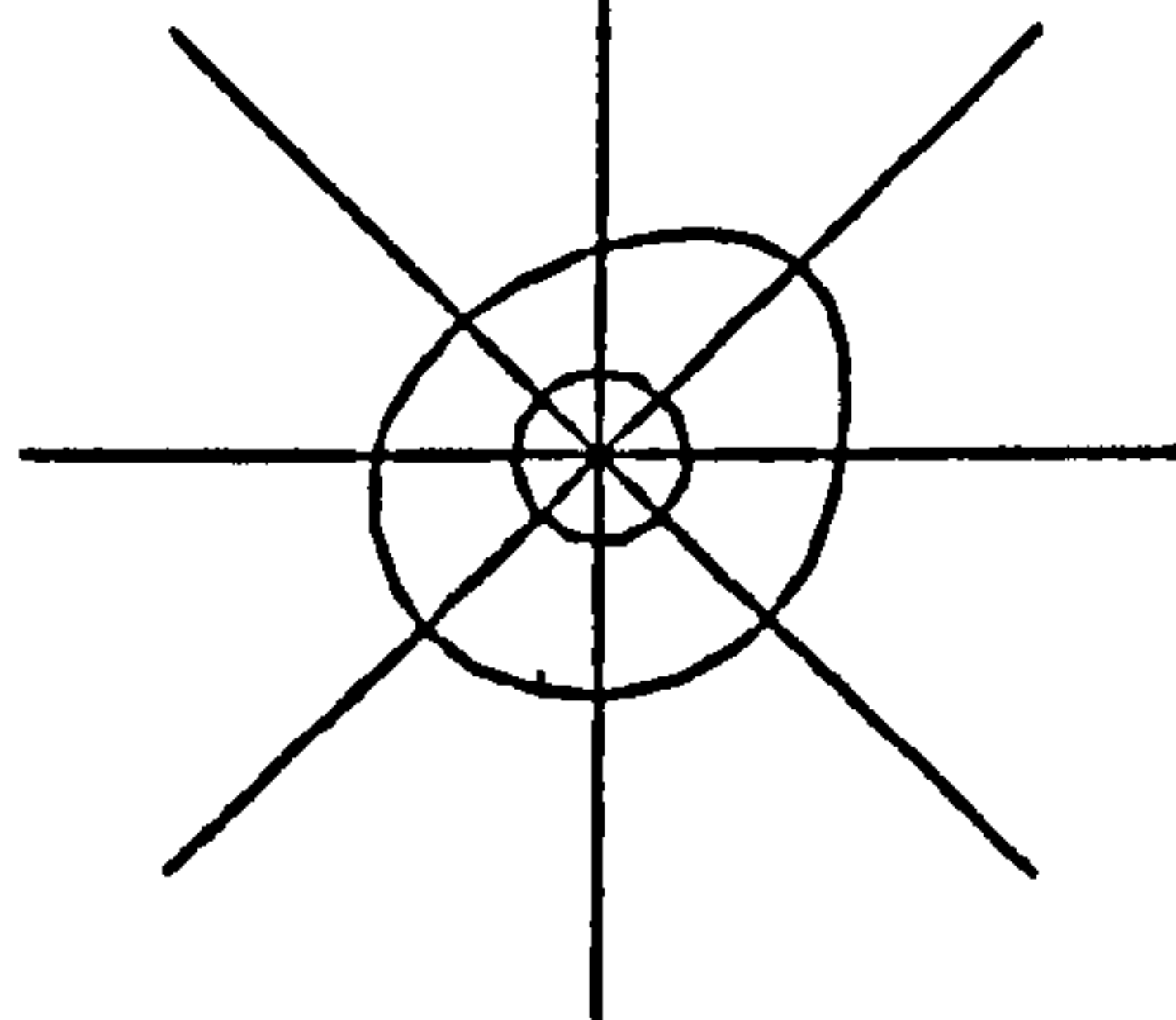
AT TIME=1/8 OF WAVE PERIOD



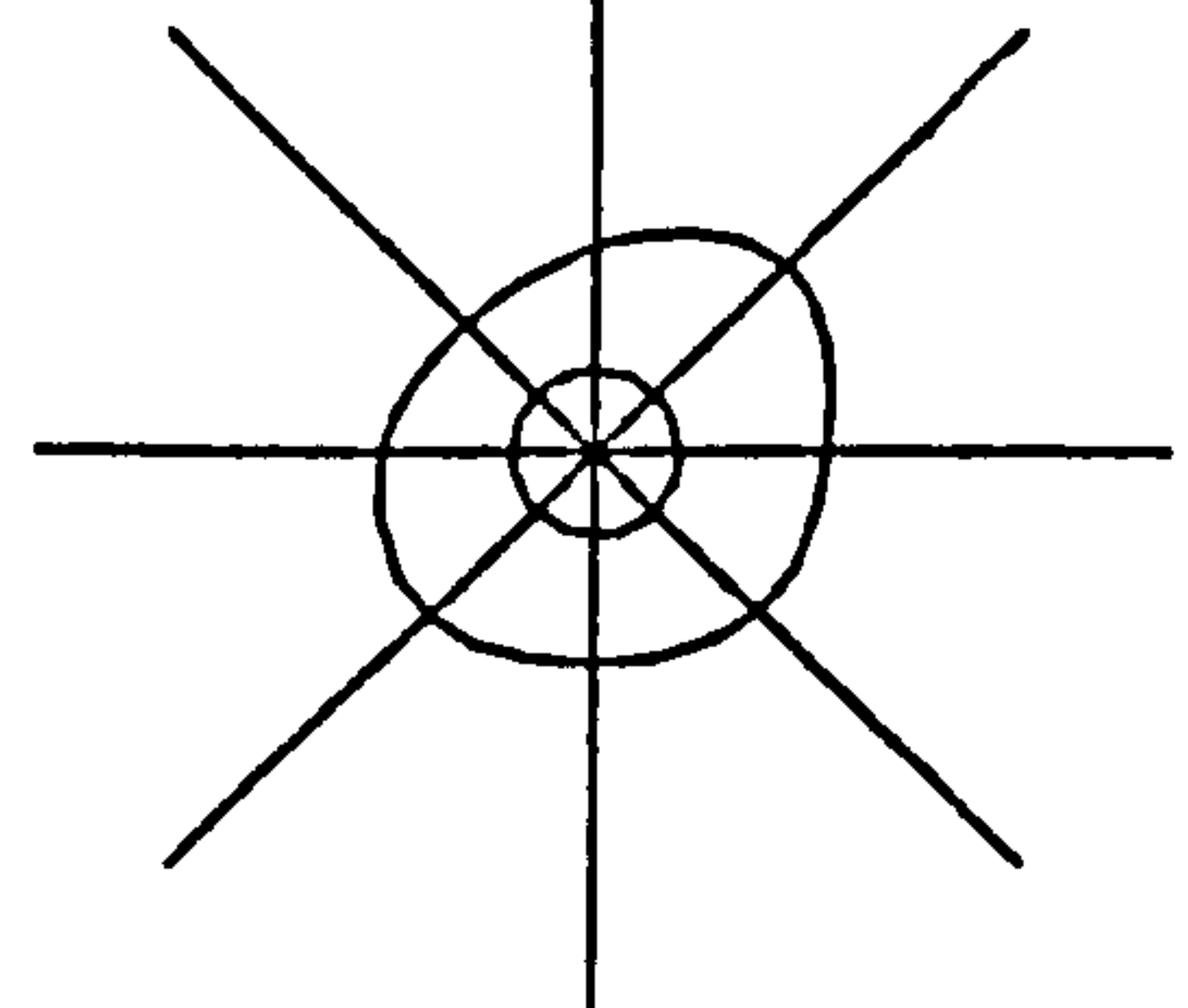
AT TIME=5/8 OF WAVE PERIOD



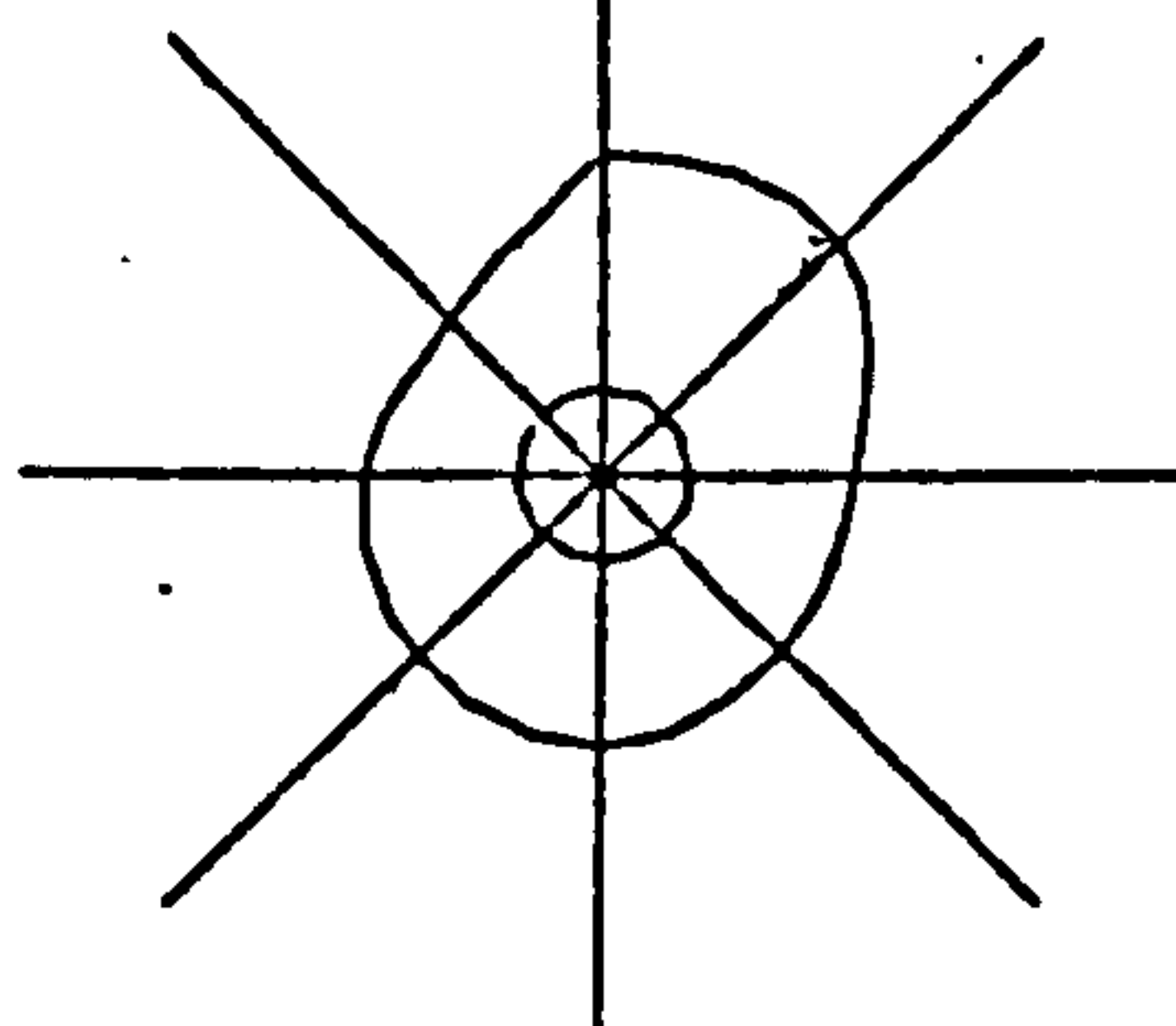
AT TIME=2/8 OF WAVE PERIOD



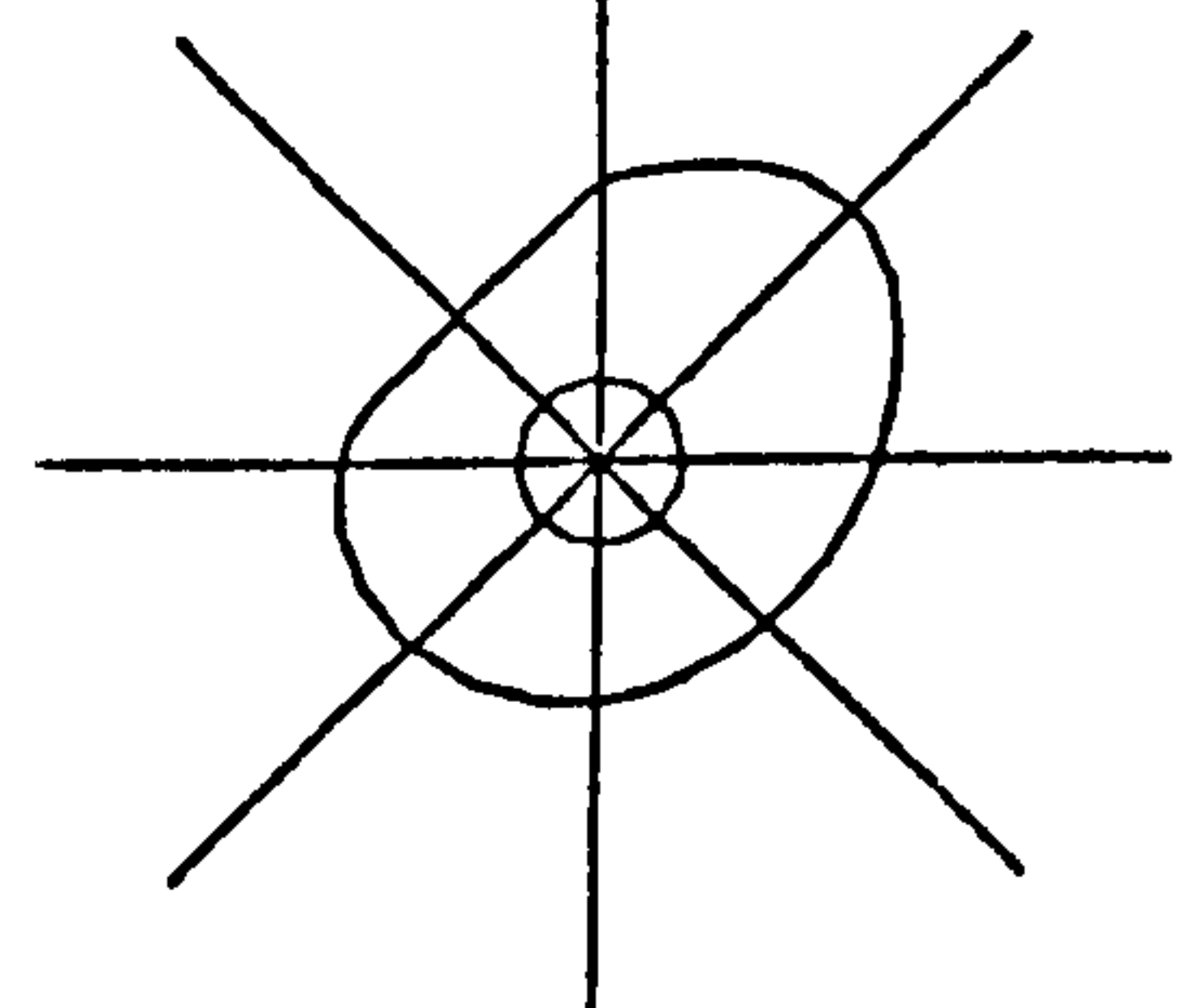
AT TIME=6/8 OF WAVE PERIOD



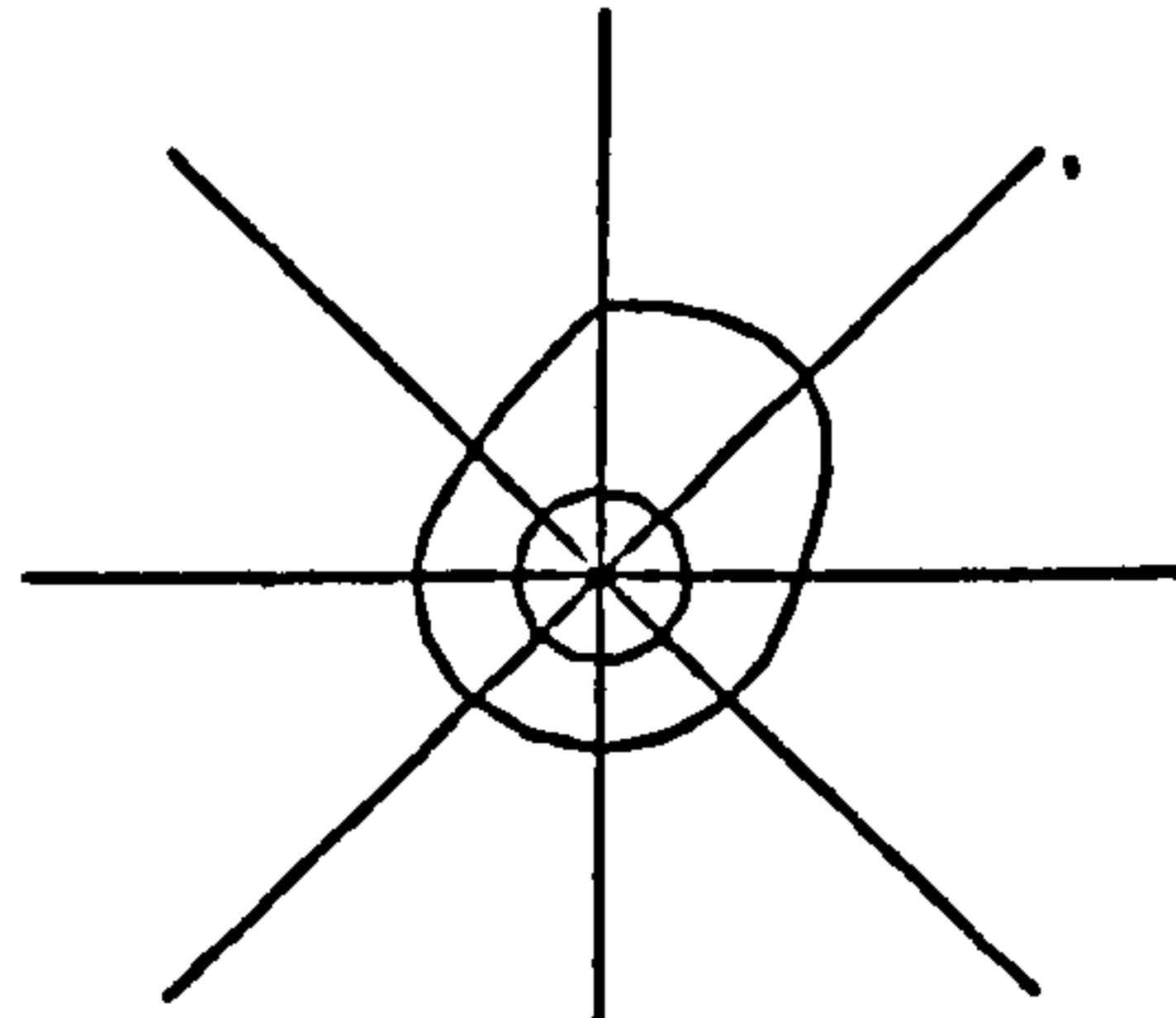
AT TIME=3/8 OF WAVE PERIOD



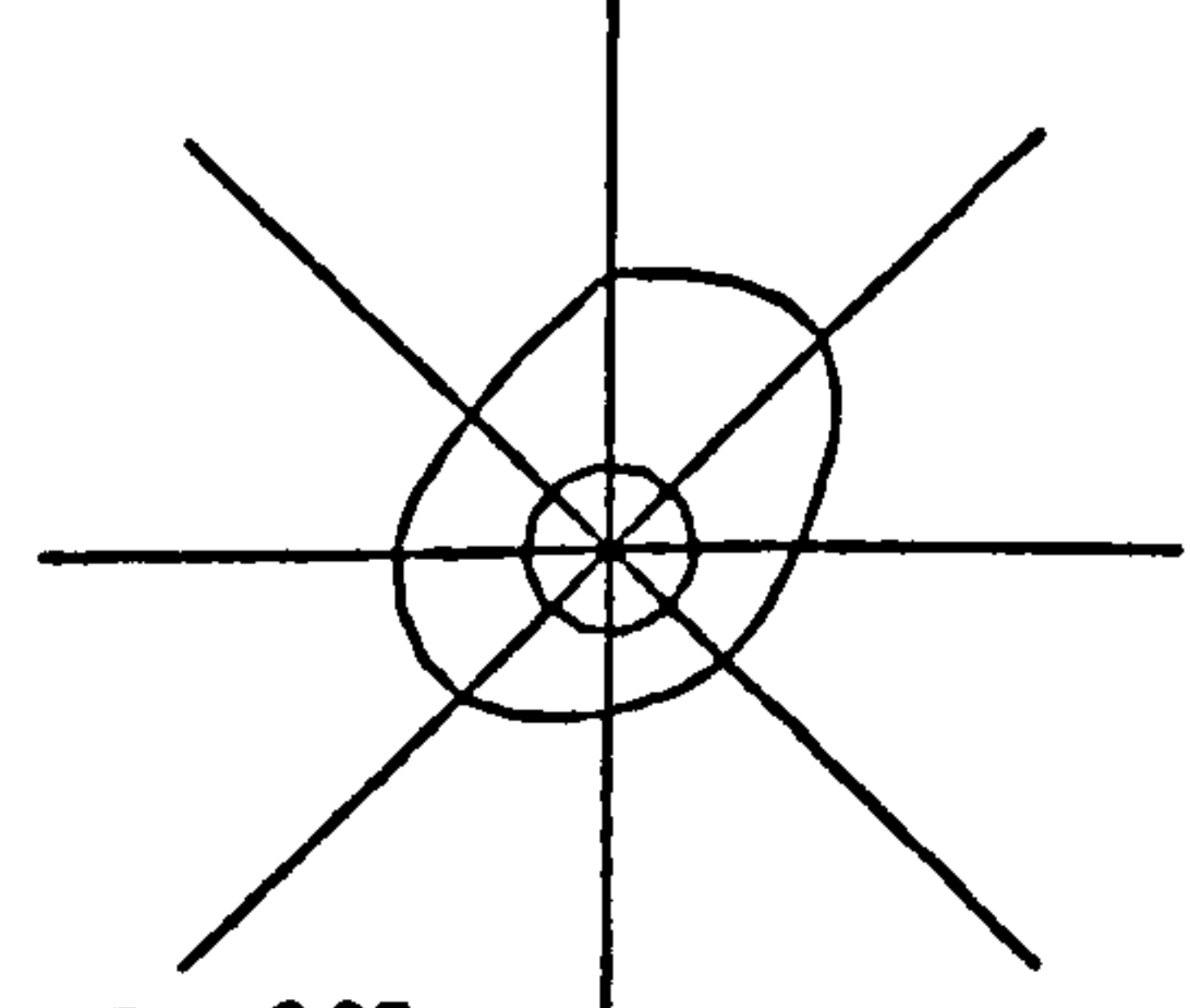
AT TIME=7/8 OF WAVE PERIOD



AT TIME=4/8 OF WAVE PERIOD



AT TIME=8/8 OF WAVE PERIOD



Direction of Wave  
Propagation

PRESSURE DISTRIBUTION AT LEVEL=0.05

Figure (5.2.4) - Pressure Distribution across the Structure during the Wave Cycle for Fixed Structure.



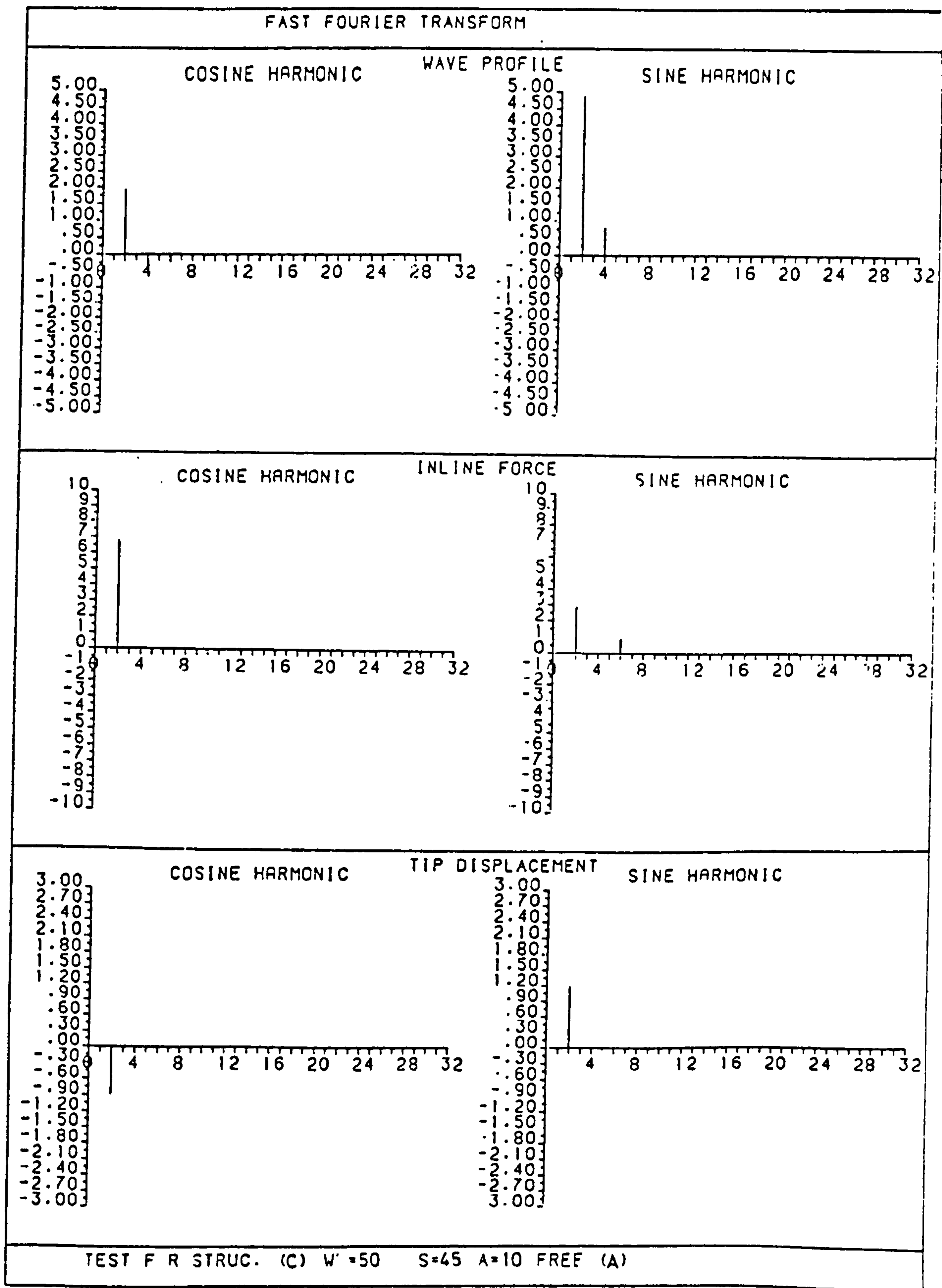


Figure (5.2.5) - Fast Fourier Transform for the Wave Profile, the In-Line Force and the Tip Displacement for Free Structure.

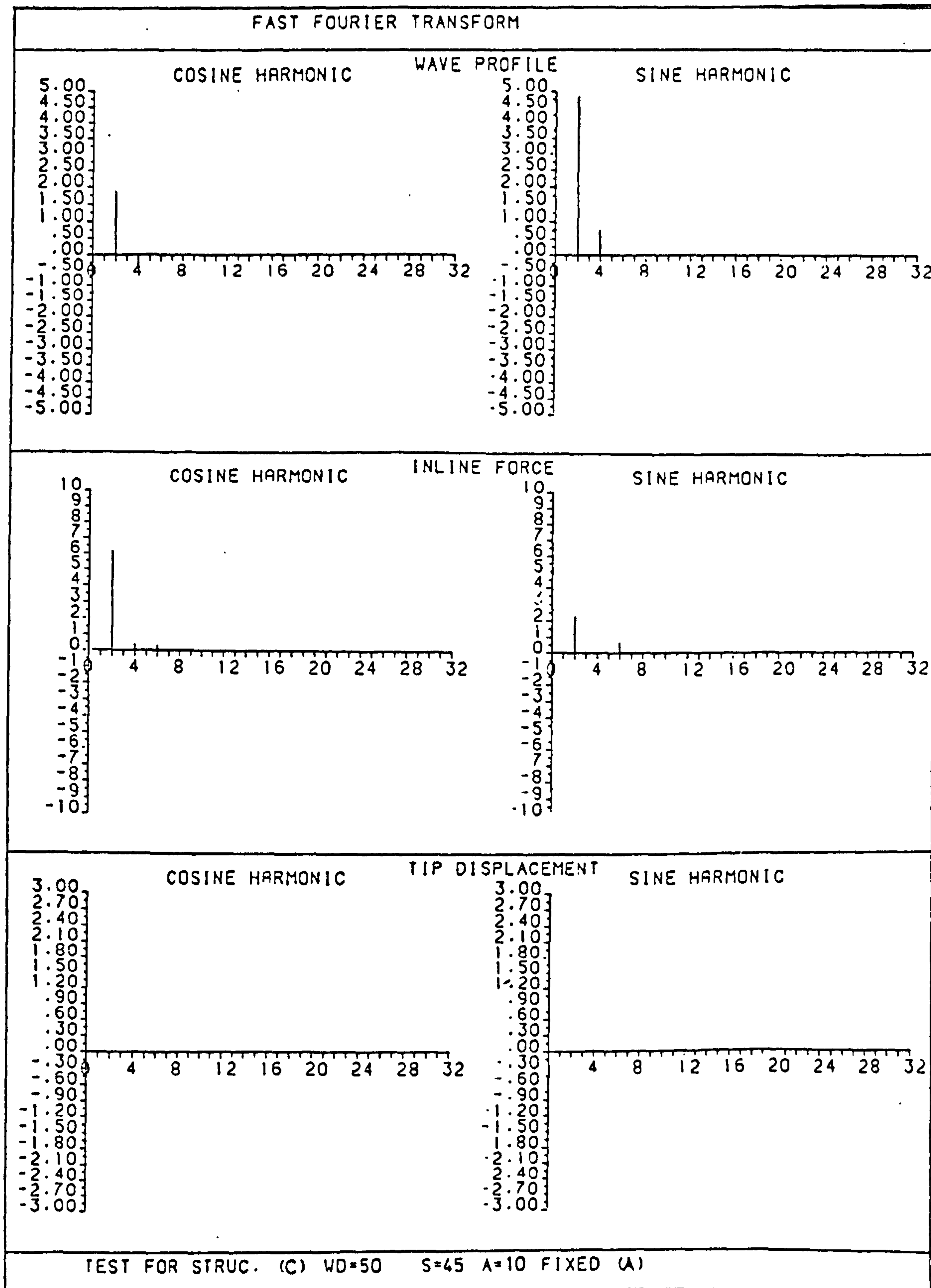


Figure (5.2.6) - Fast Fourier Transfor for the Wave Profile, the In-Line Force and the Tip Displacement for Fixed Structure.



tests. Also they show the difference in the force between the two cases, and the existence of the third sine harmonic in the force as it would be expected (see Keulegan and Carpenter<sup>(27)</sup>).

Detailed analyses were conducted for all tests. The analysis of the data obtained from each test may be divided into three sections. These three sections were wave properties, forces on structure and dynamic behaviour.

#### 5.2.1 WAVE PROPERTIES

The measured wave profile was processed and wave properties were defined. The processing of the wave profile was carried out by digitizing the electric signal from the wave probe at 0.02 of a second. As the waves generated used in the tests were not purely sinusoidal waves as it is shown in Figure (4.4.1), sinusoidal interpolation was used to generate, from the number of data points obtained from one cycle of the wave, an exact 64 data points in wave cycle, in order to use the Fast Fourier Transformation. See Appendix (C) for sinusoidal interpolation.

From the F.F.T. the amplitudes of each sine and cosine harmonics contained in the wave profile were determined. The wave profile was represented mathematically by Equation (3.2.10).

The wave period was obtained directly from the time increment between the wave cycle. Wave height was defined as the difference between the crest elevation and the trough elevation.

Figure (5.2.7) shows a typical case of the calculated wave profile using Equation (3.2.10) and substituting for the first three harmonics only and the measured one.

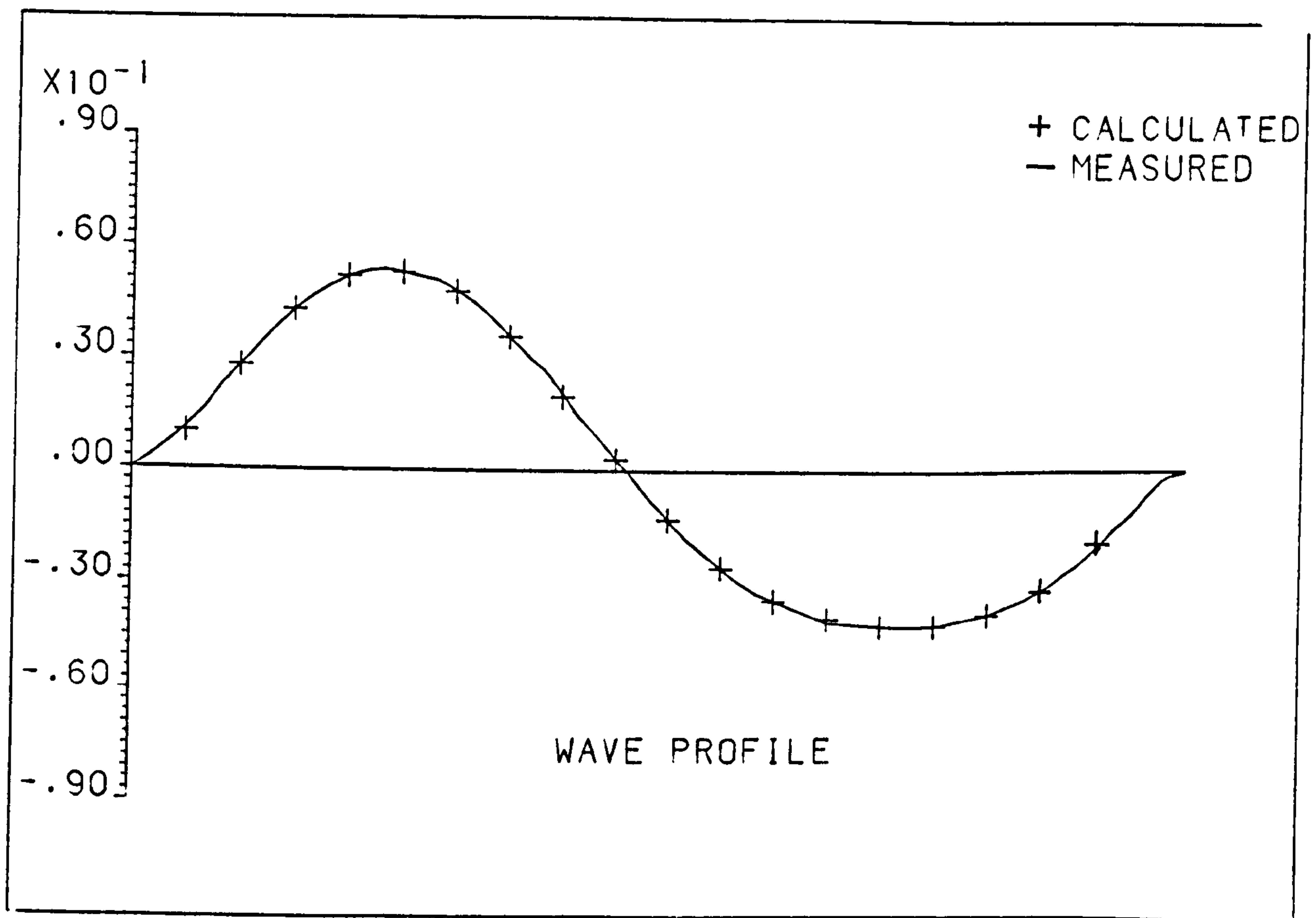


FIGURE (5.2.7) - The Measured and calculated Wave Profile.



Checks were made for the measured and calculated wave lengths using linear wave theory, from the Equation (3.2.13).

Equation (3.2.13) was solved by Newton's Raphson's iteration method getting the wave length of the first harmonic and comparing with the measured, the maximum difference was about 6%.

### 5.2.2 THE FORCES ON STRUCTURE

The signals from the eight pressure transducers located at one level of the structure were digitized at 0.02 of the second simultaneously with the wave profile, bending moment and tip displacement signals.

The force acting on the measured level of the structure at any time can be obtained from Equation (3.4.3). The numerical integration of this equation was carried out by using Simpson's rule:

$$dF(t) = \frac{1}{3} \Delta (2 \times \text{Odd value} + 4 \times \text{Even value}) ds \quad (5.2.4)$$

∴ the  $dF(t)$  in the direction of the wave propagation (in-line force) will be

$$dF(t) = \frac{1}{3} \frac{\pi D}{8} \left[ (2 \times \delta P_I \cos \frac{\pi}{4}(I-1) + 4 \delta P_J \cos \frac{\pi}{4}(J-1)) \right] ds$$

... .. (5.2.5)

where    I    =    1, 3, 5, 7  
              J    =    2, 4, 6, 8

The values of the  $dF_x(t)$  for the wave cycle had been represented mathematically in the same way as of the wave profile.

The measured bending moments were digitized. The digitized bending moments were used to compare the measured and calculated. The bending moments were calculated by using Equation (3.2.20). The values of  $C_D$  and  $C_M$  appearing in the equation were calculated from the highest level and taken as constant along the length of the structure. The difference between the calculated and measured bending moments varied from one test to another with maximum difference of 17.5%. Some tests gave good agreement between the measured and calculated bending moments as shown in Figure (5.2.8).

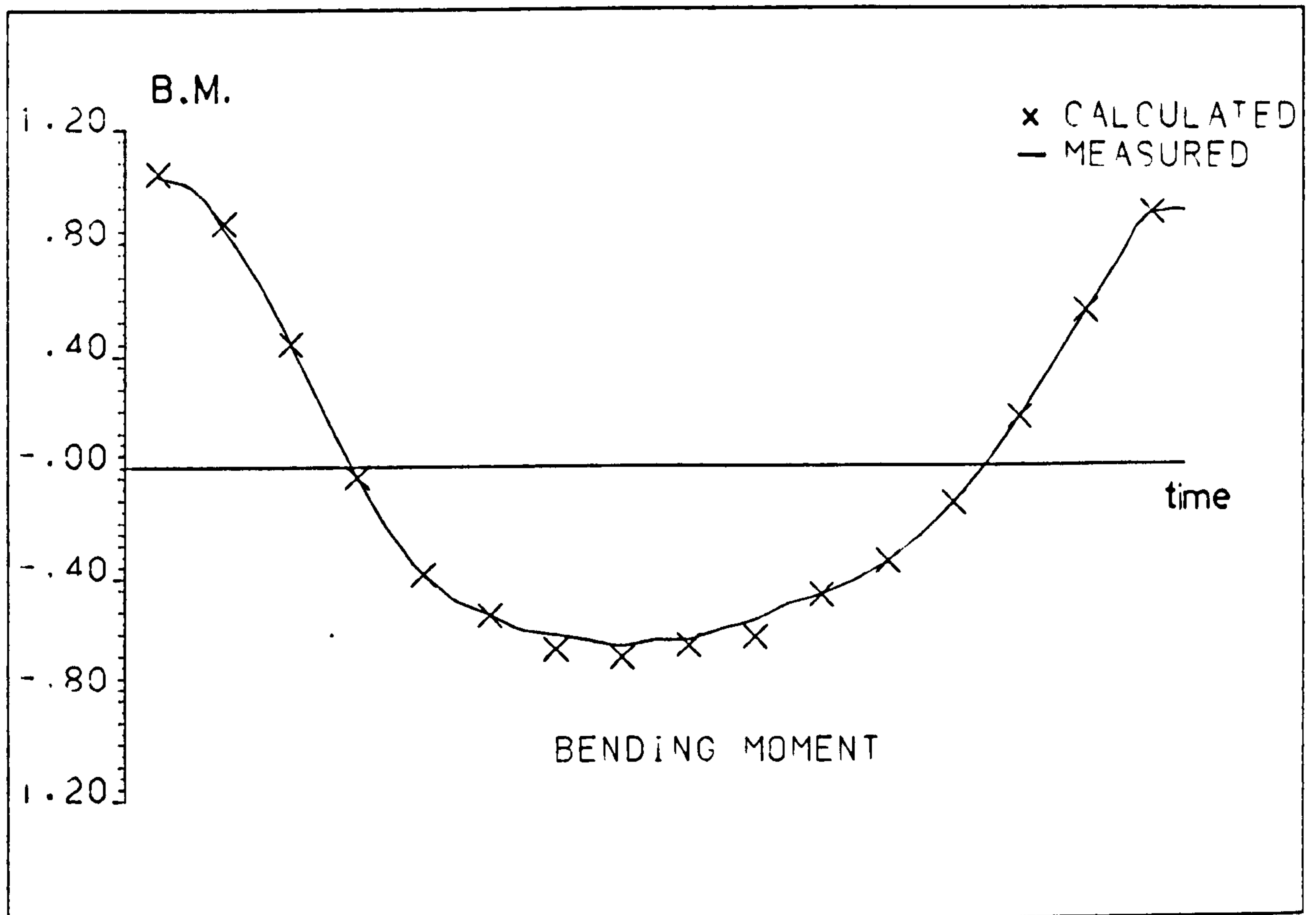


FIGURE (5.2.8) - The Calculated and Measured Bending Moments.

### 5.2.3 STRUCTURE DYNAMIC RESPONSE

The tip displacement values of  $x(t)$  had been digitized and represented mathematically in the same way as those of the wave profile and in-line force.

The mathematical representation of the tip displacement was used to calculate the structure velocity and acceleration at the measured level of pressure by Equations (3.4.7) and (3.4.8).



### 5.3 THE RESULTS FROM THE EXPERIMENTS

After the data had been analysed it was subjected to the appropriate theoretical approach to obtain the final results. The results obtained can be divided into two parts, the first part is the waves and the corresponding forces on the structures and the second part is the structural response due to the acting forces and the surrounding environment.

#### 5.3.1 WAVES AND THE CORRESPONDING FORCES ON THE STRUCTURES

In the present study, the experimental waves were nearly sinusoidal, the position parameter ( $h/T^2$ ) was varied between ( $0.247 - 0.564 \text{ m/sec}^2$ ) and the wave parameter ( $H/T^2$ ) was varied between ( $0.079 - 0.201 \text{ m/sec}^2$ ). These values, according to the validity of the wave theory by Dean<sup>(8)</sup>, lie within the region of the Airy theory. Also referring to Howell<sup>(5)</sup> the condition required to satisfy the linearization of the boundary condition is  $H/2k^2h^3 < 1$ , which allows for using linear wave theory without significant difference from the higher order. Linear wave theory was applicable as  $H/2k^2h^3$  for this study was varied between ( $0.03 - 0.074$ ). Finally according to the classification of the water wave length to the relative depth ( $h/L$ ) the waves used

in this work can be classified as intermediate waves as  $h/L$  varies between  $(1/7 - 1/2.3)$ .

From the above it can be concluded that the linear wave theory using the intermediate equation as shown in Chapter Three gives the most accurate theory to calculate the kinematic properties of the wave for the waves used.

As the structure used in this investigation had a small diameter relative to the wave length, the hydrodynamic forces were calculated by Morison's Equation (3.2.18) and the modified Morison's Equation (3.2.19).

The Keulegan-Carpenter number of the water wave was calculated on the basis of the maximum water velocity at the still water level. The forces corresponding to the wave acting on the structure were used to evaluate the values of the forces coefficients  $C_D$  and  $C_M$ . The average values of the drag and inertia coefficients for the cycle had been calculated according to a least squares fit between the experimental force history and that predicted by Morison's equation using Equation (3.2.18) and (3.2.19). Although the forces were measured at some distance from the still water level, the forces coefficients were related to the Keulegan-Carpenter number at the still water level.

For each structure the forces coefficients corresponding to the waves were represented as follows:

1. The forces coefficients  $C_D$  and  $C_M$  for fixed structures due to wave
2. The percentage ratio of the value of  $C_D$  for a free structure to that for a fixed structure ( $C_{DP}$ ) and the same for  $C_M(C_{MP})$
3. The percentage ratio of the values of  $C_D$  and  $C_M$  calculated by the modified Morison's equation to those calculated by Morison's equation ( $C_{DD}$  and  $C_{MD}$ ) when the structures were free to vibrate.

The characteristics of the waves used in the tests and the corresponding forces as represented above for each structure are shown in Tables (5.2 through 5.11).

For the case of more than one level of pressure measured along the structure the tables show:

1. For the fixed structures the drag coefficients decrease with depth while the inertia coefficients increase with depth for the tested waves. These are due to the reduction of the water particle



velocity along the structure and consequently the reduction of the K-C number, as it shows later that the  $C_D$  decreases with the decrease of the K-C number while  $C_M$  increases with the decrease of K-C number, and due to the reduction of the vorticity with depth. The variation of  $C_D$  and  $C_M$  with depth should be taken into consideration for the determination of bending moment at the base of the structure especially for the case of deep water.

2. The percentage ratio of the drag coefficients for free structures to those for fixed structures slightly decreases with depth. The corresponding percentage ratio of the inertia coefficients behaves similarly. This can be attributed to the decrease of the effect of the vortices with depth, the forward movement of the separation points of the flow round the structure with depth and the reduced structural response with depth.
3. The percentage ratio of the drag coefficients calculated by modified Morison's equation to those calculated by Morison's equation increases with depth, similarly the corresponding ratio of inertia coefficients. These are due to the increase of the ratio of the relative velocity of the water particle to that of the structures' velocity, as the water particle velocity decreases exponentially with

STR. DIAMETER=0.1100 M STR. LENGTH=0.6080 M														
NATURAL FREQ. IN AIR=58.000 DAMPING COEFF. IN AIR=0.043														
=====														
TEST WATER	WAVE	WAVE	KEULEGAN-	REYNOLDS	LEVEL									
NO. DEPTH	HEIGHT	LENGTH	PERIOD	CARPENTER	FROM	CD	CM	Z	CD	FR	CD	FR	CM	FR
METER	METER	METER	SEC.	NUMBER	NUMBER	SWL	FIXED	FIXED	CD	FX	CD	FR	CM	FX
=====														
1	0.500	0.0800	3.2500	1.6700	3.040	22026.0	0.110	0.784	2.037	116.10	100.1500	103.32	99.9500	
2	0.500	0.0740	2.4400	1.3500	2.473	22167.0	0.110	0.716	2.239	107.37	99.9200	101.02	99.9400	
3	0.500	0.1100	1.9150	1.1500	3.635	38244.0	0.110	0.826	1.963	110.22	100.6400	102.16	99.9800	
4	0.525	0.0840	3.2000	1.6500	3.449	25289.0	0.135	0.810	1.967	111.25	100.5500	103.65	100.0600	
5	0.525	0.0770	2.4930	1.3700	2.454	25798.0	0.135	0.709	2.252	106.86	99.8590	100.81	99.8000	
6	0.525	0.1150	1.8880	1.1400	3.728	39569.0	0.135	0.839	1.942	108.22	100.7900	101.39	99.9500	
7	0.470	0.0551	3.1545	1.6600	2.008	14638.1	0.090	0.662	2.411	100.00	100.0000	100.00	100.0000	
8	0.470	0.0730	2.4220	1.3600	2.493	22176.9	0.080	0.719	2.214	107.77	100.1000	101.85	99.8600	
9	0.470	0.1000	1.9165	1.1600	3.321	34642.9	0.080	0.800	1.980	111.02	100.4000	104.44	99.7000	
10	0.450	0.0543	3.1502	1.6800	1.874	13498.7	0.060	0.654	2.548	100.00	100.0000	100.00	100.0000	
11	0.450	0.0663	2.3899	1.5600	2.231	19850.1	0.060	0.686	2.314	104.42	99.7700	100.75	99.7200	
12	0.450	0.0970	1.8977	1.1600	3.269	34094.4	0.060	0.799	1.993	110.82	100.0000	103.95	99.7410	
=====														

Table (5.2) - Wave Characteristics and the Wave Force Coefficients for Structure (A).

STR. DIAMETER=0.1100 M STR. LENGTH=0.8080 M														
NATURAL FREQ. IN AIR=36.940 DAMPING COEFF. IN AIR=0.040														
=====														
TEST NO.	WATER DEPTH	WAVE HEIGHT	WAVE PERIOD	KEULEGAN- CARPENTER	REYNOLDS NUMBER	LEVEL FROM SWL	CD FIXED	CM Z	CD FR	CD FR(R)	CM FR	CM FR(R)	CM FR	CM FR(R)
METER	METER	METER	SEC.	NUMBER										
=====														
1	0.500	0.0790	2.4400	1.3500	2.682	24039.0	0.068	0.742	2.106	113.75	100.3200	136.91	100.0200	
2	0.500	0.1200	1.9510	1.1500	3.757	39534.0	0.068	0.850	1.922	110.79	100.5300	133.25	99.8400	
3	0.500	0.0990	2.2070	1.2600	3.177	30510.0	0.068	0.792	1.988	112.74	100.2400	135.36	99.9300	
4	0.525	0.0660	2.5020	1.3600	2.182	19411.0	0.093	0.668	2.291	114.15	99.7300	139.56	99.9000	
5	0.525	0.1140	1.9610	1.1600	3.748	39100.0	0.093	0.838	1.934	111.07	100.5300	133.23	99.8000	
6	0.525	0.1330	1.5200	1.0000	3.926	47506.0	0.093	0.856	1.900	108.37	100.7900	132.99	99.7600	
7	0.550	0.0749	2.5336	1.3600	2.594	23082.0	0.119	0.726	2.226	113.90	100.2000	137.51	99.7780	
8	0.550	0.1057	1.9771	1.1600	3.439	35876.1	0.119	0.821	1.977	112.05	100.1000	134.59	99.8400	
9	0.550	0.1290	1.5274	1.0000	3.775	45677.5	0.119	0.852	1.917	110.58	101.3000	133.10	99.8800	
=====														

Table (5.3) - Wave Characteristics and the Wave Force Coefficient for Structure (B).





STR. DIAMETER=0.0605 M STR. LENGTH=0.8350 M													
NATURAL FREQ. IN AIR=21.200 DAMPING COEFF. IN AIR=0.028													
=====													
TEST NO.	WAVE HEIGHT METER	WAVE LENGTH METER	WAVE PERIOD SEC.	KEULEGAN- CARPENTER NUMBER	REYNOLDS NUMBER	LEVEL FROM	CD FIXED	CM FIXED	CD FR CD FX	CD FR(R) CD FX	CM FR CM FX	CM FR(R) CM FX	
=====													
1	0.500	0.0930	2.1800	1.2500	5.524	16176.0	0.050	1.019	1.758	118.34	101.0000	109.28	99.9200
							0.150	0.978	1.837	118.27	101.2000	109.11	99.9700
-----													
2	0.500	0.1040	1.9150	1.1500	6.105	19431.0	0.050	1.044	1.740	117.76	101.1500	107.71	99.9900
							0.150	1.020	1.770	117.71	101.3200	107.67	100.1000
-----													
3	0.500	0.1480	1.3300	0.9500	8.399	32359.0	0.050	1.115	1.675	113.68	102.1400	104.68	100.3400
							0.150	1.109	1.679	113.62	102.2600	104.54	100.2700
-----													
4	0.525	0.0980	2.4800	1.3500	5.466	14820.0	0.075	0.982	1.810	118.45	100.9000	109.56	99.4680
							0.175	0.964	1.842	118.38	101.0000	109.46	99.6220
-----													
5	0.525	0.1190	1.9300	1.1500	7.576	24113.0	0.075	1.072	1.723	115.65	101.6000	105.34	99.6900
							0.175	1.058	1.733	115.44	101.7300	105.27	99.7600
-----													
6	0.525	0.1440	1.5200	1.0000	7.904	28929.0	0.075	1.106	1.688	114.93	101.6100	104.98	100.3700
							0.175	1.096	1.705	114.67	101.9000	104.82	100.3300
-----													

Table (5.5) - Wave Characteristics and Wave Force Coefficients for Structure (D).

STR. DIAMETER=0.0574 M    STR. LENGTH=0.7350 M NATURAL FREQ. IN AIR=20.000    DAMPING COEFF. IN AIR=0.064														
=====														
TEST NO.	WATER DEPTH	WAVE HEIGHT	WAVE PERIOD	KEULEGAN- CARPENTER	REYNOLDS NUMBER	LEVEL FROM SWL	CD FIXED	CM	CD FR	CD FR(R)	CM FR	CM FR(R)	CM FR	CM FR(R)
METER	METER	METER	SEC.	NUMBER	NUMBER									
=====														
1	0.525	0.1080	1.9600	1.1500	6.742	19148.2	0.120	1.054	1.719	111.18	101.3300	101.60	99.9000	
							0.170	1.052	1.720	111.14	101.3500	101.56	99.9800	
							0.270	1.050	1.731	111.12	101.3900	101.54	99.8000	
-----														
2	0.525	0.1360	1.5200	1.0000	8.130	26787.7	0.120	1.111	1.672	107.68	102.1000	100.19	100.4000	
							0.170	1.110	1.680	107.65	102.1200	100.17	100.3000	
							0.270	1.104	1.690	107.64	102.2000	100.16	100.1000	
-----														
3	0.525	0.1200	1.7400	1.0300	7.308	22295.7	0.120	1.062	1.725	109.75	101.4500	100.87	100.1000	
							0.170	1.061	1.728	109.72	101.4000	100.84	100.0000	
							0.270	1.057	1.730	109.70	101.4500	100.82	100.2000	
-----														
4	0.500	0.0900	1.9200	1.1500	5.879	16698.6	0.095	1.010	1.730	112.27	101.0500	103.08	99.9000	
							0.145	1.008	1.790	112.25	101.0000	103.04	99.8500	
							0.245	1.002	1.801	112.24	101.0000	103.02	99.3600	
-----														
5	0.500	0.1250	1.5100	1.0000	7.271	25955.3	0.095	1.062	1.700	109.95	101.3000	100.90	100.0700	
							0.145	1.056	1.710	109.92	101.2000	100.88	100.2000	
							0.245	1.054	1.730	109.93	101.3000	100.86	100.3000	
-----														
6	0.500	0.1050	1.2600	1.0300	6.520	19893.4	0.095	1.048	1.738	111.45	101.2500	102.00	99.9500	
							0.145	1.046	1.740	111.41	101.1000	101.95	99.8100	
							0.245	1.044	1.750	111.41	101.1000	101.95	99.8000	
-----														

Table (5.6) – Characteristics and the Wave Force Coefficients for Structure (E) with no Mass at the Top.



STR. DIAMETER=0.0574 M STR. LENGTH=0.7350 M														
NATURAL FREQ. IN AIR=15.130 DAMPING COEFF. IN AIR=0.068														
=====														
TEST NO.	WATER DEPTH METER	WAVE HEIGHT METER	WAVE PERIOD SEC.	KEULEGAN-CARPENTER NUMBER	REYNOLDS NUMBER	LEVEL FROM	CD FIXED	CM FIXED	CD FR	CD FR(R)	CM FR	CM FR(R)	CM FR	CM FR(R)
=====														
1	0.525	0.1080	1.9600	1.1500	6.742	19148.2	0.120	1.054	1.721	111.76	101.3300	102.17	99.9500	
							0.170	1.054	1.723	111.73	101.3200	102.15	99.9500	
							0.270	1.050	1.731	111.72	101.3300	102.12	99.9700	
-----														
2	0.525	0.1360	1.5200	1.0000	8.130	26787.7	0.120	1.112	1.680	108.25	102.0500	100.67	100.4500	
							0.170	1.111	1.682	108.22	102.0800	100.64	100.5000	
							0.270	1.104	1.690	108.21	102.0700	100.63	100.5200	
-----														
3	0.525	0.1200	1.7400	1.0600	7.308	22295.7	0.120	1.064	1.728	110.37	101.3800	101.42	100.0500	
							0.170	1.063	1.729	110.34	101.4000	101.39	100.0700	
							0.270	1.057	1.730	110.32	101.3800	101.38	100.0600	
-----														
4	0.500	0.0900	1.9200	1.1500	5.879	16098.6	0.095	1.012	1.790	112.82	101.0000	103.67	99.9100	
							0.145	1.009	1.790	112.79	101.0300	103.64	99.9200	
							0.245	1.002	1.801	112.77	101.0400	103.62	99.9400	
-----														
5	0.500	0.1250	1.5100	1.0000	7.271	25955.3	0.095	1.062	1.700	110.50	101.2800	101.50	99.9900	
							0.145	1.057	1.715	110.46	101.3000	101.45	99.9900	
							0.245	1.054	1.730	110.44	101.3000	101.46	99.9700	
-----														
6	0.500	0.1050	1.2800	1.0300	6.520	19893.4	0.095	1.048	1.738	112.01	101.1000	102.57	99.9200	
							0.145	1.046	1.740	111.97	101.1500	102.54	99.9200	
							0.245	1.044	1.750	111.95	101.1400	102.53	99.9400	
-----														

Table (5.7) - Wave Characteristics and the Wave Force Coefficients for Structure (E) with 1010 Grs at the Top.

STR. DIAMETER=0.0574 M STR. LENGTH=0.7350 M														
NATURAL FREQ. IN AIR=12.690 DAMPING COEFF. IN AIR=0.072														
=====														
TEST NO.	WATER DEPTH METER	WAVE LENGTH METER	WAVE PERIOD SEC.	KEULEGAN-CARPENTER NUMBER	REYNOLDS NUMBER	LEVEL FROM SWL	CD FIXED	CM FIXED	CD FR	CD FR(R)	CM FR	CM FR(R)	CM FR	CM FR(R)
=====														
1	0.525	0.1080	1.9600	1.1500	6.742	19148.2	0.120	1.055	1.721	112.14	101.3100	102.79	99.9000	
							0.170	1.051	1.721	112.10	101.3100	102.76	99.9200	
							0.270	1.050	1.731	112.09	101.3000	102.75	99.9300	
-----														
2	0.525	0.1360	1.5200	1.0000	8.130	26787.7	0.120	1.112	1.681	108.83	101.9000	101.10	100.3000	
							0.170	1.111	1.683	108.80	101.9100	101.06	100.3000	
							0.270	1.104	1.690	108.79	101.9000	101.04	100.3300	
-----														
3	0.525	0.1200	1.7400	1.0800	7.308	22295.7	0.120	1.064	1.728	110.94	101.4200	101.97	100.1000	
							0.170	1.062	1.727	110.90	101.4100	101.95	100.1000	
							0.270	1.057	1.730	110.88	101.4100	101.94	100.1200	
-----														
4	0.500	0.0900	1.9200	1.1500	5.879	16693.6	0.095	1.013	1.793	113.43	101.0300	104.25	99.8900	
							0.145	1.009	1.791	113.40	101.0400	104.21	99.8800	
							0.245	1.002	1.801	113.38	101.0300	104.19	99.9100	
-----														
5	0.500	0.1250	1.5100	1.0000	7.271	25955.3	0.095	1.061	1.710	111.13	101.2700	102.09	100.1000	
							0.145	1.060	1.720	111.10	101.3000	102.06	100.1000	
							0.245	1.054	1.730	111.11	101.3000	102.05	100.1000	
-----														
6	0.500	0.1050	1.2800	1.0800	6.520	17893.4	0.095	1.050	1.736	112.58	101.2000	103.15	99.9500	
							0.145	1.045	1.740	112.55	101.2300	103.11	99.9700	
							0.245	1.044	1.750	112.53	101.1800	103.13	99.9900	
-----														

Table (5.8) ~ Wave Characteristics and Wave Force Coefficients for Structure (E) with 2020 Grs at the Top.

STR. DIAMETER=0.0574 M STR. LENGTH=0.8350 M														
NATURAL FREQ. IN AIR=17.650 DAMPING COEFF. IN AIR=0.063														
=====														
TEST NO.	WATER DEPTH METER	WAVE HEIGHT METER	WAVE PERIOD SEC.	KEULEGAN-CARPENTER NUMBER	REYNOLDS NUMBER	LEVEL FROM SWL	CD FIXED	CM FIXED	CD FR	CD FR(R)	CM FR	CM FR(R)	CM FX	CM FR
=====														
1	0.525	0.1080	1.9600	1.1500	6.742	19148.2	0.120	1.073	1.718	114.76	101.3500	104.35	100.0000	
							0.170	1.068	1.720	114.74	101.4000	104.32	100.2000	
							0.270	1.056	1.735	114.72	101.3000	104.30	100.2000	
-----														
2	0.525	0.1360	1.5200	1.0000	8.130	26787.7	0.120	1.130	1.650	112.30	102.2000	102.38	100.4000	
							0.170	1.128	1.650	112.25	102.4000	102.35	100.5000	
							0.270	1.104	1.690	112.24	102.4000	102.33	100.2000	
-----														
3	0.525	0.1200	1.7400	1.0800	7.308	22295.7	0.120	1.075	1.720	113.90	101.5000	103.35	100.1500	
							0.170	1.074	1.723	113.88	101.1000	103.32	100.3000	
							0.270	1.058	1.730	113.86	101.0000	103.31	100.4000	
-----														
4	0.500	0.0900	1.9200	1.1500	5.879	16698.6	0.095	1.007	1.770	115.90	101.0700	106.11	99.9100	
							0.145	1.008	1.780	115.87	101.1100	106.08	99.9500	
							0.245	1.002	1.801	115.86	101.2000	106.07	99.9400	
-----														
5	0.500	0.1250	1.5100	1.0000	7.271	25955.3	0.095	1.060	1.710	114.00	101.3200	103.53	100.1000	
							0.145	1.056	1.714	113.98	101.2000	103.50	100.2000	
							0.245	1.054	1.730	113.96	101.5000	103.50	100.3000	
-----														
6	0.500	0.1050	1.2800	1.0300	6.520	19893.4	0.095	1.048	1.737	115.11	101.2400	104.76	99.9700	
							0.145	1.050	1.740	115.08	101.6000	104.73	99.7000	
							0.245	1.044	1.750	115.09	101.6000	104.72	99.8000	
-----														

Table (5.9) – Wave Characteristics and Wave Force Coefficients for Structure (F) with no Mass at the Top.



STR. DIAMETER=0.0574 M STR. LENGTH=0.8350 M														
NATURAL FREQ. IN AIR=13.460 DAMPING COEFF. IN AIR=0.065														
=====														
TEST NO.	WATER DEPTH METER	WAVE HEIGHT METER	WAVE PERIOD SEC.	KEULEGAN- CARPENTER NUMBER	REYNOLDS NUMBER	LEVEL FROM SWL	CD FIXED	CM FIXED	CD FR FX	CD FR(R) FX	CM FR FX	CM FR(R) FX	CM FR FX	CM FR(R) FX
=====														
1	0.525	0.1080	1.9600	1.1500	6.742	19148.2	0.120	1.096	1.710	115.37	101.3100	104.98	99.9500	99.9500
							0.170	1.092	1.710	115.34	101.2000	104.95	99.9900	99.9900
							0.270	1.068	1.725	115.32	101.2400	104.93	99.9900	99.9900
-----														
2	0.525	0.1360	1.5200	1.0000	8.130	26787.7	0.120	1.118	1.619	112.85	102.0700	103.09	100.3700	100.3700
							0.170	1.116	1.620	112.82	101.9000	103.07	100.2000	100.2000
							0.270	1.092	1.670	112.81	101.8000	103.06	100.2000	100.2000
-----														
3	0.525	0.1200	1.7400	1.0800	7.308	22295.7	0.120	1.103	1.705	114.41	101.4800	104.05	100.0100	100.0100
							0.170	1.100	1.700	114.38	101.2000	104.02	100.2000	100.2000
							0.270	1.074	1.720	114.36	101.2500	104.00	100.1700	100.1700
-----														
4	0.500	0.0900	1.9200	1.1500	5.879	16698.6	0.095	1.037	1.797	116.45	101.0500	106.62	99.9000	99.9000
							0.145	1.032	1.800	116.42	101.1300	106.59	99.9900	99.9900
							0.245	1.008	1.810	116.40	101.1600	106.57	100.1000	100.1000
-----														
5	0.500	0.1250	1.5100	1.0000	7.271	25955.3	0.095	1.086	1.630	114.63	101.3000	104.05	99.9300	99.9300
							0.145	1.080	1.630	114.60	101.7000	104.01	99.9000	99.9000
							0.245	1.056	1.730	114.58	101.5000	104.00	99.9700	99.9700
-----														
6	0.500	0.1050	1.2300	1.0300	6.520	19893.4	0.095	1.068	1.742	115.66	101.1800	105.37	99.9500	99.9500
							0.145	1.056	1.740	115.62	101.2000	105.34	100.0000	100.0000
							0.245	1.044	1.750	115.63	101.1000	105.32	100.1000	100.1000
-----														

Table (5.10) - Wave Characteristics and Wave Force Coefficients for Structure (F) with 1010 Grs at the Top.

STR. DIA=ETER=0.0574 M STR. LENGTH=0.8350 M														
NATURAL FREQ. IN AIR=11.520 DAMPING COEFF. IN AIR=0.070														
=====														
TEST NO.	WATER DEPTH METER	WAVE LENGTH METER	WAVE PERIOD SEC.	KEULEGAN-CARPENTER NUMBER	REYNOLDS NUMBER	LEVEL FROM S/L	CD FIXED	CM FIXED	CD FR	CD FR(R)	CM FR	CM FR(R)	CM FR	CM FR(R)
=====														
1	0.525	0.1080	1.2600	1.1500	6.742	19148.2	0.120	1.080	1.719	115.98	101.2800	105.53	99.8000	99.8000
							0.170	1.074	1.721	115.95	101.3000	105.49	99.9500	99.9500
							0.270	1.062	1.737	115.96	101.2000	105.47	100.0100	100.0100
-----														
2	0.525	0.1360	1.5200	1.0000	8.130	26787.7	0.120	1.128	1.680	113.46	101.9800	103.62	100.3200	100.3200
							0.170	1.126	1.660	113.41	101.8000	103.59	100.2000	100.2000
							0.270	1.120	1.670	113.40	101.5000	103.57	100.1700	100.1700
-----														
3	0.525	0.1200	1.7400	1.0800	7.308	22295.7	0.120	1.092	1.716	115.07	101.4500	104.61	100.1100	100.1100
							0.170	1.080	1.720	115.05	101.3700	104.58	100.2000	100.2000
							0.270	1.074	1.737	115.03	101.3000	104.56	100.2200	100.2200
-----														
4	0.500	0.0900	1.9200	1.1500	5.879	16698.6	0.095	1.038	1.790	117.08	101.0300	107.24	99.8700	99.8700
							0.145	1.032	1.801	117.05	101.1000	107.21	99.9000	99.9000
							0.245	1.008	1.812	117.04	101.0200	107.19	100.0200	100.0200
-----														
5	0.500	0.1250	1.5100	1.0000	7.271	25955.3	0.095	1.074	1.726	115.22	101.2000	104.67	100.1500	100.1500
							0.145	1.068	1.730	115.19	101.2000	104.63	100.2000	100.2000
							0.245	1.056	1.739	115.17	101.1000	104.64	100.1500	100.1500
-----														
6	0.500	0.1050	1.2300	1.0300	6.520	17893.4	0.095	1.055	1.753	116.28	101.2100	105.91	99.9600	99.9600
							0.145	1.056	1.755	116.27	101.1100	105.88	99.9900	99.9900
							0.245	1.050	1.760	116.25	101.0900	105.86	100.0500	100.0500
-----														

Table (5.11) - Wave Characteristics and Wave Force Coefficients for Structure (F) with 2020 Grs at the Top.

depth while the structure velocity decreases sinusoidally with depth, for the case of the drag coefficient and similarly for the acceleration in the case of the inertia coefficient.

The Reynolds numbers of the tests varied from  $(1.09 \times 10^4 \text{ to } 4.7 \times 10^4)$ . Figures (5.3.1a) and (5.3.1b) show the variation of  $C_D$  and  $C_M$  with Reynolds numbers,  $1/D$ .

The relationship between the waves and the corresponding forces can be shown by plotting the results of the dimensionless parameter (Keulegan-Carpenter number) and the coefficients representing the forces.

Figure (5.3.2a) and Figure (5.3.2b) show the variation of the drag coefficients and the variation of the inertia coefficients for the fixed structure versus the Keulegan-Carpenter numbers respectively.

Figures (5.3.3a through 5.3.12a) show the variation of the percentage ratio of  $C_D$  for free structures to that for fixed structures for each structure tested and Figure (5.3.13) shows the same variation of the ratio for all the tested structures with Keulegan-Carpenter numbers. Figures (5.3.3b through 5.3.12b) show the variation of the percentage ratio of the



$C_M$  for free structures to that for fixed structures for each structure tested and Figure (5.3.14) shows the same variation of the ratio for all tested structures with Keulegan-Carpenter number.

Figure (5.3.15a) and Figure (5.3.15b) show the variation of the percentage ratio of the  $C_D$  calculated by the modified Morison's equation to that calculated by Morison's equation and similarly for  $C_M$  with Keulegan-Carpenter numbers respectively.

The data presented in the figures cited above exhibit certain characteristics which will be discussed below.

(a) THE VARIATION OF THE FORCE COEFFICIENTS ( $C_D$  AND  $C_M$ ) FOR FIXED STRUCTURE WITH KEULEGAN-CARPENTER NUMBER

The drag coefficient  $C_D$  increases with increasing K-C numbers used in the tests (the range of K-C number used was (1.874 - 10.604)), while the  $C_M$  decreases with increasing K-C number for the same range. These results agree with the previous results of Keulegan and Carpenter 1968 (27). The results show less scattering and that is because of the method used in measuring the local force for a segment of the structure which minimizes the error; arising due to the

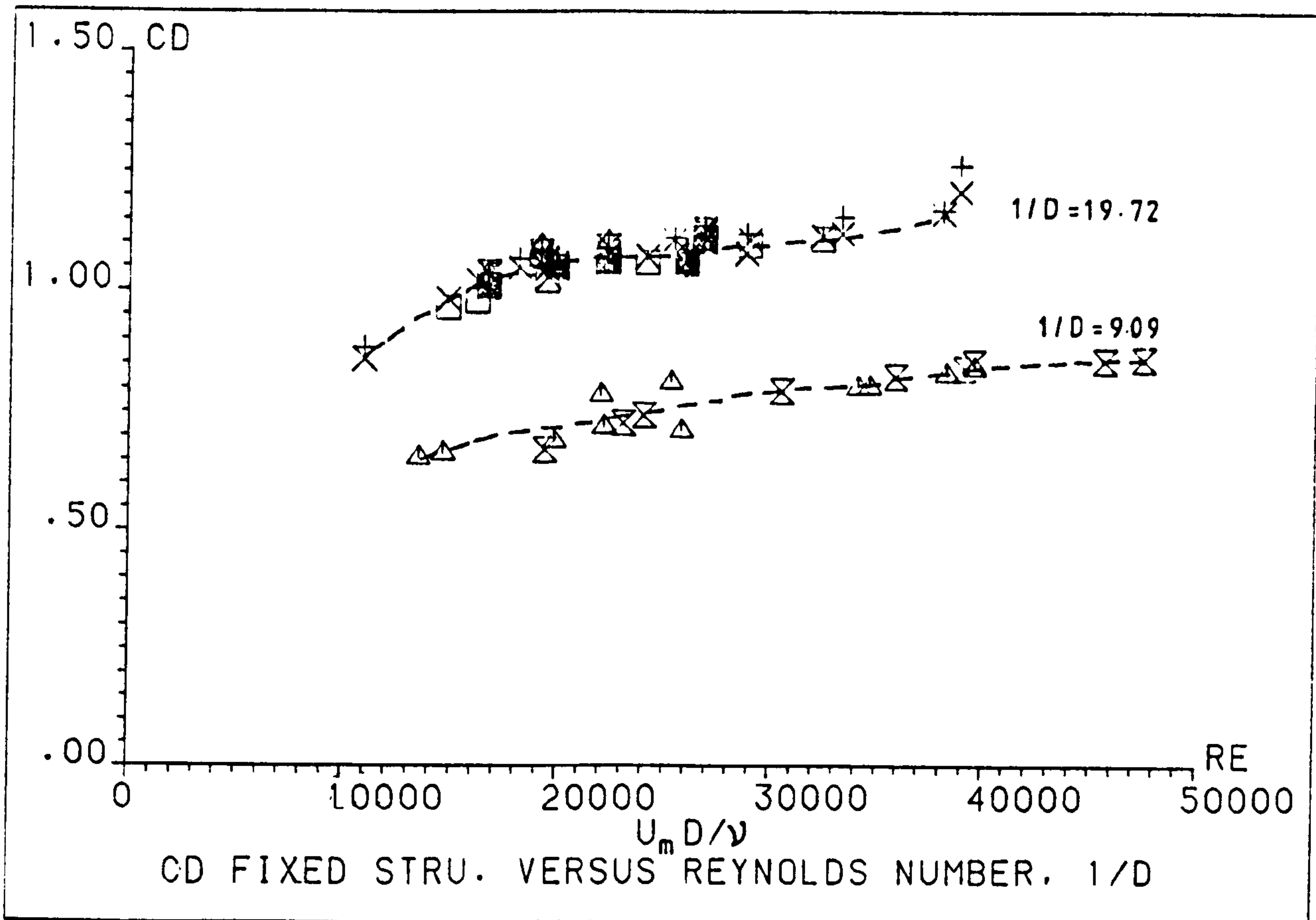


Figure (5.3.1a) - Variation of  $C_D$  with Reynolds Number,  $1/D$ .

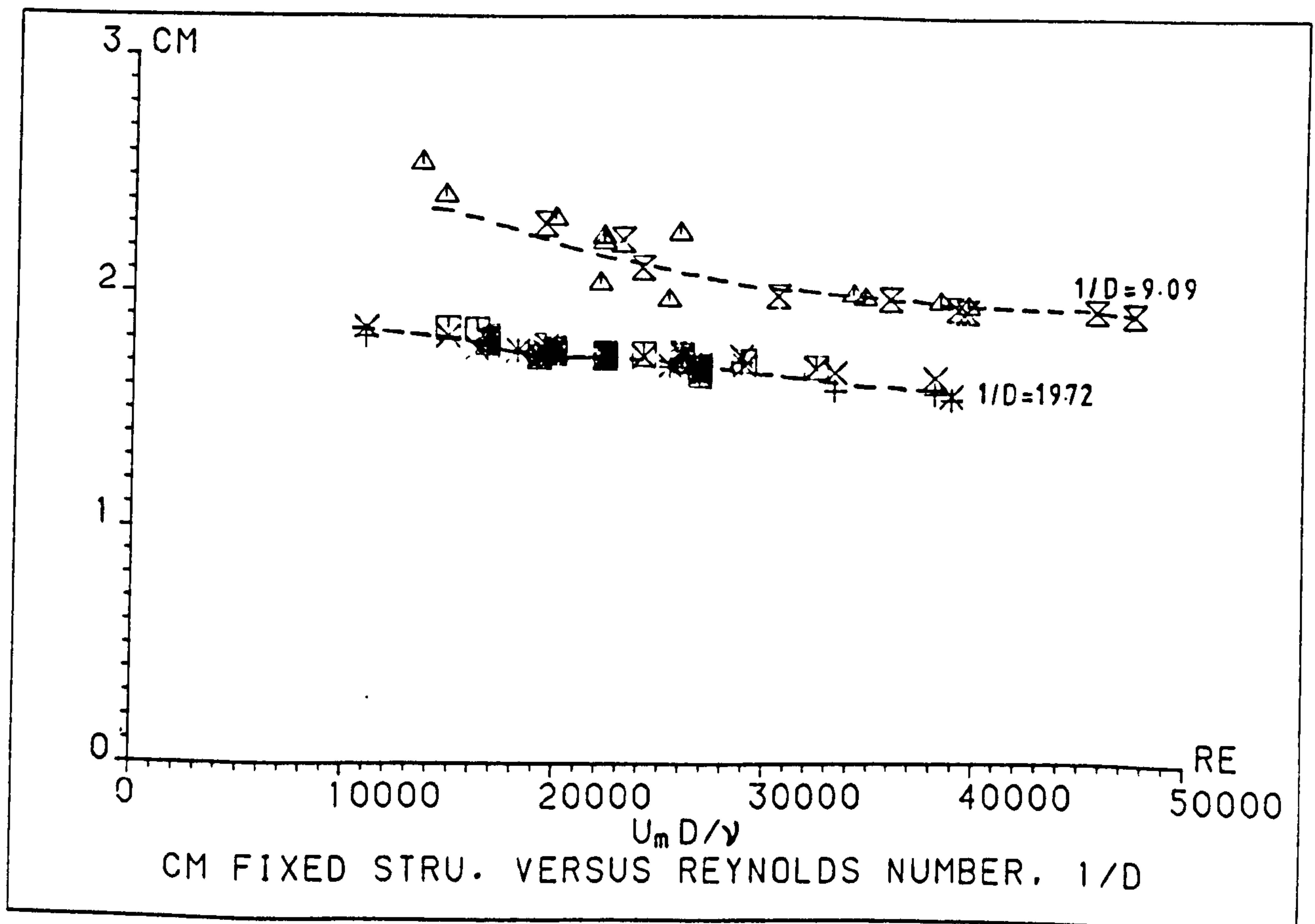


Figure (5.3.1b) - Variation of  $C_M$  with Reynolds Number,  $1/D$ .

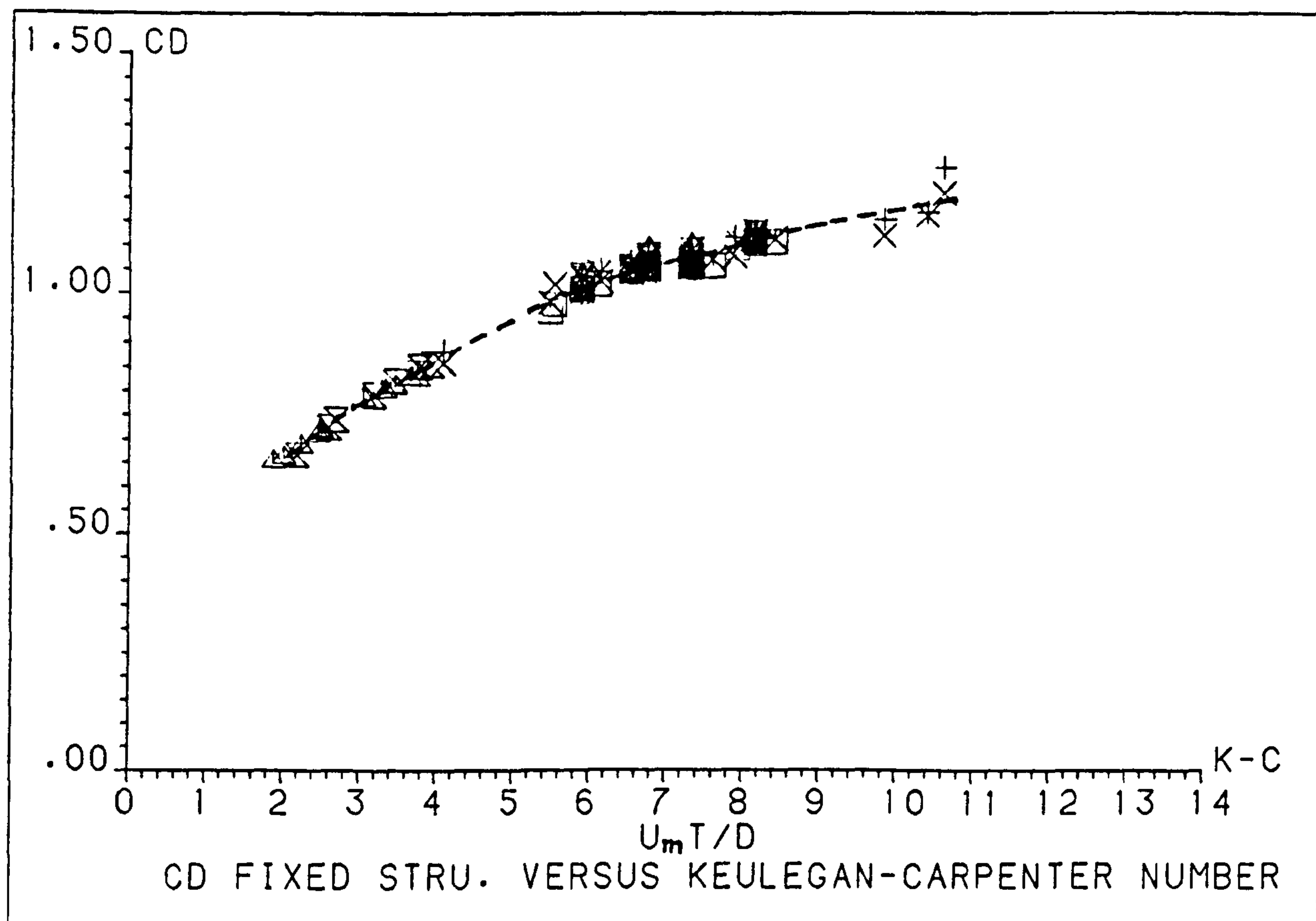


Figure (5.3.2a) - Variation of  $C_D$  with Keulegan-Carpenter Number.

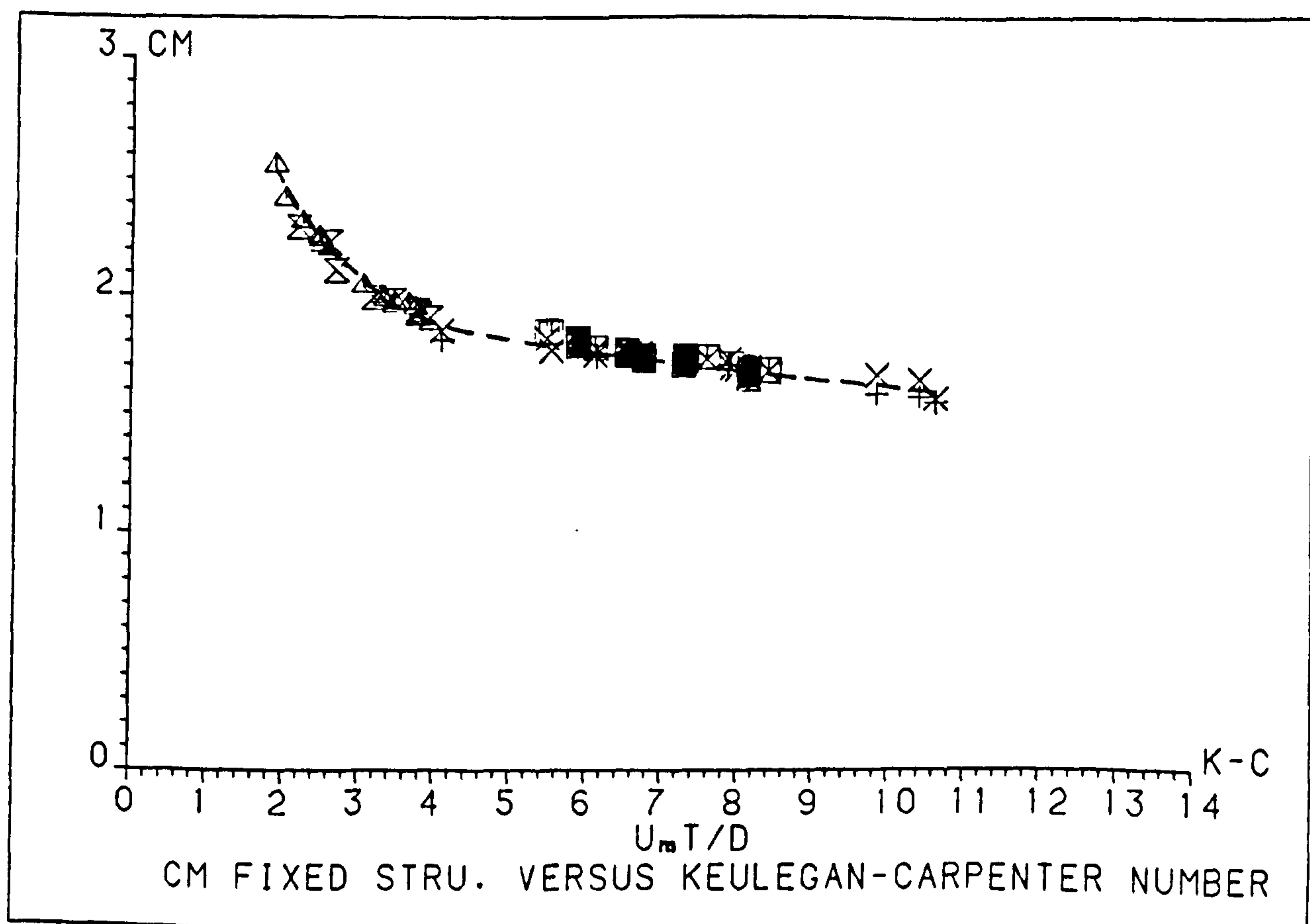


Figure (5.3.2b) - Variation of  $C_M$  with Keulegan-Carpenter Number.



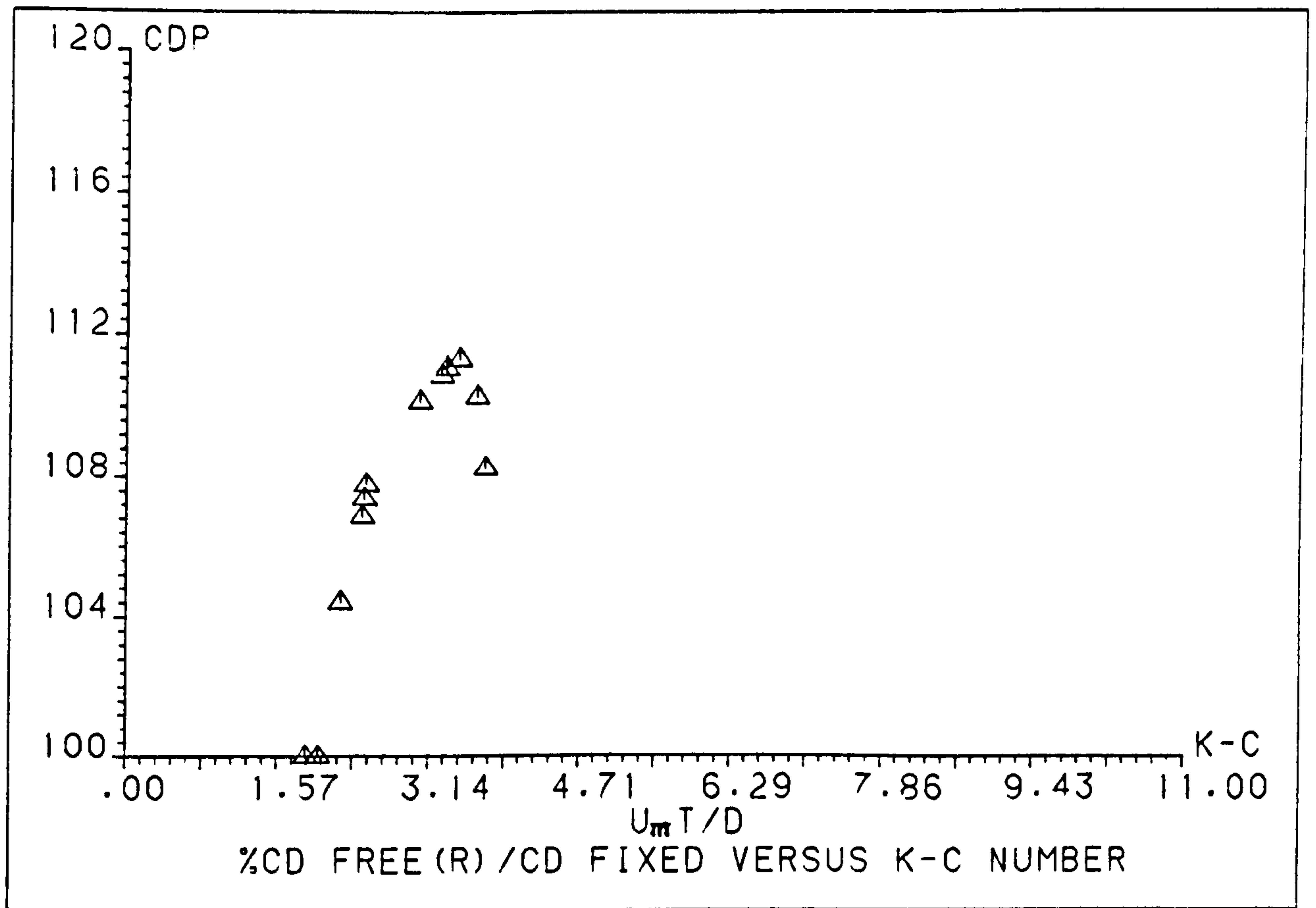


Figure (5.3.3a) - Variation of % ( $C_D$  Free (R)/ $C_D$  Fixed) with K-C Number for Structure A.

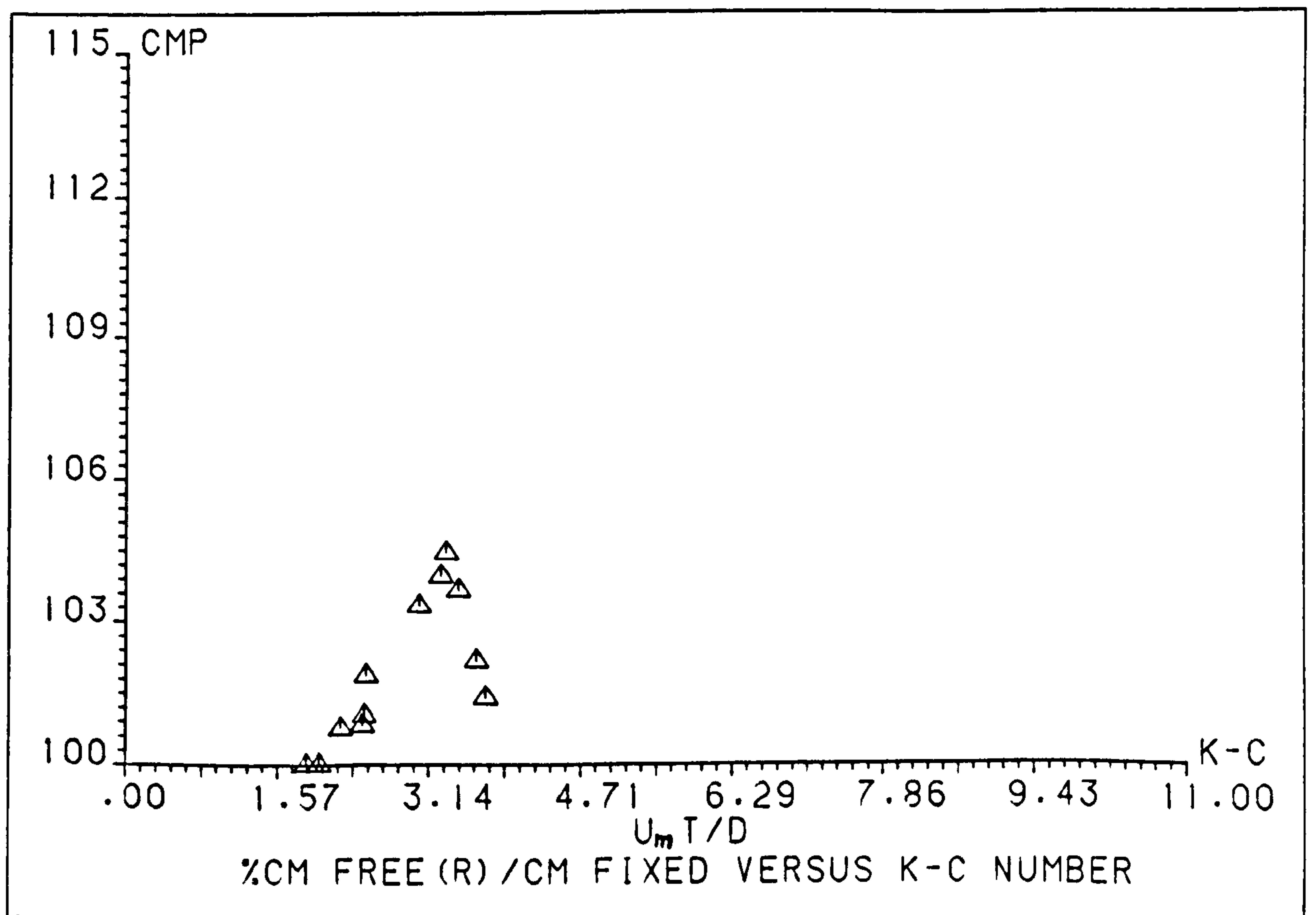


Figure (5.3.3b) - Variation of % ( $C_M$  Free (R)/ $C_M$  Fixed) with K-C Number for Structure A.

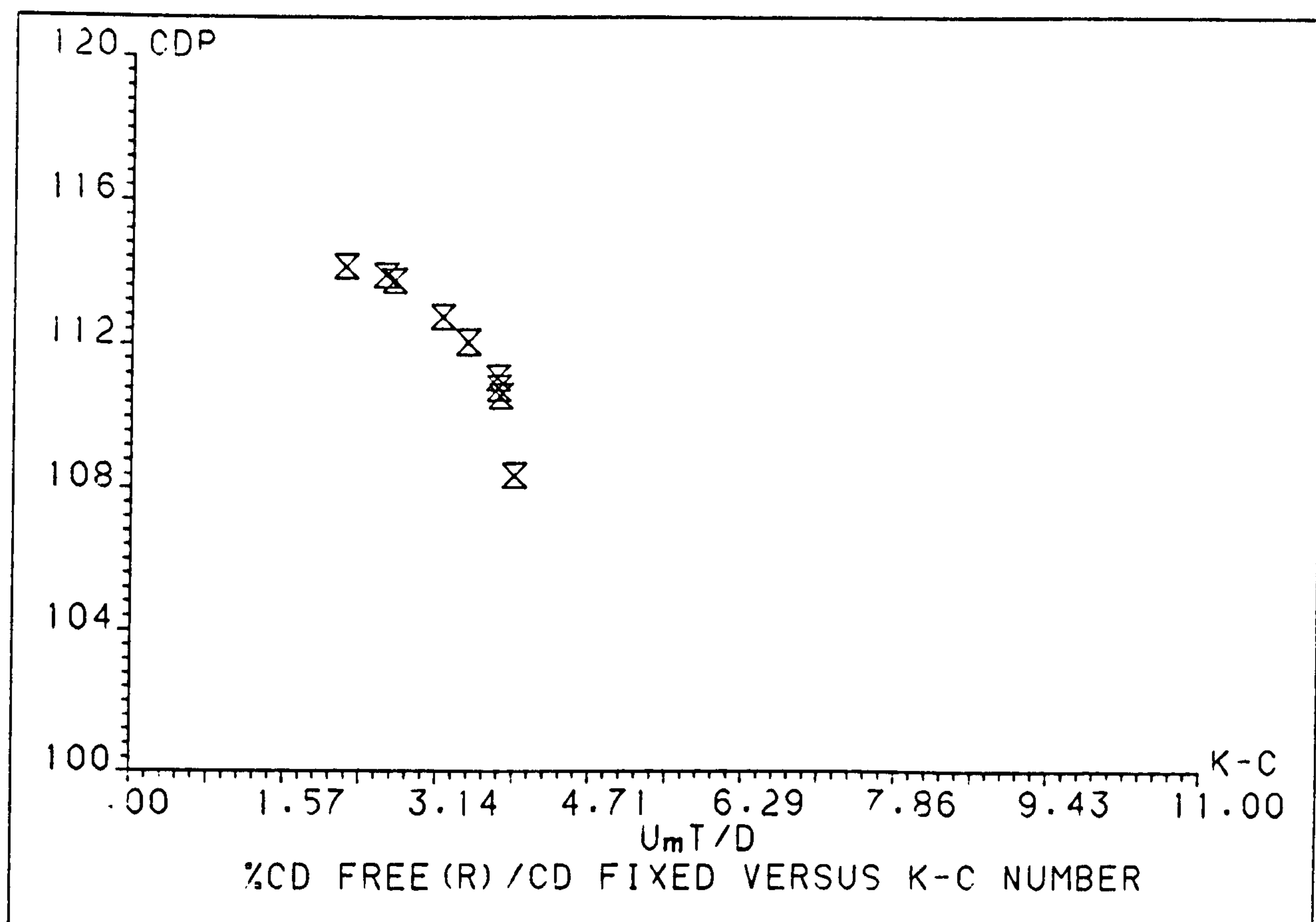


Figure (5.3.4a) - Variation of  $\% (C_D \text{ Free (R)} / C_D \text{ Fixed})$  with K-C Number for Structure B.

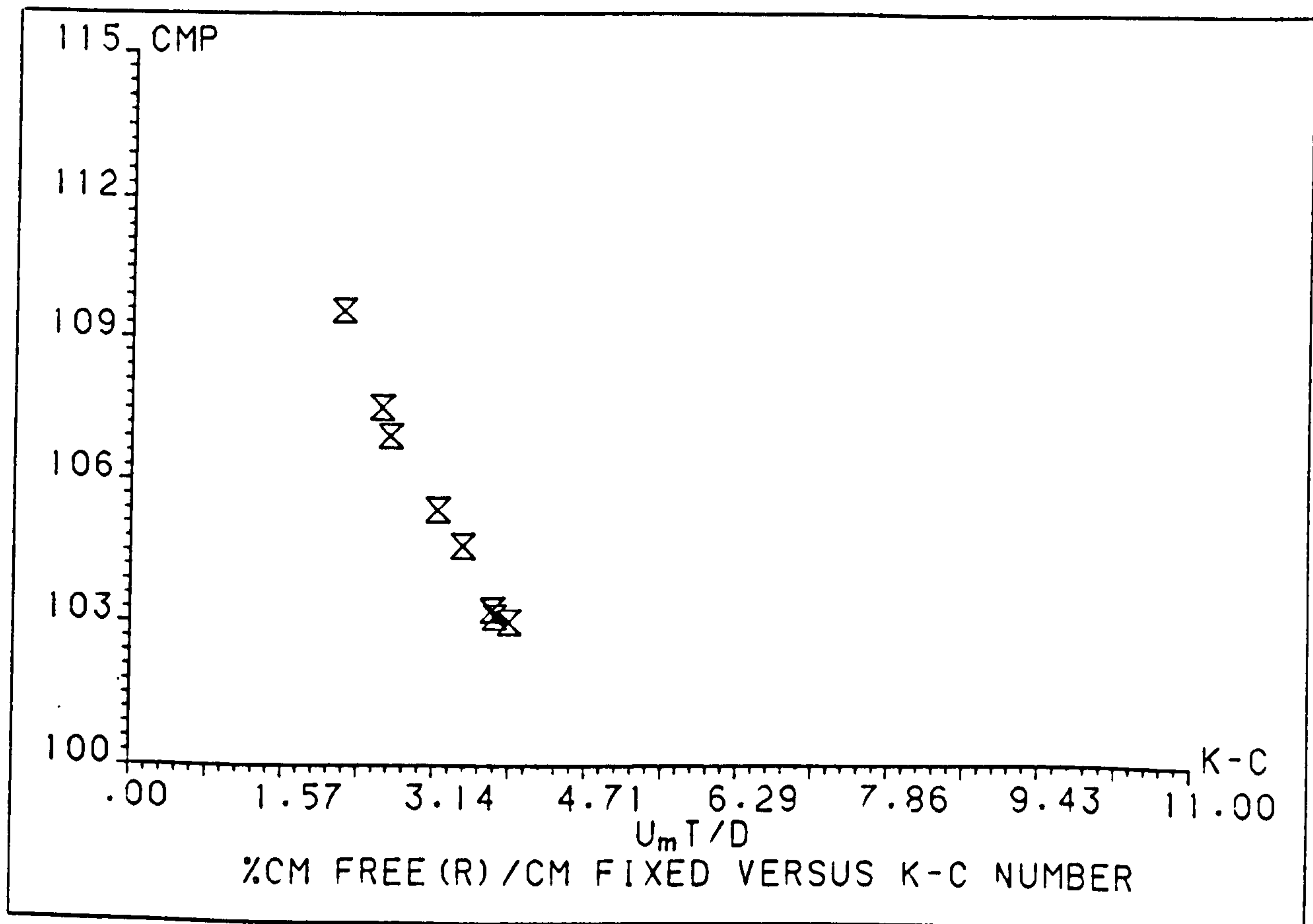


Figure (5.3.4b) - Variation of  $\% (C_M \text{ Free (R)} / C_M \text{ Fixed})$  with K-C Number for Structure B.

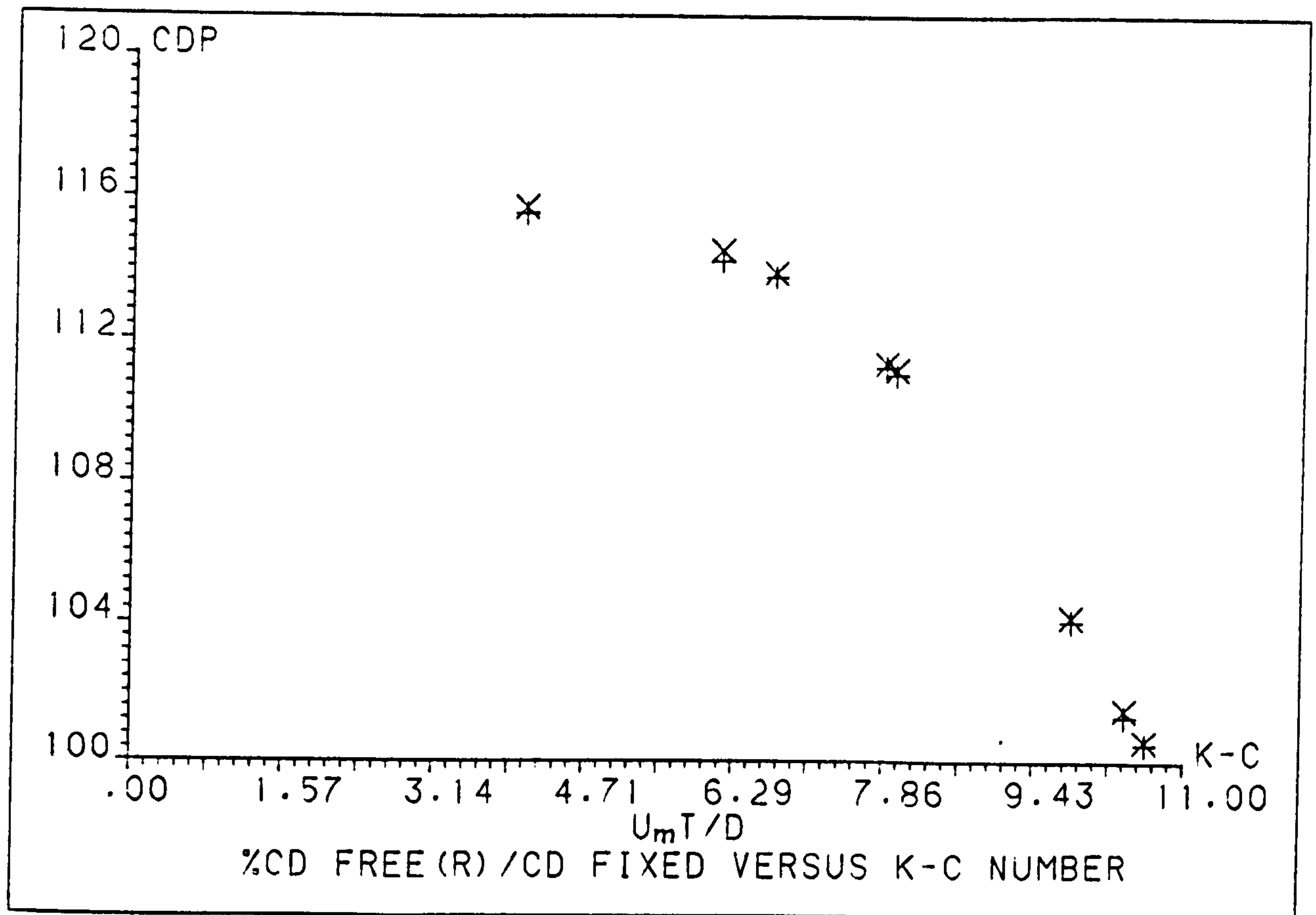


Figure (5.3.5a) - Variation of % ( $C_D$  Free (R)/ $C_D$  Fixed) with K-C Number for Structure C.

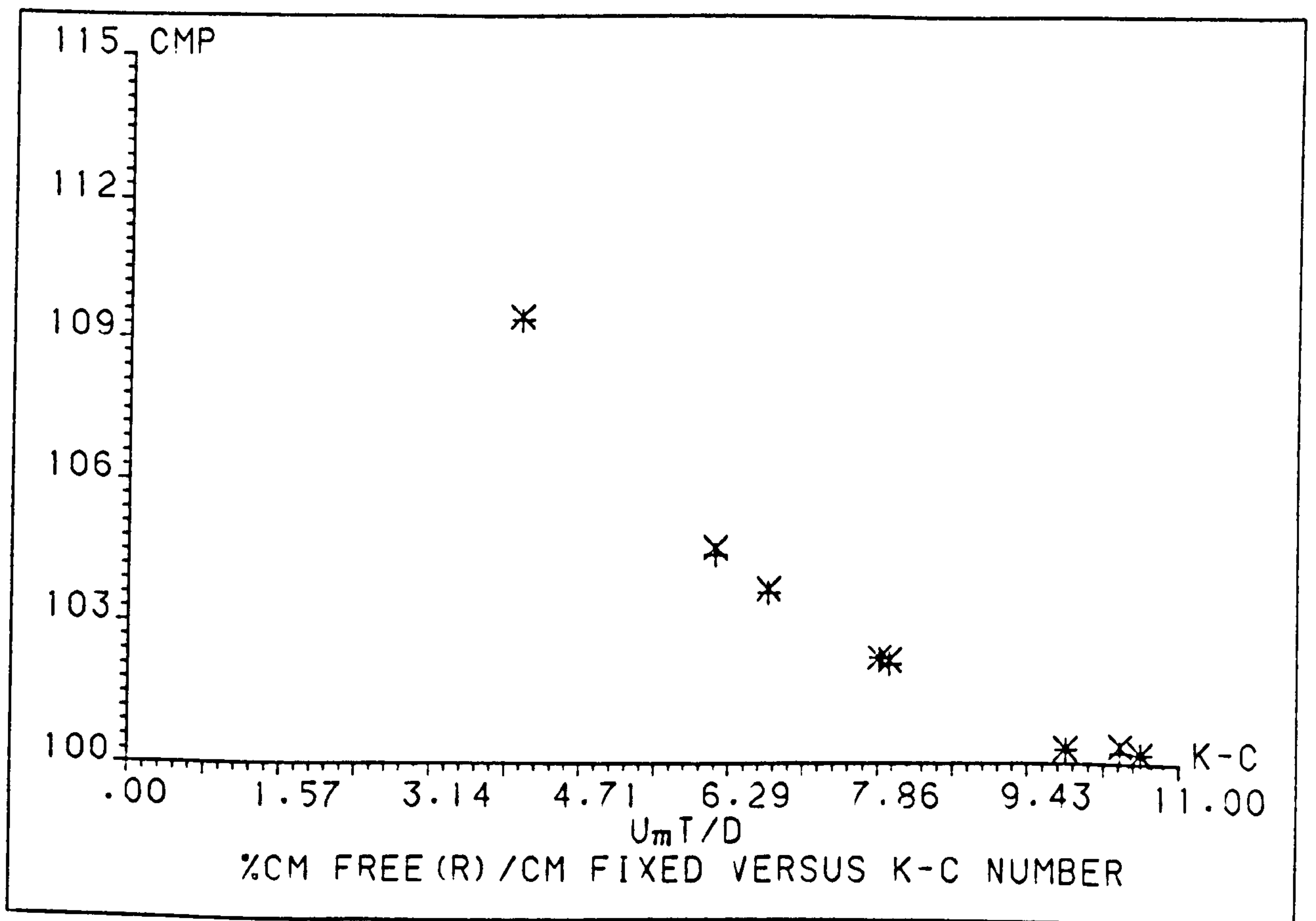


Figure (5.3.5b) - Variation of % ( $C_M$  Free (R)/ $C_M$  Fixed) with K-C Number for Structure C.



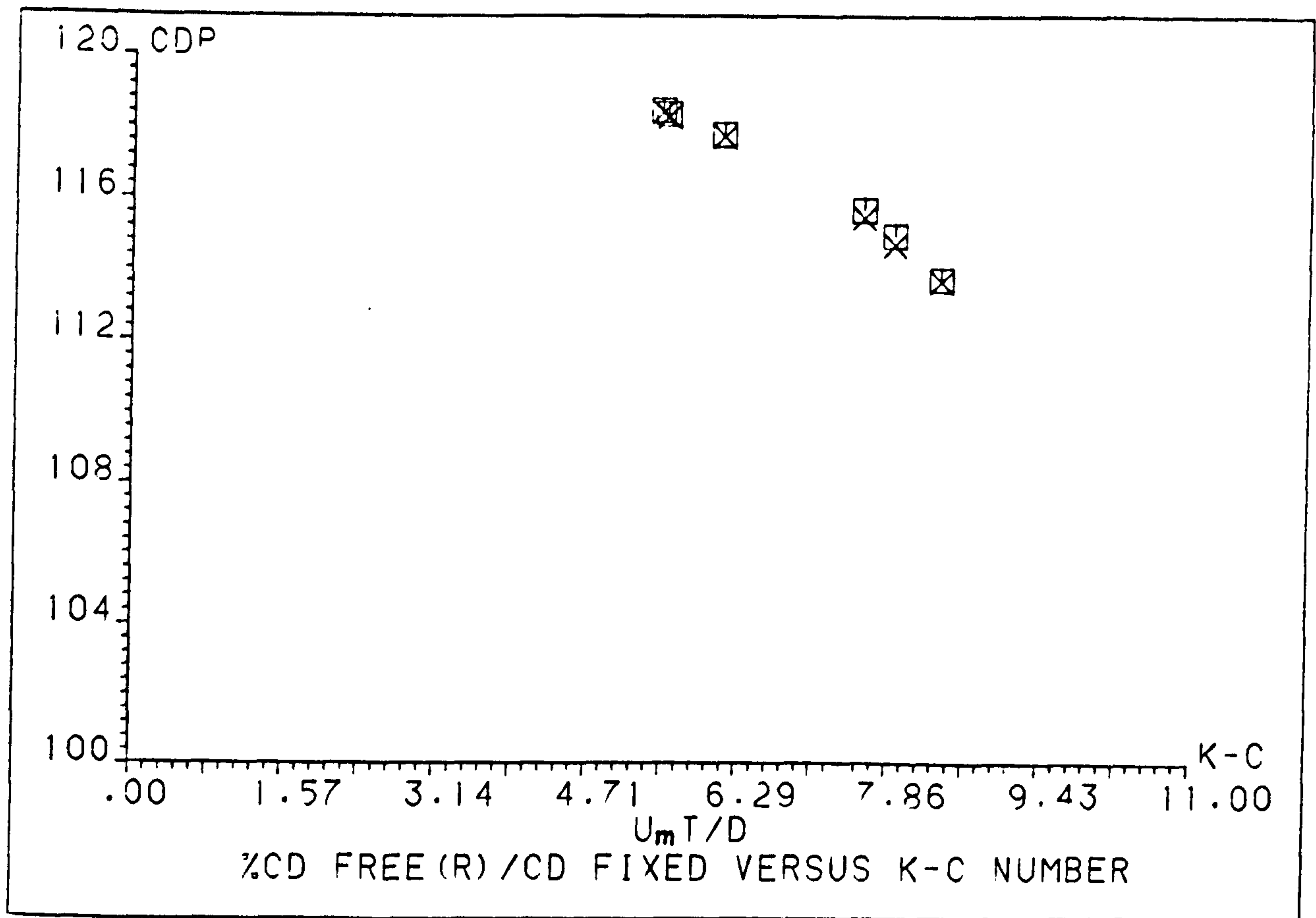


Figure (5.3.6a) - Variation of % ( $C_D$  Free (R) /  $C_D$  Fixed) with K-C Number for Structure D.

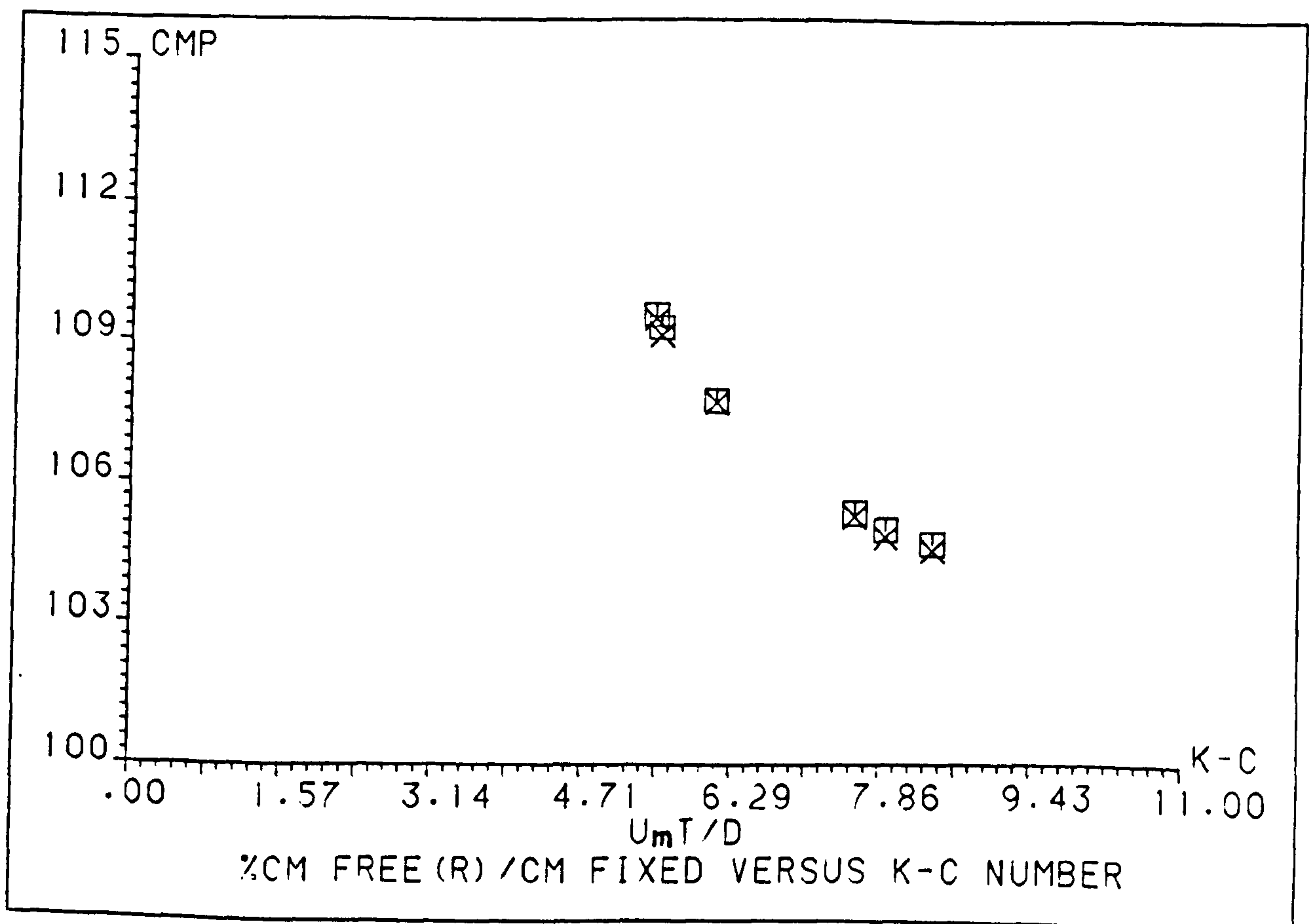


Figure (5.3.6b) - Variation of % ( $C_M$  Free (R) /  $C_M$  Fixed) with K-C Number for Structure D.

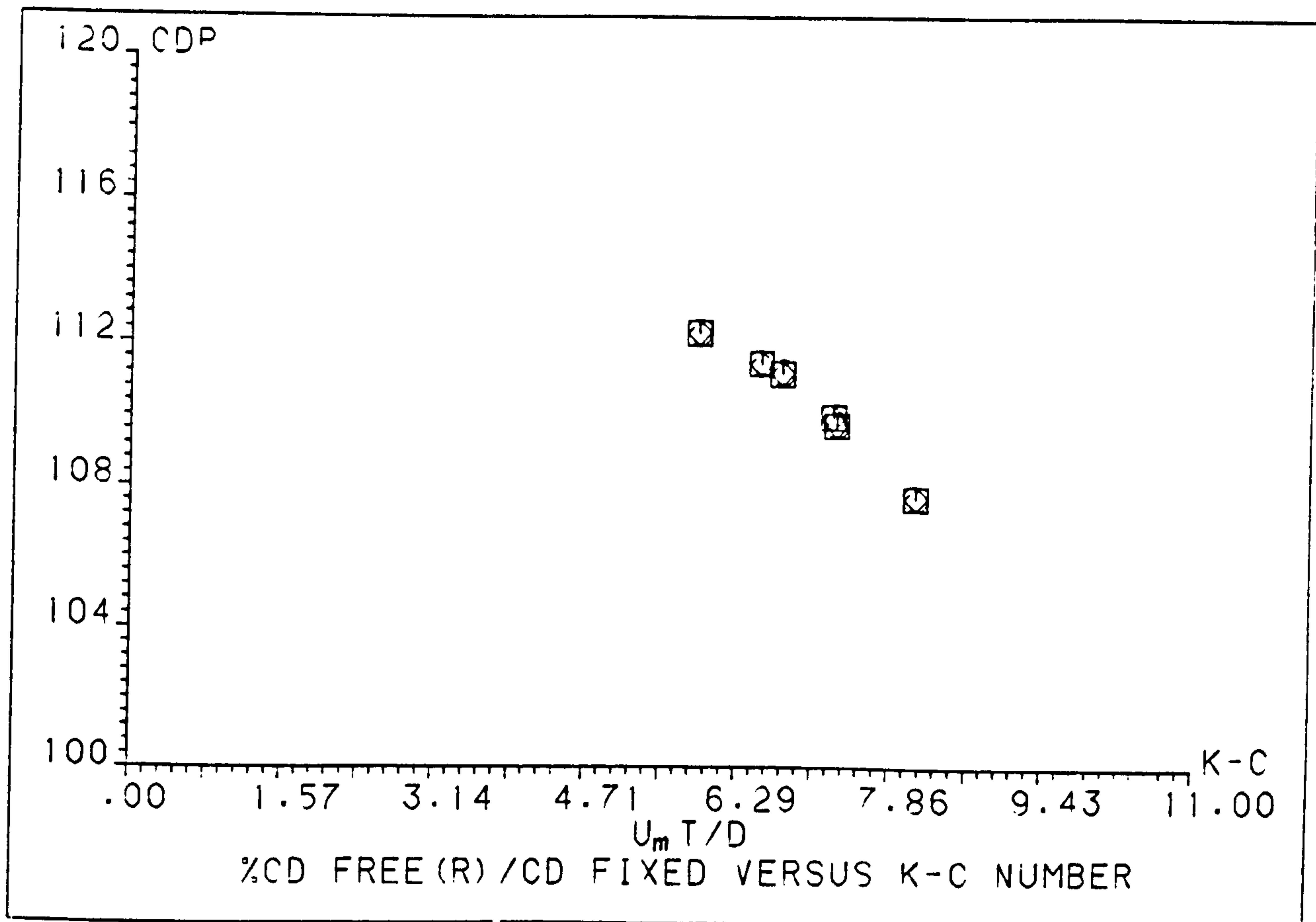


Figure (5.3.7a) - Variation of  $\% (C_D \text{ Free (R) / } C_D \text{ Fixed})$  with K-C Number for Structure E with no Mass at Top.

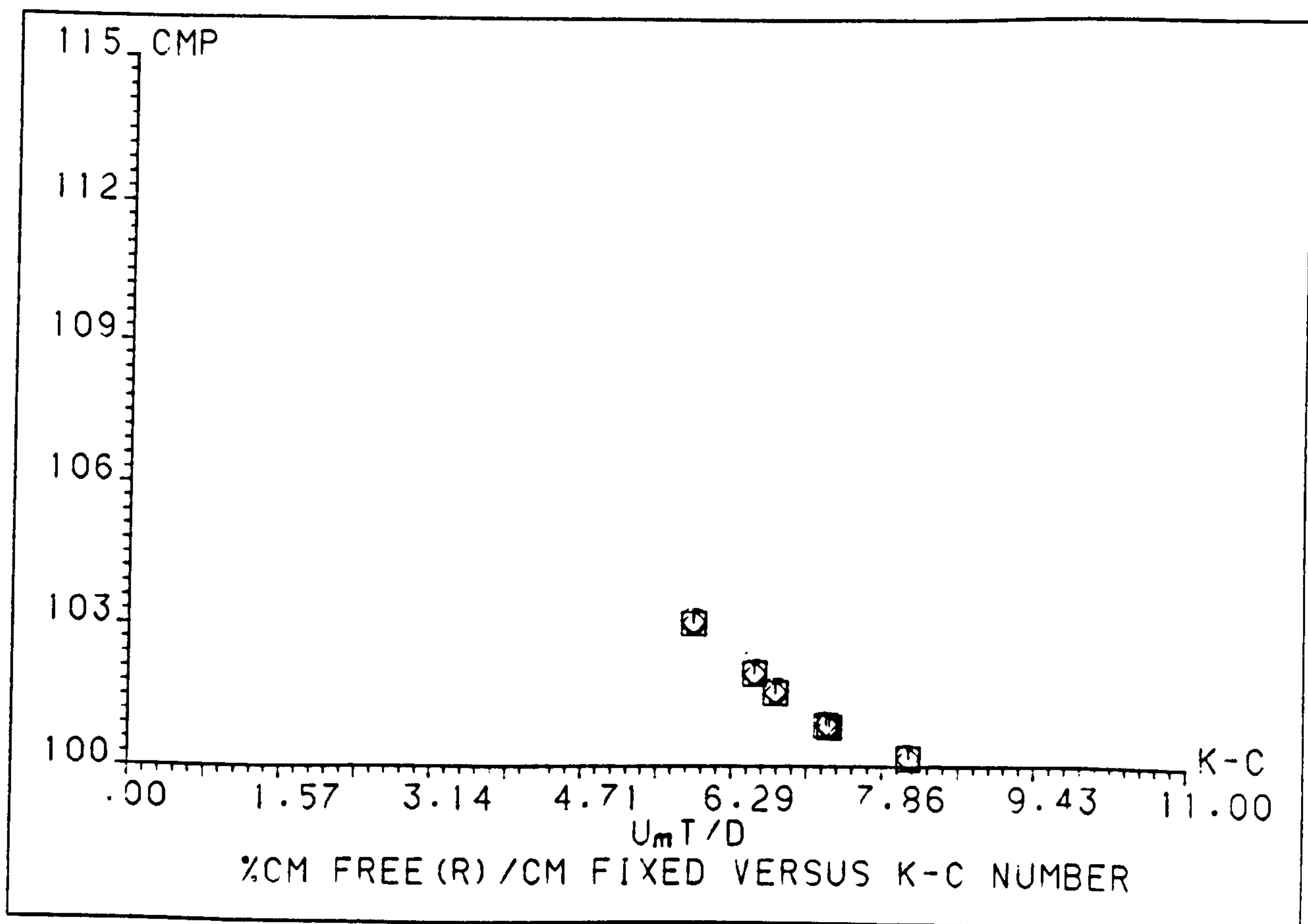


Figure (5.3.7b) - Variation of  $\% (C_M \text{ Free (R) / } C_M \text{ Fixed})$  with K-C Number for Structure E with no Mass at Top.

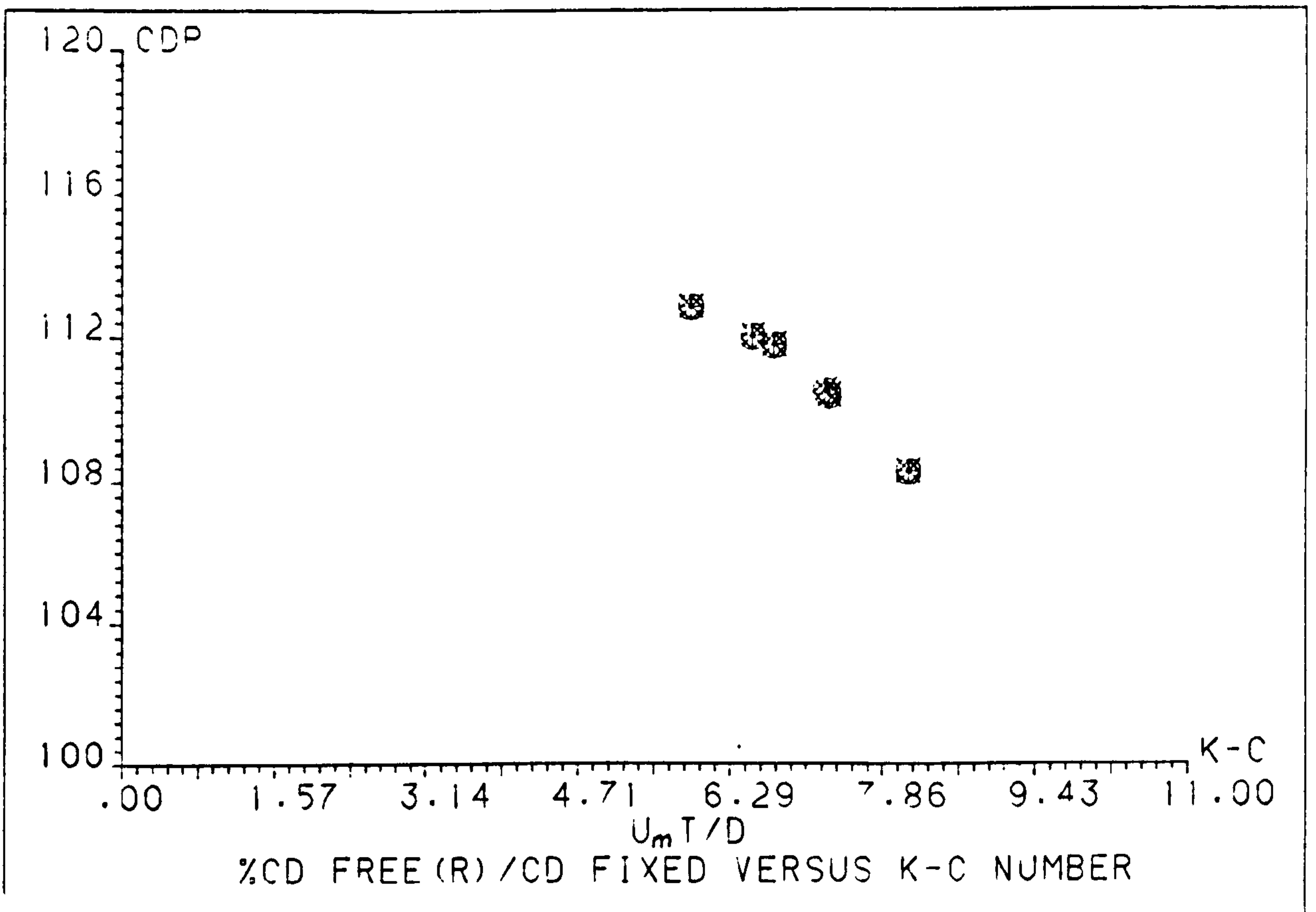


Figure (5.3.8a) - Variation of % ( $C_D$  Free (R)/ $C_D$  Fixed) with K-C Number for Structure E with 1010 Grs at Top.

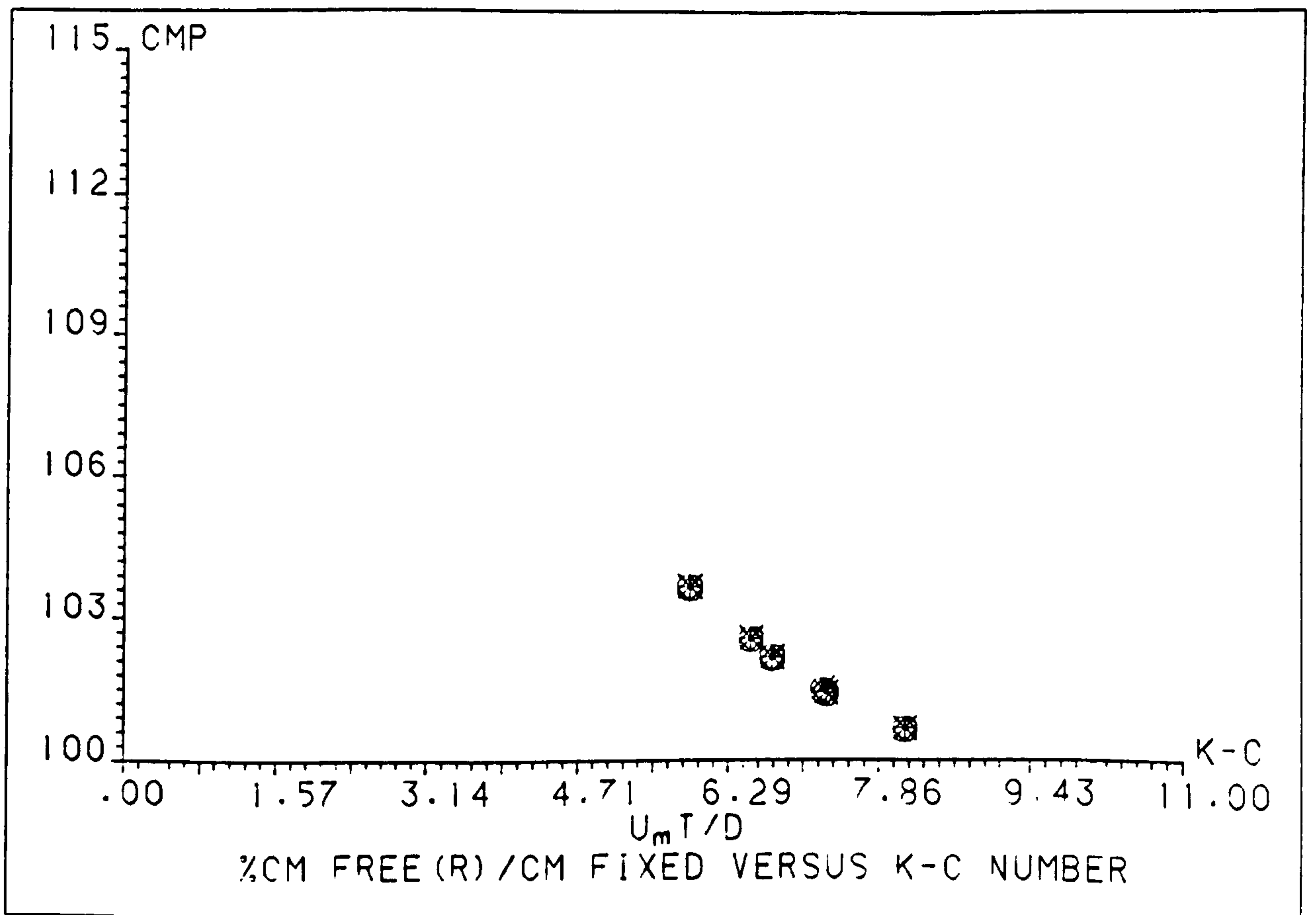


Figure (5.3.8b) - Variation of % ( $C_M$  Free (R)/ $C_M$  Fixed) with K-C Number for Structure E with 1010 Grs at Top.



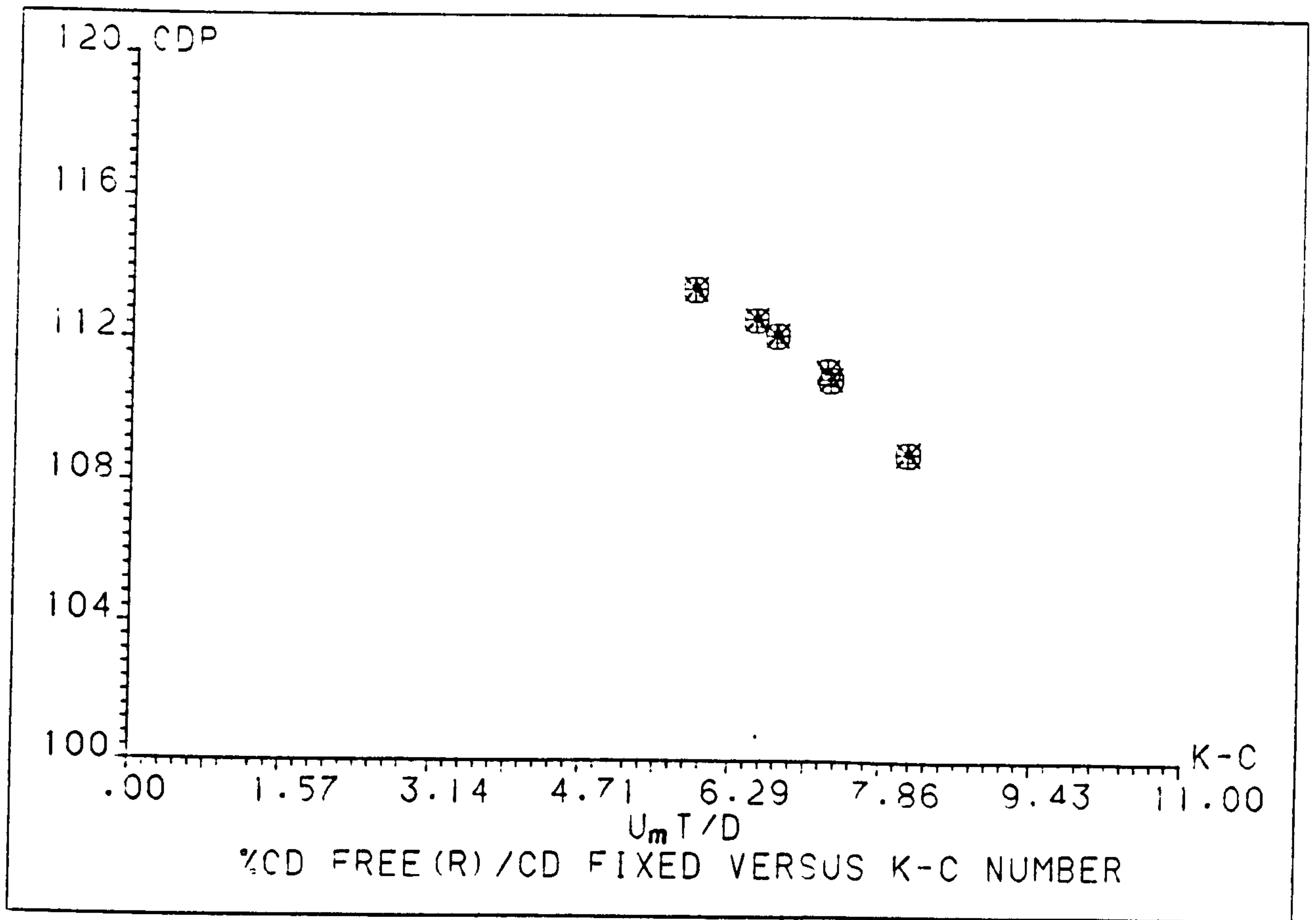


Figure (5.3.9a) - Variation of  $\% (C_D \text{ Free (R)} / C_D \text{ Fixed})$  with K-C Number for Structure E with 2020 Grs at Top.

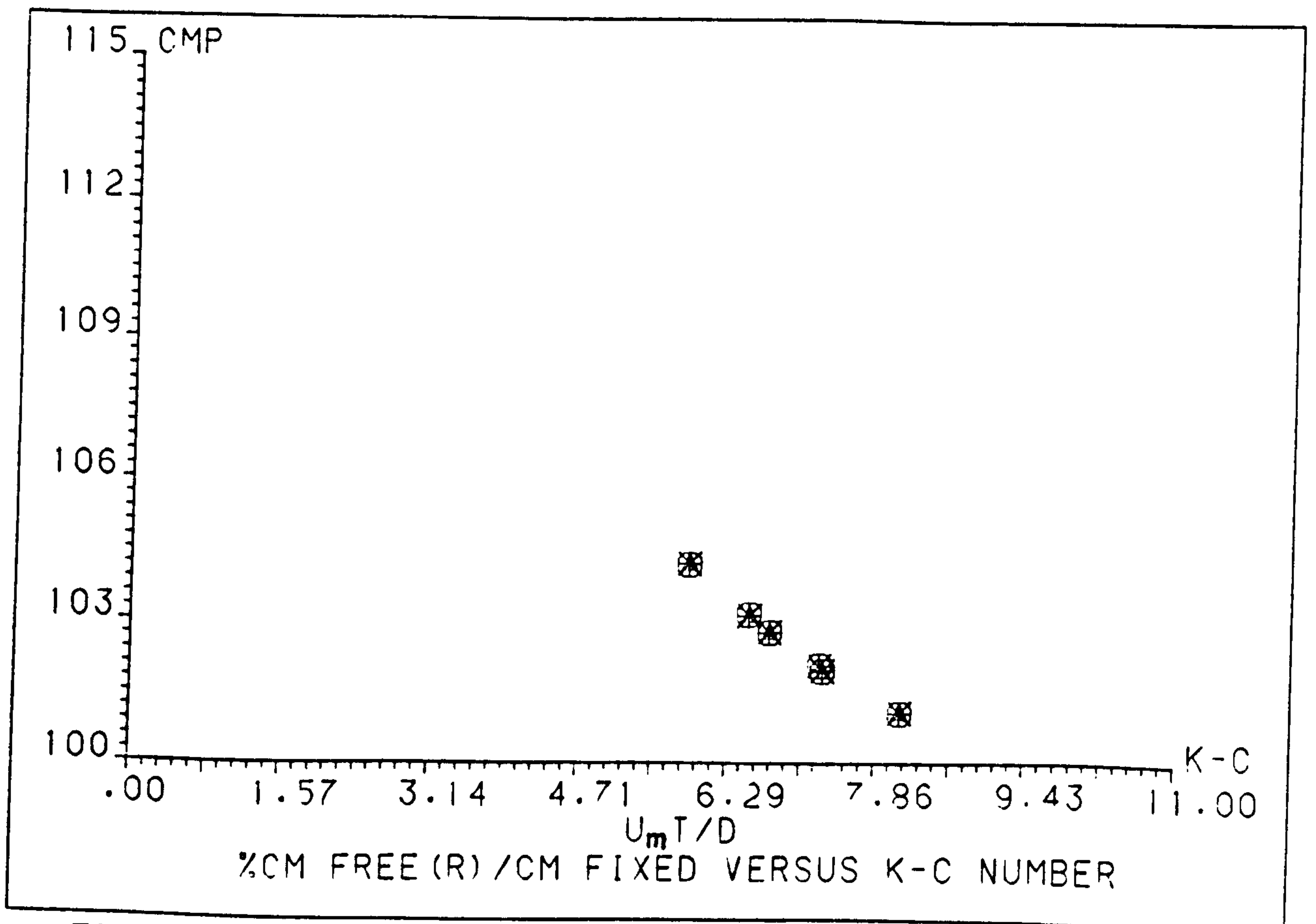


Figure (5.3.9b) - Variation of  $\% (C_M \text{ Free (R)} / C_M \text{ Fixed})$  with K-C Number for Structure E with 2020 Grs at Top.

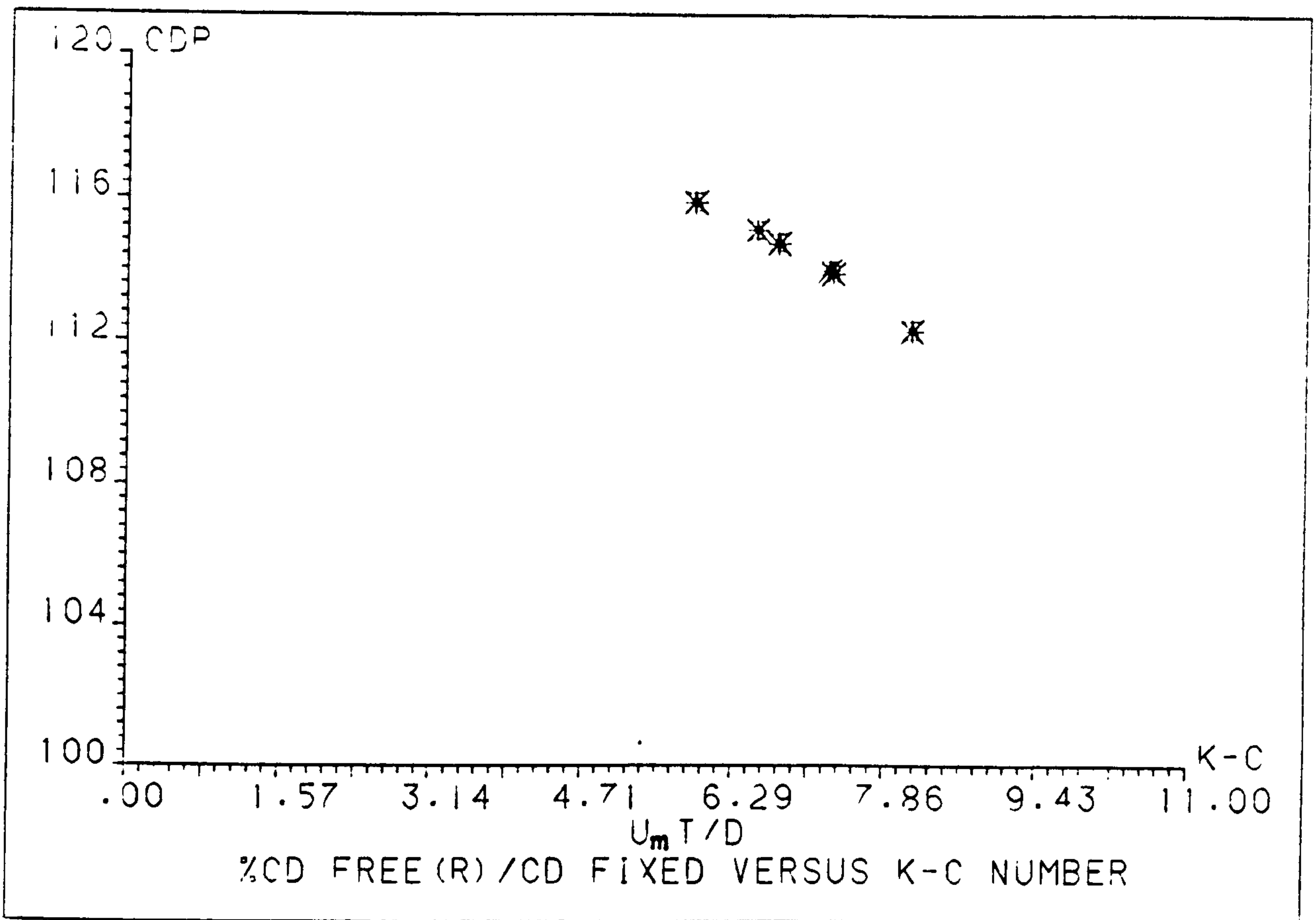


Figure (5.3.10a) - Variation of  $\% (C_D \text{ Free (R)} / C_D \text{ Fixed})$  with K-C Number for Structure F with no Mass at Top.

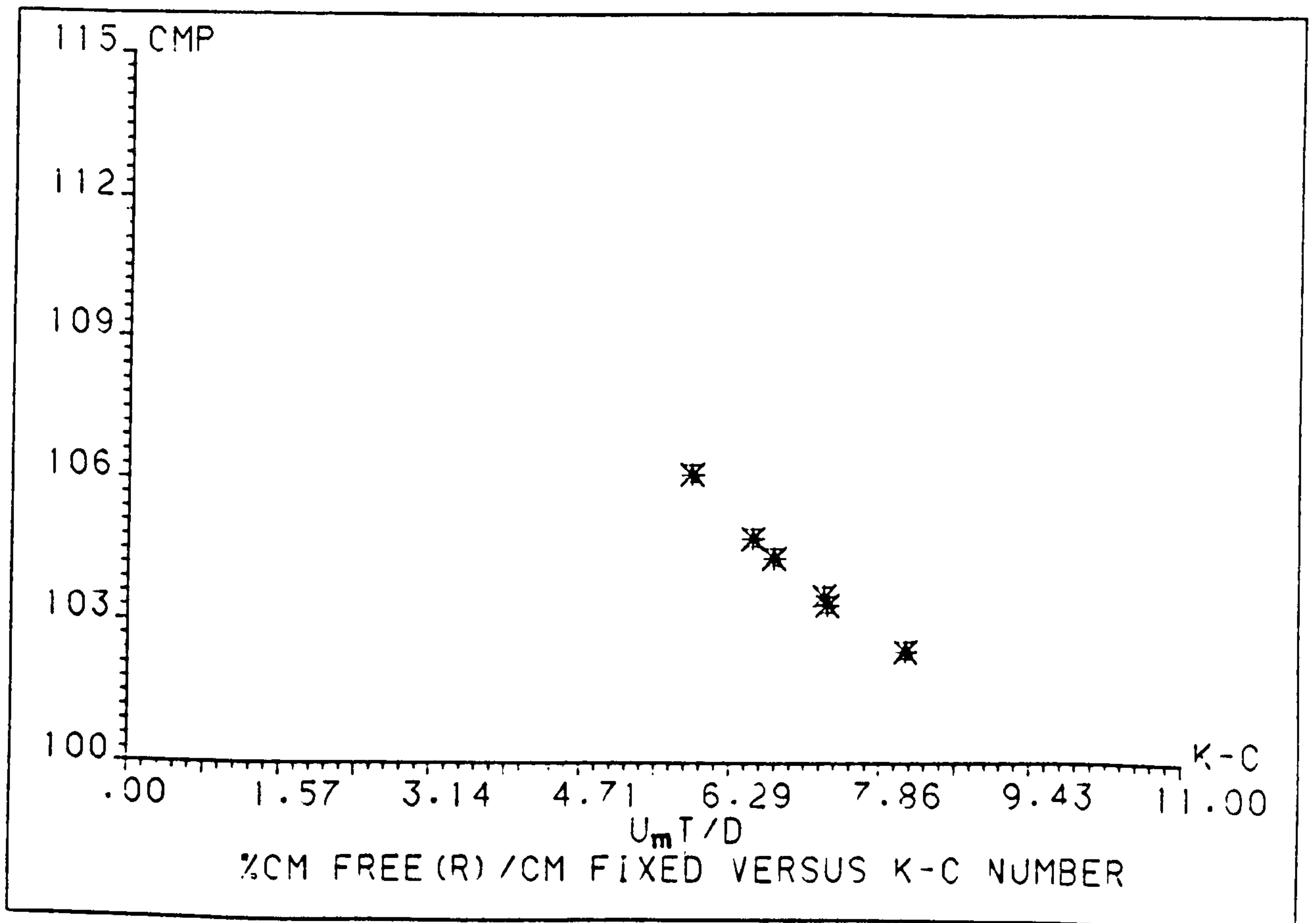


Figure (5.3.10b) - Variation of  $\% (C_D \text{ Free (R)} / C_D \text{ Fixed})$  with K-C Number for Structure F with no Mass at Top.

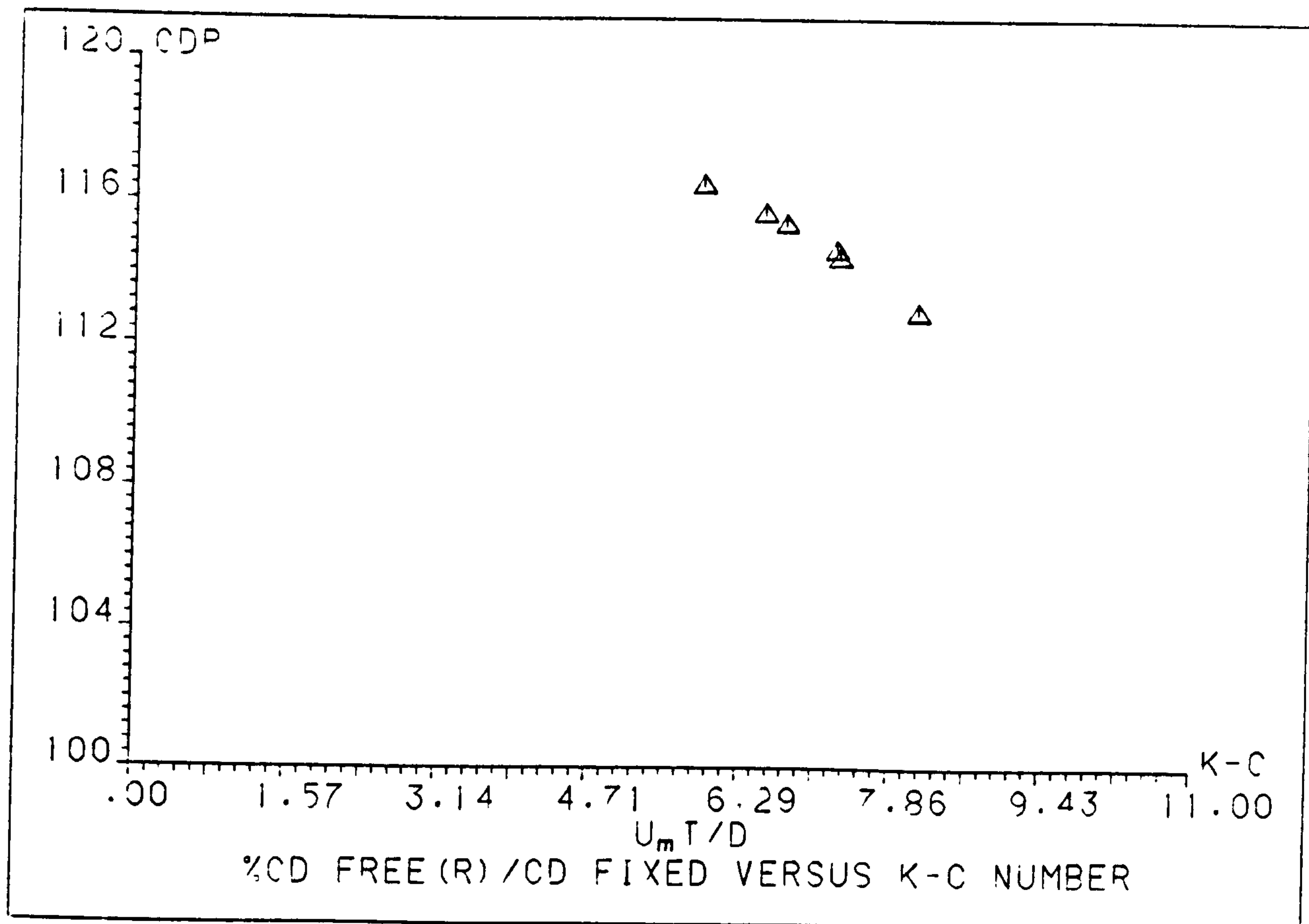


Figure (5.3.11a) - Variation of % ( $C_D$  Free (R)/ $C_D$  Fixed) with K-C Number for Structure F with 1010 Grs at Top.

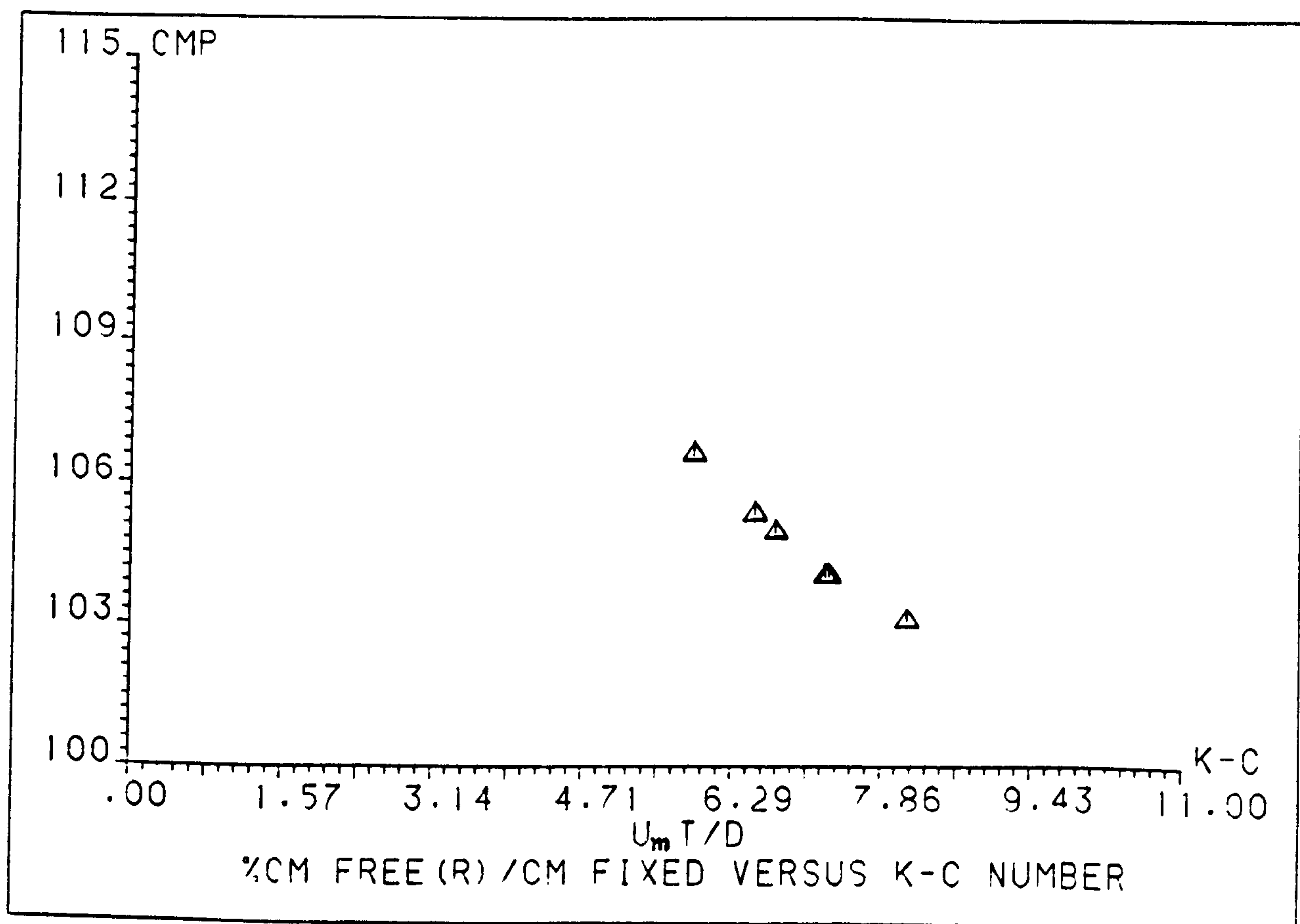


Figure (5.3.11b) - Variation of % ( $C_M$  Free (R)/ $C_M$  Fixed) with K-C Number for Structure F with 1010 Grs at Top.



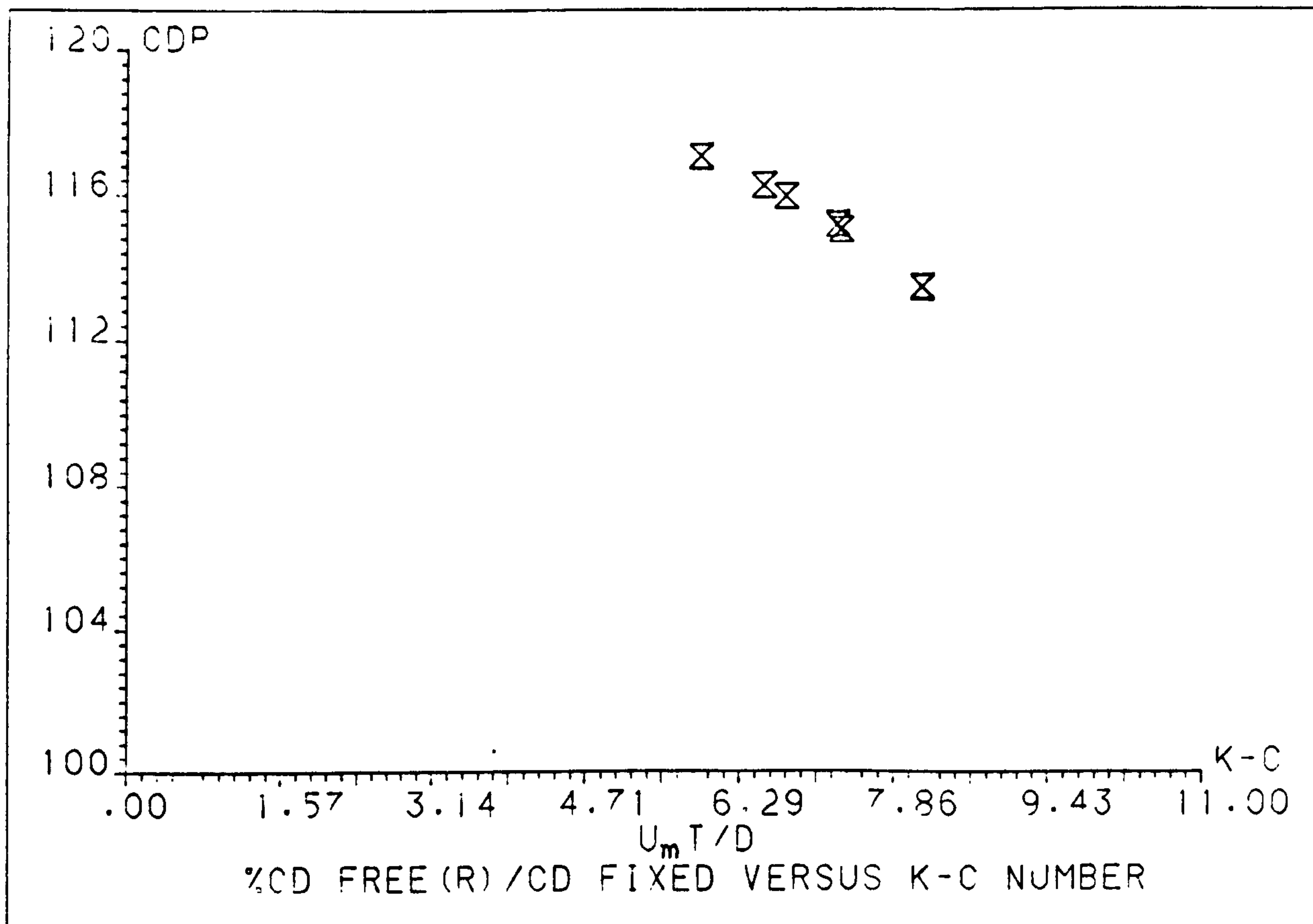


Figure (5.3.12a) - Variation of % ( $C_D$  Free (R)/ $C_D$  Fixed) with K-C Number for Structure F with 2020 Grs at Top.

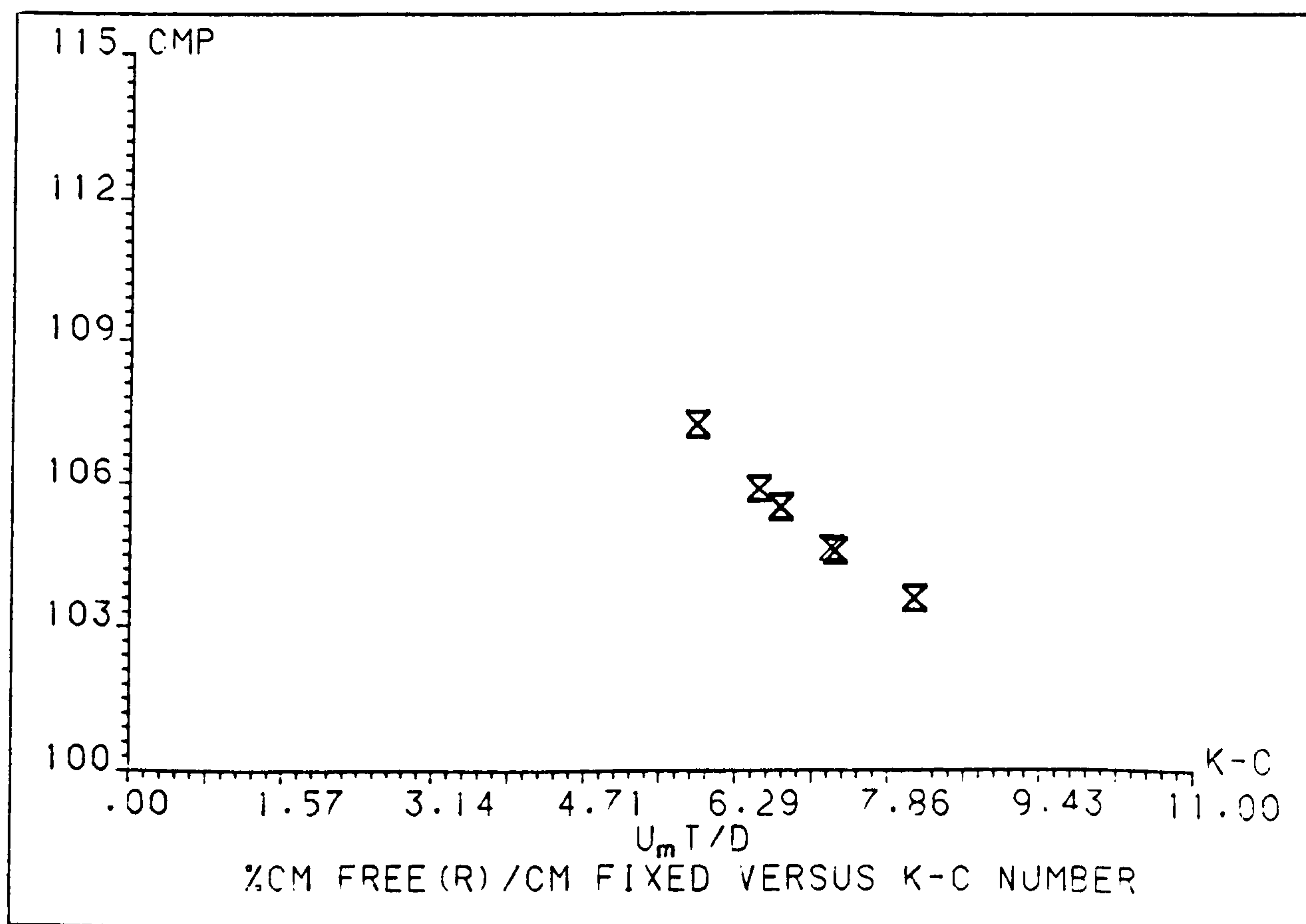


Figure (5.3.12b) - Variation of % ( $C_M$  Free (R)/ $C_M$  Fixed) with K-C Number for Structure F with 2020 Grs at Top.

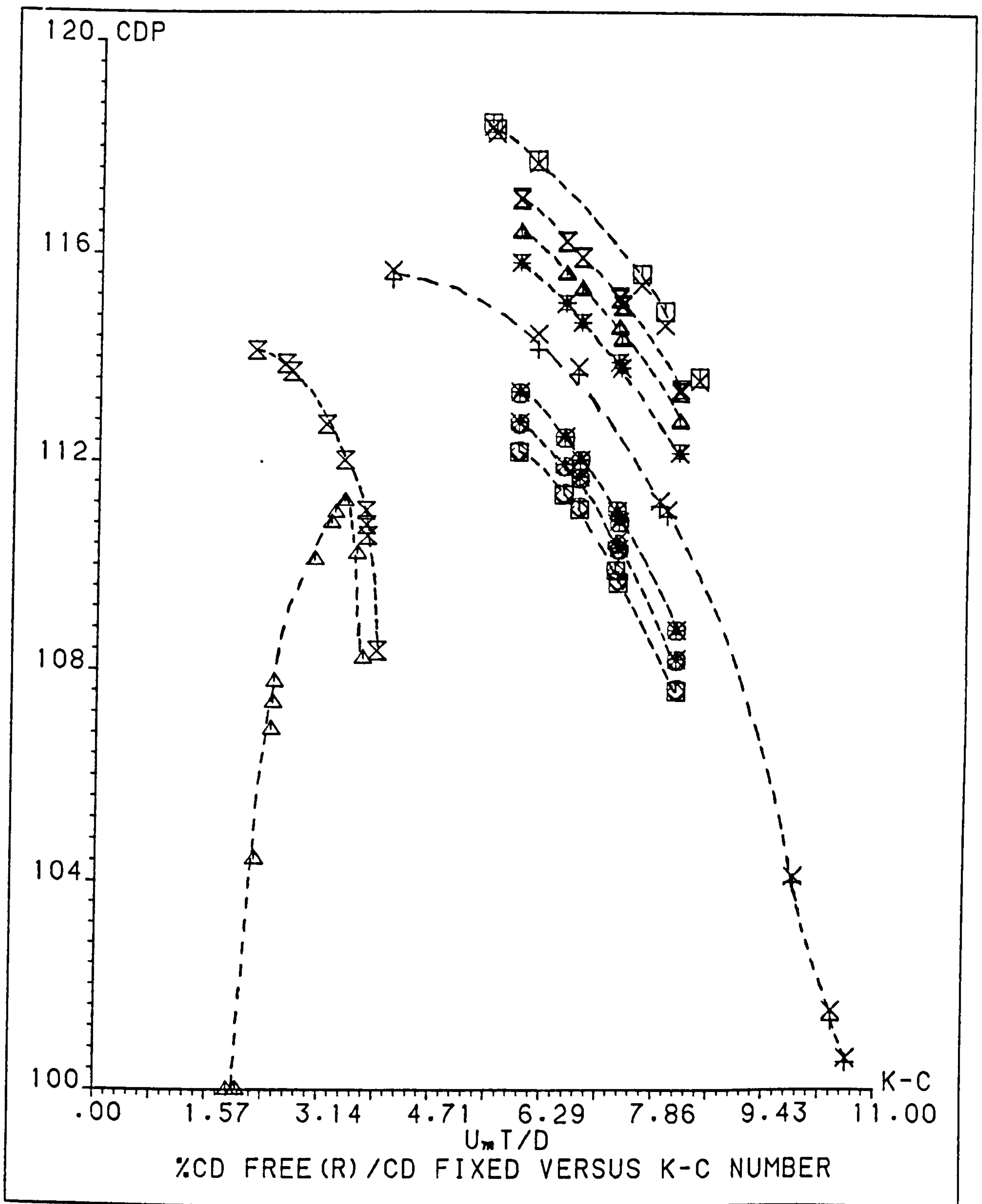


Figure (5.3.13) - Variation of % ( $C_D$  Free (R)/ $C_D$  Fixed) with K-C Number for all Structures.

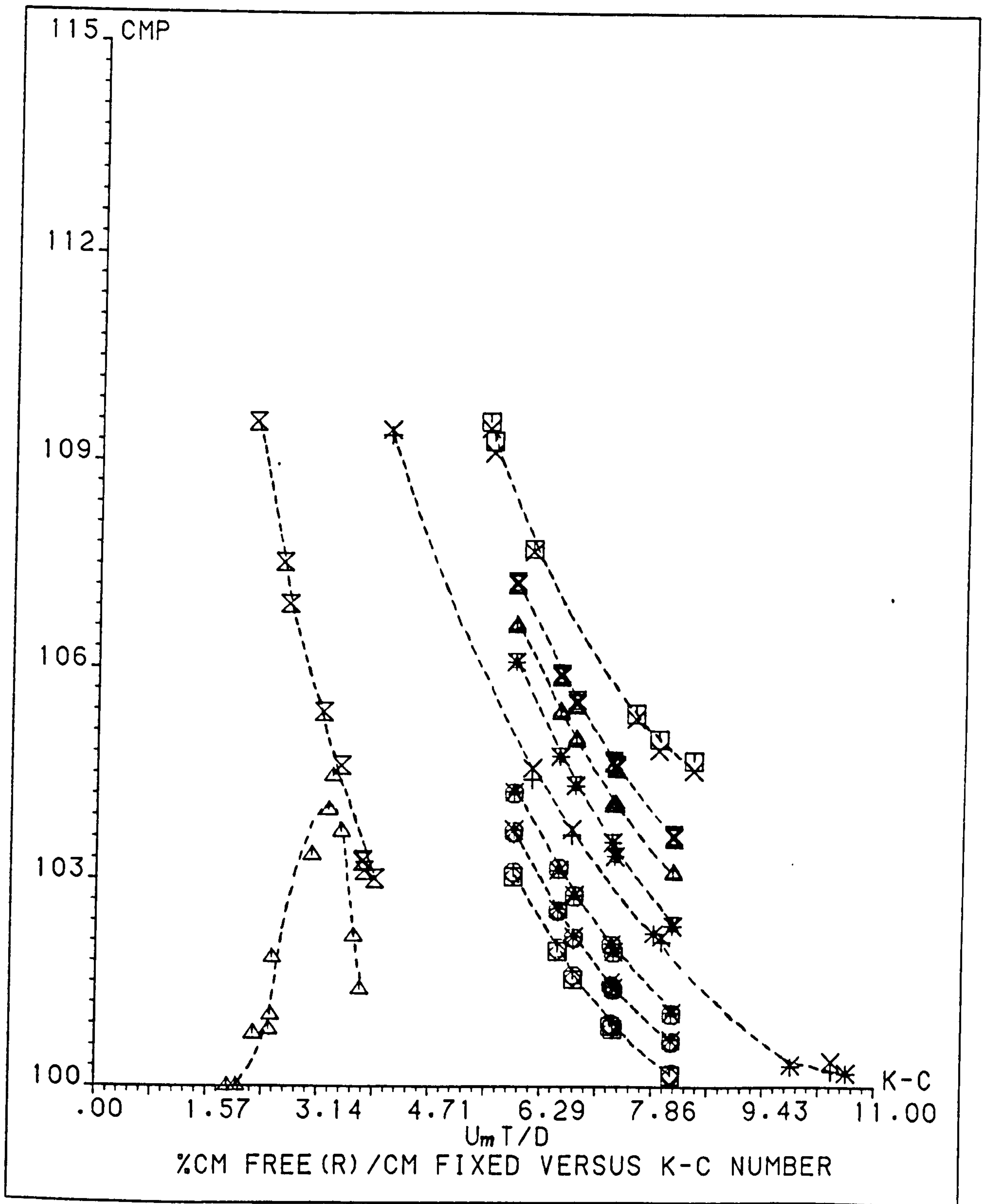


Figure (5.3.14) - Variation of % ( $C_M$  Free (R)/ $C_M$  Fixed) with K-C Number for all Structures.



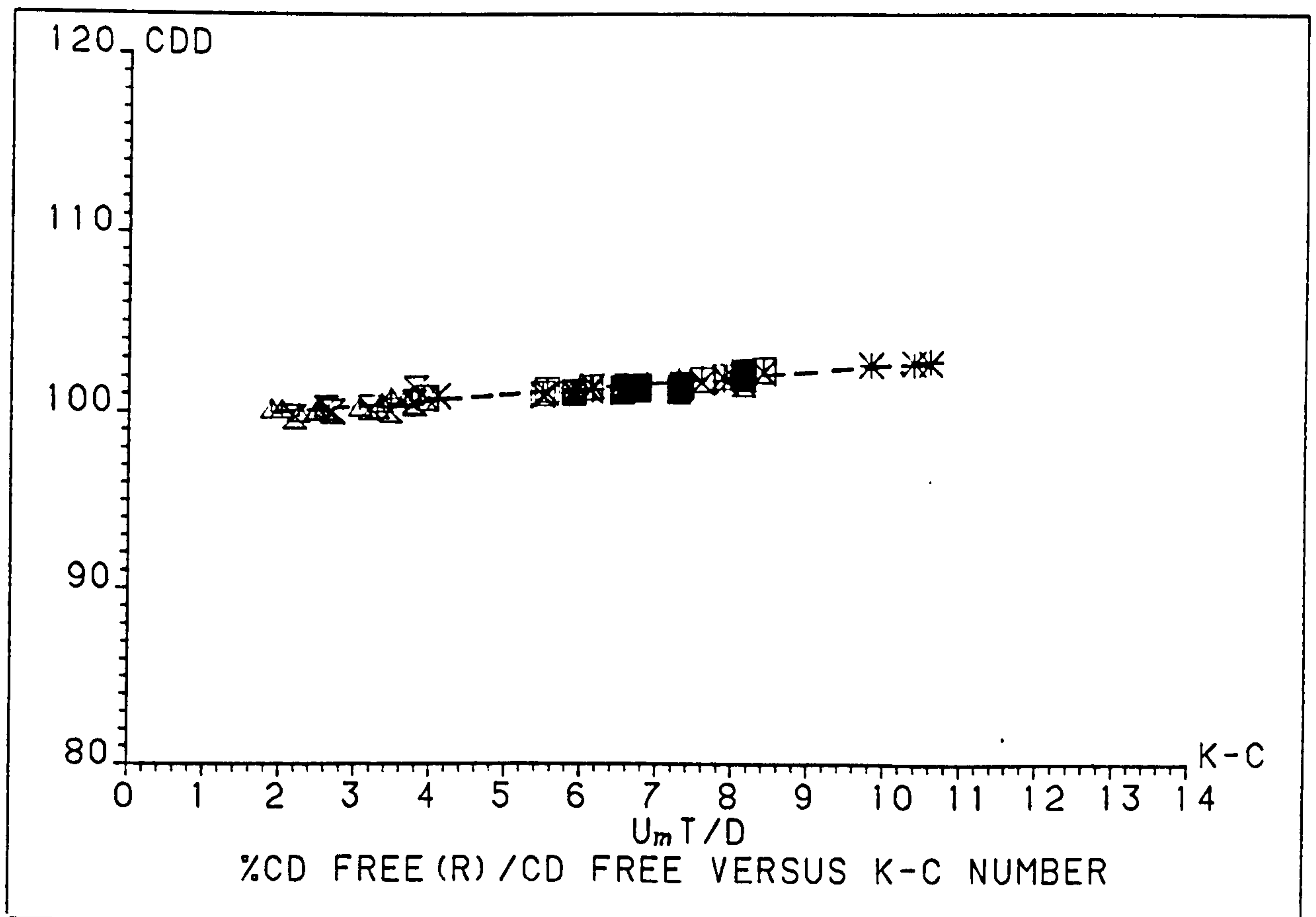


Figure (5.3.15a) - Variation of  $\% (C_D \text{ Free (R)} / C_D \text{ Free})$  with K-C Number for all Structures.

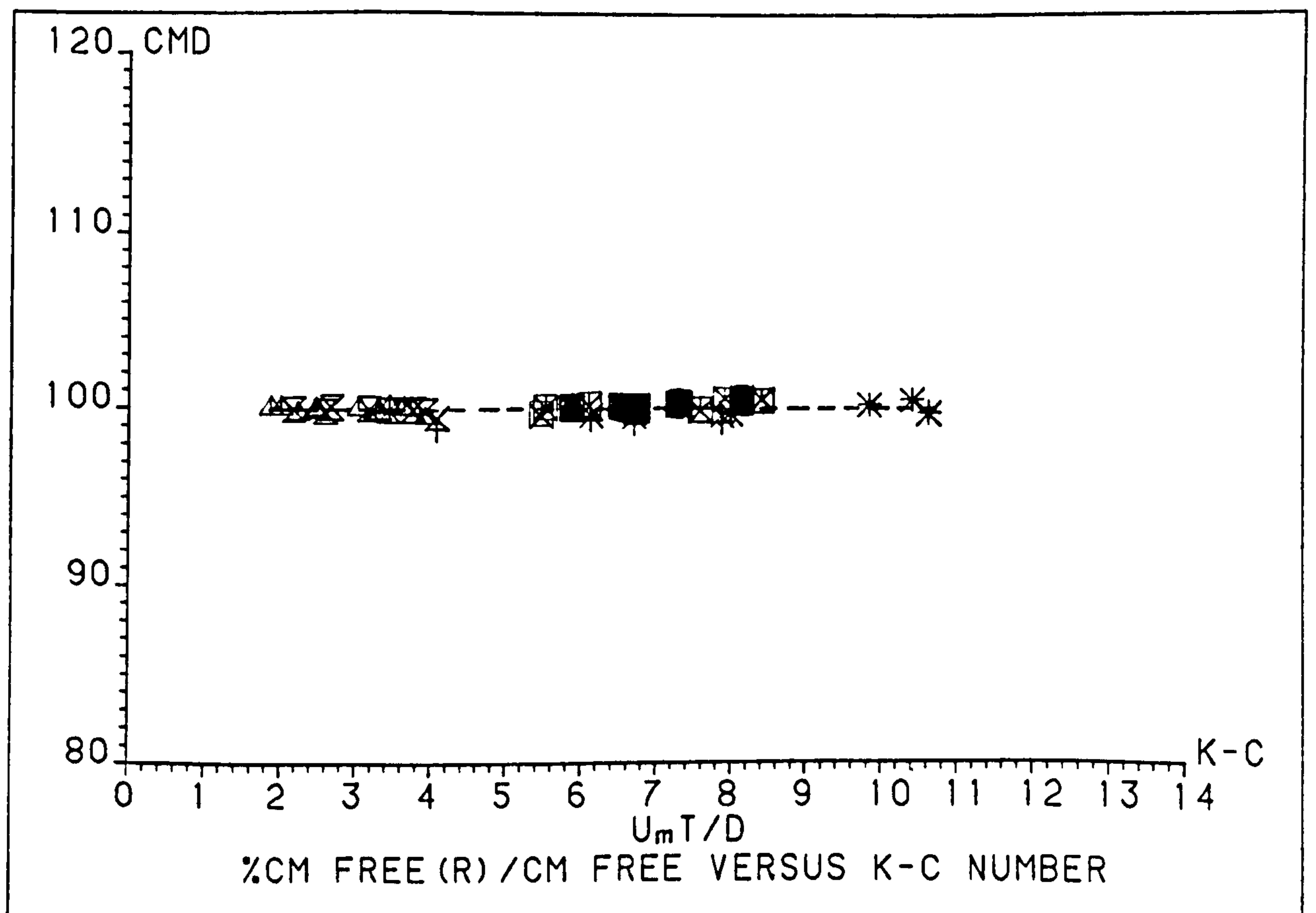


Figure (5.3.15b) - Variation of  $\% (C_M \text{ Free (R)} / C_M \text{ Free})$  with K-C Number for all Structures.

variation of the value of  $C_D$  and  $C_M$  along the submerged part of the cylinder.

- (b) THE VARIATION OF THE PERCENTAGE RATIO OF THE FORCE COEFFICIENTS FOR FREE STRUCTURES TO THOSE FOR FIXED STRUCTURES WITH KEULEGAN-CARPENTER NUMBERS.

The variations of the percentage ratio of  $C_D$  for free structures to that for fixed structures with the K-C numbers have negative gradients with negative second derivatives for all structures with the exception of structure A (relatively stiff). In this case, for low K-C numbers there is no difference between  $C_D$  (free) and  $C_D$  (fixed) with the increasing value of K-C numbers. The percentage ratio  $C_D$  (free): $C_D$  (fixed) then increases up to a definite maximum. Thereafter the behaviour of the  $C_D$  ratio is similar to that described above for other less stiff structures. The variations of the percentage ratio of the  $C_M$  have the same behaviour as that of the  $C_D$  for all structures with the exception that they have positive second derivatives.

The percentage ratios of the drag coefficient are greater than the corresponding percentage ratios of the inertia coefficient.

With decreasing structural stiffness, it is apparent that the rate of variation of the force coefficient ratios with the K-C numbers decreases.

For a particular value of K-C number it is apparent that, with decreasing structural stiffness, the ratios of the force coefficients increase.

This increase in the value of the force coefficients for free structures compared to those for fixed structures could be attributed to the movement of the structure and consequently the shift of the separation points in the upper stream direction towards the front of the cylinder and the increase of the wake size, thereby leading to an increase of the force. Similarly this increase occurs when the flow reverses its direction (see Figures (5.3.3) and (5.3.4)).

The negative gradient variation of the force coefficients with the K-C numbers could be due to the change of the level of vorticity in the fluid near the structure. The change of the level of vorticity is due to the increase of the K-C numbers combined with the increase of the amplitude of the structure's response



The reason for the lessening of the rate of change of the force coefficients ratio with the decreasing of the structural stiffness could be due to the increase of the phase angle shift of the structure's response to the wave force.

(c) THE VARIATION OF THE PERCENTAGE RATIO OF THE FORCE COEFFICIENTS CALCULATED BY MODIFIED MORISON'S EQUATION TO THOSE CALCULATED BY MORISON'S EQUATION WITH THE K-C NUMBERS

The variation of the percentage ratio of the  $C_D$  slightly increased with K-C numbers while no variation is noticed for the percentage ratio of  $C_M$  with the K-C numbers. This shows that for the tested waves and structures the ratio of the squared values of the relative velocity to the squared values of the water wave particle velocity is very small and decreases with the increase of the K-C numbers while the value of the ratio of the relative accelerations to the water wave particle accelerations is negligible.

### 5.3.2 STRUCTURE'S RESPONSE TO THE WAVE FORCES

The structures' response results obtained from the experiments conducted for the structures together with the computed values are presented below. The structures' responses were represented by the non-dimensional parameter  $X/D$  where  $X$  is the amplitude of vibration and  $D$  is structure diameter.

As the structures' responses should be related to non-dimensional parameters which contain the necessary variables to represent the structures' dynamic properties as well as the water waves. As the reduced velocity is normally used to relate the structure's response in the transverse direction due to the transverse force, because the drag component of the in-line force and the transverse force are due to the separation of flow around the structure and the formation of eddies, the structure's response in the direction of the wave can also be related to the reduced velocity. Therefore the reduced velocity was used as the non-dimensional parameter which satisfied the above condition. The reduced velocity was calculated for each test by:

$$VD = U_m/D \times FN \quad \dots \dots \dots (5.3.1)$$

where  $U_m$  = maximum water particle velocity  
 $FN$  = structure natural frequency

Also the reciprocal of reduced velocity was calculated for each test, as it was used by T. Sarpkaye and R. L. Shoaff 1979 (113).

Because the reduced velocity does not include the effect of damping of the structure, the dimensionless damping was calculated for each test by:

$$2\bar{M}\xi/\rho D^2L_s \quad \dots \quad \dots \quad \dots \quad \dots \quad \dots \quad (5.3.2)$$

- where  $\bar{M}$  = effective mass
- $\xi$  = damping coefficient
- $\rho$  = water density
- $L_s$  = structure length

The response parameter has been introduced by multiplying the dimensionless damping by the reciprocal of the reduced velocity

$$DM = (2\bar{M}\xi/\rho D^2L_s) (D \times FN/U_m) \quad \dots \quad \dots \quad \dots \quad (5.3.3)$$

Each tested structure is presented in a table (Tables 5 - 12 through 5 - 21). Each table shows the following parameters:-

1. The above non-dimensional parameters



2. The ratio of the force frequency to the structure natural frequency
3. The percentage ratio of  $C_D$  for the free structure to that for fixed structure
4. The percentage ratio of  $C_M$  for the free structure to that for fixed structure
5. The calculated phase shift between the structure's response and the applied force
6. The structure's response calculated by using the wave forces acting on the fixed structure (Method B)
7. The structure's response calculated by using the wave forces acting on the free structure (Method A)
8. The structure's response measured from the experimental tests.

The structures' responses calculated by using the wave forces acting on the structures when they were free to vibrate, the ratio of the frequency of the force to the natural frequency of the structure, the calculated phase shift between the structure's response and the applied load and the percentage ratio of  $C_D$



STRUCTURE (A)											
TEST	REDUCED 1/REDUCED	VELOCITY	DAMPING	PARAMETER	NATURAL FREQ.	CD FX	CM FX	PHASE	STRUCTURE RESPONSE	STRUCTURE RESPONSE	STRUCTURE RESPONSE
NO.	VELOCITY										
1	0.03285	30.4396	0.0000017	2.0400307	0.0108067	110.10	103.32	0.0010	0.006979	0.007210	0.007040
2	0.03307	30.2432	0.0233960	2.3704560	0.0133708	107.37	101.02	0.0013	0.007735	0.007820	0.007640
3	0.05706	17.5266	0.0624611	1.0447317	0.0156961	110.22	102.16	0.0015	0.013044	0.013390	0.012440
4	0.03793	26.3636	0.0692044	1.6244600	0.0109993	111.25	103.65	0.0011	0.006955	0.007203	0.006920
5	0.03547	28.1907	0.0345571	2.3237230	0.0132473	106.66	100.61	0.0013	0.010309	0.010390	0.010304
6	0.03935	16.3502	0.0645521	1.0677126	0.0159200	108.22	101.39	0.0016	0.013970	0.014148	0.013964
7	0.02208	45.2893	0.0739562	3.5756679	0.0109929	100.00	100.00	0.0010	0.005336	0.005360	0.005323
8	0.03344	29.9008	0.0702426	2.1003103	0.0134176	107.77	101.85	0.0012	0.006949	0.007073	0.006924
9	0.05224	19.1426	0.0597975	1.1446728	0.0157312	111.02	104.44	0.0014	0.009809	0.010242	0.009665
10	0.02047	48.8590	0.0611279	3.9636270	0.0109218	100.00	100.00	0.0010	0.004947	0.004950	0.004876
11	0.03011	33.2133	0.0697751	2.3174618	0.0134916	104.42	100.75	0.0012	0.006463	0.006509	0.006440
12	0.05169	19.3450	0.0562251	1.0876711	0.0158178	110.82	103.95	0.0014	0.006507	0.006841	0.008539

Table (5.12) - Structure's Response to the Wave Force for Structure A.



STRUCTURE (C)									
TEST	REDUCED 1/REDUCED	VELOCITY	DAMPING	PARAMETER	NATURAL FREQ.	CD FX	CM FX	PHASE	STRUCTURE
				RESPONSE					STRUCTURE
									RESPONSE
									RESPONSE
									MEASURED
1	0.12834	7.7919	0.0353260	0.2752620	0.0314901	115.53	109.37	0.0021	0.025731
2	0.22322	4.3817	0.0293724	0.1287125	0.0372405	114.20	104.39	0.0025	0.047718
3	0.33674	2.9097	0.0207382	0.0794037	0.0428260	111.20	102.22	0.0029	0.061550
4	0.21642	4.6207	0.0326135	0.1506949	0.0323185	113.74	103.00	0.0023	0.033137
5	0.30253	3.3055	0.0238020	0.0952051	0.0379391	111.00	102.09	0.0027	0.060071
6	0.40202	2.1010	0.0221021	0.0477757	0.0436300	100.52	100.19	0.0031	0.033303
7	0.40437	2.4730	0.0253946	0.0623009	0.0411706	104.00	100.29	0.0031	0.083264
8	0.46199	2.1646	0.0249626	0.0540332	0.0444642	101.31	100.22	0.0033	0.092158

Table (5.14) - Structure's Response to the Wave Force for Structure C.



STRUCTURE (D)									
TEST	REDUCED 1/REDUCED	DIMENSIONLESS RESPONSE	FORCE FREQ.	CD FR	CM FR	PHASE	STRUCTURE RESPONSE	STRUCTURE RESPONSE	STRUCTURE RESPONSE
NO.	VELOCITY	DAMPING	NATURAL FREQ.	CD FR	CM FR	SHIFT	RESPONSE	RESPONSE	RESPONSE
1	0.23343	4.2830	0.0208698	0.1151580	0.0422610	115.27	109.11	0.0026	0.045001
2	0.23142	3.5534	0.0255770	0.0908379	0.0459358	117.71	107.67	0.0029	0.060577
3	0.46705	2.1411	0.0220203	0.0471473	0.0556005	113.02	104.54	0.0035	0.053482
4	0.21842	4.5782	0.0321031	0.1409989	0.0399537	118.38	109.40	0.0020	0.040339
5	0.35536	2.8140	0.0200053	0.0750309	0.0469021	115.44	105.27	0.0031	0.073616
6	0.42633	2.3456	0.0251967	0.0591363	0.0539374	114.67	104.32	0.0030	0.090153

Table (5.15) - Structure's Response to the Wave Force for Structure D.







STRUCTURE ( E )									
TEST	REDUCED 1/REDUCED	DIMENSIONLESS	RESPONSE	PARAMETER	NATURAL FREQ.	CD FX	CM FX	SHIFT	STRUCTURE RESPONSE
-----									
NO.	VELOCITY	DAMPING							STRUCTURE RESPONSE
-----									
1	0.47622	2.0999	0.0017065	0.1295760	0.0708692	111.72	102.12	0.0101	0.039545
2	0.60265	1.5091	0.0504488	0.0851871	0.0614996	108.21	100.63	0.0116	0.053877
3	0.55147	1.8133	0.0013062	0.11111721	0.0754626	110.32	101.38	0.0106	0.045277
4	0.41385	2.4163	0.0033232	0.1578422	0.0705243	112.77	103.62	0.0099	0.032372
5	0.58976	1.6956	0.0555992	0.0942738	0.0611030	110.44	101.46	0.0114	0.044015
6	0.48973	2.0420	0.0598628	0.1222372	0.0750954	111.95	102.53	0.0106	0.036645
-----									
									0.040381
									0.039159
									0.053370
									0.044960
									0.032317
									0.043428
									0.036570
-----									

Table (5.17) - Structure's Response to the Wave Force for Structure E with  
1010 Grs at Top.



STRUCTURE (E)									
TEST	REDUCED 1/REDUCED	DIMENSIONLESS	RESPONSE	FORCE FREQ.	CD FR	CM FR	PHASE	STRUCTURE RESPONSE	STRUCTURE RESPONSE
NO.	VELOCITY	DAMPING	PARAMETER	NATURAL FREQ.	CD FR	CM FR	SHIFT	METHOD (B)	METHOD (A)
1	0.61833	1.6173	0.0630163	0.110035	0.0920175	112.09	102.31	0.0141	0.039703
									0.040796
									0.039511
2	0.86039	1.1623	0.0620493	0.0721179	0.1058201	108.79	101.04	0.0163	0.054185
									0.054733
									0.054025
3	0.71604	1.3966	0.0675067	0.0942782	0.0979816	110.88	101.94	0.0150	0.045478
									0.046376
									0.045233
4	0.52069	1.9205	0.0709266	0.1362158	0.0887311	113.38	104.19	0.0132	0.032537
									0.033902
									0.032734
5	0.74202	1.3477	0.0612004	0.0644764	0.1920408	111.11	102.05	0.0153	0.044468
									0.045373
									0.044137
6	0.61616	1.6230	0.0647588	0.1051013	0.0944822	112.53	103.13	0.0141	0.036743
									0.037687
									0.036637

Table (5.18) - Structure's Response to the Wave Force for Structure E with  
2020 Grs at Top.







STRUCTURE ( F )											
TEST	REDUCED	1/REDUCED	DIMENSIONLESS	RESPONSE	FORCE	FREQ.	CD	FX	CM	FX	PHASE
-----											
NO.	VELOCITY	VELOCITY	DAMPING	PARAMETER	NATURAL	FREQ.	CD	FX	CM	FX	SHIFT
-----											
1	0.54866	1.8226	0.0551943	0.1005987	0.0816493	115.32	104.93	0.0113	0.059118	0.052573	0.050453
2	0.76344	1.3099	0.0400760	0.0011388	0.0933967	112.81	103.06	0.0131	0.060254	0.068300	0.066210
3	0.63536	1.5739	0.0537632	0.0846189	0.0669414	114.36	104.00	0.0121	0.056992	0.059269	0.055773
4	0.47424	2.1087	0.0595726	0.1256178	0.0808145	116.40	106.57	0.0111	0.041445	0.044171	0.040324
5	0.67532	1.4797	0.0433272	0.0722493	0.0929368	114.38	104.00	0.0127	0.055498	0.057711	0.054666
6	0.56118	1.7820	0.0544557	0.0970374	0.0360526	113.63	105.32	0.0113	0.046850	0.049352	0.047214

Table (5.20) - Structure's Response to the Wave Force for Structure F with  
1010 Grs at Top.







for the free structures to that of the fixed structures as well as the percentage ratio of  $C_M$  were plotted against the two non-dimensional parameters (the reciprocal of the reduced velocity and the response parameter).

The variation of the structures' responses with the reciprocal of the reduced velocity is shown in Figure (5.3.16a). The variation of the structures' responses the response parameter is shown in Figure (5.3.16b). The figures show that the structures' responses can be represented by these non-dimensional parameters. The structural responses increase with the decrease of these non-dimensional parameters. The response parameter represents more accurately the structural response as the graph shows less scattered results.

Figures (5.3.17a) and (5.3.17b) show the variation of the phase shift with the reciprocal of the reduced velocity and the response parameter respectively.

The variation of the ratio of the force frequency to the structure frequency with the reciprocal of the reduced velocity and with the response parameter are shown in Figures(5.3.18a) and (5.3.18b), respectively.

Although the variation of the structure's response is better represented by the response parameter, the variation of the phase shift and the variation of the ratio of the force frequency to the structure frequency are better represented by the reciprocal of the reduced velocity. The variations of these three parameters with respect to the reciprocal of the reduced velocity and response parameter have the same pattern.

The variation of the percentage ratio of the drag coefficient calculated for the free structures to that calculated for fixed structures with the reciprocal of the reduced velocity is shown in Figure (5.3.19). The variation of this percentage ratio with the response parameter is shown in Figure (5.3.20). This variation has a positive gradient with a negative second derivative for all the structures.

Figures (5.3.21) and (5.3.22) show the variation of the percentage ratio of the inertia coefficient calculated for free structures to that calculated for fixed structures with reciprocal of the reduced velocity and with the response parameter respectively. The variations have positive gradients with positive second derivatives for all structures. The variation of the percentage ratio of the force coefficients with the reciprocal of the reduced velocity is clearer than that with the response parameter.



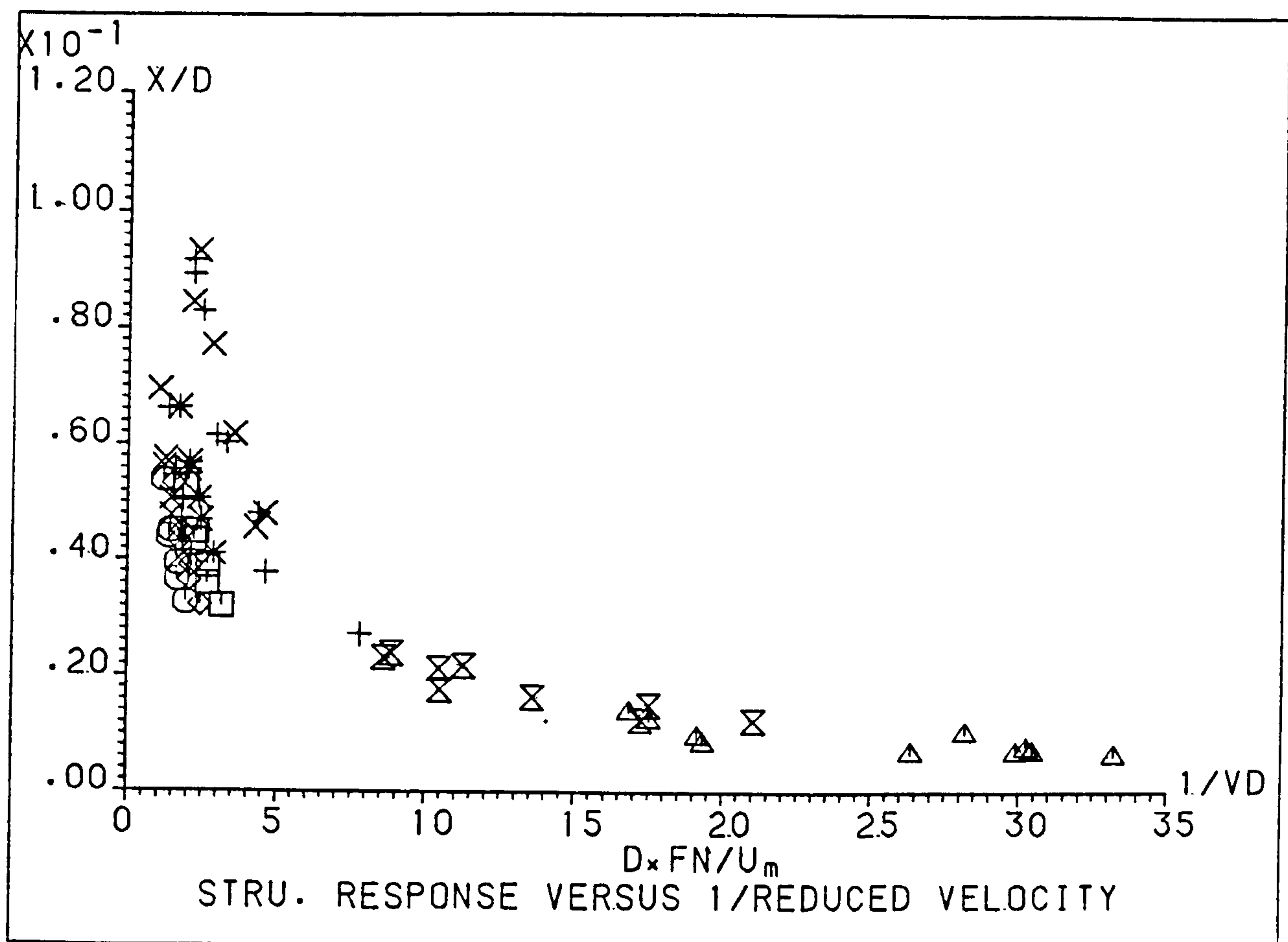


Figure (5.3.16a) - Variation of the Structures' Response ( $X/D$ ) with the Reciprocal of Reduced Velocity.

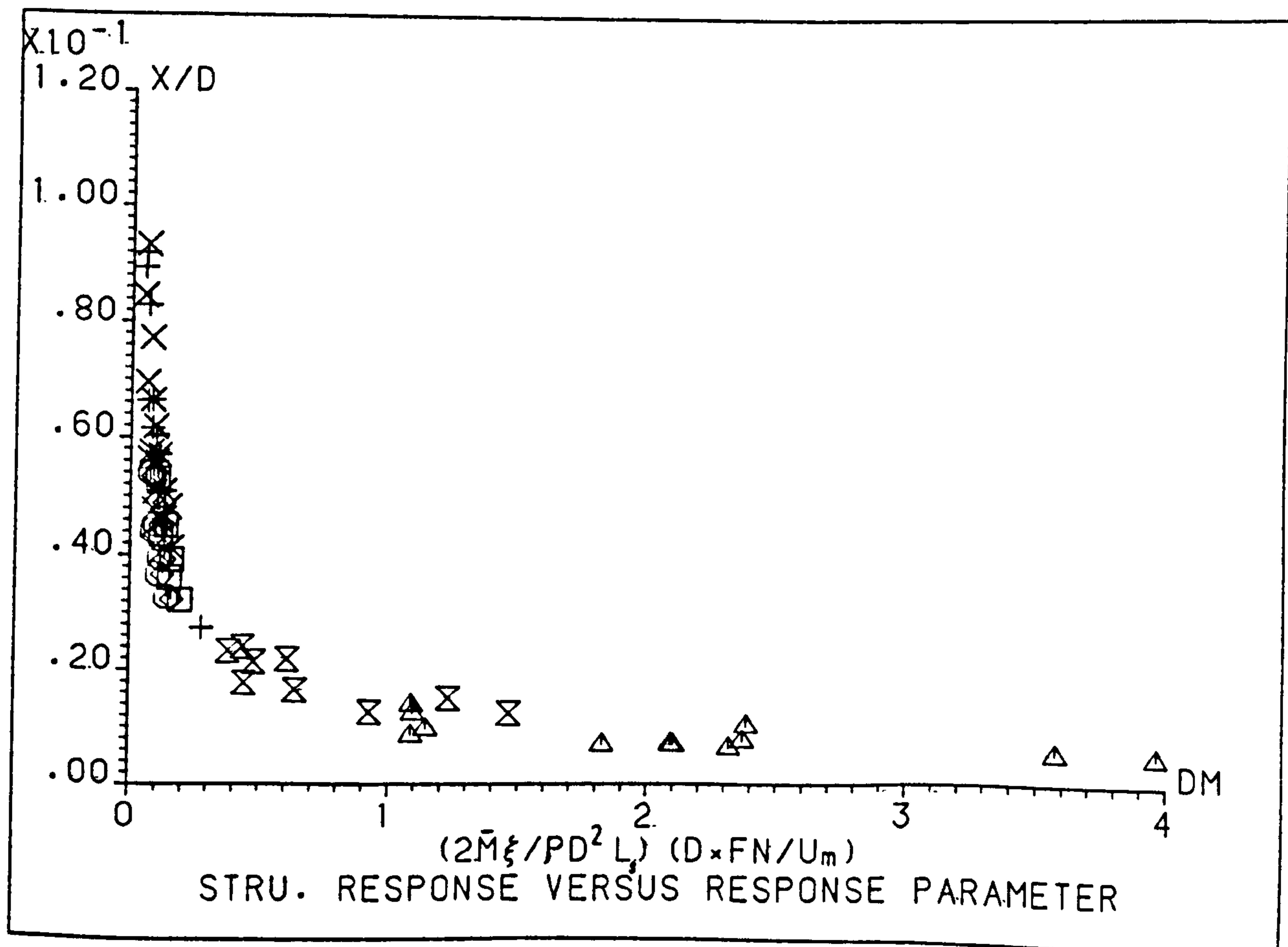


Figure (5.3.16b) - Variation of the Structures' Response ( $X/D$ ) with the Response Parameters.

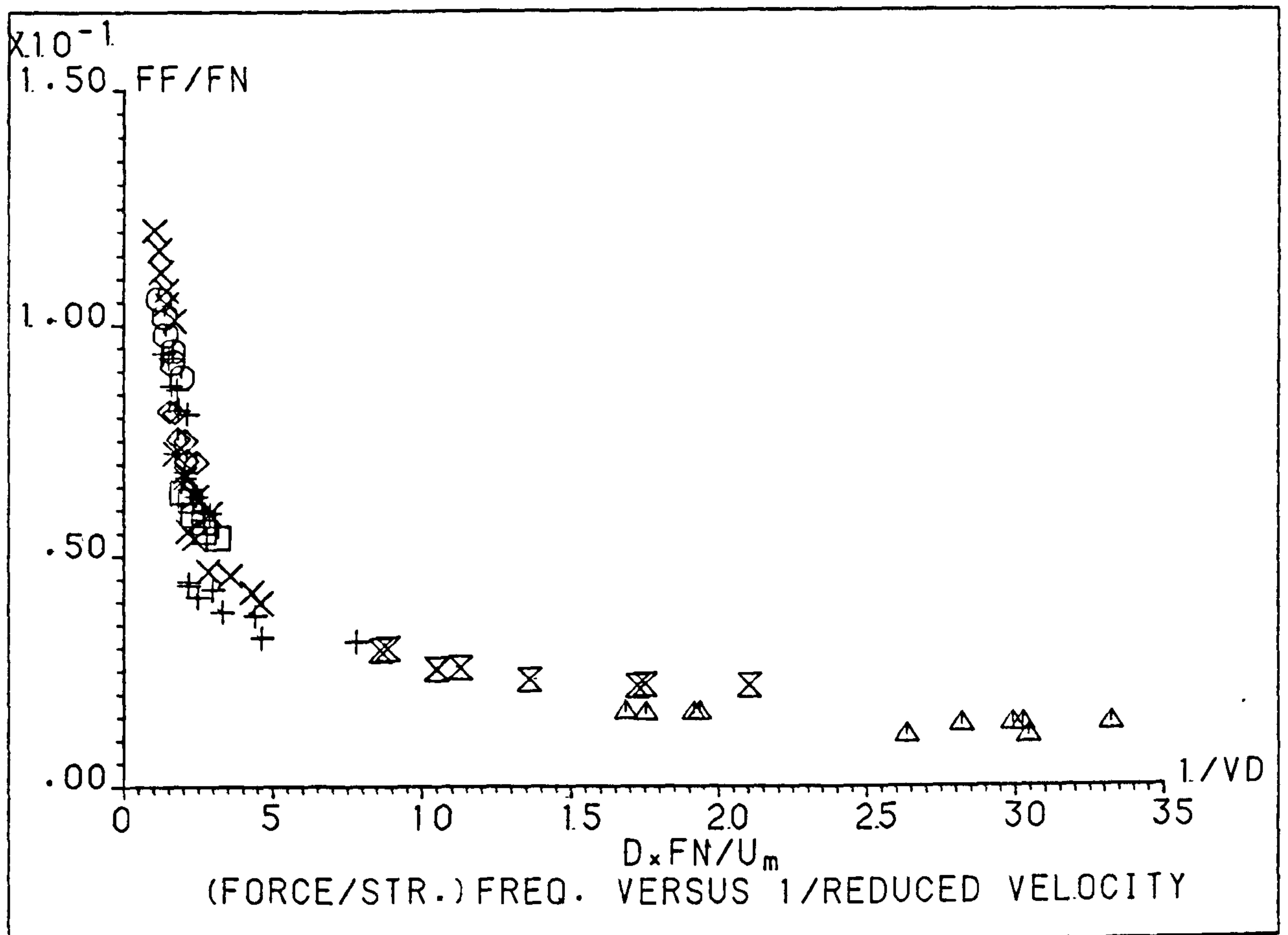


Figure (5.3.17a) - Variation of the (Force Frequency/Natural Frequency) with the Reciprocal of Reduced Velocity.

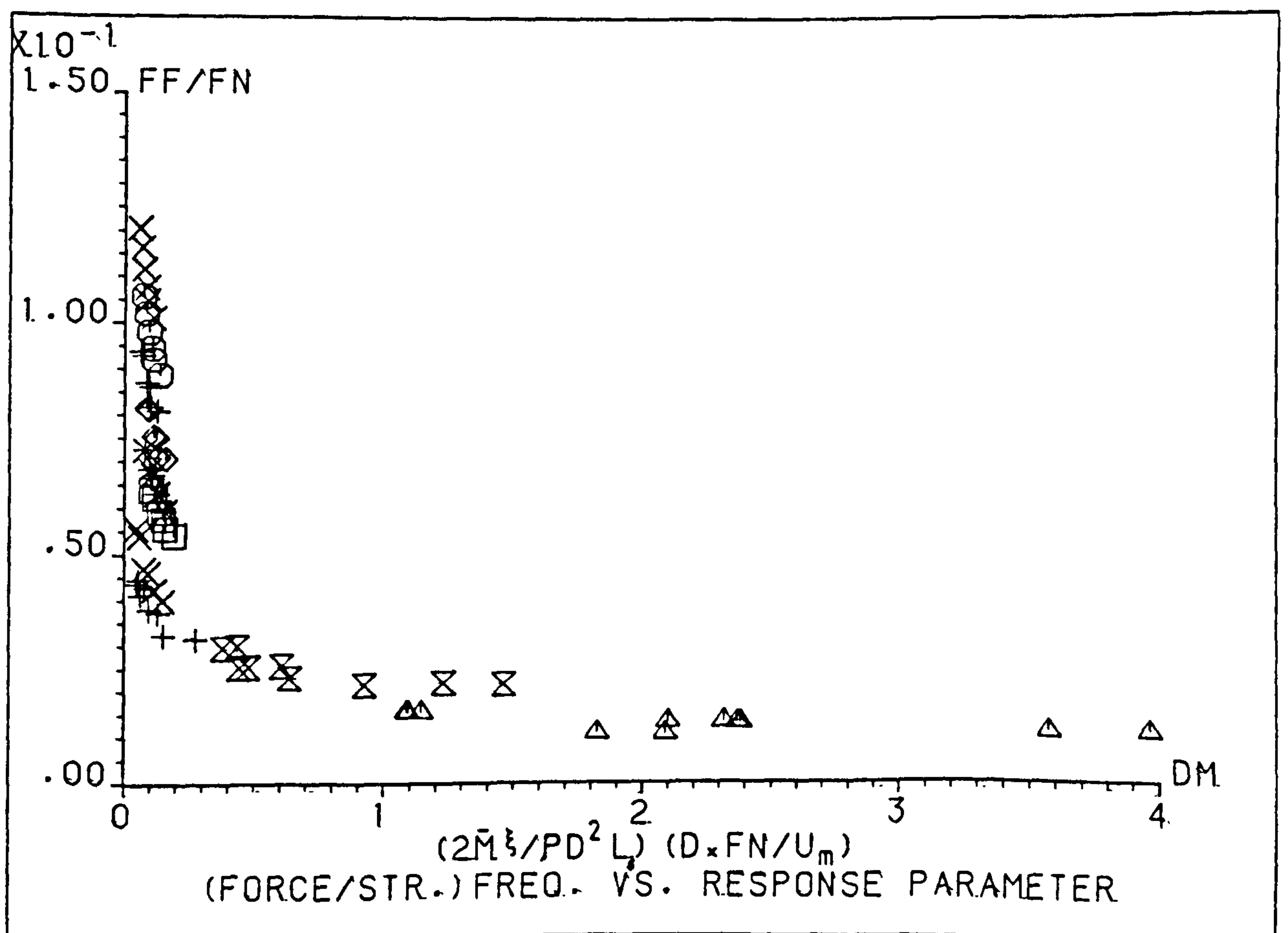


Figure (5.3.17b) - Variation of the (Force Frequency/Natural Frequency) with the Response Parameters.

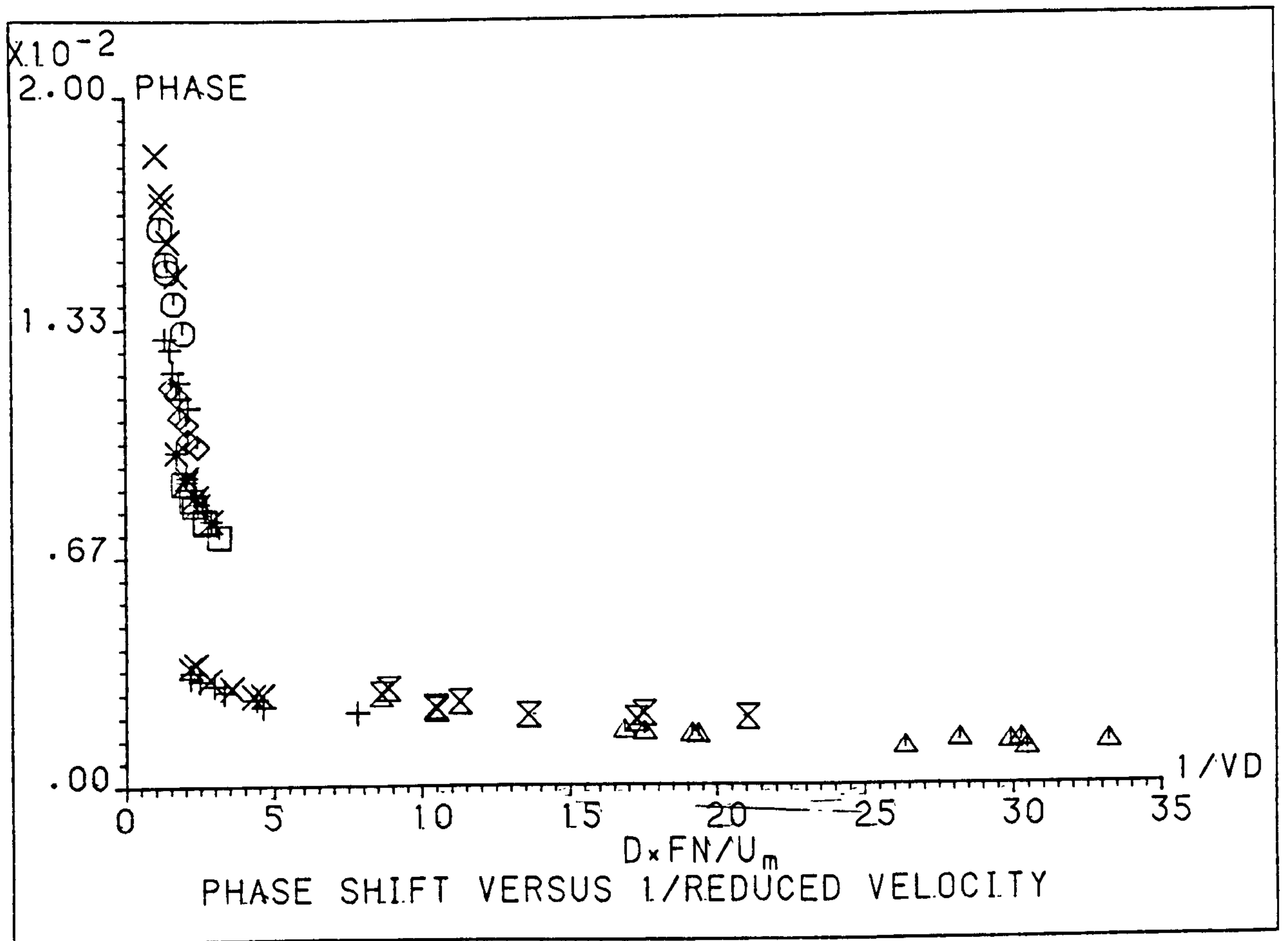


Figure (5.3.18a) - Variation of the Phase Shift between the Structure's Response and the Force with the Reciprocal of Reduced Velocity.

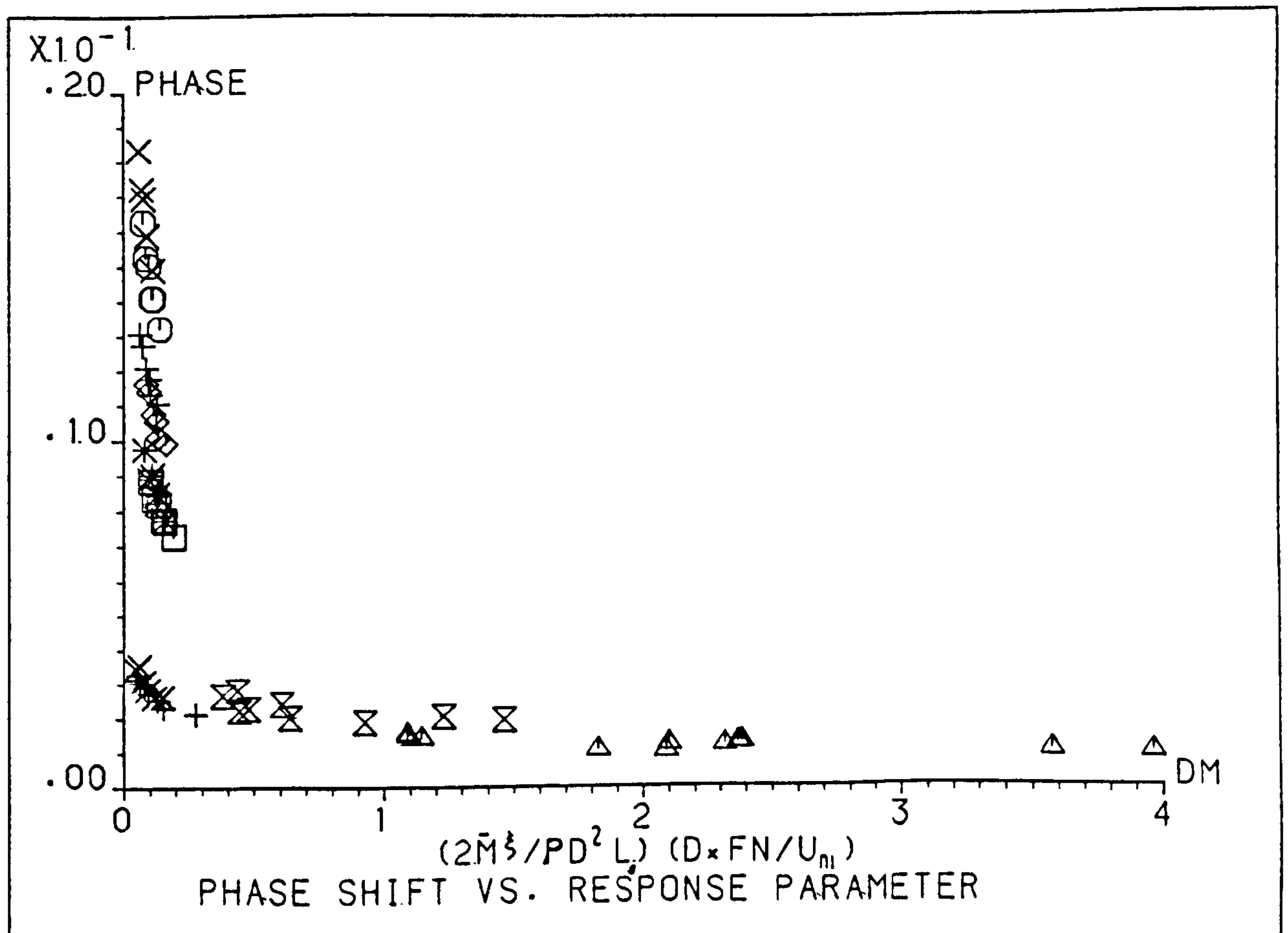


Figure (5.3.18b) - Variation of the Phase Shift between the Structure's Response and the Force with the Response Parameters.



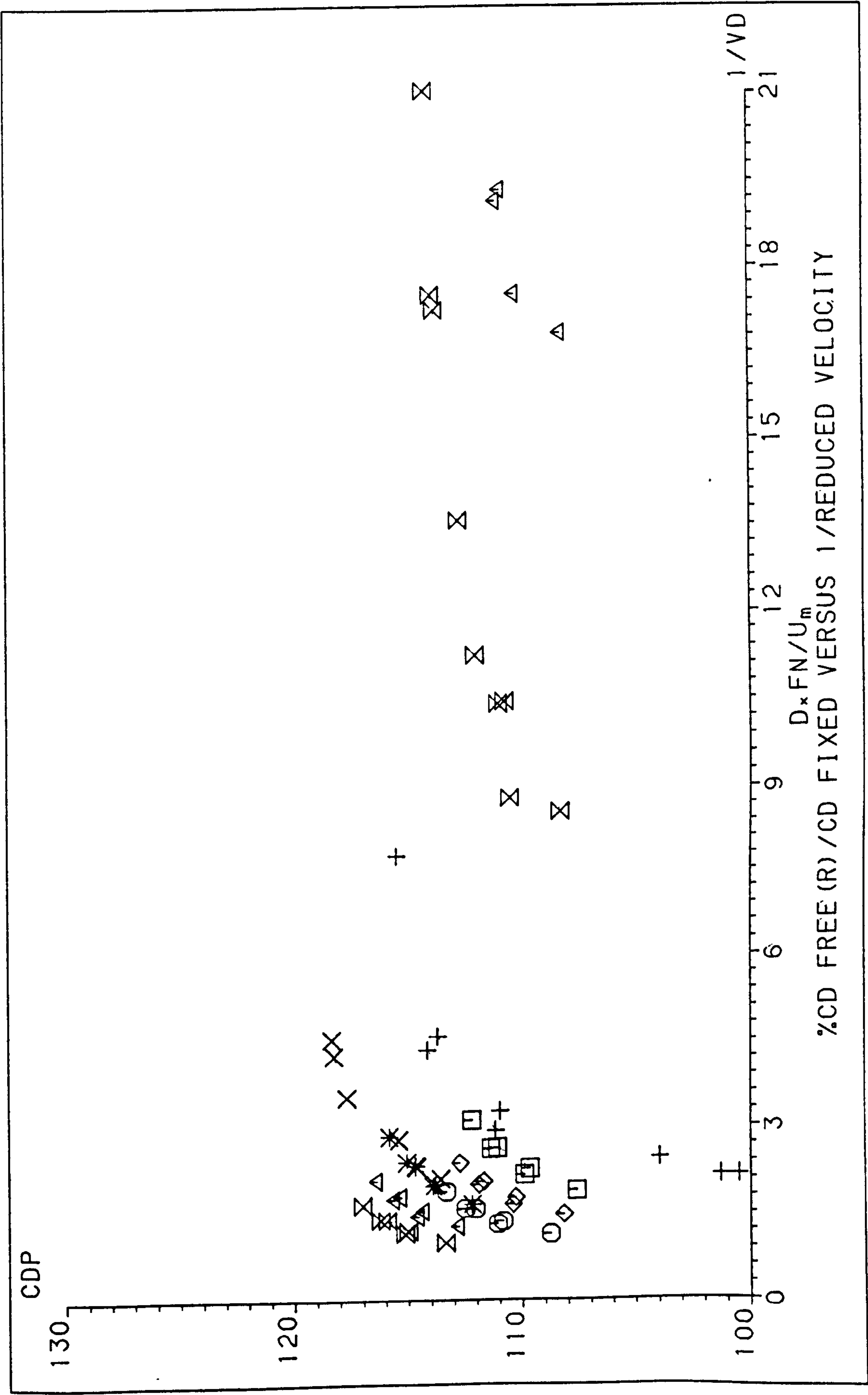


Figure (5.3.19) - Variation of ( $\% C_D$  Free(R)/ $C_D$  Fixed) with the Reciprocal of Reduced Velocity.

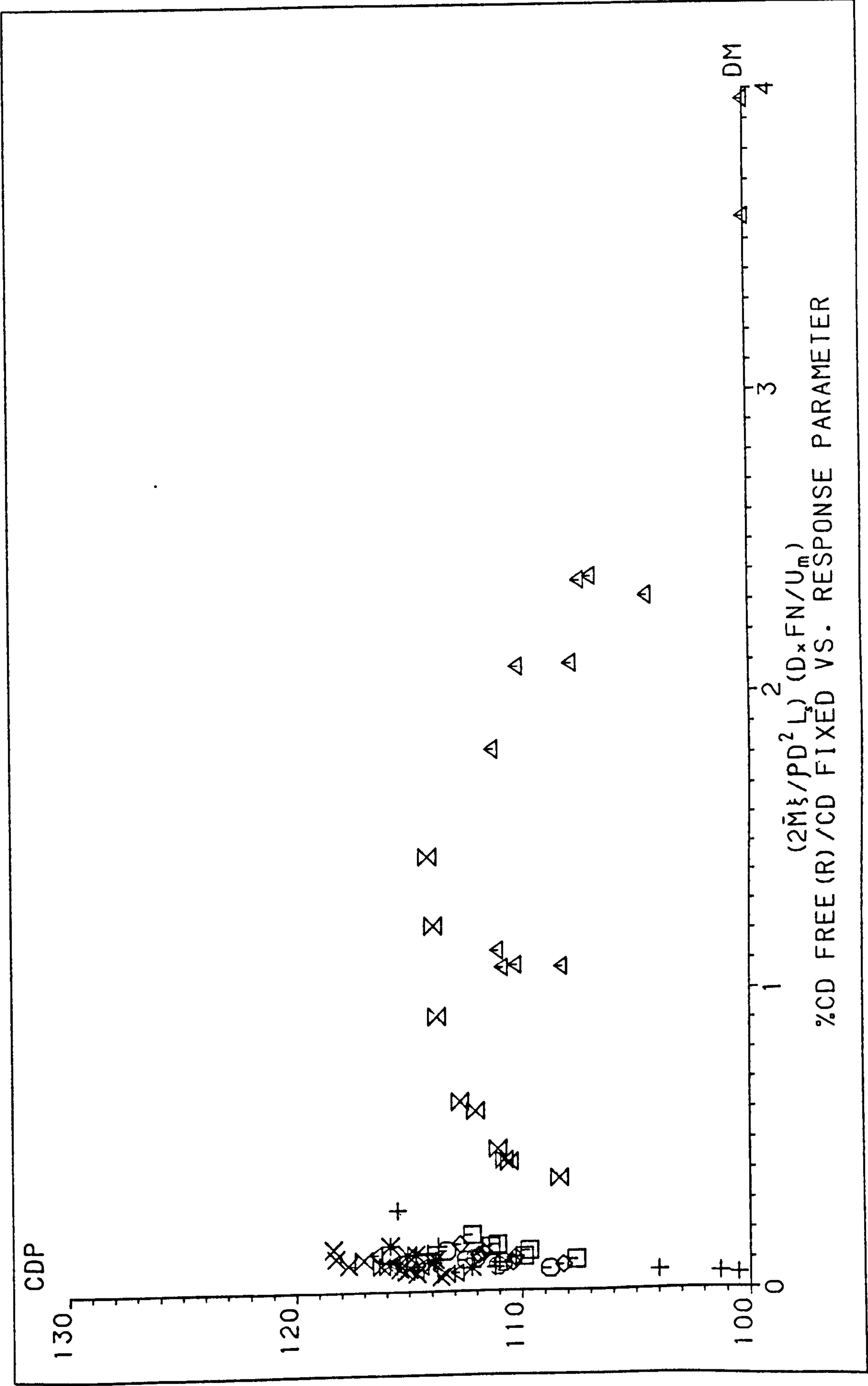


Figure (5.3.20) - Variation of  $(\% C_D \text{ Free}(R)/C_D \text{ Fixed})$  with the Response Parameter.

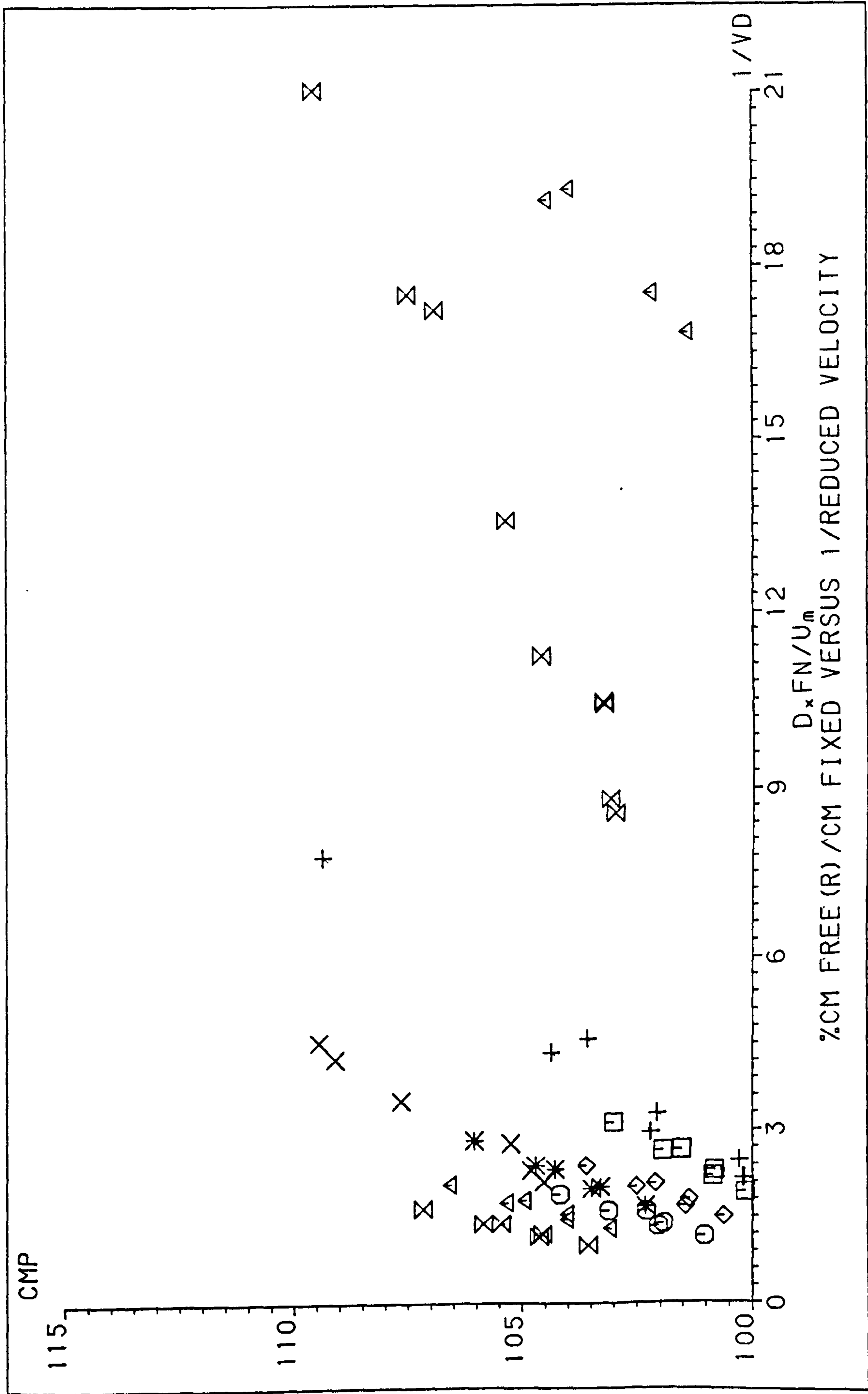


Figure (5.3.21) - Variation of  $(\% C_M \text{ Free}(R)/C_M \text{ Fixed})$  with the Reciprocal of Reduced Velocity.



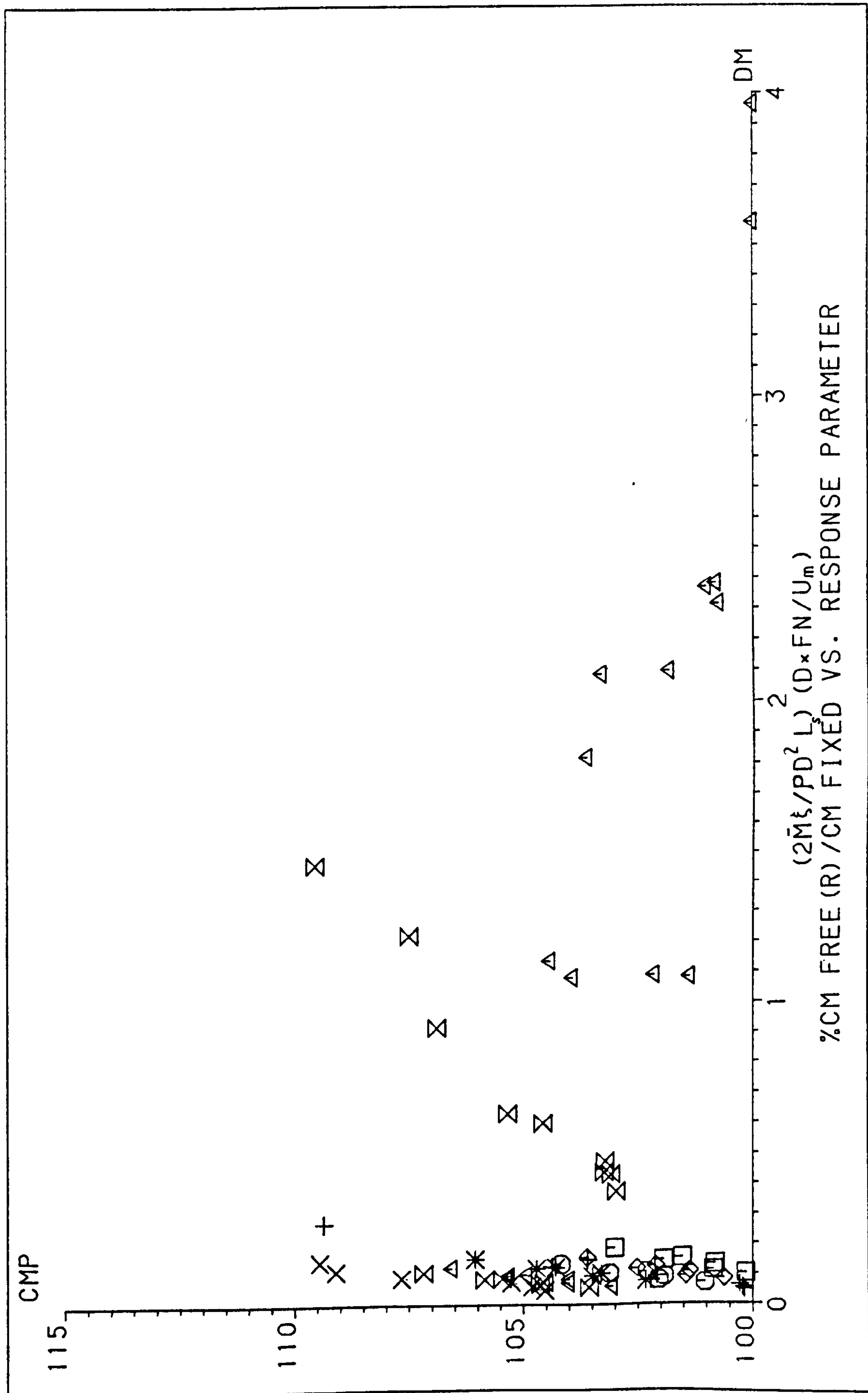


Figure (5.3.22) - Variation of  $(\% C_M \text{ Free}(R)/C_M \text{ Fixed})$  with the Response Parameter.

The variations of the percentage ratio of  $C_D$  and also of  $C_M$  with respect to the reduced velocity have a similar pattern to the variations with the K-C numbers. This similarity in the behaviour emphasises the previous explanation of the water wave structure interaction.

The variation of the relative displacement  $X/D$  with the time of one wave cycle is shown in Figures(5.3.23) through (5.3.32) for one test of each structure when the water depth was 0.5 meter and the wave period was 1.15 seconds. In these figures the relative displacements are represented by the following symbols:

- The measured displacement divided by the structure diameter.
- o The calculated relative displacement using the values of  $C_D$  and  $C_M$  for free structure and taking into consideration the water wave/structure interaction in the dynamic equation.
- + The calculated relative displacement using the values of  $C_D$  and  $C_M$  for fixed structure and using the damping coefficient in water without taking into consideration the water wave/structure interaction in the dynamic equation.

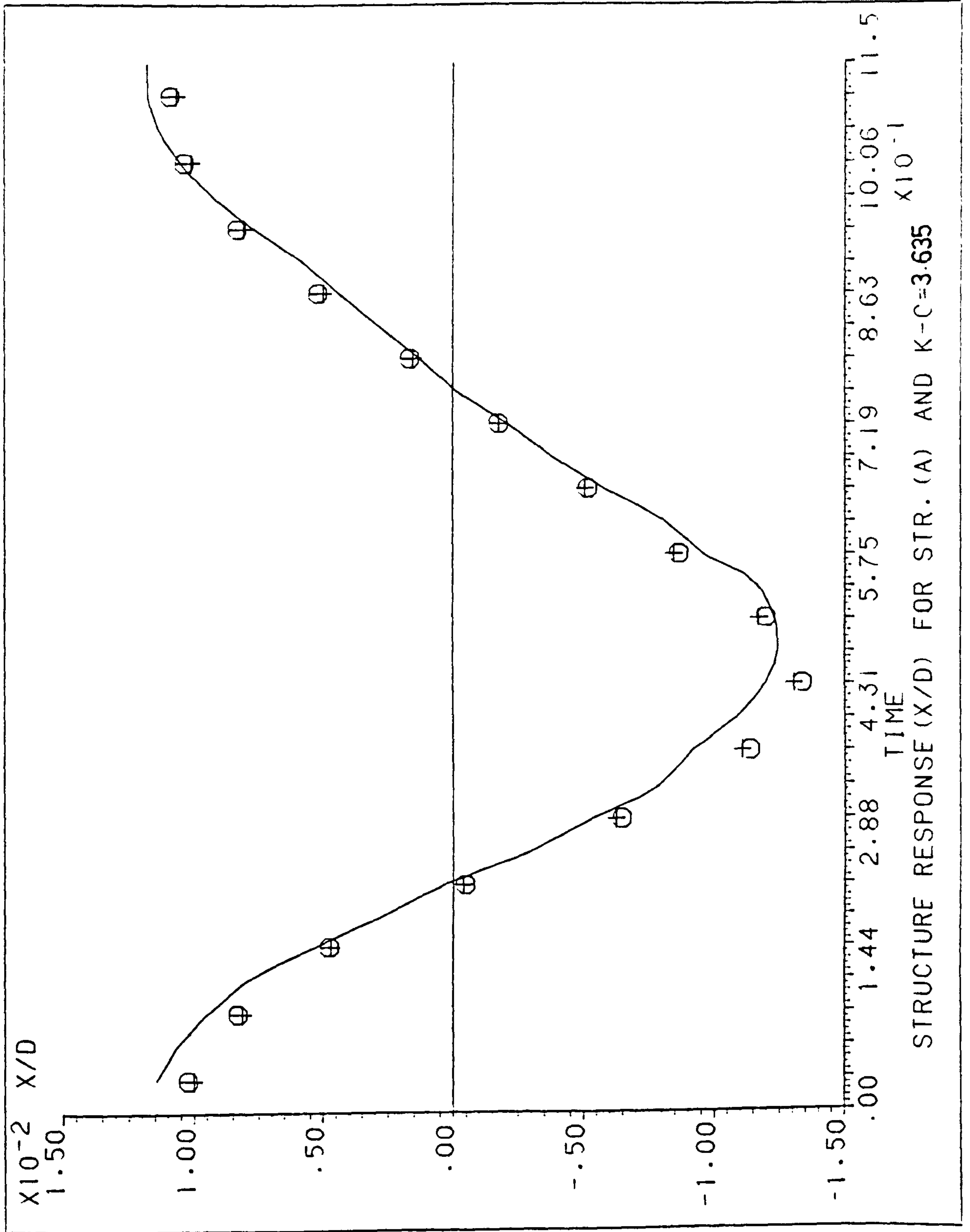


Figure (5.3.23) - Structure's Response (X/D) during the Wave Cycle for Structure A.



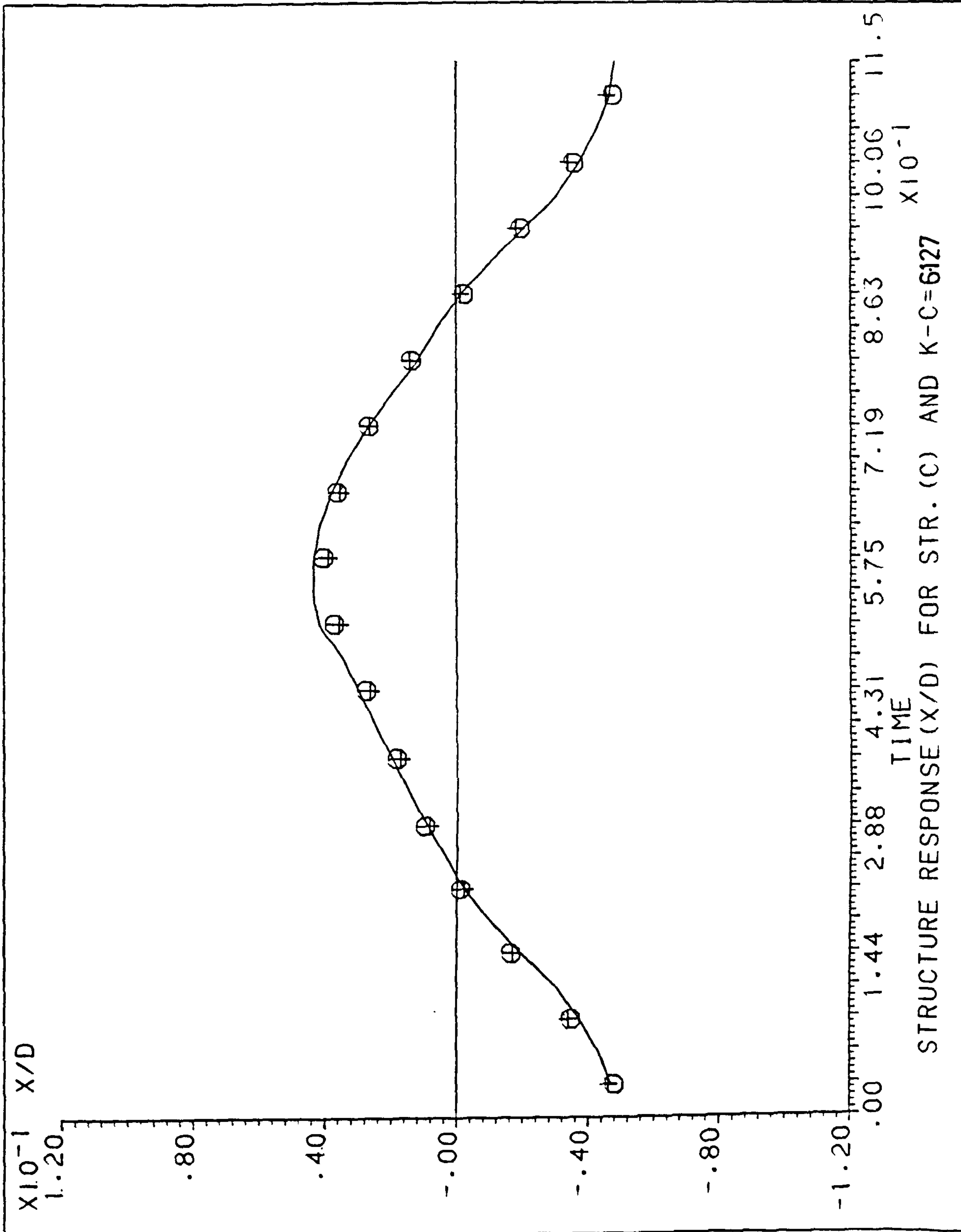


Figure (5.3.25) - Structure's Response (X/D) during the Wave Cycle for Structure C.

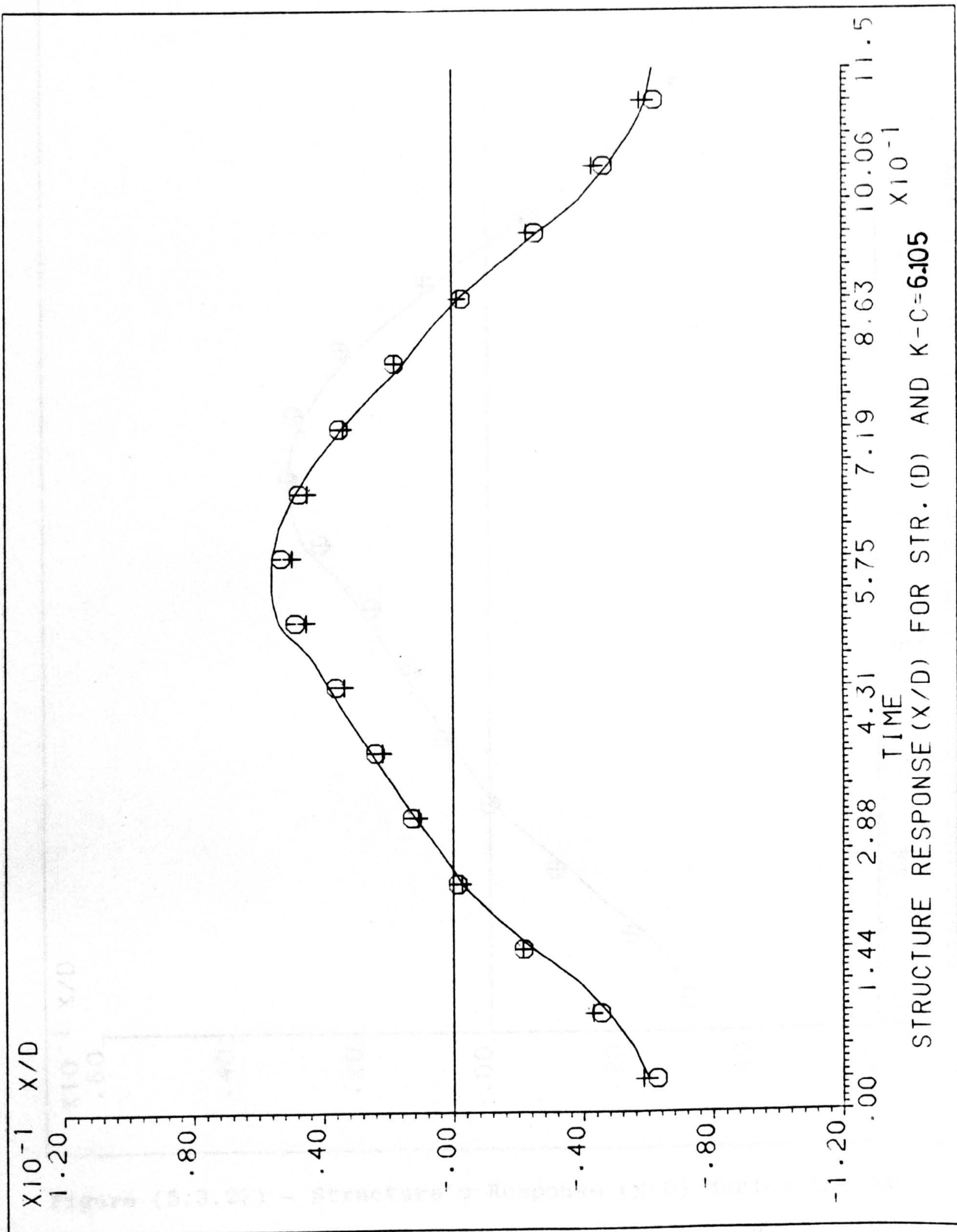


Figure (5.3.26) - Structure's Response (X/D) during the Wave Cycle for Structure D.



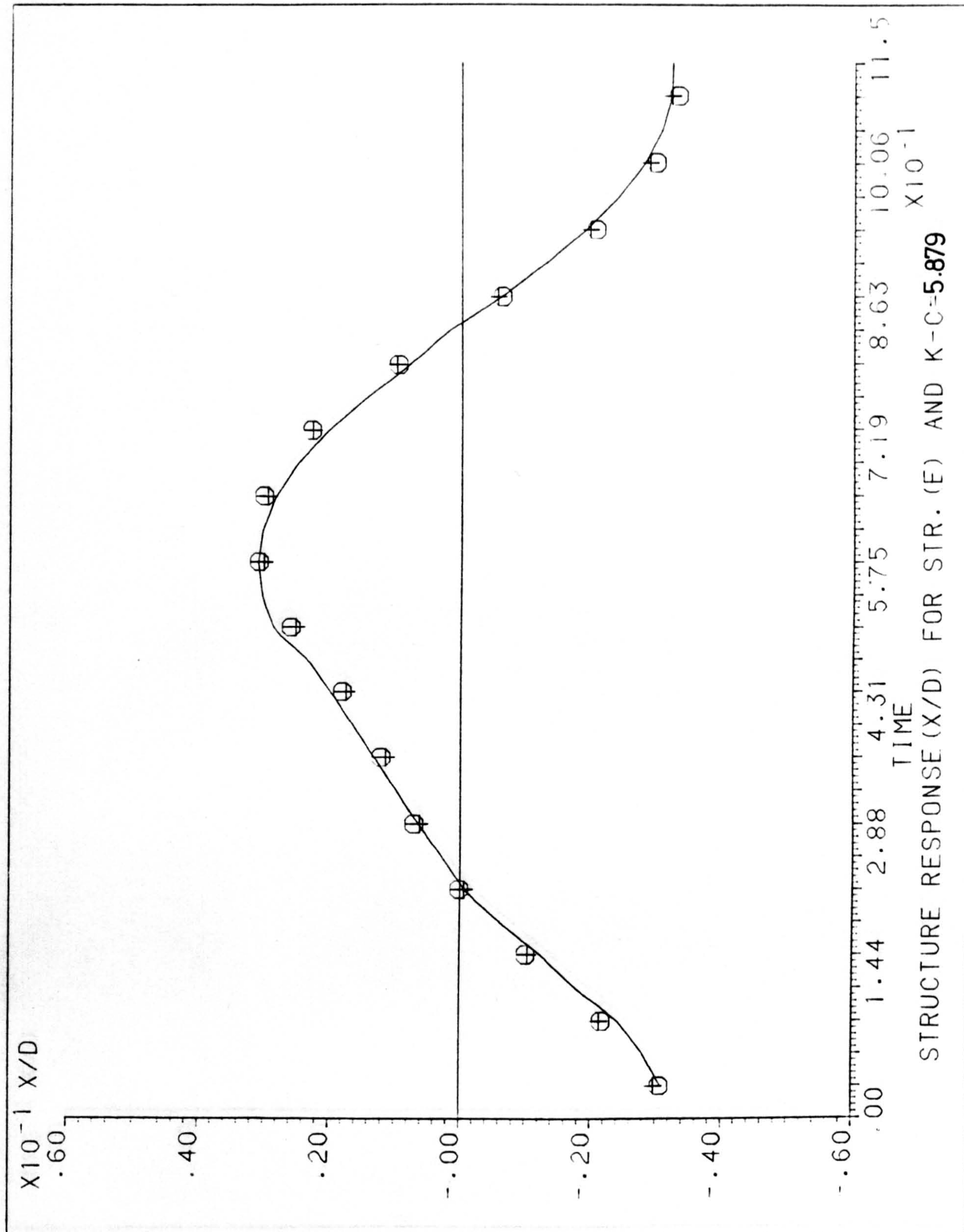


Figure (5.3.27) - Structure's Response (X/D) during the Wave Cycle for Structure E with no Mass at Top.



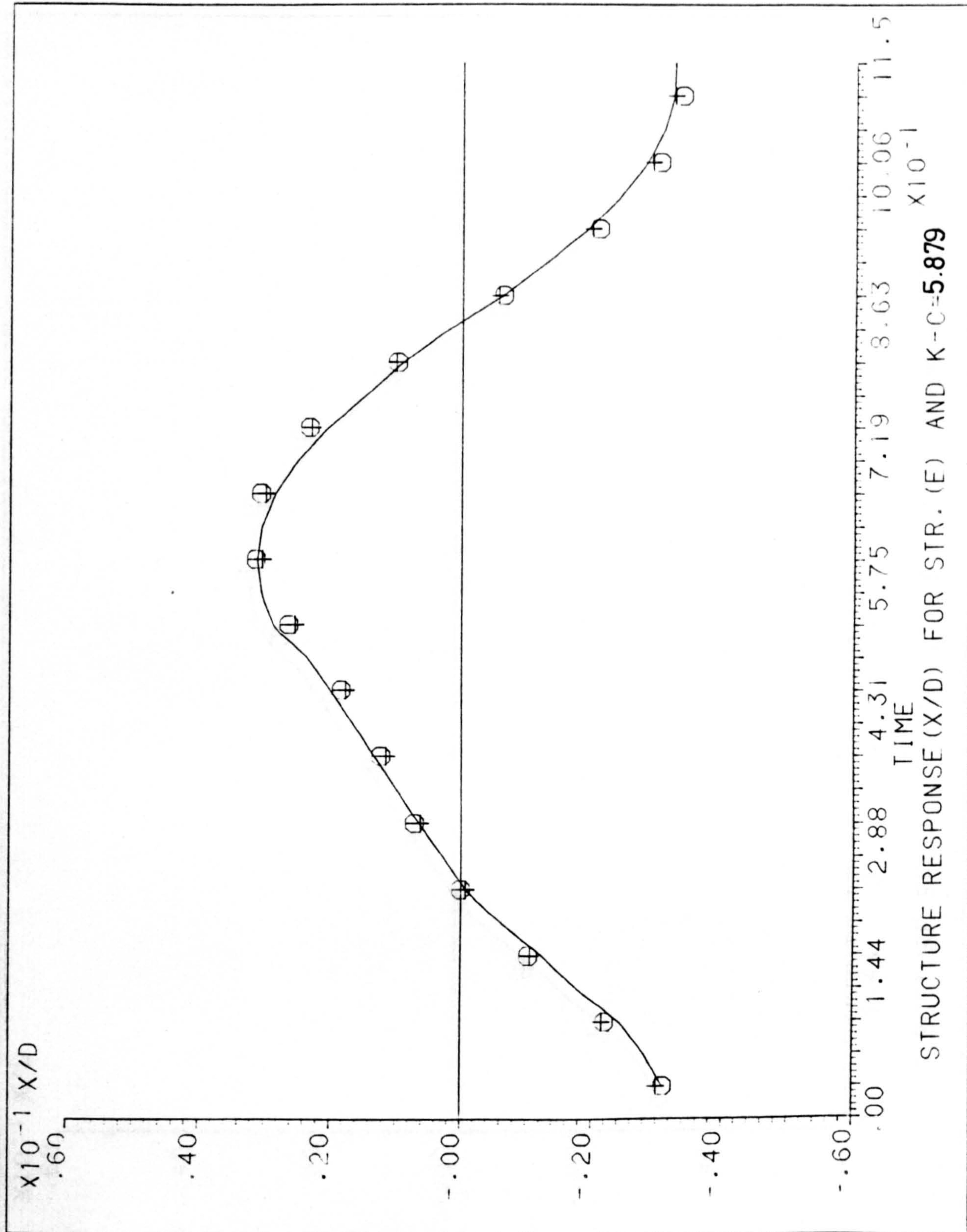


Figure (5.3.28) - Structure's Response (X/D) during the Wave Cycle for Structure E with 1010 Grs at Top.



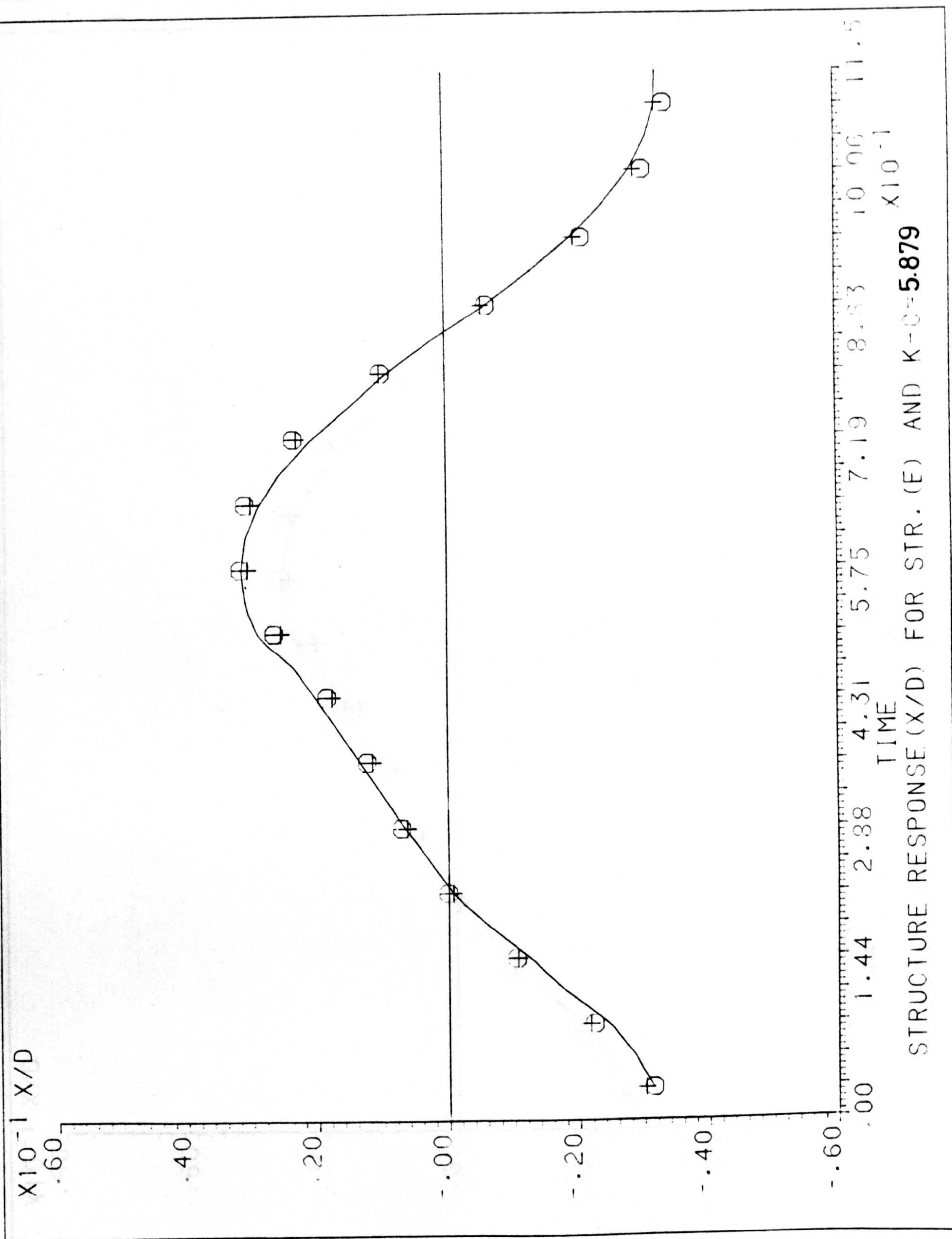


Figure (5.3.29) - Structure's Response (X/D) during the Wave Cycle for Structure E with 2020 Grs at Top.



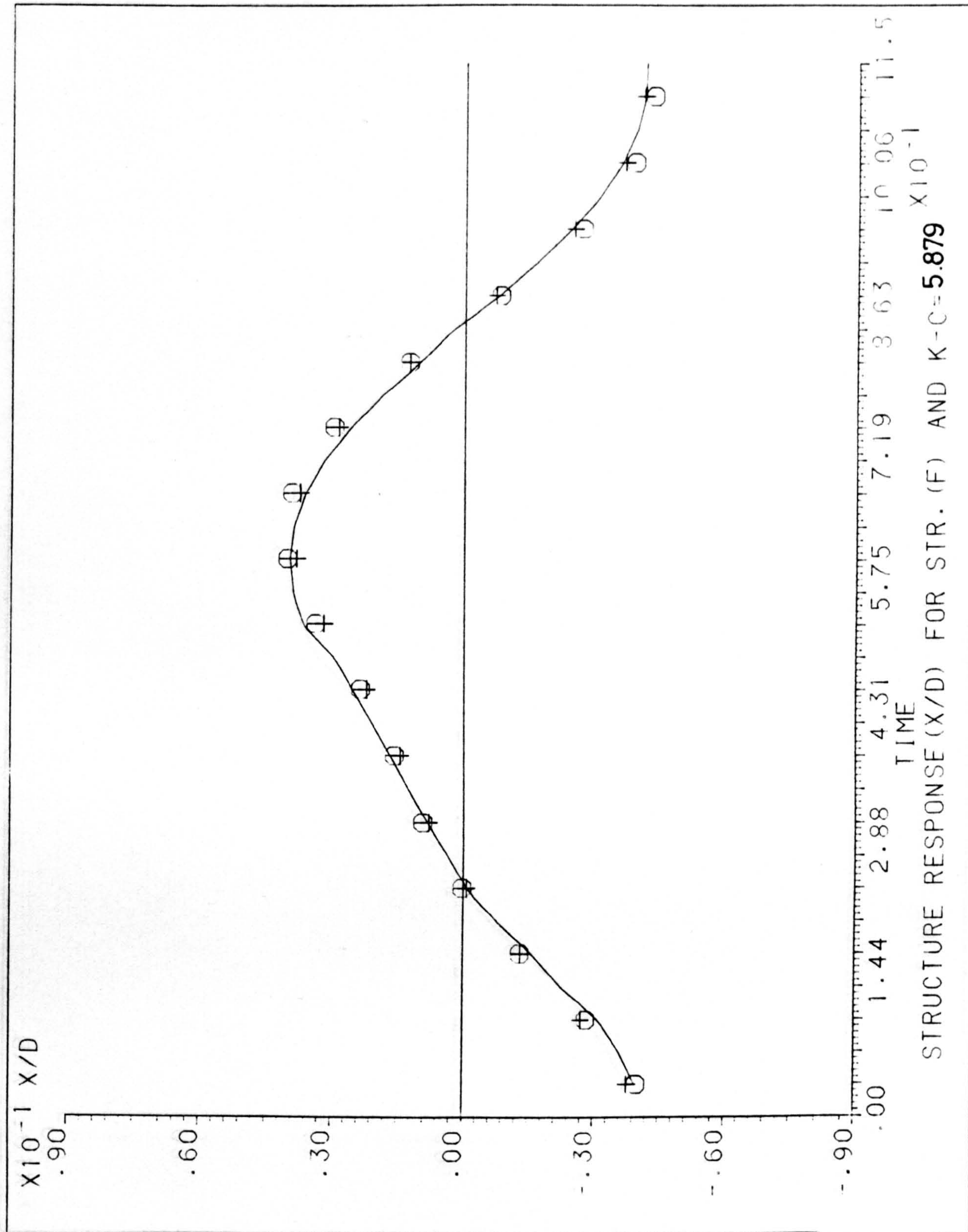


Figure (5.3.30) - Structure's Response (X/D) during the Wave Cycle for Structure F with no Mass at Top.



Results for the other tests are shown in Appendix (D)

The figures show that there are insignificant differences between the two calculated relative displacements, the greatest difference being 11.08%. Also the difference between the calculated relative displacement using finite elements and the measured relative displacement is small, with a maximum difference of 9.63%.

8.1.2 The theoretical model used in this study was

(a) The structural model is an equivalent mass arrangement (pipe element) consisting of lumped masses, the force being applied to the mass node.



## CHAPTER SIX

### SUMMARY AND CONCLUSION

- 6.1.1 Theoretical and experimental investigations were carried out in a regular wave regime to study the wave force and the associated structural response on a circular cylinder pier. The cylinders were tested under three different conditions (a) fixed at the bottom and the top end free to vibrate as a cantilever (b) fixed at both ends top and bottom, (c) fixed at the bottom but free to vibrate, top end being free carrying an added mass. The experimental study was conducted in a wave regime defined by Keulegan-Carpenter number ( $U_m T/D$ ) i.e. from 1.87 to 10.69. The maximum amplitude of the structural response ( $X/D$ ) at the top of the cylinder varied from 0.0049 to 0.098. The ratio of the force frequency to the structural natural frequency was low to avoid resonance.
- 6.1.2 The theoretical model used in this study were
- (a) The structural model is an equivalent beam arrangement (pipe element) consisting of lumped masses, the force being applied to the mass node.



- (b) The damping model for the structure is based on the mass and stiffness damping. In the case when the water wave/structure interaction is ignored and the value of  $C_D$  and  $C_M$  were taken for a fixed structure, the value of the relative damping coefficient taken from the water damping test was used.
- (c) The direct approach method was used in the iterative solution of the nonlinear differential equation of motion in the case of water wave/structure interaction.
- (d) The mode superposition technique with few modes was used in the two-dimensional analysis of the structural response in the time domain.

6.2.1 The local force coefficients  $C_D$  and  $C_M$  were calculated at certain depth of the structure (where the pressure could be measured). This depth varied from 0.06 to 0.12 metres from the still water level (see Tables 5.2 to 5.11). For some structures, there were more than one level where the local force coefficients were calculated. It was found that the magnitude of the drag coefficient decreases with depth and that of the



inertia coefficient increases with depth (e.g. in the Table 5.5 Test 1, the value of  $C_D$  at 0.05 metres from the still water level was 1.019 and at level 0.15 was 0.978 and the corresponding  $C_M$  value was 1.758 and 1.837).

6.2.2 When the structures were fixed at the top i.e. not allowed to vibrate, the value of the calculated local drag coefficient  $C_D$  varied from 0.654 to 1.261 and that of the inertia coefficient  $C_M$  varied from 2.548 to 1.544 as the Keulegan and Carpenter number varied from 1.87 to 10.69 (see Figures 5.3.2a and 5.3.2b). The order of the magnitude of the value of  $C_D$  and  $C_M$  obtained agree with the previous published results (Hogben et al 1977<sup>(53)</sup>), (Aagaard and Dean 1969<sup>(114)</sup>)  $C_D$  varied from 0.5 - 1.2 and  $C_M$  was constant and equal to 1.33, Keulegan and Carpenter 1958<sup>(27)</sup>  $C_D$  varied from 0.7 to 1.3 and  $C_M$  varied from 2.6 to 1.6, Morison et al 1950<sup>(25)</sup>  $C_D$  varied from  $1.626 \pm 0.414$  and  $C_M$  varied from  $1.508 \pm 0.197$  and Paape and Breusers 1967<sup>(115)</sup>  $C_D$  varied from 0.5 to 2.0 and  $C_M$  varied from 1.0 to 2.5).

6.2.3 When the structures were free at the top i.e. free to vibrate, the values of  $C_D$  and  $C_M$  were calculated by two methods, first by Morison's equation and second by modified Morison's equation. The second



method producing the larger value of the drag coefficient with a maximum ratio ( $C_D$  modified Morison/ $C_D$  Morison) of 102.7% while the inertia coefficient  $C_M$  showed no differences between the above two methods (see Figures 5.3.15a and 5.3.15b).

- 6.2.4 There is a difference between the magnitude of the drag coefficient of the "free" structure and that of the "fixed" structure under a particular set of wave conditions, the former being greater in magnitude than the latter. The maximum ratio of the drag coefficient for the free structure to that of fixed structure ( $C_D$  Free/ $C_D$  Fixed) was 118.45% (see Figure 5.3.13). It was found that the inertia coefficient exhibited a similar pattern of behaviour. The maximum ratio of the inertia coefficient for free structure to that of fixed structure ( $C_M$  Free/ $C_M$  Fixed) was 109.56% (see Figure 5.3.14). These differences in the magnitude of the force coefficients decrease with increasing depth from the still water level (see Tables 5.4 to 5.11).

The difference in magnitude of the drag coefficients is greater than the corresponding difference in magnitude of the inertia coefficients. Both differences in value are attributed to the vibration of the structure and consequently the



change in the flow field round the structure (see Figures 5.2.3 and 5.2.4). Therefore these differences are dependent upon the structural response ( $X/D$ ) and Keulegan-Carpenter number ( $U_m T/D$ ). There is a decrease in magnitude with increasing Keulegan-Carpenter number for the same structure because the increase of the level of vorticity in the fluid field near the structure. For constant Keulegan-Carpenter number their magnitude increase with decreasing structural stiffness.

No differences in the ratio of  $C_D$  Free/ $C_D$  Fixed and the ratio of  $C_M$  Free/ $C_M$  Fixed were noticed when the structural response ( $X/D$ ) was less than 0.006. As the structural response increases to a value in excess of 0.006 the differences in coefficients start to increase sharply until a peak is reached at  $X/D$  of 0.01, thereafter the differences decrease with increasing structural response as shown in Table (5.12).

For the tested structures and waves, the wave force acting on the free structure was greater than that of the fixed structure. The maximum difference was 9.5%.



- 6.2.5 The magnitude of the relative damping coefficient is greater in water than in air and increases with increasing water depth. For the same structure, the magnitude of the relative damping coefficient increases with increasing added mass at the top of the structure i.e. decreasing structure stiffness (see Table (5.1)).
- 6.2.6 Also from Table (5.1) it can be seen that the natural frequency of the structure in air had a higher value than that in water. The value of the structural natural frequency in water decreases with increasing water depth.
- 6.2.7 The dynamic analysis using the first three modes in the mode superposition technique (as suggested by Molhatra and Penzien 1970<sup>(85)</sup>) and using the damping matrix as proportional to the mass and stiffness matrix, gives a more accurate representation of the problem of the structural response (deflection) for a cantilever structure when the ratio of the forcing frequency to the structure's frequency is very small ( $\ll 1$ ) (i.e. 0.13). The maximum difference between the measured and the calculated structural response using the modified Morison's equation (Method A) is 9.87%. The maximum difference between the measured and calculated structural response using Morison's equation (Method B) is 7.45% (see Tables 5.12 to 5.21).



6.2.81 The maximum difference between the calculated structural response using Method A and Method B is 9.56%.

6.2.9 The structural response ( $X/D$ ) is better represented by the non-dimensional response parameter  $(2\bar{M}\xi/\rho D^2 L_s) (D FN/U_m)$  than by the reciprocal of the reduced velocity  $(D FN/U_m)$  as shown in Figures(5.3.16a - 5.3.16b).

### 6.3 RECOMMENDATION

Additional research is needed, under the same condition ( $FF/FN \ll 1$ ) for structures with dynamic properties differing from those investigated herein. In addition a continuation of research is needed under different condition ( $FF/FN > 1$ ) and less than the second resonance for structure of similar dynamic properties to those investigated.



## REFERENCES

1. Inquiry into the Collapse of Texas Tower No. 4. Hearings before the Senate Preparedness Investigating Sub-Committees, Committee on Armed Services, U.S. Senate, 87th Congress, First Session, U.S. Govt. Printing Office, May 3, 4, 10, 11 and 17, 1961.
2. H. R. Bronnan, T. R. Loftin and J. H. Whitfield "Deepwater Platform Design" Annual OTC Conference 1974, Paper No. OTC 2120.
3. A. D. K. Laird "Water Forces on Flexible Oscillating Cylinders". Journal of the Waterways and Harbors Division, ASCE, Vol. 88, No. WW3, Proc. Paper 3234, August, 1962, pp 125-137.
4. A. D. K. Laird "Flexibility in Cylinder Groups Oscillated in Water" Journal of the Waterways and Harbors Division, ASCE, Vol. 92, No. WW3, Proc. Paper 4884, August, 1966, pp 69-85.
5. D. Howell "Equations for Water Wave and Approximation Behing Them" Waves on Beaches and Resulting Sediment Transport, Edited by Meyer, Academic Press New York, London 1972.



6. J. J. Stoker "Water Waves" Interscience Publishers INC, New York, 1957.
7. J. V. Wehausen and D. V. Laiton "Surface Waves" Handbuch der Physik, Bd. IX.
8. E. V. Laiton "Limiting Conditions for Cnoidal and Stokes Wave", Journal of Geophysical Research, Vol. 67, No. 4, April 1962.
9. B. W. Wilson "Origin and Effects of Long Period Waves in Ports", XIX International Navigational Congress Section II Comm. Vol. 1, (1957).
10. R. G. Dean "Stream Function Wave Theory; Validity and Application", Proc. of the ASCE Specialty Conference on Coastal Engineering 1965, Chapter 12, pp 269-299.
11. R. G. Dean "Relative Validities of Water Wave Theories", Proc. ASCE, Jour. of Waterway and Harbors Division, Vol. 96, No. 1, Feb. 1970.
12. R. G. Dean "Evaluation and Development of Water Wave Theories for Engineering Application", U.S. Army, Corps of Engineers Coastal Engineering Research Centre Report, No. 1, 1974.



13. H. Nishimura and M. Isobe "On the Validities of Finite Amplitude Wave Theories", International Conference on Water Resources Engineering, Bangkok, Thailand, 1978.
14. R. L. Wiegel "Oceangraphical Engineering", Prentice-Hall, Inc. 1964.
15. R. L. Wiegel "Waves and Wave Spectra and Design Estimates", Deep-Sea Oil-Production Structures, January 23-27, 1978.
16. C. J. Garrison and S. Rao "Interaction of Wave With Submerged Objects", Jour. of Waterway, Harbors and Coastal Eng. Div, May 1977, WW2, pp 259-277.
17. R. L. P. Verley "Wave Forces on Structures an Introduction", BHRA Report No. TN1319, 1975.
18. R. C. MacCamy and R. A. Fuchs "Wave Force on Piles: A Diffraction Theory", U. S. Army Corps of Engineers, Beach Erosion Board, Tech. Memo No. 69, 1954.
19. Spring and Munkmeyer, "Interaction of Plane Waves with Vertical Cylinders", Coastal Eng. Conference, ASCE, Vol. III, 1974, pp 1828-1847.



20. S. K. Chakrabarti, "Wave Forces on Multiple Vertical Cylinders", Jour. of Waterway, Port, Coastal and Ocean Div. ASCE, Vol. 104, 1978, WW2 pp 147-161.
21. C. J. Garrison, "Hydrodynamics of Large Objects in the Sea, Part I - Hydrodynamic Analysis", Jour. of Hydronautics, Vol. 8, No. 1, January 1974, pp 5-12.
22. C. J. Garrison and R. Stacey, "Wave Loads on North Sea Gravity Platforms: A comparison of Theory and Experiment", Offshore Technology Conference 1977, Paper No. OTC 2794, pp 513-524.
23. H. Raman, P. G. V. Rao and P. Venkatanarasaiah, "Diffraction of Nonlinear Waves by a Circular Cylinder", Acta Mechanica, 23, 1975, pp 145-158.
24. S. K. Chakrabarti, "Wave Forces on Pile Including Diffraction and Viscous Effects", Jour. of Hydraulics Division, ASCE, Aug. 1973, Vol. 99, HY8, pp 1219-1233.
25. J. R. Morison et al, "The Force Exerted by Surface Waves on Piles", Petroleum Transaction, AIME, Vol. 189, 1950, pp 149-154.
26. R. D. Blevins, "Flow-Induced Vibration", Van Nostrand Reinhold Company (1977).



27. G. H. Keulegan and L. H. Carpenter, "Forces on Cylinders and Plates in an Oscillating Fluid", National Bureau of Standard (Journal of Research) Vol. 60, Nos. R. P 2857 (1968).
28. R. L. Wiegel et al, "Ocean-Wave Force on Circular Cylindrical Piles", Proceeding Paper 1199, ASCE, April, (1957).
29. H. A. Agerschau and J. J. Edens, "Fifth and First Order Wave Force Coefficient for Cylindrical Piles", ASCE Coastal Engineering Speciality Conference Santa Barbara, October (1965), pp 219-248.
30. R. O. Reid, "Correlation of Water Level Variations with Wave Forces on a Vertical Pile for Non-Periodic Waves", Proc. Sixth Conf. on Coastal Eng. Chap. 46, pp 749-786, 1957.
31. B. W. Wilson, "Analysis of Wave Force on a 30 inch Diameter Pile Under Confused Sea Conditions", Coastal Engineering Research Centre, U. S. Army Tech. Memo 15, 1965.
32. R. G. Dean and P. M. Aagaard, "Wave Forces: Data Analysis and Engineering Calculation Method", Jour. of Petroleum Technology, March 1970.



33. D. J. Evans, "Analysis of Wave Force Data", Jour. of Petroleum Technology, March 1970.
34. J. D. Wheeler, "Method for Calculating Force Produced by Irregular Waves", Jour. of Petroleum Technology, March 1970.
35. K. Y. Kim and H. C. Hibbard, "Analysis of Simultaneous Wave Force and Water Partical Velocity Measurement", OTC Paper No. 2192, Houston, 1975.
36. J. C. Heideman, O. A. Olsen and P. I. Johansson, "Local Wave Force Coefficient", Civil Engineering in the Oceans IV, ASCE, pp 684-699, 1979.
37. C. L. Bretschneider, "Probability Distribution of Wave Force", Proc. ASCE 93, WW2, pp 5-26, (May 1967).
38. G. G. Susbielles et al, "Wave Forces on Pile Sections due to Irregular and Regular Waves", Proc. Offshore Technol. Conf. Paper OTC 1379, 1971.
39. S. K. Chakrabarti, "Wave Forces on a Randomly Orient Tube", Proc. OTC Paper No. OTC 2190, 1975.



40. J. D. Gaston and R. D. Ohmart, "Effect of Surface Roughness on Drag Coefficients"; Civil Engineering in the Ocean IV", ASCE, pp 611-621, 1979.
41. T. Sarpkaya, "Vortex Shedding and Resistance in Harmonic Flow about Smooth and Rough Circular Cylinders at High Reynolds Number", Report No. NPS - 59SL76021, Naval Postgraduate School, Monterey, CA (1976a).
42. T. Sarpkaya, "In-Line and Transverse Forces on Smooth and Sand-Roughened Cylinder in Oscillatory Flow at High Reynolds Number", Report No. NPS - 59SL76022, Naval Postgraduate School, Monterey, CA (1976b).
43. G. G. Stokes, "On the Effect of the International Friction of Fluid on the Motion of Pendulums", Cambridge Phil. Trans. Vol. IX, Part 2, p 8, 1945.
44. T. Sarpkaya, "In-Line and Transverse Forces on Cylinders in Oscillatory Flow at High Reynolds Numbers", Journal of Ship Research, Vol. 21, No. 4, pp 200-216, (1977a).
45. T. Sarpkaya et al, "Wave Force on Rough-Walled Cylinders at High Reynolds Number", Offshore Technology Conference 1977, Vol. III, Paper No. OTC 2901, pp 175-184.



46. D. J. Maull and M. G. Milliner, "Sinusoidal Flow Past a Circular Cylinder", Journal of Coastal Engineering, Vol. 2, pp 149-168, (1978).
47. P. W. Bearman and J. M. R. Graham, "Hydrodynamic Forces on Cylindrical Bodies in Oscillatory Flow", Proc. of the Second International Conference on Behaviour of Offshore Structures BOSS 79, London, Paper No. 24, pp 309-322 (1979).
48. S. K. Keim, "Fluid Resistance to Cylinders in Accelerated Motion", Journal of the Hydraulics Div. ASCE Vol. 83, No. HY6 (1956).
49. A. D. K. Laird and C. A. Johnson, "Drag Forces on Accelerated Cylinders", Journal of Petroleum Tech. Vol. 8, pp 65-67, (1956).
50. A. D. K. Laird et al, "Water Forces on Accelerated Cylinders," Jour. of Waterways and Harbor Div. ASCE, WW1, pp 99-119 (1959).
51. C. Dalton et al, "The Forces on Cylinder oscillating Sinusoidally in Water II, Further Experiments", Offshore Technology Conference 1976, Paper No. OTC 2538.



52. T. Sarpkaya and C. J. Garrison, "Vortex Formation and Resistance in Unsteady Flow", Journal of Applied Mechanics, Vol. 30, Series E, No. 1, pp 16-24 (1963).
53. N. Hogben et al, "Estimation of Fluid Loading on Offshore Structures", Proc. Institution of Civil Engrs. Vol. 63, Part 2, pp 515-562 (1977).
54. N. Hogben, "Wave Loads on Structures", Proc. International Conference on the Behaviour of Offshore Structure, Vol. 1, pp 187-219 (1976).
55. D. D. Bidde, "Laboratory Study of Lift Forces on Circular Piles", Jour. Waterwats Harbors and Coastal Eng. Div. ASCE, Vol. 97, No. WW4, pp 595-614, 1971.
56. R. Wiegel and Delmonte, "Wave Induce Eddies and Lift Forces on Circular Cylinders", Univ. of Calif. Berkeley, Tech. Report No. HEL 9-19, 1972.
57. M. De St. Q. Isaacson, "The Forces on Circular Cylinders in Waves", PhD Thesis Submitted to the Dept. of Engineering, Univ. of Cambridge (1974).



58. M. F. Zedan and F. Rajbi, "Lift Forces on Cylinders Undergoing Hydroelastic Oscillation in Waves and Two-Dimensional Harmonic Flows", International Symposium on Hydrodynamics in Ocean Engineering, The Norwegian Institute of Technology, 1981.
59. J. A. Mercier, "Large Amplitude Oscillation of a Circular Cylinder in a Low Speed Stream", PhD Dissertation, Stevens Institute of Technology (1973).
60. T. Sarpkaya, "Forces on Cylinder and Spheres in an Oscillating Fluid", Journal of Applied Mechanics, ASCE, Vol. 42, pp 32-37, 1975.
61. D. J. Maull and M. G. Milliner, "The Forces on Circular Cylinder having a Complex Periodic Motion", In Mechanics of Wave-Induced Forces on Cylinders, (ed T. L. Shaw), Pitman, London, pp 440-502, 1979.
62. B. Berge and J. Penzien, "Three-Dimensional Stochastic Response of Offshore Towers to Wave Forces", OTC 1974, Paper No. OTC 2050, pp 173-183.



63. T. Moon, S. Haver and T. Vinje, "Stochastic Dynamic Response Analysis of Off-Shore Platform, with Particular Reference Gravity Type Platforms", OTC 1975, Paper No. OTC 2407, pp 707-716.
64. J. Penzien and W. S. Tseng, "Three-Dimensional Dynamic Analysis of Fixed Offshore Platforms", Deep-Sea Oil-Production Structure, Univ. of California, Berkeley (23-27) Jan. 1978.
65. A. S. Veletsos and Y. T. Wei, "Lateral and Rocking Vibration of a Footing", J. of the Soil Mechanics and Foundation Division ASCE, Vol. 97, No. SM9, pp 1227-1249, September 1971.
66. J. E. Luco and R. A. Westmann, "Dynamic Response of Circular Footings", J. of the Engineering Mechanics Division, ASCE, Vol. 97, No. EM5, pp 1381-1395, October 1971.
67. J. E. Luco, "Impedance Functions for a Rigid Foundation on a Layered Medium", Nuclear Engineering and Design, Vol. 31, No. 2, pp 204-217, 1974.
68. M. Novak, "Dynamic Stiffness and Damping of Piles", Canadian Geotechnical Jour. Vol. 11, pp 574-598, 1974.



69. E. Kausel, and J. M. Roessel, "Dynamic effects of Circular Foundation", J. of the Engineering Mechanics Division, ASCE, Vol. 101, No. EM6, pp 771-785, December 1975.
70. N. C. Tsai and G. W. Housner, "Calculation of Surface Motions of a Layered Half-Space", Bulletin of the Seismological Society of America, Vol. 60, No. 5, pp 1625-1651, October 1970.
71. J. Lysmer and R. L. Kuhlemeyer, "Finite Element Model for Infinite Media", J. of the Engineering Mechanics Division, ASCE, Vol. 95, No. EM4, pp 859-877, August 1969.
72. E. R. Taylor, "A Preliminary Study of Structure Dynamic of Gravity Platform", Proc. Seventh Ann. OTC Houston, Paper 2406, III, pp 695-706 (1975).
73. D. C. Angenides and J. J. Conner, "A Probabilistic Model for Stiffness Degradation of Steel Jacket Structure", Proc. BOSS 1979, London, Vol. 2.
74. K. Bell et al, "Analysis of a Wave Structure Soil System Case of Study of a Gravity Platform", Proc. BOSS 1976, Norway, Vol. 2, pp 846-863.



75. R. E. Taylor, "Structure Dynamics of Offshore Platform", Proc. Conference on Offshore Structure, Paper 10, Organised by Inst. of Civil Eng. London (7-8 October, 1974).
76. B. J. Watt, "Dynamic Analysis of Concrete Gravity Structure", Deep-Sea Oil-Production Structure, Univ. of California, Berkeley (23-27), Jan. 1978.
77. J. Penzien, "Structure Dynamics of Fixed Offshore Structure", Proc. BOSS 1976, Vol. 1.
78. R.W. Clough and J. Penzien, "Dynamics of Structures", McGraw Hill Ltd 1975.
79. N. J. Heaf, "The Effect of Marine Growth on the Performance of Fixed Offshore Platforms in the North Sea", 11th Annual of OTC Conference 1979, Paper No. OTC 3386.
80. N. R. Maddox, "Fatigue Analysis for Deep Water Fixed-Bottom Platforms", 6th Annual OTC in Houston, Tex. May 6-8, 1974, Paper No. OTC 2051.
81. J. H. Nath and D. R. F. Harleman, "Dynamics of Fixed Tower in Deep-Water Random Wave", Proc. ASCE Jour. of Waterways and Harbor Division (November 1969) pp 535-555.



82. D. R. Harleman et al, "Dynamic Analysis of Offshore Structure", Presented at the 1963 ASCE Eight Conf. on Coastal Engineering, Mexico City, Mexico.
83. J. H. Nath and D. R. F. Harleman, "The Dynamic Response of Fixed Offshore Structure to Periodic and Random Waves", M.I.T. Hydrodynamics Laboratory Report No. 102, (Jan. 1967).
84. W. C. Nolan and V. C. Honsinger, "Wave Induced Vibrations in the Fixed Offshore Structures", M.S. Thesis, M.I.T. May (1962).
85. A. K. Molhotra and J. Penzien, "Analysis of Tall Open Structures Subjected to Stochastic Excitation", Conference on Dynamic Waves in Civil Engineering, University of Wales, Swansea (1970).
86. S. C. Wu, "The Effects of Current on Dynamic Response of Offshore Platforms", 8th Annual OTC Conference Houston, Tex. May 3-6, 1976, Paper No. OTC 2540.
87. R. King, "The Added Mass of Cylinder", BHRA Report, No. TN 1100 (April 1971).



88. D. N. Jenssen et al, "Gravity Platform Tower Vibration", 9th Annual OTC in Houston, Tex. May 2-5, 1977, Paper No. OTC 2905.
89. T. Sarpkaya, "A Critical Assessment of Morison Equation", International Symposium on Hydrodynamics in Ocean Engineering, The Norwegian Institute of Technology, 1981.
90. Hallam et al, "Dynamics of Marine Structures: Method of Calculating the Dynamic Response of Fixed Structure Subject to Wave and Current Action", CIRIA Underwater Engineering Group, Report UR8, 1978.
91. J. H. Vugts and D. J. Hayes, "Dynamic Analysis of Fixed Offshore Structure", Eng. Structure Vol. 1 1979, pp (114-120).
92. Skop, Ramberg and Ferer, "Added Mass and Damping Forces on Circular Cylinder", NRL Report 7970, June 1976.
93. R. King, "The Hydrodynamic Damping of Natural Vibrations on a Cantilever Cylinder in Water", BHRA Report RR 1122, (1972).



94. T. F. Ogilvie, "Recent Progress Toward the Understanding and Prediction of Ship Motions", Proc. 5th Symp. Naval Hydrodynamics, Berge, Norway, pp 3-80, Sept. (1964).
95. S. Cherry and A. G. Brady, "Determination of Structural Damping Properties by Statistical Analysis of Random Vibrations", Proc. of the Third World Conference on Earthquake Engineering, New Zealand, (1965).
96. A. P. J. Jeary and P. E. Winney, "Determination of Structural Damping of a Large Multi-Flue Chimney From the Response to Wind Excitation", Proc. of the Institution of Civil Engineers TN 65, 53, pp 569-579 (1972).
97. E. H. Vanmarcke, "Estimation of Dynamic Properties of Offshore Structures", Third Annual Offshore Technology Conference, Houston, Texas, (1971).
98. J. A. Ruhl and R. M. Berdahl, "Forced Vibration Tests of Deep Water Platform", 11th Annual OTC Paper No. OTC 3514, (1979).
99. J. A. Ruhl, "Offshore Platform: Observation Behaviour and Comparison with Theory", 8th Annual OTC Paper No. OTC 2553, (1976).



100. R. L. P. Verley, "An Experimental Investigation into Hydrodynamic Damping in Waves", BHRA Project No. RP 13104, 1978.
101. R. L. P. Verley and G. Moe, "The Effect of Cylinder Vibration on the Drag Force and the Resultant Hydrodynamic Damping" Mechanics of Wave-Induced Force on Cylinder", Pitman Advanced Publishing Program (1979), (T.L. Shaw, Ed).
102. R. L. P. Verley, "Oscillations of Cylinder in Still Water", The Royal Norwegian Council for Scientific and Industrial Research, Report No. 602417, 1978.
103. R. B. Dean, P. R. Fish and N. J. Heaf, "Water Structure Interaction Analysis of Hydrodynamic Damping in Offshore Structure", Atkins Research and Development, A Report for L.E.A. (Offshore) Ltd. and the E.E.C. 1979.
104. W. Schumm, "Dynamic Analysis of Deep Water Platform", Inst. Symp. on Integrity of Offshore Structure, Paper 2, Glasgow (6-7 April 1978).



105. J. H. Vugts and I. M. Hines, "Model Superposition V Direct Solution Techniques in the Dynamic Analysis of Offshore Structure", Proc. of the 2nd Conference on the BOSS, London, August 1979.
106. N. Krylov and N. Bogoliuboy, "Introduction to Nonlinear Mechanics: Approximate Asymptotic Methods", Trans. by S. Lefshetz in Annals of Mathematical Studies, Vol. 11, Princeton Univ. Press (1947).
107. J. S. Bendat and A. G. Piersol, "Random Data Analysis and Measurement Procedures", Wiley-Interscience (1971).
108. S. Timoshenko, "Strength of Materials", Part II, Advanced Theory and Problems, 3rd Edition, Van Nostrand Company, Inc, Princeton, J.N. (1956).
109. E. L. Wilson and J. Penzien, "Evaluation of Orthogonal Damping Matrices", International Journal for Numerical Methods in Engineering, Vol. 4, pp 5-10 (1972).
110. Eagleson and Dean, "Small Amplitude Wave Theory", Chapter A of Estuary and Coastline Hydrodynamics", McGraw-Hill Book Co. (1966), (A. T. Ippen, Ed).



111. Maxwell and Harrington, "Effect of Velocity on Tensile Impact Properties of Polymethyl Methacrylate", ASME Transactions, May (1952).
112. Den Hartog, "Mechanical Vibrations", McGraw-Hill, New York (1956).
113. T. Sarpkaya and R. L. Shoaff, "Numerical Modeling of Vortex-Induced Oscillation", Civil Engineering in the Oceans IV, ASCE, PP 504-517, (1979).
114. P. M. Aagaard and R. G. Dean, "Wave Forces: Data Analysis and Engineering Calculation Method", Proc. 7th Offshore Techd. Conf, Houston, Paper OCT 1008, (1969).
115. A. Paape and H. N. C. Breusers, "The Influence of Pile Dimension on Forces Exerted by Waves", Proc. 10th Coastal Engineering Conference, Tokyo (1967).

Figure (1a) shows the strain gauges fixed on the sensing element and the connection of the strain gauges.

After the pressure transducer was completely built, the outer part of the plate was discarded.



# A P P E N D I X A

## PRESSURE TRANSDUCER

### SENSING ELEMENT

The sensing element was a circular disc of 48 mm diameter which was a part of a brass plate. The brass plate was 100 mm square and 0.02 mm thick. It had to be absolutely flat and without initial strain. The plate was dipped in acid etch until its thickness was reduced to between 0.015 to 0.0125 mm. The plate was pulled from each corner to give initial tension and remained in this condition until the pressure transducer was completed. Four strain gauges were fixed at each side of the sensing element. They were FL-6-11 Tokyo Kenkyoio wireless type. Connecting wires had been soldered of 36 standard wire gauge enamel self-fluxing. The strain gauges were connected together through four pine holes which can be punched from the top before the strain gauges were mounted. After the connection of the strain gauge the four pine holes were sealed and the sensing element were sprayed with flexible varnish making the thickness of the sensing element increased to 0.025 mm.

Figure (1A) shows the strain gauges fixed on the sensing element and the connection of the strain gauges.

After the pressure transducer was completely built the outer part of the plate was discarded.



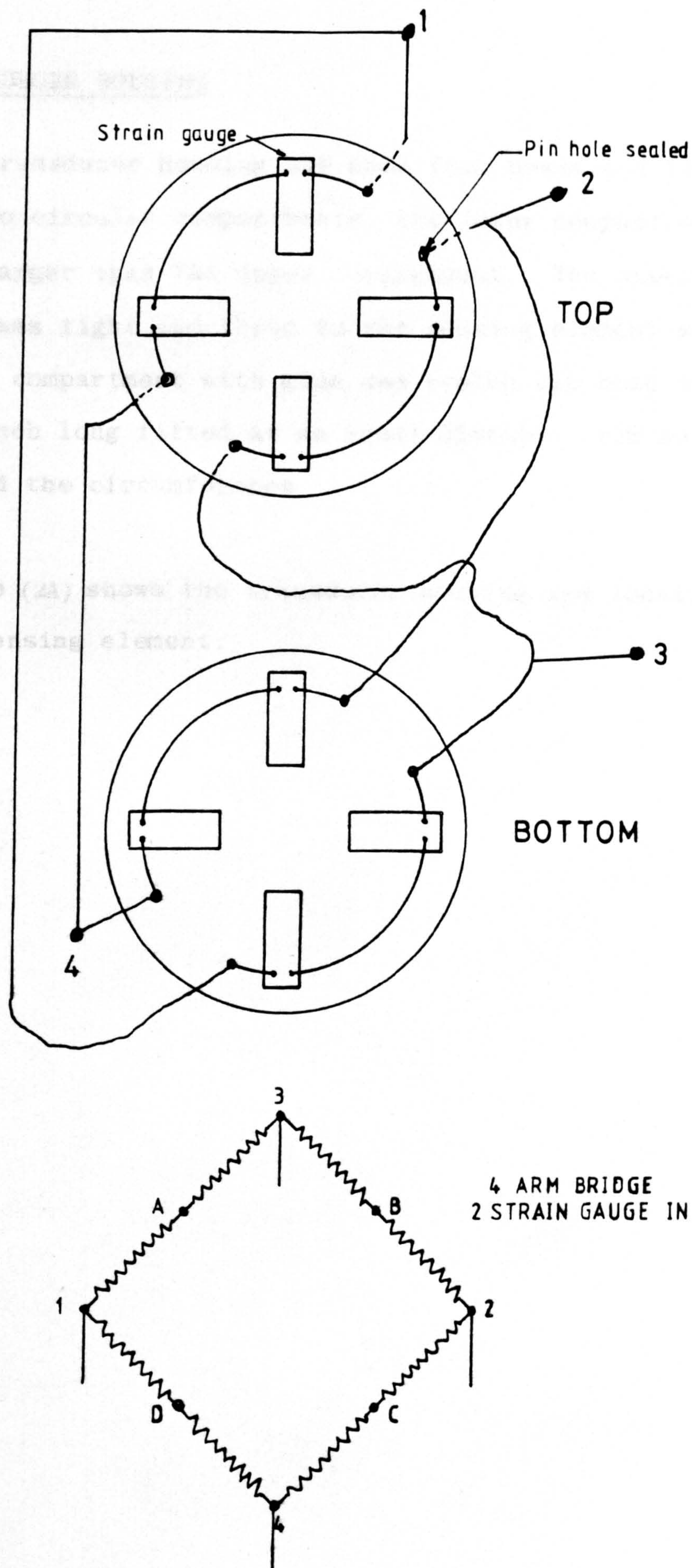


Figure (1A) - The Sensing Element.



## TRANSDUCER HOUSING

The transducer housing was made from brass and it consisted of two circular compartments, the lower compartment which was larger than the upper compartment. The upper compartment was tight and fixed to the sensing element and the lower compartment with glue and twelve cap head screws 0.5 inch long fitted at an equal distance from each other around the circumference.

Figure (2A) shows the transducer housing and location of the sensing element.

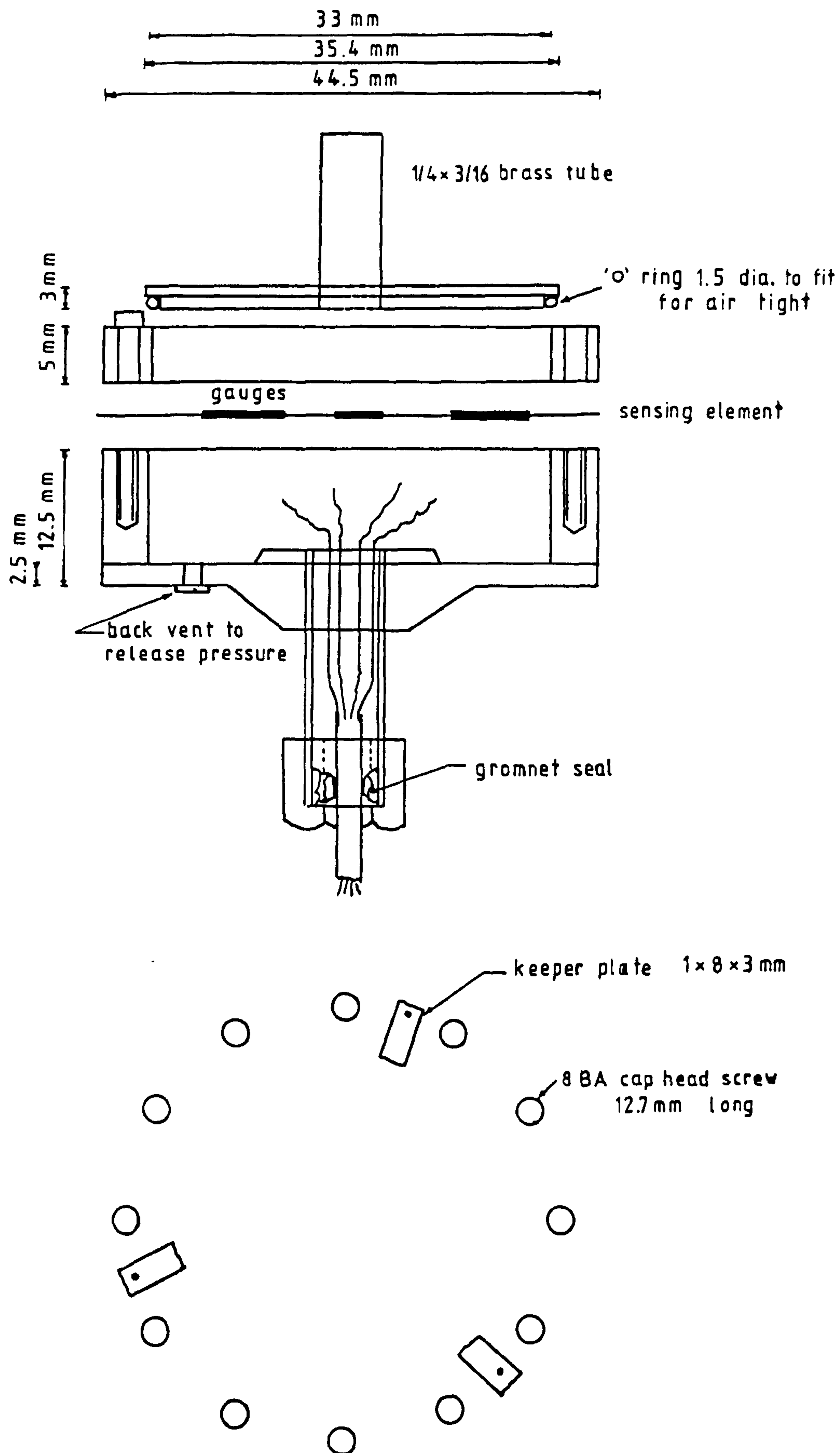


Figure (2A) - The Transducer Housing.



## A P P E N D I X B

### PREAMPLIFIER

A linear amplifier produces at its output a waveform which is a perfect copy, but of greater amplitude. The most important class of linear amplifier i.c. is the operational amplifier which features high gain, high input resistance, low output resistance and narrow bandwidth extending to d.c.

The 741 is typical of the operational amplifier generally, so that the design methods, circuits and bias arrangements can be used with small modification.

Figure (1B) shows the circuits used for an inverting preamplifier. The components used in this circuit were:

R = potentiometer resistance of 200 k $\Omega$  0.5 Watt

R<sub>1</sub> = 390 k $\Omega$  resistance of 0.25 Watt

R<sub>2</sub> = 68 k $\Omega$  resistance of 0.25 Watt

R<sub>3</sub> = 470 k $\Omega$  resistance of 0.25 Watt

C = Capacitors 0.1  $\mu$ F

$$\begin{aligned}\text{The voltage gain} &= \frac{R_3}{R_2} \times \frac{R_3}{R_2} \\ &= \frac{470}{68} \times \frac{470}{68} = 47.77\end{aligned}$$

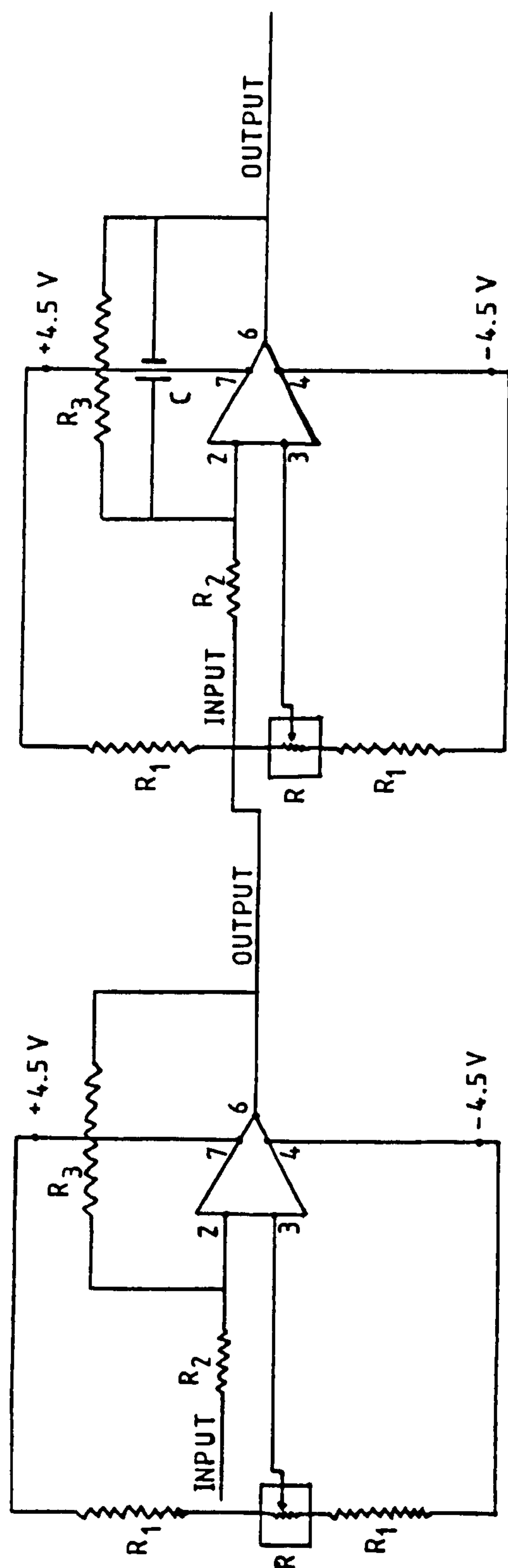
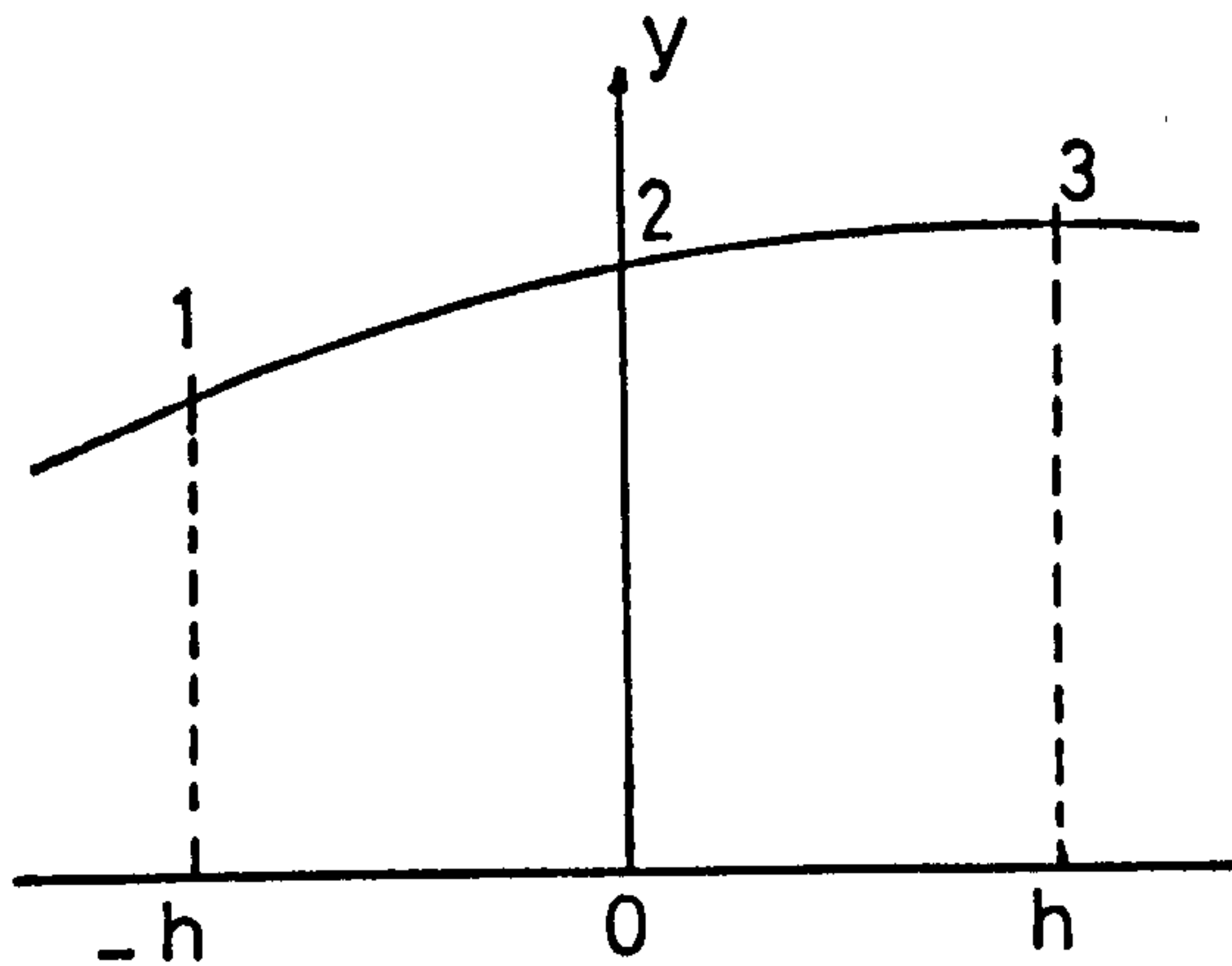


Figure (1B) - The Preamplifier Circuits.



# APPENDIX C

## SINUSOIDAL INTERPOLATION



Let  $y = a \sin (bx + c)$

at point 1  $y_1 = a \sin (-bh + c)$

at point 2  $y_2 = a \sin c$

at point 3  $y_3 = a \sin (bh + c)$

$$\begin{aligned} \therefore y_1 + y_3 &= a \sin (-bh + c) + a \sin (bh + c) \\ &= 2a \sin c \cos bh \\ &= 2y_2 \cos bh \end{aligned}$$

$$\therefore b = \frac{1}{h} \cos^{-1} \left[ \frac{y_1 + y_3}{2y_2} \right]$$

$$\begin{aligned} y_3 - y_1 &= a \sin (bh + c) - a \sin (-bh + c) \\ &= 2a \cos c \sin bh \end{aligned}$$

$$= 2y_2 \cot c \left[ 1 - \left( \frac{y_1 + y_3}{2y_2} \right)^2 \right]^{1/2}$$

$$\therefore C = \tan^{-1} \left[ \frac{2y_2}{y_3 - y_1} \left\{ 1 - \left( \frac{y_1 + y_3}{2y_2} \right)^2 \right\}^{1/2} \right]$$

and

$$a = \frac{y_2}{\sin c}$$

care should be taken to ensure that  $y_2 \neq 0$



## A P P E N D I X D

THE VARIATION OF THE RELATIVE DISPLACEMENTS  $x/d$   
WITH TIME FOR ONE CYCLE OF THE WAVE

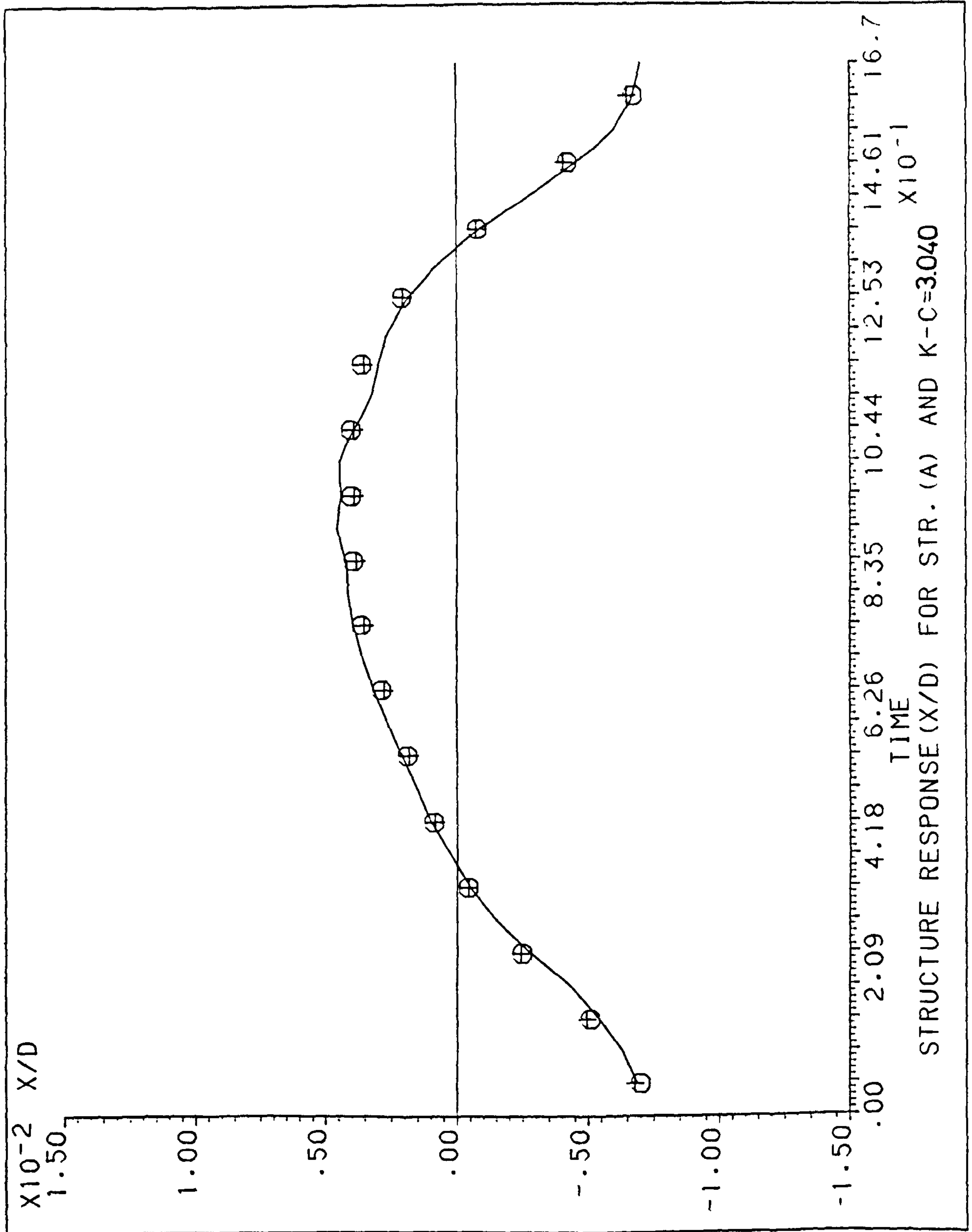


Figure (1D) - Structure's Response (X/D) during the Wave Cycle for Structure A ( $K-C = 3.04$ ).



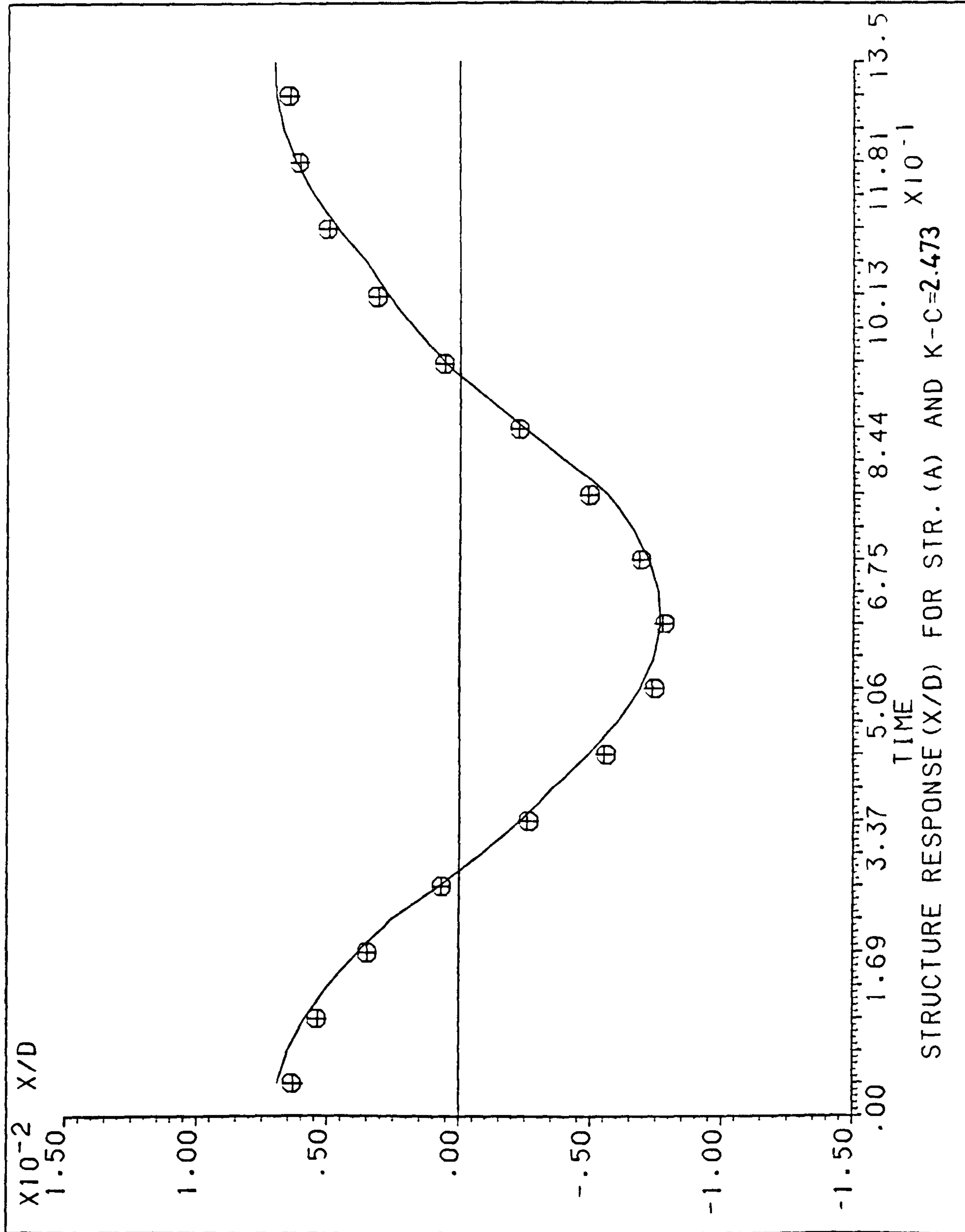


Figure (2D) - Structure's Response (X/D) during the Wave Cycle for Structure A (K-C = 2.473).

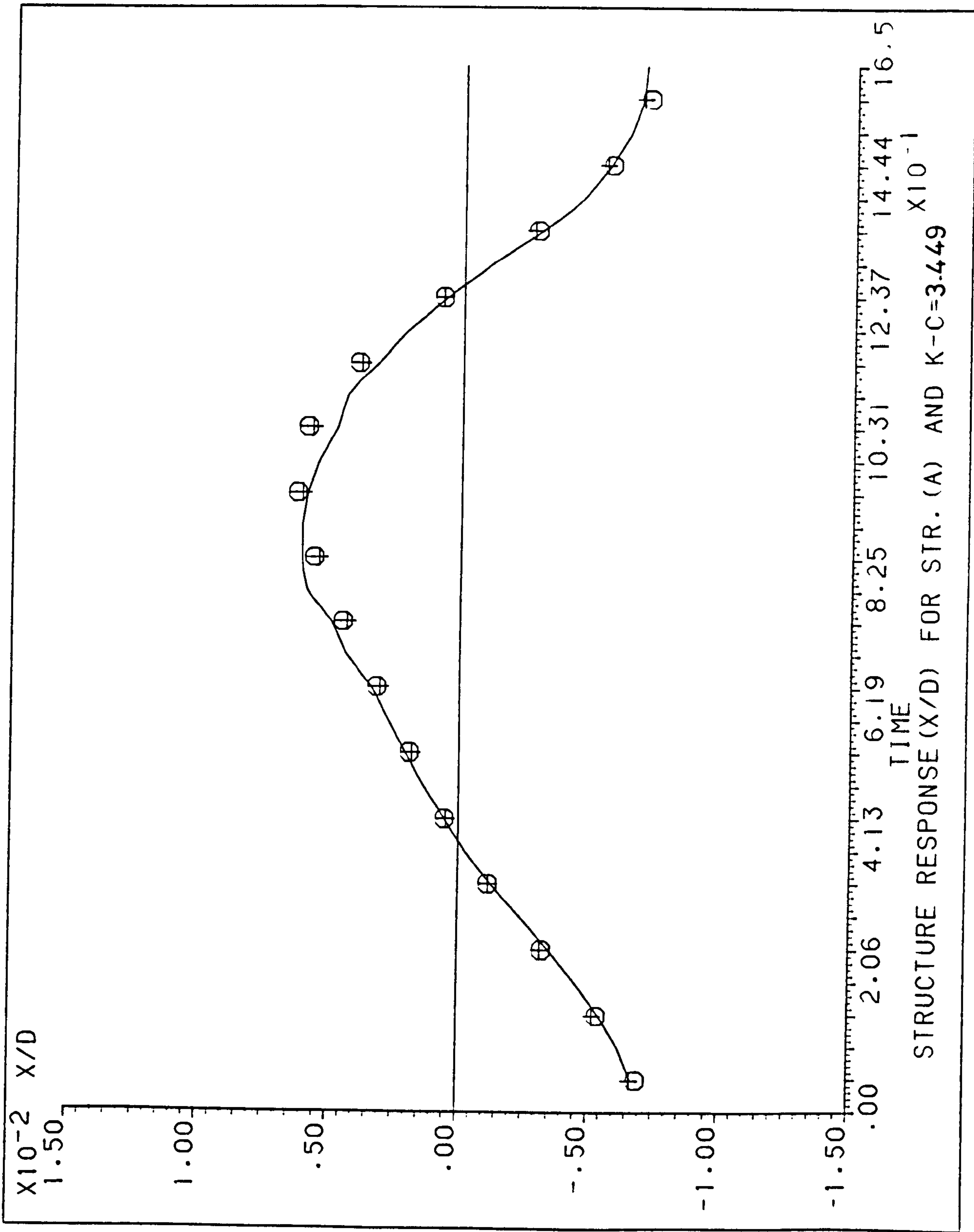


Figure (3D) - Structure's Response (X/D) during the Wave Cycle for Structure A ( $K-C = 3.449$ ).



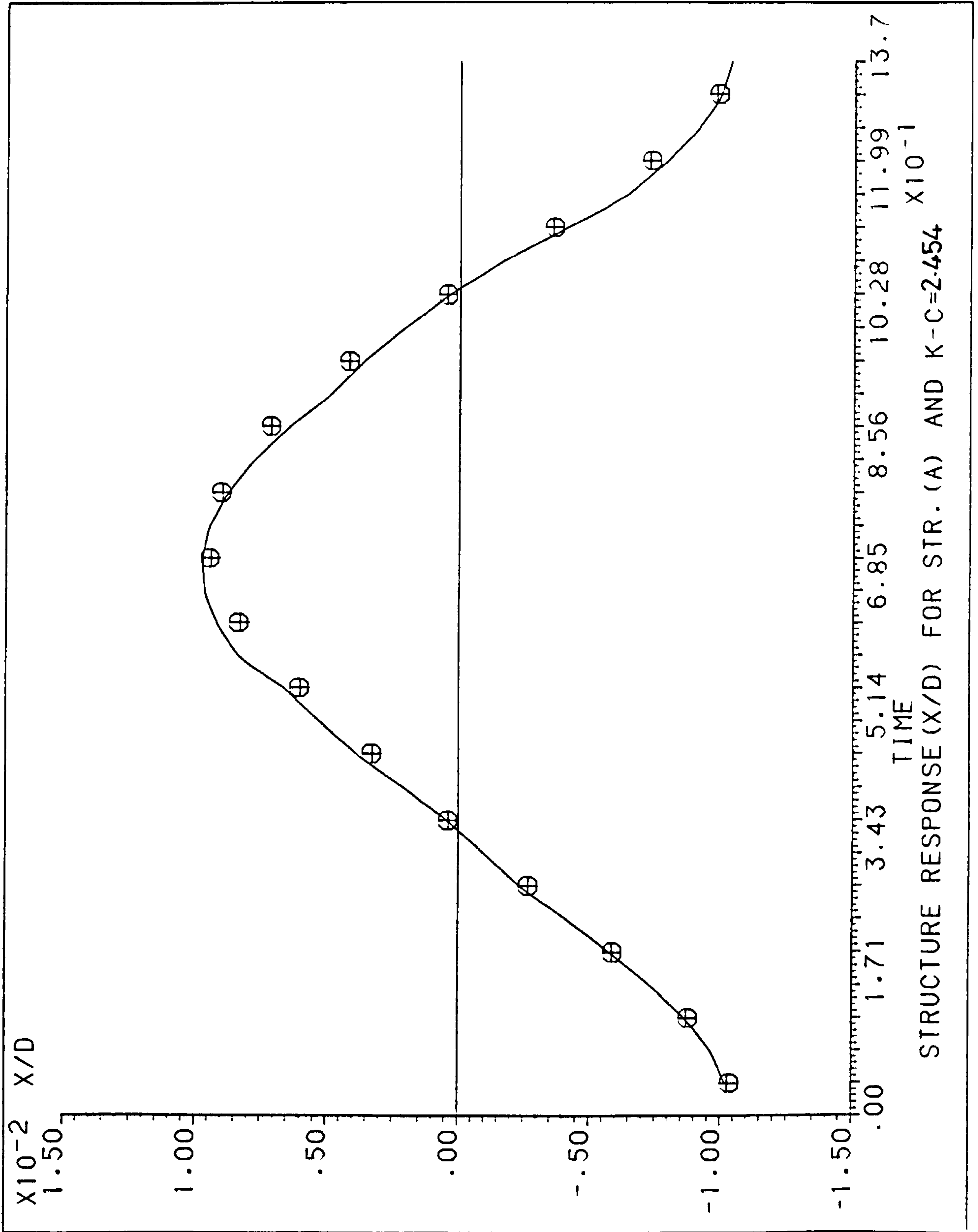


Figure (4D) - Structure's Response (X/D) during the Wave Cycle for Structure A (K-C = 2.454).

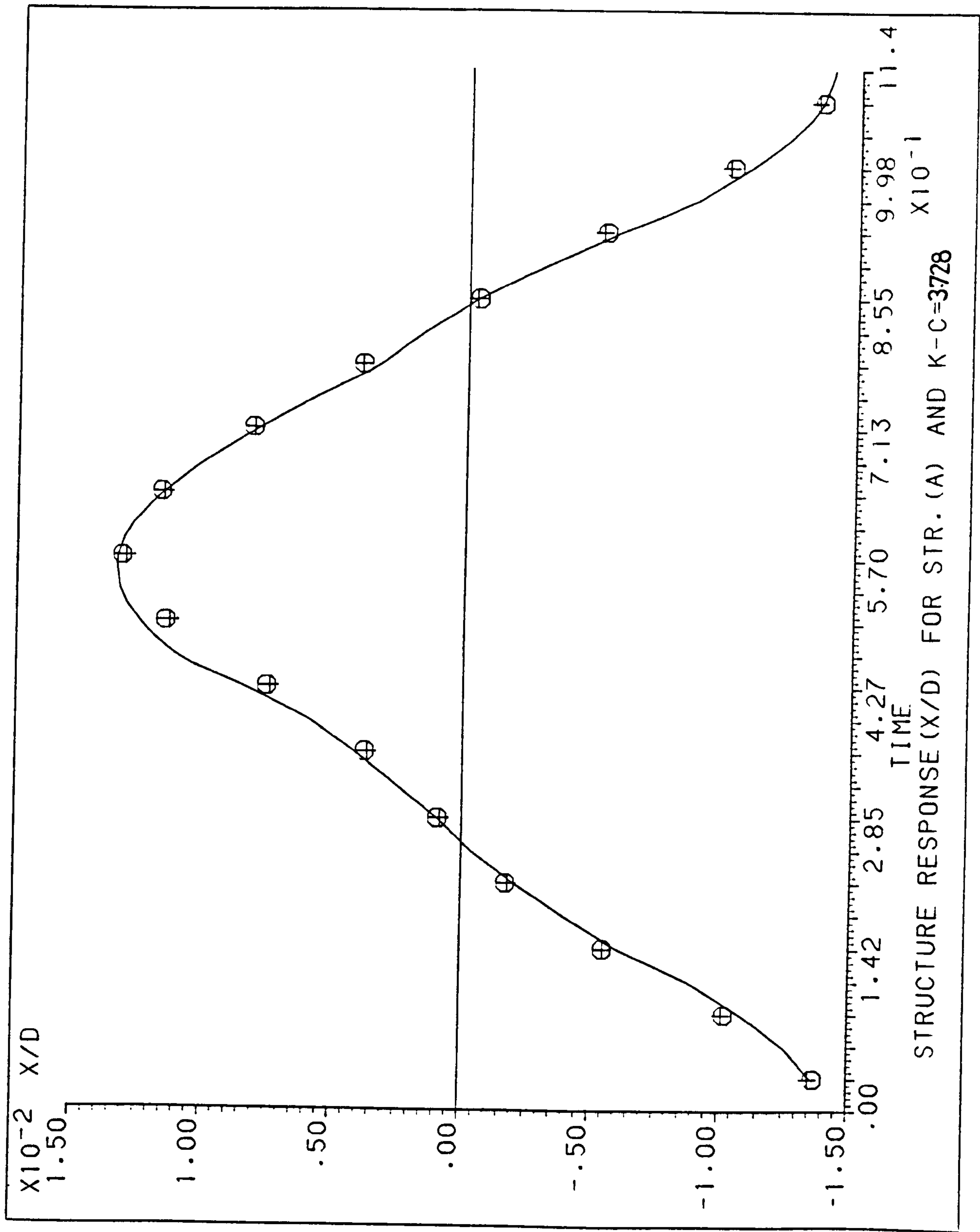


Figure (5D) - Structure's Response (X/D) during the Wave Cycle for Structure A (K-C = 3.728).



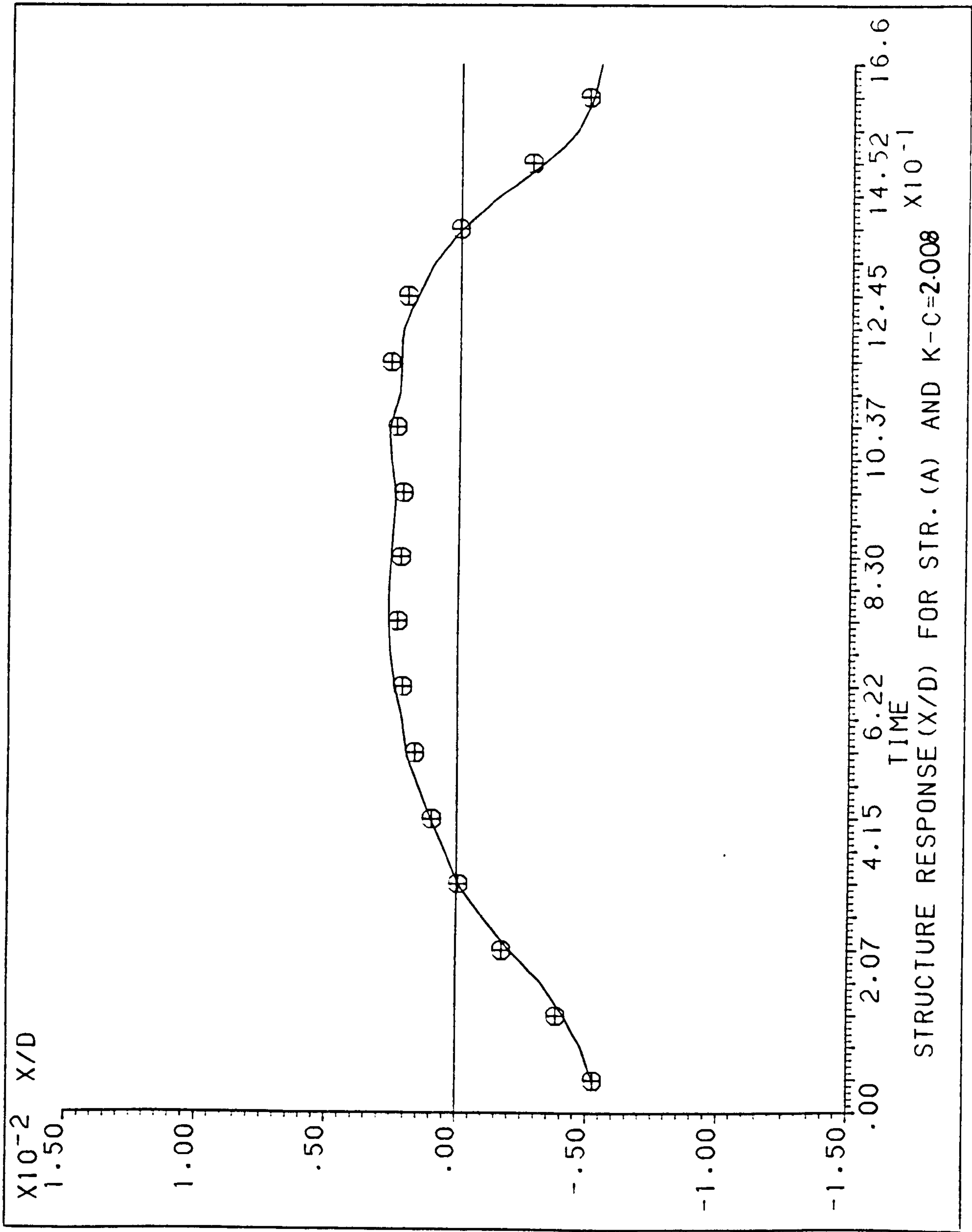


Figure (6D) - Structure's Response (X/D) during the Wave Cycle for Structure A (K-C = 2.008).

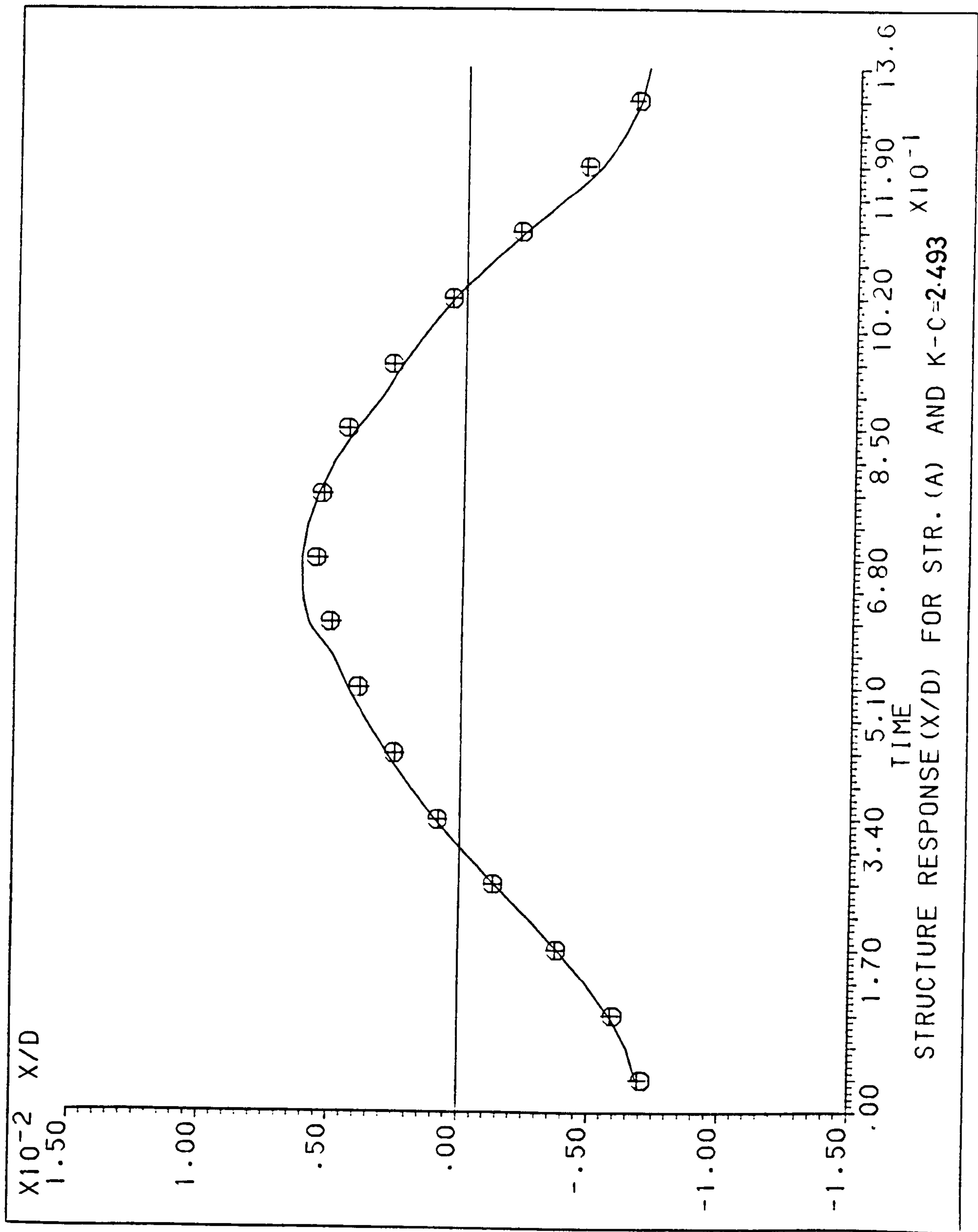


Figure (7D) - Structure's Response (X/D) during the Wave Cycle for Structure A ( $K-C = 2.493$ ).



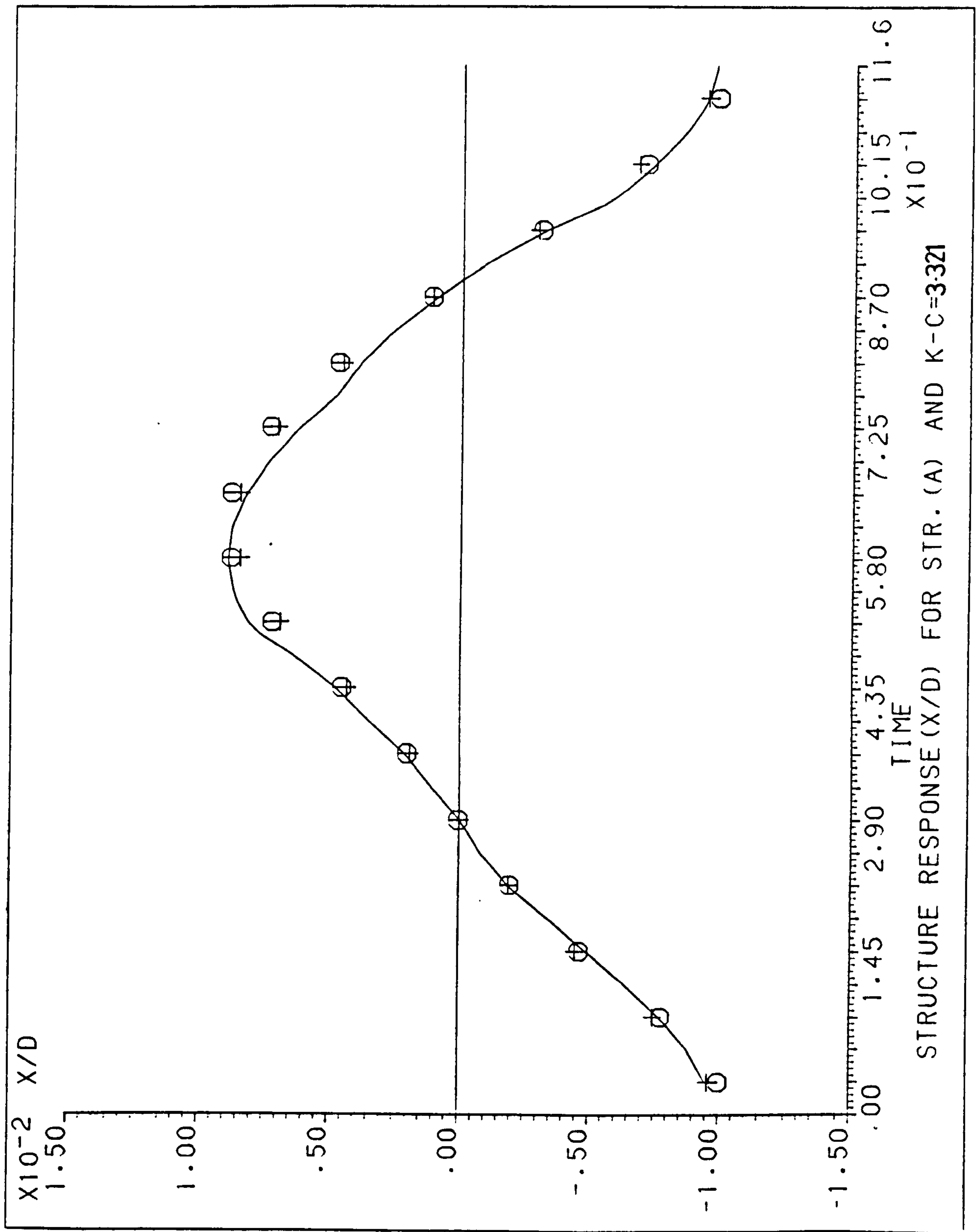


Figure (8D) - Structure's Response (X/D) during the Wave Cycle for Structure A (K-C = 3.321).

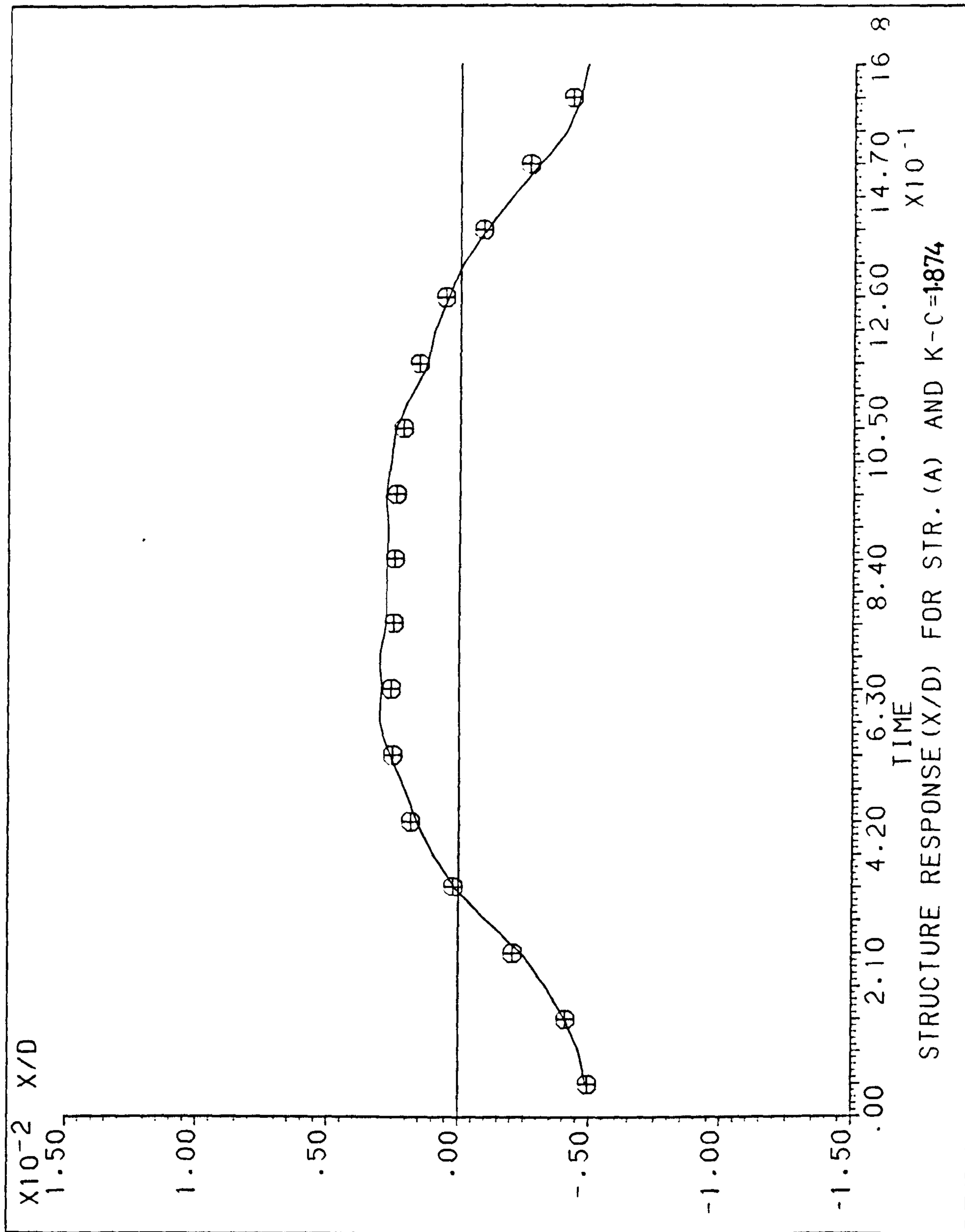


Figure (9D) - Structure's Response (X/D) during the Wave Cycle for Structure A (K-C = 1.874).



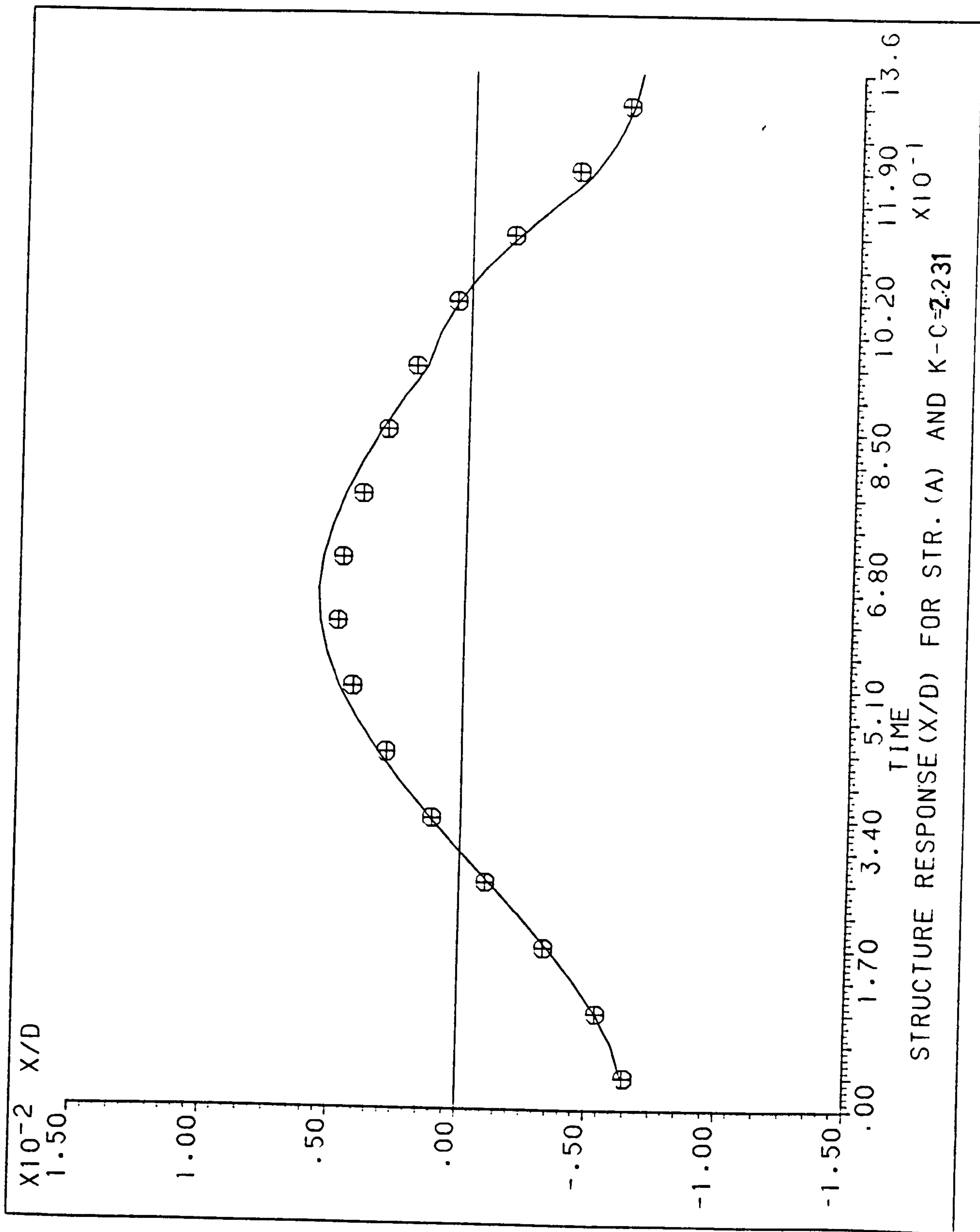


Figure (10D) - Structure's Response (X/D) during the Wave Cycle for Structure A ( $K-C = 2.231$ ).

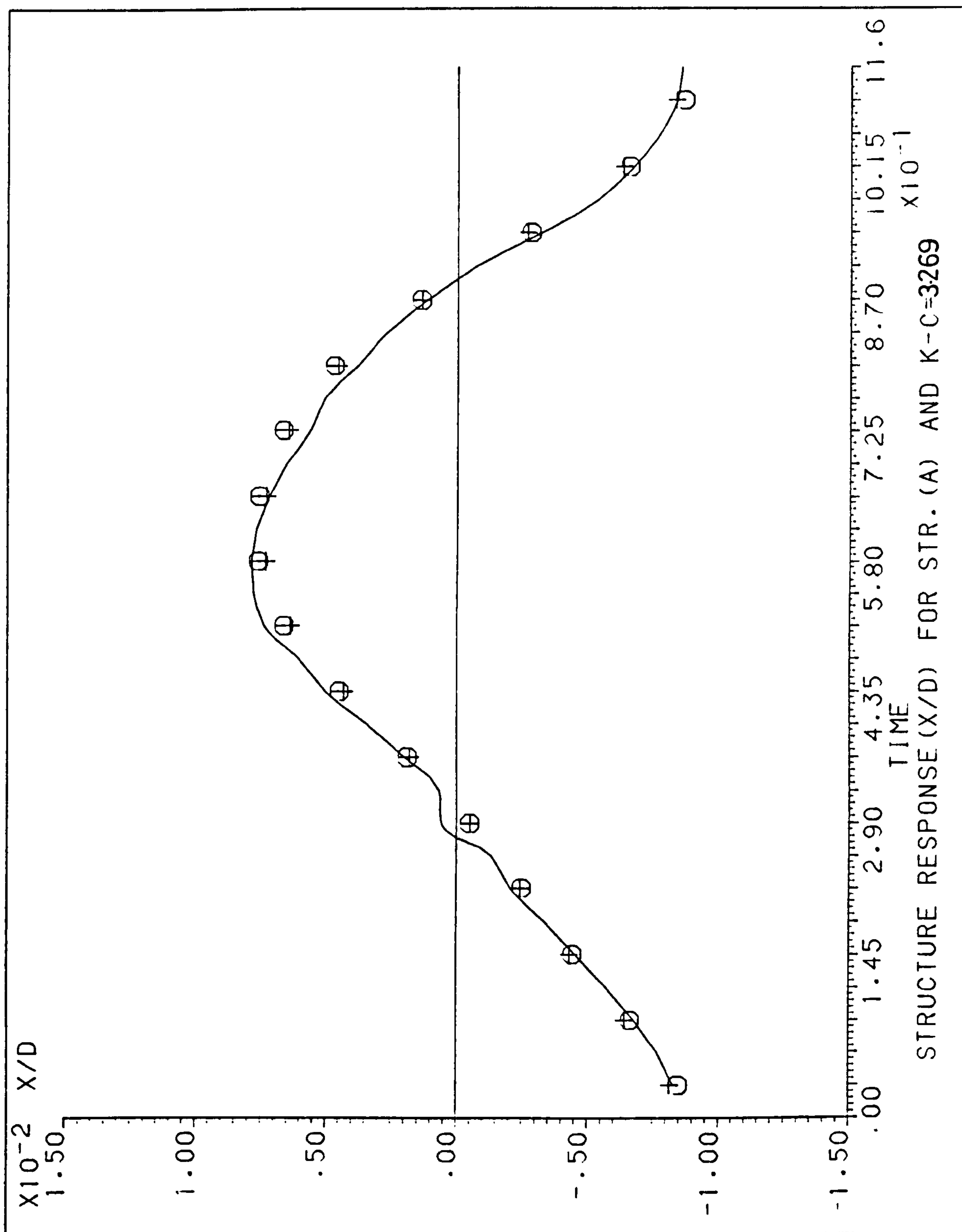


Figure (11D) - Structure's Response (X/D) during the Wave Cycle for Structure A (K-C = 3.269).



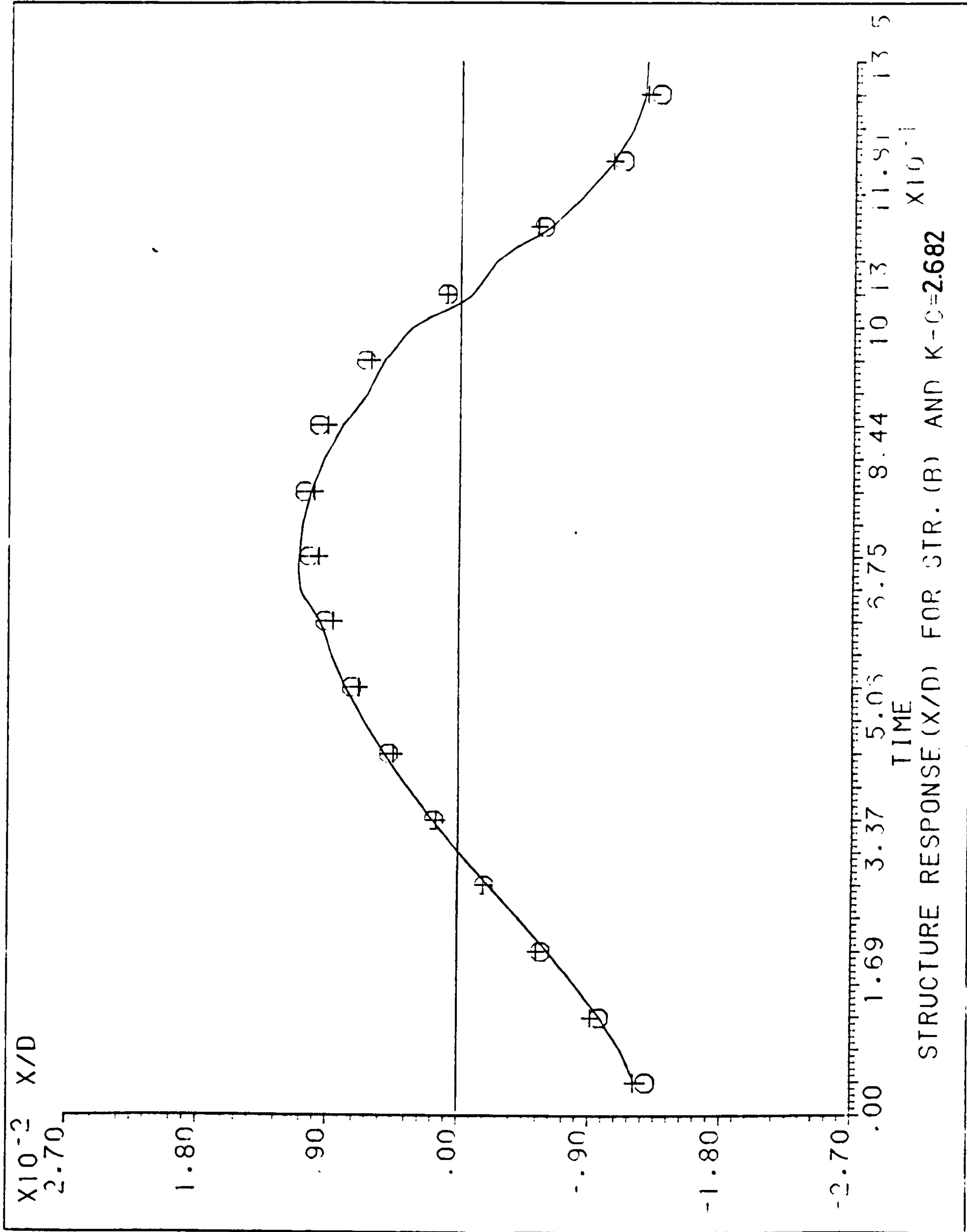


Figure (12D) - Structure's Response (X/D) during the Wave Cycle for Structure B (K-C = 2.682).

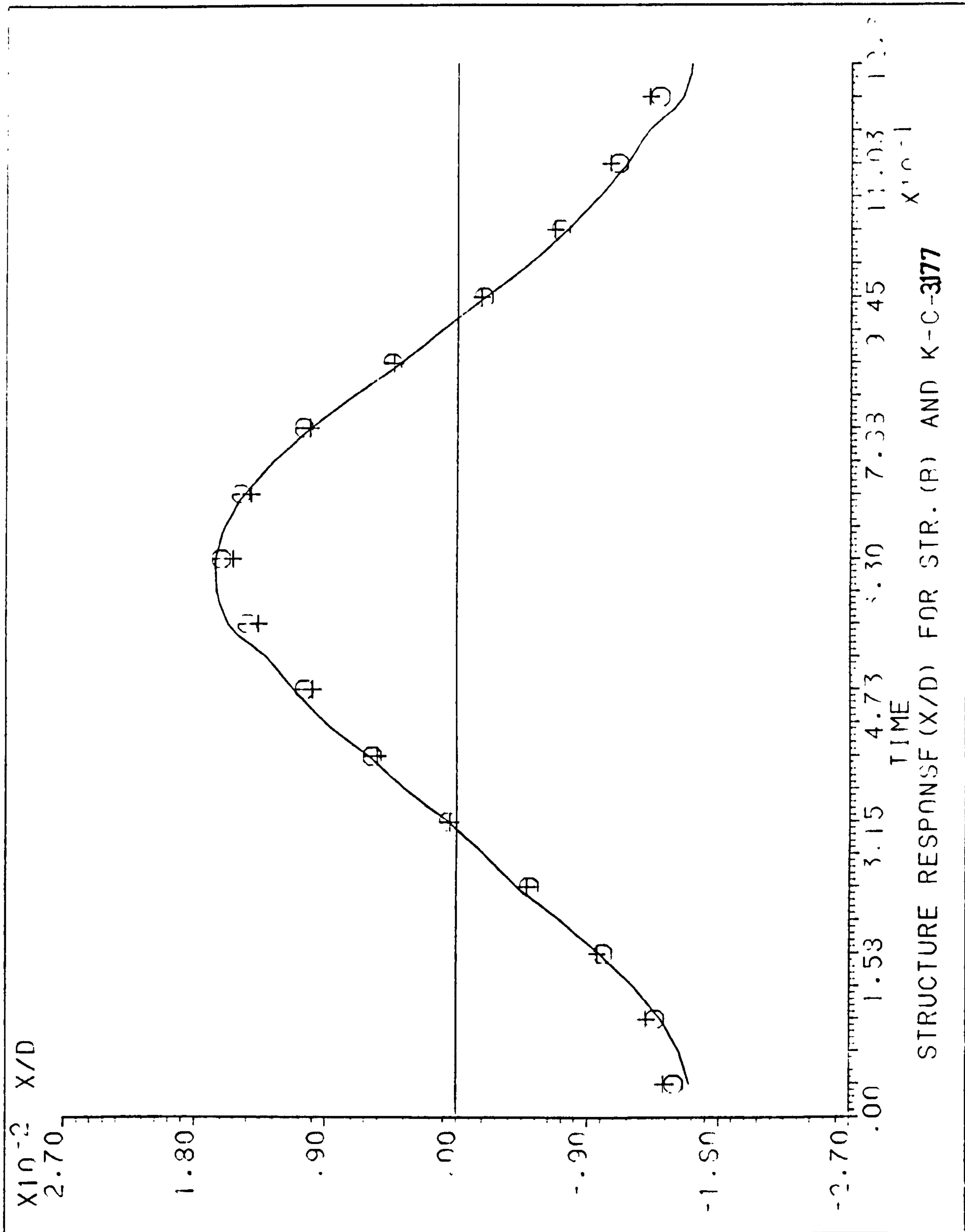


Figure (13D) - Structure's Response (X/D) during the Wave Cycle for Structure B (K-C = 3.177).



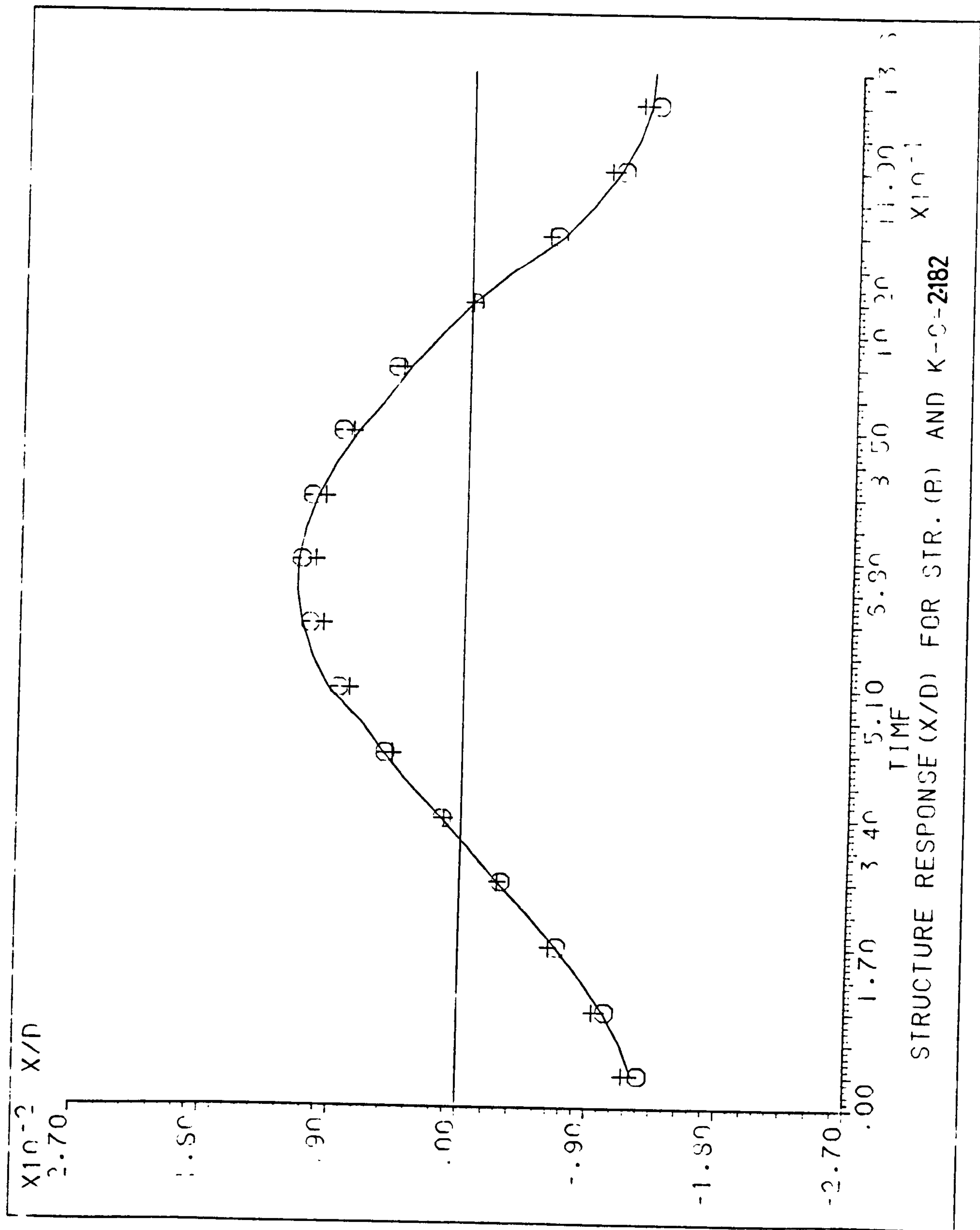


Figure (14D) - Structure's Response (X/D) during the Wave Cycle for Structure B (K-C = 2.182).

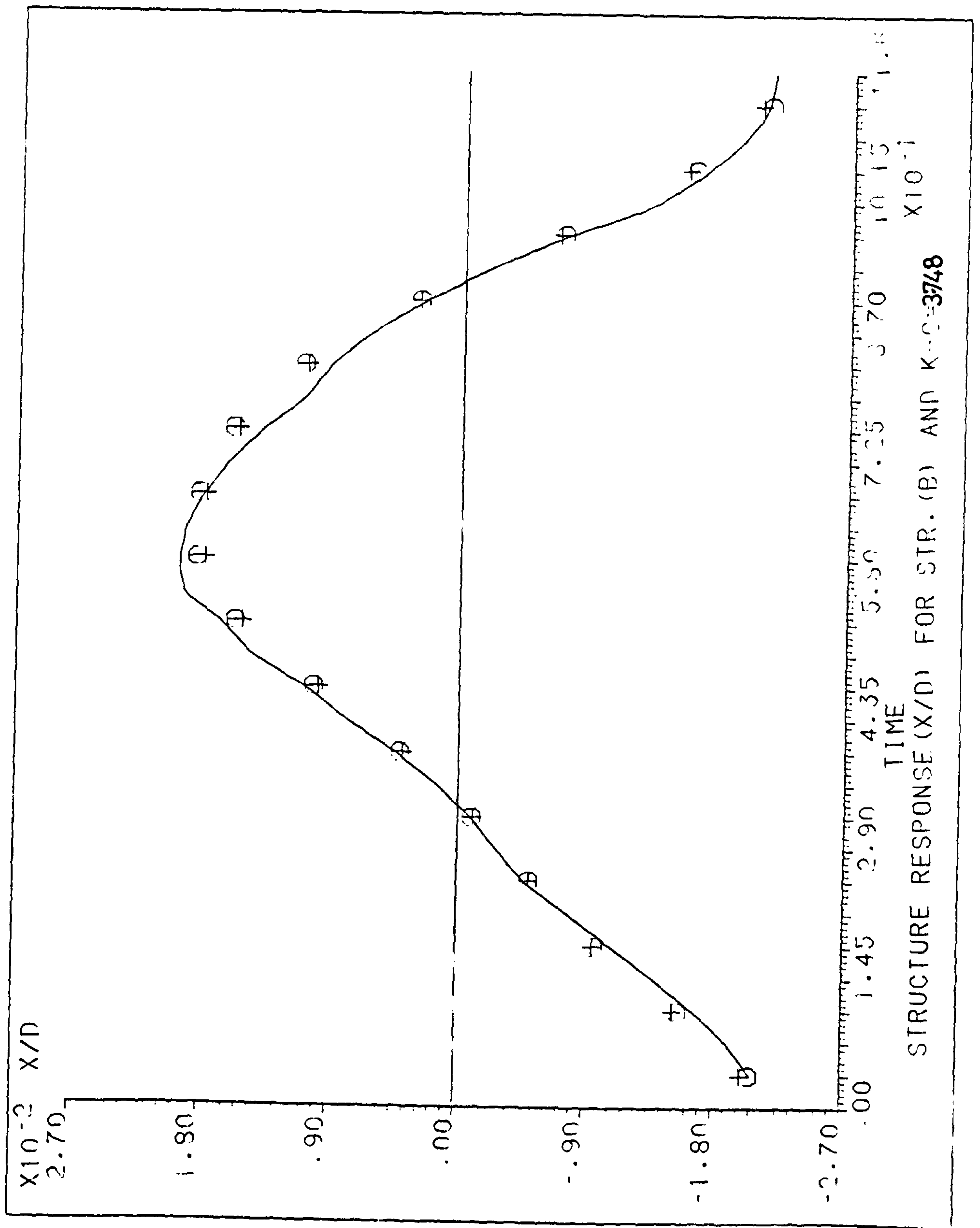


Figure (15D) - Structure's Response (X/D) during the Wave Cycle for Structure B (K-C = 3.748).



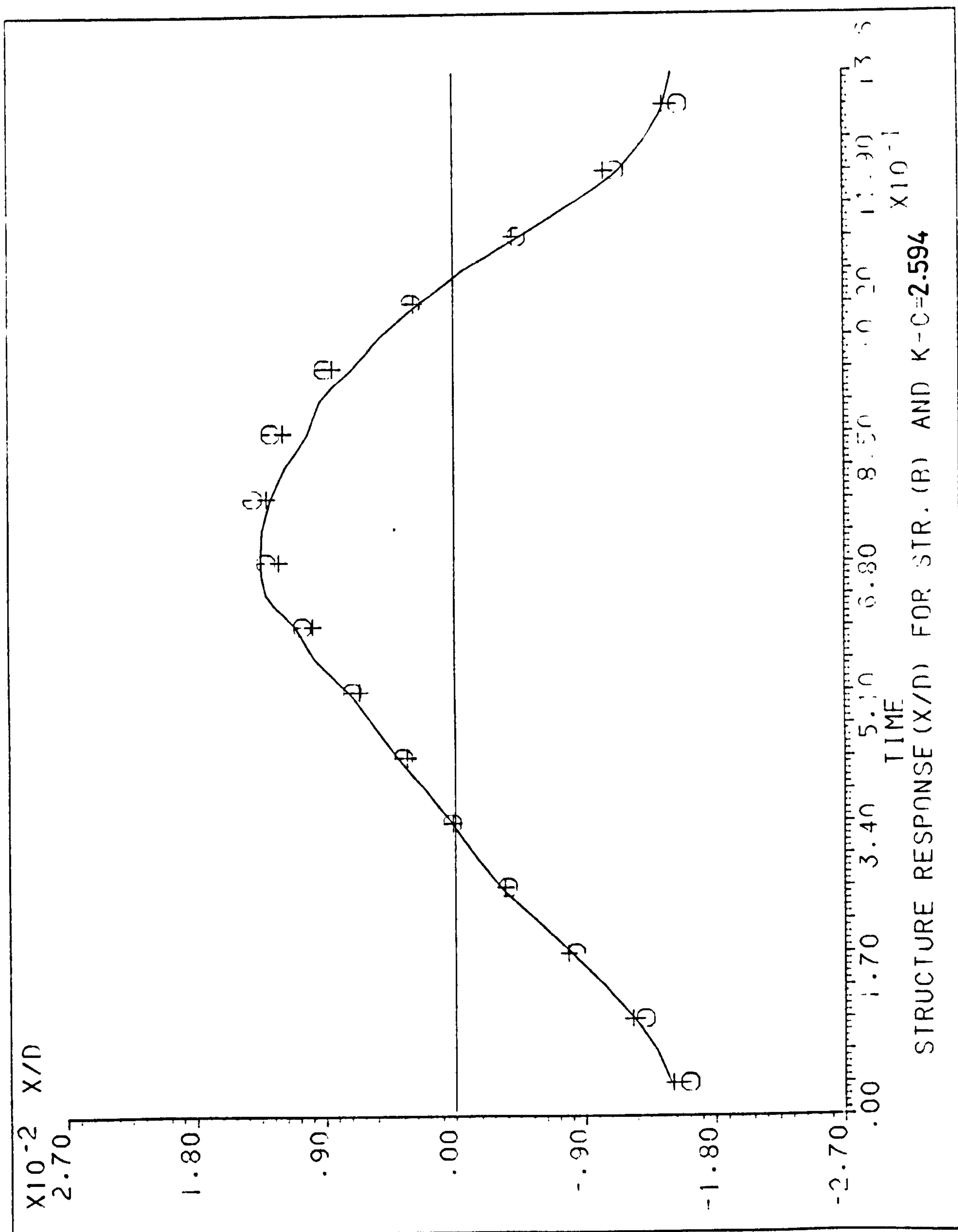


Figure (17D) - Structure's Response (X/D) during the Wave Cycle for Structure B (K-C = 2.594).

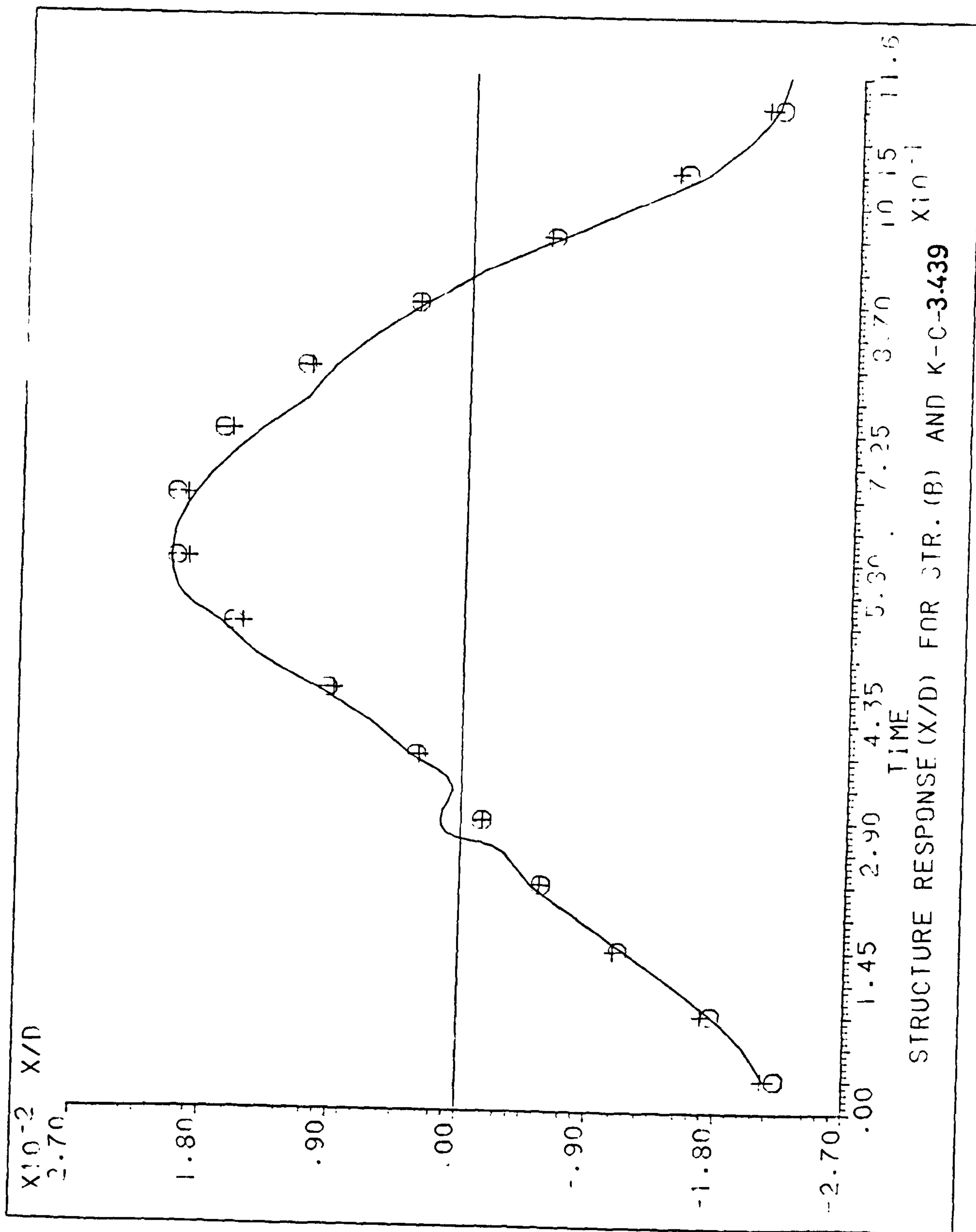


Figure (18D) - Structure's Response (X/D) during the Wave Cycle for Structure B (K-C = 3.439).



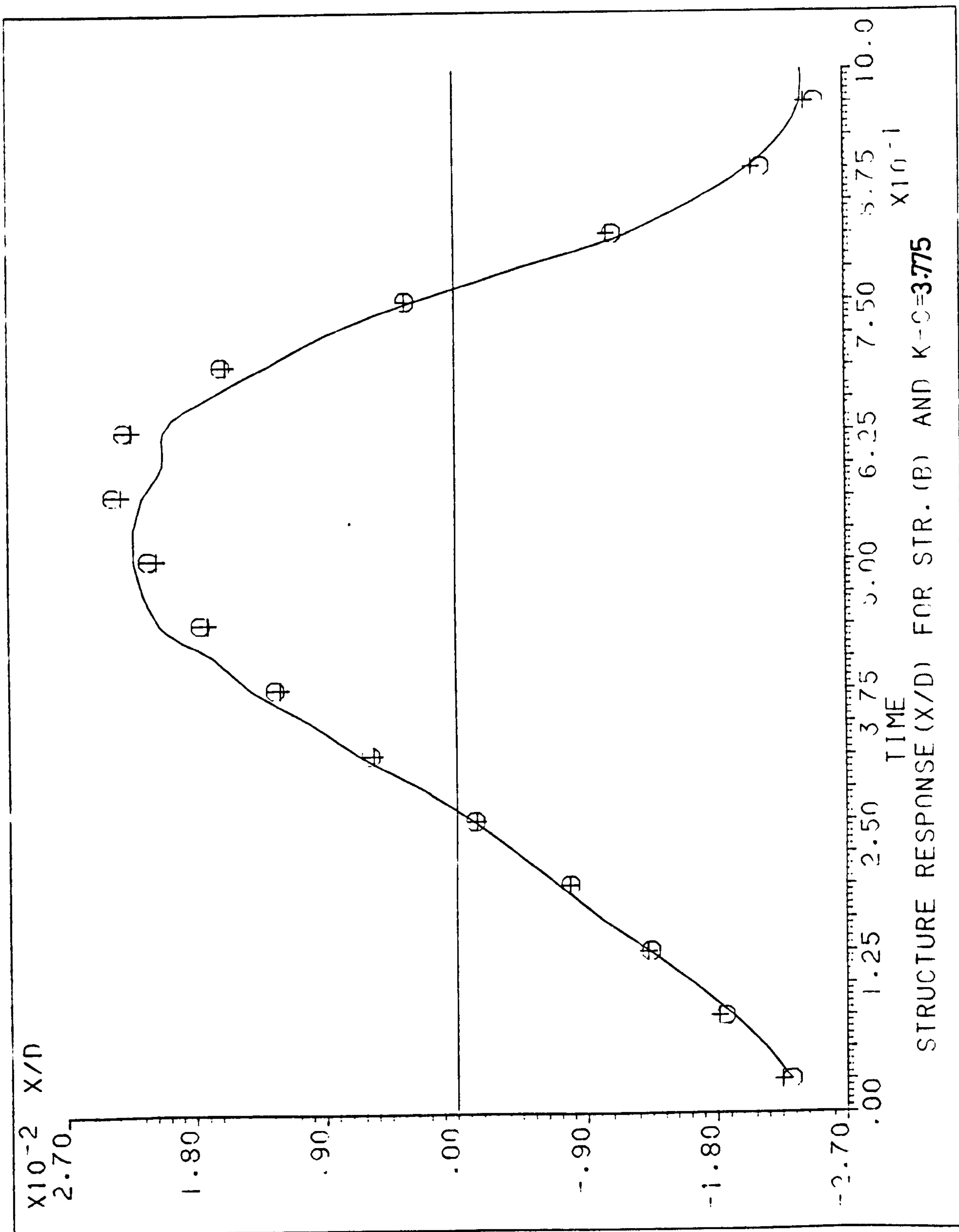


Figure (19D) - Structure's Response (X/D) during the Wave Cycle for Structure B (K-C = 3.775).

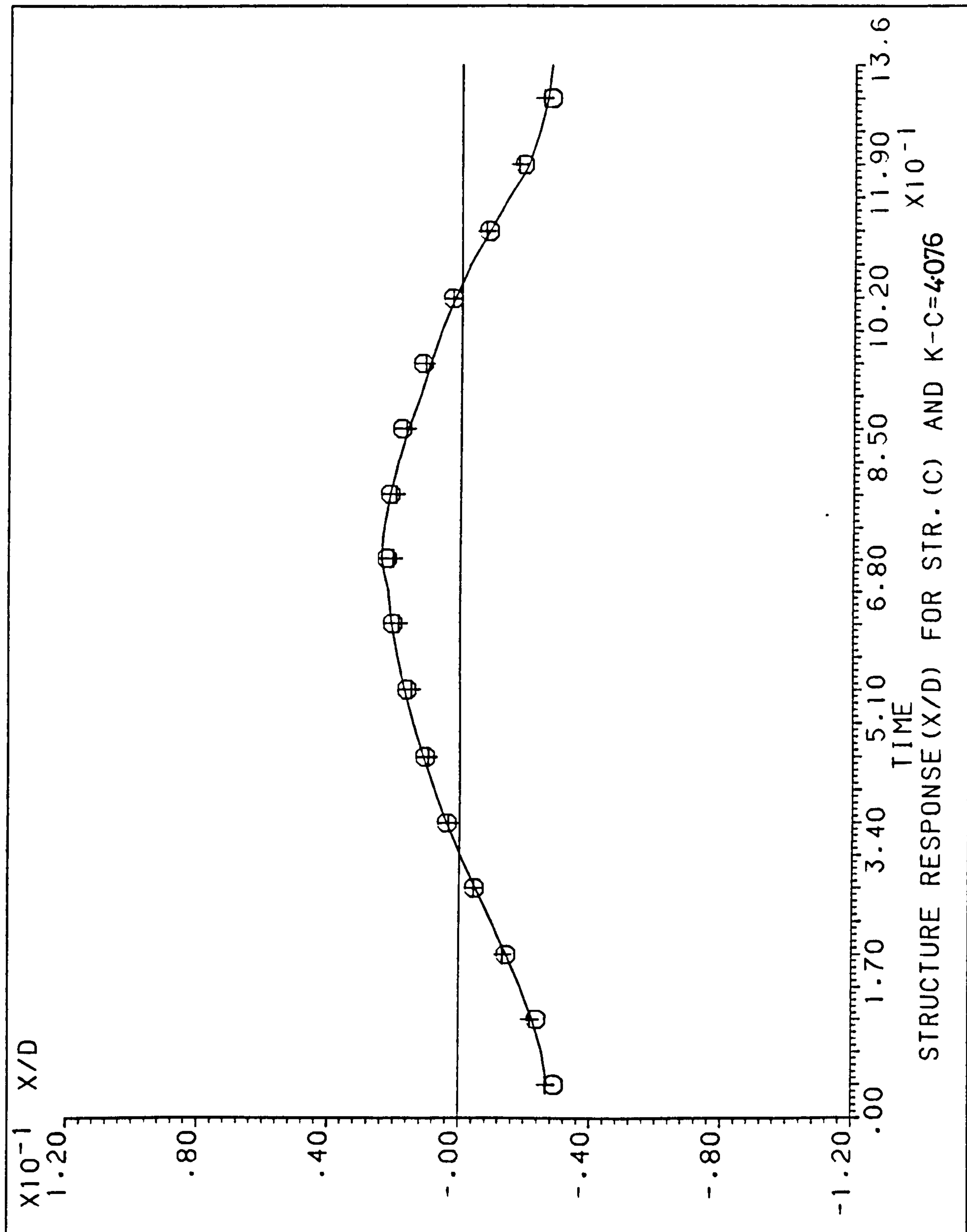


Figure (20D) - Structure's Response (X/D) during the Wave Cycle for Structure C (K-C = 4.076).



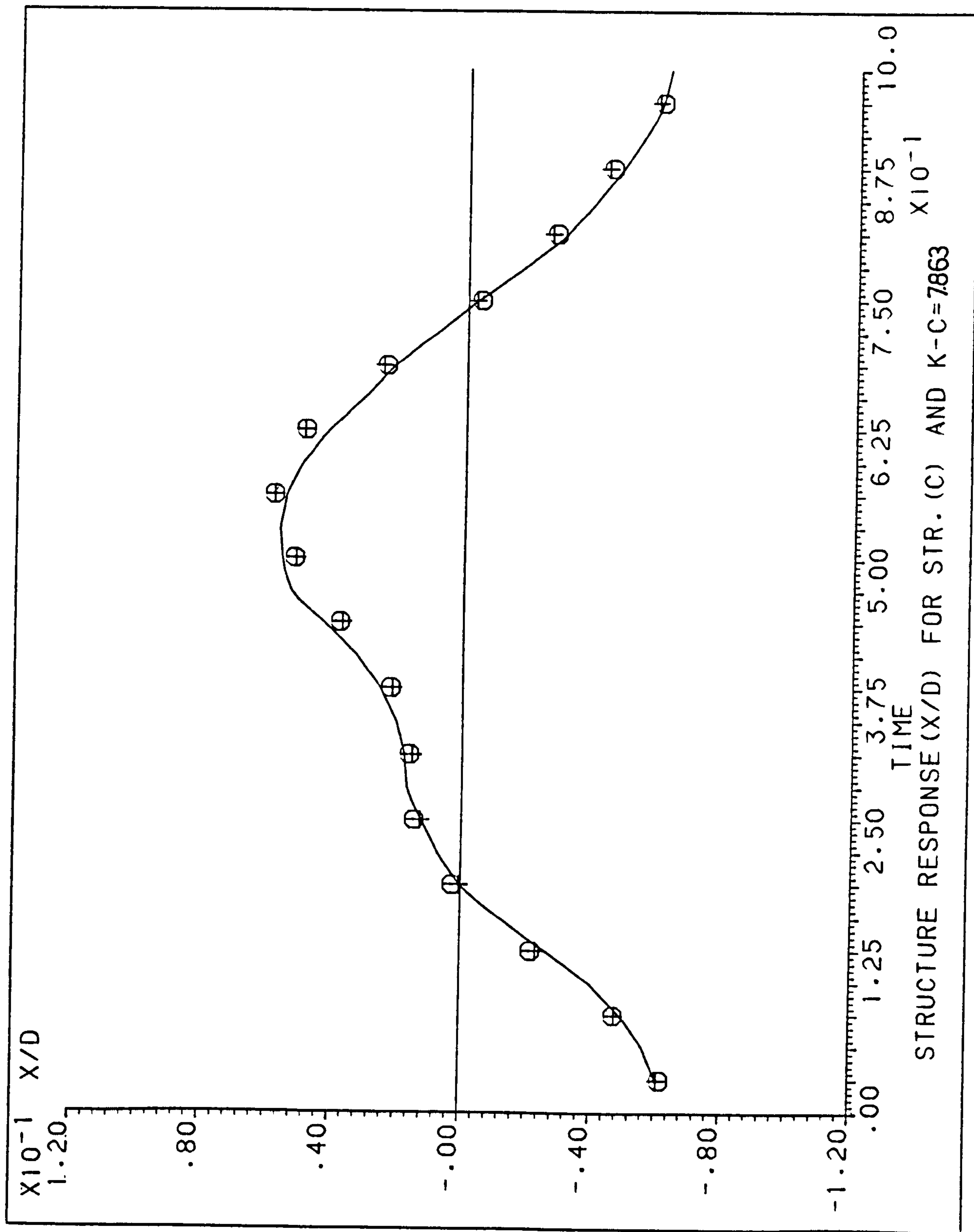


Figure (21D) - Structure's Response (X/D) during the Wave Cycle for Structure C (K-C = 7.863).

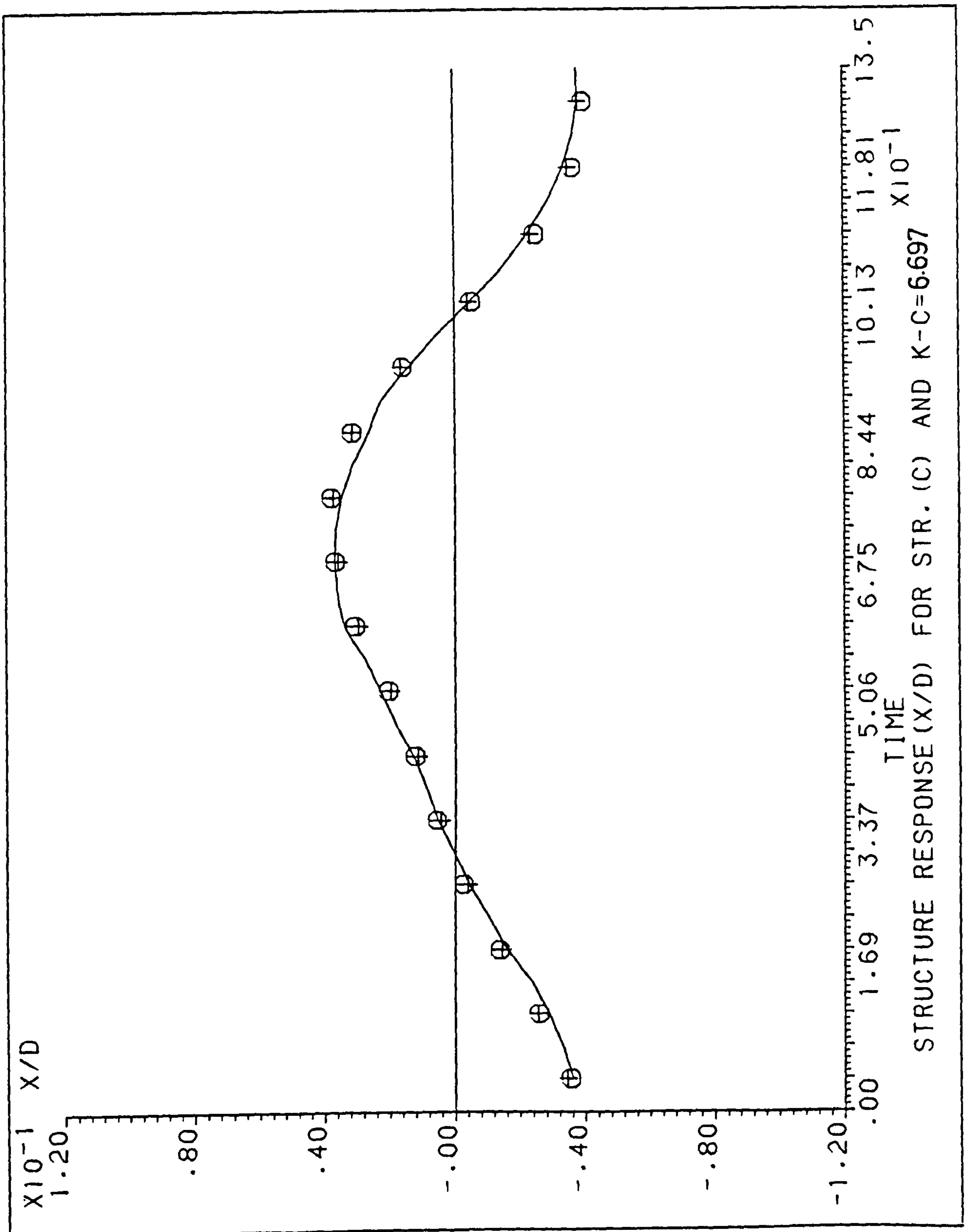


Figure (22D) - Structure's Response (X/D) during the Wave Cycle for Structure C (K-C = 6.697).



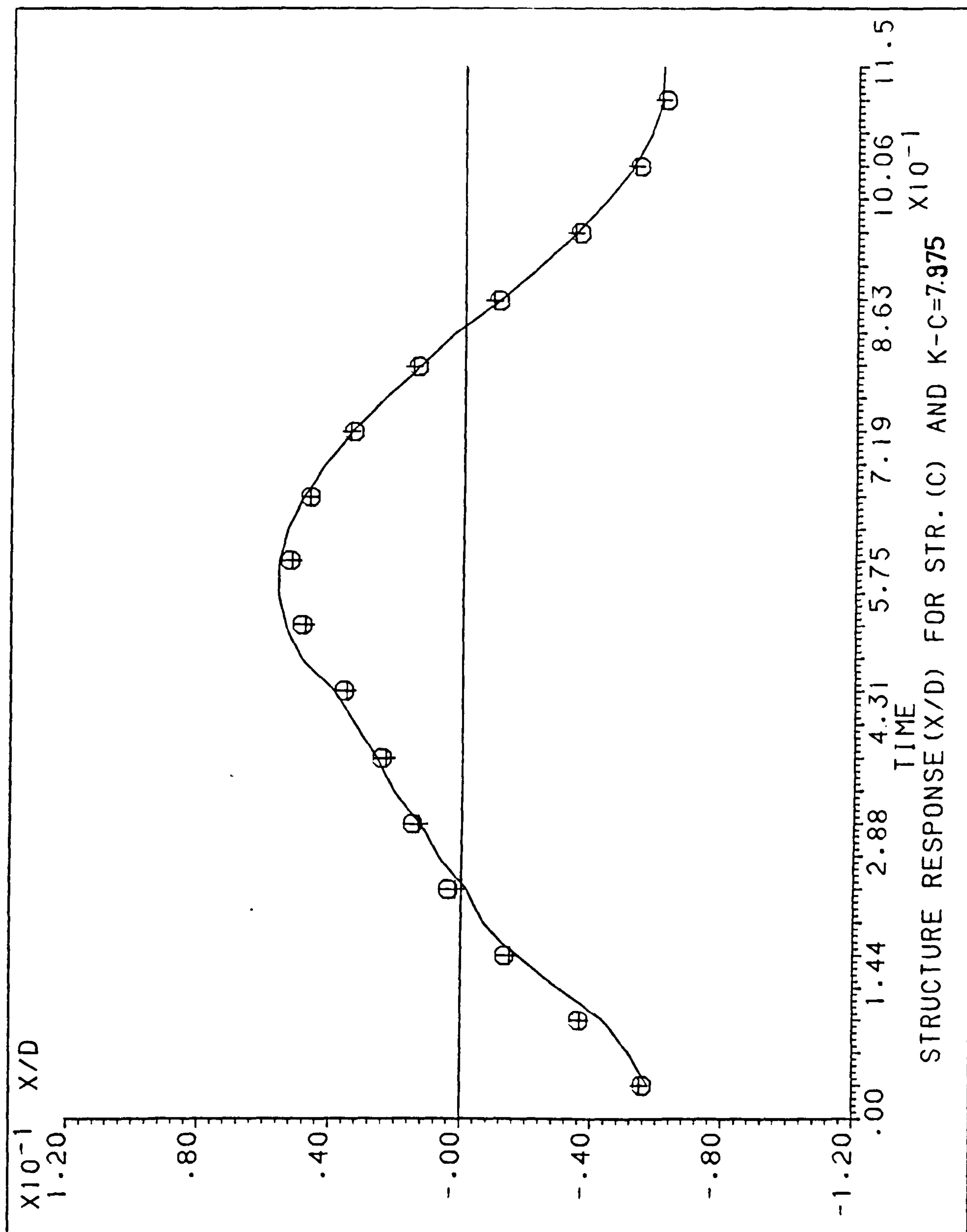


Figure (23D) - Structure's Response (X/D) during the Wave Cycle for Structure C (K-C = 7.975).

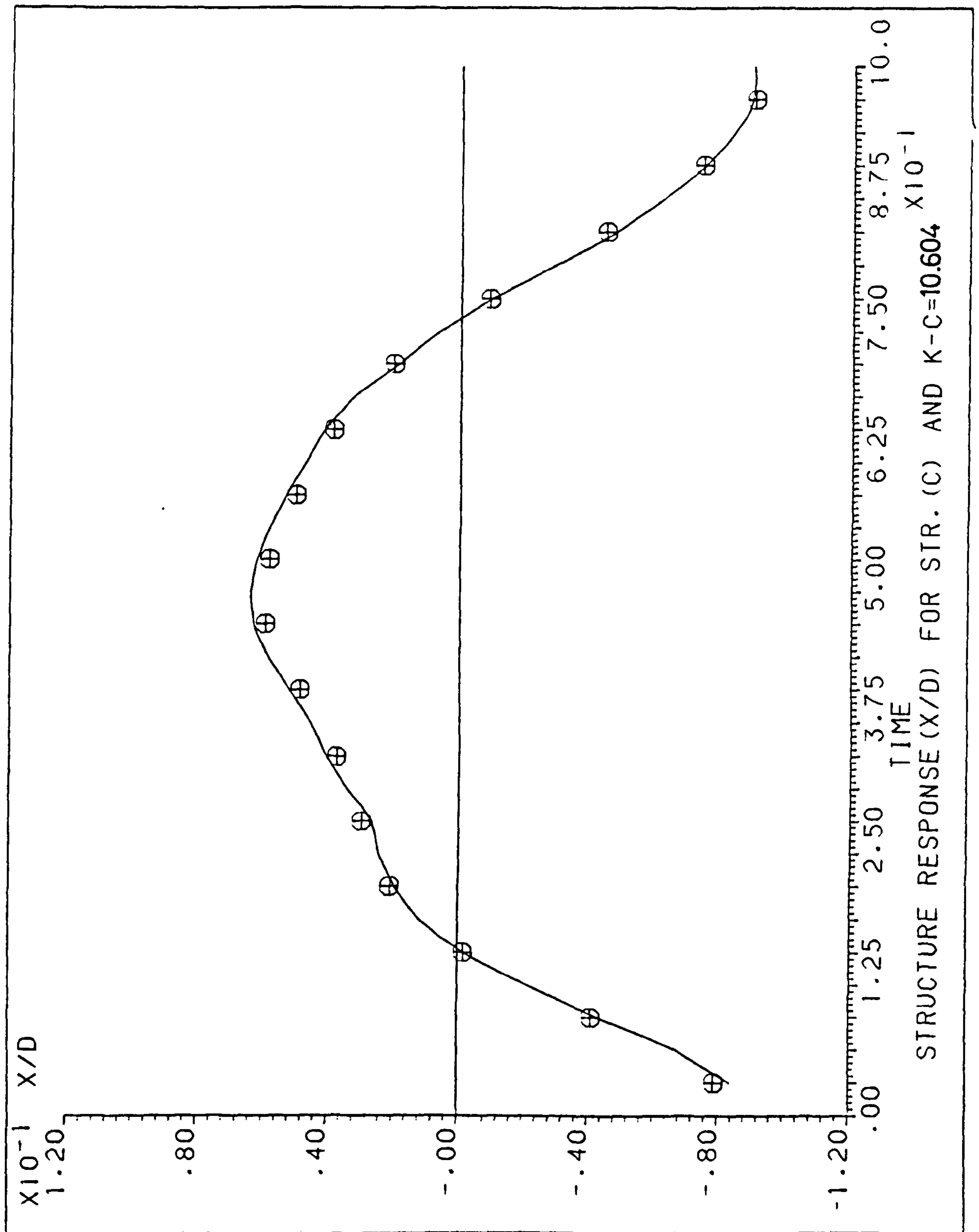


Figure (24D) - Structure's Response (X/D) during the Wave Cycle for Structure C (K-C = 10.604).



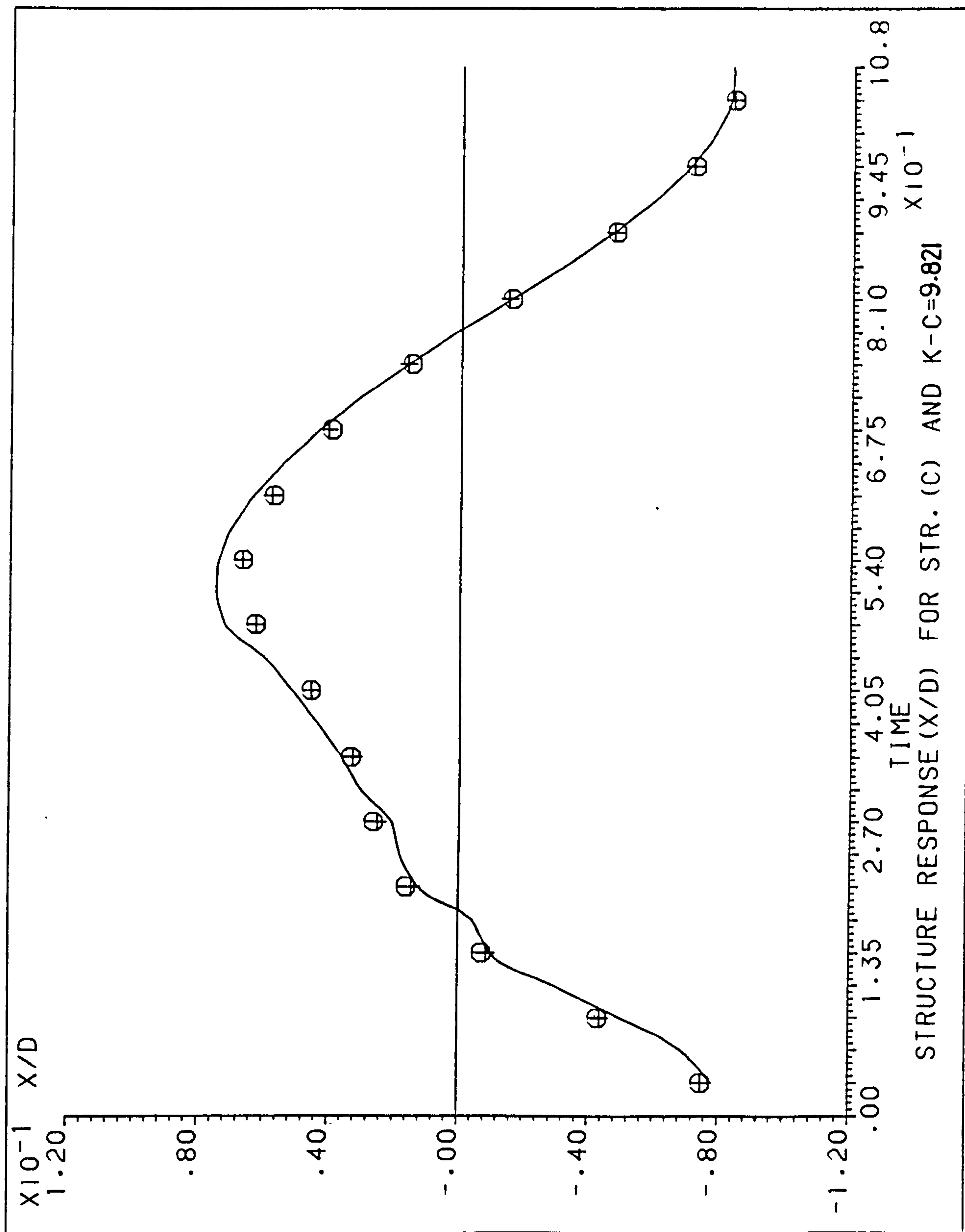


Figure (25D) - Structure's Response (X/D) during the Wave Cycle for Structure C (K-C = 9.821).

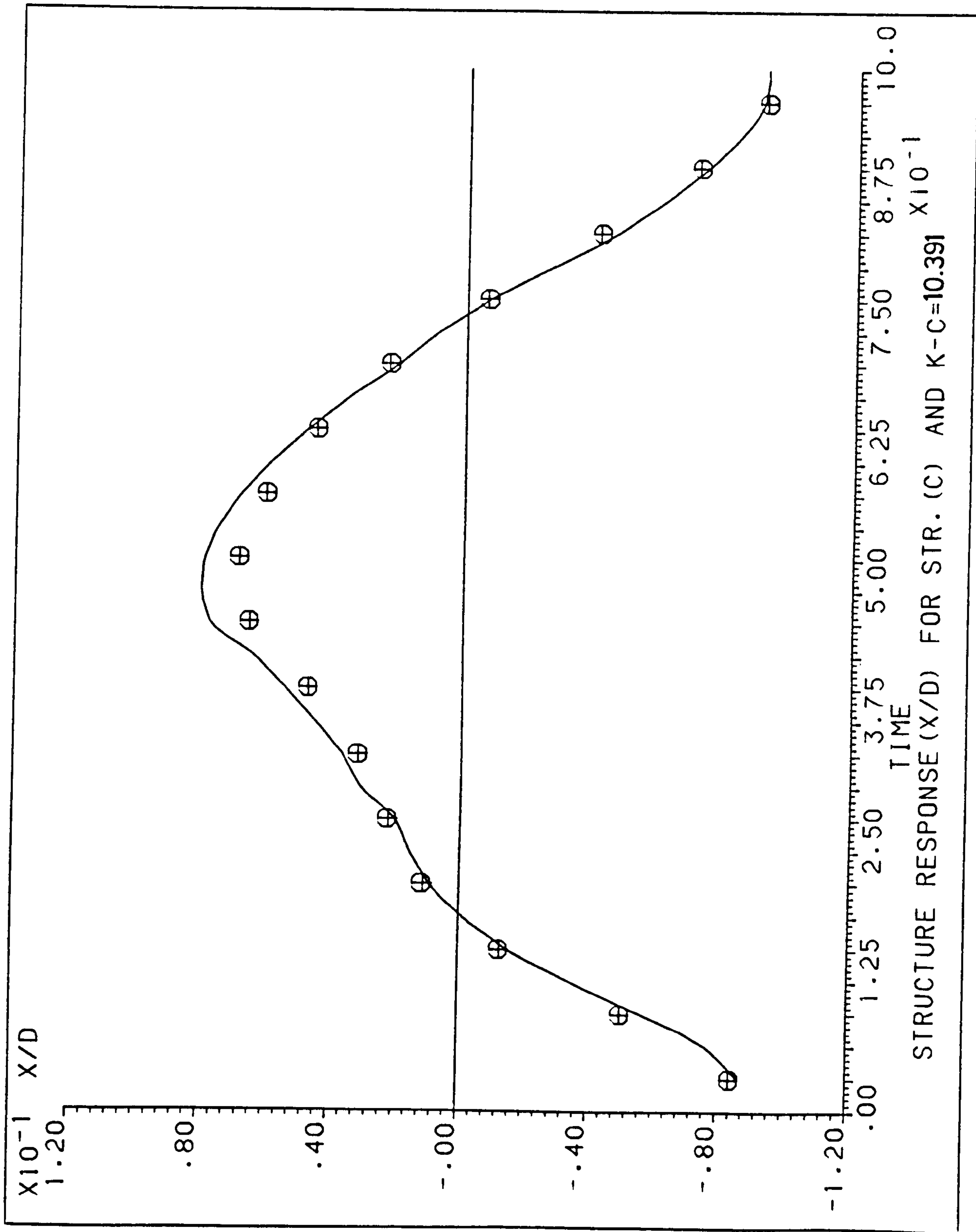


Figure (26D) - Structure's Response (X/D) during the Wave Cycle for Structure C ( $K-C = 10.391$ ).



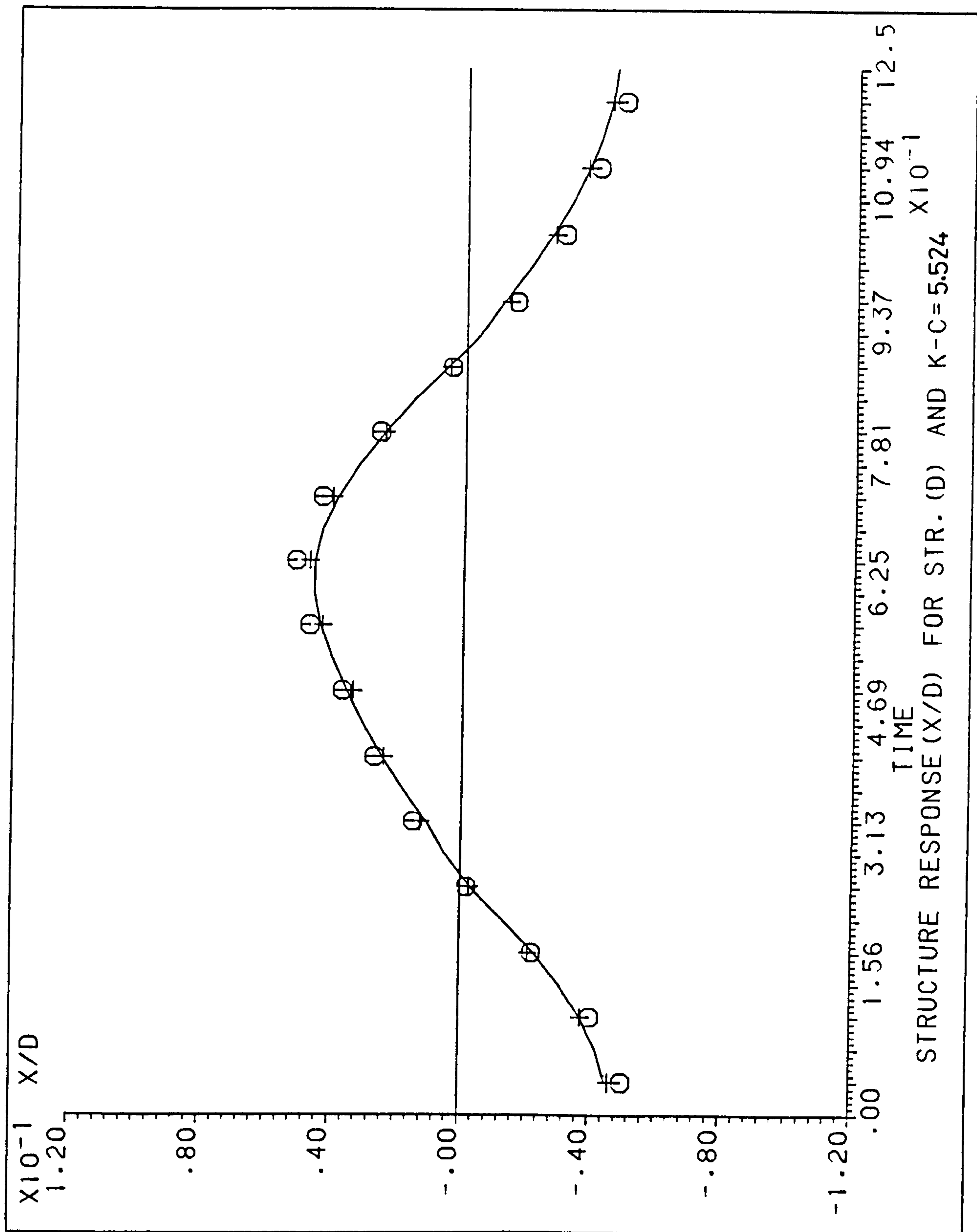


Figure (27D) - Structure's Response (X/D) during the Wave Cycle for Structure D (K-C = 5.524).

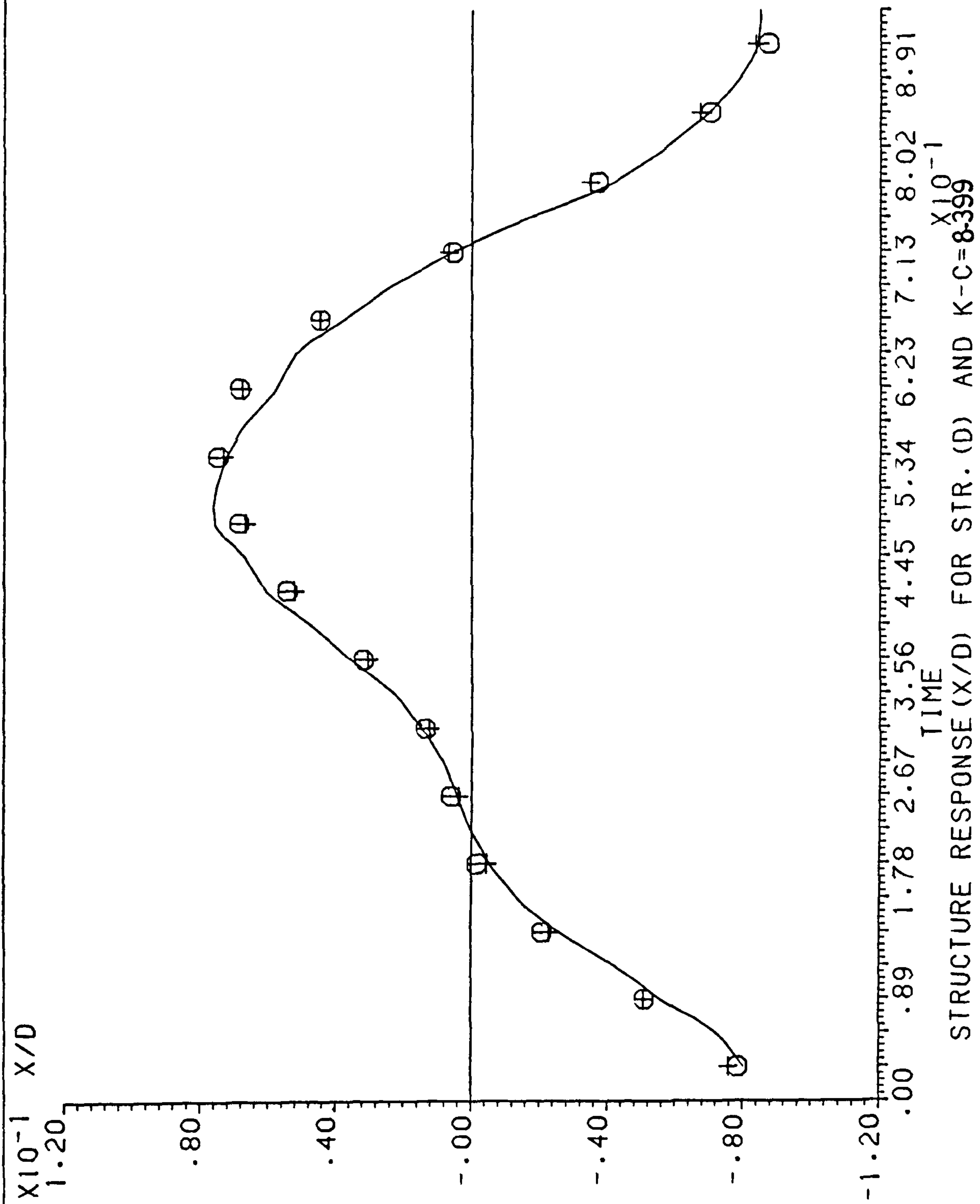


Figure (28D) - Structure's Response (X/D) during the Wave Cycle for Structure D ( $K-C = 8.399$ ).



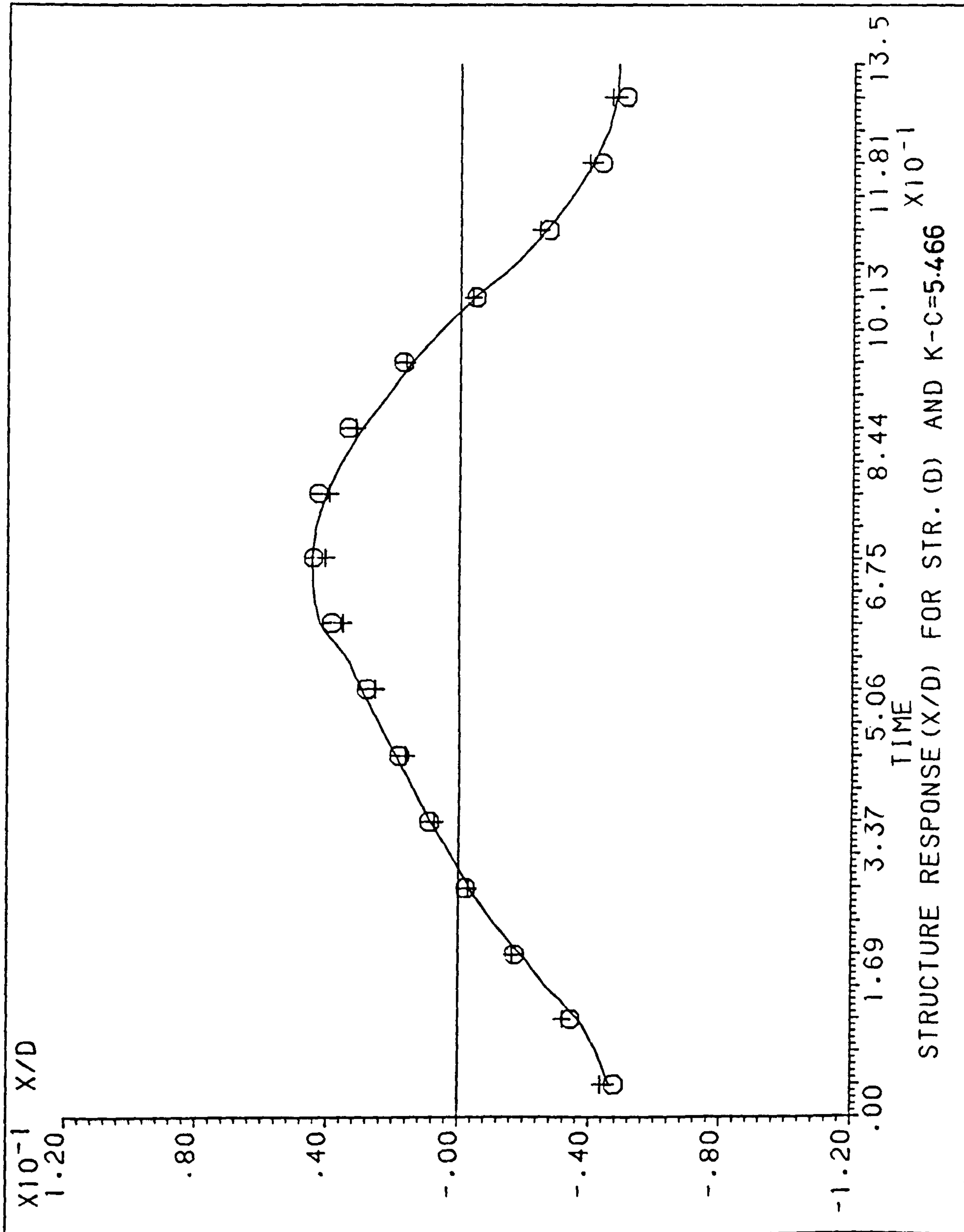


Figure (29D) - Structure's Response (X/D) during the Wave Cycle for Structure D (K-C = 5.466).

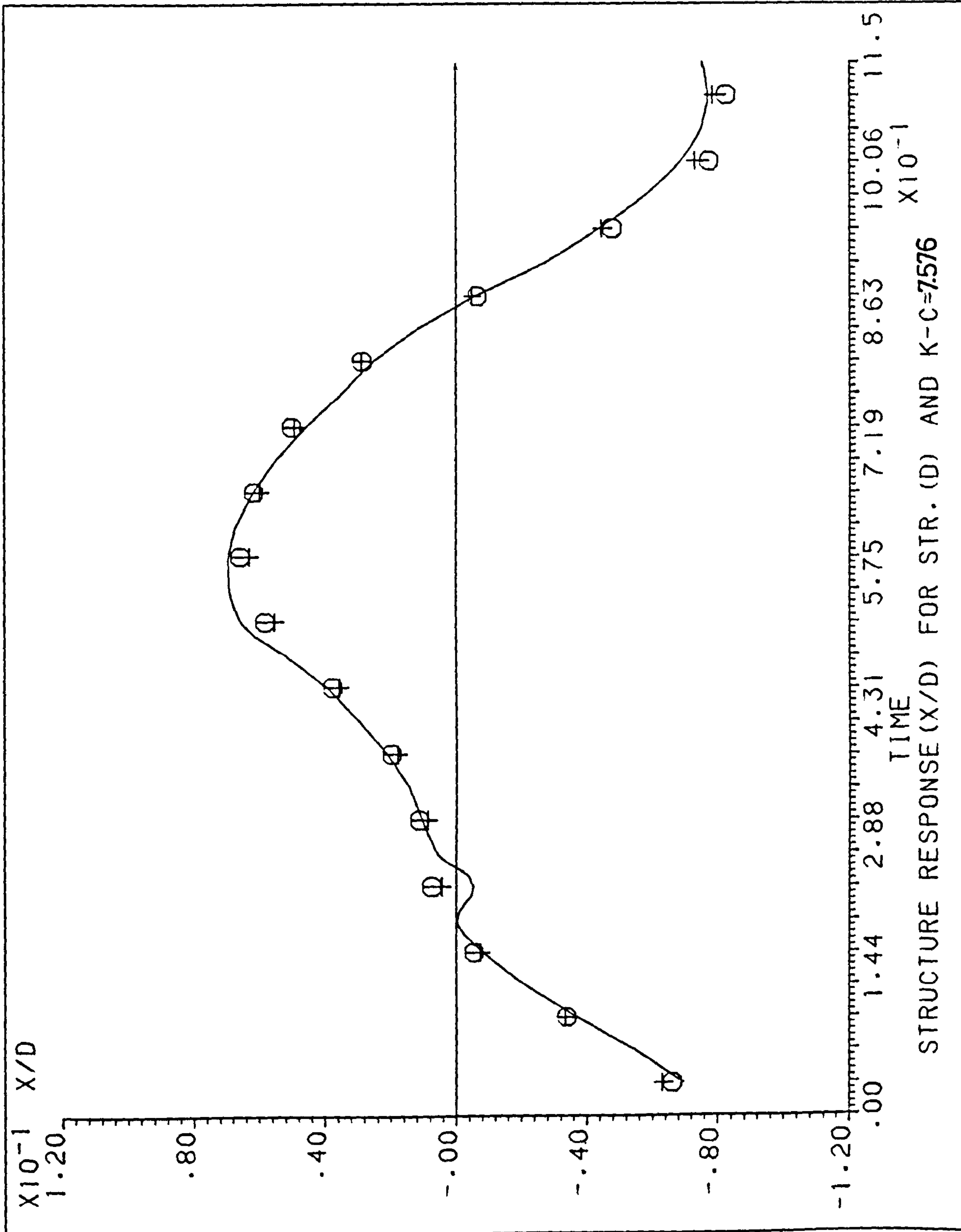


Figure (30D) - Structure's Response (X/D) during the Wave Cycle for Structure D (K-C = 7.576).



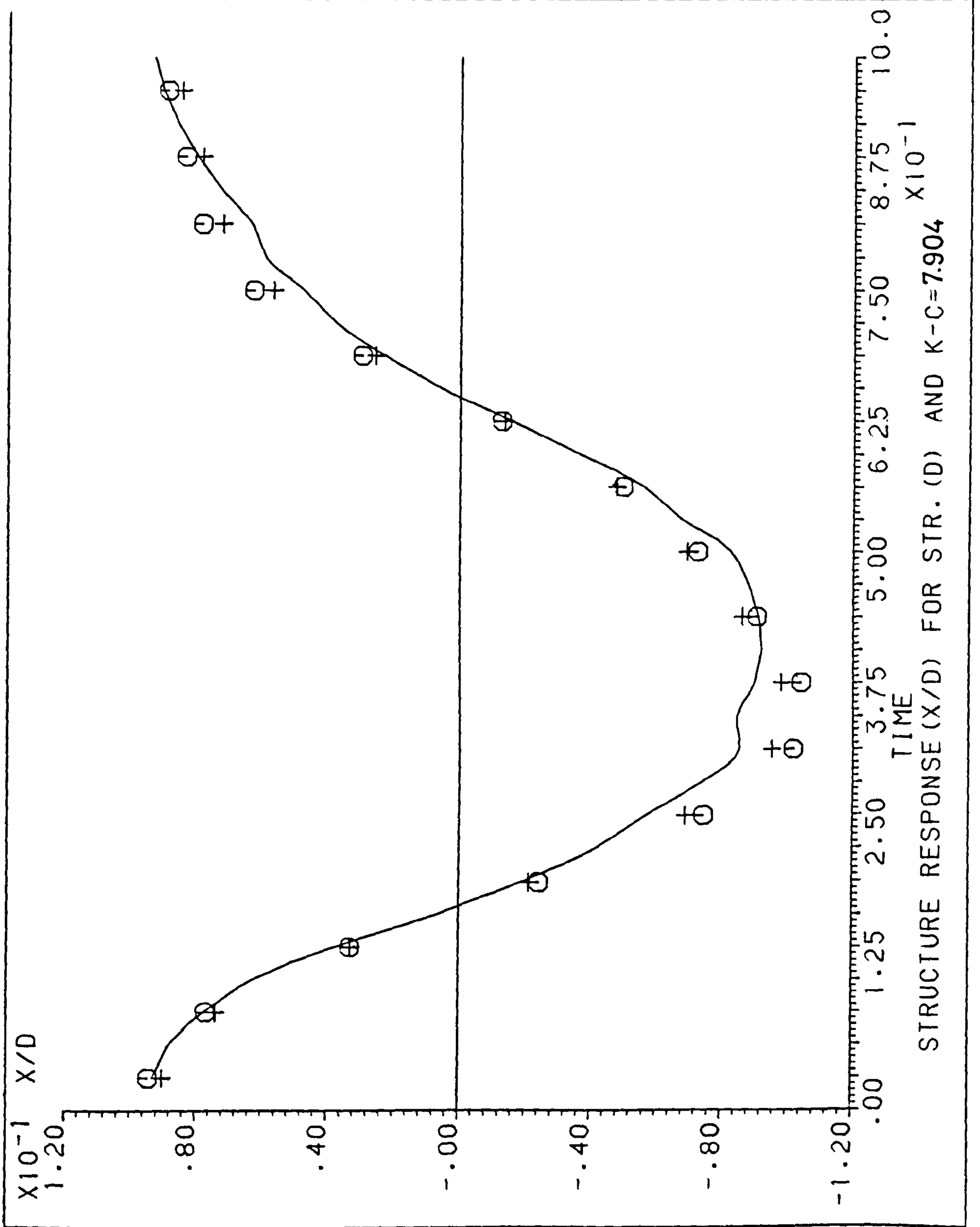


Figure (31D) - Structure's Response (X/D) during the Wave Cycle for Structure D ( $K-C = 7.904$ ).

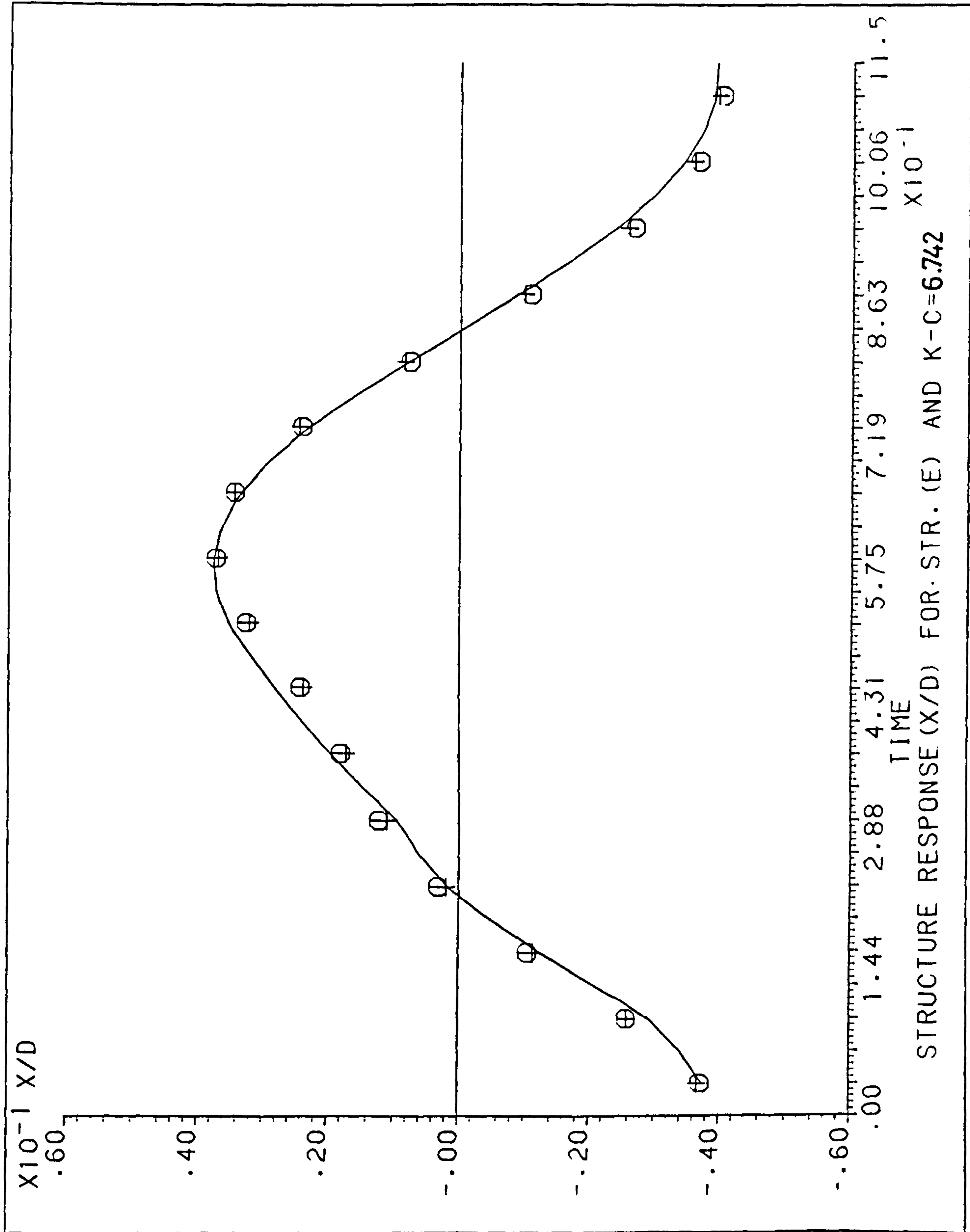


Figure (32D) - Structure's Response (X/D) during the Wave Cycle for Structure E with no Mass at Top (K-C = 6.742).



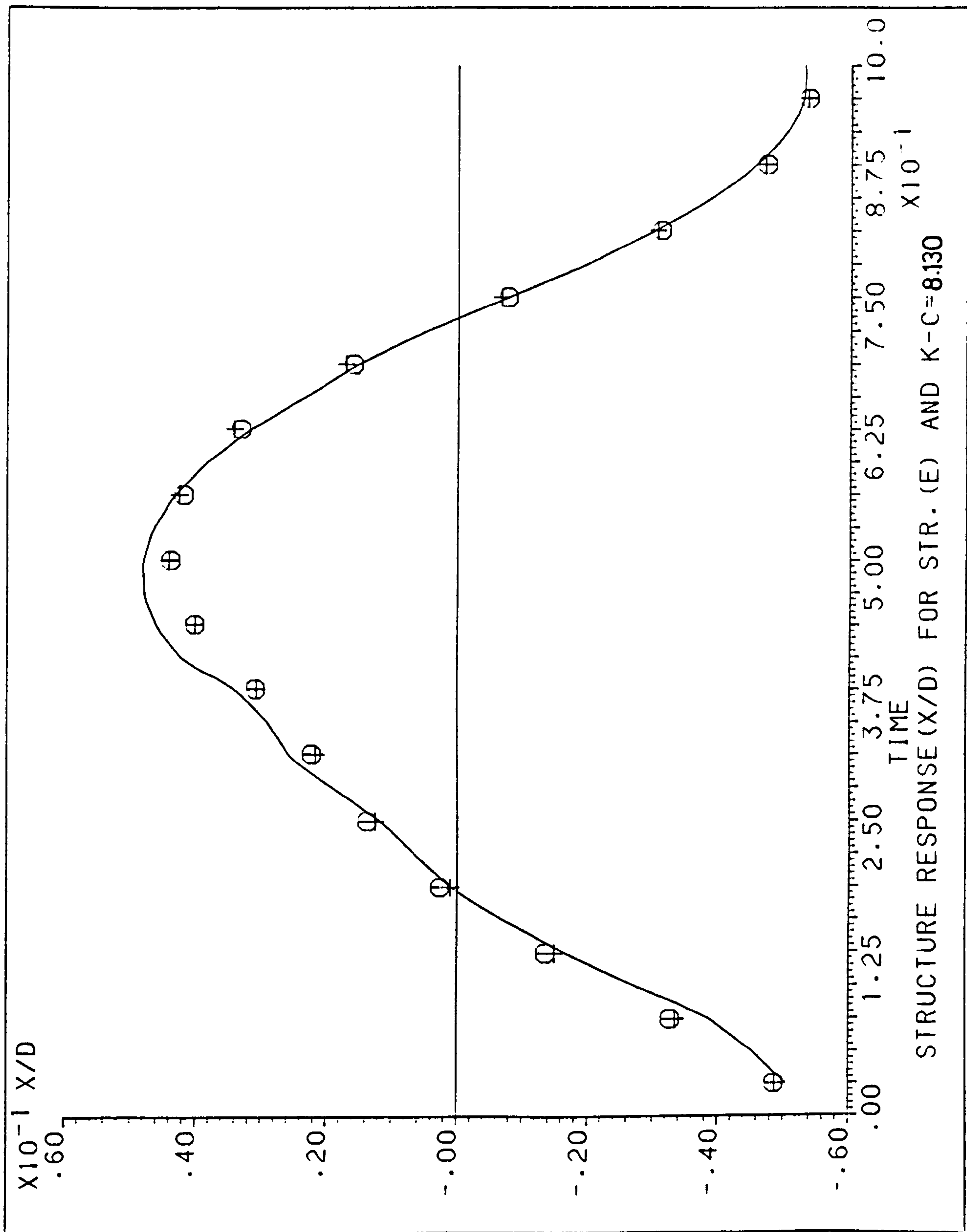


Figure (33D) - Structure's Response (X/D) during the Wave Cycle for Structure E with no Mass at Top (K-C = 8.13).

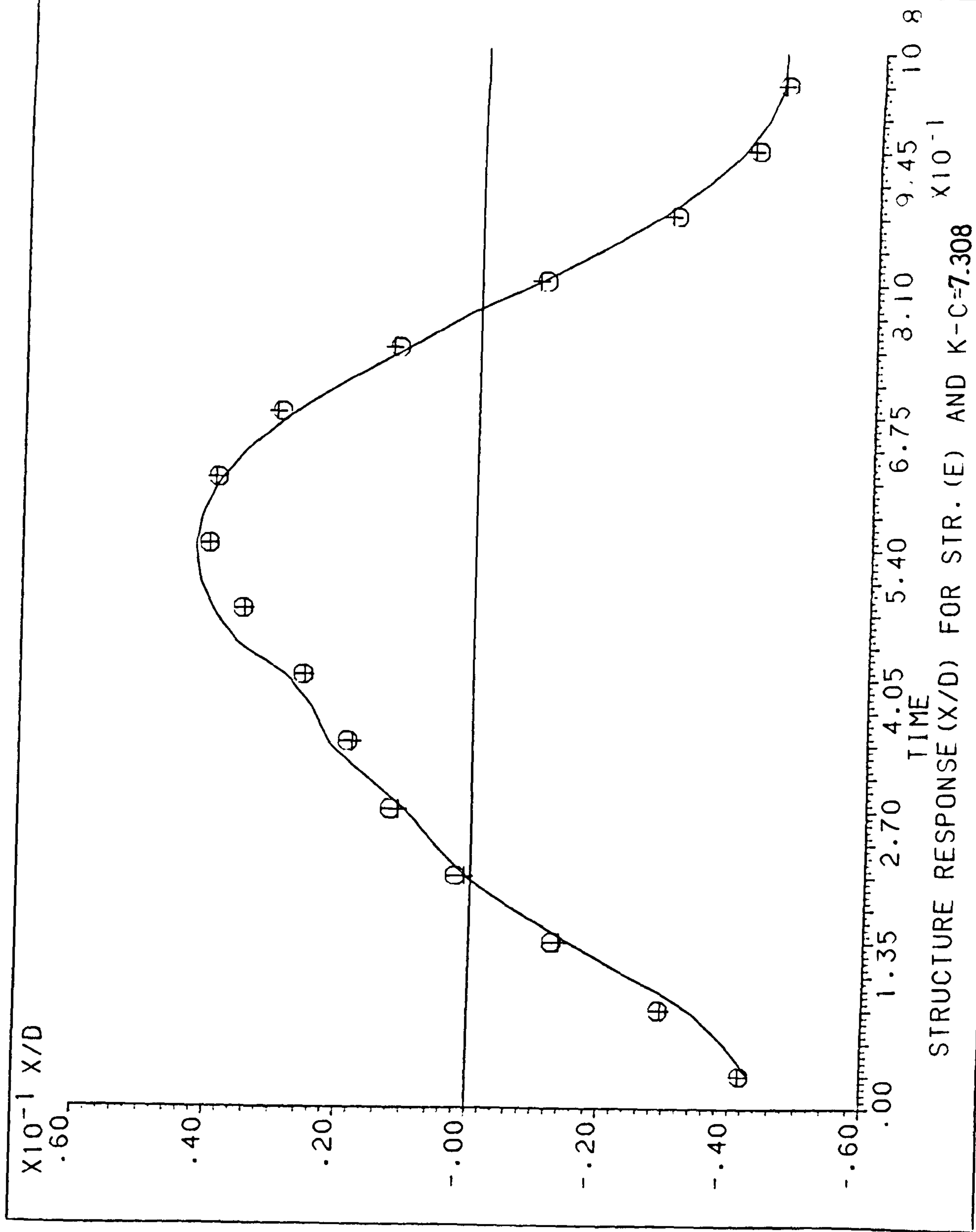


Figure (34D) - Structure's Response(X/D) during the Wave Cycle for Structure E with no Mass at Top (K-C = 7.308).



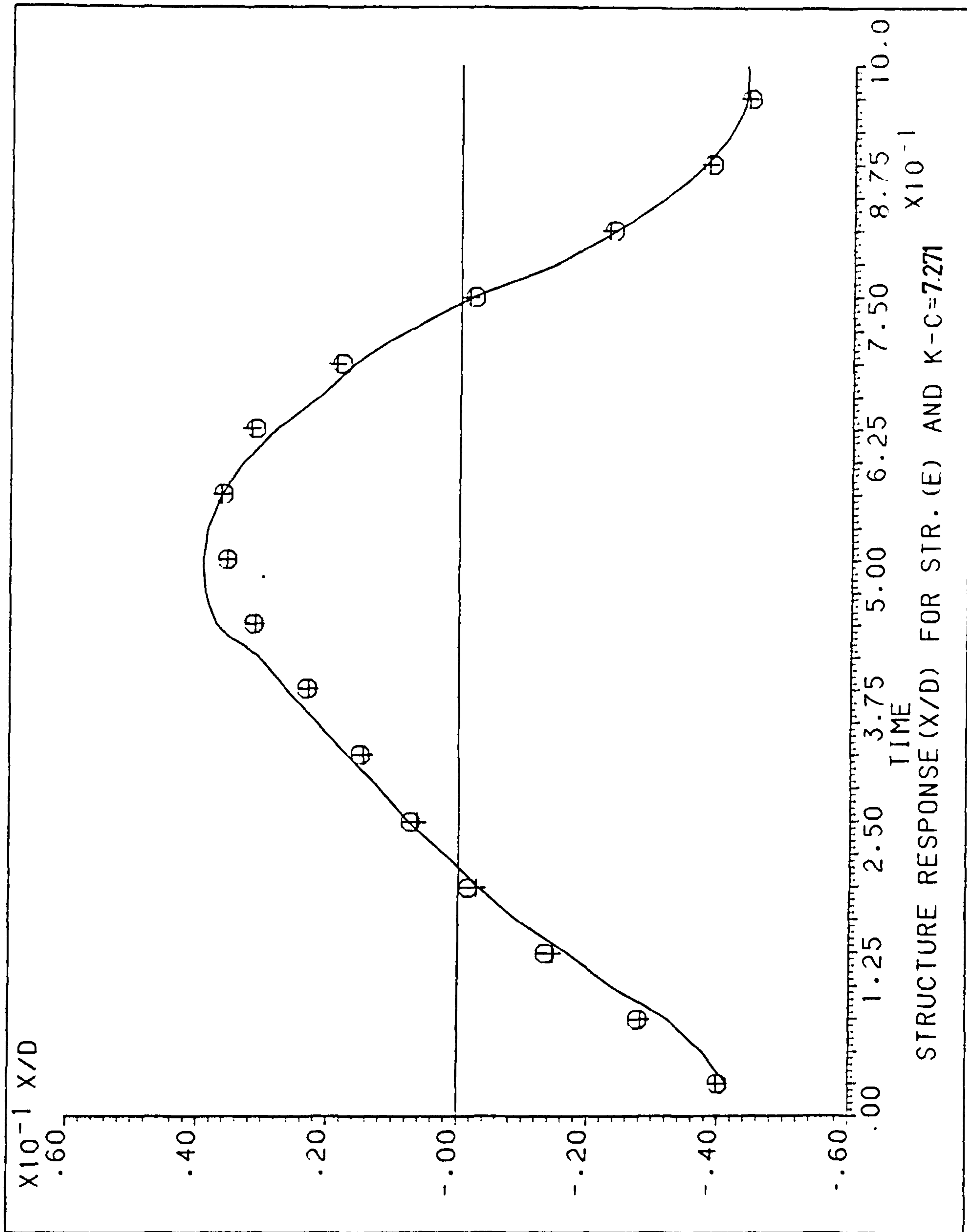


Figure (35D) - Structure's Response (X/D) during the Wave Cycle for Structure E with No Mass at Top (K-C = 7.271).

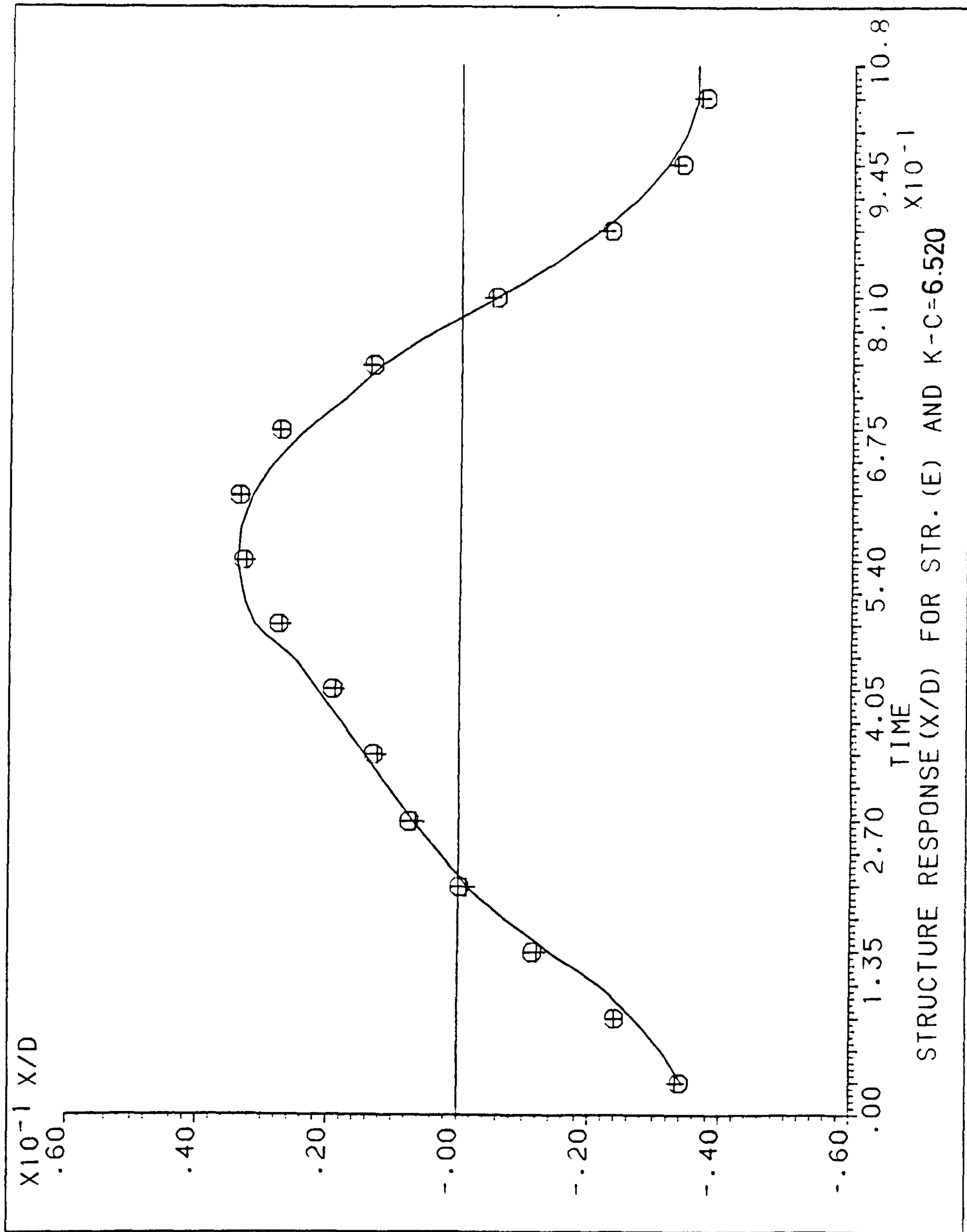


Figure (36D) - Structure's Response (X/D) during the Wave Cycle for Structure E with no Mass at Top (K-C = 6.520).



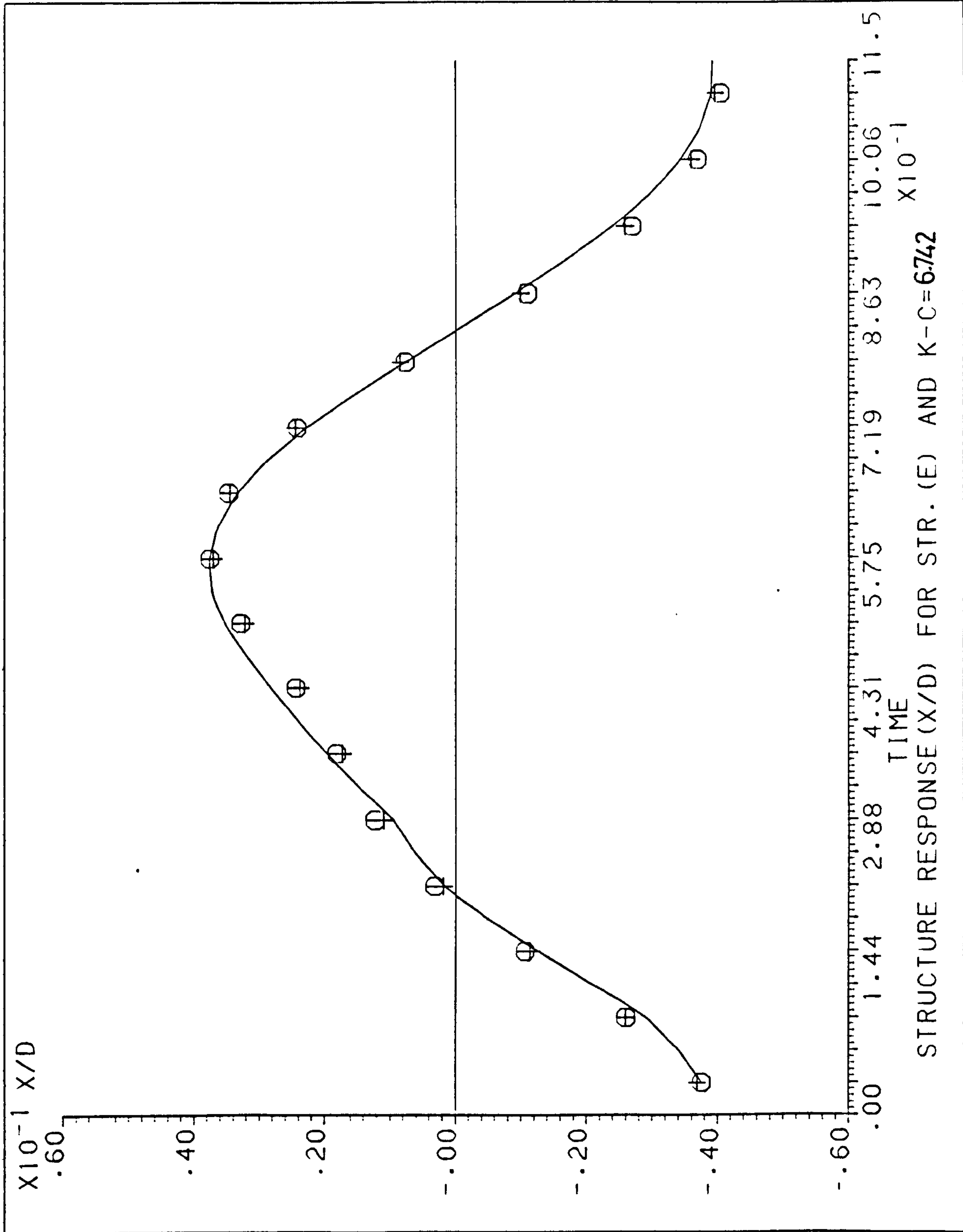


Figure (37D) - Structure's Response (X/D) during the Wave Cycle for Structure E with 1010 Grs at Top (K-C = 6.743).

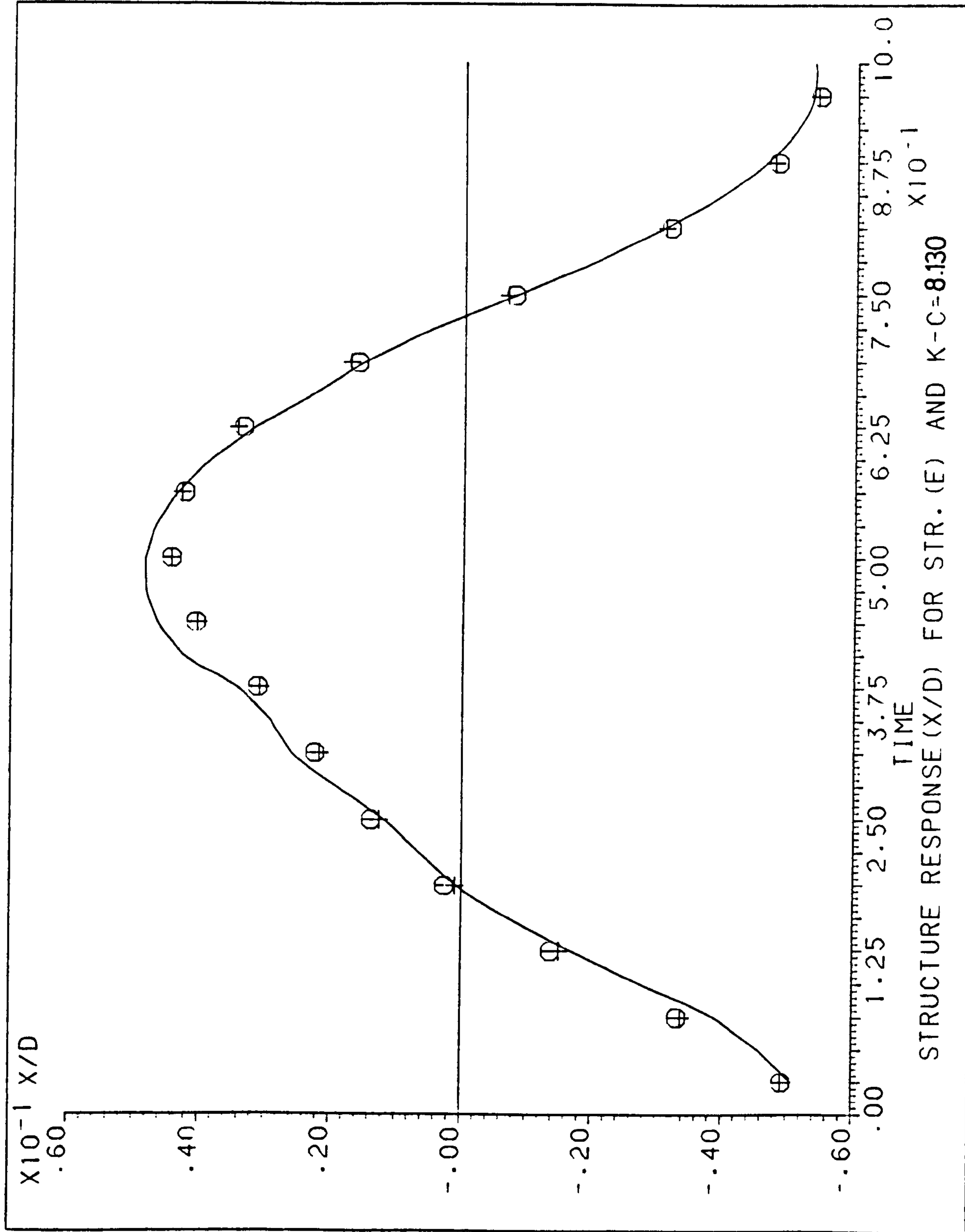


Figure (38D) - Structure's Response (X/D) during the Wave Cycle for Structure E with 1010 Grs at Top (K-C = 8.130).



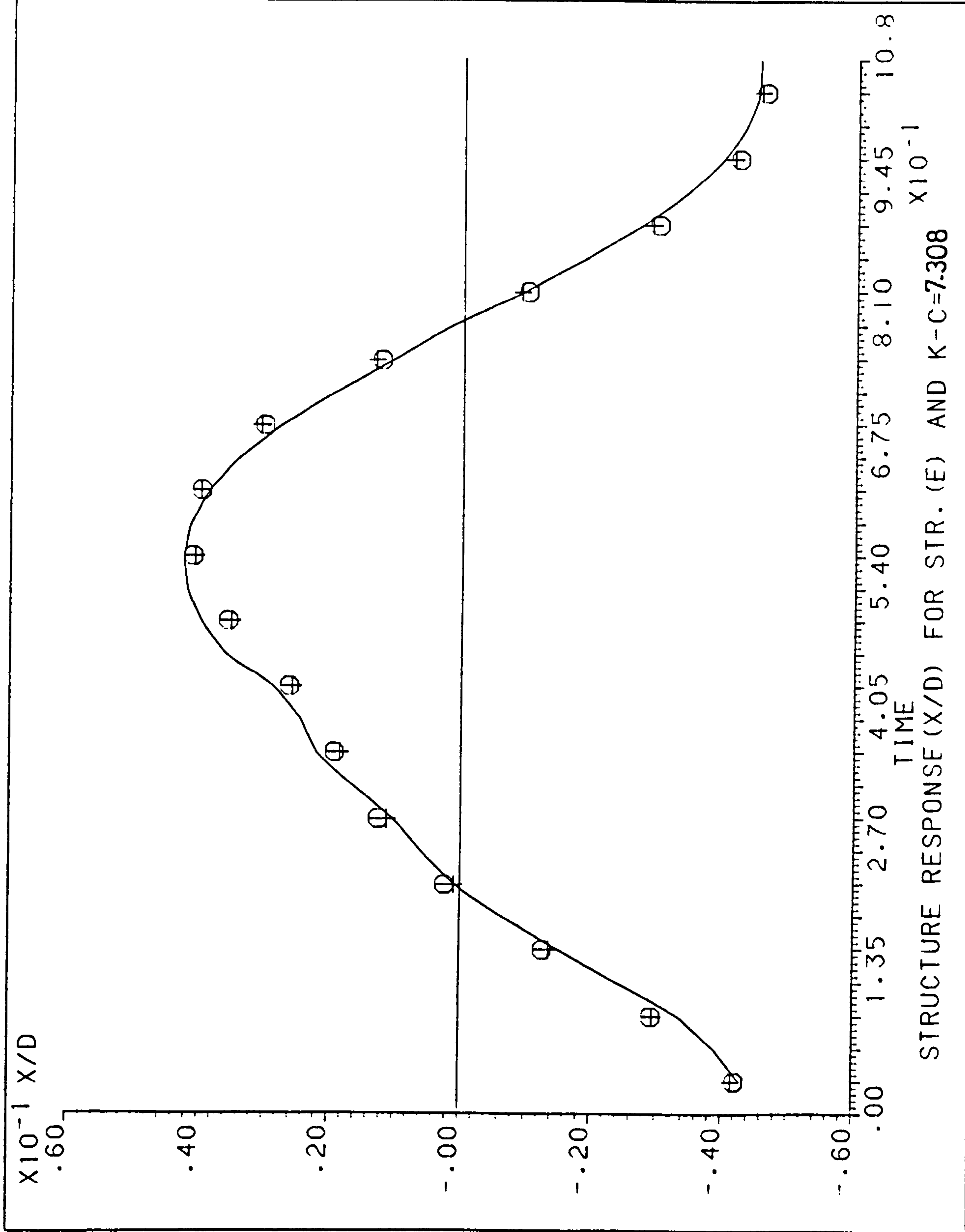


Figure (39D) - Structure's Response (X/D) during the Wave Cycle for Structure E with 1010 Grs at Top (K-C = 7.308).

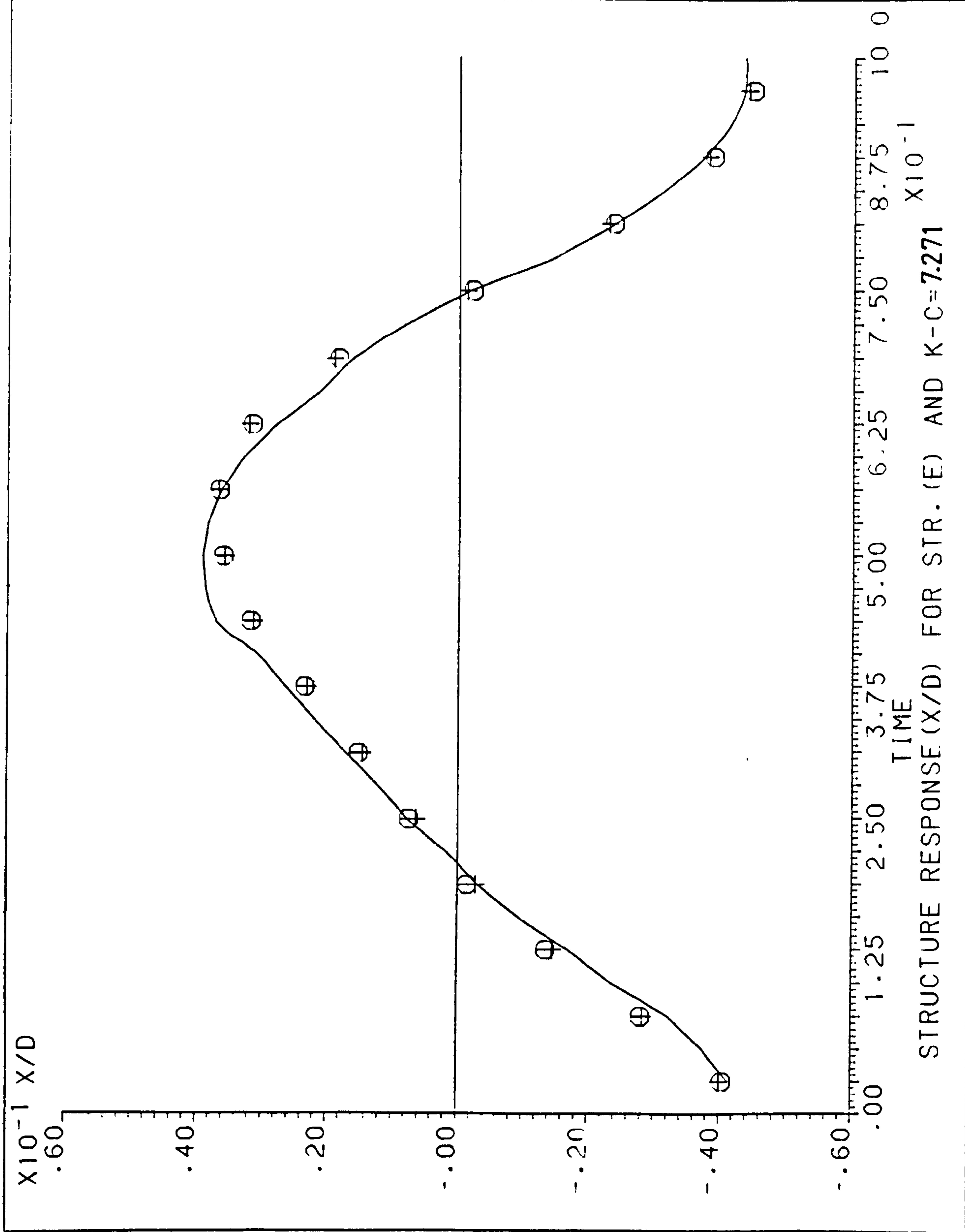


Figure (40D) - Structure's Response (C/D) during the Wave Cycle for Structure E with 1010 Grs at Top (K-C = 7.271).



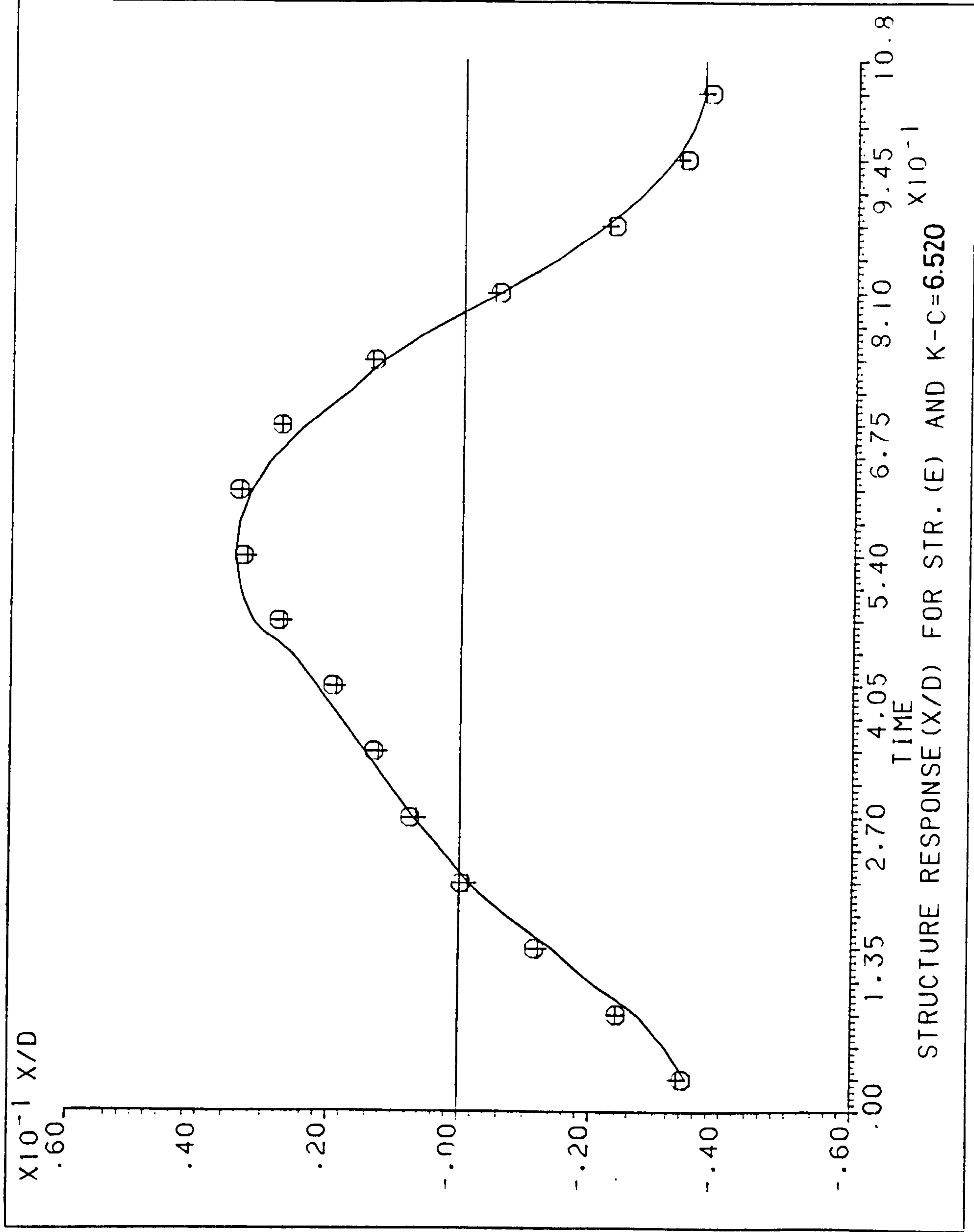


Figure (41D) - Structure's Response (X/D) during the Wave Cycle for Structure E with 1010 Grs at Top (K-C = 6.520).

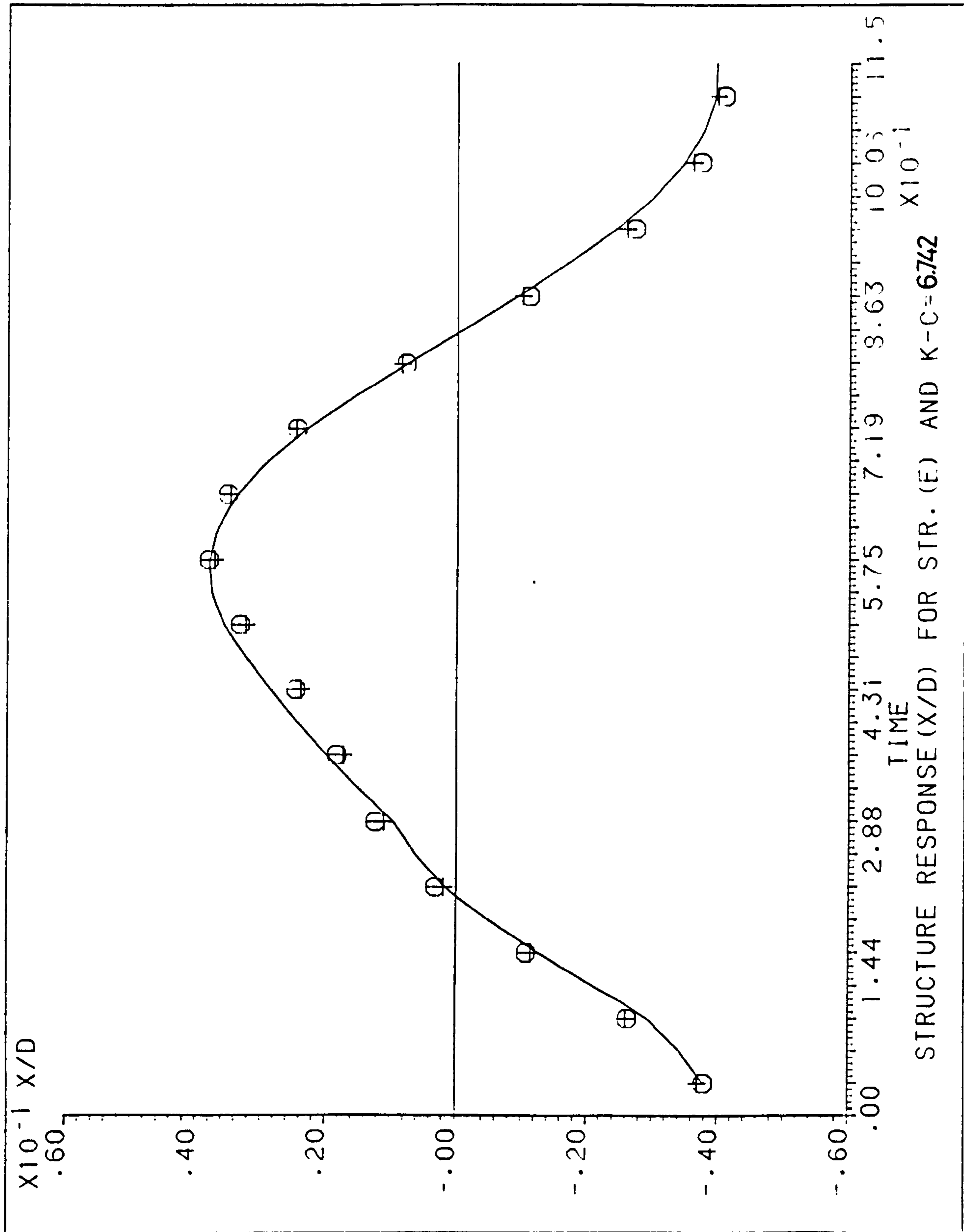


Figure (42D) - Structure's Response (X/D) during the Wave Cycle for Structure E with 2020 Grs at Top (K-C = 6.742).



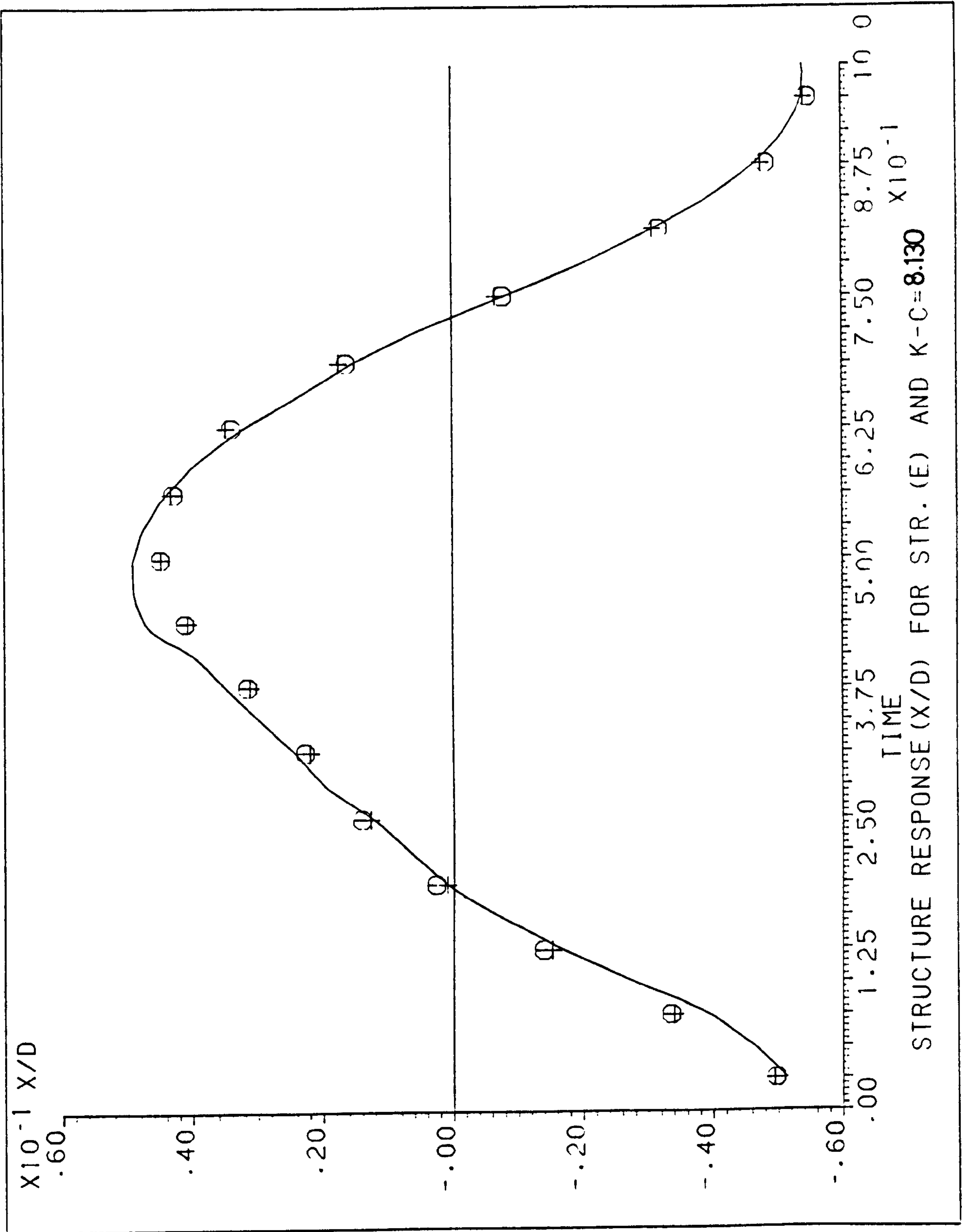


Figure (43D) - Structure's Response (X/D) during the Wave Cycle for Structure E with 2020 Grs at Top (K-C 8.130).

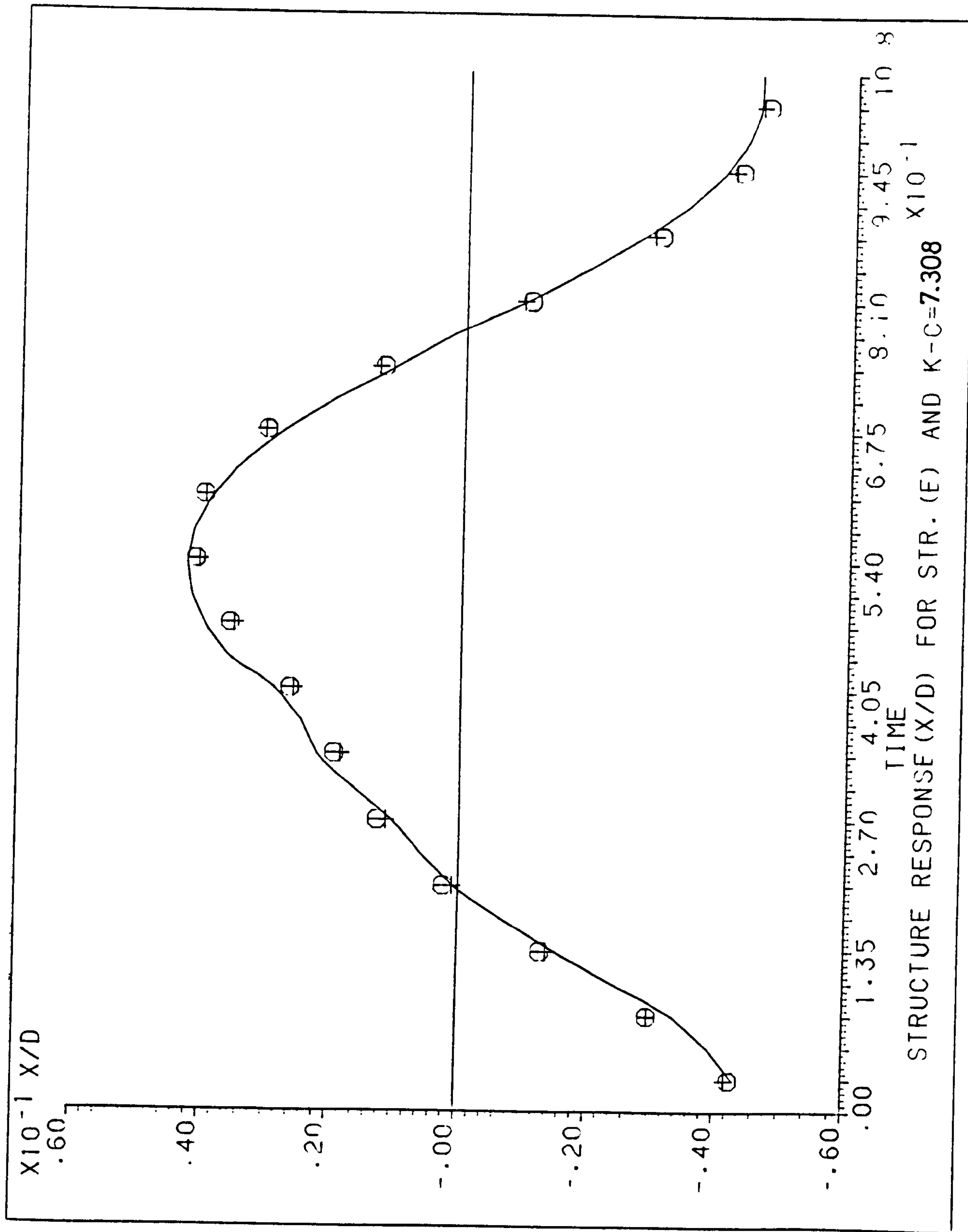


Figure (44D) - Structure's Response (X/D) during the Wave Cycle for Structure E with 2020 Grs at Top (K-C = 7.308).



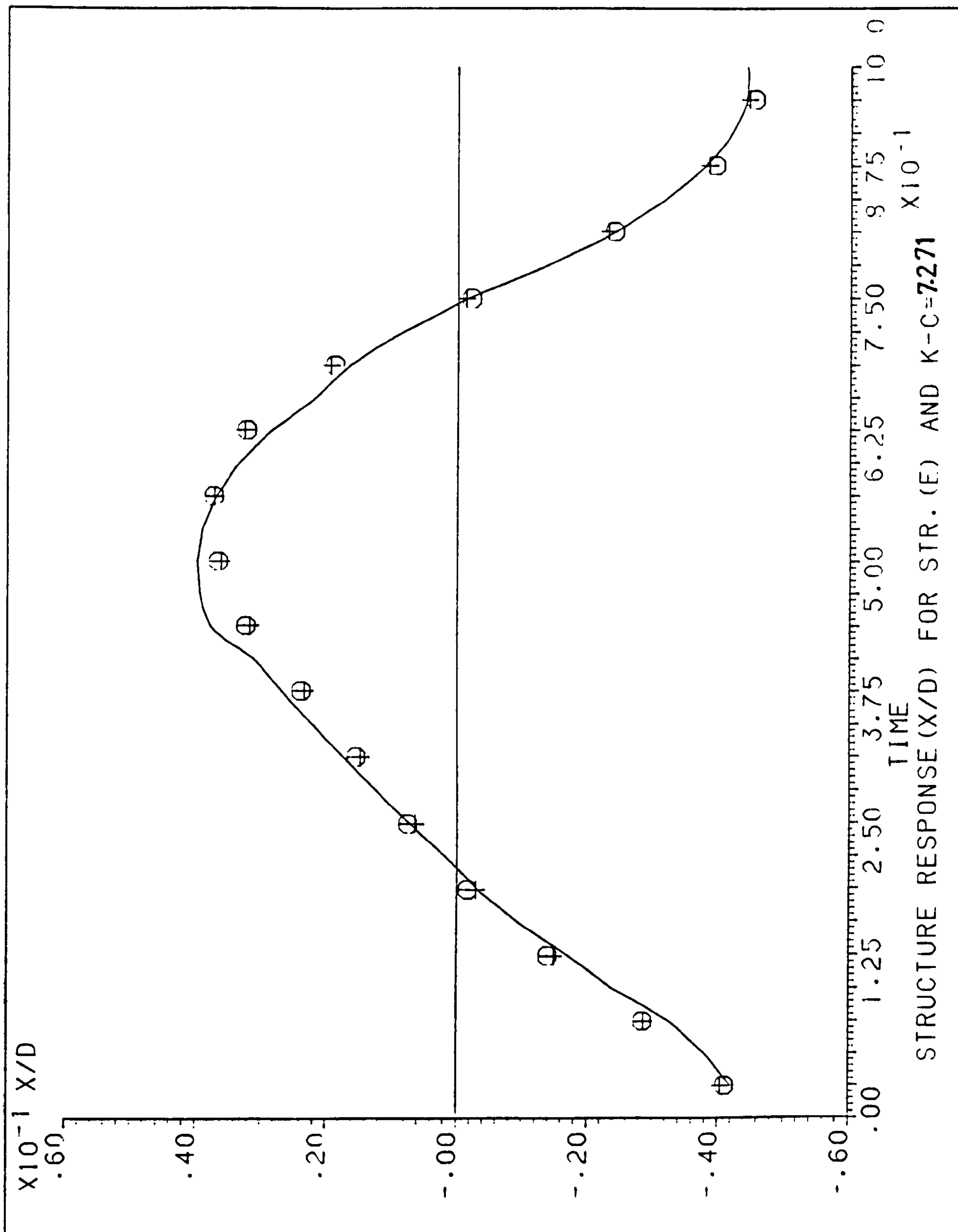


Figure (45D) - Structure's Response (X/D) during the Wave Cycle for Structure E with 2020 Grs at Top (K-C = 7.271).

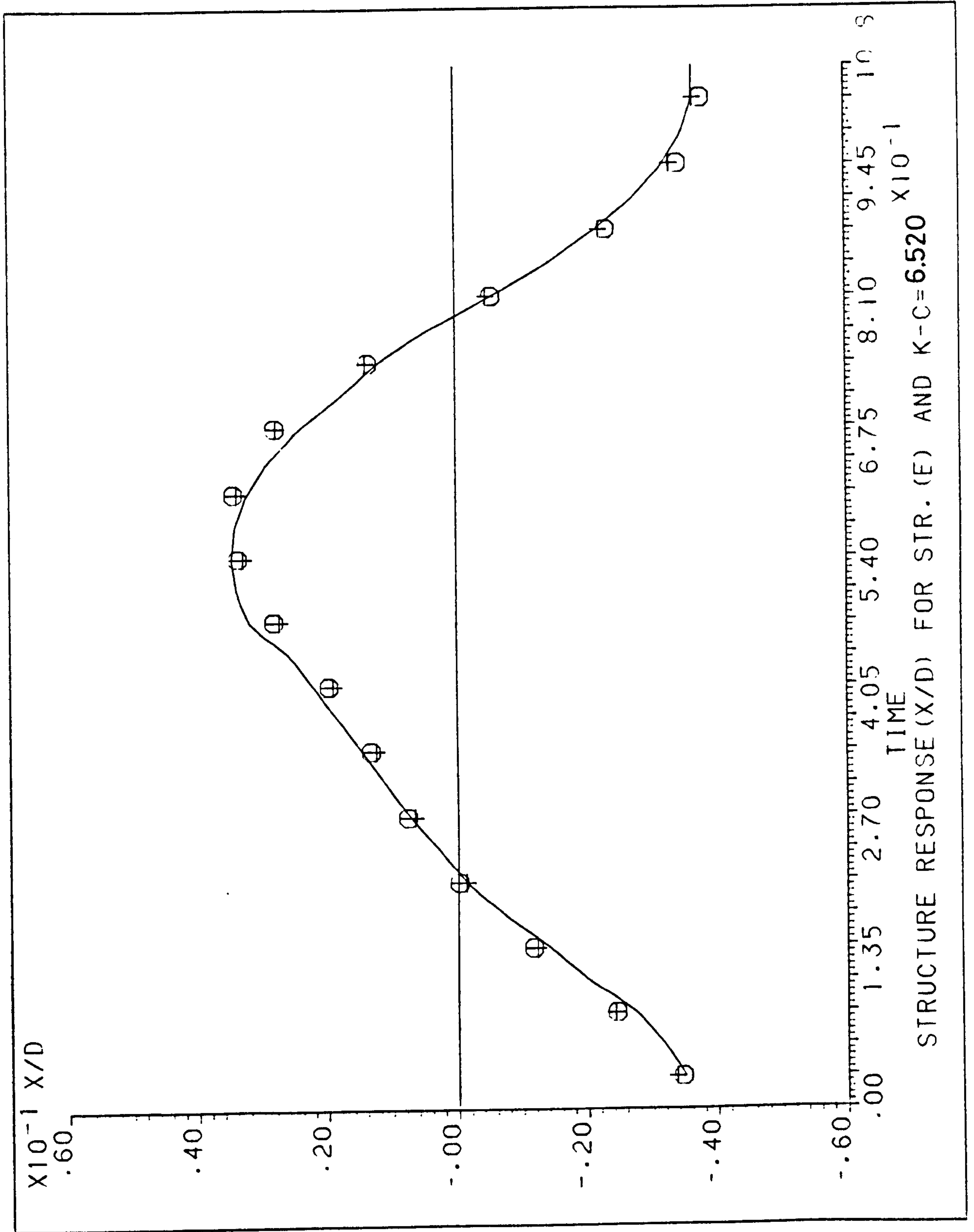


Figure (46D) - Structure's Response (X/D) during the Wave Cycle for Structure E with 2020 Grs at Top (K-C = 6.520).



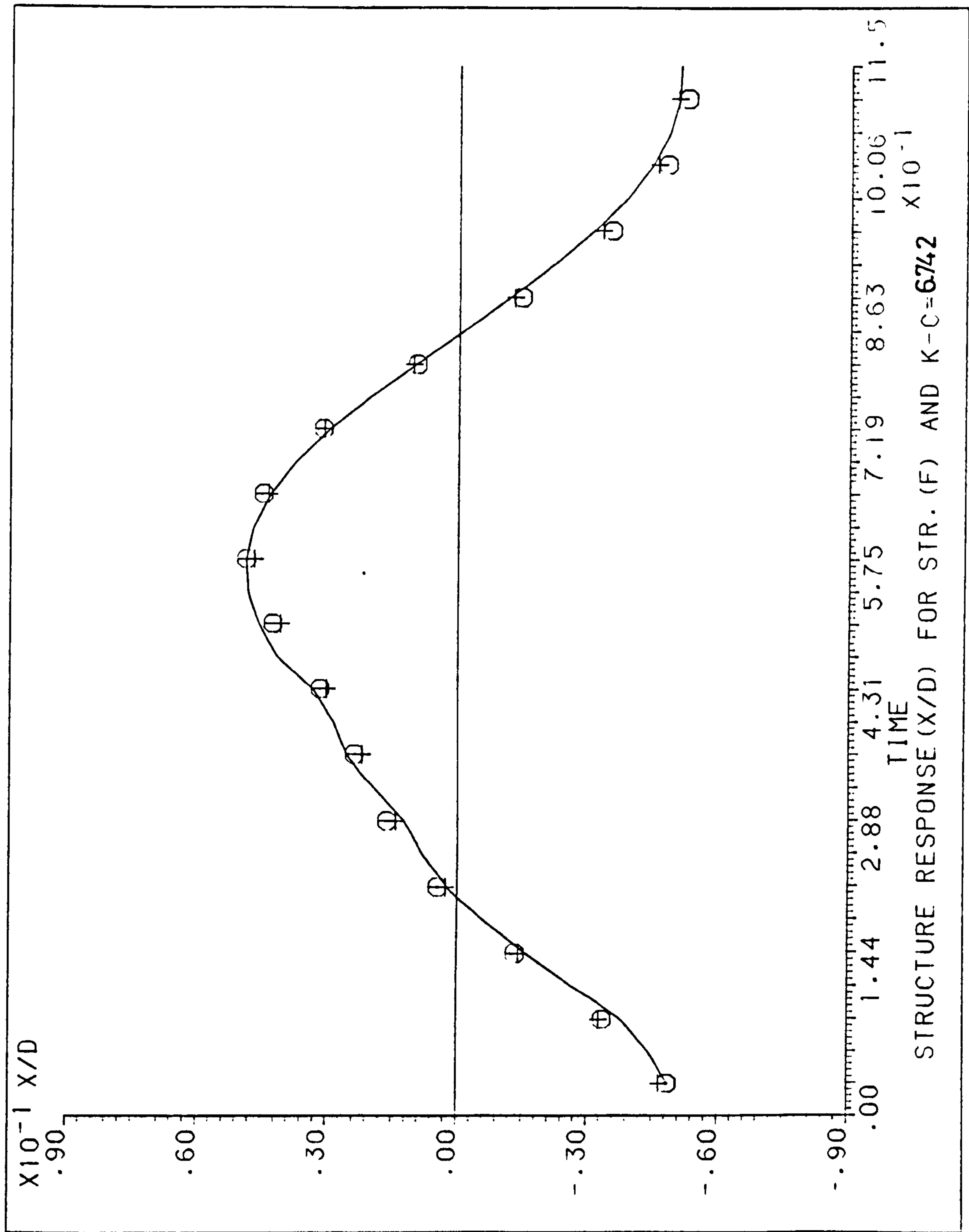


Figure (47D) - Structure's Response (X/D) during the Wave Cycle for Structure F with no Mass at Top ( $K-C = 6.742$ ).

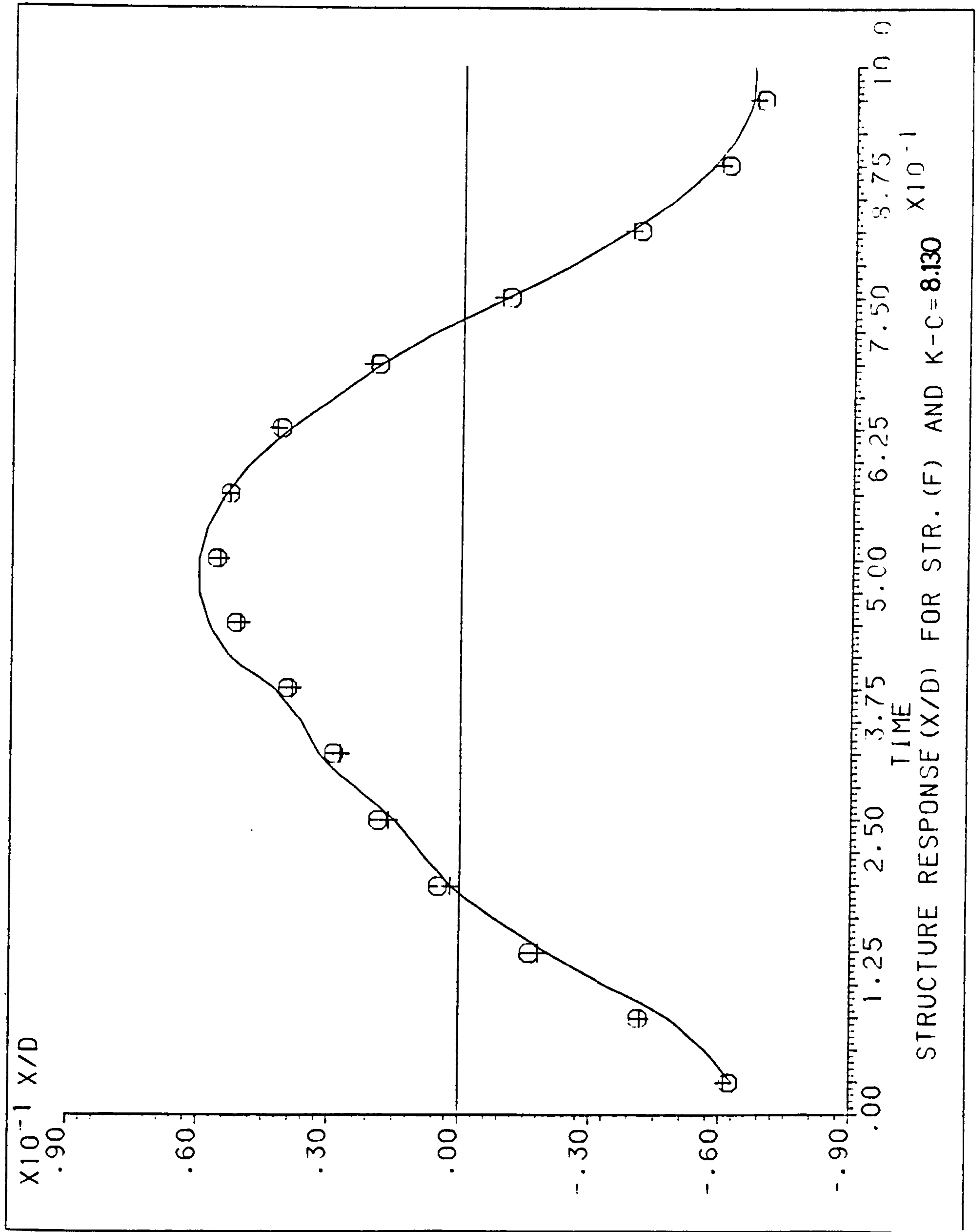


Figure (48D) - Structure's Response (X/D) during the Wave Cycle for Structure F with no Mass at Top (K-C = 8.130).



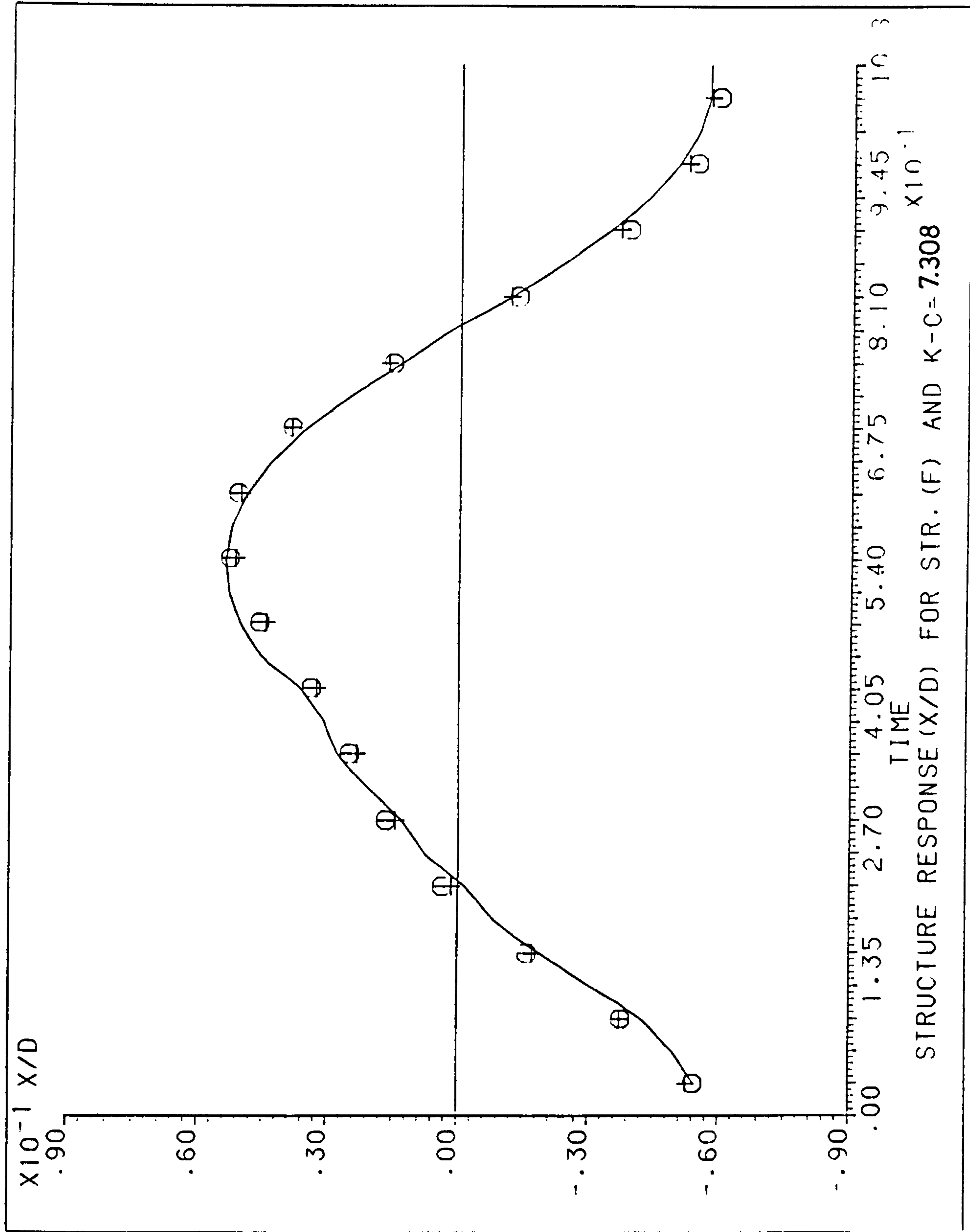


Figure (49D) - Structure's Response (X/D) during the Wave Cycle for Structure F with no Mass at Top ( $K-C = 7.308$ ).

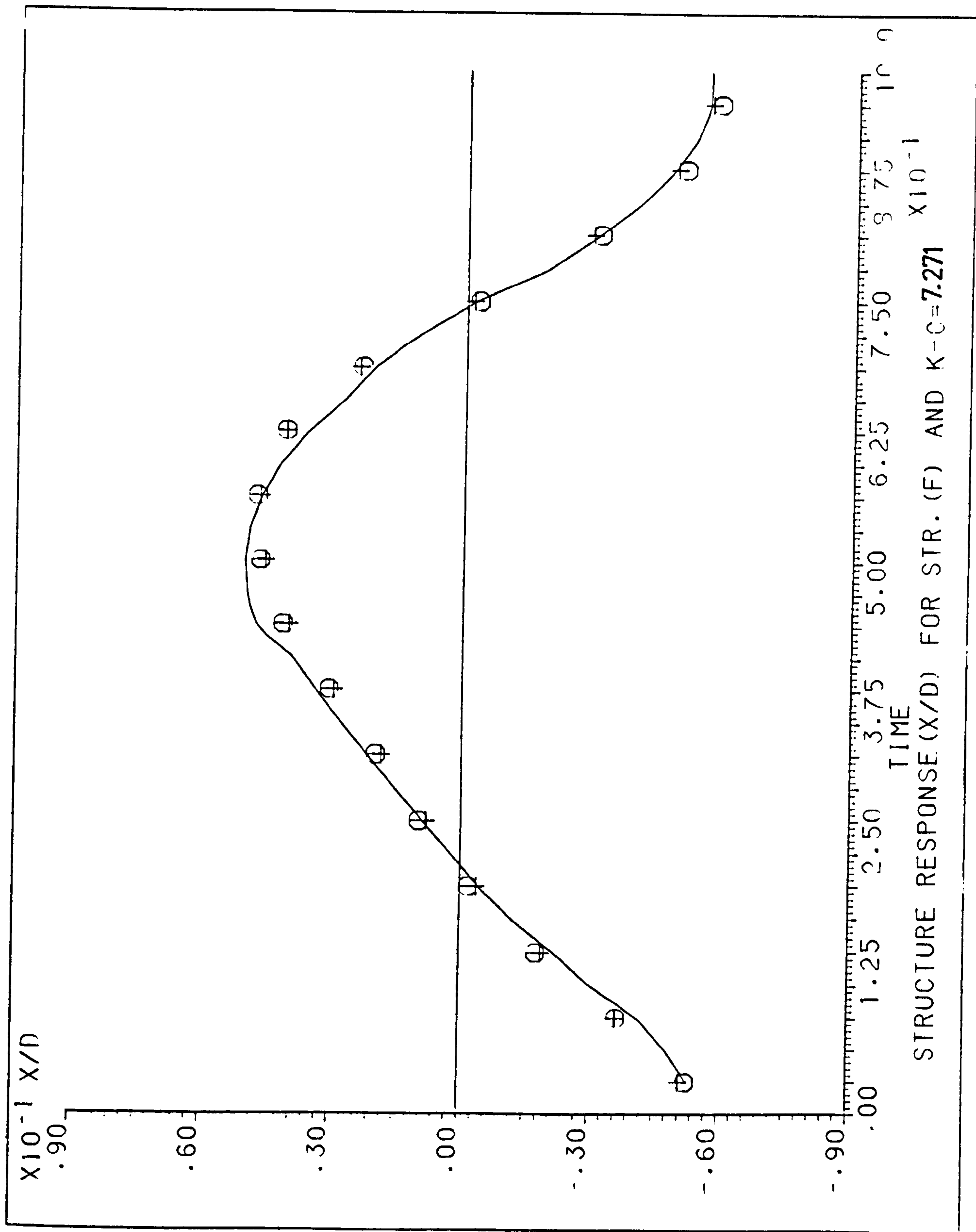


Figure (50D) - Structure's Response (X/D) during the Wave Cycle for Structure F with no Mass at Top ( $K-C = 7.271$ ).



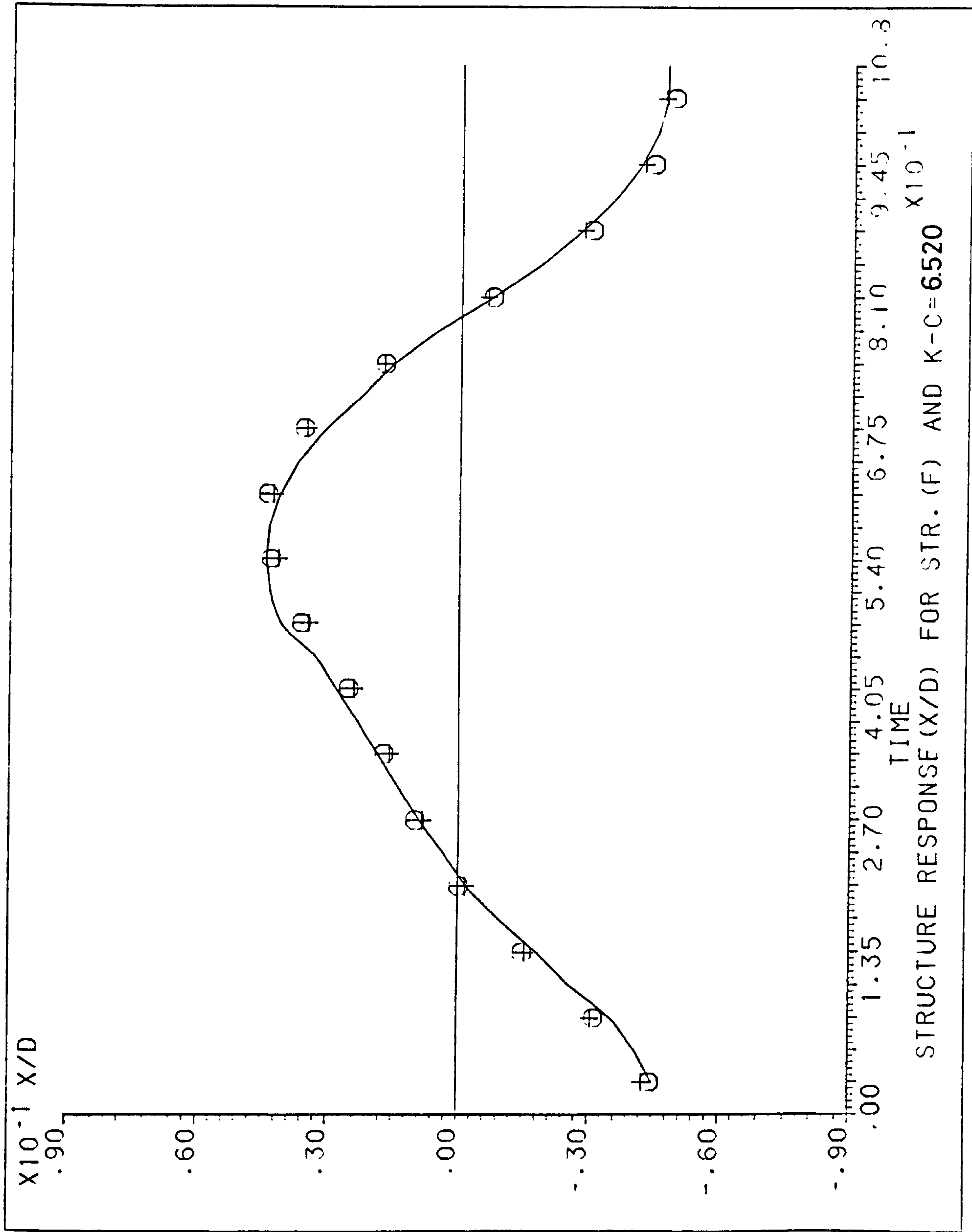


Figure (51D) - Structure's Response (X/D) during the Wave Cycle for Structure F with no Mass at Top (K-C = 6.520).

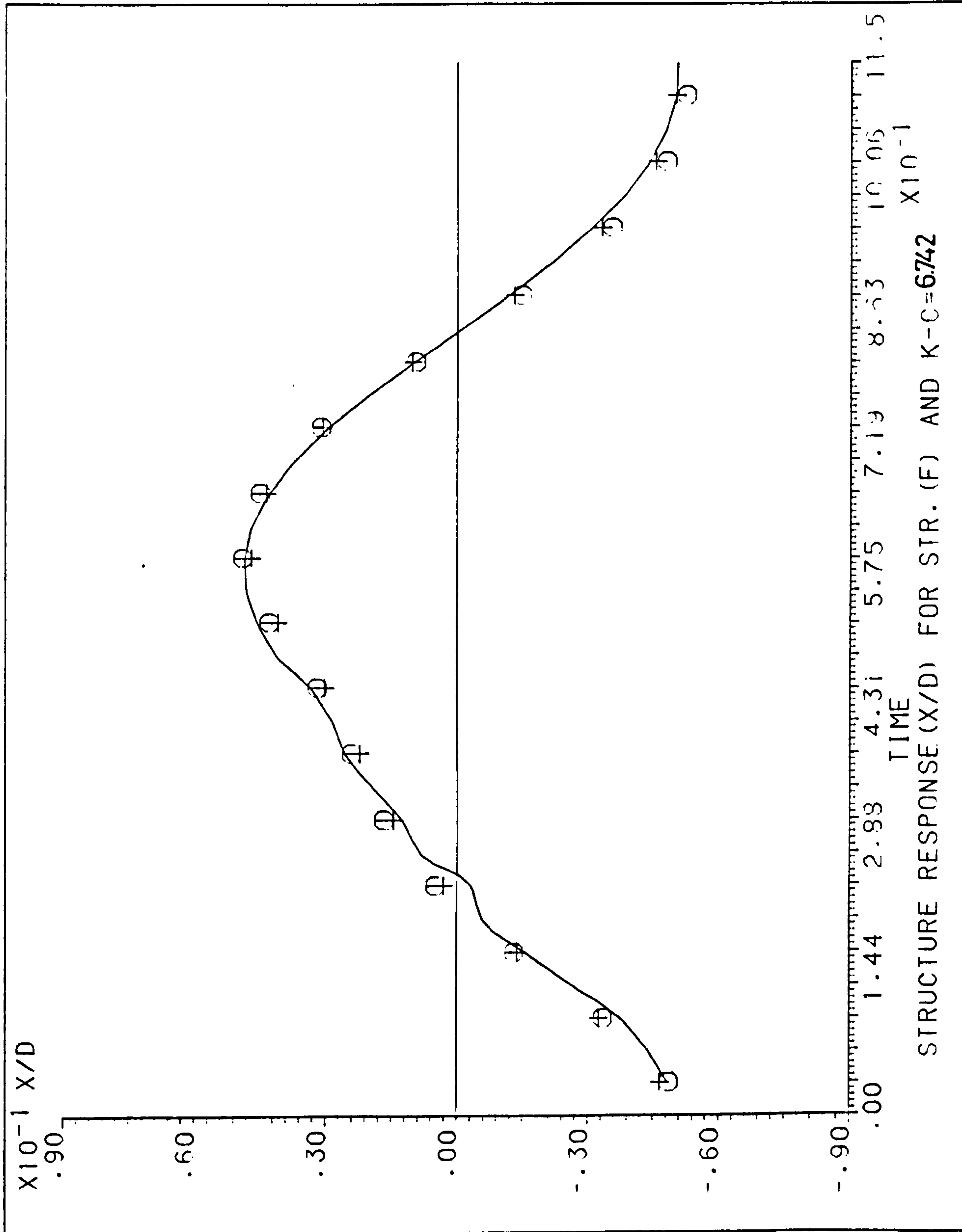


Figure (52D) - Structure's Response (X/D) during the Wave Cycle for Structure F with 1010 Grs at Top (K-C = 6.742).



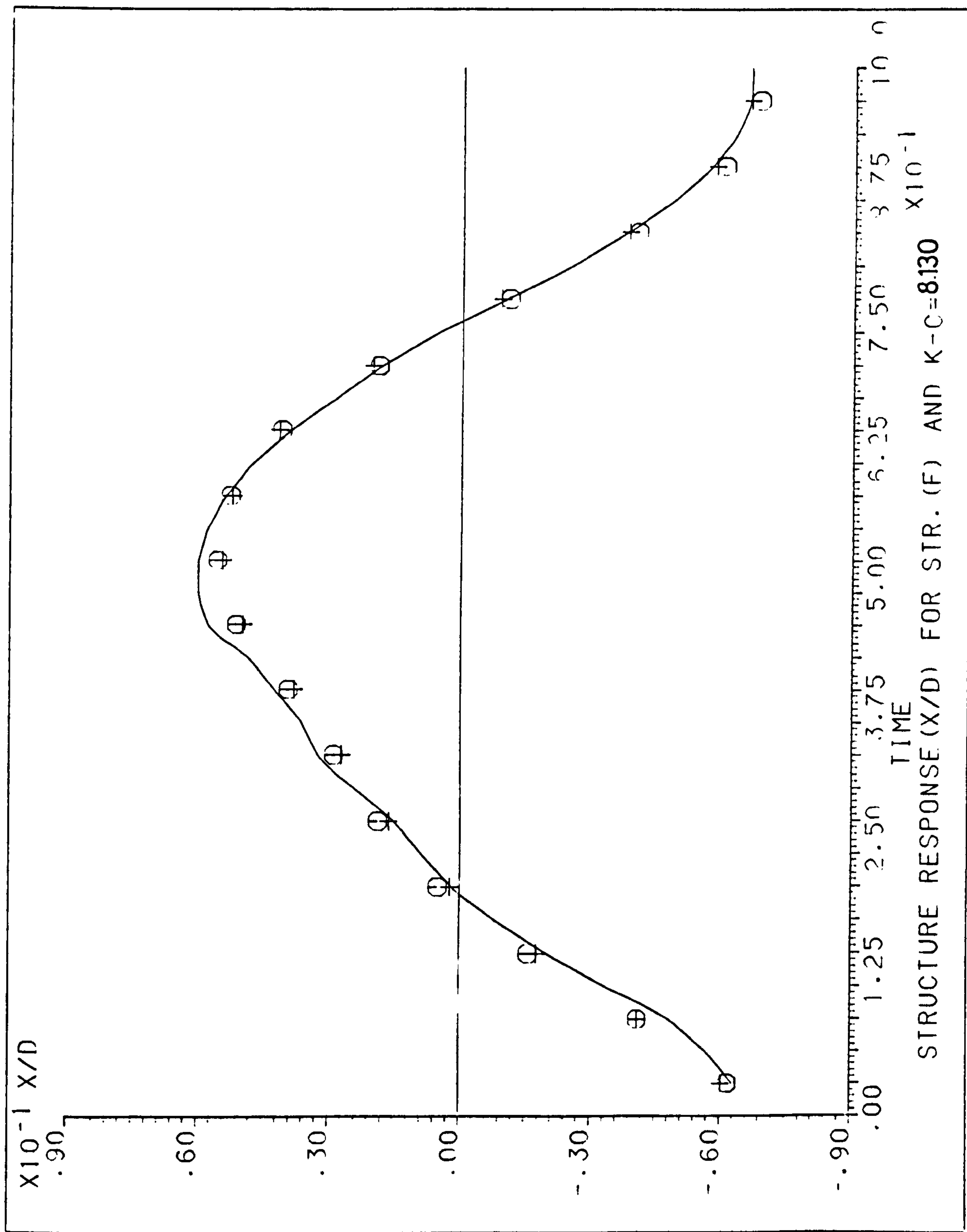


Figure (53D) - Structure's Response (X/D) during the Wave Cycle for Structure F with 1010 Grs at Top (K-C = 8.130).

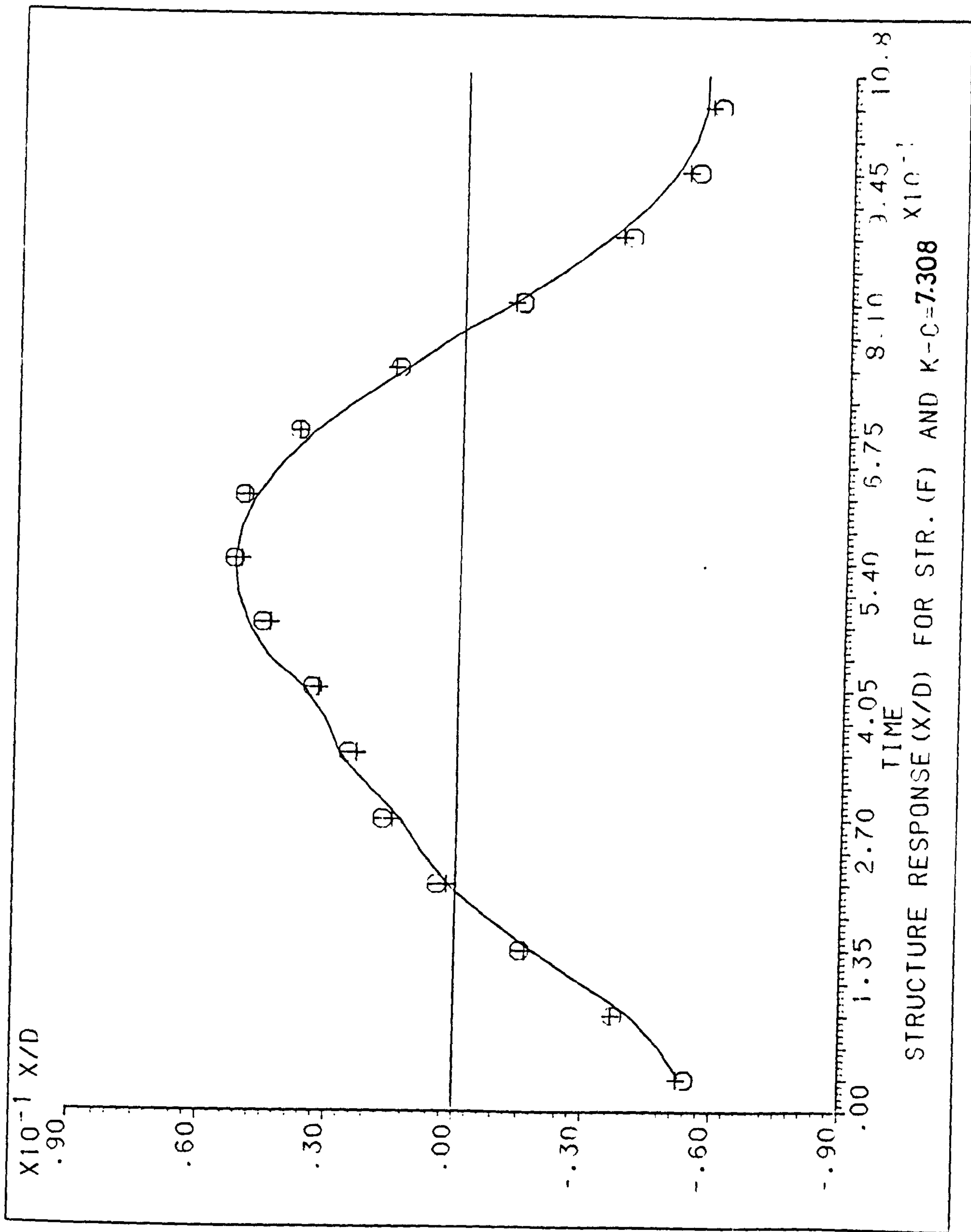


Figure (54D) - Structure's Response (X/D) during the Wave Cycle for Structure F with 1010 Grs at Top (K-C = 7.308).



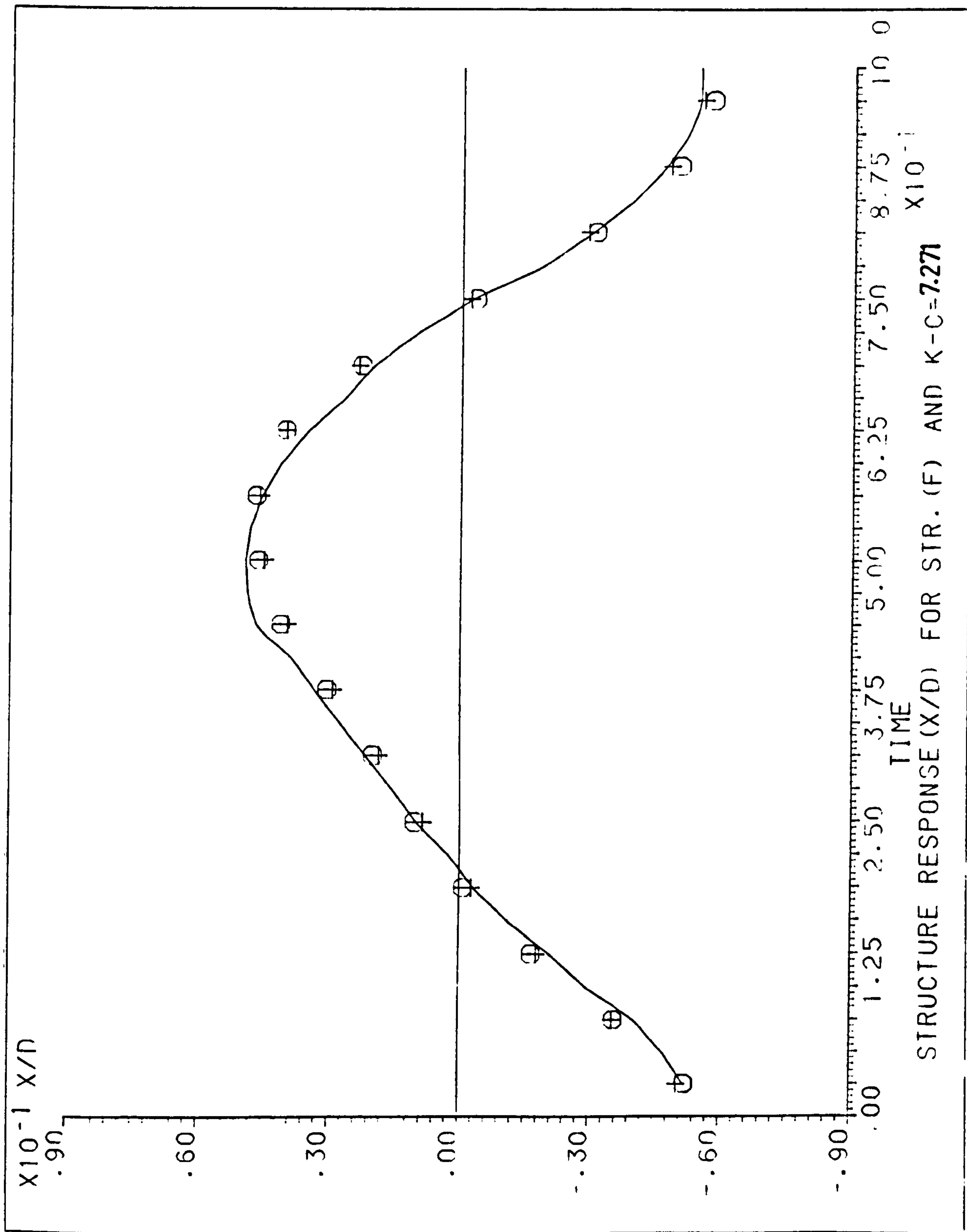


Figure (55D) - Structure's Response (X/D) during the Wave Cycle for Structure F with 1010 Grs at Top ( $K-C = 7.271$ ).

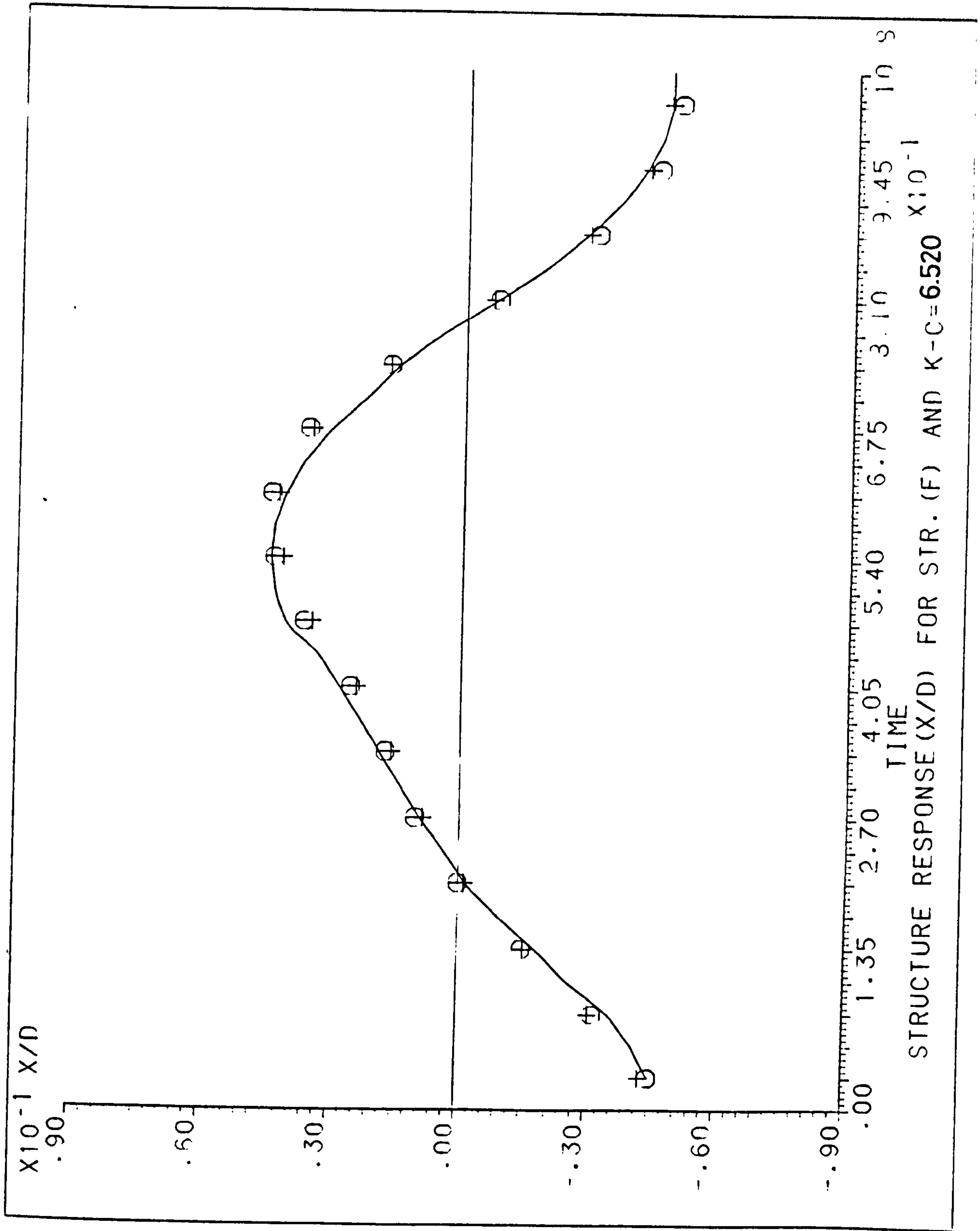


Figure (56D) - Structure's Response (X/D) during the Wave Cycle for Structure F with 1010 Grs at Top ( $K-C = 6.520$ ).



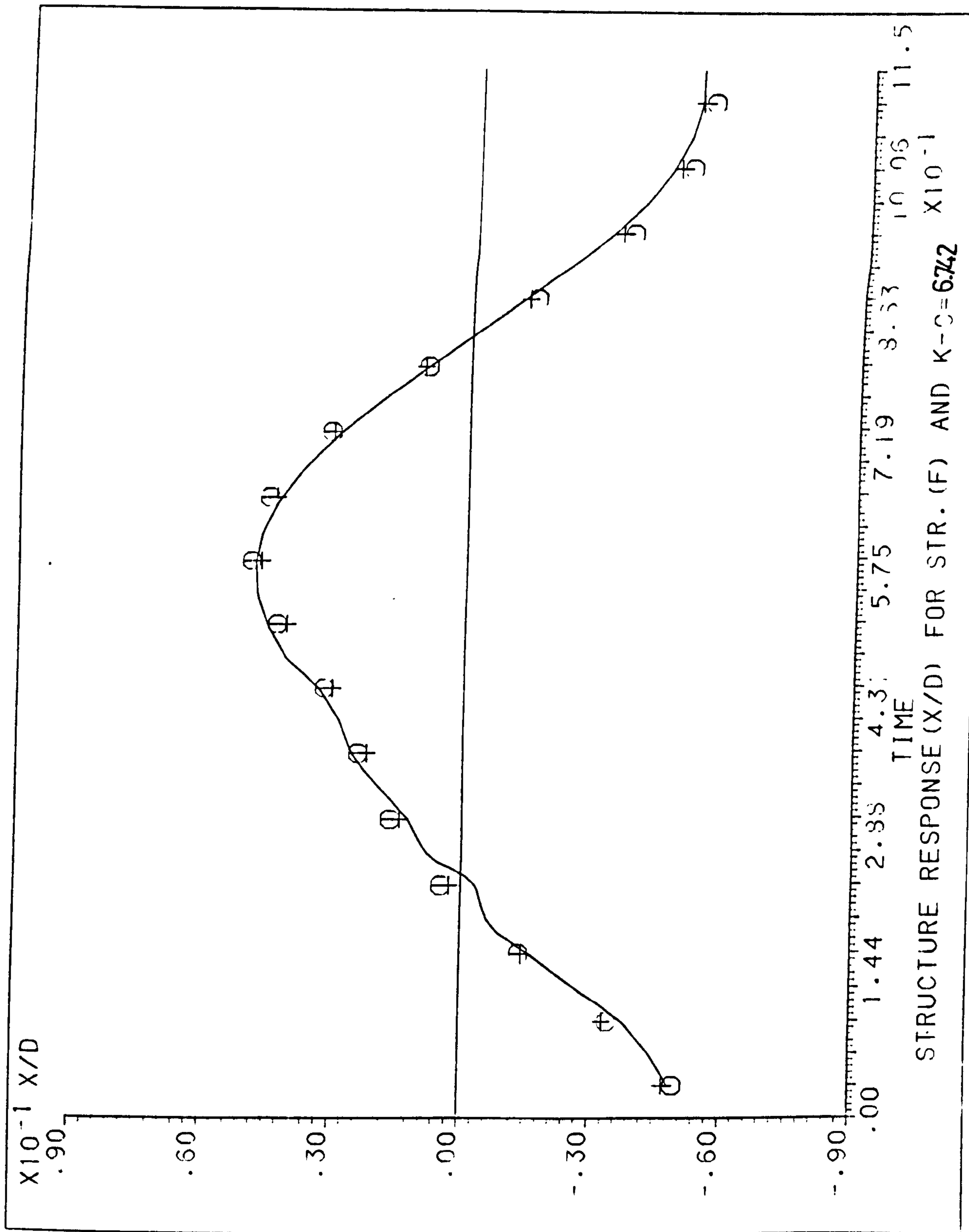


Figure (57D) - Structure's Response (X/D) during the Wave Cycle for Structure F with 2020 Grs at Top (K-C = 6.742).

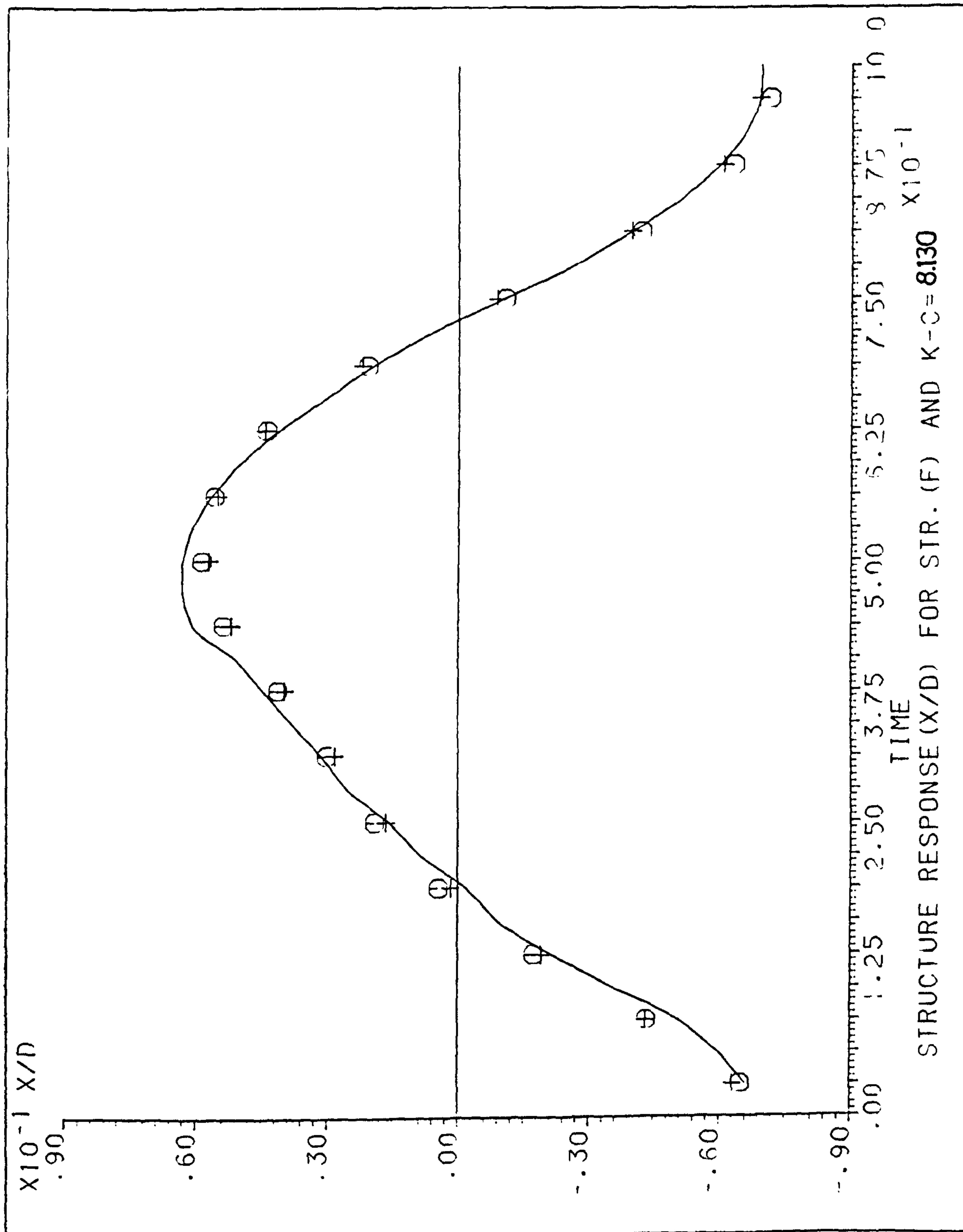


Figure (58D) - Structure's Response (X/D) during the Wave Cycle for Structure F with 2020 Grs at Top (K-C = 8.130).



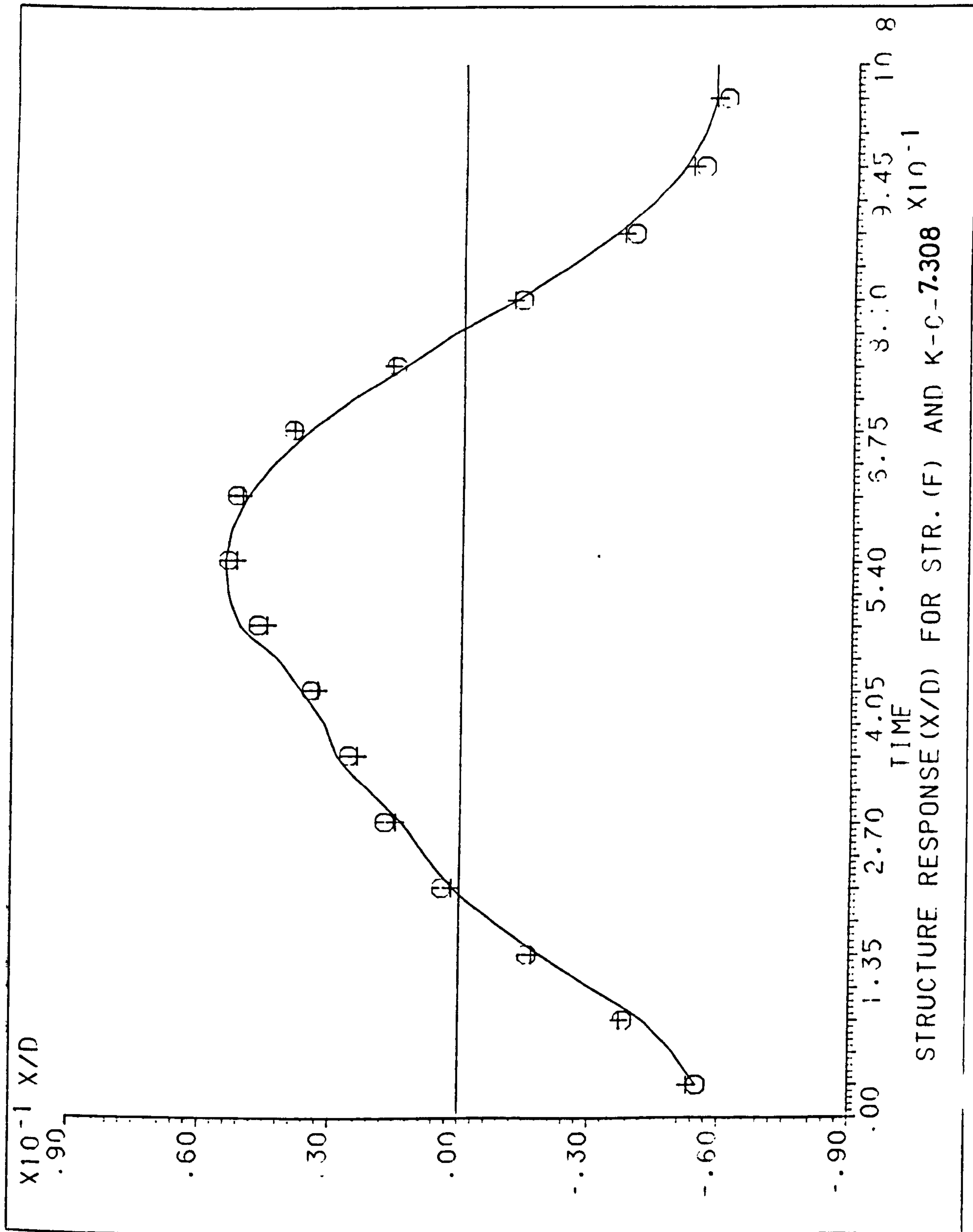


Figure (59D) - Structure's Response (X/D) during the Wave Cycle for Structure F with 2020 Grs at Top (K-C = 7.308).

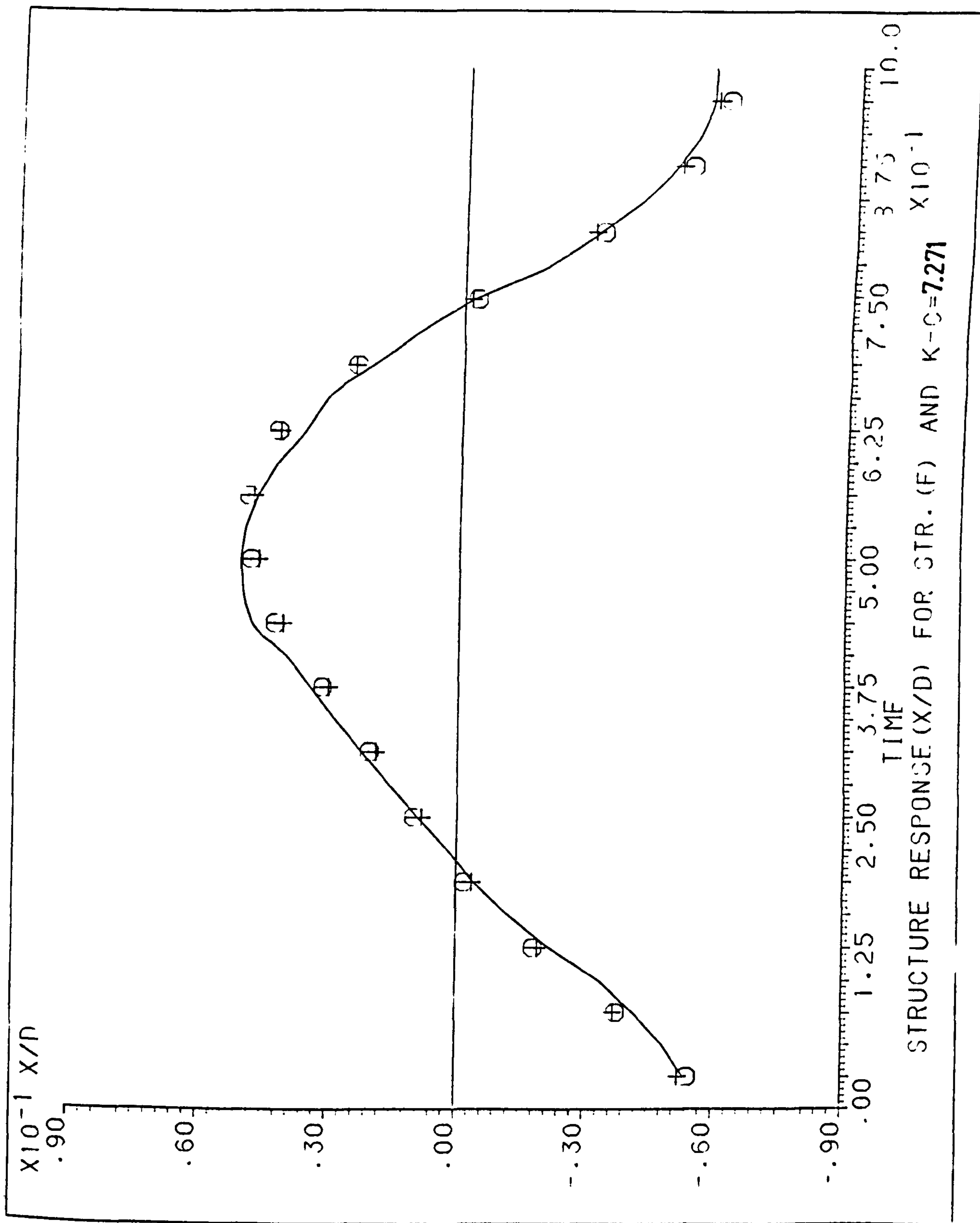


Figure (60D) - Structure's Response (X/D) during the Wave Cycle for Structure F with 2020 Grs at Top ( $K-C = 7.271$ ).



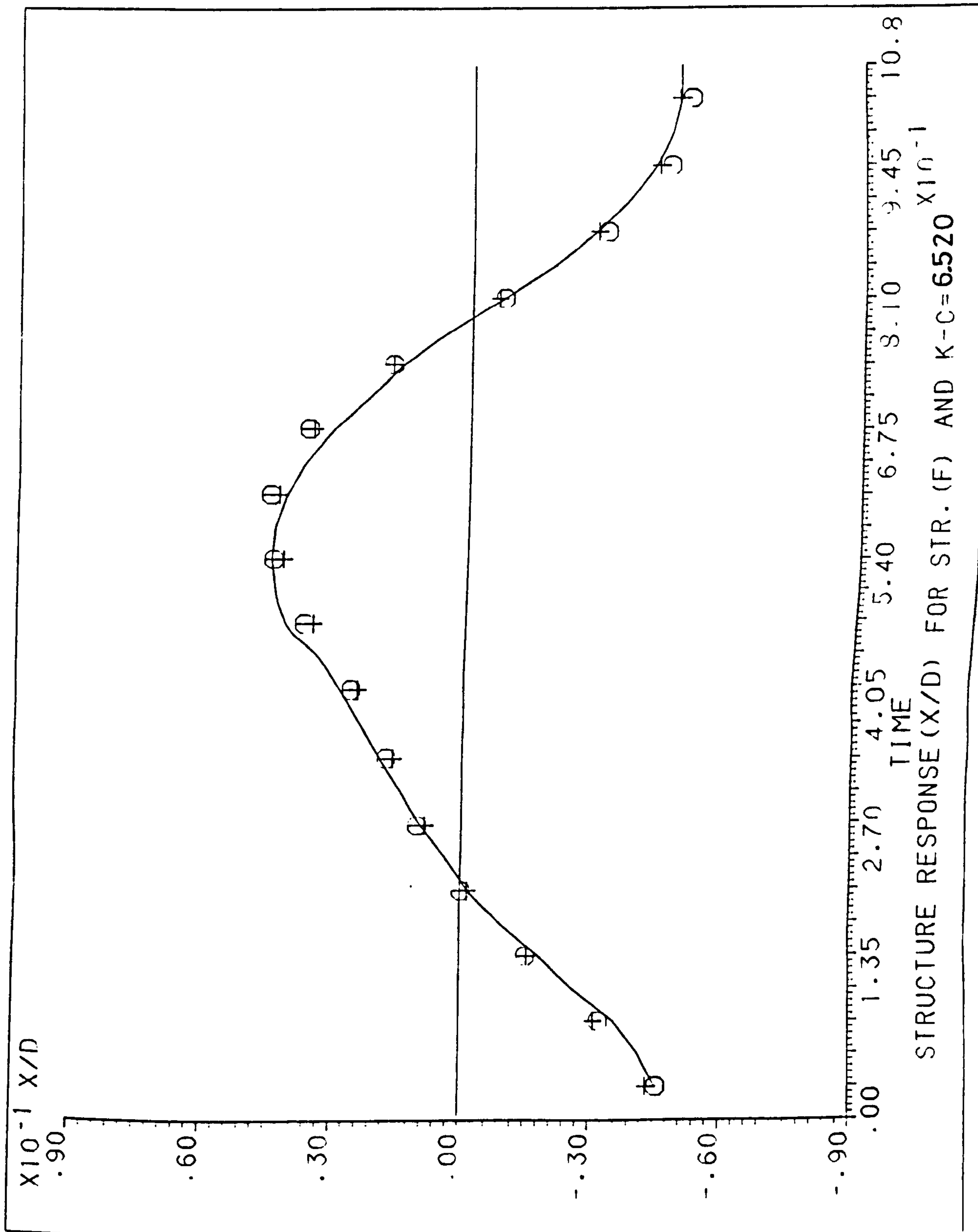


Figure (61D) - Structure's Response (X/D) during the Wave Cycle for Structure F with 2020 Grs at Top ( $K-C = 6.520$ ).

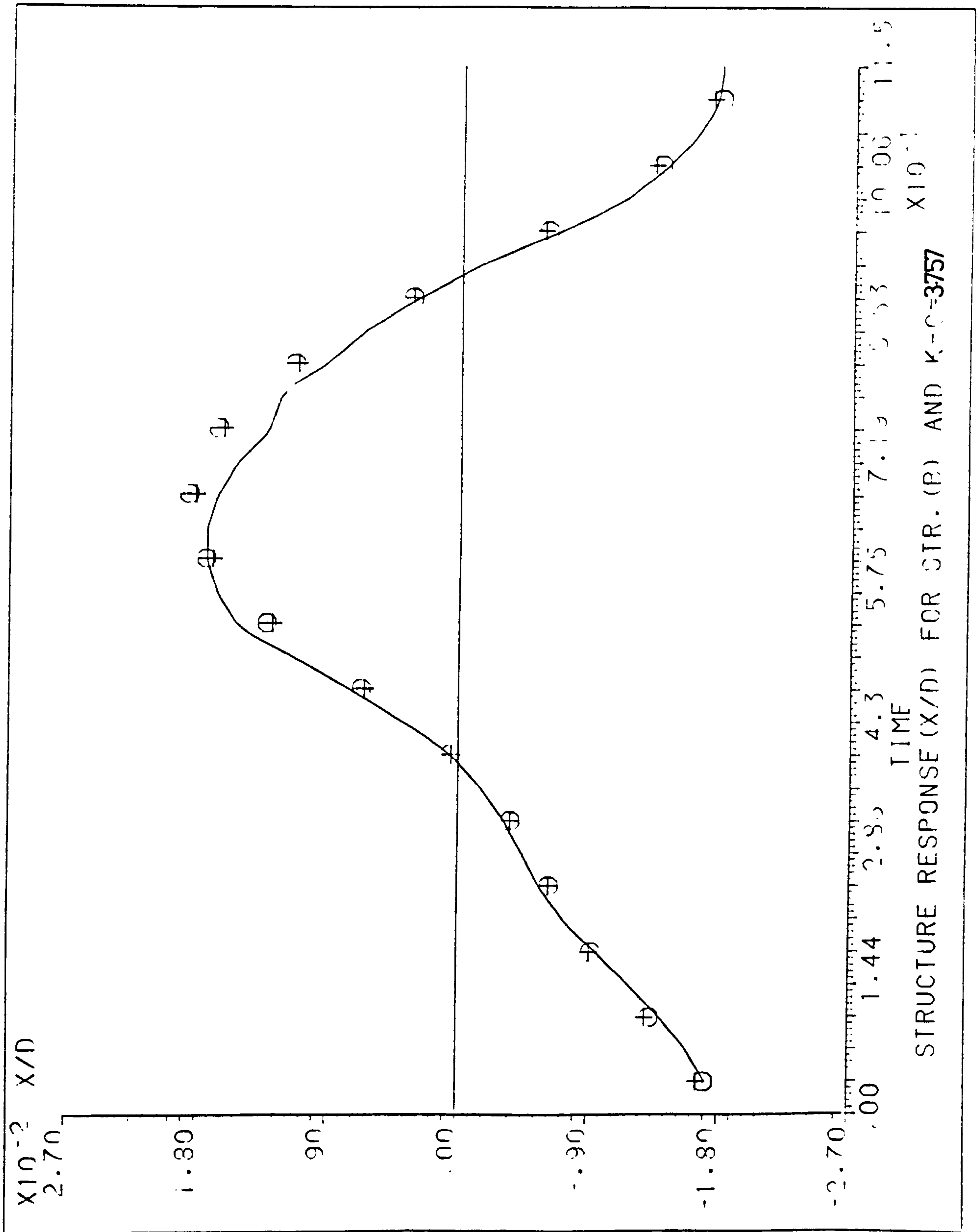


Figure (5.3.24) - Structure's Response (X/D) during the Wave Cycle for Structure B.



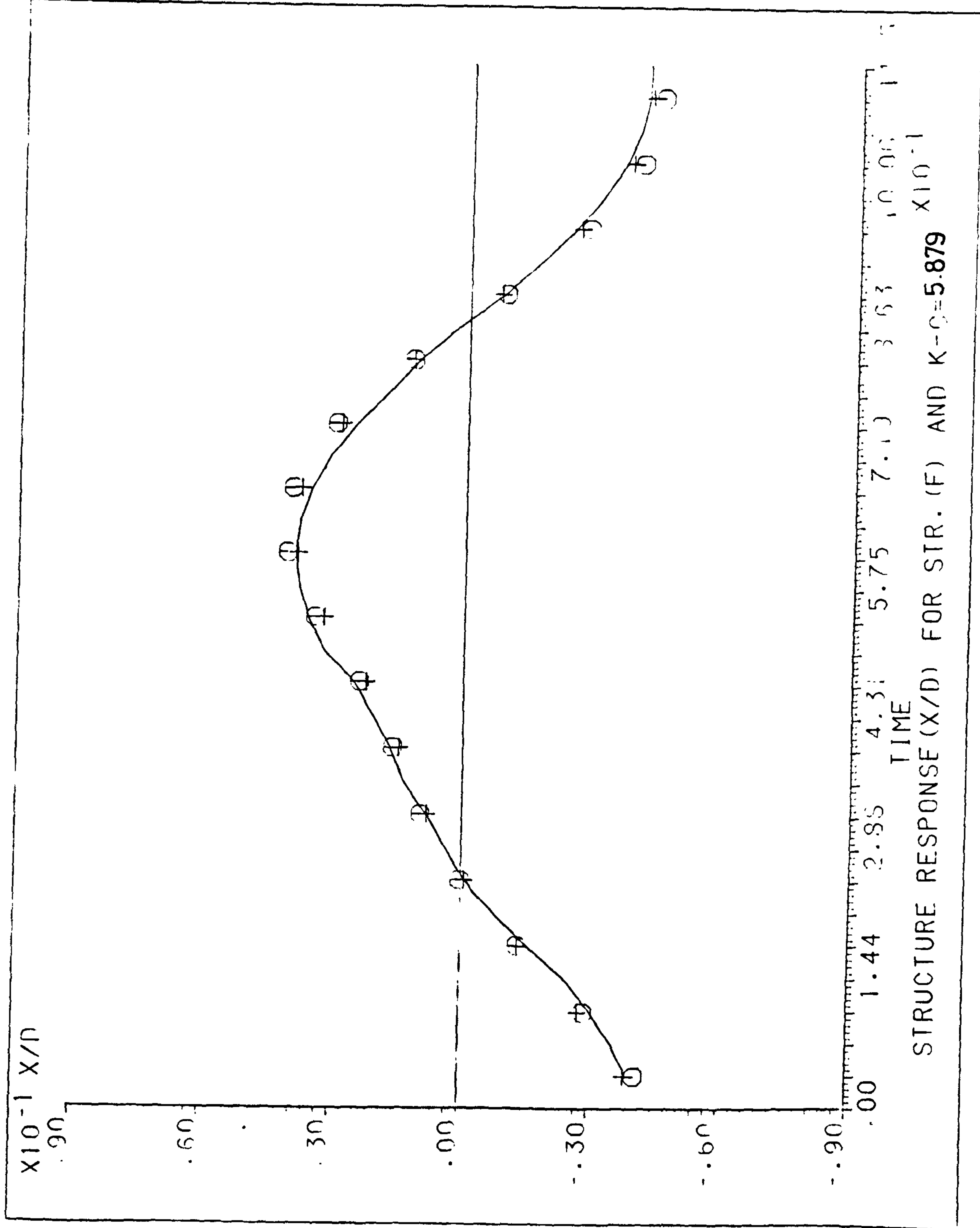


Figure (5.3.31) - Structure's Response (X/D) during the Wave Cycle for Structure F with 1010 Grs at Top.

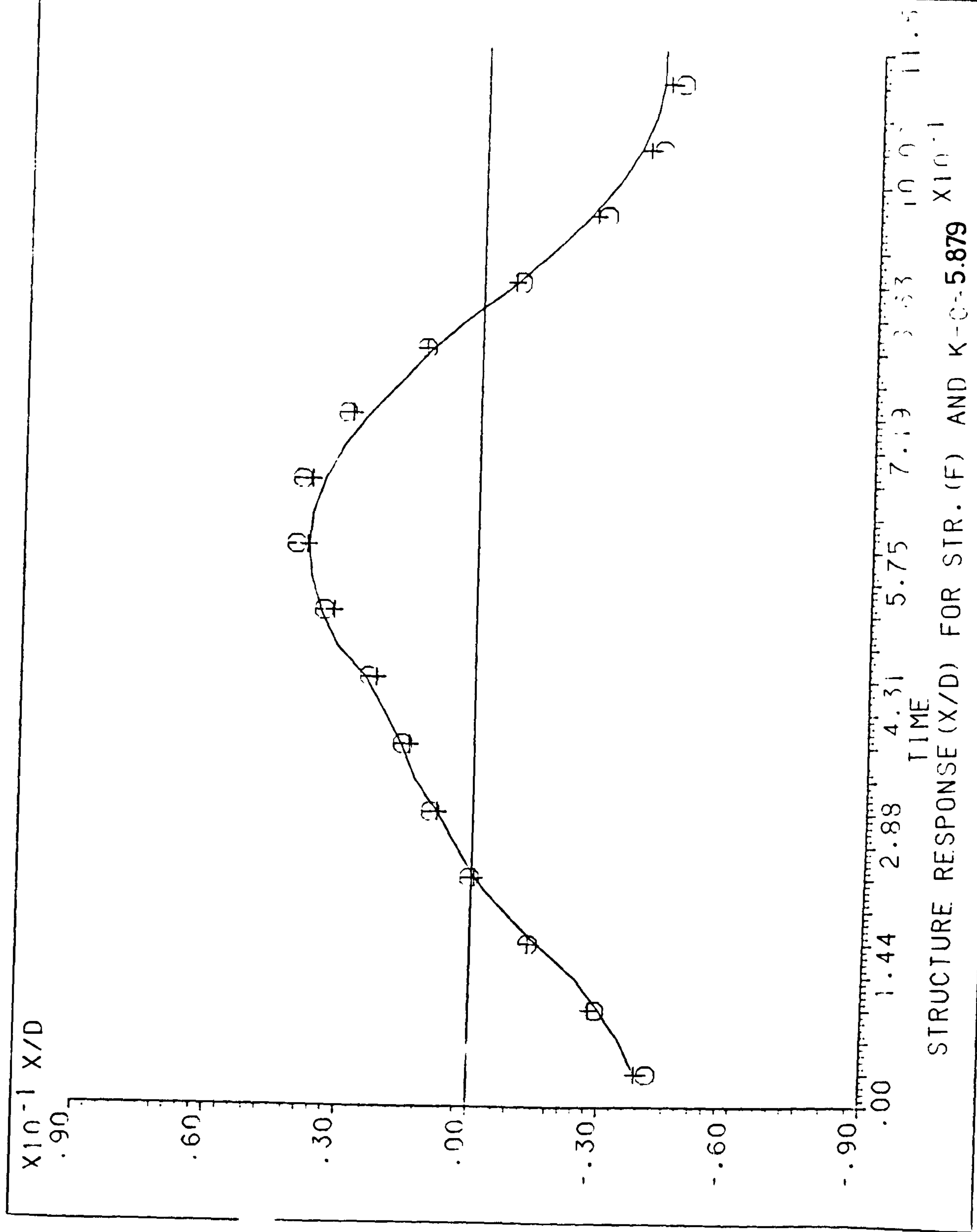


Figure (5.3.32) - Structure's Response (X/D) during the Wave Cycle for Structure F with 2020 Grs at Top.



**BEST COPY**

**AVAILABLE**

Variable print quality

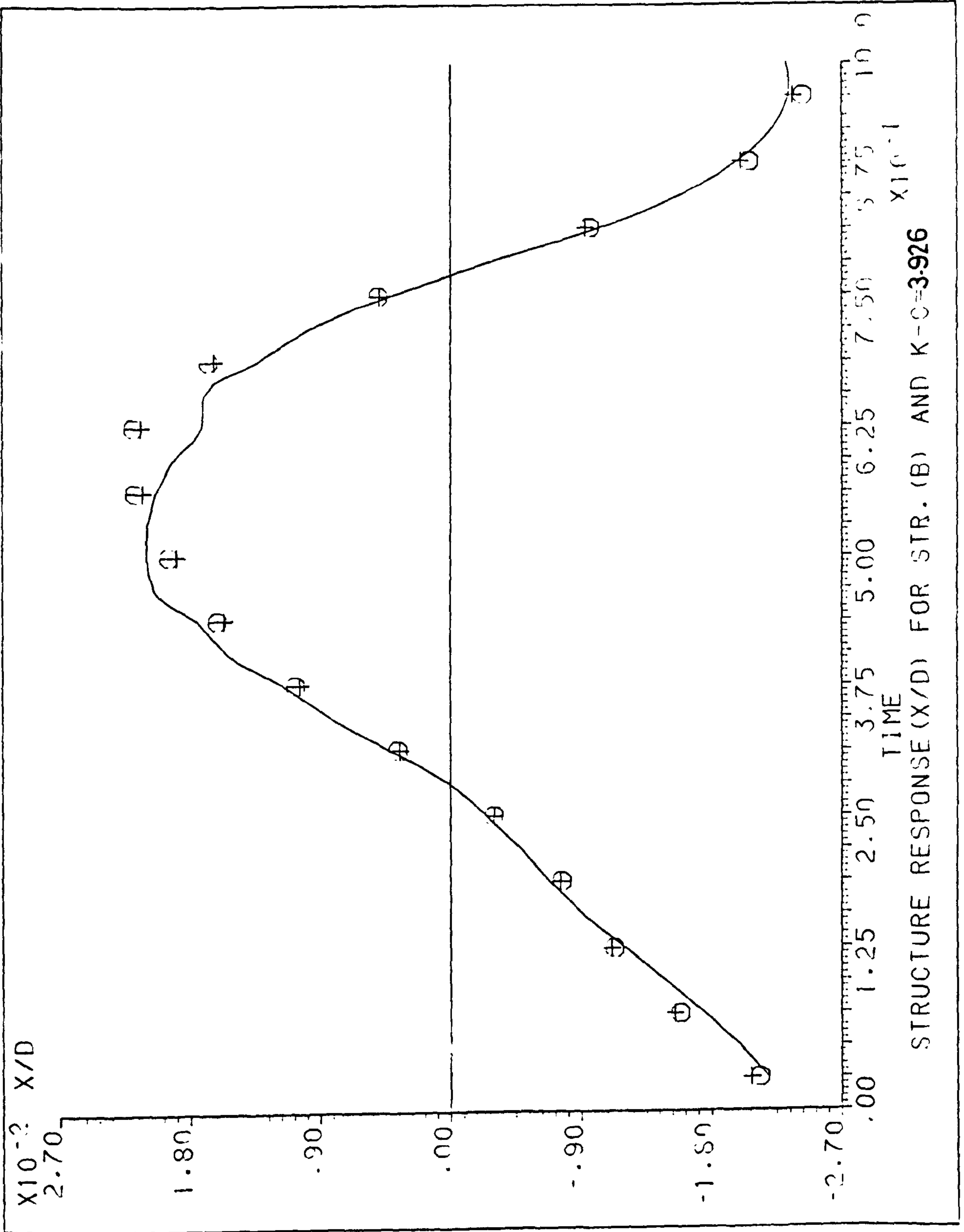


Figure (16D) - Structure's Response (X/D) during the Wave Cycle for Structure B (K-C = 3.926).